ИЗБРАННЫЕ ТРУДЫ АКАДЕМИКА Н.С. ЗЕФИРОВА В ОБЛАСТИ МЕДИЦИНСКОЙ ХИМИИ

# ИЗБРАННЫЕ ТРУДЫ АКАДЕМИКА Н.С. ЗЕФИРОВА В ОБЛАСТИ МЕДИЦИНСКОЙ ХИМИИ

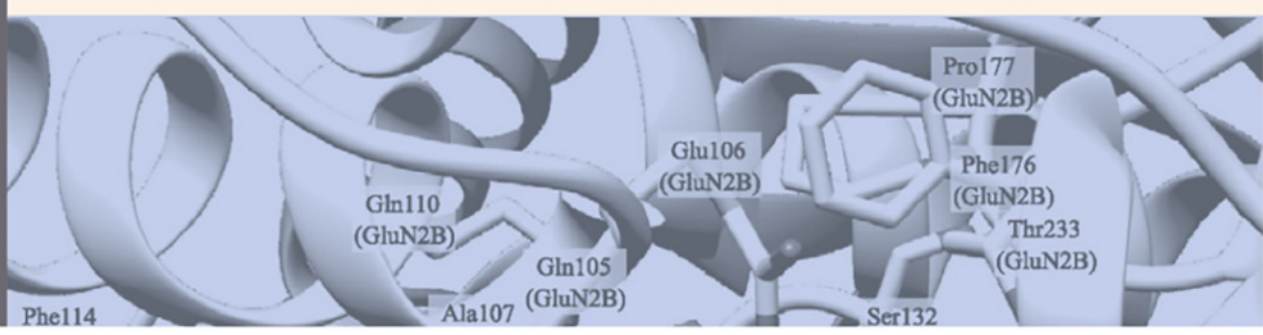

# Избранные труды академика Н.С. Зефирова в области медицинской химии

2025

УДК 541.69:54
ББК 24: 52.8

**Избранные труды академика Н.С. Зефирова в области медицинской химии.** Под общей редакцией академика С.О. Бачурина и профессора О.Н. Зефировой – ФИЦ ПХФ и МХ РАН, 2025, 364 с.

Книга содержит избранные статьи в области медицинской химии с авторством академика Н.С. Зефирова, опубликованные в открытой печати (в российских и зарубежных научных журналах). Материал в книге систематизирован по разделам: предмет и стратегии медицинской химии; избранные работы в области медицинской химии препаратов для лечения нейродегенеративных заболеваний; избранные работы по созданию противоопухолевых агентов; избранные работы в области медицинской химии препаратов для терапии нарушений окислительного статуса организма; избранные работы по созданию веществ с различными видами биологической активности; избранные работы в области развития методов компьютерного моделирования и QSAR. Книга содержит также Введение с кратким описанием научной деятельности академика Н.С. Зефирова.

*Составители:* академик **С.О. Бачурин,** д.х.н., проф. **О.Н. Зефирова,** д.х.н., проф. **Е.Р. Милаева,** к.х.н. **В.А. Палюлин**

*Набор, графика и компьютерная верстка*
к.х.н. **Е.В. Бовина**

**ISBN 978-5-91845-122-9**

# Введение

С течением времени наука претерпевает постоянные изменения в своем развитии: возникают новые области исследований, новые задачи и тенденции. К семидесятым годам двадцатого века произошло окончательное формирование междисциплинарного научного направления – медицинской химии (medicinal chemistry, drug design) с ее специфическим понятийным аппаратом, и с этого момента началось ее стремительное развитие в мире. В нашей стране фактическим инициатором образования и соответствующих исследований по тематике медицинской химии стал выдающийся химик-органик, академик Николай Серафимович Зефиров.

**Николай Серафимович Зефиров** (13.09.1935–28.04.2017) – личность поистине эпохального масштаба для российской науки. Его вклад в теорию и практику органической химии и органического синтеза (см. книгу «Органическая химия в работах Н.С. Зефирова») огромен: под его руководством на кафедре органической химии Московского государственного университета имени М.В. Ломоносова осуществлены синтезы многих оригинальных гетероциклических, полициклических, спироциклических и каркасных структур, в том числе уникальных; открыто явление конкурентного ковалентного связывания нуклеофугных анионов в карбокатионных процессах, дальнейшее изучение которого в свою очередь привело к открытию нескольких новых реакций и позволило ввести в практику органического синтеза многие новые реагенты (например, μ-оксодифенилиодозотрифлат – реагент Зефирова), а также синтезировать труднодоступные классы соединений. Широко известны исследования Н.С. Зефирова в области стереохимии, им открыты новые конформационные эффекты («хоккейных клюшек»; координационной стабилизации неустойчивых конформаций; существования ваннообразных конформаций дигетеробициклононанов и др.). В процессе изучения стереохимии и региоселективности реакций электрофильного присоединения было открыто явление увеличения эффективной электрофильности слабых электрофилов («допинг-присоединение»). Работы Николая Серафимовича в области теоретической органической химии и органического синтеза от-

мечены многочисленными престижными премиями и наградами, в том числе зарубежными; в разные годы он был членом редколлегий ведущих международных химических журналов: *Tetrahedron*, *Tetrahedron Letters*, *Tetrahedron Asymmetry*, *Synthesis*, *Physical Organic Chemistry*, *Журнал органической химии*, *Химия гетероциклических соединений* и др.

Будучи человеком творчески «ненасытным» и обладая неукротимой энергией, Н.С. Зефиров постоянно стремился к расширению спектра научных исследований. Под его руководством уже во второй половине XX века стали развиваться работы по изучению общих принципов генерации органических реакций с помощью компьютера и созданию оригинальных программ компьютерного синтеза. Совместно с С.С. Трачем была выполнена одна из фундаментальных разработок в области математической химии – предложен формально-логический подход к описанию органических реакций, примененный для классификации новых процессов. В начале 1990-х гг. Н.С. Зефиров стал уделять большое внимание решению общей проблемы поиска количественных соотношений структуры и свойств органических веществ. Эти работы позже создали математическую базу для получения соединений с целевыми свойствами, в том числе потенциальных лекарственных препаратов.

Вклад Н.С. Зефирова в развитие медицинской химии в России – его выдающееся достижение, поскольку во многом благодаря ему в нашей стране эта область химии оформилась в самостоятельное научное направление. В конце 1990-х гг. на одной из конференций Николай Серафимович познакомился с профессором университета г. Перуджи (Италия) Роберто Пелличчари (впоследствии президентом Европейского общества медицинской химии) и заинтересовался его работами по дизайну структур лекарств. Последовавшее затем глубокое изучение соответствующей литературы в сочетании с уникальным научным чутьем Николая Серафимовича позволили ему ощутить мощь и перспективы нового направления органической химии на стыке с биологией, фармакологией и математической химией. В значительной степени ориентированию на развитие направленного синтеза новых биологически активных соединений способствовало то, что с 1989 года он возглавлял Институт физиологически активных веществ РАН, который имел хорошую научную базу и задел в области оценки биологической активности вновь синтезируемых органических соединений.

Важнейшим делом национального масштаба, в котором проявилось стратегическое видение Зефировым развития отечественной медицинско-химической научной школы, стала организация им в 1998 году первого в нашей стране курса лекций по этому предмету для студентов МГУ. Появилась отдельная специализация «Медицинская химия», а в МГУ, ИФАВ РАН и ИОХ РАН были сформированы группы исследователей, работающих в области дизайна физиологически активных соединений. Эти работы включали в себя выполнение всех фундаментальных логических этапов дизайна лекарств: *выбор молекулярной мишени – предсказание структуры – синтез – биотестирование – оптимизацию*. Уже в

мае 2004 года в Москве впервые прошла Международная конференция по комбинаторной и медицинской химии под эгидой Европейского общества медицинской химии. Одним из участников этой конференции был профессор Камиль Вермут (1933–2015) – экс-президент медицинско-химической секции IUPAC, автор фундаментального труда «The practice of Medicinal Chemistry».

В 2011 году по инициативе Н.С. Зефирова была введена специальность ВАК по медицинской химии, – потребовались колоссальная энергия и авторитет Зефирова, чтобы отстоять право медицинской химии на существование в качестве самостоятельной научной дисциплины, внедрить ее в реестр специальностей ВАК, в государственные образовательные стандарты, в приоритетные направления развития академической науки и прикладных разработок. При активном содействии Николая Серафимовича и его единомышленников курсы лекций и исследования медицинско-химической направленности появились и в других научно-исследовательских институтах и университетах нашей страны. Он стал одним из главных организаторов цикла общероссийских конференций по медицинской химии, – в 2013-м году была проведена Первая Всероссийская конференция MedChemRussia с международным участием. Н.С. Зефиров был инициатором также ряда Российских и международных симпозиумов по компьютерному молекулярному моделированию и прогнозированию биологической активности химических соединений.

В течение 17 лет (с 1989 по 2006 гг.) Н.С. Зефиров возглавлял Институт физиологически активных веществ РАН в Черноголовке и многие годы был заведующим лабораторией математической химии в Институте органической химии им. Н.Д. Зелинского РАН. Огромной заслугой Николая Серафимовича было создание в 2014 году в МГУ имени М.В. Ломоносова первой в России кафедры медицинской химии и тонкого органического синтеза, в задачи которой входила подготовка специалистов для фармацевтической отрасли страны – разработчиков лекарственных веществ. Войдя в медицинскую химию уже в зрелом возрасте, Н.С. Зефиров вместе со своими более молодыми коллегами из Московского Университета и ИФАВ РАН активно участвовал и в литературных изысканиях, и в планировании уникальных разработок по созданию новых перспективных лекарственных кандидатов для лечения заболеваний центральной нервной системы, онкологических заболеваний и др.

Николай Серафимович работал над первым русскоязычным глоссарием терминов медицинской химии, который был составлен в 2000 г., а впоследствии неоднократно расширялся и редактировался (О.Н. Зефирова, К.В. Балакин, М.Ю. Красавин, В.А. Палюлин, В.В. Поройков, Е.В. Радченко, Н.Ф. Салахутдинов, А.А. Спасов, В.П. Фисенко, С.О. Бачурин. Глоссарий русскоязычных терминов в медицинской химии. *Известия Академии наук. Серия химическая*, 2019, № 12, 2381-2395).

*Стрельба по мишеням*

*Размышления над молекулярной мишенью*

*«Личный пример — не просто лучший метод убеждения, а единственный» (А. Швейцер)*

*На торжественном заседании, посвященном 30-летию ИФАВ РАН*

Академик Зефиров был одним из виднейших и авторитетнейших членов Российской академии наук, он всегда осознавал себя частью мирового научного сообщества, не знающего политических границ и национальных разделений. Сегодня Николай Серафимович стал частью Российской и мировой истории науки. В данной книге представлены некоторые, наиболее интересные и значимые статьи по тематике медицинской химии, написанные Н.С Зефировым и работавшими под его руководством авторскими коллективами в начале XXI-го столетия.

# Раздел I. Предмет и стратегии медицинской химии

## Введение

Первые публикации по медицинской химии имели своего рода «разъясняющий» характер и были призваны познакомить широкий круг химиков со спецификой этой области науки [1, 2]. Эту же задачу выполняли и обзорные статьи с авторством Николая Серафимовича Зефирова с описанием и анализом соотношений структура–активность для лигандов различных молекулярных мишеней (пример такого обзора см. [3]) или об использовании различных молекулярных фрагментов в дизайне лекарственных веществ [4–7].

## Список статей раздела

**1.** Зефирова О.Н., Зефиров Н.С. Медицинская химия (Medicinal Chemistry). I. Краткий исторический очерк, определения и цели // *Вестник Моск. ун-та. Сер. 2. Химия.* 2000. Т. 41. № 1. С. 43-47.

2. Зефирова О.Н., Зефиров Н.С. Медицинская химия (Medicinal Chemistry). II. Методологические основы создания лекарственных препаратов //*Вестник Моск. ун-та. Сер. 2. Химия*. 2000. Т. 41. № 2. С. 103-108.

Также для примера в данном разделе представлены первые страницы обзоров:

3. Зефирова О.Н., Нуриева Е.В., Рыжов А.Н., Зык Н.В., Зефиров Н.С. Таксол: Синтез, биоактивные конформации и соотношение структура–активность для его аналогов // ЖОрХ. 2005. Т. 41. № 3. С. 329-361.

4. Зефирова О.Н., Зефиров Н.С. Физиологически активные соединения, взаимодействующие с глутаматными рецепторами // ЖОрХ. 2000. Т. 36. № 9. С. 1231-1258.

5. Зефирова О.Н., Зефиров Н.С. Физиологически активные соединения, взаимодействующие с серотониновыми (5-гидрокситриптаминовыми) рецепторами // Успехи химии. 2001.Т.70. № 4. С. 382-407.

6. Zefirova O.N., Diikov A.G., Zyk N.V., Zefirov N.S. Ligands of the colchicine site of tubulin: A common pharmacophore and new structural classes // Russ. Chem. Bull. 2007. V. 56. P. 680-688.

7. Зефирова О.Н., Зефиров Н.С. Направленное применение мостиковых группировок в дизайне физиологически активных веществ // Изв. АН Сер. Хим. 2013. № 2. С. 329-341.

*ВЕСТН. МОСК. УН-ТА. СЕР. 2. ХИМИЯ. 2000. Т. 41. № 1, 43-47*

УДК 541.69:54(091)

# МЕДИЦИНСКАЯ ХИМИЯ (MEDICINAL CHEMISTRY). I. КРАТКИЙ ИСТОРИЧЕСКИЙ ОЧЕРК, ОПРЕДЕЛЕНИЯ И ЦЕЛИ

**О.Н. Зефирова, Н.С. Зефиров** ***(кафедра органической химии)***

Рассмотрена краткая история возникновения медицинской химии, определено место этой дисциплины среди смежных областей наук и рассмотрены основные задачи, решаемые этой наукой.

> «Бесчисленными путями наука (своими разнообразными дисциплинами – химией, биологией, медициной, токсикологией, экологией и компьютерными науками) вовлечена в изучение взаимодействия органических соединений со всеми формами жизни, биообразованиями и биомолекулами. Размах этих работ значительно более грандиозен, чем это обычно представляется... Как назвать эту новую область науки – не совсем ясно, но ее гигантскую, все более возрастающую важность отрицать невозможно».
>
> *Corwin Hansch (1993)*

*Медицинская химия (Medicinal chemistry)* – область органической химии, связанная с проблемой конструирования лекарственных препаратов *(drug design)*. Она зародилась в конце XIX–начале XX века и по-настоящему сформировалась к семидесятым годам нынешнего столетия, когда возникла соответствующая система понятий и определений. В последнее время эта химическая дисциплина развивается исключительными темпами. Цель настоящей работы заключается в том, чтобы проследить в общих чертах историю возникновения этой новой области химии, дать краткое описание и определить ее место среди других смежных с ней областей.

## Краткая история создания лекарственных препаратов

С древнейших времен в качестве источника лекарственных препаратов использовали в основном готовое растительное или животное сырье (классическим примером является *кора хинного дерева* – эффективное средство против малярии). Однако в средние века получила свое развитие идея применения химических средств для лечения болезней. Инициаторами этой идеи были алхимики, использовавшие производные *ртути, мышьяка, сурьмы, меди, цинка* и т. д., хотя препараты такого рода, принимаемые в неподходящих дозах, часто оказывались более опасными, чем сама болезнь.

В XVI в. швейцарский врач Парацельс изучил действие на организм многих веществ минерального и растительного происхождения и явился основателем *«иатрохимии»* – направления, стремившегося поставить химию на службу медицине [1].

В XIX в. существенно усовершенствовались методы химического анализа, что привело к попыткам найти в известных растениях активные ингредиенты, ответственные за лечебные свойства. Так, в начале XIX в. были выделены *хинин, морфин* и др. [2, 3].

Во второй половине XIX в., благодаря созданию структурной теории (Кекуле, Бутлеров, Купер), а также исследованиям многих химиков-органиков, началось бурное развитие органической химии, и это привело к подлинной революции в области синтеза лекарств. Во второй половине XIX в. появились чисто синтетические лекарственные препараты, например, синтетические галогенпроизводные (с 1869 г. *хлораль* стал применяться в качестве седативного и успокаивающего средства [4]) и *салициловая кислота,* используемая в качестве обезболивающего средства.

К концу прошлого века синтез лекарств приобрел уже промышленные масштабы. В 1888 г. фирма Байера выпустила эффективное жаропонижающее средство *фенацетин,* а в 1899 г. – известное противовоспалительное лекарство *аспирин (ацетилсалициловую кислоту)* [5].

Важно подчеркнуть, что к этому времени уже была осуществлена структурная идентификация таких соединений, как жиры, белки и углеводы, т.е. соединений, молекулы которых являются основными мишенями действия лекарственных препаратов.

Фенацетин

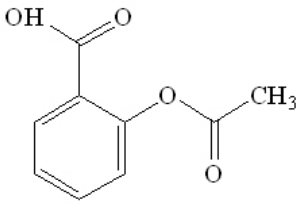

Аспирин

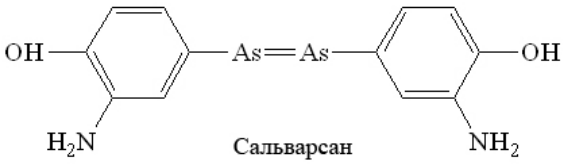

Сальварсан

В 1909–1910 гг. немецкий ученый Пауль Эрлих синтезировал *сальварсан* – первое эффективное средство против сифилиса, что обусловило возникновение концепции химиотерапии[1] [6]. Эта концепция предполагала уже не просто воз-

[1] Иногда называют хемотерапия.

можность использования химических веществ для лечения патологий (болезней), но и *необходимость модификаций структур* предполагаемых лекарственных соединений с тем, чтобы максимально эффективно воздействовать на пораженный орган.

Эрлих разработал также теорию рецепторов и структурных изменений физиологически активных органических соединений, происходящих при взаимодействии с рецептором, которая (вместе с его концепцией химиотерапии) явилась отправной точкой современной медицинской химии.

За период с конца XIX до начала 70-х годов XX в. химики создали многие тысячи аналогов, пытаясь воспроизвести и улучшить созданное природой. Были синтезированы *барбитураты* в качестве гипнотических средств [7], *ртутьорганические соединения,* обладающие свойствами диуретиков [8], *сульфамиды* – первые эффективные антибактериальные препараты [9, 10].

Возобновление в конце 30-х годов Флори и Чейном забытых работ по *пенициллину* (найденному Флемингом в 1928 г.), а также выделение стрептомицина Ваксманом в 1944 г. открыло эру антибиотиков [11].

В 50–60-е годы были созданы многие психотропные препараты, такие как сильные транквилизаторы *(хлорпромазин, мепробамат)* [12, 13], *хлордиазепоксид* (первый представитель класса бензодиазепинов), а также антидепрессанты (например, *имипрамин),* в результате чего появилась возможность лечения депрессий, шизофрении и других нервных расстройств [14].

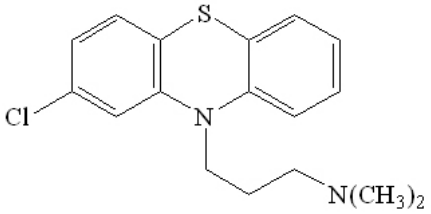


Хлорпромазин (Аминазин)

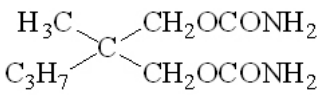


Мепробамат

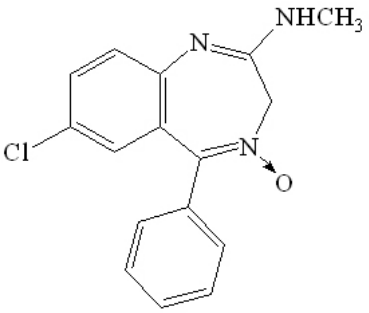


Хлордиазепоксид

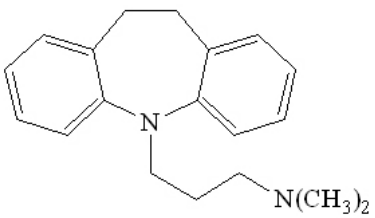


Имипрамин

В 50-х–60-х годах были синтезированы *резерпин* [15] и *метилдофа* – соединения, оказывающие антигипертензивное (гипотензивное) действие и применяемые для лечения сердечно-сосудистых заболеваний.

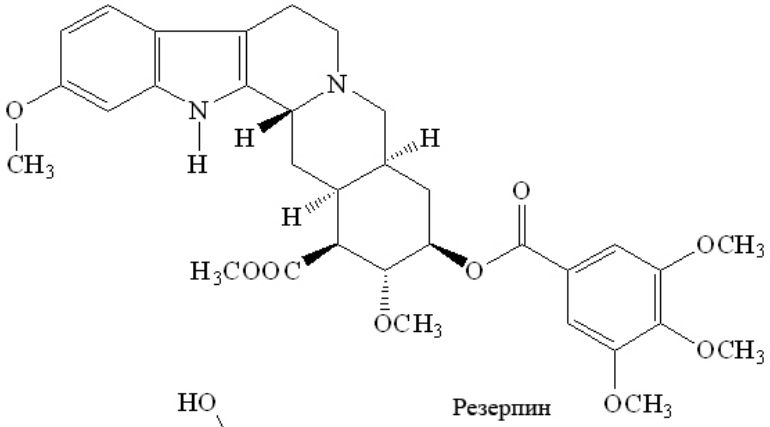


Резерпин

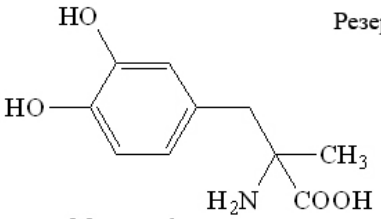


Метилдофа

Подчеркнем, что подавляющее большинство работ по созданию вышеупомянутых лекарственных препаратов было сделано без всякого «осознанного конструирования», методом «проб и ошибок», когда химики-органики в значительной степени произвольно заменяли одни химические группы другими. Однако постепенно на основании полученных результатов возникало понимание того, *какой стратегии и тактики нужно придерживаться, чтобы сконструировать лекарственное соединение.* Проникновение компьютерных методов в органическую химию привело к бурному развитию методов расчета структуры молекул (геометрии и конформаций, зарядов и карт электростатического потенциала, молекулярных орбиталей, топологических индексов и т.д.), в силу чего количественное описание структурных особенностей даже очень сложных молекул биологического уровня становилось обычным инструментом химика-органика. Поэтому в 70-х годах была создана методологическая основа для возникновения и использования рациональных подходов к синтезу физиологически активных веществ *(drug design),* что и привело к формированию медицинской химии с ее современным аппаратом.

## Что такое медицинская химия (medicinal chemistry)

В качестве отправной точки для обсуждения вопроса о предмете «медицинская химия» и ее месте среди смежных областей наук, рассмотрим раннее определение этой науки, данное комиссией IUPAC [16].[2]

[2] *Medicinal chemistry* concerns the discovery, the development, the identification and the interpretation of the mode of action of biologically active compounds at the molecular level. Emphasis is put on drugs, but the interests of the *medicinal chemistry* are not restricted to drugs but include

«Предметом *медицинской химии* является открытие, разработка и идентификация биологически активных соединений, а также интерпретация механизма их действия на молекулярном уровне. Основной акцент делается на лекарства, но интересы *медицинской химии* не ограничиваются лекарствами, а включают биологически активные соединения вообще. Предметом *медицинской химии* является также изучение, идентификация и синтез продуктов метаболизма этих лекарств и родственных соединений».

Из этого (не очень четкого!) определения ясно, что медицинская химия – наука междисциплинарная и находится на границе (с пересечением) *органической химии* с такими уже сформировавшимися и признанными науками, как *биохимия, биоорганическая химия, фармакология* и *фармацевтическая химия.*

Чем же отличается предмет *медицинской химии* от предмета исследований вышеперечисленных наук о жизни? Что касается сравнения с *биохимией* и *биоорганической* химией, то различия становятся понятными просто на основании определений последних, взятых из соответствующих учебников.

*Биологическая химия – а)* «наука о структуре химических веществ, входящих в состав живой материи, их превращении и физико-химических процессах, лежащих в основе жизнедеятельности» [17]; *б)* «наука, изучающая химическую природу веществ, входящих в состав живых организмов, их превращения, а также связь этих превращений с деятельностью органов и тканей» [18].

*«Биоорганическая химия* изучает строение и биологические функции важнейших компонентов живой материи, в первую очередь биополимеров и низкомолекулярных биорегуляторов, уделяя главное внимание выяснению закономерностей взаимосвязи между структурой и биологическим действием» [19].

Итак, ни *биологическая,* ни *биоорганическая* химия не претендуют на решение проблемы создания лекарств, хотя и важны, например, для понимания их действия.

Иначе обстоит дело, если рассматриваются определения таких научных областей, как *фармакология* и *фармацевтическая химия.*

*«Фармакология* [от греческого *Pharmakon* (лекарство) и *Logos* (учение)] – наука о взаимодействии лекарственных веществ с организмом и о путях изыскания новых лекарственных средств. Основными разделами фармакологии являются *фармакодинамика* и *фармакокинетика»* [20]. Есть и более короткое определение: *«Фармакология* – наука о лекарствах» [21].

*«Фармацевтическая химия* – наука, которая, базируясь на общих законах химических наук, исследует способы получения, строение, физические и химические свойства лекарственных веществ, взаимосвязь между их химической

bioactive compounds in general. *Medicinal chemistry* is also concerned with the study, identification, and synthesis of the metabolic products of these drugs and related compounds.

структурой и действием на организм, методы контроля качества лекарств и изменения, происходящие при их хранении» [22].

Видно, что формальное определение, данное *фармакологии,* избыточно широкое, настолько, что охватывает как задачи *фармацевтической,* так и *медицинской* химии. Однако после изучения реальных концепций и материалов, данных в учебниках по *фармакологии* и по *фармацевтической химии,* становится понятным, что данные области науки не дают ответа на главный вопрос, какую структуру надо синтезировать, чтобы создать лекарственное (физиологически активное) соединение, – вопрос, занимающий в *медицинской химии* центральное место. Иными словами, эти науки не дают ответ на вопрос: какую структурную формулу спрогнозировать для конкретного кандидата в лекарство.[3]

Существует еще одна область науки, о которой нельзя не упомянуть, говоря о *медицинской химии.* Это... медицинская химия! Это не ошибка, это еще одна медицинская химия. В классификации, предложенной Российским фондом фундаментальных исследований, в секции «Биология и медицинская наука» в разделе «Физиология и фундаментальная медицинская наука» указан подраздел *«Медицинская химия; фармакология»* [23].

В чем тут дело? Дело в том, что в данном случае речь идет о другой области науки, той, что на английском языке называется «medical chemistry».

Исчерпывающий ответ на вопросы, связанные с возникновением этой науки и проблем, решаемых ею, дается в работе [24]. Говоря об историческом значении этой области науки, автор, в частности, отмечает: *«Медицинская химия,* пришедшая на смену иатрохимии на рубеже XVIII–XIX вв., выполнила важную историческую функцию. В ее рамках в медицину были введены теоретические основы новой химии... В рамках *медицинской химии* началось использование данных *физиологической химии* для объяснения различных патологий». В результате произошло «растворение *патологической химии* в смежных направлениях – *клинической* и *медицинской химии».*

Таким образом, существуют две научные дисциплины, носящие на русском языке название медицинская химия. Медицинская химия, являющаяся аналогом medical chemistry, – это, в сущности, «биохимия патологических состояний». Одним из основных предметов ее исследований является разработка различных аналитических методов, используемых в диагностических целях, и поэтому ее действительно можно считать разделом медицины.

[3] В зарубежной литературе иногда встречается такая точка зрения, что «медицинская химия» – это новая область науки, пришедшая на смену «фармацевтической химии», названной так потому, что первооткрывателями лекарственных соединений часто были фармацевты. Однако в нашей стране «фармацевтическая химия» существует как самостоятельная дисциплина. Существуют учебники и курсы по «фармацевтической химии», задачи и цели которой, как показано выше, во многом не совпадают с таковыми для «медицинской химии».

Медицинская химия, рассматриваемая в настоящем обзоре *(medicinal chemistry,* от слова *«medicine»* – лекарство, по-французски *«chimie therapeutique»,* по-немецки *«Arzneimittelforschung»)* – это, подчеркнем еще раз, другая наука, не являющаяся разделом биологии, а являющаяся в первую очередь специфическим разделом органической химии на стыке с биохимией, биоорганической химией и фармакологией.[4]

Действительно, органическая химия имеет одну принципиальную особенность – свой специфический язык, а именно язык структурных формул. Медицинская (химиотерапевтическая) задача обычно формулируется на совершенно другом языке (например, на языке биохимии), и она непонятна или неприемлема для химика-органика, который знает, как синтезировать вещества, но не получает от смежных дисциплин указание, вещество какой структуры нужно синтезировать для решения данной задачи. Именно этим было обусловлено возникновение специальной дисциплины – *медицинской химии,* ставшей посредником, позволяющим перевести формулировку задач с языка биохимии и фармакологии на структурный язык органической химии. При этом медицинская химия имеет свою собственную систему понятий и определений [25], что и делает ее самостоятельной дисциплиной.

Поясним данную мысль на конкретном примере. Пусть сформулирована медицинская (химиотерапевтическая) задача о создании препарата для лечения заболеваний, сопровождающихся образованием язвы желудка. Для решения этой задачи химик может располагать следующей медицинской и биохимической информацией:

1. Одним из факторов, способствующих возникновению и развитию данного заболевания является повышенное выделение соляной кислоты. В случае тяжелых форм заболевания (частые повторные кровотечения, значительное кислотообразование и т.д.) обычная терапия (использование антацидных препаратов, например, гидроокисиалюминия и др.) часто оказывается неэффективной;
2. выделение желудочного сока регулирует эндогенный медиатор – *гистамин* – посредством связывания с $H_2$-рецептором. Уменьшить выделение кислоты можно созданием специфического антагониста $H_2$-рецептора, блокирующего его действие.

Это типичная медицинская, биологическая и биохимическая информация. Для химика-органика вопрос стоит так: можно ли на основании этих данных

[4] Терминологическая путаница из-за того, что две разные дисциплины имеют одно название на русском языке («медицинская химия»), может иметь негативные последствия, так как препятствует осознанному развитию дисциплины, эквивалентной «medicinal chemistry».

предложить конкретную структуру такого антагониста? Очевидно, что ответ отрицателен. Более того, на основании этой информации химик-органик не может предположить даже класс соединений. Взять производные пиридина, или адамантана, или гексоз, или ароматических аминов? Возникают еще многие сотни тысяч «или». С каких структур следует хотя бы начинать?

Этот пример показывает, что медико-биохимическая информация такого типа, несмотря на ее безусловную важность и ценность, тем не менее явно недостаточна для того, чтобы химик-органик смог предложить структуру (химическую формулу) соответствующего физиологически активного соединения и приступил к синтезу.

И здесь на сцену выходит *медицинская химия.* Именно *медицинская химия* играет роль своеобразного переводчика биохимической информации на язык структурных формул, в результате чего становится возможным создание необходимого химического соединения. В вышеприведенном конкретном примере таким соединением явился *циметидин*.[5] [26].

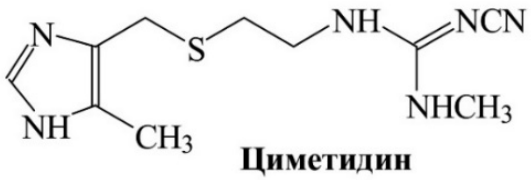


**Циметидин**

Перевод биохимической информации на язык органической химии не так прост, как это может показаться на первый взгляд. Органическая химия имеет дело с двумя фундаментальными проблемами:

1. структурные манипуляции (сюда входит и органический синтез, и изучение механизмов реакций, и поиск новых реакций и реагентов и т. д.);
2. соотношение структуры и свойства. Нетрудно видеть, что медицинская химия адресуется ко второй проблеме: *как, зная целевое свойство, предсказать необходимую для этого структуру* и уже далее реализовать ее в синтезе. Для решения этой проблемы создан свой специальный понятийный аппарат, и все это делает медицинскую химию фундаментальной химической дисциплиной [25].

Итак, общие цели медицинской химии формулируют смежные химико-биологические науки. Предметом же *медицинской химии (medicinal chemistry)* являются поиск и создание физиологически активных веществ, выявление взаимо-

[5] Отметим, что исторически при создании противоязвенного препарата существование $H_2$-рецептора гистамина сначала только предполагалось, т.е. даже в этой биохимической информации не было полной уверенности. И тем не менее, применение рациональных подходов к созданию нужного соединения оказалось возможным.

связи между химической структурой и физиологической активностью и, наконец, решение обратной задачи: конструирование необходимых структур, обладающих заданным свойством.

**СПИСОК ЛИТЕРАТУРЫ**


1. *Köstner. I.* // Theophrastus Bombastus von Hohenheim, genannt Paracelsus. Leipzig, 1989.
2. *Pelletier J., Caventou E.* // Ann. Chim. Phys. [2]. 1820. 15. P. 291.
3. *Sertamer F. W. A.* // J. Pharm. 1805. 13. P. 234.
4. *Liebreich O.* // Klin. Wochenschr. 1869. 6. P. 325.
5. *Вейссманн Дж.* // В мире науки. 1991. № 3. С. 54.
6. *Эрлих П, Хата С.* // Экспериментальная химиотерапия спириллезных заболеваний. М., 1911.
7. *Impens E.* // Deut. Med. Wochenschr. 1912. 38. P. 945.
8. *Saxl R, Heilig R.* // Wien. Klin. Wochenschr. 1920. 33. P. 943.
9. *Gelmo R.* // J. Prakt. Chem. 1908. 77. P. 369.
10. *Domagk G.* // Deut. Med. Wochenschr. 1935. 61. P. 250.
11. *Шемякин М. М., Хохлов А. С., Колосов М. Н, Бергельсон Л. Д., Антонов В. К.* // Химия антибиотиков. М., 1961.
12. *Courvoisier S., Foumel J., Ducrot R., Kolsky M., Koetchet P.* // Arch. Intern. Pharmacodyn. 1953. 92. P. 305.
13. *Berger F. M.* // J. Pharmacol. Exp. Ther. 1954. 112. P. 413.
14. *Hafliger F., Burckhardt V.* Psychopharmacological Agents. Part 1. N. Y., L., 1964.
15. *Woodward R. B., Bader F E., Bickle H, Frey A. J., Kierstad R. W.* // J. Am. Chem. Soc. 1956. 78. P. 2023.
16. *Wermuth C. G.* // The practice of Medicinal Chemistry. N. Y., 1996. P. 5.
17. *Строев Е. А.* // Биологическая химия. М., 1986. С. 5.
18. *Березов Т. Т, Коровкин Б. Ф.* // Биологическая химия. М., 1990. С. 6.
19. *Овчинников Ю. А.* // Биоорганическая химия. М., 1987. С. 8.
20. Краткая медицинская энциклопедия. Т. 3. М., 1990. С. 288.
21. *Маркова И. В., Нижинцев М. В.* // Фармакология. СП., 1997. С. 4.
22. *Беликов В. Г.* // Фармацевтическая химия. М., 1993.1. С. 5.
23. Российский Фонд Фундаментальных Исследований. Конкурсы 1998 года, подраздел 04-370. Поиск. № 26 (424). 21-27 июня 1997 года.
24. *Шамин А. Н.* // История биологической химии: Формирование биохимии. М., 1993. С. 227.
25. *Зефирова О. Н, Зефиров Н С.* // Вести. Моск, ун-та. Сер. 2, Химия. 2000. 41
26. *Durant G., Emmett J. C. Ganellin C. R.* Second Symposium on Histamine – Receptor Antagonists. / Eds. W. L. Burland, M. A. Simkins. Amsterdam-Oxford, 1977.


*Поступила в редакцию 03.09.98*

*ВЕСТН. МОСК. УН-ТА. СЕР. 2. ХИМИЯ. 2000. Т. 41. № 2, 103-108*

УДК 541.69:001.8

# МЕДИЦИНСКАЯ ХИМИЯ (MEDICINAL CHEMISTRY). II. МЕТОДОЛОГИЧЕСКИЕ ОСНОВЫ СОЗДАНИЯ ЛЕКАРСТВЕННЫХ ПРЕПАРАТОВ

**О. Н. Зефирова, Н. С. Зефиров** ***(кафедра органической химии)***

Обсуждены методологические аспекты медицинской химии и охарактеризована система ее научных понятий. Подробно рассмотрены вопросы, связанные со стратегией поиска, конструирования и оптимизации соединений-лидеров и разработки лекарственных препаратов.

> Имеется $10^{180}$ возможных биологически активных веществ, $10^{18}$ вероятных лекарственных препаратов, $10^7$ известных соединений, $10^6$ коммерчески доступных соединений, $10^6$ соединений в базах данных фирм, $10^4$ соединений в базах данных по лекарствам, $10^3$ коммерческих лекарств и $10^2$ коммерчески выгодных лекарств.
>
> *Weininger*

В предыдущей части [1] мы рассмотрели предмет медицинской химии. Цель настоящей работы заключается в том, чтобы охарактеризовать систему научных понятий, используемых в медицинской химии. Мы покажем, что медицинская химия, проникнутая структурными концепциями конструирования лекарств *(drug design),* стала новой областью химического знания, со своими научными понятиями и своей научной методологией.

Как правило, процесс поиска и конструирования лекарственных препаратов включает в себя три основные стадии:

I. Поиск и конструирование соединений-лидеров *(lead-compounds)*[6];

II. Оптимизация соединения-лидера;

III. Разработка лекарственного препарата.

Стратегия поиска лекарственных препаратов зависит от накопленных знаний об уже известных препаратах, мишенях их действия и т.д. Стратегия поиска (особенно *компьютерного)* соединений с максимальной и специфической биологической активностью зависит от наличия исходных данных. Различные варианты состояния начальной информации можно условно разделить на четыре основные категории:

1. Структуры как рецептора[7], так и лиганда неизвестны;

[6] В отечественной литературе «соединение-лидер» иногда называют «базовое соединение».

[7] Здесь понятие «рецептор» употребляется в широком смысле. Это может быть любая макромолекула – мишень лекарственного вещества в организме, а понятие «лиганд» предполагает любое эндогенное соединение, взаимодействующее с этим рецептором в организме.

2. Известна только структура рецептора (структура лиганда неизвестна);
3. Известна только структура лиганда (структура рецептора неизвестна);
4. Известны структуры как рецептора, так и лиганда.

Рассмотрим эти вопросы более детально.

## Поиск и конструирование соединений-лидеров

Первая стадия поиска и конструирования лекарственных препаратов состоит, как правило, в идентификации и синтезе новых физиологически активных веществ (ФАВ), обычно называемых «соединениями-лидерами» *(lead-compound).* Соединение-лидер – это своего рода структурный прототип будущего лекарства, т.е. соединение, обладающее определенной физиологической активностью, на базе которого и будет создаваться лекарство [2].

Соединение-лидер может быть найдено случайно, и в истории создания лекарственных препаратов таких примеров очень много. Именно так был открыт, например, *нитроглицерин,* приведший к синтезу многих эфиров алифатических спиртов с азотной кислотой, и *пенициллин,* на основе которого были синтезированы его многочисленные аналоги и производные.

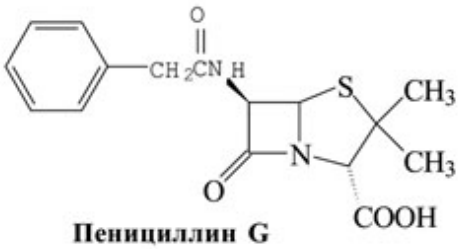


**Пенициллин G**

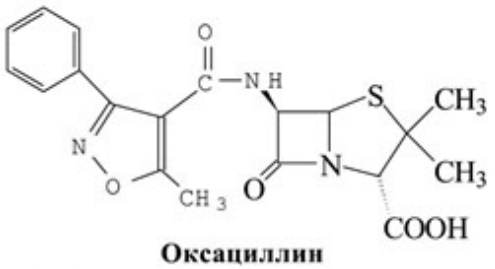


**Оксациллин**

***(один из аналогов пенициллина)***

Однако обычно начальный поиск связан с систематическим тестированием («скринингом») различных веществ на активность. Выделено два вида систематического скрининга: *а)* исследование в одном биологическом тесте достаточно большого количества соединений; *б)* изучение нескольких соединений с оригинальной структурой на многих биологических тестах. Обычно это дорогие и трудоемкие методы, сильно ограничивающие полную проверку гигантского потенциального набора органических веществ.

При скрининге иногда используют термин *hit-compound,* означающий своего рода «попадание в цель» – нахождение соединения, проявляющего физиологическую активность. Затем проводится тестирование круга соединений с похожей структурой, из которых потом и выбирается соединение-лидер.

В принципе соединение-лидер может быть не только получено органическим синтезом, но и выделено из природных источников. В поисках соединений-лидеров методом систематического скрининга нередки обращения к источникам

так называемой «народной медицины». Иными словами, источниками молекул для тестирования на биологические свойства могут быть как продукты химического синтеза, так и природные соединения, имеющие молекулы с очень необычной и сложной структурой.

Примером соединения-лидера, найденного с помощью систематического скрининга природных соединений, является *таксол* – эффективное противораковое средство [3].

В современной медицинской химии существует несколько стратегий направленного поиска соединения-лидера.

## Тотальный («through put») скрининг

С развитием компьютерной и робототехники был разработан так называемый *тотальный или сплошной скрининг,* который представляет собой одновременный автоматизированный и миниатюризованный анализ *in vitro* нескольких сотен и даже тысяч соединений в 30–50 биологических тестах. Метод сплошного скрининга, как правило, используется для тестов с замещением лигандов, меченных радиоактивными атомами, и ингибированием ферментов.

Развитие методов сплошного скрининга вызвало к жизни новое направление в органическом синтезе – *синтез «комбинаторных библиотек».* Последние представляют собой смесь большого (часто очень большого) числа соединений, полученных однотипным методом с использованием серий аналогичных реагентов и имеющих регулируемый состав. Эта смесь подвергается тотальному скринингу, после чего проводится идентификация тех структур смеси, которые проявляют биологическую активность [4].

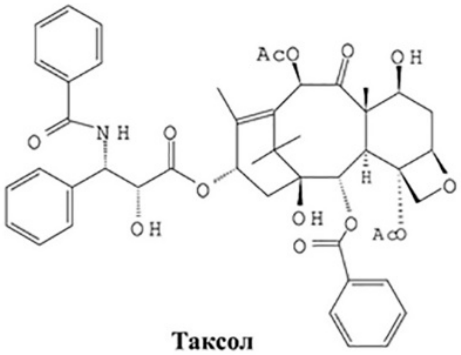

**Таксол**

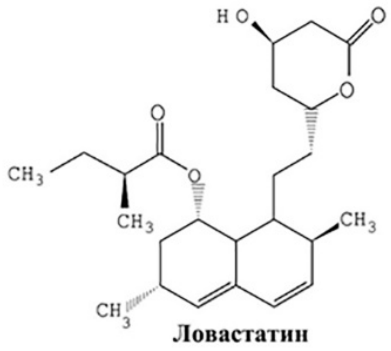

**Ловастатин**

Среди успехов метода сплошного скрининга можно отметить получение *ловастатина,* ставшего соединением-лидером для нового поколения препаратов, снижающих уровень холестерина в крови [5].

## Использование в качестве соединения-лидера уже известного (часто выпущенного на рынок) лекарства

Очевидно, что в этом случае генерируемые структуры, как правило, достаточно похожи на свой прототип (так называемые *терапевтические копии).* Тем не менее этот подход имеет специфические аспекты, обусловливающие его применение. Например, если соединением- лидером служит известное лекарство, имеющее достаточно выраженный побочный эффект, разрабатываться будет именно это «неосновное» свойство. Например, в 80-х годах было показано, что антиадренергические препараты β-адреноблокаторы), например, *атенолол,* обладают также гипотензивным эффектом. Поэтому похожая структура была использована в качестве соединения-лидера для создания антигипертензивных препаратов, которые, однако, не обладали бы β-блокаторной активностью.

Это привело к созданию *кромакалима* – первого соединения, действующего исключительно на активацию калиевых каналов (чем и обусловлена его активность как антигипертензивного средства) [6].

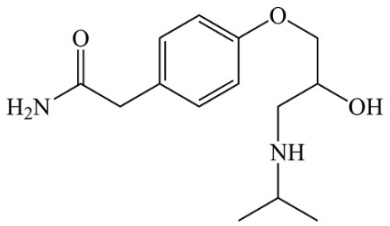


**Атенолол**

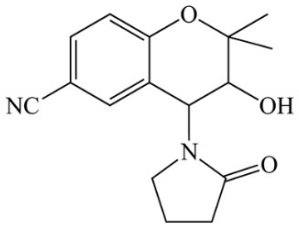


**Кромакалим**

## Рациональное конструирование соединения-лидера

К началу 70-х годов появилась реальная возможность сознательного конструирования соединений-лидеров, основываясь на информации, полученной благодаря достижениям биоорганической химии, молекулярной биологии (в особенности благодаря установлению структур некоторых рецепторов и ферментов методом рентгеноструктурного анализа). Целенаправленное конструирование особенно эффективно в том случае, когда известны структуры как рецептора, так и лиганда.

Во-первых, в этом случае, применяется компьютерное совмещение полости рецептора или фермента и гипотетических молекул *(компьютерное моделирование, docking)* с целью достижения как максимального совмещения размеров молекулы с размером полости, так и максимального взаимного связывания за счет учета водородных связей, электростатического притяжения, липофильных взаимодействий и т.д. Важным моментом «докинга» может явиться поиск подходящего трехмерного молекулярного фрагмента в соответствующей структурной базе данных. Во-вторых, если субстратом рецептора или фермента является пептидная молекула, то можно по аналогии сконструировать непептидную молекулу

*(пептидомиметик),* которая выступала бы в качестве ингибитора данного фермента. Классическим примером является использование *N-сукцинил-L-пролина* в качестве соединения-лидера для создания антигипертензивного препарата на основании знания механизма ферментативной реакции превращения ангиотензина I в ангиотензин II (последний повышает кровяное давление путем сужения сосудов). *Каптоприл* – искусственный ингибитор конвертирующего фермента – был синтезирован на основе вышеуказанного соединения в 1975 г., считается одним из первых «спроектированных» лекарственных препаратов [7].

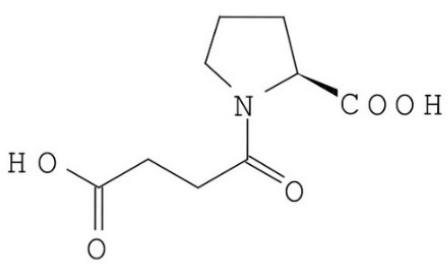


**N-сукцинил-L-пролин**

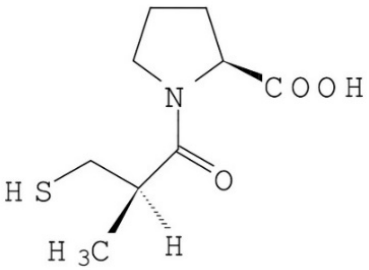


**Каптоприл**

## Оптимизация соединения-лидера

Вторая стадия конструирования лекарственного соединения – оптимизация – состоит в создании синтетической модификации структуры соединения-лидера с целью повышения его активности, уменьшения токсичности и улучшения селективности действия. Подходы, используемые на этой стадии создания лекарственных препаратов, включают изменения структуры молекулы, приводящие к лучшему соответствию между молекулой и ее мишенью в организме, например ферментом или рецептором. Такие подходы часто включают в себя также синтез структурных аналогов соединения-лидера, о чем уже упоминалось выше.

Поскольку количество возможных аналогов очень велико, в настоящее время широко применяют рациональные подходы, позволяющие предсказывать, какие заместители нужно использовать. Основными методами, используемыми медицинскими химиками на этой стадии разработки, являются вышеупомянутое компьютерное моделирование и *QSAR* (Quantitative Structure–Activity Relationship или «количественное соотношение структура–активность») [8, 9] – математический аппарат, позволяющий проводить корреляции структур химических соединений с их биологической активностью. *QSAR* предполагает идентификацию и количественное выражение структурных параметров или каких-либо физико-химических свойств физиологически активных веществ в виде *дескрипторов* с целью выявления факта влияния каждого из них на биологическую активность. Если такая зависимость имеет место, то возможно составление уравнений, позволяющих просчитать заранее биологическую активность новых аналогов, что,

в свою очередь, позволит сократить количество аналогов, которые должны быть синтезированы.

Отметим, что обнаружение аналога, не попадающего под корреляцию, означает, что для проявления молекулой биологической активности важны какие-то другие ее характеристики; в таком случае этот аналог может стать новым соединением-лидером для последующей разработки. Поэтому *QSAR* применяется для поиска соединений-лидеров в случае, когда известна только структура лиганда, а структура рецептора не известна.

Основными дескрипторами, наиболее часто применяемыми в *QSAR,* являются:

*липофильность* (способность растворяться в липидах), необходимая в первую очередь для оценки способности лекарства преодолевать клеточные мембраны*;*

*электронные эффекты,* влияющие на ионизацию или полярность соединения*;*

*стерические особенности структуры,* играющие важную роль при оценке прочности связывания исследуемого соединения в активном центре фермента или рецептора*;*

*фрагментные дескрипторы,* оценивающие вклад различных частей молекулы в общее свойство (в благоприятных случаях это может привести к формулировке гипотезы о фармакофорной группе – функциональной группе, определяющей проявление определенной физиологической активности данным веществом*).*

Итак, стратегия поиска соединений-лидеров и их оптимизация с помощью методов *QSAR и компьютерного моделирования* зависит от наличия исходных данных.

В благоприятном случае, разрабатывая (на основании небольшого количества химических соединений с известной активностью) количественную модель структура–активность *(QSAR),* предсказывающую необходимые структурные формулы, и/или формулируя структурную (или даже трехмерную) фармакофорную гипотезу, позволяющую выявить относительное расположение химических групп, важных для проявления веществом биологической активности, можно добиться резкого ограничения круга синтезируемых соединений в поиске лекарственного препарата.

Методы современного компьютерного конструирования многообразны и не ограничиваются только рассмотренными выше. Так, в случае, когда известна структура рецептора, но не найдено соединение-лидер, способное взаимодействовать с активным центром, эффективным оказывается поиск 3D-структур в

больших базах данных, с тем чтобы идентифицировать *малые фрагменты молекул,* которые могут взаимодействовать со специфическими областями рецептора, а также *связывающие (мостиковые) фрагменты* определенного размера и геометрии, которые смогут удерживать функциональные группы в нужной ориентации. Возможно использование подходов математической химии, например использование кластерного анализа и методов поиска 2D- и 3D-аналогий для идентификации потенциальных лидеров. Подход, известный под названием «оценка несходства» *(diversity assessment),* также может быть использован для идентификации непохожих соединений и их исследования методами комбинаторной химии.

## Разработка лекарственного соединения

Третья стадия – стадия разработки лекарственного соединения – включает в себя улучшение его фармацевтических и фармакокинетических свойств таким образом, чтобы сделать лекарство удобным для клинического использования (например, повысить его растворимость в воде или химическую стабильность, пролонгировать его действие и др.). При этом иногда приходится прибегать к структурной модификации и даже специальному синтезу новых структур. В этом случае возможны следующие подходы:

*Создание биоизостерических соединений (биоизостер* – химическая группа, которая способна заменить другую химическую группу, не сильно изменив при этом трехмерную молекулярную структуру и тем самым физиологическую активность) [34].

*Создание пролекарств (pro-drug)* – соединений, не обладающих выраженной физиологической активностью, но способных превратиться в активные соединения либо посредством ферментативной реакции, либо химическим (без участия белкового катализатора) путем (например, соединение *азатиоприн* является пролекарством *6-меркаптопурина,* обладающего цитостатическими и иммунодепрессивными свойствами).

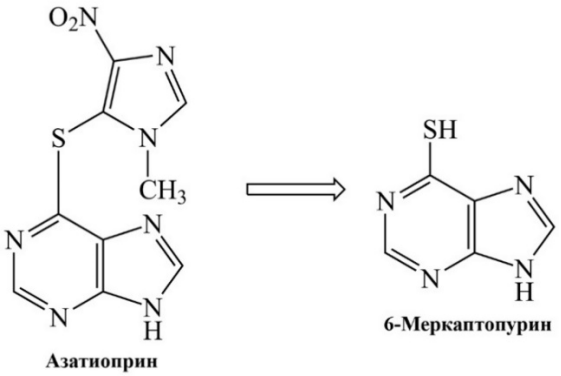


Азатиоприн 6-Меркаптопурин

В организме азатиоприн медленно превращается в 6-меркаптопурин [11], что приводит к пролонгированию действия последнего.

Создание *«мягких лекарств» (soft drugs)* – соединений, фармакологический эффект которых локализован в определенном месте (их распределение в других местах приводит к быстрой деструкции или инактивации). Этот стратегический прием был, например, использован при создании лекарств против глаукомы [12].

Создание *«двойных лекарств» (twin drugs)* – физиологически активных соединений, содержащих две фармакофорные группы, объединенные ковалентно в одну молекулу (такое определение исключает комбинацию двух лекарств в одну молекулу соли).

В качестве примера *идентичного* двойного лекарства, представляющего собой комбинацию двух одинаковых составляющих, приведем симметричную молекулу BDHP, активность которой приблизительно в десять раз выше, чем активность составляющих ее молекул *нитрендипина* (антагониста кальциевых каналов) [12].

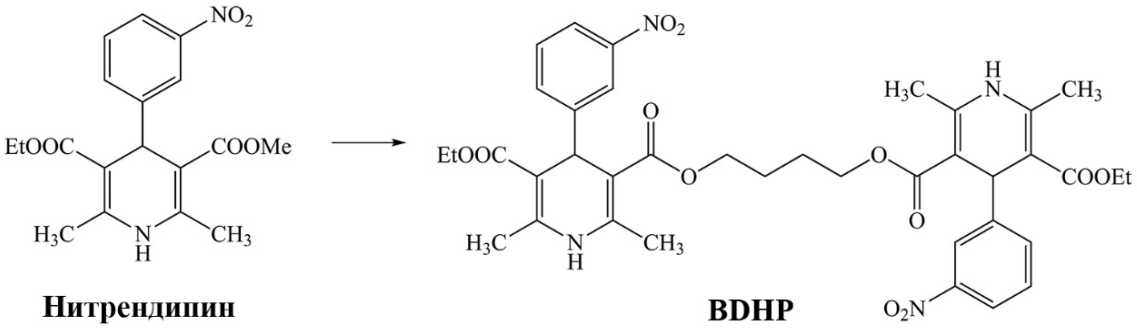


**Нитрендипин** **BDHP**

*Двойные лекарства* могут быть и *неидентичными* (имеющими в качестве составляющих различные структуры). В частности, возможно конструирование сложных «бинарных» структур, содержащих в своем составе несколько функционально значимых частей молекулы. Здесь возможны самые различные комбинации. Например, если известен фермент, разрушающий лекарственный препарат в организме, то возможно конструирование бинарной молекулы, содержащей в своей структуре как фрагмент этого лекарства, так и фрагмент молекулы ингибитора данного фермента. При расщеплении этой молекулы в организме ингибирование фермента приведет к пролонгированию действия данного лекарства.

Подчеркнем, что каждый из вышеупомянутых типов модификаций, улучшающих активность и фармакокинетические свойства соединения, приводит, строго говоря, к созданию *новой химической структуры.* Нужно иметь в виду, что новое химическое соединение может обладать меньшей активностью или иметь другой фармакологический профиль. Поэтому эта часть исследований часто неотделима от QSAR-стадии.

## Некоторые успехи медицинской химии (medicinal chemistry)

Именно с возникновением *медицинской химии* с начала 70-х годов началась новая эра в создании лекарственных препаратов. Этот период по праву можно назвать «второй химиотерапевтической революцией» [14], так как лекарства

стали создаваться с использованием арсенала средств медицинской химии. В результате направленного синтеза физиологически активных веществ с заданными свойствами были получены β-*адреноблокаторы* (для лечения сердечно-сосудистых заболеваний) [15] и β-*адреностимуляторы, кальциевые антагонисты* (антигипертензивные средства) [16], а также *блокаторы $H_2$ рецепторов гистамина* (средства против язвенной болезни), противовирусные препараты *ацикловир* и *азидотимидин* (применяющиеся, в частности, для лечения больных с синдромом приобретенного иммунодефицита – СПИДа).

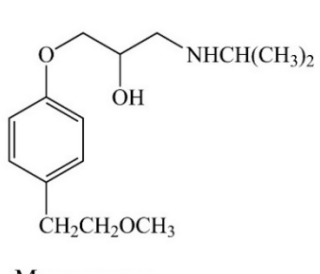


Метопролол
(β1-адреноблокатор)

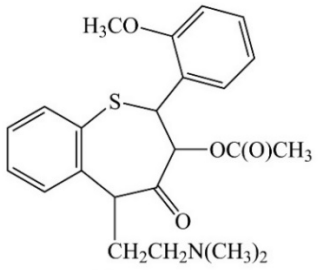


Дилтиазем
(антагонист ионов кальция)

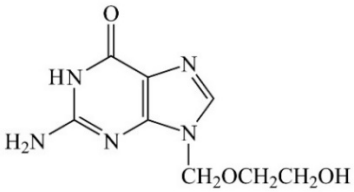


Ацикловир

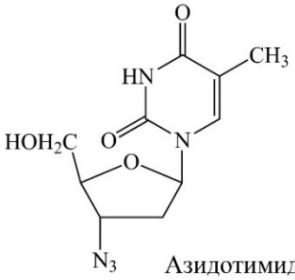


Азидотимидин

Приведем также один из последних примеров конструирования лекарственного препарата против СПИДа, проведенного фирмами *«Agouron Pharmaceuticals»* и *«Eli Lilly»* [17].

Мишенью для конструируемого лекарственного препарата был выбран фермент – вирусная протеаза *(HIVPr),* играющая важную роль в развитии вируса иммунодефицита. Ингибитор этой протеазы должен был обладать как антивирусной активностью, так и хорошей фармакокинетикой. Конструирование стало возможным благодаря наличию структурной информации о комплексе этого фермента с лигандом.

На основе компьютерного моделирования и поиска в базах данных был предложен ингибитор непептидной природы, прочно связывающийся с *HIVPr* и имеющий структуру **1**. Однако это соединение-лидер не годилось непосредственно для практического применения уже хотя бы в силу плохой растворимости в воде. Используя методы структурной оптимизации, авторами было найдено соединение *вирацепт,* которое в настоящее время выходит на рынок как оральный биоактивный ингибитор *HIVPr* для лечения СПИДа.

В заключение нужно отметить, что несмотря на огромное количество лекарственных средств, используемых в настоящее время в химиотерапии, медицинским химикам еще предстоят поиски соединений для лечения болезни Альцгеймера, артрита, болезни Паркинсона, различных видов рака, цирроза, СПИДа, генитального герпеса, хореи Гентингтона, гриппа и других патологий, для лечения которых пока не найдены достаточно эффективные препараты.

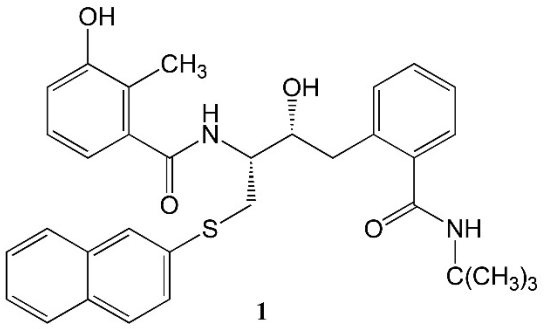


1

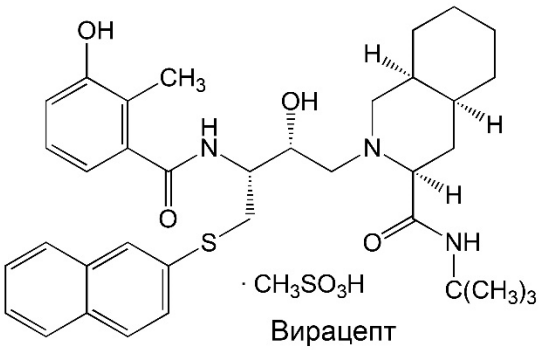


Вирацепт

Иногда проблемой при создании таких соединений является отсутствие адекватных моделей для определения биологической активности. Часто трудности при конструировании подобных лекарственных препаратов обусловлены незнанием структуры их биологической мишени в организме. Однако, несмотря на все трудности, *рациональное* проектирование лекарств – перспективное, интеллектуально емкое и крайне привлекательное направление химической науки на стыке органической, биологической и математической (компьютерной) химии. И хотя новый подход не заменяет собой всех традиционных методов поиска терапевтических средств, «метод проектирования изменяет самые основы практической деятельности научных исследований, которые сродни искусству» [18].

**СПИСОК ЛИТЕРАТУРЫ**

1. *Зефирова О. Н., Зефиров Н. С.* // Вестн. Моск. ун-та. Сер. 2. Химия. 2000. 41. С.
2. Medicinal Chemistry: Principles and Practice / Ed. F. D. King, R.S. Chem., Cambridge, 1994. P. 182.
3. *Suffness M.* Annual Reports in Medicinal Chemistry / Ed. J. A. Bristol, San Diego, 1993. P. 305.
4. *Gordon E. M., Barrett R. W., Dower W. J., Fodor S. P. W., Gallop M. A.* // J. Med. Chem. 1994. 37. P. 1385.
5. *Endo A.* // J. Med. Chem. 1985. 28. P. 401.
6. *Evans J. M., Fake C. S., Hamilton T. C., Poyser R. H., Showell G. A.* // J. Med. Chem. 1984. 27. P. 1127.
7. *Cushman D. W., Cheung H. S., Sabo E. F., Ondetti M. A. //* Biochemistry. 1977. 16. P. 5485.
8. *Hansch C., Leo A.* // Exploring QSAR. Fundamentals and Applications in Chemistry

and Biology. / American Chemical Society. Washington, 1995.

9. *Kubinyi H.* // QSAR: Hansch analysis and related approaches. / VHC, N. Y., 1993.
10. *Cramer R. D., Clark R. D., Patterson D. E., Ferguson A. M. //* J. Med. Chem. 1996. 39. P. 3060.
11. *Parker C. W., Vavra J. B.* // Progr. Hematol. 1969. 6. P. 1.
12. *Sugrue M.* // J. Med. Chem. 1997. 40. P. 2793.
13. *Jodyn A. P., Luchowski E., Triggle D. J.* // J. Med. Chem. 1988. 31. P. 1489.
14. *Mauvemay R. Y., Moleyre J.* // La seconde revolution therapeutique. Paris, 1975.
15. *Южаков С. Д.* // Хим.-фарм. журн. 1980. № 3. С. 18.
16. *Елисеев О. М.* // Тер. арх. 1990. №10. С. 126.
17. *Kaldor S. W., Kalish V. J., Davies J. F, Bhasker V. S, et al.* // J. Med. Chem. 1997. 40. P. 3979.
18. В мире науки. 1990. № 3. С. 49.

*Поступила в редакцию 03.09.98*

*Журнал органической химии. 2005. Т. 41. Вып.*

УДК 541.69

*Посвящается академику РАН В.И.Минкину в связи с его 70-летием*

# ТАКСОЛ: СИНТЕЗ, БИОАКТИВНЫЕ КОНФОРМАЦИИ И СООТНОШЕНИЕ СТРУКТУРА–АКТИВНОСТЬ ДЛЯ ЕГО АНАЛОГОВ

**© О.Н.Зефирова,[1@] Е.В.Нуриева,[1] А.Н.Рыжов,[2] Н.В.Зык,[1] Н.С.Зефиров[1]**

[1]*Московский государственный университет имени М.В.Ломоносова*
*119992, Москва, Ленинские гор; факс: (095) 939–3026*
[2]*Институт органической химии имени Н.Д.Зелинского*
*Российской Академии наук, Москва*

Поступило 16 VIII 2004

*Описаны синтезы и предполагаемые биологически активные конформации молекулы природного противоопухолевого соединения – таксола, систематизированы данные исследований структура–активность для его аналогов.*

## 1. Введение

Среди соединений, обладающих противоопухолевой активностью, важное место занимает дитерпеновый алкалоид коры *Taxus brevifolia* таксол **1**[*] и некоторые его аналоги [1,2]. Клеточной мишенью их действия является белок тубулин, способный к полимеризации с образованием микротрубочек – структур, играющих важную роль в процессе деления клетки и в формировании ее цитоскелета. Таксол вызывает неконтролируемую полимеризацию тубулина и стабилизацию микротрубочек [3], нарушая, таким образом, процесс быстрого неконтролируемого деления раковых клеток.[*]

[*]Другое название этой молекулы – паклитаксел.

[*]Ряд соединений, например, алкалоиды семейства *Vinca rosea*, также способны к взаимодействию с тубулином, однако в отличие от таксола они ингибируют процесс сборки микротрубочек.

Слева направо: Н.В.Зык, О.Н.Зефирова, Н.С.Зефиров, Е.В.Нуриева.

Ольга Николаевна Зефирова родилась в Москве, окончила химический факультет Московского государственного университета имени М.В.Ломоносова в 1987 г., кандидат химических наук с 1991 г., доцент кафедры физической химии химического факультета МГУ имени М.В.Ломоносова. Преподает спецкурс «Медицинская химия» на химфаке МГУ.

Евгения Владимировна Нуриева родилась в г. Петропавловск-Камчатский, окончила Чувашский государственный университет имени И.Н.Ульянова в 2000 г., аспирантка кафедры органической химии химического факультета МГУ имени М.В.Ломоносова.

Антон Николаевич Рыжов родился в 1981 г. в Московской обл., окончил химический факультет Московского государственного университета имени М.В.Ломоносова в 2001 г., аспирант Института органической химии имени Н.Д.Зелинского РАН.

Николай Васильевич Зык родился в 1941 г. в Брянской обл., окончил химический факультет Московского государственного университета имени М.В.Ломоносова в 1969 г., кандидат химических наук с 1975 г., доктор химических наук с 1990 г., профессор, зав.лабораторией биологически активных органических соединений кафедры органической химии химического факультета МГУ имени М.В.Ломоносова.

Николай Серафимович Зефиров родился в 1935 г. в г. Ярославле, окончил химический факультет Московского государственного университета имени М.В.Ломоносова в 1958 г., кандидат химических наук с 1961 г., доктор химических наук с 1966 г., заведующий кафедрой органической химии химического факультета МГУ имени М.В.Ломоносова. В 1997 году инициировал открытие специализации «медицинская химия» (drug-design). Академик РАН с 1987 г., директор Института физиологически активных веществ РАН.

*Область научных интересов авторов*: органическая и медицинская химия, компьютерное моделирование и QSAR для дизайна физиологически активных веществ.

*ЖУРНАЛ ОРГАНИЧЕСКОЙ ХИМИИ, 2000, том 36, № 9, с. 1231-1258*

**УДК 547.466.64 : 541.69**

# ФИЗИОЛОГИЧЕСКИ АКТИВНЫЕ СОЕДИНЕНИЯ, ВЗАИМОДЕЙСТВУЮЩИЕ С ГЛУТАМАТНЫМИ РЕЦЕПТОРАМИ

**О. Н. Зефирова, Н. С. Зефиров**[@]

*Химический факультет, Московский Государственный Университет, Ленинские горы, Москва, 119899*

*Систематизированы структурные данные по органическим соединениям, проявляющим активность по отношению к рецепторам глутаминовой кислоты и рассмотрены вопросы дизайна таких соединений.*

**1. Введение** . . . . . .
**2. Передача нервного импульса - основные понятия** . . . . . .
**3. Ионотропные глутаматные рецепторы** . . . . . .
***I. NMDA подтип.*** . . . . . .
***II. AMPA - КАИНАТНЫЙ подтип.*** . . . . . .
**4. Метаботропные глутаматные рецепторы** . . . . . .
***I. Классификация метаботропных глутаматных рецепторов*** . . .
***II. Соединения, взаимодействующие с метаботропными глутаматными рецепторами*** . . . .

## 1. ВВЕДЕНИЕ.

Целью настоящего обзора является представление для химической аудитории имеющихся данных о структуре физиологически активных веществ, взаимодействующих с *глутаматными рецепторами* и анализ зависимости активности для этих соединений от структуры. В последнее время было показано, что нейропередача с участием глутаминовой кислоты играет важную роль в процессах памяти, развитии когнитивных (познавательных) способностей, в возникновении некоторых нейродегенеративных нарушений и т. д. [1]. Избыточная активация глутаматных рецепторов является одним из факторов патогенеза таких заболеваний, как эпилепсия, мозговая ишемия и гипогликемия, травма центральной нервной системы, болезнь Альцгеймера и др. Это и явилось причиной необычайно возросшего в последнее десятилетие интереса к созданию химических соединений, блокирующих активацию глутаматных рецепторов [2].

Тем не менее, эта проблема не очень хорошо известна широкому кругу химиков-органиков. Дело в том, что, во-первых, она формулируется в литературе на языке медицинской [3,4][*] или даже биоорганической химии и, во-вторых, освещается в журналах, не являющихся для химиков приоритетными. Мы надеемся, что публикация настоящего обзора позволит именно химикам-органикам внести новый принципиальный вклад в развитие этой области медицинской химии.

[*] Медицинская химия, проникнутая структурными концепциями конструирования лекарств (*drug design*), стала новой областью химического знания, со своими научными понятиями и своей научной методологией. Предметом медицинской химии является поиск и структурный дизайн физиологически активных веществ, выявление взаимосвязи между химической структурой и активностью и, наконец, решение обратной задачи структура-свойство, а именно, конструирование необходимых структур, обладающих заданным свойством [4].

*Успехи химии* **70** (4) 2001 © 2001 Российская академия наук, Отделение общей и технической химии Российской академии наук

УДК 541.69

# Физиологически активные соединения, взаимодействующие с серотониновыми (5-гидрокситриптаминовыми) рецепторами

**О.Н.Зефирова, Н.С.Зефиров**

*Московский государственный университет им. М.В.Ломоносова, Химический факультет 119899 Москва, Ленинские горы, факс (095)939–3026*

Систематизированы данные по структурам органических соединений, проявляющим активность по отношению к рецепторам серотонина, и рассмотрены вопросы дизайна таких соединений.
Библиография — 296 ссылок.

## Оглавление

I. Введение 382
II. Классификация серотониновых рецепторов 382
III. Лиганды серотониновых рецепторов 5-$HT_{1A}$-подтипа 383
IV. Лиганды серотониновых рецепторов 5-$HT_{1B}$- и 5-$HT_{1D}$-подтипов 388
V. Лиганды серотониновых рецепторов других 5-$HT_1$-подтипов 392
VI. Лиганды серотониновых рецепторов 5-$HT_2$-подтипов 392
VII. Лиганды серотониновых рецепторов 5-$HT_3$-подтипа 397
VIII. Лиганды серотониновых рецепторов 5-$HT_4$-подтипа 400
IX. Лиганды серотониновых рецепторов других подтипов 402

## I. Введение

Проблемы дизайна физиологически активных веществ обсуждаются в литературе на языке медицинской химии,† поэтому они, как правило, не очень хорошо известны широкому кругу химиков, занимающихся органическим синтезом. Задачей настоящего обзора является систематизация имеющихся в литературе данных по дизайну физиологически активных веществ, взаимодействующих с серотониновыми рецепторами, и анализ влияния химической структуры этих соединений на их активность.

Известно, что физиологическая роль серотонина (5-гидрокситриптамина (**1**), 5-HT) в головном мозге человека заключается в регуляции различных психоэмоциональных реакций. Кроме того, серотонин участвует в контроле терморегуляции, процессов сенсорного восприятия, в частности, чувствительности к боли и др. В последнее время было показано, что нарушения обмена серотонина и/или функций серотонинових регуляторов имеют отношение к патогенезу шизофрении, депрессивных и тревожных состояний, алкоголизма, наркомании и т.п.

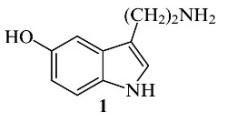

**1**

Эти факты явились причиной значительно возросшего в последнее десятилетие интереса к созданию химических соединений, так или иначе участвующих в процессе нейропередачи с участием серотонина.

Мы надеемся, что настоящий обзор, в котором обобщаются структурные подходы к созданию соединений, взаимодействующих с серотониновыми рецепторами, вдохновит химиков-синтетиков внести принципиально новый вклад в развитие этой области медицинской химии.

## II. Классификация серотониновых рецепторов

Серотонин (**1**) — биогенный амин с чрезвычайно широким спектром биологической активности по отношению к центральной нервной системе и другим органам и тканям. В центральной нервной системе человека он выполняет функции нейромедиатора, т.е. химического соединения, осуществляющего передачу информации от одной нервной клетки к другой.[3] В процессе этой передачи молекулы нейромедиа-

**О.Н.Зефирова**. Кандидат химических наук, доцент кафедры органической химии химического факультета МГУ.
Телефон: (095)939–4878, e-mail: olgaz@org.chem.msu.ru
**Н.С.Зефиров**. Академик, заведующий той же кафедрой, директор ИФАВ РАН. Телефон: (095)939–1620,
e-mail: zefirov@org.chem.msu.ru, zefirov@org.chem.msu.su
Область научных интересов авторов: органическая и физическая органическая химия, медицинская химия, в частности, создание лигандов глутаматных, серотониновых и ацетилхолиновых рецепторов, а также разработка методов компьютерного моделирования и QSAR для дизайна физиологически активных веществ.

**Дата поступления 22 января 2001 г.**

† Предметом медицинской химии является поиск и структурный дизайн (drug design)[1,2] физиологически активных веществ, выявление взаимосвязи между химической структурой и активностью и, наконец, решение обратной задачи структура – свойство, т.е. конструирование необходимых структур, обладающих заданным свойством.

680 *Russian Chemical Bulletin, International Edition, Vol. 56, No. 4, pp. 680—688, April, 2007*

# Ligands of the colchicine site of tubulin: a common pharmacophore and new structural classes

*O. N. Zefirova,* A. G. Diikov, N. V. Zyk, and N. S. Zefirov*

*Department of Chemistry, M. V. Lomonosov Moscow State University, 1 Leninskie Gory, 119992 Moscow, Russian Federation. Fax: +7 (495) 939 0290. E-mail: olgaz@org.chem.msu.ru*

Structure—activity relationships for ligands of the colchicine site of tubulin were analyzed based on their common pharmacophore. The role of the elucidation of the three-dimensional structure of the colchicine site of tubulin on the development of studies aimed at the search for the ligands of this site is analyzed.

**Key words:** structure—activity relationship, pharmacophore, colchicine, podophyllotoxin, combretastatin, tubulin polymerization inhibitors.

## Introduction

The cell protein tubulin is one of the most important molecular targets of antitumor agents. Two subunits of this protein, *viz.*, α- and β-tubulins, form α,β-dimers, which can undergo polymerization to give microtubules. The control over cell division processes is among their important and various functions in cells. Inhibition of these processes by intervening into the tubulin system of tumor cells provides the basis of one of types of antitumor therapy.[1]

Antitumor agents can bind to different sites of tubulin and cause either its uncontrolled polymerization (for example, taxol and its analogs) or inhibit tubulin polymerization. The alkaloids vincristine and vinblastine belong to the second type of agents.[1] Tubulin polymerization is inhibited also by colchicine (**1**) and its analogs. The action of colchicine is based on binding in a particular site of tubulin (the colchicine site), resulting in deformation of the α,β-dimer structure, which hinders the tubulin assembly into microtubules.

Numerous natural and synthetic ligands of the colchicine site of tubulin are exhaustively listed in a review[2] (including structural classes that are beyond the scope of the present review). There is also a group of compounds for which binding to the colchicine site is only assumed (for example, the toxin 7,11-*epi*-thyrsiferol[3] or pyrimidinylpyrazole derivatives[4]).

It should be emphasized that the vast majority of the aforementioned compounds were found by screening or with the use of purely empirical structure—activity relationships. Quite a few attempts to quantitatively describe these relationships and to use them for the prediction of active compounds were made (see, for example, Refs 5 and 6). The reason for this is the absence, for a long time, of complete and reliable data on the three-dimensional structure of the colchicine site of tubulin. In 2004, the structure of a complex of a colchicine derivative with β-tubulin was established by X-ray diffraction.[7] In our opinion, this publication has marked a new stage in studies aimed at the search for active tubulin polymerization inhibitors. The present review gives a brief illustration of the possibilities provided by this publication both for explaining the known empirical structure—activity relationships for ligands of the colchicine binding site and analyzing recent trends (2004—2006) in the search for such compounds.

## Pharmacophore groups of inhibitors of the colchicine site of tubulin

The structure elucidation of the α,β-tubulin complex with *N*-deacetyl-*N*-(2-mercaptoacetyl)colchicine (DAMA-colchicine) and the α,β-tubulin complex with podophyllotoxin[7] confirmed the earlier hypothesis that colchicine (**1**) and podophyllotoxin (**2**) bind to β-tubulin at its interface with α-tubulin. An X-ray diffraction study demonstrated that the trimethoxyphenyl groups of both DAMA-colchicine and podophyllotoxin are located in the β-tubulin structure in the vicinity of the amino acid residue Cysβ239.* The width of the colchicine site is approximately 4—5 Å, and the volume of this site is confined in β-tubulin by helix 7 (H7) containing Cysβ239. The involvement of α-tubulin in the formation of the

* In the study,[7] this amino acid residue was denoted Cysβ241; however, this residue is numbered differently in some other publications.

Published in Russian in *Izvestiya Akademii Nauk. Seriya Khimicheskaya,* No. 4, pp. 655—662, April, 2007.

1066-5285/07/5604-0680 © 2007 Springer Science+Business Media, Inc.

*ISSN 0002-3353 Известия Академии наук. Серия химическая, 2013, № 2* 329

УДК 547.518

# Направленное применение мостиковых группировок в дизайне физиологически активных веществ*

***О. Н. Зефирова,* Н. С. Зефиров***

*Московский государственный университет им. М. В. Ломоносова, Химический факультет, Российская Федерация, 119991 Москва, Воробьевы горы, 1/3.*
*Факс (459) 939 0290. E-mail: olgaz@org.chem.msu.ru*
*Институт физиологически активных веществ Российской академии наук, Российская Федерация, 142432 Черноголовка Московской обл., Северный проезд, 1.*
*E-mail: zefirov@org.chem.msu.ru*

В обзоре систематизированы примеры направленного использования мостиковых группировок в дизайне лекарств с целью биоизостерической замены, ограничения конформационной подвижности или увеличения липофильности соединения-лидера, а также в качестве пространственных шаблонов, удерживающих связывающие группировки.

**Ключевые слова:** мостиковые структуры, дизайн лекарств, конформационная подвижность, липофильность, бивалентные соединения, биоизостерическая замена.

Анализ литературы показывает, что мостиковые группировки, т.е. би- или полициклы, кольца которых содержат больше двух общих атомов (соответственно мостик содержит больше одного атома), используются в ходе создания физиологически активных веществ достаточно редко**. При этом большинство таких исследований представляют собой работы по поиску и оптимизации структур соединений-лидеров***, изначально содержащих мостиковую группировку и найденных в основном в ходе скрининга разнообразных библиотек структур, принадлежащих университетам, фармацевтическим компаниям, научным группам и др., или в результате случайных находок. Часто введение подобных группировок обусловлено синтетическими преимуществами.

В ходе систематического скрининга были найдены мостиковые соединения-лидеры, взаимодействующие, например, с эстрогеновыми[3], мелатониновыми[4], хемокиновыми[5] и многими другими молекулярными мишенями. При дальнейшей оптимизации мостиковая группировка уже присутствует в соединении-лидере и обычно не меняется. Типичным примером подобных исследований является работа[6], в которой на базе соединения **1**, найденного с помощью скрининга [5] непептидного лиганда хемокинового рецепторного белка CXCR3, проводили вариации в основном немостиковой части молекулы и изучали соотношение структура—активность в рамках синтезированных серий соединений.

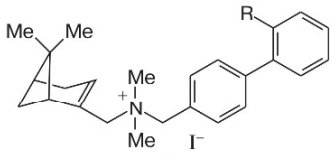


**1**

К подобному типу исследований можно отнести и многочисленные исследования, базирующиеся на структурах природных соединений-лидеров с мостиковыми группировками, такими как кокаин, морфин, эпибатидин, атропин и др., которые найдены либо случайно, либо в ходе скрининга природных веществ (см., например, лит.[7—14]). В таких работах мостиковый фрагмент часто либо не затрагивается, как при создании конформационно ограниченных аналогов эпибатидина (**2**, схема 1)[12], либо подвергается незначительным изменениям: «сдвигу» гетероатомов (см. аналоги кокаина **3**, схема 2)[13], замене одного бициклического фрагмента другим, близким по структуре (например, тропанового фрагмента — хинуклидиновым[11]).

* Посвящается академику Российской академии наук С. М. Алдошину в связи с его 60-летием.

** Отметим, что обсуждаемые в обзоре мостиковые (bridged) группировки следует отличать от каркасных (caged) структур; применение последних, главным образом адамантана, имеет свою специфику и в данном обзоре не рассматривается[1,2].

*** Соединение-лидер (*англ.* lead-compound) — структурный прототип будущего лекарства, т.е. химическое соединение, которое обладает желаемой, интересной, но не оптимизированной биологической активностью; с помощью последующей модификации (оптимизации) структуры соединение-лидер в принципе может быть преобразовано в клинически пригодное лекарство. Поскольку в ходе «медхимических» исследований соединение-лидер может меняться, в данном обзоре под таковым понимается непосредственный (или близкий) предшественник соединения с мостиковым фрагментом.

© 2013 «Известия Академии наук. Серия химическая», Российская академия наук, Отделение химии и наук о материалах Российской академии наук, Институт органической химии им. Н. Д. Зелинского Российской академии наук

# Раздел II. Избранные работы в области медицинской химии препаратов для лечения нейродегенеративных заболеваний

## Введение

**С.О. Бачурин**

Одним из важных направлений работ в области медицинской химии, выполненных под руководством и непосредственном участии академика Н.С. Зефирова, явились исследования по направленному синтезу и изучению связи структура–свойство в рядах соединений для лечения нейродегенеративных заболеваний (НДЗ) [1].

В целом необходимо отметить, что поиск препаратов для лечения таких НДЗ как болезнь Альцгеймера (БА), болезнь Паркинсона, боковой амиотрофический склероз и т.п. является одной из наиболее востребованных и неудовлетворенных потребностей современной неврологии и психиатрии. Так, в терапевтической практике для лечения БА наиболее активно используют всего 4 синтетических препарата: донепезил, ривастигмин, галантамин и мемантин. Три первых относятся к классу ингибиторов холинэстераз, а последний препарат – мемантин является блокатором N-метил-D-аспартат-(NMDA)-рецепт-канального комплекса – одного из подтипов глутаматных рецепторов в центральной нервной системе (ЦНС). Для лечения другого, более редкого НДЗ – бокового амиотрофического склероза (БАС) – применяют в основном два лекарства: мультитаргетный препарат рилузол и антиоксидант эдаравон, эффективность терапевтического действия которых крайне ограничена. Для лечения болезни Паркинсона в основном применяют препараты, компенсирующие дефицит нейромедиатора дофамина. При этом все эти препараты имеют выраженный симптоматический характер действия. В последние десятилетия одной из основных тенденций в поиске средств для лечения НДЗ является конструирование лекарственных соединений, направленно действующих на основные биомишени в патогенезе НДЗ. В качестве таких перспективных мишеней для препаратов с нейропротекторным типом действия в работах Н.С. Зефирова с коллегами рассматривались различные ферменты и рецепторы ЦНС, участвующие в нейромедиаторной передаче. В частности, изучались NMDA- и AMPA- *(*α-amino-3-hydroxy-5-methyl-4-isoxazole-propionic acid) подтипы ионотропных глутаматных рецепторов, участвующие как в процессах формирования памяти и когнитивных функций, так и в процессах нейродегенерации. В работе Н.С. Зефирова с соавторами было впервые (еще до получения рентгеноструктурных данных) проведено компьютерное моделирование структуры NMDA-рецептора, ответственного за «перевозбуждение»

ЦНС, приводящее к дегенерации соответствующих нейронов [2]. На основании сформированных моделей было предложено несколько хемотипов оригинальных биоизостерных соединений, способных, подобно известному специфическому блокатору NMDA-рецептора – препарату МК-801 – селективно взаимодействовать с внутриканальным сайтом этого рецептора, при этом не проявляя побочных эффектов, характерных для препарата МК-8013. Важным фундаментальным результатом этих исследований явилось объяснение блокирующего действие иона магния (в отличие от ионов кальция) на ионофорный канал, связанный с NMDA-рецептором [3]. В рамках последующих исследований впервые было проведено компьютерное моделирование центра связывания отрицательных модуляторов NMDA-рецептора и осуществлен молекулярный дизайн новых веществ, существенно отличающихся от известных по структуре и способу связывания, а также сформирована фокусированная библиотека химических соединений с потенциальными нейропротекторными и пронейрогенными свойствами [4].

Значительное внимание в работах Н.С. Зефирова уделено еще одному типу ионотропных глутаматных рецепторов – так называемым AMPA-рецепторам, участвующим в процессах формирования и консолидации памяти. Было проведено компьютерное моделирование трехмерной структуры этого типа рецепторов и на основании полученных результатов сконструирован и синтезирован новый ряд позитивных модуляторов AMPA-рецептора (так называемых «ампакинов»), одновременно действующих на пару симметричных сайтов связывания на разных субъединицах рецептора [5]. Было установлено, что полученные новые оригинальные бинарные ампакины проявляют активность в субнаномолярных концентрациях, что являлось на то время рекордным показателем для соединений такого типа действия. Соединения-лидеры в этом классе в последующем успешно прошли полные доклинические испытания и рекомендованы для проведения клинических испытаний как новый тип когнитивных стимуляторов.

Еще один подход к созданию стимуляторов памяти был реализован в работах Н.С. Зефирова с коллегами, в которых осуществлен синтез новой группы фосфорорганических биоизостеров трипептида эндогенной природы – Arg-Glu-Arg (RER). Для этого вещества, являющегося фрагментом белка APP, ранее было показано наличие способности не только улучшать, но и восстанавливать утраченную память (Rose S.P., 2011). Однако высокая гидролизуемость пептидной связи не позволяла рассматривать это соединение в качестве лекарственного кандидата. Для решения этой проблемы был разработан метод синтеза α-аминофосфонатов на основе олигопептидов в качестве аминокомпоненты каталитической трехкомпонентной реакции Кабачника–Филдса. Предложен метод синтеза фосфонопептидов включением в пептидную цепь α-аминофосфонатов и впервые получен фосфорный аналог трипептида RER [6].

Важным направлением работ Н.С. Зефирова в области оптимизации взаимодействия потенциального лекарства и активных центров ферментов явились исследования в области моделирования взаимодействия фосфорорганических лигандов с активными центрами сериновых эстераз. С использованием нескольких методов QSAR, включая методы MFTA (2D QSAR), CoMSIA (3D QSAR) и молекулярный докинг, был проведен анализ ингибиторной активности и селективности ряда О-фосфорилированных оксимов в отношении фармакологически значимых сериновых эстераз: ацетилхолинэстеразы (АХЭ), бутирилхолинэстеразы (БХЭ), нейротоксичной эстеразы (НТЭ), и карбоксилэстеразы [7]. Это позволило выявить структурные факторы, определяющие селективность и биологический эффект соединений этого ряда, и сформировать библиотеку структур, имеющих оптимальный эстеразный профиль (эффективных и селективных ингибиторов БХЭ, слабо ингибирующих АХЭ и не ингибирующих НТЭ), – как потенциальных препаратов для терапии БА.

В последние годы в мировой фармацевтической практике активно развивается подход репозиционирования известных лекарственных препаратов по новому применению, что позволяет в случае удачи резко сократить сроки и уменьшить расходы на проведение дорогостоящих клинических испытаний (Bachurin S. et al., Med. Res. Rev., 2017, Parvez et al., Ageing Res. Rev., 2023). Пожалуй, наиболее ярким примером реализации такой стратегии стали работы Н.С. Зефирова с коллегами по установлению выраженных нейропротекорных и когнитивно-стимулирующих свойств препарата Димебон, который применялся ранее в СССР и РФ в качестве антигистаминного средства [8]. Вторая фаза клинических испытаний, проведенная американской компанией Медивейшен, показала высокий терапевтический эффект Димебона при применении у больных болезнью Альцгеймера (Doody R. et al., Lancet. 2008 Jul 19;372(9634):207-15). И хотя на третьей фазе клинических испытаний из-за аномального положительного эффекта плацебо действие Димебона оказалось замаскировано (Bharadwaj PR et al., Transl. Psychiatry, 2013), высокий нейропротекторный потенциал этого препарата был многократно подтвержден затем ведущими исследовательскими группами в мире (Steele JW, Gandy S. Autophagy, 2013; Eckert SH et al., Aging Dis., 2018). Это позволяет рассматривать данный препарат как перспективу для лечения различных НДЗ (Скворцова В.И. и др., Acta Naturae, 2018; Ashraf G. et al., Curr. Neuropharm., 2023).

В настоящей главе будут представлены лишь некоторые из работ академика Н.С. Зефирова, связанные с указанными направлениями в области поиска и создания лекарственных веществ для коррекции НДЗ.

**СПИСОК СТАТЕЙ РАЗДЕЛА**


1. Бачурин С.О., Зефиров Н.С. Медицинская химия для коррекции функций мозга // *Вестник РАН*. 2010. Т.80. № 5-6. С. 497-503.
2. Tikhonova I.G., Baskin I.I., Palyulin V.A. Zefirov N.S., Bachurin S.O. Structural basis for understanding structure-activity relationships for the glutamate binding site of the NMDA receptor // *J. Med. Chem*. 2002. V.45. №18. P. 3836-3843.
3. Bachurin S., Tkachenko S., Baskin I., Lermontova N., Mukhina T., Petrova L., Ustinov A., Proshin A., Grigoriev V., Lukoyanov N., Palyulin V., Zefirov N. Neuroprotective and cognition enhancing properties of MK-801 flexible analogs. Structure-activity relationships // *Ann. N.Y Acad. Sci*. 2001.V. 939. P. 219-235.
4. Радченко Е.В., Карлов Д.С., Зефиров А.Н., Палюлин В.А., Зефиров Н.С., Пентковский В.М. Компьютерный дизайн отрицательный аллостерических модуляторов NMDA-рецептора // *ДАН*. 2013. Т. 448. № 3. С. 358-362;
   Карлов Д.С., Радченко Е.В., Палюлин В.А., Зефиров Н.С., Пентковский В.М. Молекулярный дизайн пронейрогенных и нейропротекторных соединений –аллостерических модуляторов рецепторов NMDA // *ДАН*. 2017. Т. 473. № 5. С. 608-612.
5. Лавров М.И., Григорьев В.В., Бачурин С.О., Палюлин В.А., Зефиров Н.С. Новый бивалентный положительный аллостерический модулятор AMPA-рецепторов // *ДАН.* 2015. Т. 464. № 5. С. 1–4.
6. Матвеева Е.Д., Подругина Т.А., Присяжной М.В., Бачурин С.О., Зефиров Н.С. Синтез «трипептида памяти» (Arg–Glu–Arg, RER) и реакция Кабачника–Филдса с ди- и трипептидами как метод синтеза фосфорсодержащих производных пептидов // *Изв. АН Сер. хим*. 2010. Т. 59. № 1. С. 200-208.
7. Makhaeva G.F., Radchenko E.V., Baskin I.I., Palyulin V.A., Richardson R.J., Zefirov N.S. Combined QSAR studies of inhibitor properties of O-phosphorylated oximes toward serine esterases involved in neurotoxicity, drug metabolism and Alzheimer's disease // *SAR QSAR Environ Res*. 2012. V. 23. № 7-8. P. 627-647.
8. Bachurin S., Bukatina E., Lermontova N., Tkachenko S., Afanasiev A., Grigoriev V., Grigorieva I., Ivanov Y., Sablin S., Zefirov N. Antihistamine agent dimebon as a novel neuroprotector and a cognition enhancer // *Ann. N.Y. Acad. Sci.* 2001. V. 939. № 1. P. 425-435.

*ВЕСТНИК РОССИЙСКОЙ АКАДЕМИИ НАУК, Т. 80 (5-6), СТР. 497-503, 2010*

# МЕДИЦИНСКАЯ ХИМИЯ ДЛЯ КОРРЕКЦИИ ФУНКЦИЙ МОЗГА

**Доклад члена-корреспондента РАН С.О. БАЧУРИНА и академика Н.С. ЗЕФИРОВА**

Создание новых высокоэффективных лекарственных средств для лечения различных заболеваний человека – наиболее приоритетная задача в большинстве стран мира с точки зрения как социальной значимости, так и финансовой. В денежном выражении мировой фармацевтический рынок в 2008 г. оценивался примерно в 750 млрд долл. и ожидается, что к 2012 г. его объём может достичь 912 млрд долл., что будет больше объёма мирового нефтяного рынка [1].

В связи с существенным увеличением доли пожилого населения в мире, и особенно в развитых странах, важное место в ряду современных лекарственных препаратов занимают средства для лечения возраст-зависимых заболеваний, к которым относятся многие нейродегенеративные патологии мозга, в частности болезнь Альцгеймера (БА). По различным оценкам, частота заболеваний этой болезнью у людей в возрастной группе 65–75 лет колеблется от 3 до 6%, а с увеличением возраста до 85 лет и старше превышает 35%. Проблема старческого слабоумия крайне актуальна и для нашей страны. Так, проведённые Научным центром психического здоровья РАМН эпидемиологические исследования показали, что 4.5% населения Москвы (более 70 тыс. человек) в возрасте 60 лет и старше страдают деменцией альцгеймеровского типа, причём у 1.8% обследованных (более 30 тыс. человек) выявлены выраженные и тяжёлые формы слабоумия. Эти больные требуют постороннего ухода и надзора. Экстраполяция полученных данных на население старших возрастов в целом позволяет говорить о том, что уже в настоящее время общая численность страдающих болезнью Альцгеймера в России приближается к 1 млн человек [2].

Разработка стратегий поиска и создания новых высокоэффективных лекарственных препаратов является важнейшим направлением в науках о жизни (life sciences). Ключевая роль здесь отводится современной медицинской химии, возникшей как наука в 70-х годах прошлого столетия на стыке органической химии и молекулярной медицины. В соответствии с классификацией Международного союза теоретической и прикладной химии, медицинскую химию определяют как область химической науки, связанную с выявлением, развитием, идентификацией и исследованием механизма действия биологически активных соединений на молекулярном уровне. Главное внимание при этом направлено на лекарственные препараты, но интересы медицинской химии распространяются также на изучение, выявление и синтез метаболитов лекарств и родственных соединений.

Общую схему создания лекарственного препарата обычно представляют в виде определённой последовательности стадий (рис. 1). Первые четыре из них и являются собственно содержанием работ в области медицинской химии. Анализ этой схемы позволяет сделать вывод, что из примерно сотен тысяч изначально синтезированных соединений только одно дойдёт до клинических испытаний. А из десяти веществ, отобранных для клинических исследований, только один препарат поступит на рынок в виде лекарственного средства. В этой связи важнейшей задачей медицинской химии является разработка методов предсказания перспективных соединений, обеспечение направленного синтеза, а также повышение эффективности отбора потенциальных лекарственных кандидатов на основе привлечения широкого спектра современных методов скрининга и оптимизации структуры перспективных соединений.

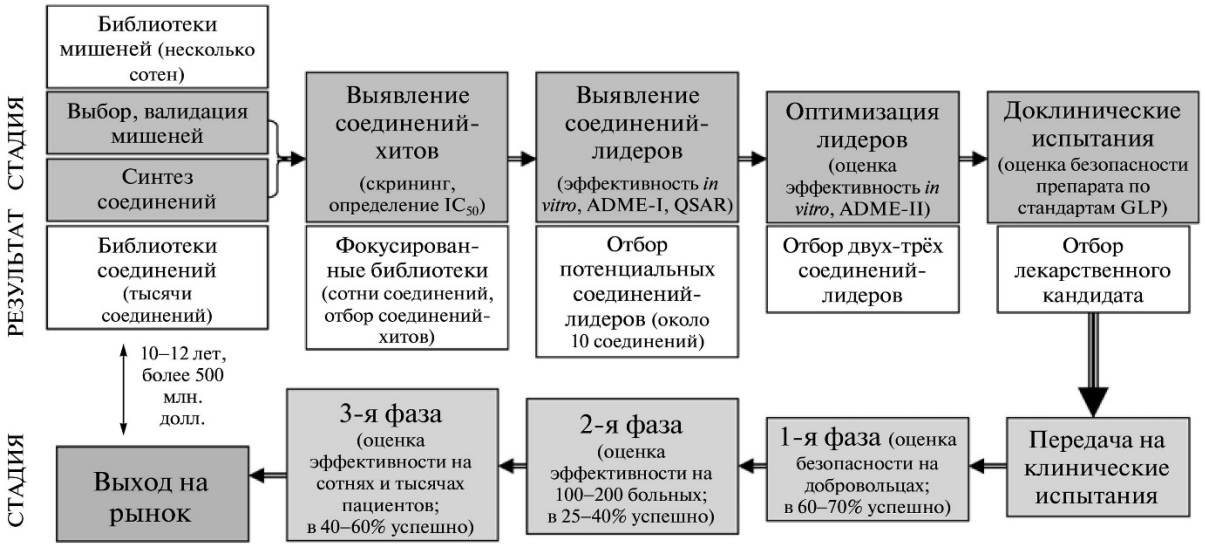


Рис. 1. Схема создания лекарственного препарата: от синтеза до рынка.
По материалам «Nature Reviews Drug Discovery» (2004-2007).

Рассмотрим современные подходы к поиску и конструированию структуры лекарств. Прогресс в медицинской химии связан с введением в научный оборот понятия «биомишень» (ДНК, фермент, рецептор, ионный канал и т.п.), свойства которой надо видоизменить за счёт действия лекарства. В тех случаях, когда есть информация о пространственном строении биомишени (как правило, белковой молекулы), применяются методы прямого конструирования, в рамках которых реализуются отдельные этапы методологии «от гена – к лекарству». Эти методы можно разделить на две группы: виртуальный скрининг в молекулярных базах данных и виртуальное конструирование лигандов. Если нет сведений о строении биомишени, но есть данные о необходимой биоактивности для серии соединений, используются методы непрямого поиска, главным образом КССА (количественная связь «структура–активность»). При отсутствии данных о структурах

лигандов и рецептора применяются методы комбинаторной химии и тестирования больших массивов соединений. Рассмотрим подробнее перечисленные подходы, начав с последнего.

В условиях, когда нет данных как о строении биомишени, так и о структуре активных соединений, поиск лекарств базируется на синтезе библиотек соединений методами комбинаторной химии и последующих массовых испытаниях биологической активности. Число синтезируемых соединений методами комбинаторной химии при наличии современной робототехники на крупных фирмах достигает десятков и даже сотен тысяч в неделю. Революцию в деле тестирования произвели современные системы высокопроизводительного скрининга (в англоязычной литературе – High Throughput Screening), позволяющие быстро проверять на широком спектре биомишеней все синтезируемые соединения. Отметим, что стоимость оборудования и необходимых расходных материалов для комбинаторной химии и особенно для систем высокопроизводительного скрининга составляет миллионы долларов. Отдельной дорогостоящей проблемой при этом становится обработка огромных массивов данных о биологической активности сотен тысяч соединений. За рубежом при государственной поддержке были созданы специальные программы (типа «Дорожная карта» в США), обеспечивающие проведение широкомасштабного скрининга веществ, синтезируемых как в университетах, так и в специализированных центрах. Это направление развивается также на крупных фармацевтических фирмах.

Методы непрямого поиска, как правило, основаны на методологии КССА. Для проведения таких исследований необходимы исходные данные, состоящие из набора химических структур с известными значениями активностей. Далее статистическими методами строится модель «структура–активность», или КССА-модель. Следующий этап заключается в генерации и дизайне новых структур с заданной активностью на базе построенных моделей. Идёт генерация большого количества гипотетических структур; предсказание для них активности на основе КССА-моделей; автоматическая селекция структур с требуемыми значениями активности; анализ их синтетической доступности; последующий синтез и практические испытания. Таким образом, процесс создания новых соединений носит итерационный характер: после синтеза и экспериментальных исследований серии соединений проводятся новые исследования КССА и затем конструируются новые структуры, осуществляется их синтез, тестирование и вновь переходят к исследованиям КССА, но уже с учётом данных для новых соединений.

Хорошие результаты дают методы, базирующиеся на топологическом совмещении структур с известной биоактивностью и на анализе её связи с локальными (атомными) параметрами (например, метод МЕТА [3]). Важным направлением разработок в области КССА стало применение методологии искусственных

нейронных сетей. Обычно нейронные сети для КССА включают входной слой нейронов (он получает рассчитанные значения дескрипторов), промежуточный и выходной слои нейронов, соответствующих прогнозируемым свойствам. Благодаря применению искусственных нейронных сетей и использованию базы данных «структура–активность» происходит оптимизация параметров нейронной сети таким образом, что в результате преобразования значений дескрипторов получаются наиболее точные значения активности. Нейросетевые модели могут воспроизводить нелинейные зависимости и обеспечивают высокую точность прогнозирования активности структур [4].

Большое значение имеет также априорная (до проведения синтеза) компьютерная оценка параметров, характеризующих всасывание, распределение, метаболизм, выделение и возможную токсичность лекарственных веществ (ADMET). Ранее оценка таких параметров осуществлялась экспериментальными методами, и значительное число веществ синтезировалось напрасно.

В последнее десятилетие большие успехи достигнуты при использовании трёхмерных подходов, основанных на картировании биомишеней путём определения формы места связывания, исходя из структурных данных о лигандах и данных об их связывании. К таким методам относится CoMFA (метод сравнительного анализа молекулярного поля) и CoMSIA (метод сравнительного анализа индексов молекулярного сходства). Эти методы позволяют сделать обоснованные выводы о строении биомишени и характере связывания с ней лигандов [5]. К сожалению, они являются составной частью дорогостоящих коммерческих программных комплексов и относительно малодоступны в России.

Рассмотрим направления, основанные на знании строения биомишени. В настоящее время в общедоступных базах данных имеются координаты атомов для тысяч белков, полученные методами рентгеноструктурного анализа или ЯМР. Эти данные могут служить в качестве базового знания о биомишенях при разработке новых лекарств. Однако для большинства белков известны лишь аминокислотная последовательность и некоторые данные точечного мутагенеза, указывающие на аминокислотные остатки в структуре белка, необходимые для связывания определённых лигандов. В этом случае возможно компьютерное построение пространственной модели белка-биомишени, например, по гомологии с белками, имеющими известную пространственную структуру. Информация же о точечных мутациях, влияющих на связывание лигандов, помогает определить сайт связывания лигандов.

Именно такие подходы активно используются при конструировании лекарственных препаратов, действующих на биологический аппарат. Ниже мы приведём лишь два примера направленного поиска и создания веществ, способных эффективно защищать нервные клетки от развития дегенеративных процессов, стимулировать сниженные когнитивные функции и память. Подобные вещества

обычно рассматриваются в качестве перспективных кандидатов для лечения различных нейродегенеративных заболеваний, в частности болезни Альцгеймера.

В области создания средств для лечения болезни Альцгеймера и родственных нейродегенеративных расстройств особое внимание в последние годы уделяется препаратам, действующим на глутаматергическую медиаторную систему ЦНС. В частности, единственный препарат, рекомендованный для терапии развитых стадий болезни Альцгеймера – мемантин, относится к блокаторам NMDA-подтипа глутаматных рецепторов [6]. Альтернативный подход к созданию высокоэффективных стимуляторов когнитивных функций связан с поиском позитивных модуляторов (в частности, ампакинов) AMPA-рецепторов – другого подтипа ионотропных глутаматных рецепторов [7], участвующих в процессах консолидации памяти и обеспечения когнитивных функций. В связи с этим представлялось крайне интересным создать структуры, способные блокировать NMDA и одновременно потенцировать AMPA-рецепторы мозга. Можно было ожидать, что такие соединения будут, с одной стороны, защищать нервные клетки от развития нейродегенеративных процессов (быть нейропротекторами), а с другой – улучшать когнитивные функции и память, ослабленные при болезни Альцгеймера или других формах деменции. Направленный дизайн, синтез и испытания этих соединений были выполнены в совместных работах Института физиологически активных веществ РАН и кафедры органической химии МГУ.

В качестве исходной точки для дизайна таких «мультицелевых» препаратов было взято модельное вещество МК-801, являющееся высокоаффинным лигандом NMDA-рецепторов, но обладающее рядом побочных эффектов именно в силу «излишней жёсткости» связывания с внутриканальным сайтом NMDA-рецептора. Метод, который применялся для генерации новых структурных аналогов МК-801, основан на концепции «привилегированных» подструктур (фрагментов) в оригинальной трактовке, заключающейся в анализе получающихся фрагментов при виртуальном раскрытии напряжённой структуры МК-801. Ожидалось, что это должно привести к потере нежелательных побочных психотомиметических эффектов, свойственных высокоаффинным блокаторам NMDA-каналов. На следующем этапе проводилась функционализация отобранных наиболее активных структур, в частности, производных дибензиламина, биоизостерны, и фрагментами известных позитивных модуляторов AMPA-рецептора (ампакины). Вводились изотиурониевые фрагменты, являющиеся в соответствии с критерием Шеридана [8] биоизостерными аналогами сульфамидной группировки, – характерного фармакофора ампакинов.

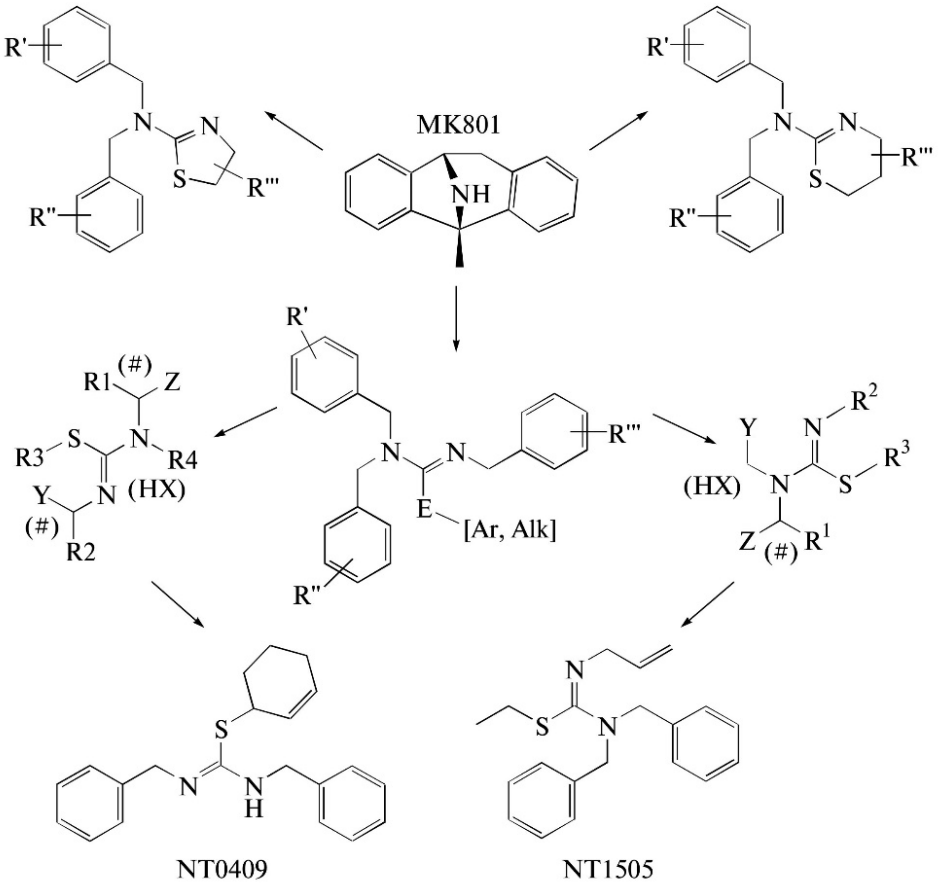


Рис. 2. Фокусированная библиотека привилегированных структур, действующих одновременно на NMDA- и AMPA-рецепторы.

В итоге была сформирована фокусированная библиотека, содержащая несколько сотен соединений, удовлетворяющих определённым структурным критериям (рис. 2). На основе результатов сравнительного докинга этих соединений на внутриканальном сайте NMDA- и на модулирующем сайте AMPA-рецепторов (рис. 3) были отобраны наиболее перспективные вещества, которые затем прошли испытания в экспериментах *in vitro* и *in vivo.* В частности, на изолированных нейронах Пуркинье была установлена способность этих соединений потенцировать активность AMPA-рецепторов, а радиолигандным методом проведена оценка аффинности этих веществ в отношении внутриканального сайта NMDA-рецептора. Отобранные соединения-хиты затем были испытаны в качестве когнитивных энхансеров на нейротоксикологической модели деменции на животных в тесте водного лабиринта. Было показано, что соединения-лидеры (препараты NT-1505 и NT-0409) проявляют свойства эффективных стимуляторов памяти и когнитивных функций у животных с искусственно вызванной деменцией. Эти препараты обладают крайне привлекательным фармакологическим профилем, что позволило предложить их в качестве перспективных средств для лечения болезни Альцгеймера и родственных заболеваний [9].

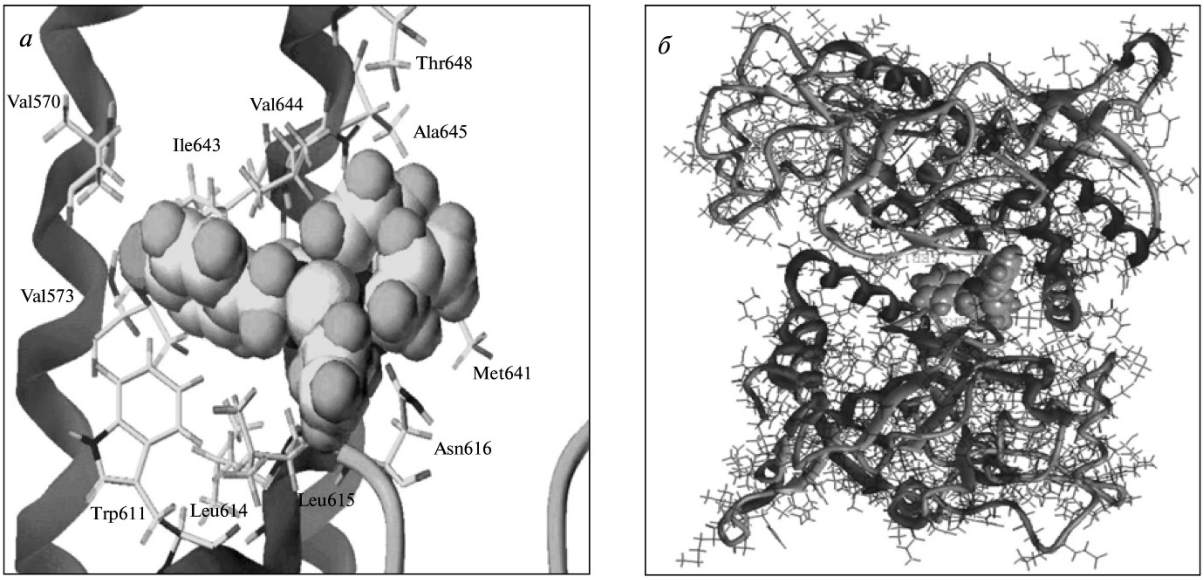


Рис. 3. Докинг соединения-лидера NT-1505 на внутриканальный сайт NMDA-рецептора (*а*) и сайт связывания позитивных модуляторов AMPA-рецептора (*б*).

Ещё одним ярким и успешным примером направленного поиска высокоэффективных препаратов для лечения патологий мозга является обнаружение принципиально новых свойств, в том числе способности восстанавливать когнитивные функции и память у отечественного антигистаминного лекарственного средства «димебон». Ещё в середине 1990-х годов коллективом исследователей из Института физиологически активных веществ РАН было установлено, что ряд производных гамма-карболинов, которые можно рассматривать как циклические аналоги некоторых эндогенных нейрорегуляторов и нейромедиаторов, проявляют способность защищать нервные клетки от гибели, индуцированной различными стрессовыми факторами. Было установлено, что один из представителей этой группы соединений – препарат димебон, созданный ранее на химическом факультете МГУ и применявшийся уже более 10 лет у нас в стране в качестве антигистаминного противоаллергического средства, обладает высокими нейропротекторными и когнитивно-стимулирующими свойствами. Димебон, как было показано, способен действовать на биомишени, участвующие в патогенезе ряда нейродегенеративных заболеваний [10]. Так, препарат выступал в качестве низкоаффинного блокатора NMDA-рецепторов, одновременно являясь позитивным модулятором AMPA-рецепторов. Он оказывал ингибирующее действие на ацетил- и бутирилхолинэстеразы, подобно тому, как действуют известные антиальцгеймеровские препараты такрин и амиридин.

Принципиально новой мишенью действия димебона стали митохондрии, в частности митохондриальные поры, принимающие участие в «запуске» процессов апоптоза и некроза. В опытах на модельных животных и в рамках пилотных клинических испытаний, проведённых на ограниченном числе пациентов с бо-

лезнью Альцгеймера, было обнаружено, что димебон существенно улучшает когнитивные функции и память [10]. В настоящее время в различных лабораториях мира получено подтверждение, что димебон способен действовать на широкий спектр биологических мишеней (рис. 4), играющих важную роль в инициации и развитии нейродегенеративных процессов в мозге.

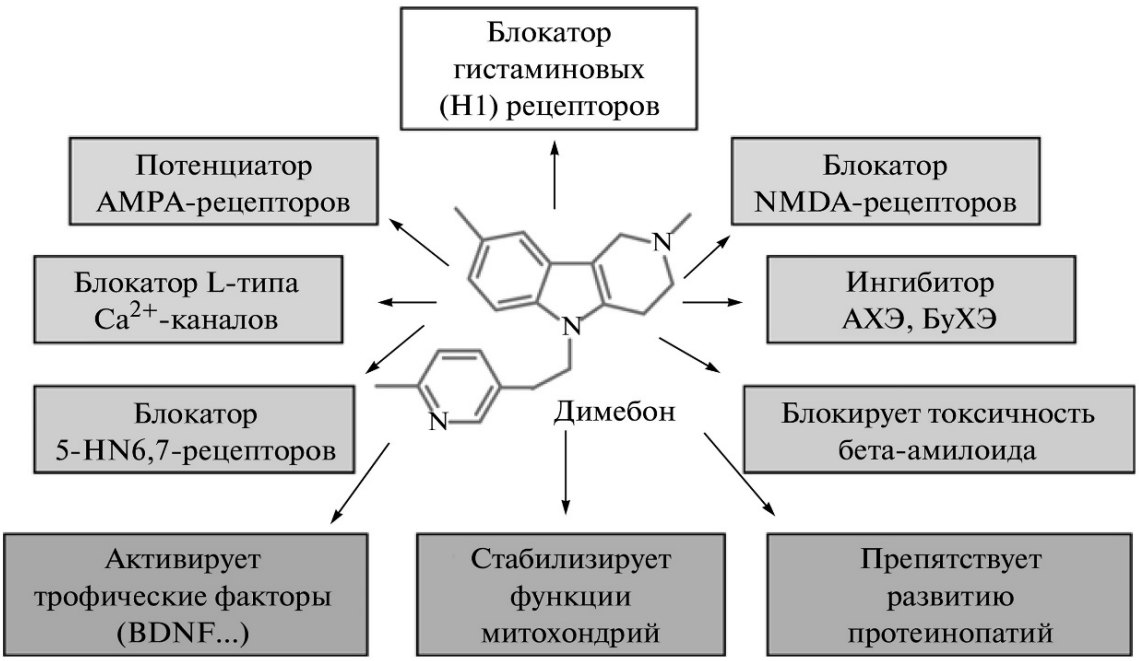


Рис. 4. Подтвержденные мишени действия препарата димебон.

Вторая фаза клинических испытаний димебона по международным стандартам GCP проводились в России американской компанией «Медивейшн» на более чем 180 пациентах с болезнью Альцгеймера. Результаты испытаний показали, что димебон по своей эффективности существенно превосходит все применяемые в настоящее время препараты. Главное его отличие от уже имеющихся препаратов состоит в том, что он способен не только задерживать развитие заболевания, но и улучшать состояние когнитивных функций больных по сравнению с уровнем на начало испытаний [11] (рис. 5). Это позволяет рассматривать димебон как первый «болезнь-модифицирующий» препарат, влияющий на патогенез болезни Альцгеймера. Успешные результаты клинических испытаний димебона нашли широкий отклик за рубежом, что ещё раз подтверждает высокий потенциал исследований, проводимых в институтах Российской академии наук [12].

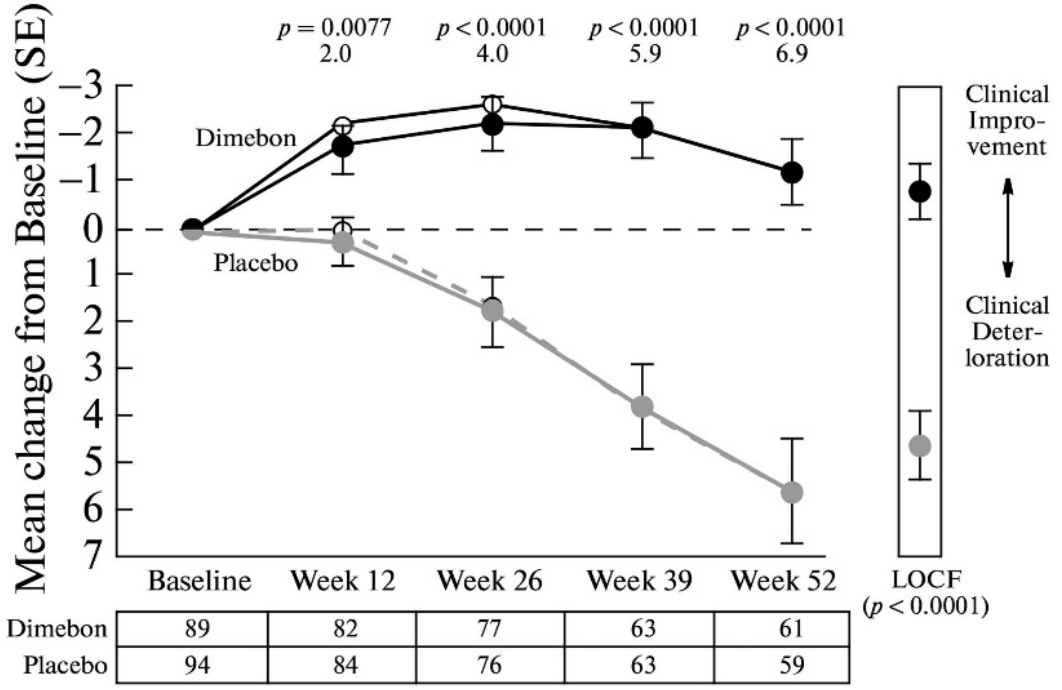


Рис. 5. Результаты клинических испытаний димебона. Улучшение памяти и когнитивных функций у больных болезнью Альцгеймера при 52-недельном лечении димебоном (верхняя кривая) по сравнению с плацебо (нижняя кривая). По оси ординат приведены средние отклонения показателей когнитивных функций от начального уровня (выше нуля – улучшение, ниже нуля – ухудшение когнитивных функций). Пунктиром показаны данные по 134 пациентам (из общего числа 182), которые по завершении шести месяцев испытаний принимали участие в следующем 12-месячном испытании.

Как известно, в 2009 г. принята Стратегия развития фармацевтической промышленности Российской Федерации до 2020 г. (Фарма-2020), которая предусматривает выведение на рынок нескольких десятков инновационных лекарств. С целью наиболее эффективной реализации имеющегося научного потенциала академических институтов по созданию оригинальных лекарственных препаратов РАН выступила с инициативой по формированию уникальной для нашей страны Национальной сети биологического скрининга. Этот проект вошёл в реестр перспективных проектов, отобранных Министерством промышленности и торговли РФ. Дальнейшие успехи и перспективы в реализации научного потенциала во многом зависят от того, будет ли он востребован отечественной фарминдустрией.

**ЛИТЕРАТУРА**

1. Pharmaceutical Market Trends, 2008–2012.
2. *Гаврилова С.И.* Фармакотерапия болезни Альцгеймера: миф или реальность // Материалы 2-й Российской конференции “Болезнь Альцгеймера и старение: от нейробиологии к терапии”. М., 1999. С. 25-44.
3. *Patyulin V.A., Radchenko E.V., Zefirov N.S.* Molecular Field Topology Analysis Method in QSAR Studies of Organic Compounds // Journ. Chem. Inf. Comput. Sci.

2000. V 40. P. 659-667.

4. *Галъберштам Н.М., Баскин И.М., Палюлин В.А., Зефиров Н.С.* Нейронные сети как метод поиска зависимостей структура–свойство органических соединений // Успехи химии. 2003. № 7.
5. *Baskin L.L., Tikhonova I.G., Patyulin V.A., Zefirov N.S.* Selectivity Fields: Comparative Molecular Field Analysis (CoMFA) of the Glycine/NMDA and AMPA Receptors // Journ. Med. Chem. 2003. V 46. P. 4063–4069.
6. *Parsons C.G. et al.* Memantine: a NMDA receptor antagonist that improves memory by restoration of homeostasis in the glutamatergic system – too little activation is bad, too much is even worse // Neuropharmacology. 2007. V 53. P. 699-723.
7. *O'Neill M.J., Dix S.* AMPA receptor potentiators as cognitive enhancers // Drugs. 2007. V 10. P. 185–192.
8. *Sheridan R.P.* The Most Common Chemical Replacements in Drug-Like Compounds // Journ. Chem. Inf. Comput. Sci. 2002. V. 42. P. 103-108.
9. Патенты РФ № 2223952, № 2223952.
10. *Bachurin S., Bukatina E., Lermontova N. et al.* Antihistamine agent Dimebon as novel neuroprotector and cognition enhancer // Ann. N.Y Acad. Sci. 2001. V. 939. P. 425-435.
11. *Doody S., Gavrilova S.I., Sano M. et al.* Dimebon improves cognition, behaviour, activities of daily living and global function in a randomised, double-blind, placebo-controlled 6-month study of patients with mild- to-moderate Alzheimer's disease // Lancet. 2008. V. 372. P. 207-215.
12. *Pollak A.* Antihistamine Shows Promise in Treating Alzheimer's // The New York Times. 2007. June 11.

*JOURNAL OF MEDICINAL CHEMISTRY, 2002, Vol. 45, No. 18, 3836-3843*

# STRUCTURAL BASIS FOR UNDERSTANDING STRUCTURE-ACTIVITY RELATIONSHIPS FOR THE GLUTAMATE BINDING SITE OF THE NMDA RECEPTOR

**Irina G. Tikhonova, Igor I. Baskin, Vladimir A. Palyulin, Nikolai S. Zefirov, and Sergey O. Bachurin**

*Department of Chemistry, Moscow State University, Moscow 119992, Russia*

We present new homology-based models of the glutamate binding site (in closed and open forms) of the NMDA receptor NR2B subunit derived from X-ray structures of the water soluble AMPA sensitive glutamate receptor. The models were used for revealing binding modes of agonists and competitive antagonists, as well as for rationalizing known experimental facts concerning structure−activity relationships: (i) the switching between the agonist and the antagonist modes of action upon lengthening the chain between the distal acidic group and the amino acid moi-

ety, (ii) the preference for the methyl group attached to the R-amino group of ligands, (iii) the preference for the D-configuration of agonists and antagonists, and (iv) the existence of "superacidic" agonists.

## Introduction

The NMDA receptor belongs to a family of ionotropic glutamate receptors and performs important functions in the central nervous system. It is involved in neuronal signaling processes, memory consolidation, and synaptic plasticity.[1,2] The neurotoxicity induced by NMDA hyperactivation leads to a number of pathological conditions, ranging from acute neurodegenerative disorders, such as stroke and trauma, to chronic neurodegenera- tive diseases, such as Huntington's disease, Parkinson's disease, Alzheimer's disease, and amyotrophic lateral sclerosis.[3-6]

At present, four sites at the NMDA receptor are considered as major targets for endogenous and exogenous ligands: (i) the glutamate site for agonists and competitive antagonists, (ii) the glycine site for coagonists and the corresponding antagonists, (iii) two or even three polyamine sites (voltage-dependent and voltageindependent, respectively) for NMDA receptor modulators, and (iv) the phencyclidine site for channel blockers (noncompetitive antagonists) (see refs 3-6). All of them display unique properties and pharmacology. This paper deals with the glutamate binding site as historically the first studied one and playing the key role in the work of the NMDA receptor. (For our recent studies on modeling the NMDA receptor ion channel and the phencyclidine binding site, see ref 7.)

A number of different agonists and antagonists have been synthesized for the glutamate binding site,[8-13] and some of them are shown in Figures 1 and 2. The structure-activity relationships for them include the following major regularities: the dependence of agonist (antagonist) activity on the length of the molecular chain, the preference for substitution on the nitrogen atom of the amino group, and the preference of the D− configuration for both agonists and antagonists.[5,14,15] It should, however, be mentioned that none of these compounds is currently used in medical practice, because of their adverse effects.[3,16,17] The latter circumstance dictates the necessity for further research with the purpose of clarifying the mechanism of action and developing new ligands that would not cause undesirable side effects.

It has been shown that the NMDA receptor is composed of at least two NR1 and at least two NR2 subunits.[18-21] Each NR1 subunit is present in one of its splice variants, while each NR2 subunit belongs to one of its four subtypes, NR2A-NR2D, leading to a big heterogeneity of the wild-type NMDA receptors and variance of their electrophysiological properties and pharmacological profiles.[19] Four or five NR1 and NR2 subunits form an ion channel, which is usually blocked by magnesium in a voltage-dependent manner.

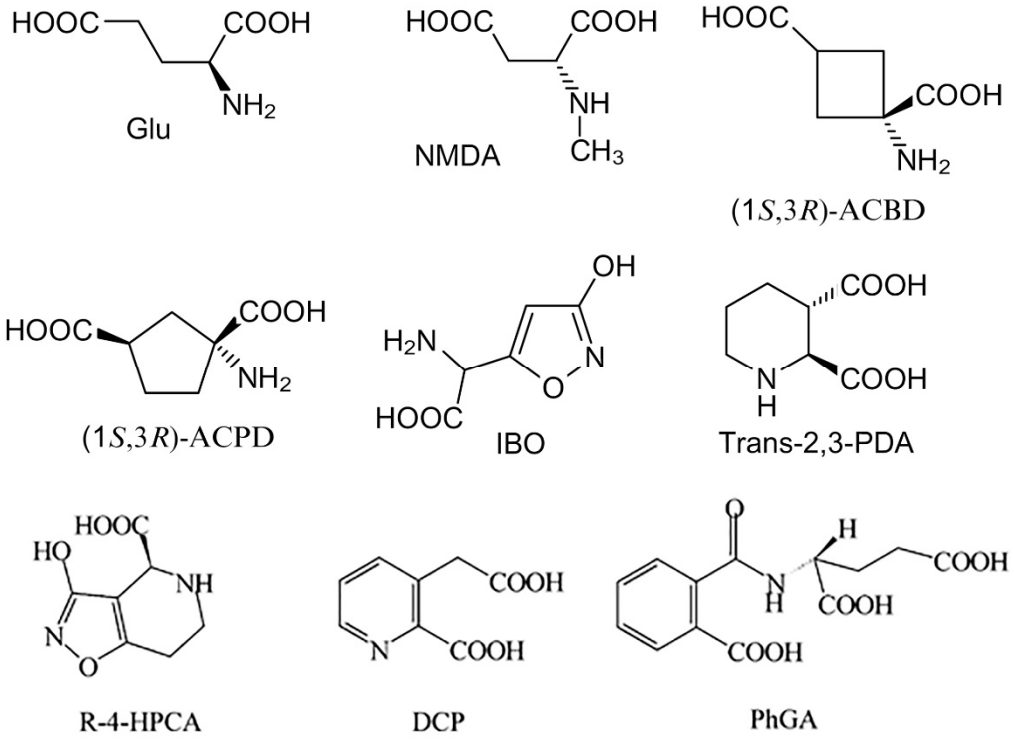


**Figure 1.** Agonists of the glutamate site of the NMDA receptor.

Upon simultaneous activation of the receptor (under the action of an agonist on the glutamate site and a coagonist on the glycine site)[18] and the release of the magnesium blockage (caused by simultaneous partial depolarization of the membrane), an influx of calcium into the cell takes place. This effect is known to be the key element in the process of long-term potentiation underlying the memory formation.

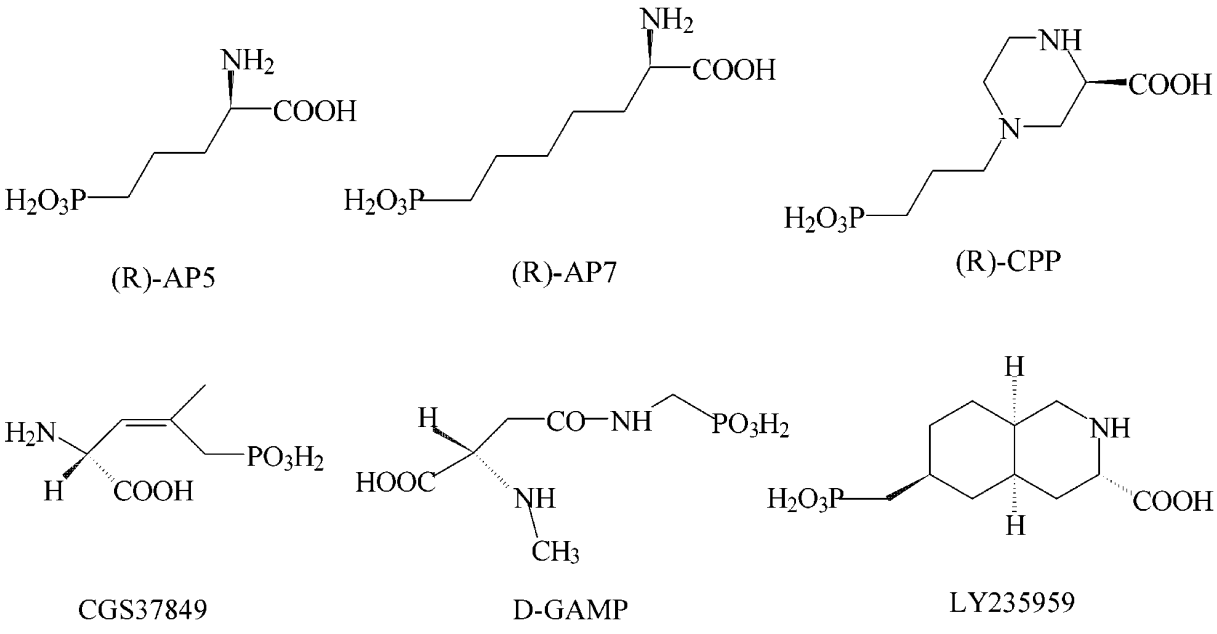


Figure 2. Antagonists of the glutamate site of the NMDA receptor.

All NR1 and NR2 subunits are characterized by the identical four domain structure: (i) the N-terminal extracellular modulatory domain (which contains a voltage-independent polyamine site); (ii) the agonist/ coagonist binding domain, which holds the glycine binding site in an NR1 subunit and the glutamate binding site in an NR2 subunit; (iii) the transmembrane channel-forming region, which hosts several partially overlapping binding sites for magnesium, zinc, phencyclidine, polyamines (voltage-dependent site), etc.; and (iv) the C-terminal intracellular regulatory domain taking part in interactions with several intracellular proteins of postsynaptic density. In the 1990s, all genes encoding the NR1 and NR2 subunits were cloned and thoroughly studied, and their amino acid sequences were identified,[22,23] which offered the prospect of their comparative modeling. On the basis of the homology of amino acid sequences between bacterial periplasmic proteins and agonist binding domains of glutamate (both ionotropic and metabotropic) receptors, a common general structure and a common activation mechanism were postulated for their ligand binding domains.[24] It was assumed that such domains could consist of two lobes and exist in two forms, open and closed, while binding of agonists/coagonists causes closure of the domain (leading to receptor activation) via the Venus flytrap mechanism. Laube and colleagues[25] made the first attempt to build three-dimensional (3D) models of the NMDA receptor glutamate and glycine sites on the basis of sequence homology with the bacterial periplasmic protein (LAOBP). They have built an approximate model of these sites in the open form of the domain and suggested the mode of agonist and antagonist binding.

Meanwhile, in 2000, the X-ray crystallographic analyses of a water soluble AMPA sensitive glutamate receptor (AMPASGR), GluR2 ligand binding core, and its complexes with different ligands exhibiting agonist, partial agonist, and antagonist activity have been made.[26] Because the homology between AMPA and NMDA receptors is much higher (~30%) than between LAOBP (~18%) and the agonist/coagonist binding domains of the NMDA receptor and X-ray structures of open and closed forms of the AMPASGR are available, we suggested that 3D structures built by means of this homology would be more correct than the previous models and hence would allow us to shed light on mechanisms of receptor activation and to reach a better understanding of structure-activity relationships for NMDA receptor ligands.[5,14,15]

In this study, molecular modeling of the glutamate site belonging to the NR2B subunit of the NMDA receptor has been carried out (for our preliminary communications, see ref 27). The obtained models were used for studying different modes of ligand binding and explaining known structure-activity relationships for its agonists and competitive antagonists. The work with the glycine site is also in progress in our laboratory and will be a matter of a separate publication.

## Materials and Methods

The multiple amino acid sequence alignment was built by means of the Clustal X program.[28] The BLOSSUM30 homology matrix was used for evaluating amino acid similarity. This sequence alignment was used as a basis for homology modeling using the Biopolymer module in the Sybyl6.6 molecular modeling package[29] on the SGI Octane workstation. The X-ray structure of the complex of the AMPASGR with glutamate (Brookhaven Protein Data Bank[30] accession code 1FTJ) was used as a template for modeling the closed form of the glutamate binding site of the NMDA receptor, while the X-ray structure of the complex of the same protein with an antagonist 6,7-dinitroquinoxaline-2,3-dione (DNQX, Brookhaven Protein Data Bank[30] accession code 1FTL) was used as a template to model the open form of the same binding site.

In the course of molecular modeling, a template protein was mutated to a goal protein in accordance with the following procedure. All aligned nonidentical amino acids were "mutated" to each other by changing their side chains while keeping main chain atoms unchanged and fixed at their original position in space. Internal torsion angles in side chains of new amino acids were chosen to be most appropriate for a given amino acid in a given secondary structure state (which remains unchanged while "mutating" residues). All insertions and deletions were handled by defining "loops" containing all residues being inserted and several atoms neighboring to positions of insertion or deletion, followed by searching the Brookhaven Protein Data Bank[30] for them. After that, search results were visually inspected, and the main chain atoms of those loops, which (i) the geometry of the main chain atoms neighboring to the deletion or insertion positions underwent smaller changes, (ii) the amino acid sequence possessed the strongest homology to the required sequence, and (iii) no unfavorable spatial hindrance between atoms belonging to the loop and to the remaining part of the protein could be expected, were inserted in the protein model followed by adding appropriate side chains in accordance with the aforementioned procedure. After that, all proline residues and side chains of all other residues were "fixed" by finding new values for several torsion angles so as to remove spatial overlap between atoms. This was followed by adding hydrogen atoms capable of forming hydrogen bonds. After that, the protein was subjected to energy minimization using the Tripos force field as implemented in the SYBYL package.[29] Then, the protein was solvated with a box of water molecules and reminimized with the AMBER 6.0[31] program SANDER using the Cornell et al. force field.[32] This was followed by a short 20 ps molecular dynamics simulation at 300 K using the same SANDER program. The complexes of the protein with D-AP5 and L-Glu were subjected to longer molecular dynamics simulations (100 ps).

The stereochemical quality of the protein models was checked using the PROCHECK program[33,34] with a pseudoresolution of 1.9 A. The sequence–structure compatibility of the protein models was assessed using the Verify3D[35] program.

**Ligands.** All ligands were built interactively using Sybyl6.6. The carboxyl and amino groups of ligands were ionized, since in this form they usually occur under physiological conditions. Atomic charges in ligands were computed with the Gasteiger-Marsili method.[36]

**Docking.** A putative binding pocket was determined on the basis of known data on site-directed mutagenesis.[25] Each ligand was placed into the binding pocket and orientated taking into account the X-ray structures of the AMPASGR-ligand complexes. A manual docking procedure was applied, and the obtained receptor-ligand complexes were optimized using the Tripos force field. Different conformations and orientations of each ligand within the binding pocket were explored, and each time, the ligand-protein complex was reminimized.

## Results and Discussion

**Alignment of Amino Acid Sequences.** The multiple amino acid sequence alignment for modeling the glutamate site of the NMDA receptor was built between the primary sequences of all representatives of the ionotropic glutamate receptors family, namely, NR1 (Swiss Protein Data Bank[37] accession code P35437), NR2A (Q08948), NR2B (Q13224), NR2C (Q14957), NR2D (Q15399), GLUR1 (P42261), GLUR2 (P42262), GLUR3 (P42263), GLUR4 (P48058), GLUR5 (P39086), GLUR6 (Q13002), KA1 (Q16099), and KA2 (Q16478) subunits and the sequence of the water soluble AMPASGR. A section of this alignment containing only the primary sequences of the NR2B subunit (chosen by us for modeling the glutamate site of the NMDA receptor) and AMPASGR (serving as a template for comparative modeling) and spanning the sequence region homologous to the whole molecule of AMPASGR is depicted in Figure 3.

```
              *  * * *        * *                 *   *          * * *    * *
AMPA : NKTVVVTTILESPYVMMKKNHEMLEG----------------NERYE----------GYCVDLAAEIAK :   43
NR2B : DDHLSIVTLEEAPFVIV-ESVDPLSGTCMRNTVPCQKRIVTENKTDEEPGYIKKCCKGFCIDILKKISK :  413
                  |  |
                 413

           * * *  *  ** *        **** ** *   *      ***   **** *** **   *** *
AMPA : HCGFKYKLTIVGDGKYGARDADTKIWNGMVGELVYGKADIAIAPLTITLVREEVIDFSKPFMSLGISIM :  112
NR2B : SVKFTYDLYLVTNGKHGKKING--TWNGMIGEVVMKRAYMAVGSLTINEERSEVVDFSVPFIETGISVM :  537
                       ||                                |      |
                       486                              512    519

                          *   *           **   ***    *         *  **
AMPA : IKKG--∫--∫T-PIESAEDLSKQT------EIAYGTLDSGSTKEFFRRSKIAVFDKMWTYMRSAEPSVF :  168
NR2B : VSRSNG∫--∫VDQVSGLSDKKFQRPNDFSPPFRFGTVPNGSTERNIRNN----YAEMHAYMG----KFN :  710
                                          |    ||
                                         686

        *            *   *             *   *     * *    * *****  * *     * *
AMPA : VRTTAEGVARVRKSKGKYAYLLESTMNEYIEQRKP-CDTMKVG-G-NLDSKGYGIATPKGSSLGNAVNL :  243
NR2B : QRGVDDALLSLKTGK-LDAFIYDAAVLNYMAGRDEGCKLVTIGSGKVFASTGYGIAIQKDSGWKRQVDL :  778
                                  |                  |
                                 735                757

       * * *   *    *   *      *
AMPA : AVLKLNEQGLLDKLKNKWWYDKGEC------------ :  259
NR2B : AILQLFGDGEMEELEALWLTG--ICHNEKNEVMSSQLD :  814
```

Figure 3. Sequence alignment used for building models.

The whole multiple alignment of all sequences can be obtained in the Supporting Information. It is noteworthy mentioning that the use of the pairwise alignment between the latter two sequences instead of the multiple sequence alignment between all subunits of ionotropic glutamate receptors does not lead to construction of a correct molecular model, since it does not detect the transmembrane channel-forming region inside a primary sequence of the NR2B subunit.

**Assessment of Models Quality.** Analysis of the model in open and closed forms using PROCHECK[33,34] revealed good stereochemistry. Standard deviations of all main chain and side chain stereochemical parameters were within or better than the expected values;[33] ~73% of the residues in the closed form and ~70% in the open form adopted the most favored main chain torsion angles, and only ~1% (in the open form) and ~2% (in the closed form) of residues lied in unfavorable regions. No short intramolecular contacts were detected. Energy profiles analysis using Verify 3D[35] displayed that negative score regions (30-31 (432-433), 34-36 (436-438), 37-45 (439-446)) were found in the model, but they were localized at the loops far from the binding sites that could not influence on the validity of the structural sites affecting ligand selectivity (Figure 4).

**Structure of Receptor Binding Site.** On the basis of the sequence homology with AMPASGR, 3D models of the glutamate site in the open and closed forms were obtained. It is common knowledge that receptors exert their biological action by changing their conformations upon binding ligands-agonists. However, the issue of the exact number of such conformations is a matter of hot discussion.[38,39] Although the most popular point of view implies the existence of two main conformations,[40] a ligand binding "active" and a ligand-free "nonactive" one, numerous works suggest the existence of multiple (or even a continuum of) conformational states involved in receptor activation.[38,39] An X-ray study of the AM-PASGR complexes with different ligands suggests the existence of at least three principal conformational states[26] of the ligand binding region: (i) "closed" conformations adopted by complexes with agonists, (ii) "half-open" conformations stabilized by partial agonists, and (iii) "open" conformations in the ligand-free form and in complexes with antagonists. The main distinction between these forms is expressed by an angle between two lobes comprising the protein globule forming the ligand binding domain. However, comparison of X-ray structures of AM-PASGR complexes with two AMPA receptor agonists, glutamate and AMPA, reveals a rather small difference between them (rms of fitting between the complexes is only 0.66 A for all atoms), so one can suggest that it is sufficient to use only one conformation of the glutamate binding site for modeling its interactions with agonists. The difference between open conformations is even smaller (rms of fitting between the ligand-free "apo" and DNQX bound forms is 0.55 A for all atoms), so we assume that

considering only one conformation of this site is also sufficient for modeling its interactions with antagonists. So, in accordance with the principle of Ockham's Razor,[41] we conclude that the model with two conformational states, one for complexes with agonists and one for complexes with antagonists, may be adequate for pharmacology studies and therefore can be adopted for the purposes of this work.

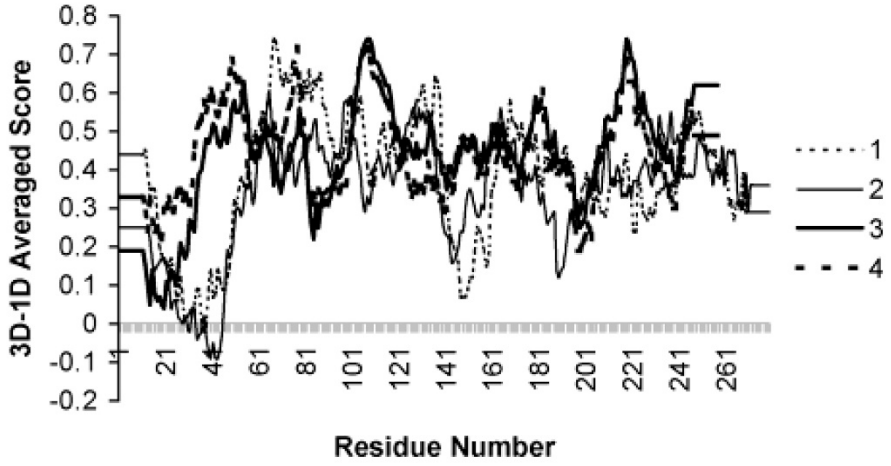


**Figure 4.** Verify 3D plots of the models of the NMDA receptor glutamate site closed (1) and open (2) forms in comparison with X-ray structures of AMPASGR complexes with an agonist (3) and antagonist (4).

In this study, the X-ray structure of the complex of AMPASGR with glutamate (access code 1FTJ in the Brookhaven Protein Data Bank[30]) was used for modeling the closed agonist binding form of the glutamate site of the NMDA receptor, while the X-ray structure of the complex of AMPASGR with AMPA receptor antagonist 6,7-dinitroquinoxaline-2,3-dione (access code 1FTL in the Brookhaven Protein Data Bank[30]) was used for modeling the antagonist binding open form of the same site. Molecular modeling has shown that the glutamate binding domain of the NMDA receptor consists of two lobes composed of β-sheets covered with R-helices. In the model, these two lobes are connected with a hinge region (Figure 5a,b). In a real receptor, there is also a transmembrane channel-forming region coming from one of these lobes, so the switch between the open and the closed states of the glutamate binding domain causes the switch between the open and the closed states of the NMDA receptor ion channel through an indirect mechanism involving mutual rotation of different subunits (see Discussion in ref 26). Agonist-induced closure of the glutamate site leads to the activation of the receptor and opening of the channel, while the antagonist-induced opening of the same site leads to the closure of the channel.

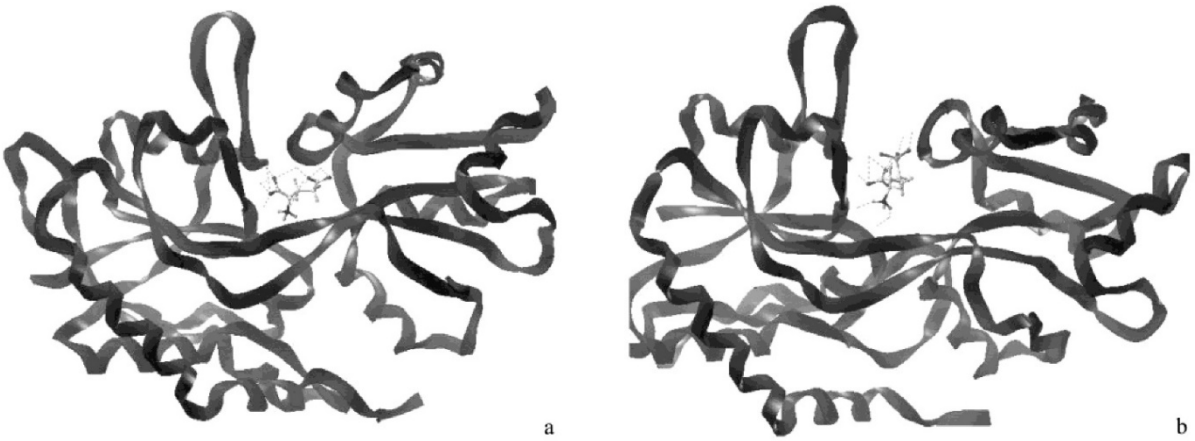


**Figure 5.** Binding of agonist glutamate (a) and antagonist R-AP5 (b) to the NMDA receptor glutamate binding site after molecular dynamics simulation.

**Binding Modes of Agonists and Antagonists.** In accordance with site-directed mutagenesis experiments,[25] amino acid residues E413, K485, S512, R519, S690, T691 in NR2B are important for receptor functioning, and this may take place if they are either involved in binding agonists or in gating mechanism, or they are important for proper protein folding.[42] From the analysis of the binding mode of AMPASGR with glutamate, one can reveal residues forming hydrogen bonds and ion bridges with ligand (R94 in AMPASGR interacts with R-carboxyl group, E191 and P87 are bonded to amino group, and S140 and T141 bind to *Y*-carboxyl group). Considering the positions of the corresponding amino acid residues in the multiple alignment, it can be found that residue R519 in NR2B (corresponds to R94 in AMPASRG), S690 (S140), and T691 (T141) are conservative in NR2B and AMPASGR; however, S512 in NR2B corresponds to P87 in AM- PASGR. Residue E191 in AMPASGR, which participates in hydrogen bond formation with the amino group of glutamate, corresponds to D732 in NR2B (no mutagenesis data have been reported for this case). All of these facts were taken into account when docking the agonists and antagonists shown in Figures 1 and 2 to this site. These docking experiments revealed that the optimal orientation could be achieved when the R-carboxyl group of agonists was allowed to form a salt bridge with R519 and hydrogen bonds with S690 and T514, while the protonated amino group is hydrogen-bonded to E413 and S512, in accordance with Laube's et al. model.[25] However, the distal acidic function of agonists, in contradiction to Laube's et al. model,[25] is predicted in our model to form hydrogen bonds with S690 and T691. One can suggest that the difference between Laube's et al. and our models might partially be accounted for by the fact that Laube et al. built all of their models, including even complexes with agonists, for the open form of the glutamate binding site, although in reality agonists make stable complexes with the closed form. In the case of antagonists, we have found that the R-acidic moiety and amino group interact with the same residues as agonists, whereas a distal group (phosphonic in R-AP5) forms salt bridges with K485 and K488.

To improve results of docking and study the role of water in ligand binding, we have performed molecular dynamics studies of protein complexes with glutamate and AP5 (Figure 6a,b). The results of these studies have shown that in both cases the amino group interacts preferably with D732, while the docking procedure predicts binding of this group with E413 (see above). Both residues are located in the vicinity of this amino group but at opposite sides. It is possible that both residues contribute to binding this group; however, the 100 ps dynamics did not reveal a reverse switch from D732 to E413. The molecular dynamics simulations have also allowed refinement of the position of the distal group in AP5: it forms a hydrogen bond with the main chain NH moiety belonging to S690, and it is also bound to K485 directly and to K488 through a water molecule. Different interaction modes result in dissimilar arrangement of agonists and antagonists in the glutamate binding domain. Figure 5a,b illustrates the general arrangement of agonists and antagonists inside the glutamate site for the cases of glutamate and R-AP5. Glutamate, the native agonist, lies deeply in the binding pocket approximately in parallel with the hinge region, interacts with both lobes of the domain, and causes them to approach each other (see Figure 5a). An antagonist R-AP5 is, on the contrary, oriented perpendicularly with respect to the hinge region, and its distal group prevents the lobes from closure (see Figure 5b). Detailed analysis of the binding pocket made it possible to account for the structure-activity relationships discovered in various pharmacological and electrophysiological studies.[5,14,15]

Switch between the Agonist and Antagonist Activity of Ligands upon Lengthening the Chain between the Amino Acid Moiety and the Distal Anionic Group. The dependence of the agonist and antagonist activity of ligands acting on the glutamate site of the NMDA receptor upon the distance between two acidic groups was discussed in the literature.[5] In particular, a shorter distance is needed for a ligand to exhibit agonist activity, while antagonists are characterized by a longer distance between them (compare formulas in Figures 1 and 2). This fact can easily be explained on the basis of molecular models. It is seen in Figure 6a that the distal carboxyl of the native agonist glutamate lies in the vicinity of a small pocket formed by four hydrophobic residues: V714, Y731, F729, and V686. One can suggest that the wall of this pocket limits the size of agonists. Antagonists do not fit to the size of the binding pocket, so they have to turn around and bind to K485 and K488 (see Figure 6b). This might explain the switch between the agonist and the antagonist activity of ligands upon lengthening the chain between the amino acid moiety and the distal anionic group. It can also be predicted from this study that it is impossible to find a lengthy or a bulky agonist for this binding site.

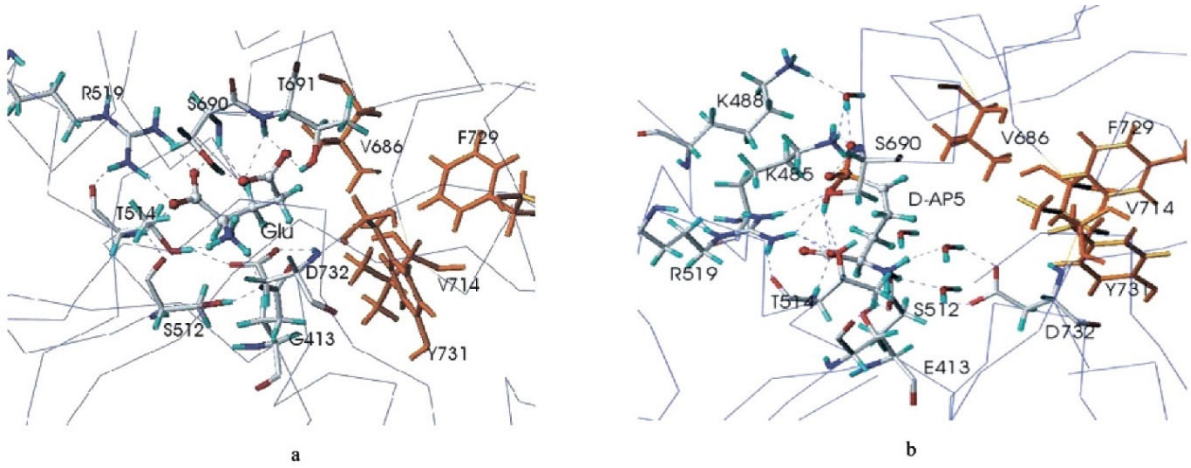


**Figure 6.** Binding mode of agonists (a) and antagonists (b) to the NMDA receptor glutamate site.

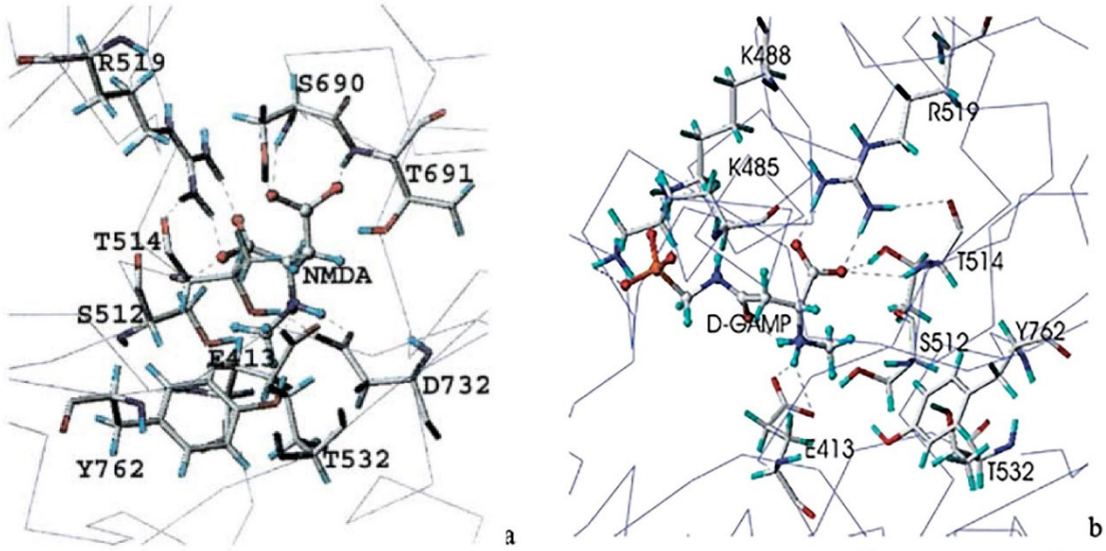


**Figure 7.** Binding of NMDA (a) and D-GAMP (b) to the glutamate site.

**Preference for Substitution at the Nitrogen Atom in the Amino Group.** Using our models, one can explain the following structure-activity relationship: the preference for substitution at the nitrogen atom in the amino group for both agonists and antagonists. The binding of NMDA and D-GAMP to the glutamate site is shown in Figure 7a,b. In both cases, there is a small hydrophobic pocket for the $CH_3$ group formed by Y762 and T514. This might explain this experimental fact.

**Preference for the D-configuration in Agonists and Antagonists.** To explain the preference for the D-configuration of the chiral center in both agonists and antagonists, L-forms of agonist NMDA (i.e., NMLA and N-methyl-L-aspartate) and antagonist AP5 were docked to the models of the binding site (Figure 8a,b). We have found that the reason for preference for the D-configuration is different for agonists and antagonists. For the case of agonists, there is a steric repulsion between NMLA and residues H486 and S512 that hinders binding. Comparing binding of L-AP5 (Figure 8b) and D-AP5, it can be noted that the distal negatively charged phosphonic group in the

D-configuration is closer to positively charged K485 and K488 than for the L-configuration. So, electrostatic ligand-protein interaction is more favorable for the D-configuration of antagonist AP5.

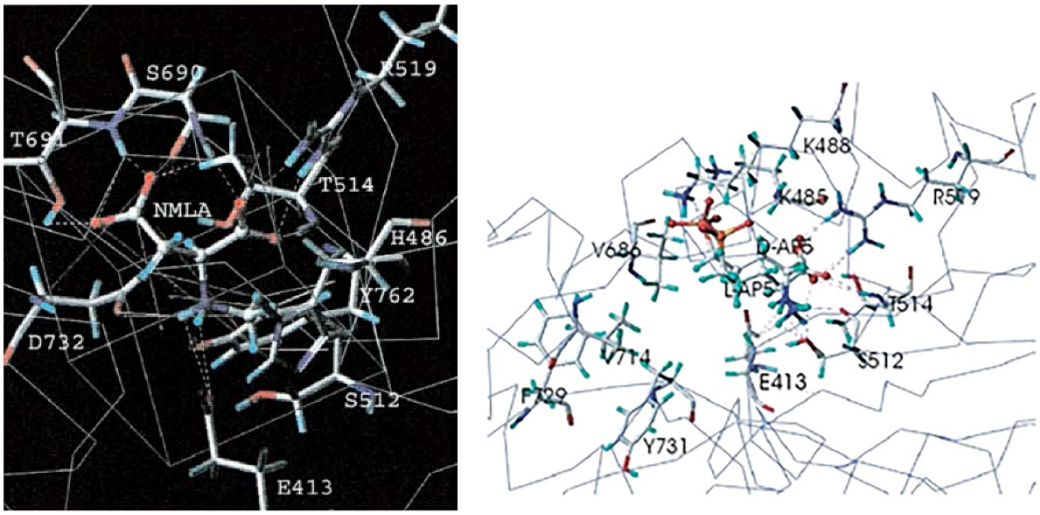


a b

**Figure 8.** Docking of NMLA (a) and L-AP5 (b) to the glutamate site.

**Superacidic Agonists.** In this study, we have suggested the binding mode of selective superacidic agonist N-phthalamoyl-L-glutamic acid (PhGA).[5] This compound does not possess the pharmacophore (consisting of two acidic and one amino group) that is common for almost all ligands of the glutamate site of the NMDA receptor. Using models, we can see the important role of the carboxyl group attached to the benzene ring. This group plays the role of the distal acidic group of agonists and binds to S690 and T691 (see Figure 9). This explains the crucial role of this group for binding to the NMDA receptor known from the experiment.[9]

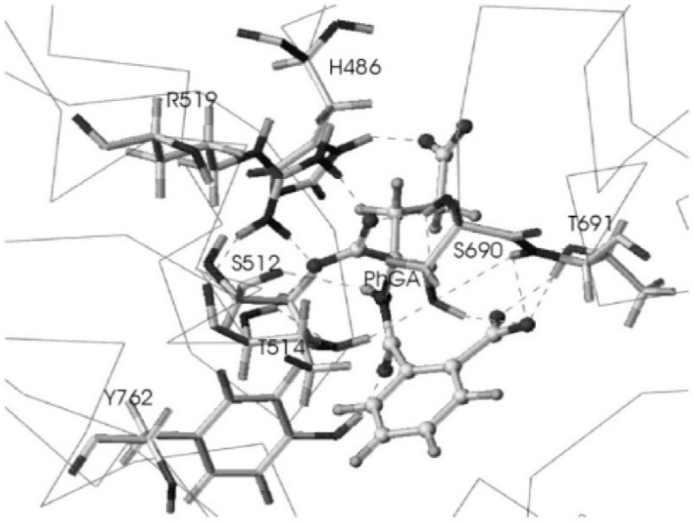


**Figure 9.** Binding of PhGA to the glutamate site.

**Receptor Subtype Specificity between Different NR2 Subunits.** At the present time, not one of the known ligands of the glutamate site is selective with respect to

different NR2 subunit subtypes. Examination of molecular models can explain this fact. The distance between the ligands and the nearest nonconservative among NR2A-D subtype amino acids (G713 in NR2B) exceeds 7.5 A, and there is no free space between them (they are screened by conservative V714). So, it seems that it is hardly possible to design subtype selective ligands acting on the glutamate site.

## Conclusion

Relatively high homology within the group of glutamate ionotropic receptors allowed us to use the results of the X-ray analysis of AMPASGR for molecular modeling of the NMDA receptor glutamate site. The models obtained satisfactorily explain the structure-activity relationships for binding a series of agonists and competitive antagonists of the glutamate site. These models can reveal the key residues that interact with ligands. Further studies in this direction would validate these models, which could subsequently be used for de novo drug design. Coordinates of the model in open and closed forms will be submitted to the Brookhaven Protein Data Bank.

**Acknowledgment.** We thank Tripos GmbH (Muinich, Germany) and the V. N. Orekhovich Institude of Biomedical Chemistry of the Russian Academy of Medical Sciences for scientific and technical assistance. We acknowledge the University of California, San Francisco for providing Amber 6.

**REFERENCES**

1. Parsons, C. G.; Danysz, W.; Quack, G. Glutamate in CNS Disorders as a Target for Drug Development: An Update. *Drug News Perspect.* 1998, *11*, 523-579.
2. Nakanishi, N. S. Molecular diversity of glutamate receptors and implications for brain function. *Science* 1992, *258*, 31-37.
3. Dingledine, R.; Borges, K.; Bowie, D.; Traynelis, S. F. The Glutamate receptor ion channels. *Pharmacol. Rev.* 1999, *51*, 7-61.
4. Bräuner-Osborne, H.; Egebjerg, J.; Nielsen, E. 0.; Madsen, U.; Krogsgaard-Larsen, P. Ligands for glutamate receptors: design and therapeutic prospects. *J. Med. Chem.* 2000, *43*, 2609-2645.
5. Petrov, V. I.; Piotrovsky, L. B.; Grigoriev, I. A. *Exitatory Amino Acids*; Volgograd Medical Academy: Volgograd, 1997; p 168.
6. Zefirova, O. N.; Zefirov, N. S. Physiologically active compounds acting on glutamate receptors. *Zh. Org. Khim. (Russ.)* 2000, *36*, 1273-1300.
7. (a) Bachurin, S.; Tkachenko, S.; Baskin, I.; Lermontova, N.; Mukhina, T.; Petrova, L.; Ustinov, A.; Proshin, A.; Grigoriev, V.; Lukoyanov, N.; Palyulin, V.; Zefirov, N. Neuroprotective and Cognition-enhancing Properties of MK-801 Flexible Analogues. Structure-Activity Relationships. *Ann. N. Y. Acad. Sci.* 2001, *939*, 219-236. (b) Baskin, I. I.; Palyulin, V. A.; Zefirov, N. S. Molecular Modeling of the NMDA Receptor Ion Channel. *Proceedings of the*

*II Russian Congress "Molecular Modeling"*, Moscow, Russia, April, 2001; p 52.

8. Johnson, R. L.; Koerner, J. E. Excitatory amino acid neurotransmission. *J. Med. Chem*. 1988, *31*, 2057-2066.
9. Kiskin, N. I.; Tsynderenko, A. Ya.; Dumpis, M. A.; Piotrovsky, L. B.; Krishtal, O. A. A novel selective NMDA agonist, *N*- phthalamoyl-L-glutamic acid. *Neuroreport* 1991, *2*, 29-32.
10. Shinozaki, H.; Ishida, M.; Shimamoto, K.; Ohfune, Y. A conformationally restricted analogue of L-glutamate, the (2*S*,3*R*,4*S*) isomer of L-α-(carboxycyclopropyl)glycine, activates the NMDA- type receptor more markedly than NMDA in isolated rat spinal cord. *Brain Res*. 1989, *480*, 355-359.
11. Curry, K.; Peet, M. J.; Magnuson, D. S.; McLennan, H. Synthesis, resolution, and absolute configuration of the isomers of the neuronal excitant 1-amino-1,3-cyclopentanedicarboxylic acid. *J. Med. Chem*. 1988, *31*, 864-867.
12. Madsen, U.; Ferkany, J. W.; Jones, B. E.; Ebert, B.; Johansen, T. N.; Holm, T.; Krogsgaard-Larsen, P. NMDA receptor agonists derived from ibotenic acid. Preparation, neuroexcitation and neurotoxicity. *Eur. J. Pharmacol*. 1990, *189*, 381-391.
13. Allan, R. D.; Hanrahan, J. R.; Hambley, T. W.; Johnston, G. A. R.; Mewett, K. N.; Mitrovic, A. D. Synthesis and activity of a potent *N*-methyl-D-aspartic acid agonist, *trans*-1-aminocyclobu- tane-1,3-dicarboxlic acid, and related phosphonic and carboxylic acids. *J. Med. Chem*. 1990, *33*, 2905-2915.
14. Davies, J.; Evans, R. H.; Francis, A. A.; Jones, A. W.; Smith, D. A.; Watkins, J. C. Conformational aspects of the actions of some piperidine dicarboxylic acids at excitatory amino acid receptors in the mammalian andamphibian spinal cord. *Neurochem. Res*. 1982, *7*, 1119-1133.
15. Davies, J.; Evans, R. H.; Jones, A. W.; Smith, D. A.; Watkins, J. C. Differential activation and blockade of excitatory amino acid receptors in the mammalian and amphibian central nervous systems. *Comp. Biochem. Physiol*. 1982, *72*, 211-224.
16. Hargreaves, R. J.; Hill, R. G.; Iversen, L. L. Neuroprotective NMDA antagonists: the controversy over their potential for adverse effects on cortical neuronal morphology. *Acta Neurochir Suppl.* 1994, *60*, 15-19.
17. Sveinbjornsdottir, S.; Sander, J. W.; Upton, D.; Thompson, P. J.; Patsalos, P. N.; Hirt, D.; Emre, M.; Lowe, D.; Duncan, J. S. The excitatory amino acid antagonist D-CPP-ene (SDZ EAA-494) in patients with epilepsy. *Epilepsy Res*. 1993, *16*, 165-174.
18. Hollmann, M.; Heinemann, S. Cloned glutamate receptors. *Annu. Rev. Neurosci*. 1994, *17*, 31-108.
19. Kutsuwada, T.; Kashiwabuchi, N.; Mori, H.; Sakimura, K.; Kushiya, E.; Araki, K.; Meguro, H.; Masaki, H.; Kumanishi, T.; Arakawa, M.; Mishina, M. Molecular diversity of the NMDA receptor channel. *Nature* 1992, *358*, 36-41.
20. Meguro, H.; Mori, H.; Araki, K.; Kushiya, E.; Kutsuwada, T.; Yamazaki, M.; Kumanishi, T.; Arakawa, N.; Sakimura, K.; Mishina, M. Functional characterization of a heteromeric NMDA receptor channel expressed from cloned cDNAs. *Nature* 1992, *357*, 70-74.
21. Monyer, H.; Sprengel, R.; Schoepfer, R.; Herb, A.; Higuchi, M.; Lomeli, H.; Burnashev, N.;

Sakmann, B.; Seeburg, P. H. Heteromeric NMDA receptors: molecular and functional distinction of subtypes. *Science* 1992, *256*, 1217-1221.

22. Le Bourdelles, B.; Wafford, K. A.; Kemp, J. A.; Marshall, G.; Bain, C.; Wilcox, A. S.; Sikela, J. M.; Whiting, P. J. Cloning, functional coexpression, and pharmacological characterisation of human cDNAs encoding NMDA receptor NR1 and NR2A subunits. *J. Neurochem.* 1994, *62*, 2091-2098.
23. Zimmer, M.; Fink, T. M.; Franke, Y.; Lichter, P.; Spiess, J. Cloning and structure of the gene encoding the human *N*-methyl- D-aspartate receptor (NMDAR1). *Gene* 1995, *159*, 219-223.
24. O'Hara, P. J.; Sheppard, P. O.; Thogersen, H.; Venezia, D.; Haldeman, B. A.; McGrane, V.; Houamed, K. M.; Thomsen, C.; Gilbert, T. L.; Mulvihill, E. R. The ligand-binding domain in metabotropic glutamate receptors is related to bacterial peri- plasmic binding proteins. *Neuron* 1993, *11*, 41-52.
25. Laube, B.; Hirai, H.; Sturgess, M.; Betz, H.; Kuhse, J. Molecular determinants of agonist discrimination by NMDA receptor subunits: analysis of the glutamate binding site on the NR2B subunits. *Neuron* 1997, *18*, 493-503.
26. Armstrong, N.; Gouaux, E. Mechanisms for activation and antagonism of an AMPA-sensitive glutamate receptor: crystal structures of the GluR2 ligand binding core. *Neuron* 2000, *28*, 165-181.
27. (a) Zefirov, N. S.; Baskin, I. I.; Palyulin, V. A. Molecular modeling of ionotropic and metabotropic glutamate receptors: A route to design of new neuroprotectors. *Book of Abstracts, Second IndoUS Workshop on Mathematical Chemistry with Applications to Drug Discovery, Environmental Toxicology, Chemoinformatics and Bioinformatics*, May 30-June 3, 2000, Duluth, MN; p 72. (b) Tikhonova, I. G.; Baskin, I. I.; Palyulin, V. A.; Zefirov, N. S. Computer-assisted modeling of 3D structure of the NMDA receptor NR2B subunit glutamate site. *Dokl. Akad. Nauk (Russ.)* 2002, *382* (4), 550-553; English translation *Dokl. Biochem. Biophys.* 2002, *382* (1-6), 38-42. (c) Baskin, I. I.; Belenikin, M. S.; Tikhonova, I. G.; Palyulin, V. A.; Zefirov, N. S. Computational approaches to molecular modeling of glutamate receptors. *Book of Abstracts, the II Russian Congress "Molecular Modeling"*, Moscow, Russia, April 2001; p 20.
28. Thompson, J. D.; Gibson, T. J.; Plewniak, F.; Jeanmougin, F.; Higgins, D. G. The CLUSTAL_X windows interface: flexible strategies for multiple sequence alignment aided by quality analysis tools. *Nucleic Acids Res.* 1997, *25* (24), 4876-4882.
29. *Sybyl 6.6*; Tripos Assoc.: St. Louis, MO.
30. Abola, E. E.; Bernstein, F. C.; Bryant, S. H.; Koetzle, T. F.; Weng, J. Protein data bank. In *Crystallographic Databases - Information Content, Software Systems, Scientific Applications*; Allen, F. H., Bergerhoff, G., Sievers, R., Eds.; Data Commission of the International Union of Crystallography: Bonn, Cambridge, Chester, 1987; pp 107-132.
31. Case, D. A.; Pearlman, D. A.; Caldwell, J. W.; Cheatham, T. E., III; Ross, W. S.; Simmerling, C. L.; Darden, T. A.; Merz, K. M.; Stanton, R. V.; Cheng, A. L.; Vincent, J. J.; Crowley, M.; Tsui, V.; Radme, R. J.; Duan, Y.; Pitera, J.; Massova, I.; Seibel, G. L.; Singh, U. C.; Weiner, P. K.; Kollman, P. A. *AMBER 6*; University of California: San Francisco, 1999.
32. Cornell, W. D.; Cieplak, P.; Bayly, C. I.; Gould, I. R.; Merz, K. M., Jr.; Ferguson, D. M.;

Spellmeyer, D. C.; Fox, T.; Caldwell, J. W.; Kollman, P. A. A second generation force field for the simulation of proteins, nucleic acids, and organic molecules. *J. Am. Chem. Soc.* 1995, *117*, 5179-5197.
33. Laskowski, R. A.; MacArthur, M. W.; Moss, D. S.; Thornton, J. M. PROCHECK: A program to check the stereochemical quality of protein structures. *J. Appl. Crystallogr.* 1993, *26*, 283-291.
34. Rullmann, J. A. C. *AQUA*; Utrecht University: The Netherlands, 1996.
35. Lüthy, R.; Bowie, J. U.; Eisenberg, D. Assessment of protein models with three-dimensional profiles. *Nature* 1992, *356*, 8385.
36. Gasteiger, J.; Marsili, M. Iterative Partial Equalization of Orbital Electronegativity - A Rapid Access to Atomic Charges. *Tetrahedron* 1980, *36*, 3219-3228.
37. Bairoch, A.; Apweiler, R. The SWISS-PROT protein sequence database and its supplement TrEMBL in 2000. *Nucleic Acids Res*. 2000, *28*, 45-48.
38. Tuček, S. Is the R and R* dichotomy real? *TiPS* 1997, *18,* 414-415.
39. Kenakin, T. Agonist-specific receptor conformations. *TiPS* 1997, *18*, 416-417.
40. Leff, P. The two-state model of receptor activation. *Trends Pharmacol. Sci*. 1995, *16*, 89-97.
41. Hoffmann, R.; Minkin, V. I.; Carpenter, B. K. Ockham's Razor and Chemistry. *HYLE* 1997, *3*, 3-28.
42. Colquhoun, D. Binding, gating, affinity, and efficacy: The interpretation of structure-activity relationships for agonists and of the effects of mutating receptors. *Br. J. Pharmacol*. 1998, *125*, 924-947.

*ANNALS OF THE NEW YORK ACADEMY OF SCIENCES, 2001, V. 939, P: 219-236*

# NEUROPROTECTIVE AND COGNITION-ENHANCING PROPERTIES OF MK-801 FLEXIBLE ANALOGS STRUCTURE–ACTIVITY RELATIONSHIPS

**S. Bachurin, S. Tkachenko, I. Baskin, N. Lermontova, T. Mukhina, L. Petrova, A. Ustinov, A. Proshin, V. Grigoriev, N. Lukoyanov, V. Palyulin, N. Zefirov**

*Institute of Physiologically Active Compounds RAS, 142432, Chernogolovka, Russia*

Neuroprotective and biobehavioral properties of a series of novel open chain MK-801 analogs, as well as their structure-activity relationships have been investigated. Three groups of compounds were synthesized: monobenzylamino, benzhydrylamino, and dibenzylamino (DBA) analogs of MK-801. It was revealed that DBA analogs exhibit pronounced glutamate-induced calcium uptake blocking properties and anti-NMDA activity. The hit compound of DBA series, NT-1505, was investigated for its ability to improve cognition functions in animal model of Alzheimer's disease type dementia, simulated by treating animals with cholinotoxin AF64A.

The results from an active avoidance test and a Morris water maze test showed that experimental animals, treated additionally with NT-1505, exhibited much better learning ability and memory than the control group (AF64A treated) and close to that of the vehicle group of animals (treated with physiological solution). Study of NT-1505 influence on locomotor activity revealed that it is characterized by a spectrum of behavioral activity radically different from that of MK-801, and in contrast to the latter one does not produce any psychotomimetic side effects in the therapeutically significant dose interval. The computed docking of MK-801 and its flexible analogs on the NMDA receptor elucidated the crucial role of the hydrogen bond formed between these compounds and the asparagine residue for magnesium binding in the NMDA receptor. It was suggested that strong hydrophobic interaction between MK-801 and the hydrophobic pocket in the NMDA receptor-channel complex determines much higher irreversibility of this adduct compared to the intermediates formed between this site and Mg ions or flexible DBA derivatives, which might explain the absence of PCP-like side effects of the latter compounds.

# INTRODUCTION

It is generally recognized that specific blockade of calcium ion influx via hyper-activated glutamate receptor-channel complexes (GluR), in particular NMDA subtype receptors, can provide efficient protection against diverse group of neurological disorders related to glutamate excitotoxicity, such as brain ischemia and Alzheimer's disease (AD). In the latter, it is considered that NMDA receptor antagonists may provide efficient protection of neurons against neurotoxic action of beta-amyloid peptide (Aβ), realized, in part, by potentiating the excitotoxic effects of endogenous glutamate.[1] On the other hand, it is assumed that glutamate receptor agonists (in particular, AMPA subtype receptor agonists) can exhibit strong cognitive enhancing effects due to activation of glutamatergic neurotransmission that is otherwise reduced in the course of AD.[2] Such dualism in the properties of glutamatergic compounds explains the interest to these substances as promising neuroprotectors and cognition enhancers. Previously it had already been revealed that the well known noncompetitive NMDA receptor antagonist, MK-801, shows strong neuroprotective properties in cell culture experiments. However, the therapeutic potential of MK-801 is diminished by side remarkable psychotomimelic effects associated with its high affinity interaction with the intrachannel binding site (ICS) of the NMDA receptor.[3] In contrast to MK-801, the low affinity open channel blockers, such as amantadine, memantine, or ARL 15896, often show better therapeutic indices because of their rapid blocking kinetics and strong voltage dependency.[4,5] The goal of the study reported here was to provide: (1) focused synthesis of flexible analogs of MK-801, (2) a computational estimate of the binding of MK-801 and its flexible analogs to the NMDA receptor by the molecular docking method, and (3) a study of neuroprotective and behavioral (in particular, cognition-enhancing)

properties of series of novel open chain MK-801 analogs whose side effects were expected to be minimized due to less rigid interaction of ICS with flexible molecules relative to MK-801.

## METHODOLOGY OF DIRECTED SEARCH FOR NEUROPROTECTORS AND COGNITION ENHANCERS

To screen and study the action of potential neuroprotectors and cognition enhancers among wide spectrum of GluR ligands a battery of *in vitro* and *in vivo* tests and models was used in the present study. This set of tests includes:

1. Inhibition of total and specific glutamate-stimulated calcium ion ($Ca^{2+}$) uptake in rat brain synaptosomes;
2. Study of the ability of the compound to prevent the development of NMDA-induced convulsion and lethality in experimental animals – as a measure of anti- NMDA activity.
3. Animal behavioral study of the cognition-enhancing properties for the most promising compounds in an active avoidance test and in a water maze test, after artificial cholinergic neurodegeneration in rat brain induced by a specific synthetic cholinotoxin, ethylcholine aziridinium ion (AF64A).

As a first step the ability of each compound to inhibit glutamate-induced $Kz^{2+}$ uptake (in rat brain synaptosomes) and to manifest anti-NMDA activity was estimated. This permitted us to limit the total number of potentially promising structures and to create a uniform date bases for QSAR analysis and docking. In the second stage of our research, the most promising compounds ("hit compounds") were studied for their neuroprotective and cognition enhancing properties in animal models of AD-type degeneration.

## TOTALLY OPEN CHAIN ANALOGS OF MK-801 STRATEGY FOR TEMPLATE GENERATION AND SYNTHESIS

Disclosure of the MK-801 bicycle leads to the generation of two types of compounds: (1) open chain analogs as a result of breaking one cycle (see FIGURE 1): and (2) totally open chain analogs as a result of breaking two cycles (see FIGURE 2). Open chain analogs include two groups of compounds: the isoquinoline series and the isoindoline series (FIG. 1). The molecular shapes of these molecules are very similar to MK-801, and some of the compounds display properties of high affinity open channel blockers and associated side effects, such as isoquinoline FR-115427.

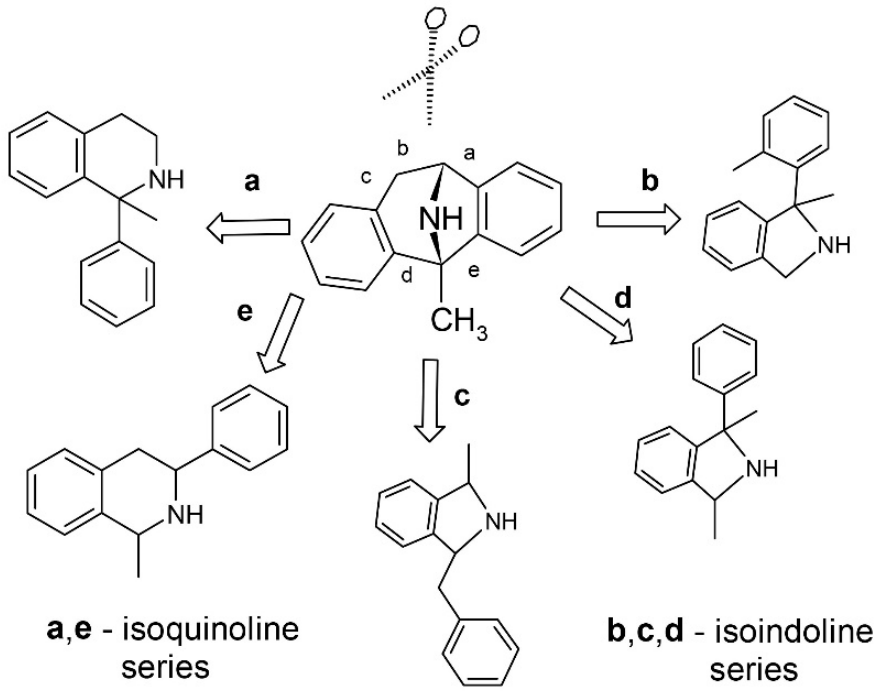


FIGURE 1. Template generation for isoquinoline and isoindoline series.

Four templates result from the further opening of isoquinoline and/or isoindoline cycles to form totally open chain types of MK-801 analogs: monobenzylamine. benzhydryl amine, phenethylamine, and dibenzylamine series (FIG. 2).

These compounds are very similar, but essentially more flexible molecules, relative to MK-801. Focusing libraries contained 100200 substances were synthesized in each series, forming a total of about 600 compounds. The functional variation[7] in each series included changes "around" the template (introduction of substituents to aryl, and/or alkyl, and/or nitrogen, and bioisosteric substitution of aryls in the template) but not involving a change of template (e.g., transformation of the template into novel cycles).

# MOLECULAR DOCKING

## Homology Modeling

Amino acid sequences of human GLUR1 (Swiss Protein Data Bank accession number P42261), GLUR2 (P42262), GLUR3 (P42263), GLUR4 (P48058), GLUR5 (P39086), GLUR6 (Q13002), GLUR7 (Q13003), KA1 (Q16099), KA2 (Q16478), NR2A (Q12879), NR2B (Q13224), NR2C (Q14957). NR2D (O15399), and NR1 (P35437) subunits were multiply aligned with the amino acid sequence of the $K^+$ channel from *Streptomyces lividans*[8] (KcsA $K^+$ channel, Brookhaven Protein Data Bank[9] accession number 1BL8) using the program Clustal X.[10-12] The BLOSUM 30 homology matrix was used to evaluate amino acid similarity. This sequence alignment was used as the basis for homology modeling using the Biopolymer module in SYBYL 6.5.[13]

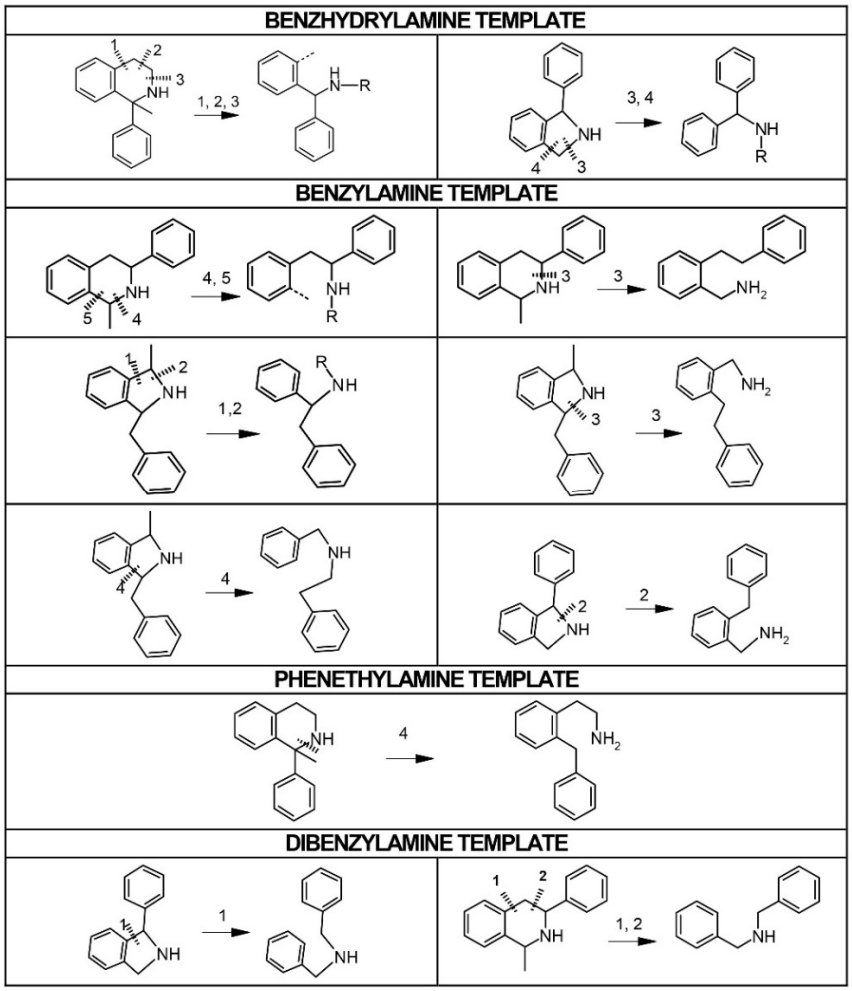


FIGURE 2. Opening of isoquinoline and/or isoindoline cycles leads to the generation of total open-chain templates (benzhydrylamines, benzylamines, and dibenzylamines.

The X-ray structure of the KcsA $K^+$ channel was used as a template for building a NR1/NR2B/NR1/NR2B tetramer of the NMDA receptor. Chains A and K from the $K^+$ channel were "mutated" to NR2B subunits, whereas chains < and D were mutated to NR1 subunits in accord with the following procedure. All aligned non-identical amino acids were mutated to each other by changing their side chains while keeping main chain atoms unchanged and fixed at their original positions in space. Internal torsion angle values in side chains of new amino acids were chosen to be those most appropriate for a given amino acid in a given secondary structure state (which remains unchanged by mutating residues). All insertions and deletions were handled by defining "loops" containing all residues being inserted and several neighboring atoms to the positions of insertion or deletion were followed by searching for them in the Brookhaven Protein Data Bank. Subsequently, that search results were visually inspected, and main chain atoms of those *loops* for which (1) the geometry of the main chain atoms neighboring the deletion or insertion positions underwent smaller changes,

(2) the amino acid sequence possessed the strongest homology to the required sequence, and (3) no unfavorable spatial hindrance between atoms belonging to the *loop* and to the remaining part of the protein could be expected, were inserted in the protein model and followed by adding appropriate side chains in accord with the aforementioned procedure. Next, all proline residues and side chains of all other residues were "fixed" by finding new values for several torsion angles so as to remove the spatial overlap between atoms. This was followed by adding hydrogen atoms that were capable of forming hydrogen bonds. The protein was then subjected to 5,000 steps of constrained energy minimization, with all main chain atoms fixed in space using the Tripos force field, as implemented in the SYBYL package. This was followed by 5,000 steps of constrained minimization without fixing the main chain atoms, but keeping the mutual spatial arrangement of several oxygen atoms at the narrowest part of the pore unchanged so as to preserve the requirements for effective ion conduction.

## Docking Ligands

All ligands were manually docked lo the putative binding silo followed by 500 steps of energy minimization for the entire protein-ligand complex. Interactive docking was carried out by means of the Sybyl 6.5 molecular-modeling package running on a SGI Octane workstation.

## Sequence Alignment

In order to avoid chance effects and increase validity of the alignment used for predicting the three-dimensional structure of the NMDA receptor channel, we included all members if the ionotropic glutamate receptor family subunits into multiple alignment of amino acid residues, along with the amino acid sequence of the $K_+$-channel. Since all sequences have different numbering for the residues, we introduced a uniform numbering for them, the rows are labeled in the multiple alignment diagram with the abbreviation C.N. The mere existence of such multiple alignment implies that the general architecture of channel pores in subunits of all ionotropic receptors can actually be expected to be the same. Thus, the part in each sequence that is generally associated with transmembrane segment Ml corresponds to C.N. 3-21, the segment M2 has C.N. 51-71, and the amino acids in transmembrane segment M3 have C.N. 82-100. Four "fingerprint" amino acid residues (that correspond to the ion selectivity filter of the KcsA $K_+$ channel) in the nearest part of the channel pore have C.N. 67-70. The most important among them is generally believed to be the amino acid with C.N. 67 (Q/R/N site). For the case of AMPA receptors this residue can undergo RNA editing,[14] which controls the $Ca^{2+}$ permeability of these receptors. In the NMDA receptor, this amino acid in a NR2 subunit (Asn614 in NR2A, Asn615 in NR2B, Asn612 in NR2C, and Asn642 in NR2D) has been shown to take part in the voltage-dependent $Mg^{2+}$ blockage

of the receptor channel.[15] Homological residue Asn616 in NR1 has been shown to control the $Ca^{2+}$ permeability[15] of the NMDA receptor channel, as well as being involved in the voltage-dependent blockage by compounds believed to bind to the PCP blocking site in the receptor pore.[16] This residue, along with Trp611 and Ala645 in the NR1 subunit are supposed to form the PCP binding site.[16]

## Architecture of the NMDA Receptor Channel

A three-dimensional model of the NMDA receptor channel, built in accordance with the procedure considered above, is depicted in FIGURE 3. The receptor channel in this model is a heterotetramer with two-fold symmetry about a central pore. Each of its subunits consists of two transmembrane a-helices, segments M1 and M3, connected by a pore region, segment M2, that consists of a turret, pore helix, and selectivity filter. Four subunits are arranged in the heterotetramer such that one transmembrane helix (segment M3) faces the central pore and the other (segment M1) faces the lipid membrane. The transmembrane helices M3 are tilted with respect to the membrane, so that the subunits open like the petals of a flower. The M3 helices are attached to the pore region near the intracellular surface of the membrane. This region contains the selectivity filter of the channel.

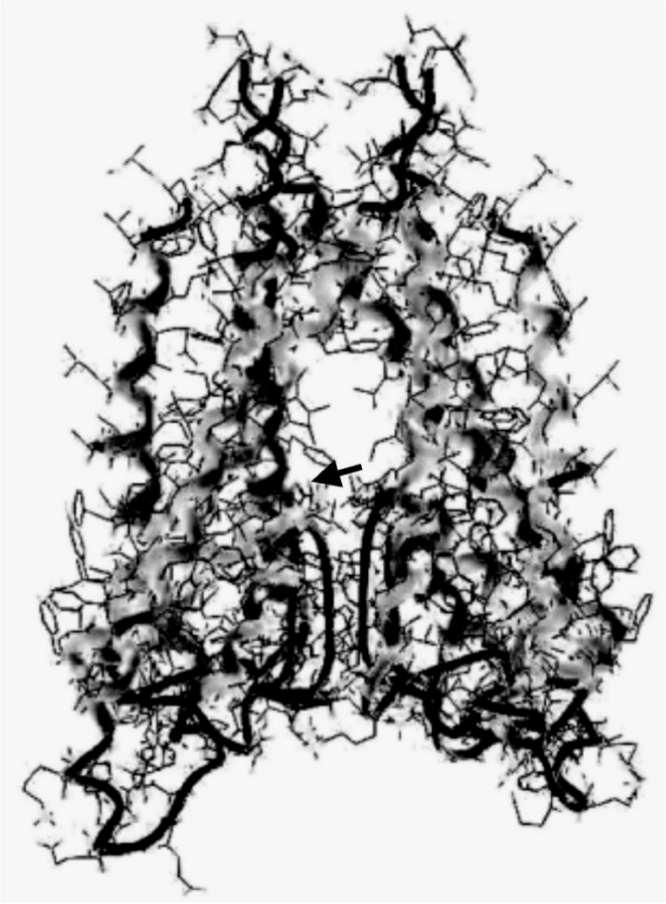

FIGURE 3. General view of the NMDA receptor channel modeled by homology (thr arrow indicates the approximate location of MK-801-binding site).

The selectivity filter is formed by four amino acids with C.N. 67-70. Sixteen main chain carbonyl oxygen atoms of these residues face the pore and take part in stabilizing dehydrated cations moving through it. In addition to the main chain atoms, the oxygen atoms of the asparagine side chains (C.N. 67) located near the entrance to the narrow pore formed by the selectivity filter amino acids may play an important role in dehydrating and stabilizing metal cations (since it controls the $Mg^{2+}$ blockage for the case of a NR2 subunit of the NMDA receptor and $Ca^{2+}$ permeability for the cases of the AMPA and the NR1 subunit of the NMDA receptor).

Two important features of the cavity inside the channel should be considered in connection with their possible pharmacological implications. First, the walls of the pore are formed by hydrophobic amino acids. And second, there is a narrow hydrophobic pocket between segments M2 and M3 just above the selectivity filter. The shape of this pocket is nearly complementary to the shape of the most potent phencyclidine binding site ligands, such as PCP and MK-801, and in the vicinity of this pocket there is the important Asn616 residue that controls the $Ca^{2+}$ permeability of the channel. The space location of this amino acid permits easy formation of a strong hydrogen bond with PCP, MK-801, and their analogs. Thus, all important features of the phencyclidine binding site pharmacophore, two hydrophobic areas (one formed by the pocket and one by the surface of the M3 helix facing the central part of the pore) arranged nearly perpendicularly to each other and the hydrogen bond acceptor part located near the corner of this triangle, are present here. We suggest that this part of the channel contains the phencyclidine binding site.

# MATERIALS AND METHODS

## Estimation of Calcium-Blocking Activity

Interaction between compounds and glutamate-dependent $Ca^{2+}$ uptake system was studied on newborn (8-11 days old) rat brain synaptosomal $P_2$-fraction. Specific $Ca^{2+}$ uptake was measured in the presence of the compound tested as a variation between $_{45}Ca^{2+}$ content in glutamate stimulated synaptosomes and $^{45}Ca^{2+}$ content in unstimulated synaptosomes according to the equation:

$$D = [(Ca4 – Ca3)/(Ca2 – Cal)] \times 100\%$$

Where Cal is the $Ca^{2+}$ influx in a blank experiment (without glutamate and tested compounds); Ca2 is the $Ca^{2+}$ influx in the presence of glutamate only (glutamate-induced $Ca^{2+}$ influx); Ca3 is the $Ca^{2+}$ influx in the presence of tested compound (without glutamate); Ca4 is the $Ca^{2+}$ influx in the presence of both glutamate and the tested compound.

## Estimation of Anti-NMDA Activity

Adult non-pedigree male mice weighing 20-24 g were used. The compounds tested were administered i.p. 30 min prior to administration of NMDA. NMDA was i.c.v. injected in doses of 0.1 μg in 1.0 μl of distilled water (pH = 7.0); this induced clonic seizures in 100% of mice. The anti-NMDA activity was determined as a dose of the compound under i.p. administration needed to prevent NMDA-induced seizures in 50% of mice. $ED_{50}$ values were calculated from the linear portions of sigmoidal curves. The $\chi$-test was used to compare $ED_{50}$ values for different treatments.

## Animal Model of AD Type Dementia

Neuronal atrophy related to the loss of cholinergic markers in some areas of human brain is known to be the most typical pathological feature of AD.[17] It was shown previously that i.c.v. injection of AF64A leads to degeneration of cholinergic neurons in the brain of experimental animals and reproduces some specific features of chronic cholinergic hypofunction, along with learning and memory impairments analogous to those observed in AD.[18-19] In our research we used a cholinotoxin-induced animal model of AD type neurodegeneration to study cognitionenhancing properties of the compounds in a Morris water maze test and in an active avoidance test.

## Experimental Design

*Compound Injections*

The experiments were performed on male Wistar rats (200-230 g weight). AF64A was prepared from commercial samples of AF64 (RBI) according to a method described elsewhere[20] and diluted with artificial cerebrospinal fluid (CSF). Before the surgery, rats were anesthetized with ether. Freshly prepared AF64A solution in a dose of 3 nmol/3 μl was injected into each of lateral cerebral ventricles of experimental rats. Control rats received 3 μl CSF. One day after the surgery AF64A injected rats received orally 2 mg/kg of Aricept (Pfizer, USA) or Memantine (RBI, Memantine HC1) or NT1505 as a suspension in 1% starch. The compounds were injected over a period of 23 days. Ten days after the first injections, animal training in the pool was started. During the training the compounds were injected 1-1.5 hours after the daily learning trials (to study their effect on long-term memory).

*Morris Water Maze Test*

Experiments were performed in a circular black swimming pool 180 cm in diameter. The surface of a removable platform (10 cm) was located 2-3 cm below the water level, so that the platform was invisible to the swimming rat. All experiments were detected by means of a video camera connected with a computer and S-VHS recorder.

The training procedures aimed at finding the hidden platform were started 10 days after the first injections, with all animals receiving two escape trials a day from two different positions. On the day 11, the daily training was interrupted and a retention test was performed only on days 14 and 26. On days 5, 11, 14, and 26 after commencing the training, the movements of the rats during the test were recorded and then analyzed with the original computerized system "Behavioral Vision".[21,22] Four parameters were analyzed: *escape latency* (the time in seconds required for the rat to find the hidden platform), *depression index* (characterizing immobility of rats in the pool and calculated as a ratio between time that the rat spent with a speed less than a threshold value to the time of swimming with the higher speed; the threshold was set experimentally at 10 cm/s), *straightness index* (characterizing the track directionality and calculated as a ratio between trajectory length and distance from the track start to the platform center, i.e., deviation of the trajectory from the straight path-vector from start position to platform), and *strategy index* (calculated as trajectory length within the non-entering zone, as a percentage of the full trajectory of animal during the trial).

*Statistical Analysis*

The results were analyzed by ANOVA followed by post hoc LSD comparisons using program package STATISTICA ver. 5.0. The level of significance was preset at $p < 0.05$. Data are presented as mean ± S.E.M.

*Active Avoidance Test*

The test procedure is described elsewhere.[23] Briefly it is as the follows: two weeks after the injection of AF64A or CSF, active avoidance training was conducted in a two-chamber shuttle box. Each chamber was 30 cm long and 20 cm wide, with a guillotine door (7x7 cm) between them, and a grid floor of steel rods 1 cm apart. A 12-W light bulb was fixed in the ceiling on each side. Before training, the animals were given a five-minute familiarization period in the darkened shuttle box with the central door open. The conditioned stimulus was a five-second light followed by the unconditioned stimulus, a 1 mA shock was delivered to the grid in the lit chamber. During the presentation of both stimuli, the door was open. After the rat either escaped or avoided the shock by crossing through to the other chamber, the door closed and a new trial sequence began. The intertrial interval was 30-60 sec. The time taken to escape or to avoid the shock (response latency) was measured. The avoidance during the conditioned stimulus (5 sec) was considered a conditioned avoidance response (CAR). Training procedure consisted of 35 trials. Data from the last 15 trials (learning test) were collected and analyzed in five-trial blocks, as percentage of CAR summarized over each block. From this was calculated the mean percentage of CAR in three blocks. Twenty-five further trials were given 24 h later (retention test). In this case, data were analyzed as the mean percentage of CAR in first two blocks of five trials. Statistical

significance was tested using an unpaired Student's /-test. $p < 0.05$ was taken as indicative of statistical significance.

## RESULTS AND DISCUSSION

The results obtained at the first stage of investigation revealed the group of compounds that manifested strong anti-NMDA and calcium-blocking activity. Examples of anti-calcium and anti-NMDA activities are presented in TABLE 1. The most interesting and promising results have been obtained in a series of newly synthesized monobenzylamine and dibenzylamine derivatives.

TABLE 1. Calcium-blocking property ($IC_{50}$) and anti-NMDA activity ($ED_{50}$) of several totally open chain analogs of MK-801 in the monobenzylamine and dibenzylamine series.

| Structure | $IC_{50}$ (μM) | $ED_{50}$ (mg/kg) | Structure | $IC_{50}$ (μM) | $ED_{50}$ (mg/kg) |
|---|---|---|---|---|---|
| **NT-1505** | **15** | **10** | LS-4206 | **11** | **30** |
| **NT-3101** | **6** | **16** | **NT-5001** | **18** | **35** |
| 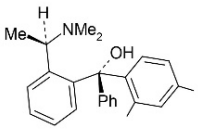 | **16** | **100** | 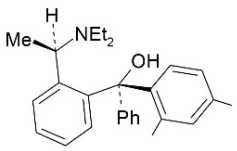 | **11** | **65** |
| 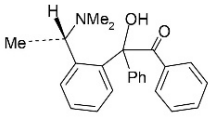 | **100** | **>100** | 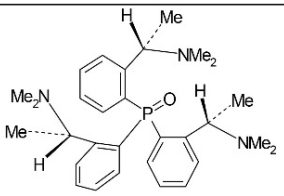 | **100** | **55** |
| 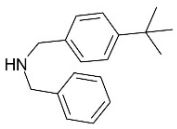 | **20** | **25** | 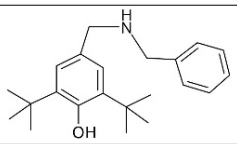 | **100** | **62** |
| 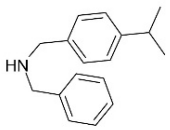 | **31** | **52** | 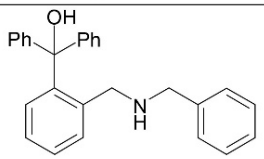 | **100** | **70** |
| 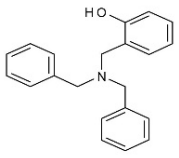 | **56** | **10** | 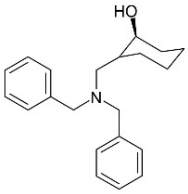 | **107** | **43** |

Structure-activity analysis in these series of compounds revealed that their biological effects depend appreciably on the substituents in the benzene rings. The introduction of a bulky *ortho*-group into the each benzene rings leads to the increase of inhibition effect. The bioisosteric substitution of the benzene ring on the heteroaryl

moiety (furyl, pyridyl, etc.) leads mainly to the appreciable stimulation of uptake. The hit compound in both series (NT-1505 and NT-3101) demonstrated a strong calcium-blocking property ($IC_{50}$ = 15.0 and 6.0 μF, respectively) and anti-NMDA activity ($ED_{50}$ = 10 and 16 mg/kg).

According to these results the most promising group of compounds, in particular, compound NT-1505, were selected for an expanded biobehavioral study. In parallel, the comparative docking study of NT-1505 and MK-801 binding with the NMDA receptor was performed.

## Binding of Ligands to the Channel

The three-dimensional structure of the complex between MK-801 and the putative PCP-binding site of the NMDA receptor is depicted in FIGURE 4. MK-801 forms two hydrogen bonds with the receptor, one with Asn616, and the other with the main chain carbonyl oxygen atom belonging to Leu615.

In addition, MK-801 binds with one of its benzene rings deeply into the hydrophobic narrow pocket and the other sticks to the hydrophobic M3 helix. The side-chain amide group of Asn 616 also forms two hydrogen bonds: one between its oxygen atom and protonated nitrogen of MK-801, and one between its amide nitrogen and the oxygen atoms belonging to the main chain of the same residue. As a result, the oxygen atom belonging to the side chain of Asn616 and the oxygen atom belonging to its main chain can no further stabilize cations inside the narrow pore formed by the selectivity filter amino acids.

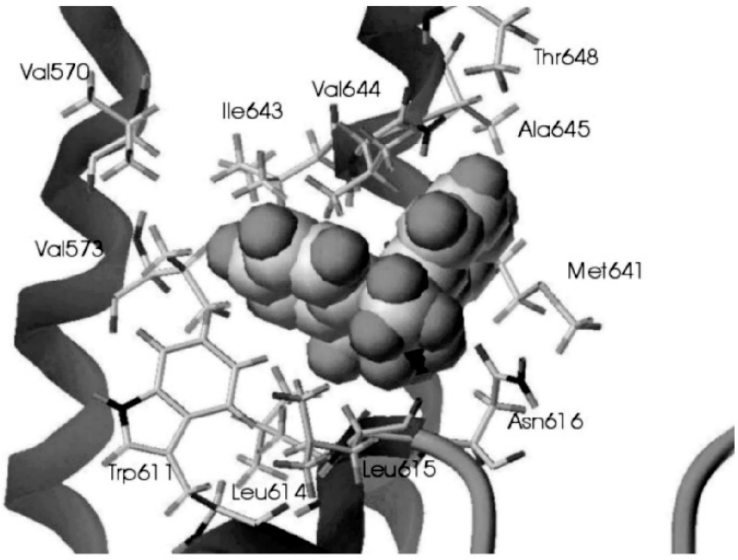


FIGURE 4. Predicted binding mode of MK-801 to the putative phencyclidine site inside the NMDA receptor channel.

The flexible MK-801 analog NT-1505 was docked to the putative PCP binding site in a conformation that mimics the spatial structure of MK-801, NT-1505 appeared to be able to bind to the same hydrophobic pocket as MK-801 in the same mode (see

FIGURE *5)*. However, it binds to the receptor with only one hydrogen bond, the opposite site is more exposed to the channel pore, and the binding involves freezing of torsion degrees of freedom. Thus, one can suppose more favorable condition for dissociation of NT-1505 upon channel closure.

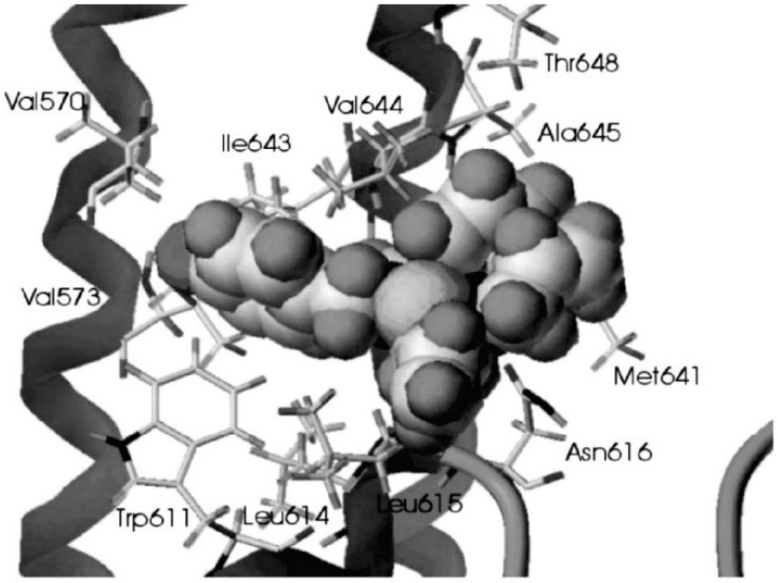


FIGURE 5. Predicted binding mode of NT-1505 to the putative phencyclidine site inside the NMDA receptor channel.

## Behavioral Properties of NT-1505

A preliminary examination of the cognition-enhancing properties of each compound and its ability to improve learning and memory from a toxin-induced animal model of dementia, studied in the active avoidance test. The results presented in FIGURE 6 indicate that rats treated with cholinotoxin AF64A demonstrate significant reduction in learning ability and pronounced memory impairment when compared to the vehicle group of animals treated with CSF (approximately 50% from the control level of CAR). Oral administration of NT1505 causes the recovery of the cognitive functions that deteriorate after the injection of neurotoxin AF64A, both in the learning test (the learning trials follow training on the same day) and in the retention test (the trials were performed the day after the training set). The compound produced statistically significant memory-enhancing effects at all doses, in the interval 0.5 to 5.0 mg/kg (orally) that lasted for at least 10 days after the learning trial.

A comparative long-term study of cognition enhancing properties of compound NT-1505 and widely used anti-Alzheimer medicines, Aricept and Memantine, was performed in a variant of the Morris water maze test in rats treated with toxin AF64A.

The superposition of swimming trajectories (start position 1) of alt groups ot rats in search of the hidden platform in the Moms water pool is presented in FIGURE 7 The

results of computer estimated indices of escape latency and track directionality (straightness index) are presented in FIGURE 8.

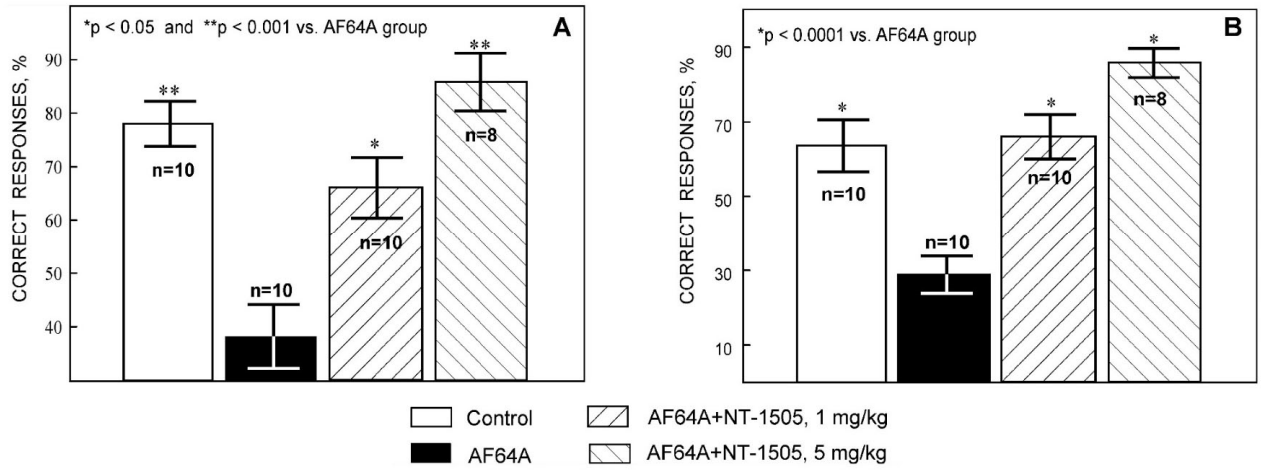


FIGURE 6. Cognition-enhancing effect of NT 1505 (n is the number of animals). A. Learning test. B. Retention test (the day after the learning trials).

Despite rather large mean escape latency observed on day 5 of the training. Aricept significantly ($p = 0.048$) decreased the time and improved the trajectory in the search of the platform, Memantine demonstrated a tendency to decrease the search time in comparison with AF64A-treated rats.

On day 11 of training, the difference between control and AF64A-injected groups in the escape latency was almost statistically significant ($p = 0.077$). The AF64A treated rats receiving Aricept and NT-1505 escaped to the platform in almost the same time and this was significantly different from the AF64A group. Two-day interruption of the training with continued injections of the compounds led to a small increase in the search time for all the rats; however, for the rats receiving Aricept, this was significantly ($p = 0.035$) less than that of AF64A-injected group.

The best values of the straightness index on day 14 was obtained for Aricept and Memantine. The rats receiving Memantine and NT-1505 had rather good values for the strategy index on day 14 (data not shown).

An eleven day break (day 26) in the training procedure after completing the compound injections led to a considerable deterioration in the spatial orientation of rats receiving Aricept, and a slight decrease for the other groups, except for NT-1505-injected rats for which the ability to find the platform remained almost the same as on day 14. The most statistically significant differences among the groups, relative to AF64A-injected rats, were obtained for the straightness index.

The depression was slightly pronounced during all experiments. However, on day 26, some rats receiving Memantine and control rats swam reluctantly, demonstrating stress or less motivation (data not shown) that could led to an increase in the escape latency.

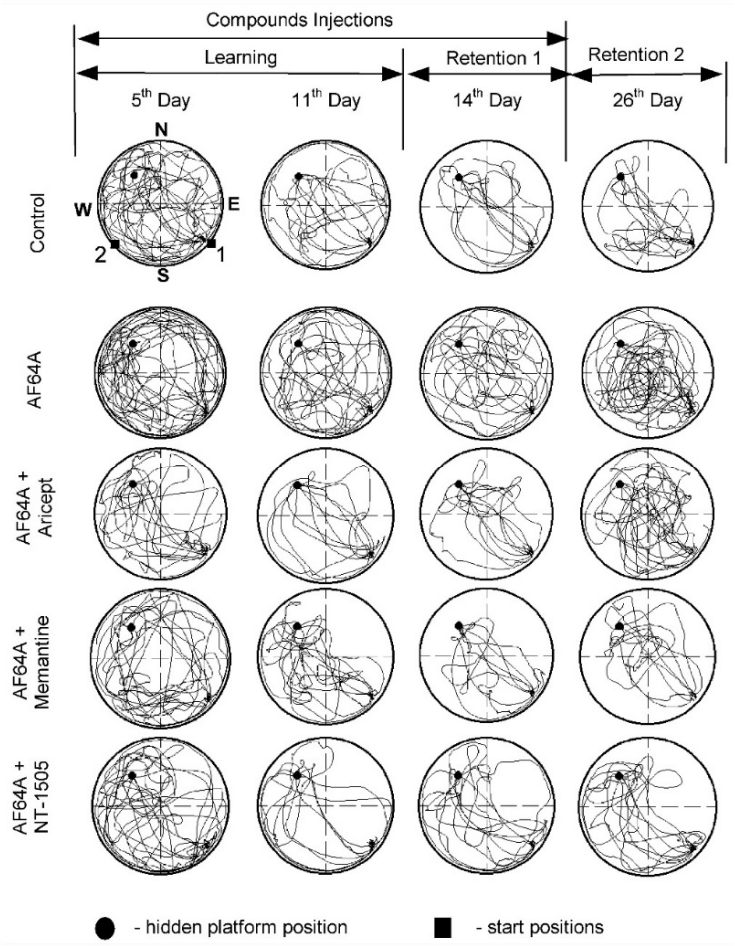


FIGURE 7. Swimming trajectories of rats receiving different compounds.

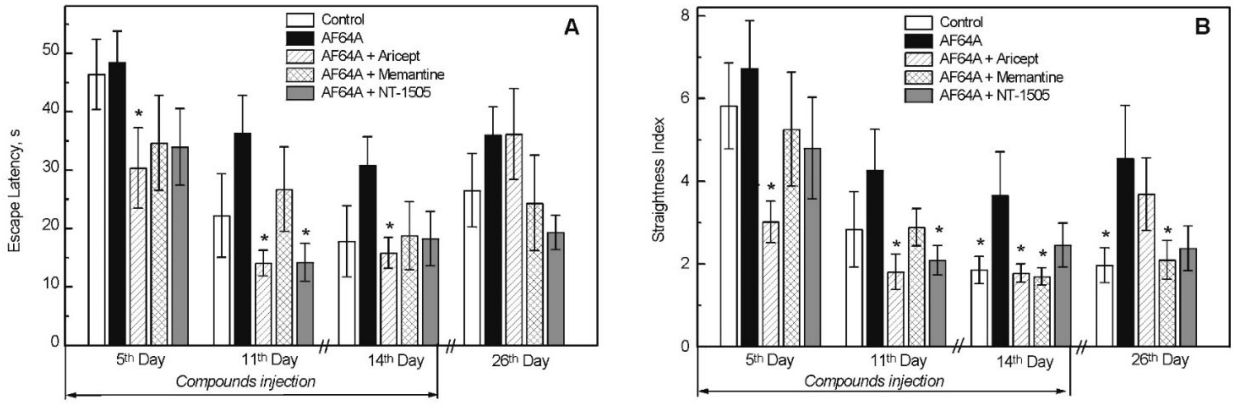


FIGURE 8. Escape latency (A) and track directionality relative to platform position (B). Start position 1. Control, $n = 10$; AF64A, $n = 10$; AF64A+Aricept, $n = 10$; AF64A+Memantine, $n = 8$ (days 5 and 26), $n = 9$ (days 11 and 14); $n$ is the number of animals; $*p < 0.05$ , versus AF64A group (ANOVA followed by post hoc comparisons).

Summarizing the results obtained at this stage, it was noted that Aricept, Memantine, and NT-1505 demonstrated statistically significant improvement in the learning ability of the experimental animals so that it became equal to the results for the control group, or even exceeded it. A significant imperfection of Aricept is its symptomatic

effect, namely, cancellation of injections (results obtained on day 26) leads to a decrease in the cognitive functions of rats down to the level of the untreated group. Memantine and NT-1505 demonstrated a prolonged effect, observed after completing their injections, that allowed us to suppose that they influence regenerative and/or compensatory processes in brain. All the above data permit us to conclude that NT-1505 improves learning of rats with partial chronic deprivation of cholinergic functions in the task of finding a hidden platform, and demonstrates a long-term effect on their retention ability after finishing training and injection of the compound. The efficiency of its influence on spatial learning in the chronic experiment is almost the same as for Aricept. However, NT-1505 causes a more prolonged effect on memory functions than Aricept, which let us assume its effect on regenerative and/or compensatory processes in brain.

To reveal possible similarities and differences between NT-1505 and MK-801, a comparative study of the effects of the compounds at various doses on locomotor activity of rats was performed. It was found that MK-801 in doses of 0.1 mg/kg and higher produces a significant psychogenic effect in animals manifesting in stereotypic behavior, ataxia, and hyperactivity (see TABLE 2).

TABL.E. 2. Side effects of MK-801 and NT-1505

| **MK-801** | | | | **NT-1505** | | | |
|---|---|---|---|---|---|---|---|
| **$ED_{50}$ (Anti-NMDA) = 0.2 mg/kg** | | | | **$ED_{50}$ (Anti-NMDA) = 10 mg/kg** | | | |
| **Dose, mg/kg** | **Stereotypic Movement** | **Ataxy** | **Activity** | **Dose, mg/kg** | **Stereotypic Movement** | **Ataxy** | **Activity** |
| **0.1** | **NO** | **NO** | ↑ | **0.5** | **NO** | **NO** | **NO** |
| **0.2** | ↑ | ↑ | ↑↑ | **1** | **NO** | **NO** | **NO** |
| **0.4** | ↑ | ↑↑ | ↑↑↑ | **5** | **NO** | **NO** | **NO** |
| **0.8** | ↑↑↑ | ↑↑↑ | ↑↑↑ | **10** | **NO** | **NO** | **NO** |
| **1.0** | ↑↑↑↑ | ↑↑↑↑ | ↑↑↑↑ | **50** | **NO** | **NO** | ↓ |

In contrast to MK-801, agent NT-1505 did not potentiate stereotypy, ataxia, or behavioral activity; that is, it did not exhibit any side effects typical of MK-801. It is important to note that the absence of MK-801-like side effects is observed over wide interval of doses, from 0.5 to 50 mg/kg, which completely covers the interval of its neurological activity (according to previously published results, NT-1505 shows anti-NMDA activity in doses 10-50 mg/kg and exhibits cognition-enhancing properties at doses of 0.5-5 mg/kg). The results obtained permit us to conclude that NT-1505 possesses strong cognition-enhancing properties, manifested in a toxin-induced animal model of AD- type degeneration and characterized by a spectrum of behavioral activity radically different from that of MK-801. In particular, it does not produce any psychotomimetic side effects over the therapeutically significant dose interval.

## REFERENCES


1. Mattson, M.P., B. Cheng, D. Davis, *et al*. 1992. β-Amyloid peptodes destabilize calcium homeostasis and render human cortical neurons vulnerable to excitotoxicity. J. Neurosci. **12**: 376-389.
2. Greenamyre, J.T., J.B. Penney, C.J. D'Amato, & A.B. Young. 1987. Dementia of the Alzheimer's type: changes in hippocampal L-[$^3$H]glutamate binding. J. Neurochem. **48**: 543-551.
3. Vanderschuren, L.J.M.J., A.N.M. Schoffelmeer, A.H. Mulder, & T.J. De Vries. 1998. Trend Dizocilpine (MK801): Pharm. Sci. **19**: 79-81
4. Blanpied, T.A., F.A. Boeckman, E. Aizenman, & J.W. Johnson. 1997. Trapping channel block of NMDA-activated responses by amantadine and memantine. J Neurophysiol. **77**: 309-323
5. Palmer, G.C., J.A. Miller, E.F. Cregan, P. Gendron, & J. Peeling. 1997. Low- affinity NMDA receptor antagonists. The neuroprotective potential of ARL 15896AR. Ann. N.Y. Acad. Sci. **825**: 220-31.
6. Parsons, C., W. Danysz, & G. Quack. 1998. Glutamate in CNS disorders as a target for drug development. Drug News Perspect. **11**: 523-579.
7. Katritzky, A., J. Kiely, N. Hebert, & C. Chassaing. 2000. Definition of Templates within Combinatorial Libraries. J. Comb. Chem. **2**: 2-5.
8. Doyle, D., J. Cabral, R. Pfuetzner, A. Kuo, J. Gulbis, S. Cohen, B. Chait, & R. MacKinnon. 1998. The Structure of the Potassium Channel: Molecular Basis of K+ Conduction and Selectivity. Science. **280**: 69-77.
9. Abola, E., F. Bernstein, S. Bryant, T. Koetzle, & J. Weng. 1987. Protein data bank. In Crystallographic Databases - Information Content, Software Systems, Scientific Applications. F. H. Allen, G. Bergerhoff, & R. Sievers, Eds: 107-132. Data Commission of the International Union of Crystallography, Bonn, Cambridge, Chester.
10. Higgins, D., & P. Sharp. 1989. Fast and sensitive multiple sequence alignments on a microcomputer. CABIOS. **5**: 151-153.
11. Higgins, D., A. Bleasby, & R. Fuchs. 1991. CLUSTAL V: improved softwarefor multiple sequence alignment. CABIOS. **8**: 189-191.
12. Thompson, J.D., D.G. Higgins, & T.J. Gibson. 1994. CLUSTAL W: improving the sensitivity of progressive multiple sequence alignment through sequence weighting, positions-specific gap penalties and weight matrix choice. Nucleic Acids Research. **22**: 4673-4680.
13. Sybyl 6.5; Tripos Assoc.: St. Louis, MO.
14. Sommer, B., M. Koehler, R. Sprengel, & P.H. Seeburg. 1991. RNA editing in brain controls a determinant of ion flow in glutamate-gated channels. Cell. **67**: 11-19.
15. Burnashev, N., R. Schoepfer, H. Monyer, J.P. Ruppersberg, W. Guenther, P.H. Seeburg, & B. Sakmann. 1992. Control by asparagine residues of calcium permeability and magnesium blockage in the NMDA receptor. Science. **257**: 1415-1419.
16. Ferrer-Montiel A.V., W. Sun, & M. Montal. 1995. Molecular design of the *N*- methyl-D-aspartate binding site for phencyclidine and dizolcipine. Proc. Natl. Acad. Sci. USA. **92**: 8021-8025.
17. Mesulam, M.M. 1996. The system level organization of cholinergic innervation in the human cerebral cortex and its alterations in Alzheimer's disease. Progress in Brain Res. **109**: 285-297.
18. Hanin, I. 1996. The AF64A model of cholinergic hypofunction: an update. Life

Sciences. **58**: 1955-1964.

19. Walsh, T., & K. Opello. 1994. The use of AF64A to model Alzheimer disease. In: Toxin-Induced Models of Neurological Disorders: 259-337. Plenum Press. N.Y., London
20. Fisher, A., C. Manti one, D. Abraham, & I. Hanin. 1982. Long-term central cholinergic hypofunction induced in mice by ethylcholine aziridinium ion (AF64F) in vivo. J. Pharm. Exp. Ther. **22**: 140-145.
21. Mukhina, T.V., N.N. Lermontova, & S.O. Bachurin. 2000. Automated system for tracking and behavioral analysis. Presented at the 3rd International Conference on Methods and Techniques in Behavioral Research "Measuring Behavior 2000". Nijmegen, The Netherlands, 15-18 August.
22. Mukhina, T.V. & S.O. Bachurin. 2000. Software-hardware complex behavioral vision ("BVision"). Russian certificate for registration of the software for PC. No. 2000610678. Date of registration, July 25, 2000.
23. Lermontova, N., N. Lukoyanov, T. Serkova, *et al*. 1998. Effect of Tacrine on Deficits in Acute Avoidance Performance Induced by AF64A in Rats. Molec. Chem. Neuropathol. **33**: 51-61.

*ДОКЛАДЫ АКАДЕМИИ НАУК, 2017, том 473, № 5, с. 608- 612*

*БИОХИМИЯ, БИОФИЗИКА, МОЛЕКУЛЯРНАЯ БИОЛОГИЯ*

УДК 544.165

# МОЛЕКУЛЯРНЫЙ ДИЗАЙН ПРОНЕЙРОГЕННЫХ И НЕЙРОПРОТЕКТОРНЫХ СОЕДИНЕНИЙ – АЛЛОСТЕРИЧЕСКИХ МОДУЛЯТОРОВ РЕЦЕПТОРА NMDA

**Д.С. Карлов, Е.В. Радченко, В.А. Палюлин, академик РАН Н.С. Зефиров**

Рецептор *N*-метил-D-аспарагиновой кислоты (NMDA) представляет собой перспективную мишень для лечения нейродегенеративных заболеваний и других повреждений мозга, а также для создания пронейрогенных соединений, способных стимулировать нейрогенез во взрослом мозге. Нами проанализирована структура сайта связывания отрицательных аллостерических модуляторов в аминоконцевом домене NMDA-рецептора и определены возможные способы их связывания, выполнен молекулярный дизайн новых модуляторов, существенно отличающихся от известных по структуре и способу связывания, а также сформирована фокусированная библиотека химических соединений с потенциальными нейропротекторными и пронейрогенными свойствами, желательным набором фармакокинетических свойств и низкой токсичностью, которые могут стать основой для разработки лекарств нового поколения.

Ионотропный глутаматный рецептор N-метил-D-аспарагиновой кислоты (NMDA) представляет собой лиганд-зависимый катионный канал, активируемый в организме глутаминовой кислотой и глицином [1]. Он участвует во многих важных нейрофизиологических процессах в центральной нервной системе, связанных с передачей быстрого синаптического возбуждения, формированием памяти и др. Антагонисты, обратимые блокаторы канала и отрицательные модуляторы этого рецептора обладают нейропротекторными свойствами благодаря снижению потока кальция в клетку и подавлению эксайтотоксического действия глутамата, что делает NMDA-рецептор перспективной мишенью для лечения нейродегенеративных заболеваний (прежде всего болезней Альцгеймера и Паркинсона), нейропатической боли, последствий ишемии, инсульта, травм мозга и других состояний [2, 3]. Кроме того, NMDA-рецептор играет важную роль в регуляции процессов нейрогенеза (главным образом на этапах пролиферации нервных стволовых клеток, миграции незрелых нейронов и их выживания) и является одной из мишеней для создания пронейрогенных соединений, способных стимулировать нейрогенез во взрослом мозге [4, 5].

Необходимо отметить, что избыточная активация или блокада ионного тока NMDA-рецептора приводят к нежелательным побочным эффектам [2], поэтому наибольший интерес для поиска потенциальных лекарственных веществ с мягким селективным действием представляют его аллостерические модуляторы, прежде всего отрицательные модуляторы, связывающиеся с аминоконцевыми доменами рецептора. Примером таких лигандов является ифенпродил (**1**) и его структурные аналоги. Ранее мы детально проанализировали его взаимодействие с рецептором и возможный механизм действия аллостерических модуляторов, структуру сайта связывания и факторы, определяющие их активность, а также разработали подходы к направленному поиску и дизайну новых активных соединений [6, 7].

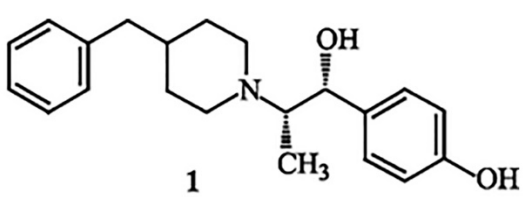


**1**

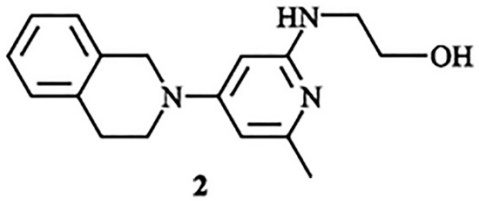


**2**

В то же время ифенпродил и родственные лиганды оказались непригодными для клинического применения из-за неприемлемых побочных эффектов, прежде всего кардиотоксичности, обусловленной действием на калиевые каналы hERG в сердечной мышце. Отказ от заряженного атома азота и/или вытянутой структуры лиганда ведет к снижению аффинности к hERG [8], поэтому большое значение имеет разработка новых структурных типов отрицательных аллостерических модуляторов NMDA-рецептора.

С учетом этого целью настоящей работы явился детальный анализ структуры сайта связывания отрицательных аллостерических модуляторов в аминоконцевом домене NMDA-рецептора, определение возможных способов их связывания и молекулярный дизайн новых классов потенциальных модуляторов с желательным набором фармакокинетических свойств и низкой токсичностью.

Моделирование молекулярной динамики аминоконцевых доменов NMDA-рецептора (подтип GluNl/GluN2B) в комплексе с ифенпродилом и без него [6] показывает, что сайт связывания модуляторов не является жестким и способен подстраиваться под изменение структуры лигандов, причем молекула ифенпродила не заполняет некоторые доступные его области. Это подтверждается результатами проведенного нами молекулярного докинга большой серии известных отрицательных модуляторов NMDA-рецептора, относящихся к разным структурным типам. Недавно опубликованные структуры комплексов аминоконцевых доменов GluNl/GluN2B с отрицательными модуляторами [9] также демонстрируют существование альтернативного способа связывания лигандов в сайте связывания ифенпродила.

Эта особенность строения сайта связывания позволяет выполнить виртуальный скрининг потенциальных лигандов, отличающихся от ифенпродила по структуре и способу связывания. Модель сайта связывания отрицательных модуляторов строили с помощью программы OpenEye Make Receptor 3.2.0.4 из пакета OEDocking [10] по структурам комплексов димерного аминоконцевого домена GluNl/GluN2B с ифенпродилом и лигандом **2**, для которого реализуется альтернативный способ связывания. Из поиска исключали область, соответствующую фенольному фрагменту ифенпродила, и в то же время включали области в средней части сайта, не занятые в комплексе с ифенпродилом. Объем разрешенной полости сайта связывания составлял 1091 $Å^3$. Общий вид сайта связывания представлен на рис. 1.

Библиотеку структур для виртуального скрининга формировали на основе базы данных по структурам доступных соединений (www.zelinsky.com, около 400 000 веществ). После стандартизации представления структур исключали соединения, содержащие токсофорные и другие нежелательные группы, а также соединения, значительно отличающиеся по своим физико-химическим свойствам от большинства лекарств (в частности, имеющие молекулярную массу больше 600 Да или прогнозируемую величину коэффициента распределения в системе октанол–вода более 6) с помощью модуля OpenEye Filter 2.5.1.4 [10]. Далее проводили определение состояния протонирования функциональных групп при физиологическом уровне pH = 7.4 и расчет зарядов на атомах с помощью метода MMFF94 в рамках программы OpenEye QUACPAC 1.6.3.1 [10]. Затем строили пространственные модели структуры соединений с помощью методов

генерации конформаций и молекулярной механики в рамках программы OpenEye OMEGA2.5.1.4 [10,11]. Полученная библиотека включала около 100 000 структур и в среднем около 40 достижимых конформаций для каждой структуры.

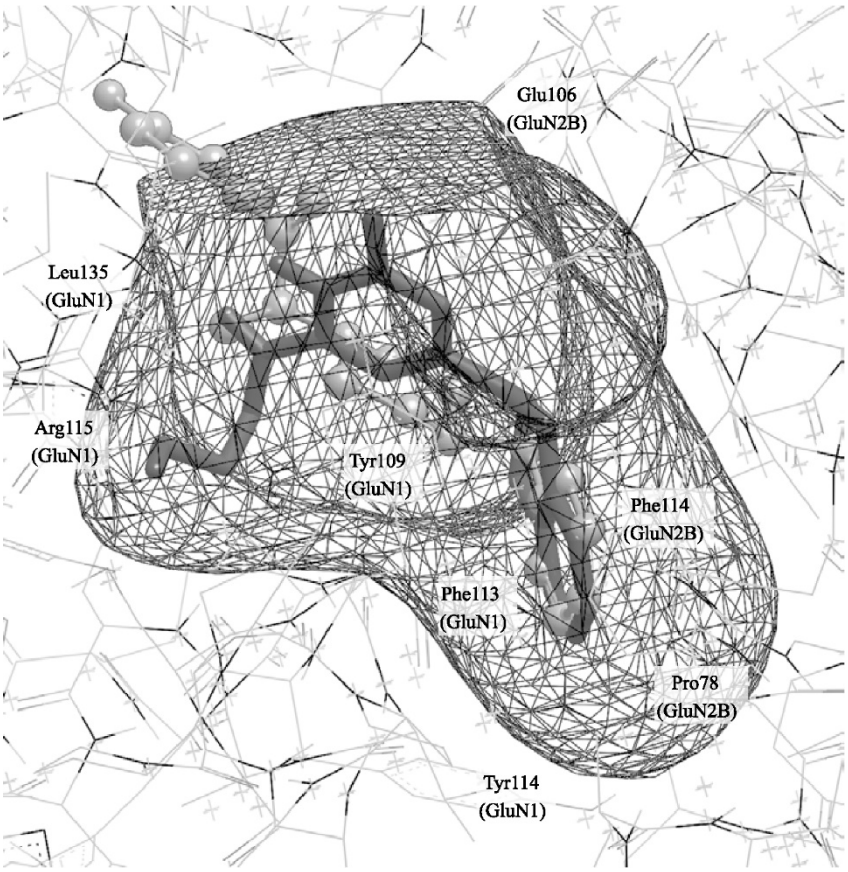


**Рис. 1**. Общий вид модели сайта связывания отрицательных модуляторов в аминоконцевом домене NMDA-рецептора. Контур разрешенной области (полости связывания) показан темно-серой сеткой, расположение молекул ифенпродила **1** и лиганда **2** в опорной структуре комплекса – светло-серой шаростержневой и темно-серой стержневой моделями соответственно.

В ходе виртуального скрининга выполняли молекулярный докинг библиотеки структур в модель сайта связывания отрицательных аллостерических модуляторов NMDA-рецептора, используя программу OpenEye FRED 3.2.0.4 из пакета OEDocking [10,12]. Величина оценочной функции *Chemgauss4* (характеризующей связывание потенциального лиганда с рецептором) для 1000 лучших соединений изменяется в интервале от –20 до –16. Далее для них выполняли прогнозирование ключевых фармакокинетических параметров и токсичности с помощью нейросетевых фрагментных моделей связи структуры со способностью вещества к проникновению через гематоэнцефалический барьер LogSS [13] (диапазон изменения прогнозируемых значений от –1,8 до 2,0), способностью вещества к всасыванию в кишечнике человека *HIA* [14] (диапазон изменения от 0 до 100%) и аффинностью к калиевому каналу кардиомиоцитов (hERG) [15] (риск кардиотоксичности, диапазон изменения от 3,2 до 8,3).

Фокусированная библиотека потенциальных пронейрогенных и нейропротекторных соединений должна включать соединения, обладающие высокой прогнозируемой активностью в отношении целевой мишени – NMDA-рецептора, а также средней или высокой способностью к проникновению через гематоэнцефалический барьер, хорошим всасыванием в кишечнике человека и низкой токсичностью. С учетом этого в качестве критериев для отбора соединений фокусированной библиотеки были выбраны следующие условия (обозначения параметров см. выше):

Полученная с использованием этих условий фокусированная библиотека включает 10 соединений. Примеры их структур **3–6** представлены ниже.

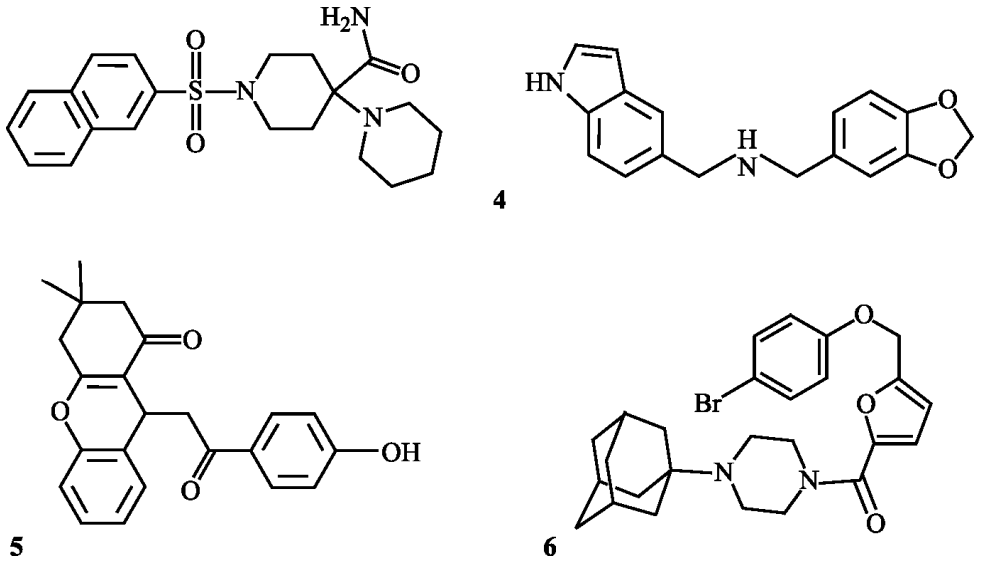

**4**

**5**

**6**

Расположение молекул соединения **6** и ифенпродила **1** в сайте связывания по результатам докинга показано на рис. 2. Видно, что их способы связывания действительно существенно различаются. Связывание рассматриваемых соединений обеспечивается главным образом гидрофобными и полярными взаимодействиями, для большинства соединений возможно также образование водородной связи.

Таким образом, нами детально проанализирована структура сайта связывания отрицательных аллостерических модуляторов в аминоконцевом домене NMDA-рецептора и определены возможные способы их связывания, выполнен молекулярный дизайн новых модуляторов, существенно отличающихся от известных по структуре и способу связывания, а также сформирована фокусированная библиотека химических соединений с потенциальными нейропротекторными и пронейрогенными свойствами, желательным набором фармакокинетических свойств и низкой токсичностью, которые могут стать основой для разработки лекарств нового поколения.

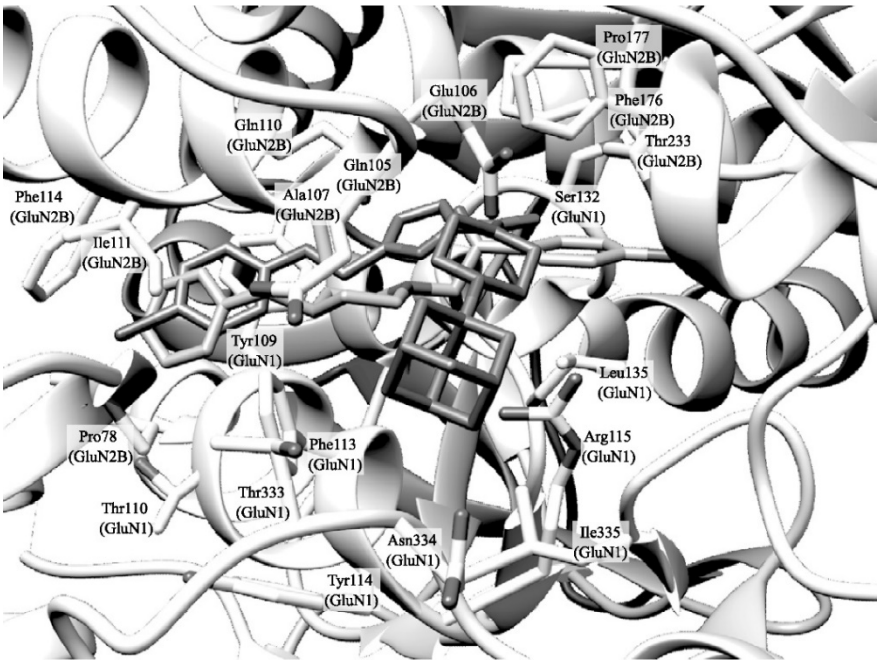


**Рис. 2.** Расположение молекул ифенпродила **1** (серый цвет) и потенциально пронейрогенного и нейропротекторного соединения **6** (темно-серый цвет) в сайте связывания отрицательных аллостерических модуляторов NMDA-рецептора по результатам докинга. Молекулы лигандов представлены стержневыми моделями. Ход основной цепи и вторичная структура белка показаны лентами, а аминокислотные остатки, расположенные на расстоянии не более 4 Å от лиганда **6**, – стержневыми моделями светло-серого цвета.

Авторы признательны фирме “OpenEye” за предоставление лицензий на программное обеспечение для молекулярного моделирования.

Работа выполнена при поддержке Министерства образования и науки Российской Федерации (проект № RFMEFI60414X0144).

**СПИСОК ЛИТЕРАТУРЫ**

1. *Traynelis S. F., Wollmuth L. P., McBain C. J., et al.* // Pharmacol. Rev. 2010. V. 62. № 3. P. 405–496.
2. *Santangelo R. M., Acker T. M., Zimmerman S. S., et al.* // Exp. Opin. Ther. Pat. 2012. V. 22. № 11. P. 1337-1352.
3. *Lai T. W, Zhang S., Wang Y.T.* // Prog. Neurobiol. 2014. V. 115. P. 157-188.
4. *Faigle R., Song H.* // Biochim. et Biophys. Acta. 2013. V. 1830. № 2. P. 2435-2448.
5. *Platel J. C., Kelsch W.* // Cell. Mol. Life Sci. 2013. V. 70. № 19. P. 3591-3601.
6. *Karlov D. S., Radchenko E. V., Zefirov A. N., et al.* // Biochem. and Biophys. Res. Communs. 2012. V. 424. № 4. P. 687-690.
7. *Радченко Е.В., Карлов Д. С., Зефиров А. Н. и др.* // ДАН. 2013. Т. 448. № 3. С. 358-362.
8. *Kawai M., Ando K., Matsumoto Y., et. al.* // Bioorg. Med. Chem. Lett. 2007. V. 17. № 20. P. 5558-5562.
9. *Stroebel D., Buhl D. L., Knafels J. D., et. al.* // Mol. Pharm. 2016. V. 89. № 5. P. 541-551.
10. OEDocking 3.2.0.4, QUACPAC 1.6.3.1, Omega 2.5.1.4, OpenEye Scientific Software.

Santa Fe (NM) www.eyesopen.com, 2009–2016.
11. *Hawkins P. C., Skillman A. G., Warren G.L., et. al.* // J. Chem. Inf. Model. 2010. V. 50. № 4. P. 572-584.
12. *McGann M.* // J. Comput.-Aided Mol. Des. 2012. V. 26. N 8. P. 897-906.
13. *Дябина А. С., Радченко Е.В., Палюлин В. А., Зефиров Н. С. //* ДАН. 2016. Т. 470. № 6. С. 720-723.
14. *Радченко Е.В., ДябинаА. С., Палюлин В.А., Зефиров Н. С.* // Изв. АН. Сер. хим. 2016. № 2. С. 576–580.
15. *Радченко Е. В., Рулев Ю. А., Сафаньяев А.Я., Палюлин В. А., Зефиров Н. С.* // ДАН. 2017. Т. 473. № 4. С. 494-497.

*Поступило в редакцию 12.07.2016 г.*

*ДОКЛАДЫ АКАДЕМИИ НАУК, 2015, том 464, № 5, с. 626-628*

*БИОХИМИЯ, БИОФИЗИКА, МОЛЕКУЛЯРНАЯ БИОЛОГИЯ*

УДК 544.165

# НОВЫЙ БИВАЛЕНТНЫЙ ПОЛОЖИТЕЛЬНЫЙ АЛЛОСТЕРИЧЕСКИЙ МОДУЛЯТОР AMPA-РЕЦЕПТОРОВ

**М.И. Лавров, В.В. Григорьев, член-корреспондент РАН С.О. Бачурин, В.А. Палюлин, академик РАН Н.С. Зефиров**

*Московский государственный университет им. М.В. Ломоносова*
*Институт физиологически активных веществ Российской Академии наук (Черноголовка Московской обл.)*

С помощью компьютерного молекулярного моделирования найден положительный аллостерический модулятор AMPA-рецепторов, обладающий рекордной экспериментально подтвержденной активностью в диапазоне пикомолярных концентраций. Он принадлежит к новому классу бивалентных лигандов AMPA-рецепторов, содержащих каркас 3,7-диазабицикло[3.3.1]нонана. Предложенная структура может служить основой для дальнейшей оптимизации и создания препаратов для лечения нейродегенеративных заболеваний, улучшения когнитивных функций и памяти.

Глутаматергическая система является главной возбуждающей медиаторной системой мозга млекопитающих и в этой связи представляет собой перспективную мишень для создания средств лечения заболеваний ЦНС [1, 2]. Среди большого числа различных типов глутаматных рецепторов значительное внимание в по-

следние годы уделяют изучению подгруппы ионотропных рецепторов, специфическим агонистом которых является (RS)-α-амино-3-гидрокси-5-метил-4-изоксазолпропионовая кислота (AMPA). Лиганды AMPA-рецепторов рассматриваются в настоящее время как потенциальный класс новых лекарственных средств для лечения таких заболеваний, как болезнь Альцгеймера, болезнь Паркинсона, шизофрения, депрессия, эпилепсия, боковой амиотрофический склероз и др. [3–5]. В ряду лигандов рецепторов AMPA особый интерес представляет группа так называемых положительных аллостерических модуляторов (ПАМ) AMPA-рецепторов, улучшающих память и когнитивные функции животных и человека, а также обладающих способностью запускать механизм экспрессии генов, отвечающих за синтез факторов роста нервной ткани, что обеспечивает проявление у этих соединений нейропротекторных свойств [5–8].

Ранее нами была экспериментально исследована серия сравнительно небольших молекул ПАМ, для которых была показана довольно умеренная активность [9]. Докинг таких соединений в димер глутаматсвязывающего домена AMPA-рецептора [10] показал возможность одновременного связывания двух молекул на небольшом расстоянии друг от друга в кармане, расположенном на интерфейсе между двумя субъединицами (рис. 1).

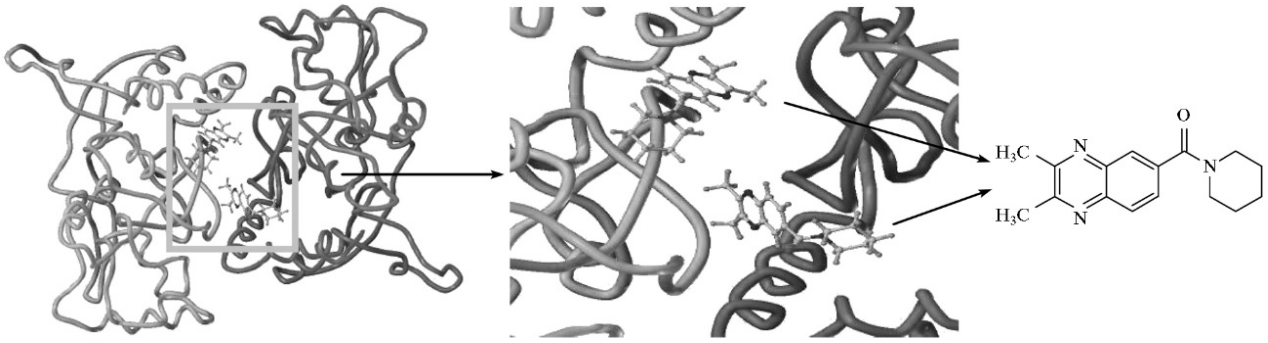


**Рис. 1.** Молекулярный докинг производного модулятора CX-516.

Похожий способ связывания был найден экспериментально (рентгеноструктурные данные) и для комплекса CTZ [11] с димером глутаматсвязывающего домена AMPA-рецептора.

На основании этих данных нами был разработан принцип конструирования новых активных лигандов, заключающийся в соединении спейсером двух небольших молекул, связывающихся с каждым из двух модуляторных сайтов димера глутаматсвязывающего домена AMPA-рецептора. При этом спейсер должен был обеспечивать необходимое расстояние между «активными фрагментами» таких молекул и позволять им принимать требуемую для оптимального связывания ориентацию, но при этом быть достаточно жестким (например, каркасным). Способ связывания конструируемых бивалентных лигандов с модуляторными сайтами AMPA-рецептора показан на рис. 2.

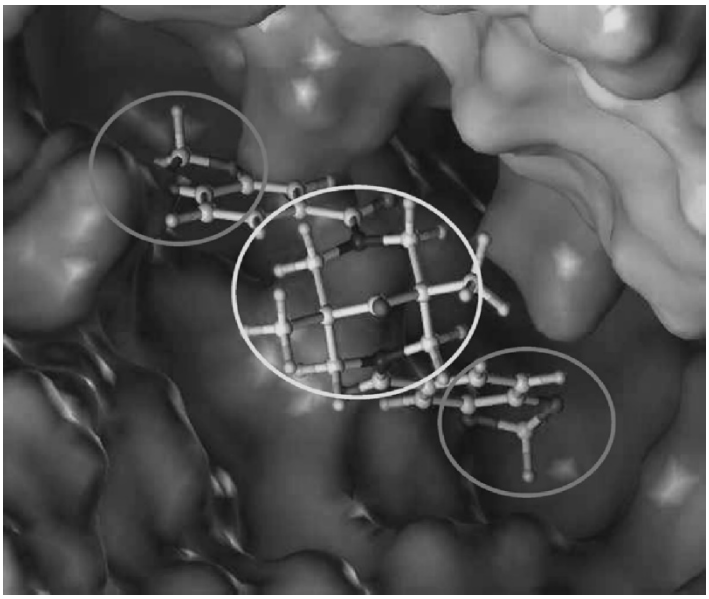

**Рис. 2.** Предпочтительная область связывания положительного аллостерического модулятора с AMPA-рецептором. Обведены «активные фрагменты» и «спейсер» (в центре).

Конструирование и оптимизацию потенциальных лигандов осуществляли с помощью пакета программ SYBYL-X2.1 [12]. Молекулярный докинг исследуемых соединений проводили в предполагаемый сайт связывания, расположенный между двумя глобулами двух субъединиц глутаматсвязывающих доменов AMPA-рецептора.

Для поиска наилучшей конформации в полости связывания мишени применяли варьирование торсионных углов лигандов методом синхронного поиска (одновременное варьирование всех торсионных углов). Процедуру докинга осуществляли с помощью программы AutoDock 4.2 [13], обеспечивающей поиск генетического алгоритма и отбор комплексов на основе оценочной функции энергий связывания. Для оптимизации структуры использовали метод моделирования de novo. Он заключается в виртуальном конструировании молекулы и оптимизации ее положения в активном центре биомишени с учетом стерических, электростатических взаимодействий, водородных связей и других факторов, обусловливающих взаимодействие лиганда с белком. В результате был подобран спейсер – каркасная структура на основе 3,7-диазабицикло[3.3.1]нонан-9-она, обеспечившая необходимую для оптимального связывания ориентацию двух ацильных заместителей, соответствующие которым исходные «монолиганды» [9, 10] обладали весьма умеренной активностью.

Таким образом, была сконструирована молекула **1**, которая, по данным моделирования, хорошо соответствовала по форме карману связывания ПАМ и по оценкам должна была проявлять значительно более высокую активность, чем известные соединения с похожим физиологическим действием.

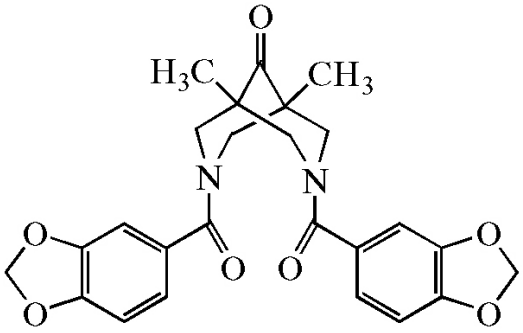

**1**

Опыты *in vitro* полностью подтвердили эти предположения. Так, в электрофизиологических экспериментах для соединения **1** начало потенциирования лежало в области пикомолярных концентраций.

Эксперименты по оценке действия вещества **1** на AMPA-рецепторы были проведены методом patch-clamp на свежеизолированных нейронах Пуркинье, выделенных из мозжечков крыс 12–15-дневного возраста. Для выделения использовали модифицированный метод. Срезы мозжечка толщиной 400–600 мкм помещали в термостатируемую камеру объемом 10 мл. Раствор для выделения имел следующий состав (в мМ): NaCl 150.0, KCl 5.0, $CaCl_2$ 2.0, $MgSO_4 \cdot 7\ H_2O$ 2.0, HEPES 10.0, глюкоза 15.0, pH 7.42. Срезы инкубировали в этом растворе в течение 60 мин, после чего этот раствор заменяли аналогичным раствором, содержащим проназу (2 мг/мл) и коллагеназу (1 мг/мл), и инкубировали в течение 70 мин. После отмывки первоначальным раствором в течение 20 мин срезы помещали в чашку Петри и разъединяли механическим способом при помощи пастеровской пипетки. Растворы непрерывно продували 100%-ном $O_2$ при температуре 34°C. Нейроны Пуркинье помещали в рабочую камеру объемом 0.6 мл. Рабочий раствор имел состав (в мМ): 150.0 NaCl, 5.0 KCl, 2.6 $CaCl_2$, 2.0 $MgSO_4 \cdot 7H_2O$, 10.0 HEPES, 15.0 глюкоза, pH 7.36.

Трансмембранные токи индуцировали активацией AMPA-рецепторов методом быстрой суперфузии путём аппликации растворов агониста этих рецепторов – каиновой кислоты (КК). Поскольку сама AMPA вызывает слишком сильную десенситизацию рецепторов, в таких экспериментах и используют КК. Регистрацию токов осуществляли при помощи боросиликатных микроэлектродов (сопротивление 2.0–4.5 МОм), заполненных раствором следующего состава (в мМ): 100.0 KCl, 11.0 ЭГТА, 1.0 $CaCl_2$, 1.0 $MgCl_2$, 10.0 HEPES, 5.0 АТФ, pH 7.2. Для регистрации использовали прибор EPC-9 («HEKA», Германия). Обработку результатов осуществляли при помощи программы Pulsefit («HEKA»).

Аппликация КК в нейронах Пуркинье индуцирует трансмембранные входящие токи. Мы обнаружили, что добавление в перфузируемый раствор соединения **1** приводит к зависимому от концентрации **1** увеличению амплитуды токов (рис. 3). Этот эффект мы зарегистрировали в диапазоне низких концентраций **1**:

$10^{-11}$–$10^{-9}$ М. При использовании бóльших концентраций **1** значения амплитуды токов возвращались к контрольному уровню.

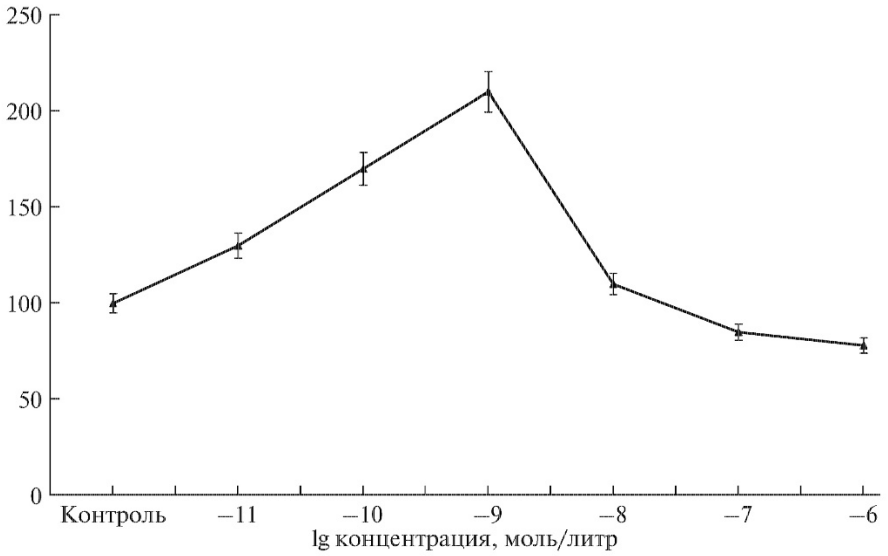


**Рис. 3.** Действие соединения **1** на токи AMPA-рецепторов в нейронах Пуркинье мозжечка крыс, исследованное электрофизиологическим методом patch-clamp; $M \pm m$, $n = 17$.

Резюмируя результаты проведенных исследований, можно сделать вывод, что соединение **1** проявляет ярко выраженный эффект, свойственный для аллостерических модуляторов AMPA-рецепторов. Наряду с этим, эффективные дозы представленного соединения значительно ниже, чем для практически всех известных на данный момент ПАМ AMPA-рецепторов (например, [14, 15]). Это дает надежду на то, что при дальнейшей оптимизации структуры удастся создать препарат широкого спектра действия для лечения и профилактики нейродегенеративных и психоневрологических заболеваний, а также для стимуляции памяти и улучшения когнитивных функций человека.

Авторы выражают благодарность за поддержку данной работы в рамках программы Президиума РАН.

**СПИСОК ЛИТЕРАТУРЫ**

1. *Watkins J.C., Evans R.H.* // Ann. Rev. Pharmacol. Toxicol. 1981. V. 21. P. 165-204.
2. *Lapidus K.A., Soleimani L., Murrough J.W.* // Novel Glutamatergic Drugs for the Treatment of Mood Disorders // Neuropsychiatr. Dis. Treat. 2013. V. 9. P. 1101-1112.
3. *O'Neill M.J., Witkin J.M.* // Curr. Drug Targets. 2007. V. 8. № 5. P. 603-620.
4. *Bleakman D., Alt A., Witkin J.M.* // CNS Neurol. Disord. Drug Targets. 2007. V. 2. P. 117-126.
5. *Григорьев В.В., Прошин А.Н., Кинзирский А.С., Бачурин С.О.* // Успехи химии. 2009. Т. 78. № 5. С. 524-534.
6. *Lynch G., Gall C.M.* // Trends Neurosci. 2006. V. 29. № 10. P. 3-9.
7. *Francotte P., de Tullio P., Fraikin P., et al.* // Recent Pat. CNS Drug Discov. 2006. V.

1. № 3. P. 239-246.
8. *Arai A.C., Kessler M.* // Curr. Drug Targets. 2007. V. 8. № 5. P. 583-602.
9. *Лавров М.И., Лаптева В.Л., Григорьев В.В. и др.* // Хим.-фарм. журн. 2012. Т. 46. № 2. С. 27-30.
10. *Тихонова И.Г., Лавров М.И., Палюлин В.А., Зефиров Н.С.* // ДАН. 2004. Т. 399. № 2. С. 268-270.
11. *Jin R., Clark S., Weeks A. M., et al.* // J. Neurosci. 2005. V. 25. P. 9027-9036.
12. SYBYL-X 2.1. 2013. www.certara.com
13. *Morris G.M., Huey R., Lindstrom W., et al.* // J. Comput. Chem. 2009. V. 30. P. 2785-2791.
14. *Timm D.E., Benveniste M., Weeks A.M., et al.* // Mol. Pharmacol. 2011. V. 80. P. 267-280.
15. *Harms J.E., Benveniste M., Maclean J.K.F., et al.* // Neuropharmacology. 2013. V. 64. P. 45-52.

*Поступило в редакцию 10.03.2015 г.*

*ИЗВЕСТИЯ АКАДЕМИИ НАУК. СЕРИЯ ХИМИЧЕСКАЯ. 2010, т. 59 (1),*

*стр. 196-204*

УДК 547.241+547.466

# СИНТЕЗ «ТРИПЕПТИДА ПАМЯТИ» (ARG–GLU–ARG, RER) И РЕАКЦИЯ КАБАЧНИКА–ФИЛДСА С ДИ- И ТРИПЕПТИДАМИ КАК МЕТОД СИНТЕЗА ФОСФОРСОДЕРЖАЩИХ ПРОИЗВОДНЫХ ПЕПТИДОВ

**Е.Д. Матвеева, Т.А. Подругина, М.В. Присяжной, С.О. Бачурин, Н.С. Зефиров**

*Московский государственный университет им. М. В. Ломоносова,*
*Химический факультет*
*Институт физиологически активных веществ Российской академии наук*

Разработаны методы синтеза потенциальных препаратов бинарного действия («twindrugs»), содержащих фрагменты антагониста глутаматных рецепторов и олигопептиды, стимулирующие когнитивные функции мозга. Синтезирован «трипептид памяти» Arg–Glu–Arg (RER), содержащий трипептидную последовательность белка $APP_{328–330}$ – предшественника β-амилоида. Разработан метод синтеза α-аминофосфонатов на основе олигопептидов в качестве ами-

нокомпоненты каталитической трехкомпонентной реакции Кабачника–Филдса. Предложен метод синтеза фосфонопептидов включением в пептидную цепь α-аминофосфонатов.

Актуальной задачей органического синтеза является создание веществ с заданными свойствами, к которым, в частности, относятся лекарства нового поколения для лечения нейродегенеративных расстройств. Одним из перспективных направлений, позволяющих решить эту проблему, является создание биоизостерных аналогов известных биологически активных веществ[1], либо синтез препаратов бинарного действия («twin-drugs») на основе так называемого «фрагментно-базируемого дизайна»[2]. Среди разных классов физиологически активных веществ в этой области известны олигопептиды, способные улучшать когнитивные функции и оказывать влияние на центральную нервную систему. Выделим среди них два примера.

Так, одним из активно исследуемых классов эндогенных пептидных регуляторов являются пептиды, подобные адренокортикотропному и меланоцитстимулирующим гормонам, которые известны под общим термином меланокортины (МК). В настоящее время синтетический гептапептид семакс (Met–Glu–His–Phe–Pro–Gly–Pro), представляющий собой лишенный гормональной активности структурный аналог адренокортикотропного гормона ($АКТГ_{4–10}$)[3], является единственным широко используемым в клинике лекарственным препаратом ноотропного действия[4].

Помимо этого, известно, что белок APP – предшественник β-амилоида (играющего, вероятно, ключевую роль в генезисе болезни Альцгеймера) – выполняет важные функции в нормальных тканях мозга и, в частности, играет специфическую роль в формировании долгосрочной памяти[5,6]. При исследовании механизма его действия была идентифицирована специфическая пентапептидная последовательность $APP_{328–332}$, а именно Aig–Glu–Aig–Met–Ser (RERMS) как активный домен, отвечающий за вышеупомянутые функции. Более того, аналогичные синтетические пентапептиды RERMS и SMRER также устраняют дефицит памяти. Наиболее интересным оказалось, что даже палиндромный трипептид Arg–Glu–Arg (RER), содержащий трипептидную последовательность $APP_{328–330}$, защищает от потери памяти, индуцированной β-амилоидом[6,7]. Показано[8,9], что как семейство производных пентапептида, отвечающего аминокислотной последовательности $APaP_{328–332}$, так и семейство производных трипептида, отвечающего аминокислотной последовательности $APP_{328–330}$, могут быть использованы как усилители когнитивных функций при лечении болезни Альцгеймера. Интересно, что «трипептид памяти» – RER (Aig–Glu–Arg) – сохраняет активность как при изменении конфигурации одного из аргининовых остатков, так и при частич-

ном ацилировании[6-8]. Отметим также, что аналогичные три- и пентапептиды являются потенциальными ингибиторами урокиназных рецепторов[10], ангиотензин-1-превращающих ферментов[11] и обладают антитромботической[9] активностью.

Ранее[12] мы разработали удобный метод синтеза антагониста первого подтипа глутаматных рецепторов 1-аминоиндан-1,5-дикарбоновой кислоты (AIDA). В продолжение этих исследований мы решили создать гибридные молекулы, содержащие как фрагменты AIDA и ее биоизостеров, аминофосфонатов[13,14], так и олигопептидную цепь, моделирующую указанный «трипептид памяти», – RER (Arg–Glu–Arg). Вместе с тем самостоятельной проблемой является создание метода синтеза фосфорных аналогов пептидов – фосфонопептидов на основе α-аминофосфонатов.

Возможный подход к синтезу α-аминофосфонатов основан на вовлечении аминокислот и их эфиров в качестве аминной компоненты в разработанный нами новый каталитический процесс[14-16]. В настоящей работе мы расширили синтетические возможности описанного метода и распространили его на ди- и трипептиды.

Хотя трипептид Arg–Glu–Arg коммерчески доступен (Cambridge Research Biochemicals Ltd; MWG-Biotech Ltd, UK), мы синтезировали его с помощью адаптированного для лабораторной практики метода пептидного синтеза[17-19] по схеме 1, исходя из производных ω-нитро-L-аргинина **(1a–c)** и α-*n*-нитрофенилового-γ-бензилового эфира *N*-Boc-L-глутаминовой кислоты (**2**). Из коммерчески доступного *N*-Boc-ω-нитро-L-аргинина **(1a)** получен бензиловый эфир *N*-Boc-ω-нитро-L-аргинина (**1b**) (выход 95%). Последующее снятие *N*-Boc-защиты в соединении **1b** приводит к бензиловому эфиру ω-нитро-L-аргинина **(1c)** с практически количественным выходом. Защитные группы исходных аминокислот были подобраны таким образом, чтобы иметь возможность снять их за одну стадию каталитическим гидрированием. Далее конденсацией *N*-Boc-защищенного *n*-нитрофенил-γ-бензилглутамата **(2)** с С-защищенным нитроаргинином (**1c**) был синтезирован дипептид глутамиларгинин (**3a**) (выход 93%). Снятием *N*-Boc-защиты получена соль дипептида **3b** с трифторуксусной кислотой. На следующей стадии *N*-Boc-защищенный нитроаргинин (**1a**) вводили в реакцию с дипептидом **3b** в присутствии дициклогексилкарбодиимида (DCC) и *N*-гидроксибензотриазола (HOBt). В результате был получен защищенный трипептид **4a** с выходом 60%. Целевой «трипептид памяти» **4b** синтезирован в виде соли обработкой трифторуксусной кислотой соединения **4a** и последующим гидрогенолизом на палладии.

Введение α-аминофосфоната в качестве С-конца пептидного фрагмента открывает путь к синтезу фосфонопептидов, физиологическая активность которых в ряде случаев оказывается на несколько порядков выше, чем активность пептидов[20,21].

Схема 1

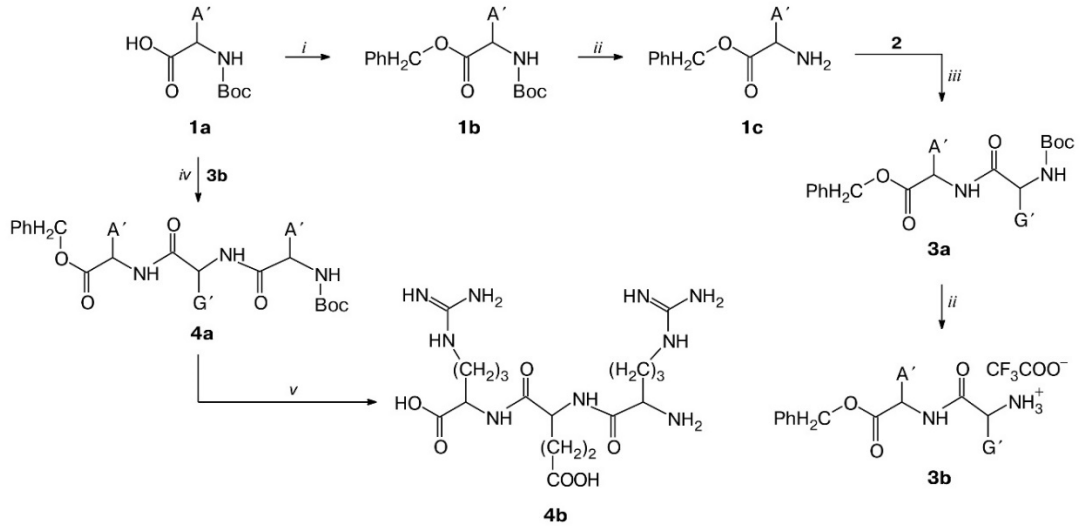

**Реагенты и условия:** *i*. $PhCH_2Cl$, DIEA, NaI, DMF; *ii*. TFA, 2 ч; *iii*. DMF, DIEA, HOBt; *iv*. DCC, $CH_2Cl_2$, HOBt, 0 °C, 2 ч; *v*. 1) TFA, 2 ч; 2) $HCOONH_4$, Pd/C, AcOH—MeOH, 48 ч.

На примере сочетания аргинина, глутаминовой кислоты и α-аминофосфоната **5** был продемонстрирован синтез фосфонопептида (схема 2). На первой стадии *N*-Boc-защищенный аргинин **(1a),** предварительно активированный DCC, был введен в реакцию с эфиром α-аминофосфоновой кислоты **5**, в результате чего был получен фосфонодипептид **6** с выходом 60%. На второй стадии конденсацией фосфонодипептида **6** с Boc-замещенным α-(*n*-нитрофенил)-γ-бензилглутаматом **(2)** был получен фосфонотрипептид **7** с выходом 90%.

Схема 2

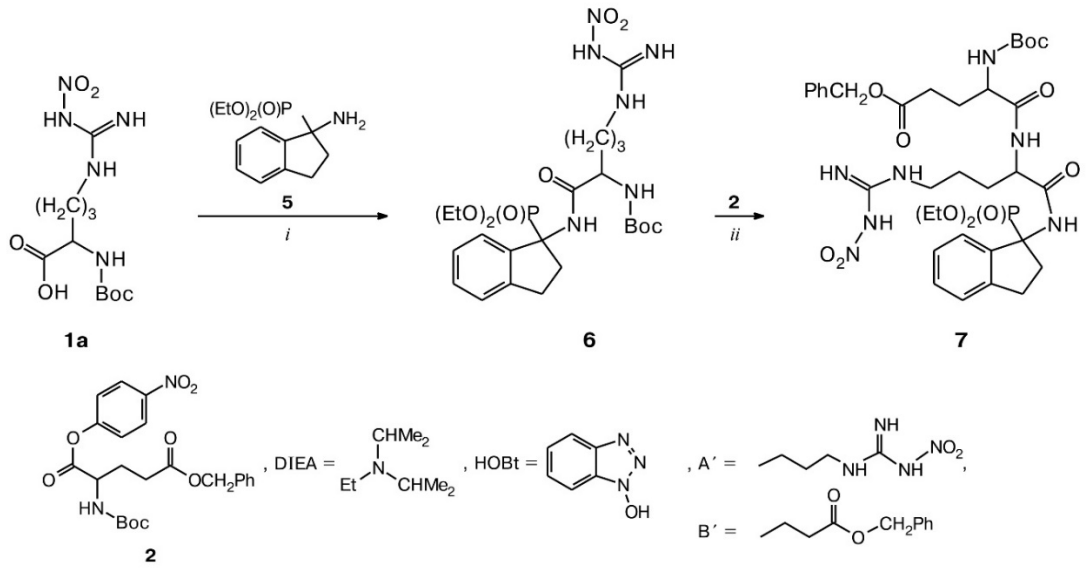

**Реагенты и условия:** *i*. 1) DCC, HOBt, $CH_2Cl_2$, 0 °C, 2 ч; 2) **5**; *ii*. 1) TFA, 2 ч; 2) DMF, DIEA, HOBt, **2**

Для оценки возможности применения пептидов как аминной компоненты в разработанном нами ранее каталитическом варианте реакции Кабачника–Фил-

дса[16] первоначально были использованы модельные дипептиды. Нами установлено, что метиловый эфир глициллейцина **(8a)** реагирует с бензальдегидом и диэтилфосфитом в условиях катализа [тетра(*трет*-бутил)фталоцианин]алюминийхлоридом ($^t$PcAlCl) с образованием соответствующего α-аминофосфоната **9a**. Реакцию проводили в метаноле при комнатной температуре в присутствии молекулярных сит 4 Å, выход дипептида **9a** составил лишь 15% из-за побочного образования соединений **10** и **11** (схема 3).

Схема 3

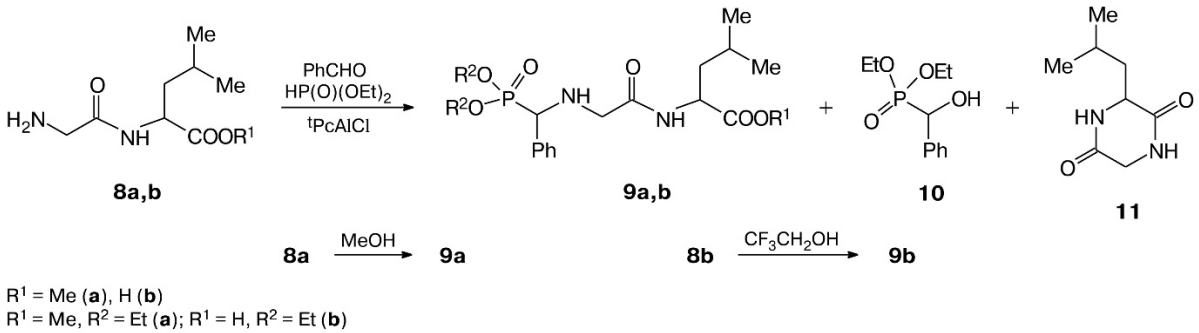


**8:** $R^1$ = Me (**a**), H (**b**)
**9:** $R^1$ = Me, $R^2$ = Et (**a**); $R^1$ = H, $R^2$ = Et (**b**)

Мы нашли, что и неэтерифицированный дипептид **8b** реагирует с бензальдегидом и диэтилфосфитом в условиях катализа фталоцианинами с образованием соответствующего α-аминофосфоната **9b**. Поскольку дипептид **8b** в метаноле практически не растворяется, реакцию проводили в кипящем 2,2,2-трифторэтаноле. Так как дипептид в такой среде представляет собой цвиттер-ион, для высвобождения аминогруппы в реакционную смесь добавляли эквимольное количество триэтиламина. В этом случае аминофосфонат **9b** был получен с выходом 75%. Побочно, по-видимому, образуются продукты переэтерификации фосфонатной группировки.

Схема 4

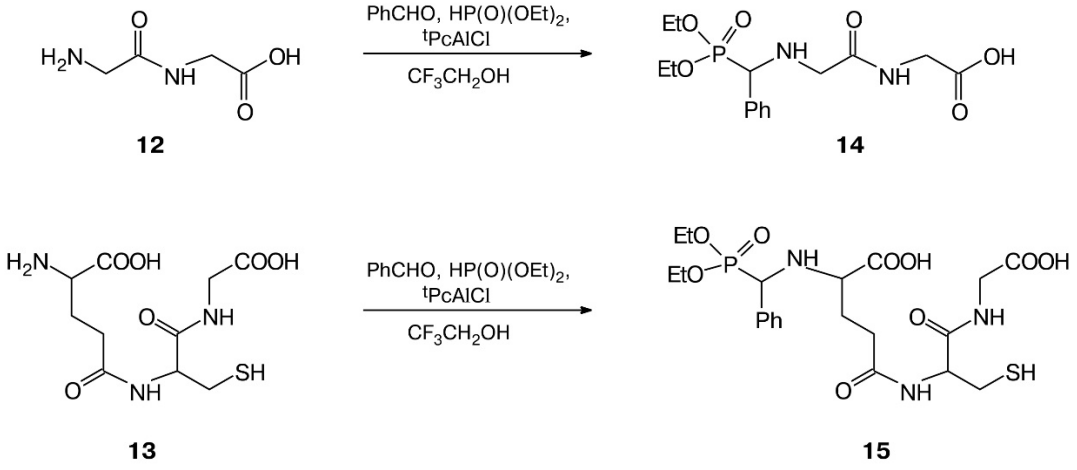


Аналогичным образом мы провели реакции с глицилглицином (**12**) и глутатионом (**13**). α-Аминофосфонаты **14** и **15** получены с выходами 70 и 40% соответственно (схема 4).

В среде трифторэтанола, по-видимому, происходит частичная переэтерификация фосфонатной группы, что зафиксировано в спектрах ЯМР $^{31}$P (появление дополнительных сигналов в области δ 20–24 м.д.).

В реакцию Кабачника–Филдса мы ввели дипептид **3b**. В качестве карбонильной компоненты был использован индан-1-он – структурный фрагмент лиганда глутаматных рецепторов AIDA[22] (схема 5). Благодаря высокой растворимости защищенного дипептида **3b** в органических растворителях, реакция легко протекает в хлористом метилене при 30°C с образованием аминофосфоната **16** с выходом 60%.

Схема 5

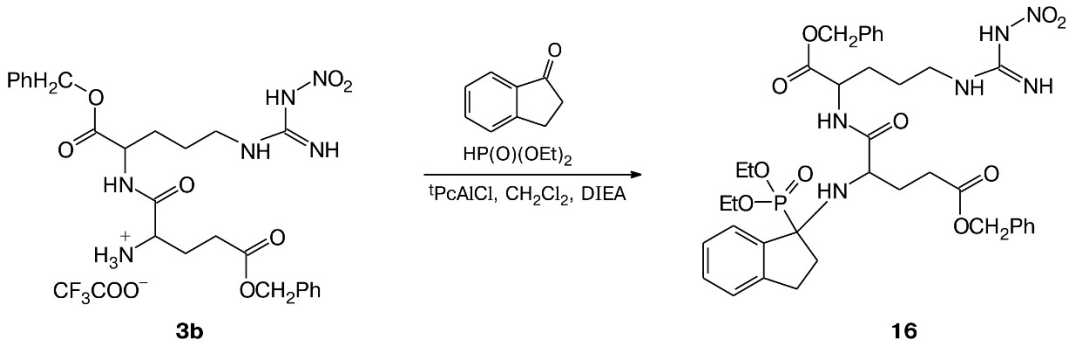


Дальнейшим шагом на пути к синтезу аналогов «трипептида памяти» стало введение в каталитическую реакцию Кабачника–Филдса трипептида **4a** в качестве аминной компоненты (схема 6). В реакции использовали индан-1-он и 5-индан-1-он в качестве карбонильной компоненты и диэтилфосфит как P–H-компоненту. После удаления Boc-группы в защищенном аргинилглутамиларгинине **4a** обработкой трифторуксусной кислотой полученную соль вводили в реакцию Кабачника–Филдса в присутствии Pc$^t$AlCl и эквимольного количества диизопропилэтиламина. В результате были получены аминофосфонаты **17** и **18** с выходами 60%. Завершающая стадия синтеза фосфорсодержащего аналога «трипептида памяти» – снятие защитных групп – была осуществлена на примере соединения **17** каталитическим гидрированием в присутствии Pd/C в водном растворе уксусной кислоты при комнатной температуре. В результате был получен искомый аминофосфонат **19** с выходом 95%.

Разработанный нами подход открывает путь к синтезу фосфонопептидов.

Все полученные олигопептиды и их фосфорные аналоги охарактеризованы методами ЯМР $^1$H, $^{13}$C, $^{31}$P, ИК-спектроскопии и масс-спектрометрии.

В ИК-спектрах соединений **6, 7, 9, 14–19** присутствуют полосы поглощения в области 1250–1260 см$^{-1}$, соответствующие группе P=O, в области 1600–1640 см$^{-1}$, соответствующие группе C=N гуанидиновых фрагментов и группе $NO_2$ (для соединений **7, 16-19),** в области 1680–1690 и 1720–1740 см$^{-1}$, характерные для амидной и кислотной групп C=O, в области 3250–3500 см$^{-1}$ – широкие полосы, соответствующие группам OH и NH.

Схема 6

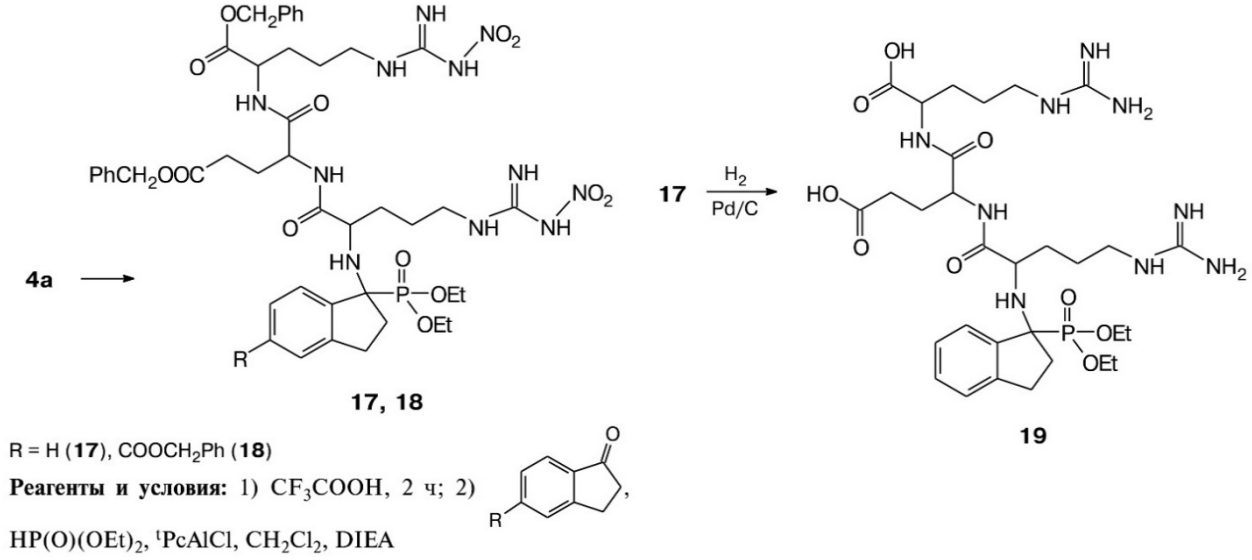


Поскольку в данном процессе мы использовали пептиды на основе оптически активных L-аминокислот, аминофосфонаты **6, 7, 9, 15–19** представляют собой смеси диастереомеров, различающихся конфигурацией атома углерода, связанного с атомом фосфора. Поэтому в спектрах ЯМР $^{31}$P, $^{1}$H и $^{13}$C этих соединений наблюдалось удвоение или уширение большинства сигналов. В спектрах ЯМР $^{31}$P соединений **6, 7, 9, 14–19** имеются сигналы в области δ 20–31 м.д., соответствующие диалкиламинофосфонатным группам.

В спектрах ЯМР $^{1}$H всех полученных аминофосфонатов **6, 7, 9, 14–19** наблюдаются сигналы неэквивалентных фосфонатных этоксигрупп – триплеты метильных групп в области δ 1.0–1.4 м.д. и мультиплеты метиленовых протонов в области δ 3.6–4.6 м.д. Сигнал протона при α-углеродном атоме аминофосфонатного узла (соединения **9, 14, 15)** проявляется в области δ 3.3–5.0 м.д. в виде двух дублетов диастереомерной пары с КССВ $^{2}J_{H,P}$ = 10.6–14.6 Гц. В соединениях **9** и **14** сигналы диастереотопных метиленовых протонов проявляются в виде двух дублетов в области δ 3.0–3.7 м.д. ($J_{AB}$ = 17.0–18.8 Гц). В результате дейтерообмена протоны гидроксильной и аминогрупп не проявляются. Сигналы, соответствующие α-протонам аминокислотных фрагментов, проявляются в области δ 3.5–4.7 м.д.

В спектре ЯМР $^{13}$C фосфорных аналогов пептидов **6, 7, 9, 15–19** присутствуют удвоенные сигналы диастереомерных смесей. α-Углеродный атом при атоме фосфора проявляется в области δ 53–69 м.д. с $J_{P,C}$ =149–165 Гц. Химические сдвиги диастереотопных этоксигрупп при атоме фосфора лежат в области δ 15.5–20 м.д. ($CH_3$) и δ 62–65 м.д. ($OCH_2$). Сигналы асимметрических атомов углерода пептидного фрагмента проявляются в области δ 51–56 м.д. Химические сдвиги атомов углерода гуанидиновых групп находятся в области δ 159–160 м.д.

(δ 155.6 м.д. для незащищенной группы соединения **19**); сигналы карбоксильных и амидных атомов углерода расположены в области δ 169–179 м.д. Остальные сигналы в спектрах ЯМР $^{13}C$ α-фосфорных аналогов пептидов соответствуют структуре углеродного скелета исходного карбонильного соединения и исходных пептидов.

Работа выполнена при финансовой поддержке Российского фонда фундаментальных исследований (проект № 08-03-00611), Совета по грантам при Президенте Российской Федерации (Целевая программа «Развитие научного потенциала высшей школы», грант 02.445.11.7468), Российской академии наук (гранты фундаментальных исследований 1-ОХНМ РАН и Ю-ОХНМ РАН, грант Президиума РАН 9П).

**СПИСОК ЛИТЕРАТУРЫ**

1. P. Ertl, *J. Chem. Inf. Comput. Sci.,* 2003, **43**, N.2, 374.
2. D. C. Rees, M. Congreve, C. W. Murray, R. Carr, *Nature Rev. Drug Discovery,* 2004, **3**, 660.
3. М. А. Пономарева-Степная, В. Н. Незавибатько, Л. В. Антонова, Л. А. Андреева, Л. Ю. Алфеева, В. Н. Потман, А. А. Каменский, И. П. Ашмарин, *Хим. фарм. журн.,* 1984, 7, 790 *[Chem. Pharm. J.* (Engl. Trend.), 1984, 7].
4. М. А. Пономарева-Степная, В. Н. Незавибатько, И. П. Ашмарин, А. А Каменский, Л. В. Антонова, Ас. № 939440, СССР, 1981.
5. R. Mileusnic, C. L. Lancashire, A N. B. Johnston, S. P. R. Rose, *Eur. J. Neurosci.,* 2000, **12**, 4487.
6. R. Mileusnic, C. L. Lancashire, S. P. R. Rose, *Ann. N. Y.Acad. Sci.,* 2005, **1048**, 149.
7. R. Mileusnic, C. L. Lancashire, S. P. R. Rose, *Eur. J. Neurosci.,* 2004, **19**, 1933.
8. R. Mileusnic, S. P. R. Rose, US Pat. 20080153759, 2008.
9. R. Mileusnic, S. P. R. Rose, Eur. Pat. EP 1381627, 2004.
10. K. Bifulco, I. Longanesi-Cattani, L. Gargiulo, O. Maglio, M. Cataldi, M. De Rosa, M. P. Stoppelli, V. Pavone, M. V. Carriero, *FEBS Lett.,* 2008, **582**, No. 7, 1141.
11. K. Katayama, H. E. Anggraeni, T. Mori, M. A. Abdulatef, S. Kawahara, M. Sugiyama, T. Nakayama, M. Maruyama, M. Muguruma, *J. Agric. FoodChem.,* 2008, **56**, № 2, 355.
12. Е. Д. Матвеева, Т. А Подругина, О. Н. Зефирова, А. С. Алексеев, С. О. Бачурин, R. Pellicciari, Н. С. Зефиров, *Журн. орган, химии.,* 2002, **38**, 1825 *[Russ. J. Org. Chem. (Engl. Transl.),* 2002, **38**].
13. V. P. Kukhar, H. R. Hudson, *Amonophosphonic and Aminophosphinic Acids: Chemistry and Biological Activity,* Ed. V. P. Kukhar, John Wiley and Son, 2000.
14. N. S. Zefirov, E. D. Matveeva, *ARKIVOC,* 2008, (i), No. 1,1.
15. Е. Д. Матвеева, Н. С. Зефиров, *Журн. орган, химии,* 2006, **42**, 1254 [Russ. *J. Org. Chem. (Engl. Transl.),* 2006, **42**].
16. Е. Д. Матвеева, Т. А. Подругина, М. В. Присяжной, И. Н. Русецкая, Н. С. Зефиров, *Изв. АН. Сер. хим.,* 2007, 768 *[Russ. Chem. Bull., Engl. Transl.,* 2007, **56**, 798].
17. H. Otsuka, K. Inoue, M. Kanayama, F. Shinozaki, *Bull. Chem. Soc. Jpn,* 1966, **39**, 882.
18. G. L. Tritsch, D. W. Woolley, *J. Am. Chem. Soc.,* 1960, **82**, № 11, 2787.

19. Y. Chen, C. Guohui, M. Zhao, C. Wang, K.Qian, S. Morris- Natschke, K. Lee, S. Peng, *Bioorg. Med. Chem.,* 2008, **16**, 5914.

20. Arendt, M. Hoffmann, A. Kolodziejczyk, A. Sobczak, T. Sokolowska, C. Wasielewski, *Pol. J. Chem.,* 1979, **53**, 447.

21. I. Ntai, B. O. Bachmann, *Bioorg. Med. Chem. Lett.,* 2008, **18**, 3068.

22. R. Pellicciary, R. Luncia, G. Constantino, M. Marinozzi, B. Natalini, P. Jakobsen, A. Kanstrup, G. Lombardi, F. Moroni, C. Thomsen, *J. Med. Chem.,* 1995, **38**, 3717.

23. С. А Михаленко, С. В. Барканова, О. Л. Лебедев, Е. А. Лукьянец, *Журн. общ. химии,* 1971, **41**, 2735 [J. *Gen. Chem. USSR (Engl. Transl.),* 1971, 41].

24. E. D. Matveeva, T. A. Podrugina, E. V. Tishkovskaya, L. G. Tomilova, N. S. Zefirov, *Synlett,* 2003, 15, 2321.

*Поступила в редакцию 21 сентября 2009*

*SAR AND QSAR IN ENVIRONMENTAL RESEARCH, VOL. 23 (7-8), 2012, 627-647*

# COMBINED QSAR STUDIES OF INHIBITOR PROPERTIES OF O-PHOSPHORYLATED OXIMES TOWARD SERINE ESTERASES INVOLVED IN NEUROTOXICITY, DRUG METABOLISM AND ALZHEIMER'S DISEASE

**G.F. Makhaeva, E.V. Radchenko, I.I. Baskin, V.A. Palyulin, R.J. Richardson and N.S. Zefirov**

*Institute of Physiologically Active Compounds, Chernogolovka, Russia; Department of Chemistry, Moscow State University, Moscow, Russia Toxicology Program, Department of Environmental Health Sciences, University of Michigan, Ann Arbor, USA*

Oxime reactivation of serine esterases (EOHs) inhibited by organophosphorus (OP) compounds can produce O-phosphorylated oximes (POXs). Such oxime derivatives are of interest, because some of them can have greater anti-EOH potencies than the OP inhibitors from which they were derived. Accordingly, inhibitor properties of 58 POXs against four EOHs, along with pair-wise selectivities between them, have been analysed using different QSAR approaches. EOHs (with their abbreviations and consequences of inhibition in parentheses) comprised acetylcholinesterase (AChE: acute neurotoxicity; cognition enhancement), butyrylcholinesterase (BChE: inhibition of drug metabolism or stoichiometric scavenging of EOH inhibitors; cognition enhancement), carboxylesterase (CaE: inhibition of drug metabo-

lism or stoichiometric scavenging of EOH inhibitors), and neuropathy target esterase (NTE: delayed neurotoxicity). QSAR techniques encompassed linear regression and backpropagation neural networks in conjunction with fragmental descriptors containing labelled atoms, Molecular Field Topology Analysis (MFTA), Comparative Molecular Similarity Index Analysis (CoMSIA), and molecular modelling. All methods provided mostly consistent and complementary information, and they revealed structural features controlling the 'esterase profiles', i.e. patterns of anti-EOH activities and selectivities of the compounds of interest. In addition, MFTA models were used to design a library of compounds having a cognition-enhancement esterase profile suitable for potential application to the treatment of Alzheimer's disease.

## 1. Introduction

Exposure of a serine esterase (EOH) to an organophosphorus (OP) compound gives rise to reactions of inhibition, spontaneous reactivation, and aging shown in Figure 1 [1].

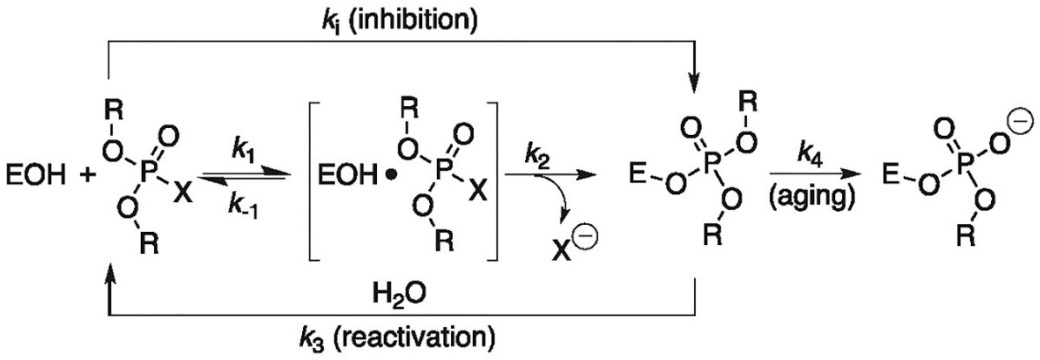


**Figure 1.** Interactions of an OP inhibitor with a serine esterase (EOH), showing inhibition, reactivation, and aging. R = substituted or unsubstituted alkyl or aryl groups, X = leaving group; $k_1$, $k_{-1}$ = rate constants for association and dissociation, respectively, of the inhibitor with the enzyme to form a Michaelis complex (shown in square brackets); $k_2$ = phosphorylation rate constant to form a covalent adduct between the inhibitor and the active site serine of the enzyme; $k_3$ = reactivation rate constant; $k_4$ = aging rate constant; $k_i$ = bimolecular rate constant of inhibition.

Because inhibition of certain EOHs can be toxic (see below), and the rate of spontaneous reactivation is extremely slow for many EOP adducts, potent nucleophiles in the form of oximes have been developed to hasten reactivation, as shown in Figure 2 [2]. Although most phosphorylated oximes (POXs) formed in oxime-mediated reactivation are unstable and readily hydrolyse to form non-inhibitory compounds [3], some POXs are more potent as EOH inhibitors than the original OP compounds from which they were derived [4,5]. Hence, considerable interest has developed in the class of POX inhibitors of EOHs [6,7].

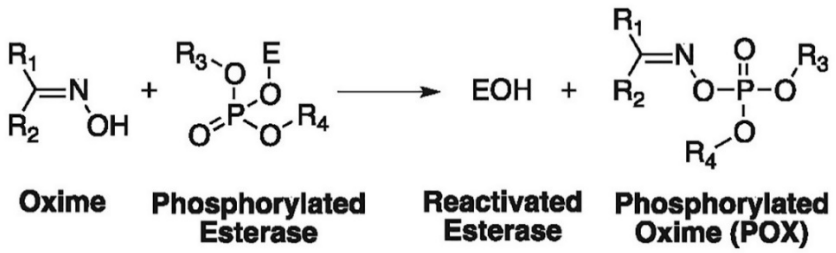


**Figure 2.** Reaction of a phosphorylated serine esterase with an oxime to form reactivated esterase and phosphorylated oxime (POX).

The particular spectrum of toxic or therapeutic effects from exposure to a given EOH inhibitor is determined in part by its 'esterase profile', i.e. a data set describing relative inhibitory potencies toward EOHs of particular interest [8,9]. As shown in Figure 3, we chose to study EOHs whose inhibition is involved in acute neurotoxicity (acetylcholinesterase (AChE) EC 3.1.1.7) [10], delayed neurotoxicity (neuropathy target esterase (NTE) 3.1.1.5) [11], and drug metabolism or stoichiometric scavenging of EOH inhibitors (butyrylcholinesterase (BChE) EC 3.1.1.8; and carboxylesterase (CaE) EC 3.1.1.1) [12,13]. In addition, inhibition of AChE and/or BChE can enhance cognitive function in Alzheimer's disease [14,15]. Analysis of the esterase profile of OP compounds, especially using modern quantitative structure-activity relationship (QSAR) methods, makes it possible to determine the contribution of different structural elements to their biological effects [7,9,16].

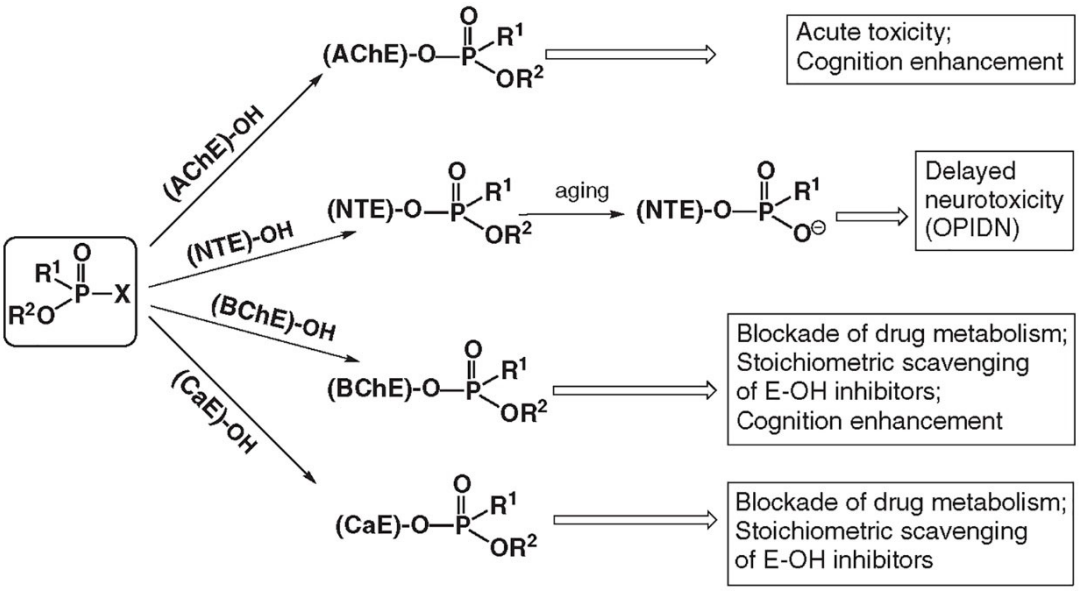


**Figure 3.** Inhibition of serine esterases by OP inhibitors yields toxic or potentially therapeutic effects. $R_1$, $R_2$ = jsubstituted or unsubstituted alkyl or aryl groups, X = leaving group. AChE = acetylcholinesterase; inhibition yields acute toxicity or cognition enhancement. NTE = neuropathy target esterase; inhibition and aging yields delayed neurotoxicity (OPIDN). BChE = butyrylcholinesterase; inhibition yields blockade of drug metabolism, stoichiometric scavenging or cognition enhancement. CaE = carboxylesterase; inhibition yields blockade of drug metabolism or stoichiometric scavenging. The –OH appended to each esterase denotes the active site serine hydroxyl group that becomes covalently organophosphorylated by OP inhibitors.

The following parameters were considered in our esterase profile analysis:

| | |
|---|---|
| (A) Inhibitor activity of POXs toward the four EOHs: | |
| (A1) AChE inhibitor activity ($A_A$) | $A_A$ = log $k_i$ (AChE) [$k_i$, $M^{-1}$ $min^{-1}$] |
| (A2) BChE inhibitor activity ($A_B$) | $A_B$ = log $k_i$ (BChE) [$k_i$, $M^{-1}min^{-1}$] |
| (A3) NTE inhibitor activity ($A_N$) | $A_N$ = log $k_i$ (NTE) [$k_i$, $M^{-1}min^{-1}$] |
| (A4) CaE inhibitor activity ($A_C$) | $A_C$ = log $k_i$ (CaE) [$k_i$, $M^{-1}min^{-1}$] |
| (S) Pair-wise inhibitor selectivity of POXs: | |
| (S1) BChE vs. AChE selectivity ($S_{BA}$) | $S_{BA}$ = log $k_i$ (BChE) – log $k_i$ (AChE) |
| (S2) NTE vs. AChE selectivity (SNA) | $S_{NA}$ = log $k_i$ (NTE) – log $k_i$ (AChE) |
| (S3) CaE vs. AChE selectivity ($S_{CA}$) | $S_{CA}$ = log $k_i$ (CaE) – log $k_i$ (AChE) |
| (S4) BChE vs. NTE selectivity (SBN) | $S_{BN}$ = log $k_i$ (BChE) – log $k_i$ (NTE) |
| (S5) CaE vs. NTE selectivity ($S_{CN}$) | $S_{CN}$ = log $k_i$ (CaE) – log $k_i$ (NTE) |
| (S6) CaE vs. BChE selectivity ($S_{CB}$) | $S_{CB}$ = log $k_i$ (CaE) – log $k_i$ (BChE) |

Thus, we have four indicators of activity and six of selectivity for a total of 10 modelling endpoints. Each of these parameters is based on the bimolecular rate constant of inhibition ($k_i$) of the inhibitor toward the enzyme(s) of interest, and each one is important for some aspect of the observed pharmacological and toxicological profile. For example, the ratio $k_i$(NTE)/$k_i$(AChE) represents the relative inhibitory potency of compounds with respect to target enzymes for delayed neurotoxicity (NTE) and acute neurotoxicity (AChE). This quotient is correlated with the ratio between the $LD_{50}$ and the neuropathic dose and can be used as a convenient index characterizing the neuropathic potential of an OP compound that can undergo aging [1,17,18]. The ratios $k_i$(BChE)/$k_i$(AChE) and $k_i$(CaE)/$k_i$(AChE) characterize the potential contributions of BChE and CaE to the suppression of acute toxicity of a compound by virtue of stoichiometric scavenging. Likewise, the ratios $k_i$(BChE)/$k_i$(NTE) and $k_i$(CaE)/$k_i$(NTE) represent the contributions of BChE and CaE to the potential suppression of delayed neurotoxicity [9]. Finally, the $k_i$(CaE)/$k_i$(BChE) ratio characterizes the inter-scavenger selectivity of a compound.

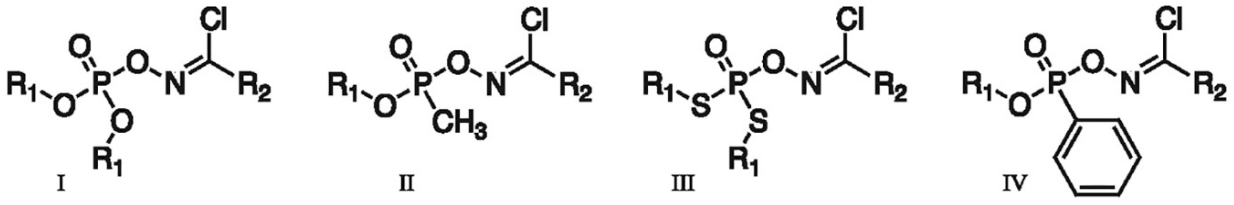


**Figure 4.** The four general structures (**I-IV**) of phosphorylated oximes (POXs) in this study.

In the present study, we tested the hypothesis that a combination of QSAR approaches could be used to analyse and predict inhibitor properties of 58 POXs (Figure 4 and Table 1) against the four EOHs of interest (Figure 3). QSAR techniques encom-

passed linear regression and backpropagation neural networks in conjunction with fragmental descriptors containing labelled atoms, Molecular Field Topology Analysis (MFTA), Comparative Molecular Similarity Index Analysis (CoMSIA), and molecular modelling. In addition, because AChE and/or BChE inhibition can result in cognition enhancement [14,15], we applied MFTA to design a library of inhibitors as potential therapeutic agents in Alzheimer's disease.

## 2. Methods

### Kinetic data on EOH inhibition

The synthesis and chemical characterization of the various POXs used in the present investigation have been described earlier [19-24]. The bimolecular rate constants of inhibition ($k_i$) were determined using human erythrocyte AChE, horse serum BChE, and pig liver CaE (Sigma, St. Louis, MO, USA), as well as hen brain NTE, which was prepared in our laboratory as described previously [25]. Detailed descriptions of the inhibition kinetics experiments have been presented elsewhere [26,27]. In brief, an enzyme sample was incubated for different time intervals with a compound of interest under conditions such that $[I]_0$ $[E]_0$, and the residual enzymatic activity was determined. The $k_i$ values were calculated according to Aldridge and Reiner [28] by linear regression using OriginPro 6.1 software [29].

The resulting data [18,26,30-33] for 58 POX compounds of general structures **I-IV** (Figure 4) along with the calculated selectivity values are presented in Table 1.

Table 1. Anti-esterase activity and selectivity of POX compounds.

| N | *Str.*[a] | $R_1$ | $R_2$ | $A_A$ | $A_B$ | $A_N$ | $A_C$ | $S_{BA}$ | $S_{NA}$ | $S_{CA}$ | $S_{BN}$ | $S_{CN}$ | $S_{CB}$ |
|---|---|---|---|---|---|---|---|---|---|---|---|---|---|
| 1 | I | $CH_3$ | $CH_3$ | 4.041 | 3.566 | 0.00 | 3.961 | -0.475 | -4.041 | -0.080 | 3.566 | 3.961 | 0.395 |
| 2 | I | $C_2H_5$ | $CH_3$ | 3.642 | 4.610 | 0.78 | 4.608 | 0.968 | -2.862 | 0.966 | 3.830 | 3.828 | -0.002 |
| 3 | I | $C_3H_7$ | $CH_3$ | 3.360 | 5.100 | 3.12 | 5.892 | 1.740 | -0.240 | 2.532 | 1.980 | 2.772 | 0.792 |
| 4 | I | $C_4H_9$ | $CH_3$ | 3.468 | 4.712 | 3.71 | 6.927 | 1.244 | 0.242 | 3.459 | 1.002 | 3.217 | 2.215 |
| 5 | I | *i*-$C_4H_9$ | $CH_3$ | 3.435 | 4.991 | 3.29 | 6.881 | 1.556 | -0.145 | 3.446 | 1.701 | 3.591 | 1.890 |
| 6 | I | $C_5H_{11}$ | $CH_3$ | 4.094 | 5.300 | 3.65 | 8.000[b] | 1.206 | -0.444 | 3.906 | 1.650 | 4.350 | 2.700 |
| 7 | I | $CH_3$ | $CH_2Cl$ | 4.964 | 5.127 | 2.33 | 5.676 | 0.163 | -2.634 | 0.712 | 2.797 | 3.346 | 0.549 |
| 8 | I | $CH_3$, $C_2H_5$ | $CH_2Cl$ | 5.081 | 5.777 | | | 0.696 | | | | | |
| 9 | I | $C_2H_5$ | $CH_2Cl$ | 4.833 | 6.241 | 3.30 | 6.733 | 1.408 | -1.533 | 1.900 | 2.941 | 3.433 | 0.492 |
| 10 | I | $C_3H_7$ | $CH_2Cl$ | 5.248 | 7.173 | 4.12 | 7.700 | 1.925 | -1.128 | 2.452 | 3.053 | 3.580 | 0.527 |
| 11 | I | $C_4H_9$ | $CH_2Cl$ | 6.064 | 7.850 | 5.43 | 8.512 | 1.786 | -0.634 | 2.448 | 2.420 | 3.082 | 0.662 |
| 12 | I | *i*-$C_4H_9$ | $CH_2Cl$ | 5.896 | 7.898 | 5.04 | 8.079 | 2.002 | -0.856 | 2.183 | 2.858 | 3.039 | 0.181 |
| 13 | I | $C_5H_{11}$ | $CH_2Cl$ | 5.908 | 8.201 | 6.17 | 9.000[b] | 2.293 | 0.262 | 3.092 | 2.031 | 2.830 | 0.799 |
| 14 | I | $CH_3$ | $CHCl_2$ | 5.715 | 6.182 | 2.55 | | 0.467 | -3.162 | | 3.629 | | |
| 15 | I | $C_2H_5$ | $CHCl_2$ | 5.104 | 6.993 | 3.09 | 7.865 | 1.889 | -2.018 | 2.761 | 3.907 | 4.779 | 0.872 |
| 16 | I | $C_3H_7$ | $CHCl_2$ | 5.848 | 8.248 | | 8.500[b] | 2.400 | | 2.652 | | | 0.252 |
| 17 | I | $C_4H_9$ | $CHCl_2$ | 6.389 | 8.265 | | 9.000[b] | 1.876 | | 2.611 | | | 0.735 |

| | | | | | | | | | | | | | |
|---|---|---|---|---|---|---|---|---|---|---|---|---|---|
| 18 | I | $C_5H_{11}$ | $CHCl_2$ | 6.479 | | | 9.000[b] | | | 2.521 | | | |
| 19 | I | $CH_3$ | F | 4.763 | 4.622 | | 5.253 | -0.141 | | 0.490 | | | 0.631 |
| 20 | I | $C_2H_5$ | F | 5.270 | 6.097 | | 5.887 | 0.827 | | 0.617 | | | -0.210 |
| 21 | I | $C_3H_7$ | F | 5.179 | 6.778 | | 6.326 | 1.599 | | 1.147 | | | -0.452 |
| 22 | I | $C_4H_9$ | F | 5.294 | 7.587 | | 7.787 | 2.293 | | 2.493 | | | 0.200 |
| 23 | I | $C_5H_{11}$ | F | 5.994 | 7.314 | | 8.127 | 1.320 | | 2.133 | | | 0.813 |
| 24 | I | $C_2H_5$ | $C_2H_5$ | 3.467 | 4.384 | | 4.185 | 0.917 | | 0.718 | | | -0.199 |
| 25 | I | $C_2H_5$ | $C_3H_7$ | 3.632 | 4.347 | | 3.662 | 0.715 | | 0.030 | | | -0.685 |
| 26 | I | $C_2H_5$ | $C_4H_9$ | 3.777 | 5.029 | | 4.083 | 1.252 | | 0.306 | | | -0.946 |
| 27 | I | $C_2H_5$ | *i*-$C_3H_7$ | 2.783 | | | | | | | | | |
| 28 | II | $C_2H_5$ | $CH_3$ | 3.316 | 2.866 | 2.16 | 3.207 | -0.450 | -1.156 | -0.109 | 0.706 | 1.047 | 0.341 |
| 29 | II | $C_3H_7$ | $CH_3$ | 3.493 | 4.017 | 2.39 | 3.591 | 0.524 | -1.103 | 0.098 | 1.627 | 1.201 | -0.426 |
| 30 | II | *i*-$C_3H_7$ | $CH_3$ | 4.929 | 5.598 | 1.24 | 4.610 | 0.669 | -3.689 | -0.319 | 4.358 | 3.37 | -0.988 |
| 31 | II | $C_4H_9$ | $CH_3$ | 3.929 | 4.918 | 3.32 | 4.615 | 0.989 | -0.609 | 0.686 | 1.598 | 1.295 | -0.303 |
| 32 | II | $C_5H_{11}$ | $CH_3$ | 4.462 | 4.914 | 3.83 | 4.544 | 0.452 | -0.632 | 0.082 | 1.084 | 0.714 | -0.370 |
| 33 | II | $C_6H_{13}$ | $CH_3$ | 4.999 | 5.188 | 3.46 | 4.462 | 0.189 | -1.539 | -0.537 | 1.728 | 1.002 | -0.726 |
| 34 | II | $C_4H_9$ | $C_2H_5$ | 3.663 | 4.924 | | 4.462 | 1.261 | | 0.799 | | | -0.462 |
| 35 | II | $C_4H_9$ | $C_3H_7$ | 3.663 | 5.201 | | 4.013 | 1.538 | | 0.350 | | | -1.188 |
| 36 | II | $C_4H_9$ | *i*-$C_3H_7$ | 3.613 | 5.035 | | 4.124 | 1.422 | | 0.511 | | | -0.911 |
| 37 | II | $C_4H_9$ | $C_4H_9$ | 3.94 | 5.659 | | 4.326 | 1.719 | | 0.386 | | | -1.333 |
| 38 | II | $C_4H_9$ | $CH_2Cl$ | 6.544 | 7.474 | | 7.193 | 0.930 | | 0.649 | | | -0.281 |
| 39 | III | C2H5 | F | 5.911 | 6.271 | | 7.165 | 0.360 | | 1.254 | | | 0.894 |
| 40 | III | $C_3H_7$ | F | 6.068 | 6.880 | | 7.820 | 0.812 | | 1.752 | | | 0.940 |
| 41 | III | $C_4H_9$ | F | 6.230 | 7.278 | | 8.000[b] | 1.048 | | 1.770 | | | 0.722 |
| 42 | III | *i*- $C_4H_9$ | F | 6.102 | 7.015 | | 8.000[b] | 0.913 | | 1.898 | | | 0.985 |
| 43 | III | $C_5H_{11}$ | F | 6.086 | 6.161 | | 7.964 | 0.075 | | 1.878 | | | 1.803 |
| 44 | IV | $CH_3$ | $CH_3$ | 3.864 | 5.740 | 3.53 | 5.887 | 1.876 | -0.334 | 2.023 | 2.210 | 2.357 | 0.147 |
| 45 | IV | $C_2H_5$ | $CH_3$ | 3.396 | 5.643 | 4.07 | 5.783 | 2.247 | 0.674 | 2.387 | 1.573 | 1.713 | 0.140 |
| 46 | IV | *i*-$C_3H_7$ | $CH_3$ | 2.623 | 4.473 | 3.62 | 5.743 | 1.850 | 0.997 | 3.120 | 0.853 | 2.123 | 1.270 |
| 47 | IV | $C_3H_7$ | $CH_3$ | 3.512 | 5.135 | 4.47 | 6.046 | 1.623 | 0.958 | 2.534 | 0.665 | 1.576 | 0.911 |
| 48 | IV | *i*- $C_4H_9$ | $CH_3$ | 3.243 | 5.476 | 4.48 | 6.194 | 2.233 | 1.237 | 2.951 | 0.996 | 1.714 | 0.718 |
| 49 | IV | $C_4H_9$ | $CH_3$ | 3.676 | 5.746 | 5.11 | 6.509 | 2.070 | 1.434 | 2.833 | 0.636 | 1.399 | 0.763 |
| 50 | IV | $C_5H_{11}$ | $CH_3$ | 3.543 | 5.827 | 5.06 | 6.504 | 2.284 | 1.517 | 2.961 | 0.767 | 1.444 | 0.677 |
| 51 | IV | $CH_3$ | $C_2H_5$ | 3.398 | 4.941 | 3.25 | 5.945 | 1.543 | -0.148 | 2.547 | 1.691 | 2.695 | 1.004 |
| 52 | IV | $C_2H_5$ | $C_2H_5$ | 3.563 | 4.998 | 3.69 | 5.719 | 1.435 | 0.127 | 2.156 | 1.308 | 2.029 | 0.721 |
| 53 | IV | $C_2H_5$ | $C_3H_7$ | 3.266 | 5.440 | 3.91 | 5.940 | 2.174 | 0.644 | 2.674 | 1.530 | 2.030 | 0.500 |
| 54 | IV | $C_2H_5$ | *i*-$C_3H_7$ | 2.792 | 5.064 | 2.92 | | 2.272 | 0.128 | | 2.144 | | |
| 55 | IV | $C_2H_5$ | $CH_2Cl$ | 4.997 | 6.632 | 5.11 | 7.591 | 1.635 | 0.113 | 2.594 | 1.522 | 2.481 | 0.959 |
| 56 | IV | $CH_3$ | *i*-$C_3H_7$ | 3.404 | 4.974 | 2.42 | | 1.570 | -0.984 | | 2.554 | | |
| 57 | I | *i*-$C_3H_7$ | $CH_2Cl$ | 3.850 | | 2.65 | | | -1.200 | | | | |
| 58 | II | *i*-$C_4H_9$ | $CH_3$ | 3.800 | | 3.04 | | | -0.760 | | | | |

Notes: [a] General structure of the compound (I-IV) as shown in Figure 4.[b]Estimated value for highly active compound (direct determination of $k_i$ was not possible using the available techniques).

**2D QSAR modelling based on fragmental descriptors with labelled atoms**

Fragmental descriptors with labelled atoms are a special subtype of fragmental descriptors [34] in which certain atoms are marked with a label indicating their special role for a property under study [35]. In this article, only fragmental descriptors with the labelled phosphorus atom and up to seven other non-hydrogen atoms were used. This allows exact positioning of fragments within a chemical structure with reference to the unique phosphorus atom in a molecule. All descriptors were generated using the FRAGMENT block of the NASAWIN software package [36,37]. The QSAR models were built using Fast Stepwise Multiple Linear Regression (FSMLR) and Backpropagation Neural Networks (BPNN) techniques. For the BPNN models, one hidden layer of five neurons was used. The 5x4-fold double cross-validation procedure [35] was used, wherein the complete data set is systematically partitioned into training, internal test, and external test sets, so that the internal test set compounds are used to select the model, and the external test set compounds provide an independent measure of the model predictivity.

**2D QSAR modelling using MFTA**

In this approach [38,39] the bioactivity model is constructed on the basis of values of local molecular descriptors (e.g. atomic properties). Two-dimensional structures of compounds in the training set (structural formulas) are topologically superimposed to construct a molecular supergraph that provides a common frame of reference for meaningful comparison and analysis of local properties in different structures. In addition to the predictive model, constructed by partial least squares (PLS) regression and relating these properties at all positions of the molecular supergraph to the bioactivity, this method gives a graphic map of their effect on activity. The predictivity of models was estimated by means of the cross-validation technique with exclusion of 25% of training set compounds using the special stabilization procedure [40] where the $Q^2$ (cross-validation parameter) values are averaged over many random reshufflings of the cross-validation subsets, and thus provide a significant degree of independence of the actual data partitioning. It should be noted that this procedure generally gives lower $Q^2$ values than other approaches; therefore, the usual acceptance criteria are not applicable.

**3D QSAR modelling**

In this study, the CoMSIA technique [41] was used. This is based on alignment of 3D structures of compounds followed by calculation of the similarity indices for the steric, electrostatic, and hydrophobic interactions in each node of a rectangular grid. Statistical analysis of these data by means of PLS regression yields a predictive structure-activity model as well as a 3D contour map of favourable and unfavourable interaction regions around the molecules. Initial conversion from 2D to 3D structures was per-

formed via SYBYL 8.0 molecular modelling software [42] using the CONCORD feature [43]. To achieve the consistent molecular alignment necessary to obtain meaningful 3D QSAR models, the conformations of the compounds under study were normalized manually according to the model of the most active compounds (maintaining the fixed orientation of the methyl/phenyl phosphonate group), followed by additional molecular mechanics relaxation to the locally stable conformer. The key torsion angles were initially set as follows: O=P-O-N to 50°, P-O-N=C to 270°, N=C-C-Alk to 120°, and O=P-O/C/S- Alk to 50°. The resulting alignment built by rigid superimposition of the common O=P- O-N=C-Cl substructure is shown in Figure 5. The CoMSIA models were constructed for all target properties using SYBYL 8.0 software [42] with 4-fold cross-validation.

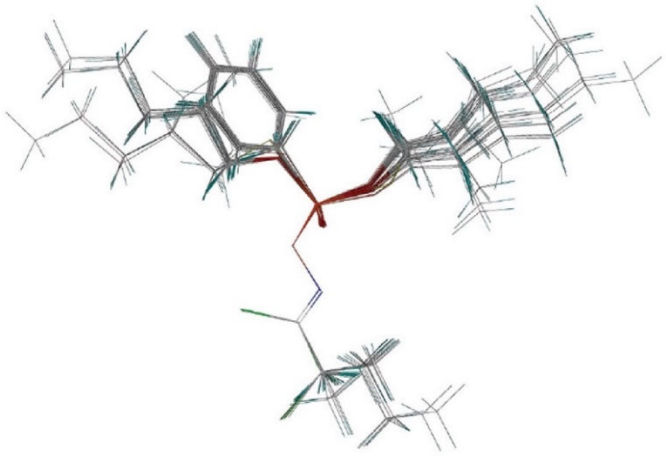

**Figure 5.** 3D alignment of the POX structures. A coloured version of this figure is available in the online edition of the paper.

## Molecular modelling

The potential binding of POXs in the active sites of two EOHs was studied using molecular modelling techniques. Our criteria for selection of EOH structures from the Protein Data Bank (PDB) included the following: same species as used in our biochemical studies or one with high (4 85%) sequence identity; high-quality X-ray structure (5 2.50 A resolution); no covalently bound ligand in the active site; no mutated residues; and well-characterized binding of ligands in a single active site. Based on these criteria, we selected mouse AChE (PDB ID: 2HA3) [44] and human BChE (PDB ID: 1P0M) [45]. Although human AChE was used in our biochemical studies, there were no human AChE structures of sufficient resolution available. The remaining mammalian AChE structures of sufficient resolution included 16 for mouse AChE, of which one containing non-covalently bound choline was chosen. Similarly, although we used horse BChE in our biochemical studies, the only mammalian structures for BChE in the PDB were mouse (two structures with covalently bound ligands) and human (22 structures; we selected the one with the best resolution and no ligands). We chose not to study CaE at this time, because there were no structures meeting all our criteria; the

two human structures met all but the last criterion, but ligand binding to the active site or sites of this enzyme are insufficiently characterized. Finally, although a homology model of the active site domain of NTE has been published [46], there are currently no X-ray structures of NTE available.

The flexible structures of several representative POX molecules were docked into the rigid enzyme structures of AChE and BChE using AutoDock 4.2 [47]. The low-energy binding poses having the appropriate ligand orientation for subsequent phosphorylation (oxime leaving group towards the exit, phosphorus atom close to active site Ser203/Ser198 hydroxyl, phosphoryl oxygen toward the oxyanion region Gly121-122/Gly116-117, respectively) were selected and further optimized using the Tripos force field in SYBYL- X 1.2 [48].

## 3. Results and discussion

### Overview of results

*Fragmental descriptors modelling*

Two kinds of descriptors were included in the QSAR study: fragmental descriptors of up to eight non-hydrogen atoms (with 'labelled' phosphorus atom) and the lipophilicity (LogP) estimated using the neural network model [36]. As described above, BPNN and FSMLR modelling techniques were used in the framework of the double cross-validation procedure. The statistical characteristics of the models are presented in Table 2.

The results clearly demonstrate rather strong correlation between log $k_i$ of all four esterases and the fragment composition and lipophilicity of their inhibitors. The QSAR models for their pair-wise selectivities are sufficiently strong to predict selectivity and reveal factors governing it (with the exception of the BChE/NTE selectivity), although their statistical performance is worse than that of the individual enzyme models.

Table 2. Statistical performance of FSMLR and BPNN models.

| | *FSMLR* | | | | *BPNN* | | | |
|---|---|---|---|---|---|---|---|---|
| *Endpoint* | *n* | $Q^2_{DCV}$ | $RMSE_{DCV}$ | $MAE_{DCV}$ | *n* | $Q^2_{DCV}$ | $RMSE_{DCV}$ | $MAE_{DCV}$ |
| $A_A$ | 58 | 0.772 | 0.536 | 0.391 | 58 | 0.793 | 0.511 | 0.374 |
| $A_B$ | 54 | 0.734 | 0.633 | 0.441 | 54 | 0.755 | 0.608 | 0.454 |
| $A_N$ | 35 | 0.778 | 0.599 | 0.487 | 35 | 0.800 | 0.569 | 0.446 |
| $A_C$ | 51 | 0.759 | 0.714 | 0.542 | 51 | 0.787 | 0.672 | 0.465 |
| $S_{BA}$ | 54 | 0.605 | 0.462 | 0.357 | 54 | 0.687 | 0.411 | 0.331 |
| $S_{NA}$ | 35 | 0.637 | 0.840 | 0.688 | 35 | 0.673 | 0.796 | 0.599 |
| $S_{CA}$ | 51 | 0.605 | 0.723 | 0.575 | 51 | 0.747 | 0.578 | 0.442 |
| $S_{BN}$ | 33 | 0.180 | 1.011 | 0.754 | 33 | 0.323 | 0.839 | 0.586 |
| $S_{CN}$ | 30 | 0.630 | 0.637 | 0.489 | 30 | 0.601 | 0.661 | 0.495 |

Note: *n* – number of compounds; $Q^2_{DCV}$ – determination coefficient for double cross-validation; $RMSE_{DCV}$ – root-mean-square error of prediction for double cross-validation; $MAE_{DCV}$ – the mean absolute error of prediction for double cross-validation.

The relative importance of descriptors was determined by the number of models into which they are selected by the FSMLR procedure. The most important descriptors (in order of decreasing importance) for each of the properties are listed in Table 3.

Table 3. The most important descriptors (in the order of decreasing importance) for each of the properties in the fragmental descriptor models.

| Endpoint | Descriptors and the sign of their influence |
|---|---|
| $A_A$ | (+) Cl–C–C=N–O–P; (–) C–C–C=N–O–P; (+) F–C=N–O–P; (+) $CH_3$–P(=O)(–O)$_2$ |
| $A_B$ | (+) LogP; (+) Cl–C–C=N–O–P; (+) F–C–C=N–O–P; (–) C–C–C=N–O–P; (+) $CH_3$-P(=O)( –O)$_2$ |
| $A_N$ | (+) LogP; (+) Ph–P(=O)(–O)$_2$; (+) Cl–C–C=N–O–P; (–) C–C–C=N–O–P; (–) C–O–P; (+) C–C–C–O–P |
| $A_C$ | (–) $CH_3$–P(=O)(–O)$_2$; (+) LogP; (–) C–C–C=N–O–P; (+) F–C–C=N–O–P; (+) Cl–C–C=N–O–P |
| $S_{BA}$ | (+) Ph–P(=O)(–O)$_2$; (+) LogP; (+) C–O–P; (–) C–C=N–O–P; (–) $CH_3$–C–O–P |
| $S_{NA}$ | (+) Ph–P(=O)(–O)$_2$; (–) C–O–P; (+) LogP; (+) $CH_3$–$CH_2$–$CH_2$–$CH_2$–O–P; (–-) C–C–C–O–P |
| $S_{CA}$ | (–) $CH_3$–P(=O)(–O)$_2$; (+) Ph–P(=O)(–O)$_2$; (–) C–O–P; (–) C–C–C–O–P; (+) $CH_3$–$CH_2$–$CH_2$–$CH_2$–O–P |
| $S_{BN}$ | (–) Ph–P(=O)( –O)$_2$; (+) C–C=N–O–P; (+) Cl–C–C=N–O–P; (–) LogP; (–) $CH_3$–P(=O)( –O)$_2$ |
| $S_{CN}$ | (+) O–P; (–) C–C–O–P; (+) C–C=N–O–P; (–) $CH_3$–P(=O)(–O)$_2$ (–) C–C–C–O–P |

*MFTA modelling*

The MFTA models were constructed for all the activity and selectivity endpoints. The structure of the molecular supergraph and the example superimposition for compound **54** are shown in Figure 6.

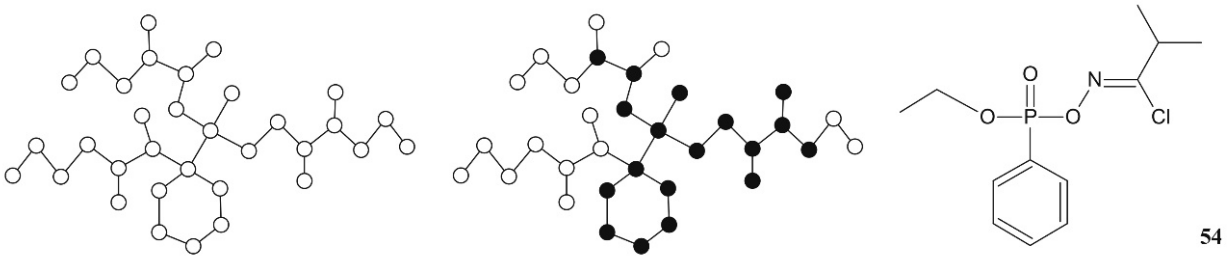


**Figure 6.** Structure of the molecular supergraph and the example superimposition for compound **54**.

Optimal results were obtained when using the following local molecular descriptors [38,39]: the effective charge, Q, on an atom, estimated by electronegativity equalization; the effective van der Waals radius, Re, which takes into account the steric requirements of the central non-hydrogen atom and other atoms bound to it; and the group lipophilicity, Lg, which takes into account the contributions of the central non-hydrogen atom and the hydrogen atoms bound to it. The statistical parameters of the

models are shown in Table 4. All of them provide good or reasonable predictivity. The activity and selectivity maps derived from them are shown in Figure 7.

Table 4. Statistical performance of the MFTA models.

| Endpoint | *n* | $N_F$ | $r^2$ | *RMSE* | $Q^2$ | $RMSE_{cv}$ |
|---|---|---|---|---|---|---|
| $A_A$ | 58 | 6 | 0.91 | 0.33 | 0.73 | 0.58 |
| $A_B$ | 54 | 6 | 0.89 | 0.40 | 0.71 | 0.67 |
| $A_N$ | 35 | 6 | 0.96 | 0.26 | 0.82 | 0.55 |
| $A_C$ | 51 | 6 | 0.94 | 0.40 | 0.83 | 0.68 |
| $S_{BA}$ | 54 | 4 | 0.83 | 0.30 | 0.69 | 0.41 |
| $S_{NA}$ | 35 | 2 | 0.80 | 0.61 | 0.70 | 0.77 |
| $S_{CA}$ | 51 | 2 | 0.80 | 0.52 | 0.72 | 0.62 |
| $S_{BN}$ | 33 | 2 | 0.67 | 0.59 | 0.46 | 0.76 |
| $S_{CN}$ | 30 | 2 | 0.70 | 0.58 | 0.48 | 0.79 |
| $S_{CB}$ | 50 | 2 | 0.62 | 0.52 | 0.44 | 0.64 |
| $A_{AN}$[a] | 35 | 6 | 0.91 | 0.24 | 0.57 | 0.53 |
| $S_{B\|AN}$[a] | 33 | 5 | 0.83 | 0.24 | 0.47 | 0.43 |

Notes: *n* - number of compounds; $N_F$ - number of factors in the PLSR model; $r^2$ - squared correlation coefficient; *RMSE* - root-mean-square error; $Q^2$ - cross-validation parameter; $RMSE_{cv}$ - root-mean-square error for cross validation.

[a] Additional objective parameters for optimization of activity profile discussed in Section 3.3.

### *CoMSIA modelling*

The CoMSIA models were constructed for some of the activity and selectivity endpoints using the steric, electrostatic and hydrophobic field descriptors. The statistical parameters of the models are shown in Table 5. Generally, the quality of the models is similar to that for the MFTA approach. The activity and selectivity maps derived from the models are shown in Figure 8.

Table 5. Statistical performance of CoMSIA models.

| Endpoint | *n* | $N_F$ | $r^2$ | *RMSE* | $Q^2$ |
|---|---|---|---|---|---|
| AA | 58 | 4 | 0.89 | 0.40 | 0.80 |
| $A_B$ | 54 | 4 | 0.87 | 0.46 | 0.76 |
| $A_N$ | 35 | 4 | 0.93 | 0.38 | 0.84 |
| SBA | 54 | 4 | 0.81 | 0.33 | 0.62 |
| SNA | 35 | 3 | 0.84 | 0.58 | 0.73 |

Notes: *n* - number of compounds; $N_F$ - number of factors in the PLSR model; $r^2$ - squared correlation coefficient; *RMSE* - root-mean-square error; $Q^2$ - cross-validation parameter.

## Discussion: Factors controlling activity and selectivity

### *Inhibitor activity*

**AChE inhibitor activity**. As can be seen from Table 3, the uniqueness of AChE among the four EOHs under study lies in the relatively low importance of total lipophilicity (LogP) of POXs for their inhibitor activity. This is in agreement with the results of the MFTA study (no dominant effect of lipophilicity in different positions). Another important factor is the potency-enhancing role of the $CCl_2$ group; this was revealed by

fragmental descriptors as well as by MFTA (electrostatic and lipophilic contributions) and CoMSIA (lipophilic field).

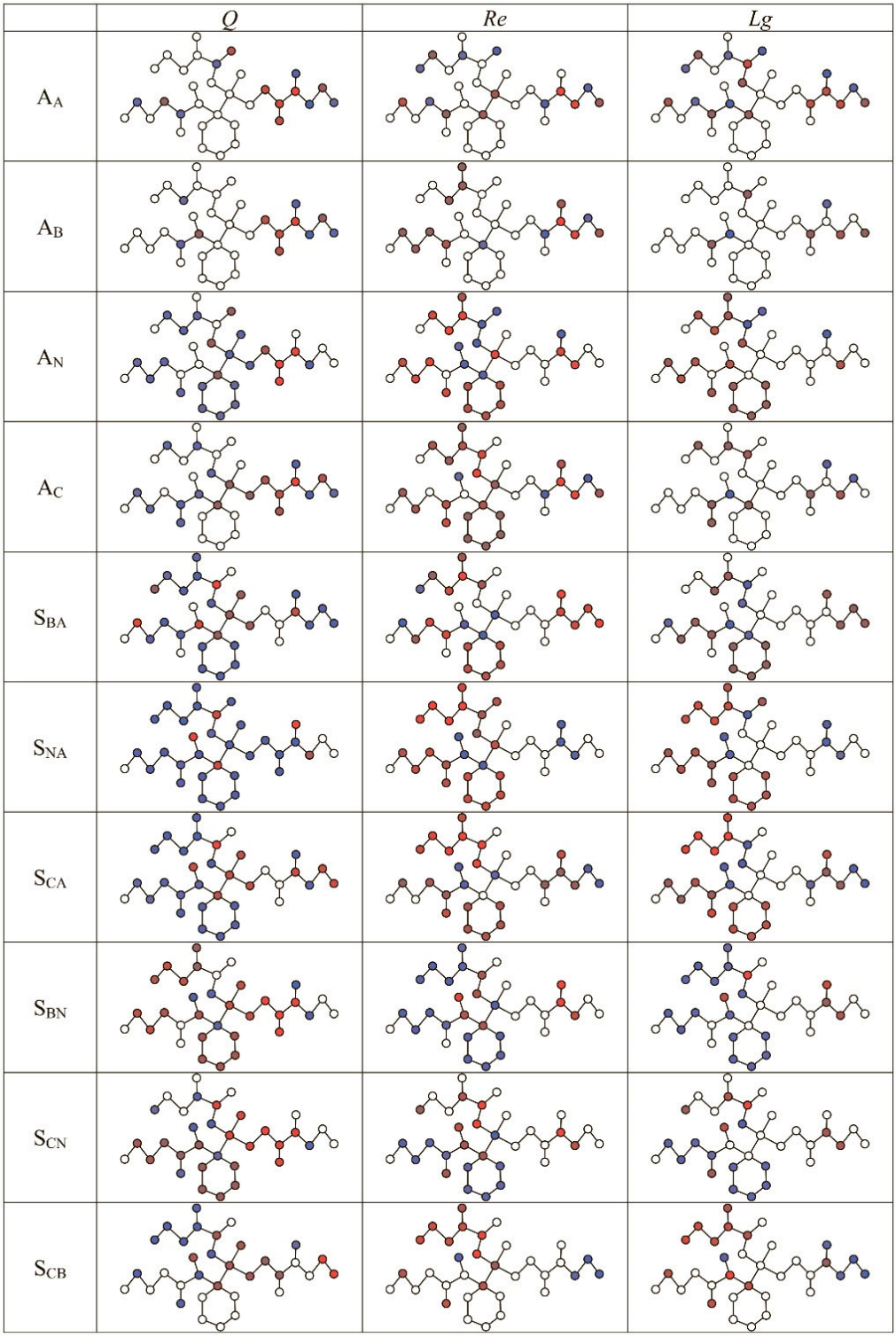


**Figure 7.** MFTA activity and selectivity maps for the esterase inhibition by POXs. A coloured version of this figure is available in the online edition of the paper. In positions marked with the black circles (red in the online edition), an increase in the descriptor, all other things being equal, tends to increase the activity (selectivity) of compounds. In positions marked with the gray circles (blue in the online edition), an increase in the descriptor, conversely, is accompanied by a probable decrease in the activity. Intensity of colours in the online edition of the paper reflects the magnitude of the influence.

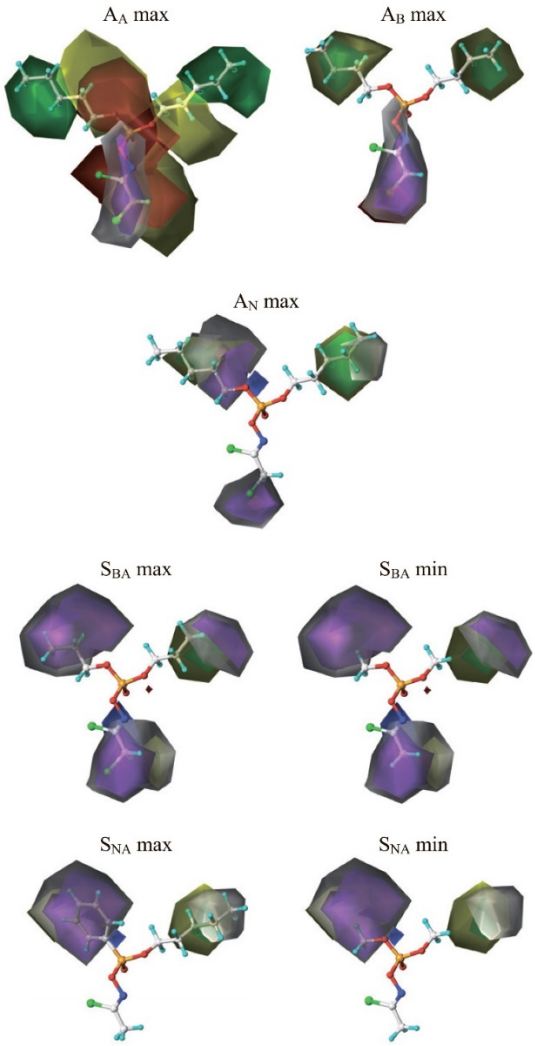


**Figure 8.** CoMSIA activity and selectivity maps for the esterase inhibition by POXs. For the steric field, in yellow-coloured regions additional steric bulk is detrimental for activity and in greencoloured regions it is favourable. For the electrostatic field, in red-coloured regions activity should be increased by additional negative charge and in blue-coloured regions by additional positive charge. For the hydrophobic field, in magenta-coloured regions activity should be increased by hydrophobic groups and in grey-coloured regions by hydrophilic groups. For the sake of clarity, in activity maps the structure of the most active compound is overlaid: **18** for AChE, **17** for BChE and **13** for NTE. In selectivity maps, two structures are shown: for $S_{BA}$, **16** is most selective to BChE and **1** is most selective to AChE; for $S_{NA}$, **50** is most selective to NTE and **1** is most selective to AChE.

The fragmental descriptor data in Table 3 also indicate the favouring influence of fluorine and the disfavouring influence of alkyl chains in the oxime moiety, as well as the favouring influence of an alkyl group attached to phosphorus. These conclusions are not as evident from the MFTA and CoMSIA analyses. Thus, the results of the three different modelling approaches verify and complement each other.

**BChE inhibitor activity**. Fragmental descriptor data in Table 3 indicate that lipophilicity is the most important factor for exerting inhibitor activity with regard to BChE (in contrast to AChE). Other structural factors revealed by regression analysis with fragmental descriptors are the same as in the case of AChE, i.e. the favouring influence

of the $CCl_2$ group and fluorine and the disfavouring influence of alkyl chains in the oxime moiety, as well as the favouring influence of an alkyl group attached to the phosphorus atom. Similar conclusions, i.e., the favouring role of the $CCl_2$ group in the oxime moiety and alkyl $C_2$-$C_5$ in the phosphoryl moiety, can be extracted from the MFTA analysis. By analysing the CoMSIA maps, one can also draw a conclusion about the favouring role of the $CCl_2$ group in the oxime moiety (from the lipophilic field map) and of long alkyl groups in the phosphoryl moiety (from the steric field map). Thus, for this kind of activity, all the different approaches completely agree with each other regarding the factors governing inhibitor activity of POXs toward BChE.

**NTE inhibitor activity**. All three methods clearly indicate the very important role of the total lipophilicity of POX inhibitors for anti-EOH activity toward NTE. Substructural analysis shown in Table 3 reveals a new factor, which also appears to be very important for this kind of activity, i.e. a phenyl group attached to the phosphorus atom, while all other substructures are actually the same as in the previous cases but with lower relative importance. This result is compatible with conclusions that can be drawn from the MFTA and CoMSIA analyses. In the latter case, the importance of an alkyl and phenyl group in the phosphoryl moiety follows from the steric and lipophilic molecular field maps.

**CaE inhibitor activity**. One can see from Table 3 that the main factors governing the inhibitor activity of POXs toward CaE are the same as in the case of AChE and BChE, but their relative importance is different: for CaE the influence of alkyl group in the phosphoryl moiety prevails over the influence of substituents in the oxime moiety. This conclusion is also in agreement with the results of the MFTA studies.

*Inhibitor selectivity*

From the discussion above it is evident that the inhibitor activity of POXs toward different EOHs is affected mostly by the same factors and structural features, and their selectivity depends on the complex interplay of subtle differences in their structures as well as in the relative importance of various factors. Thus, separate structure-selectivity models can provide a more focused picture of different factors controlling the selectivity.

**Selectivity toward BChE versus AChE**. As follows from Table 3, the major factors governing selectivity of POXs toward BChE versus AChE are the phenyl group attached to the phosphorus atom, the total lipophilicity, and the length of the phosphoryl and oxime moieties. A positive influence of the phenyl group, as well as positive influence of relatively short alkoxy groups attached to the phosphorus atom (up to $C_2$-$C_4$) and a negative influence of longer groups are also evident from the MFTA and

CoMSIA models (Figure 9). The latter factor can be explained by different sizes of the cavity inside the binding sites of these enzymes.

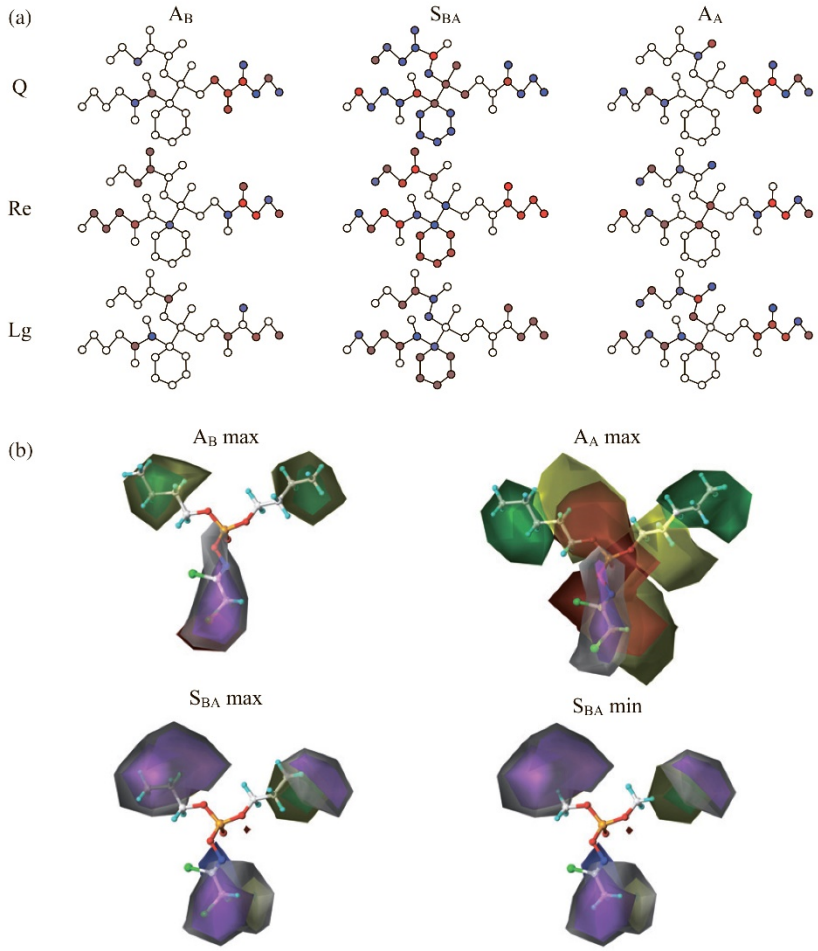


**Figure 9.** Detailed analysis of factors controlling the selectivity to BChE vs. AChE in the framework of the MFTA (a) and CoMSIA (b) approaches. For notation see Figures 7 and 8, respectively.

This is illustrated by the optimized structures of the POX-EOH complexes shown in Figure 10. In the relatively tight pocket of AChE, the long alkyl groups tend to assume a partially folded conformation, while in the larger pocket of BChE they are more extended. However, a smaller hydrophobic zone in the BChE binding site may hinder the packing of longer alkyl chains. On the other hand, for smaller low- activity compounds, the binding mode that is favourable for the reaction is not sufficiently stabilized.

**Selectivity toward NTE versus AChE**. According to the substructural analysis, the major factors influencing the selectivity toward NTE versus AChE are the phenyl and alkoxy groups attached to the phosphorus atom, as well as the total lipophilicity.

Strong positive effects of these factors are also prominently shown by the MFTA analysis (Figure 7). CoMSIA-based selectivity fields confirm the preference for phenylphosphonate groups and longer alkylphosphate chains by NTE. AChE-selective inhibitors attain a much worse match to these fields.

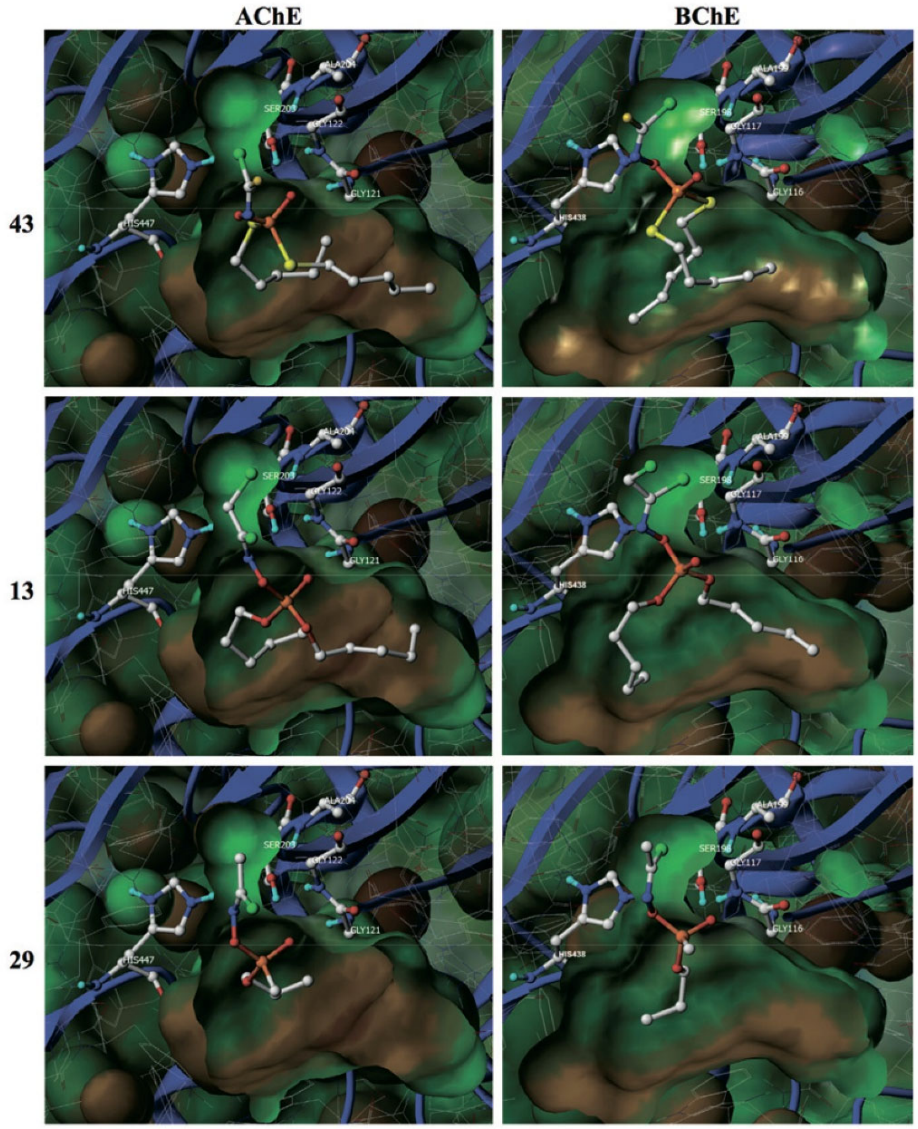


**Figure 10.** Models of the POX-EOH complexes obtained by docking to the rigid enzyme followed by molecular mechanics optimization using the Tripos force field. The Connolly surface is coloured by the molecular lipophilic potential. The following representative compounds were selected: **43** is a high-activity inhibitor slightly more selective for AChE; **13** is a high-activity inhibitor selective for BChE, and **29** is a low-activity non-selective inhibitor. For clarity of comparison, the protein conformation from the AChE-**43** complex is shown in all AChE images, and the protein conformation from the BChE-**13** complex is shown in all BChE images.

**Selectivity toward CaE versus AChE**. According to the substructural analysis presented in Table 3, the main factors governing the selectivity to CaE versus AChE are methyl, phenyl and alkoxy groups attached to the phosphorus atom. The importance of these groups follows also from the MFTA analysis. Nonetheless, some conclusions from these approaches are different. For example, the MFTA analysis indicates the importance of lipophilicity for this kind of selectivity, which is not supported by the substructural analysis.

**Selectivity toward BChE versus NTE**. Although the statistical quality of the MFTA and fragmental descriptor models for the selectivity toward BChE versus NTE is moderate, they both exactly agree on the major factors influencing this kind of selectivity: the $CCl_2$ group in the oxime moiety (positive influence), relatively short alkyl group in the phosphoryl moiety (positive influence), total lipophilicity (negative influence), and methyl and phenyl groups attached to the phosphorus atom (negative influence).

**Selectivity toward CaE versus NTE**. For the selectivity toward CaE versus NTE, the substructural analysis and MFTA lead to different conclusions. For example, MFTA suggests the importance of the $CCl_2$ group in the oxime moiety (weak positive influence) and of total lipophilicity (negative influence), which is not supported by the substructural analysis. The conclusions from these analyses are probably less reliable than in the previous cases. This underlines the importance of applying different methods and searching for consensus between them in order to draw well-grounded conclusions.

**Selectivity toward CaE versus BChE**. According to the MFTA analysis, the major factors governing the selectivity toward CaE versus BChE are a positive charge in the oxime moiety and the presence of alkyl group in the phosphoryl moiety, as well as the total lipophilicity.

## Molecular design of selective and safe esterase inhibitors

The selective BChE inhibitors suitable for use as novel anti-Alzheimer drugs should have high selectivity toward BChE, low activity toward AChE, very low or no activity toward NTE, and possibly moderate activity toward CaE. This multi-target/multi-objective optimization problem is difficult to solve based on the consideration of individual activities and selectivities. We believe [49] that in such cases it is beneficial to introduce integral parameters of positive and negative effects that are based on domain knowledge and easily interpretable. These parameters can be constructed as generalized mean values of the respective individual activities. In this study, the power-3 (cubic) mean was used as a simple function that increases monotonically with increasing individual values while being partially dominated by larger values. Other parameters, for example exponential mean or maximum/minimum values, may also be used.

Thus, we introduce the integral AChE and NTE inhibitor activity parameter as $A_{AN} = [1/2(A^3_A + A^3_N)]^{1/3}$. The main objective parameter for optimization, selectivity toward BChE versus AChE and NTE, is then defined as $S_B|_{AN} = A_B - A_{AN}$. The statistical characteristics of the MFTA models for these parameters are also shown in Table 4.

The selectivity maps for $A_B$, $A_{AN}$ and $S_B|_{AN}$ are shown in Figure 11.

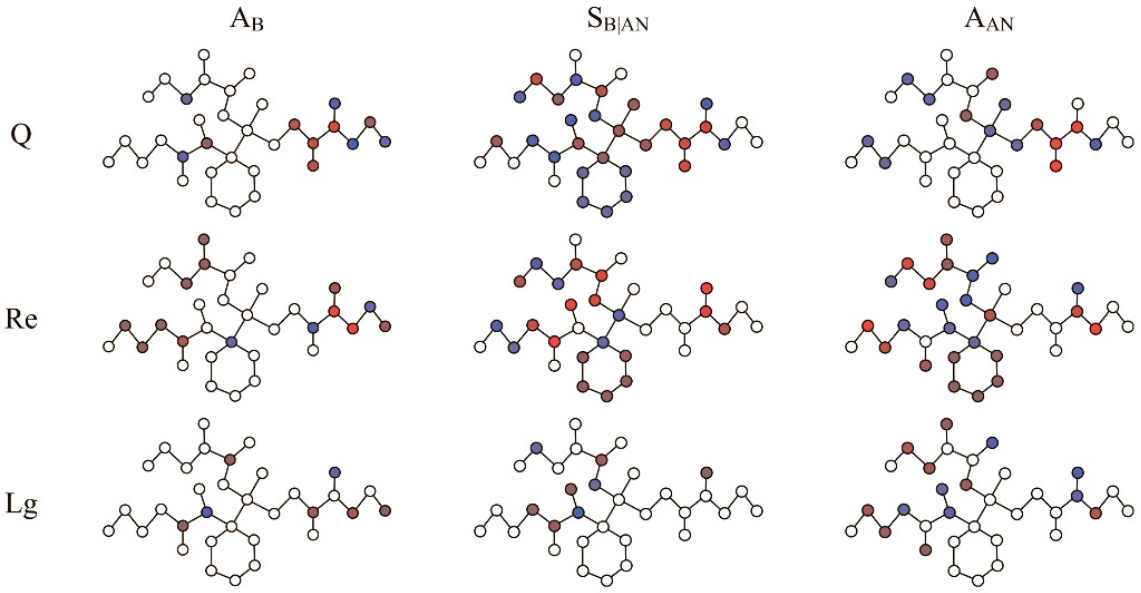


**Figure 11.** MFTA activity and selectivity maps for the activity profile optimization of POXs. For notation see Figure 7. A coloured version of this figure is available in the online edition of the paper.

It can be seen that short-chain branched alkoxy substituents are preferred, but the whole picture of influence is rather complicated. For this reason, we have performed virtual screening [39] of potential selective BChE inhibitors in a generated structure library of POXs. The library was built from the MFTA model supergraph by means of the specialized MFTA-oriented structure generator [50] developed by us. The total number of structures was 19,136. After the applicability domain filtering using the PLSR outlier scores, a set of 4631 structures was obtained that covers a wide range of activity and selectivity (Figure 12).

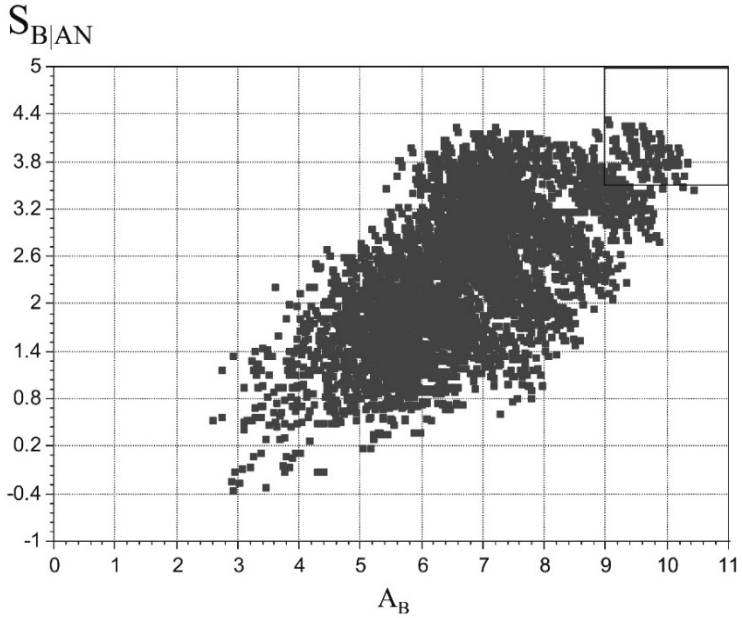


**Figure 12.** Distribution of selectivity and activity toward BChE in the generated structure library of POXs. The box in the upper right-hand corner marks the desired property range.

From it, a focused library of 116 structures was selected that provides high predicted selectivity and activity toward BChE ($S_B|_{AN} > 3.5$, $A_B > 9$); this is represented by the box in the upper right-hand corner of Figure 12. Some of the proposed structures from this focused library are shown in Figure 13.

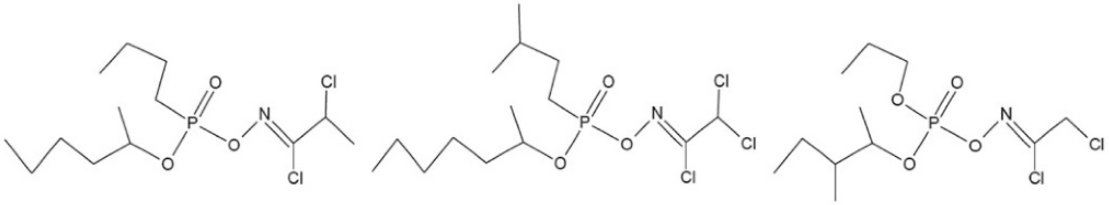

**Figure 13.** Sample structures with high predicted selectivity and activity toward BChE.

## 4. Conclusions

The relationships between the structure of POXs and their inhibitor activity and selectivity to four pharmacologically and toxicologically important EOHs were successfully analysed by means of several different approaches, including linear regression and artificial neural networks based on the fragmental descriptors, MFTA (2D QSAR), and CoMSIA (3D QSAR), as well as molecular modelling. Despite substantially different principles, all methods provide mutually consistent and complementary insights into structural features controlling the anti-EOH activity and selectivity of POXs. Moreover, MFTA models can support the design of promising compounds having a desired esterase profile, for example, novel anti-Alzheimer drugs. This work has been in a pharmacodynamic context, and further work will be required at the physiological level to determine the effectiveness of our predictions in a pharmacokinetic context.

## Acknowledgements

The authors gratefully acknowledge the support of this work by the Russian Foundation for Basic Research (RFBR, grants no. 11-03-00581 and 11-03-01174), Ministry of Education and Science of Russia (Federal Program ‘Scientists and Educators for Innovative Russia’ 2009-2013), and Russian Academy of Sciences (RAS).

## References

1. R.J. Richardson, R.M. Worden, and G.F. Makhaeva, *Biomarkers and biosensors of delayed neuropathic agents, in Handbook of Toxicology of Chemical Warfare Agents*, R.C. Gupta, ed., Academic Press/Elsevier, Amsterdam, 2009, pp. 859-876.
2. R.K. Sit, Z. Radic, V. Gerardi, L. Zhang, E. Garcia, M. Katalinic, G. Amitai, Z. Kovarik, V.V. Fokin, K.B. Sharpless, and P. Taylor, *New structural scaffolds for centrally acting oxime reactivators of phosphylated cholinesterases,* J. Biol. Chem. 286 (2011), pp. 19422-19430.

3. C.M. Thompson and R.J. Richardson, *Anticholinesterase insecticides, in Pesticide Toxicology and International Regulation*, T.C. Marrs and B. Ballantyne, eds., Wiley, New York, 2004, pp. 89-127.

4. H. Leader, A. Vincze, B. Manisterski, N. Rothschild, C. Dosoretz, and Y. Ashani, *Characterization of O,O-diethylphosphoryl oximes as inhibitors of cholinesterases and substrates of phosphotriesterases,* Biochem. Pharmacol. 58 (1999), pp. 503-515.

5. C. Luo, A. Saxena, M. Smith, G. Garcia, Z. Radic, P. Taylor, and B.P. Doctor, *Phosphoryl oxime inhibition of acetylcholinesterase during oxime reactivation is prevented by edrophonium*, Biochemistry 38 (1999), pp. 9937-9947.

6. C. Becker, F. Worek, and H. John, *Chromatographic analysis of toxic phosphylated oximes (POX): A brief overview*, Drug Test. Anal. 2 (2010), pp. 460-468.

7. E.V. Radchenko, G.F. Makhaeva, V.B. Sokolov, V.A. Palyulin, and N.S. Zefirov, *Study of the structural determinants of acute and delayed neurotoxicity of O-phosphorylated oximes by molecular field topology analysis (MFTA)*, Dokl. Biochem. Biophys. 429 (2009), pp. 309-314.

8. G. Makhaeva, I. Filonenko, S. Fomicheva, and V. Malygin, *''Esterase profiles'' of O,O-dialkyl- O-dimethyl-chloroformiminophosphates in prediction of their toxic effects*, Toxicol. Lett. 88 (Suppl. 1) (1996), p. 25.

9. G.F. Makhaeva, O.G. Serebryakova, N.P. Boltneva, T.G. Galenko, A.Y. Aksinenko, V.B. Sokolov, and I.V. Martynov, *Esterase profile and analysis of structure-inhibitor selectivity relationships for homologous phosphorylated 1-hydroperfluoroisopropanols*, Dokl. Biochem. Biophys. 423 (2008), pp. 352-357.

10. R.J. Richardson, *Anticholinesterase insecticides*, in *Comprehensive Toxicology*, Vol. 13, C.A. McQueen, ed., Elsevier, Oxford, 2010, pp. 433-444.

11. S.J. Wijeyesakere and R.J. Richardson, *Neuropathy target esterase*, in in *Hayes' Handbook of Pesticide Toxicology*, R. Krieger, ed., Academic Press/Elsevier, New York, 2010, pp. 1435-1455.

12. D.M. Maxwell and K.M. Brecht, *Carboxylesterase: Specificity and spontaneous reactivation of an endogenous scavenger for organophosphorus compounds*, J. Appl. Toxicol. 21 (2001), pp. S103-S107.

13. P. Masson and O. Lockridge, *Butyrylcholinesterase for protection from organophosphorus poisons: Catalytic complexities and hysteretic behavior*, Arch. Biochem. Biophys. 494 (2010), pp. 107-120.

14. Y. Furukawa-Hibi, T. Alkam, A. Nitta, A. Matsuyama, H. Mizoguchi, K. Suzuki, S. Moussaoui, Q.S. Yu, N.H. Greig, T. Nagai, and K. Yamada, *Butyrylcholinesterase inhibitors ameliorate cognitive dysfunction induced by amyloid-fl peptide in mice,* Behav. Brain Res. 225 (2011), pp. 222-229.

15. R.M. Lane, S.G. Potkin, and A. Enz, *Targeting acetylcholinesterase and butyrylcholinesterase in dementia*, Int. J. Neuropsychopharmacol. 9 (2006), pp. 101-124.

16. E.V. Radchenko, G.F. Makhaeva, V.V. Malygin, V.B. Sokolov, V.A. Palyulin, and N.S. Zefirov, *Modeling of the relationships between the structure of O-phosphorylated oximes*

*and their anticholinesterase activity and selectivity using molecular field topology analysis (MFTA)*, Dokl. Biochem. Biophys. 418 (2008), pp. 47-51.

17. M. Lotti and M.K. Johnson, *Neurotoxicity of organophosphorus pesticides: Predictions can be based on in vitro studies with hen and human enzymes*, Arch. Toxicol. 41 (1978), pp. 215-221.

18. V.V. Malygin, V.B. Sokolov, R.J. Richardson, and G.F. Makhaeva, *Quantitative structure-activity relationships predict the delayed neurotoxicity potential of a series of O-alkyl-O-methylchloroformimino phenylphosphonates*, J. Toxicol. Environ. Health, Part A 66 (2003), pp. 611-625.

19. V.B. Sokolov, A.N. Ivanov, T.A. Epishina, and I.V. Martynov, *Reaction of alkyl hydrogen methylphosphonites with 1,1-dichloro-1-nitrosopropane*, J. Gen. Chem. USSR (Engl. Transl.) 57 (1987), pp. 845-846.

20. V.B. Sokolov, A.N. Ivanov, T.V. Goreva, T.A. Epishina, and I.V. Martynov, *O- Alkylchloroformimino-O-alkylmethylphosphonates*, Rus. Chem. Bull. 37 (1988), pp. 989-991.

21. A.N. Ivanov, T.A. Epishina, T.V. Goreva, V.B. Sokolov, and I.V. Martynov, Reaction of dialkyl *phosphites with 1,1-dichloronitrosoalkanes,* Rus. Chem. Bull. 36 (1987), pp. 204-205.

22. I.V. Martynov, A.N. Ivanov, T.A. Epishina, and V.B. Sokolov, *Reaction of polychloronitrosoethanes with phosphorous acid derivatives*, Rus. Chem. Bull. 36 (1987), pp. 1001-1003.

23. L.A. Chepakova, V.K. Brel, G.F. Makhaeva, V.L. Yankovskaya, B.K. Beznosko, V.V. Malygin, and I.V. Martynov, *Synthesis and antiesterase activity of sulfur containing O-phosphorylated oximes*, Pharm. Chem. J. 22 (1988), pp. 143-146.

24. G.F. Makhaeva, I.V. Kononova, V.V. Malygin, Iu.E. Liashenko, V.B. Sokolov, and I.V. Martynov, *O-alkyl-O-methylchlorformimmophenylphosphonates - effective inhibitors of hen brain neurotoxic esterase*, Dokl. Akad. Nauk SSSR. 317 (1991), pp. 1009-1012 (Russ.).

25. G.F. Makhaeva and V.V. Malygin, *A stable preparation of hen brain neuropathy target esterase for rapid biochemical assessment of neurotoxic potential of organophosphates*, Chem. Biol. Interact. 119-120 (1999), pp. 551-557.

26. G.F. Makhaeva, I.V. Filonenko, V.L. Yankovskaya, S.B. Fomicheva, and V.V. Malygin, *Comparative studies of O,O-dialkyl-O-chloromethylchloroformiminophosphates: Interaction with neuropathy target esterase and acetylcholinesterase*, Neurotoxicology 19 (1998), pp. 623-628.

27. G.F. Makhaeva, A.Y. Aksinenko, V.B. Sokolov, I.I. Baskin, V.A. Palyulin, N.S. Zefirov, N.D. Hein, J.W. Kampf, S.J. Wijeyesakere, and R.J. Richardson, *Kinetics and mechanism of inhibition of serine esterases by fluorinated aminophosphonates*, Chem. Biol. Interact. 187 (2010), pp. 177-184.

28. W.N. Aldridge and E. Reiner, *Enzyme Inhibitors as Substrates*, North Holland Publishing, Amsterdam, 1972, pp. 37-52.

29. *OriginPro 6.1*, OriginLab, Northampton, MA, 2000; software available at http://www.originlab.com

30. G.F. Makhaeva, V.V. Malygin, Sh.M. Yakubov, and S.M. Gorbunov, *Investigation of the relationship between structure and antiesterase activity in the series of O-phosphorylated*

*oximes. 1. Methylphosphonates*, Pharm. Chem. J. 28 (1994), pp. 367-371.

31. G.F. Makhaeva, V.V. Malygin, Sh.M. Yakubov, and S.M. Gorbunov, *Investigation of the relationship between structure and antiesterase activity in the series of O-phosphorylated oximes. II. Dialkylphosphates and methylphosphonates*, Pharm. Chem. J. 28 (1994), pp. 620-625.

32. G.F. Makhaeva, V.V. Malygin, and I.V. Martynov, *Assessment of the neurotoxic potential of some methyl- and phenylphosphonates using a stable preparation of neuropathy target esterase from chicken brain*, Dokl. Biochem. Biophys. 377 (2001), pp. 68-71.

33. A.Kh. Plyamovaty, I.I. Vandyukova, R.R. Shagidullin, G.F. Makhaeva, V.V. Malygin, and S.M. Gorbunov, *Studies of the relationships between three-dimensional structure and anticholinesterase activity for O-phosphorylated oximes*, Pharm. Chem. J. 31 (1997), pp. 199-204.

34. Baskin and A. Varnek, *Fragment descriptors in SAR/QSAR/QSPR studies, molecular similarity analysis and in virtual screening*, in *Chemoinformatics Approaches to Virtual Screening*, A. Varnek and A. Tropsha, eds., RSC, Cambridge, 2008, pp. 1-43.

35. N.I. Zhokhova, I.I. Baskin, V.A. Palyulin, A.N. Zefirov, and N.S. Zefirov, *Fragmental descriptors with labeled atoms and their application in QSAR/QSPR studies*, Dokl. Chem. 417 (2007), pp. 282-284.

36. N.V. Artemenko, I.I. Baskin, V.A. Palyulin, and N.S. Zefirov, *Prediction of physical properties of organic compounds using artificial neural networks within the substructure approach*, Dokl. Chem. 381 (2001), pp. 317-320.

37. I.I. Baskin, N.M. Halberstam, N.V. Artemenko, V.A. Palyulin, and N.S. Zefirov, *NASAWIN - a universal software for QSPR/QSAR studies*, in *EuroQSAR 2002 Designing Drugs and Crop Protectants: Processes, Problems and Solutions*, M. Ford, D. Livingstone, J. Dearden, and H. Waterbeemd, eds., Blackwell, Malden, 2003, pp. 260-263.

38. V.A. Palyulin, E.V. Radchenko, and N.S. Zefirov, *Molecular Field Topology Analysis method in QSAR studies of organic compounds*, J. Chem. Inf. Comp. Sci. 40 (2000), pp. 659-667.

39. E.V. Radchenko, V.A. Palyulin, and N.S. Zefirov, Molecular Field Topology Analysis in drug design and virtual screening, in Chemoinformatics Approaches to Virtual Screening, A. Varnek and A. Tropsha, eds., RSC, Cambridge, 2008, pp. 150-181.

40. E.V. Radchenko, V.A. Palyulin, and N.S. Zefirov, QSAR validation, descriptor selection, and the *quest for the best models,* in XVI Eur. *Symp. on Quantitative Structure-Activity Relationships and Molecular Modelling*, Italy, September 10-17, 2006, p. 207.

41. G. Klebe, U. Abraham, and T. Mietzner, *Molecular similarity indices in a comparative analysis (CoMSIA) of drug molecules to correlate and predict their biological activity*, J. Med. Chem. 37 (1994), pp. 4130-4146.

42. *SYBYL 8.0*, Tripos International, 1699 South Hanley Rd., St. Louis, Missouri, 63144, USA, 2008; software available at http://www.tripos.com

43. *Concord*, R.S. Pearlman, distributed by Tripos International, St. Louis, Missouri, 63144, USA, 2008; software available at http://www.tripos.com

44. Y. Bourne, Z. Radic, G. Sulzenbacher, E. Kim, P. Taylor, and P. Marchot, *Substrate and product trafficking through the active center gorge of acetylcholinesterase analyzed by crystallography and equilibrium binding*, J. Biol. Chem. 281 (2006), pp. 29256-29267.

45. Y. Nicolet, O. Lockridge, P. Masson, J.C. Fontecilla-Camps, and F. Nachon, *Crystal structure of human butyrylcholinesterase and of its complexes with substrate and products*, J. Biol. Chem. 278 (2003), pp. 41141-41147.

46. S.J. Wijeyesakere, R.J. Richardson, and J.A. Stuckey, *Modeling the tertiary structure of the patatin domain of neuropathy target esterase*, Protein J. 26 (2007), pp. 165-172.

47. G.M. Morris, R. Huey, W. Lindstrom, M.F. Sanner, R.K. Belew, D.S. Goodsell, and A.J. Olson, *AutoDock4 and AutoDockTools4: Automated docking with selective receptor flexibility*, J. Comput. Chem. 30 (2009), pp. 2785-2791.

48. *SYBYL-X 1.2*, Tripos International, 1699 South Hanley Rd., St. Louis, Missouri, 63144, USA, 2010; software available at http://www.tripos.com

49. E.V. Radchenko, A.A. Melnikov, G.F. Makhaeva, V.A. Palyulin, and N.S. Zefirov, *Molecular design of O-phosphorylated oximes - selective butyrylcholinesterase inhibitors*, Dokl. Biochem. Biophys. 443 (2012), pp. 91-95.

50. A.A. Melnikov, V.A. Palyulin, E.V. Radchenko, and N.S. Zefirov, *Generation of chemical structures on the basis of QSAR Models of Molecular Field Topology Analysis*, Dokl. Chem. 415 (2007), pp. 196-199.

*NEUROPROTECTIVE AGENTS*
*Серия книг: ANNALS OF THE NEW YORK ACADEMY OF SCIENCES*
*Vol. 939, pp. 425-435 (2001)*

# ANTIHISTAMINE AGENT DIMEBON AS A NOVEL NEUROPROTECTOR AND A COGNITION ENHANCER

**S. Bachurin, E. Bukatina, N. Lermontova, S. Tkachenko, A. Afanasiev, V. Grigoriev, I. Grigorieva, Yu. Ivanov, S. Sablin, N. Zefirov**

Dimebon, launched earlier in Russia as an antihistamine drug, was evaluated as a representative of a new generation of anti-Alzheimer's drugs that have two beneficial actions: (1) to alleviate symptoms, and (2) to prevent progression of the disease. The drug demonstrated cognition and memoryenhancing properties in the active avoidance test in rats treated with the neurotoxin AF64A, which selectively destroys cholinergic neurons. Dimebon protected neurons in the cerebellum cell culture against the neurotoxic action of P-amyloid fragment (Aβ25-35, $EC_{50}$ = 25 μM). *In vitro,* Dimebon displayed $Ca^{2+}$-blocking properties ($IC_{50}$ = 57 μM, on isolated rat ileum intestine) and pronounced anticholinesterase activity ($IC_{50}$ = 7.9 μM and 42

μM for butyrylcholine esterase and acetylcholine esterase, respectively). It also exhibited strong anti-NMDA activity in the prevention of NMDA-induced seizures in mice ($EC_{50}$ = 42 ± 6 mg/kg i.p.). A beneficial effect of Dimebon in the therapy of Alzheimer's disease was demonstrated in a pilot clinical trial performed in the Moscow Center of Gerontology. Fourteen patients who participated in the trial were evaluated for their state of personality and for the severity of the disease. The evaluation included orientation (space, place, time, and patient personality), memory for the past and present, life in present, speech, irritability, and so forth. During and after the eight-week therapy with Dimebon, cognitive and self-service functions of patients improved significantly, and psychopathic symptoms, anxiety, depression, tearfulness, and headache were substantially diminished. The results of these studies suggest Dimebon as a new candidate for the therapy of Alzheimer's-like disorders.

# INTRODUCTION

Alzheimer's disease is the most common form of dementia affecting millions of people in the world. It is characterized by the progressive degeneration and death of nerve cells in certain brain regions, leading to loss of intellectual abilities, such as thinking, memory, learning skills, language, and communication. The disease is also characterized by significant psychiatric and emotional problems, such as agitation, depression, delusions, and delirium. Pathological features include general atrophy of brain with a specific loss of cholinergic neurons resulting in a deficiency of the neurotransmitter acetylcholine. The cause of the disease remains unknown. Moreover, there are no FDA-approved medications that have any effect on the progression of the disease. Conventional therapies that are currently used in clinical practice are aimed at compensating for specific symptoms (cognitive function) associated with the loss of acetylcholine, using drugs to elevate the level of this neurotransmitter, as well as to compensate for associated psychiatric and emotional symptoms. Therefore, pharmacological strategies in searching for new effective therapies are focused on drugs that, not only improve cognitive functions, but also prevent the progression of the disease.

The key event that results in the progressive degeneration of cholinergic neurons in the brain of an Alzheimer's patient is thought to be the formation of в-amyloid peptide (Ае), which induces the neurotoxic effect of excitatory amino acids, glutamate and aspartate (for a recent review see Ref. 1). The toxic action of glutamate and aspartate is mediated through the activation of *N*-methyl-D-aspartate (NMDA) receptors. This activation leads to an increase in the intracellular $Ca^{2+}$ concentration that triggers a cascade of pathological reactions causing the death of nerve cells.[2-4] The disturbances of glutamatergic neurotransmission are thought to underlie the pathomechanism and cognitive deficits of Alzheimer's disease. Therefore, antagonists of $Ca^{2+}$ channels and NMDA receptors are currently a focus of interest for their potential use as neuroprotective agents in the treatment of this disease.[1,4-7]

In this report, we introduce Dimebon, which was launched previously in Russia as an antihistamine drug, as a new neuroprotective and cognition-enhancing agent for the potential use in the therapy of Alzheimer's disease. The properties of Dime- bon as an antagonist of $Ca^{2+}$ channels and NMDA receptors are evaluated. The results of a pilot open-label clinical study of the Dimebon treatment are also presented.

# MATERIALS AND METHODS

## Materials

Dimebon was provided by NPO Organika (Novokuznetsk, Russia). β-Amyloid peptide fragment (Aβ25-35) was purchased from Bachem. All other reagents were purchased from Sigma.

## General Methods

Effect of Dimebon on $Ca^{2+}$ channels was studied using rat ileum intestine. $Ca^{2+}$- induced contractions of segments of small intestine were recorded in the absence or in the presence of varied concentration of Dimebon using dynograph R-612, Beckman, USA.

The effects of Dimebon on the catalytic activities of acetylcholine esterase and butyrylcholine esterase were determined using partially purified enzyme preparations.

The activities of both enzymes were measured in the presence of varied concentration of the drug and monitored by the accumulation of thiocholine, a product of the hydrolysis of acetylthiocholine and butyryltiocholine by acetylcholine esterase and by butyrylcholine esterase, respectively. Thiocholine was detected spectrophotometrically in the reaction with a thiol reagent, 5,5'-dithio(bis)-nitrobenzoic acid, followed by the formation of the product of this reaction with maximum of absorbance at 412 nm.

Study of the anti-NMDA effect of Dimebon was conducted on white pedigreed male mice (20-24 g). A skin flap on the head of each mouse was removed under ether anesthesia, and a hole was drilled through the skull using a fine drill bit. A solution (1.4 μl) containing 0.1 μg of NMDA was injected into the lateral ventricle of the brain using a microsyringe. The solution also contained methylene blue dye for monitoring the accuracy of the injection. The needle was immersed to a depth of 2.5 mm. After the operation, the wound was treated with a 2% novocaine solution. A solution of Dimebon in 0.2 ml of 5% aqueous dimethylsulfoxide (for experimental animals) or physiological solution (for control animals) was injected intraperitoneally 40 minutes prior to the injection of NMDA. Mice were used for pharmacological experiments two to four hours after the operation. Each dose of Dimebon was tested in a group of six to eight

animals. The $ED_{50}$ value (the dose of the agent preventing the development of convulsions and the death of 50% of the animals) was determined by a probit analysis method.[8]

## Studies on the Neural Cell Culture

Neuroprotective properties of Dimebon against neurotoxicity induced by β-amyloid were studied on a culture of cerebellar granule cells (CGC). The CGC culture is a homogeneous population of nervous cells containing acetylcholine and NMDA receptors.[9] The mature cell culture in the media containing 25 mM KCl was incubated with varied concentrations of either β-amyloid fragment (Aβ25-35), or with Dimebon, or with both. The viability of cells was monitored by computerized count and by lactate dehydrogenase activity.

## Memory and Cognitive Skills Test

Studies of memory and cognitive skills were performed in the active avoidance test in rats treated (i.c.v.) with the cholinergic toxin AF64A that selectively destroys cholinergic neurons.[10,11] Male Wistar rats (250-300 g) were anesthetized with ether and placed into a stereotaxic frame. A cannula was inserted through the skull, and the solution of toxin AF64A (3 nmol/3 μl, bilaterally, experimental group) or artificial cerebrospinal fluid (vehicle group) were infused into each of the ventricles at a rate of 2-3 μl/min.

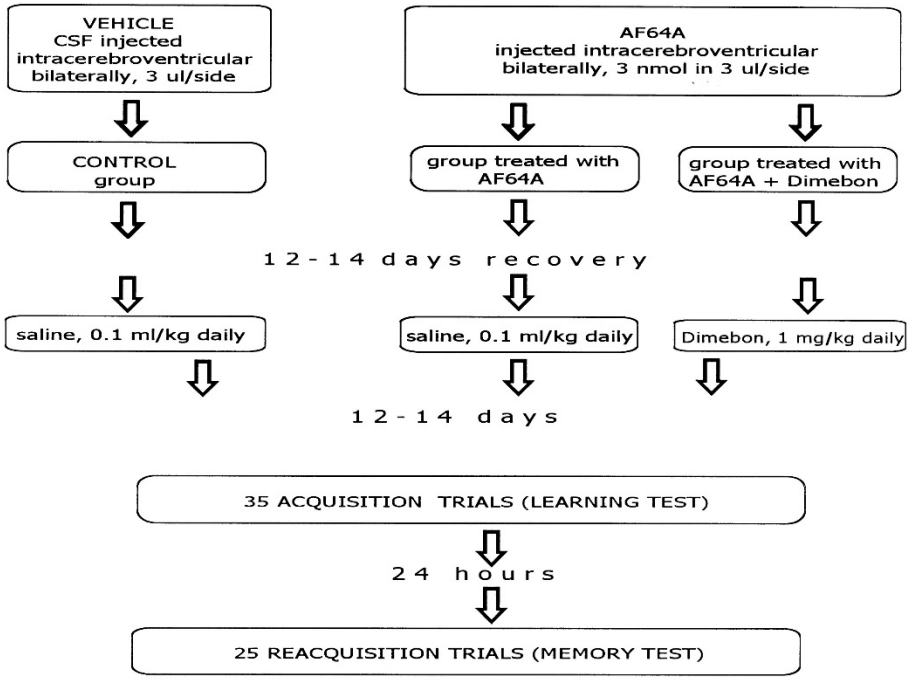


FIGURE 1. Scheme of the experiments on the evaluation of memory and learning skills of rats treated with cholinergic toxin AF64A.

On the second day after the surgery and during the next 10 days rats were injected (i.p.) daily, either with the physiological solution (vehicle group and one of the groups of AF64A treated rats) or with the solution containing 1 mg/kg Dimebon (other two groups of AF64A treated rats). Rats were allowed 12-14 days to recover from the surgery. They were then given 35 acquisition trials to perform an active conditioned avoidance response in two-way shuttle box with light and electrostimulation as conditioned and unconditioned stimulus, respectively (learning test). Within 24 hours all rats were given five reacquisition trials to test memory impairment (memory test). The scheme of trials is presented in FIGURE 1.

## Clinical Trial

Open label clinical trials were performed in the Moscow Center of Gerontology on 14 patients (1 male, 13 females, age ranging from 64 to 88 years old). All patients who participated in the trial were diagnosed with mild to moderate Alzheimer's disease. The diagnosis was made based on ICD-10 NINCDS ADRDA criteria.[12] The clinical diagnosis was confirmed by the computer tomography of the brain of each patient. Medical records indicated no dramatic change in the condition of patients for two years prior to the trial. Patients were treated for eight weeks with 60 mg (20 mg/dose, three times a day, orally) of Dimebon daily. Before the treatment, at the fourth and at the eighth week of the treatment, and on the eighth week after the treatment was discontinued, all patients were evaluated for the condition of personality and for the severity of the disease. The evaluation was performed according to the Hasegawa scale (similar to the Mini-Mental State examination) and according to the Bukatina scale (introduced in clinical practice, by one of the authors, in the Moscow Center of Gerontology). In brief, the evaluation included the orientation (in space, in place, in time, in the nearest surroundings, and the patient's personality), memory for the past and present, life in present, speech, irritability, articulation, concentration of attention, spirits, delirium, hallucinations, anxiety, headaches, dizziness, tearfulness, spontaneous activity, elementary self-service, and so forth. Statistical analysis was performed based on the Student's *t*-test and Fisher's $\phi$ criteria. During the trial patients were under continuous observation by psychiatrists, by the medical staff and by patients' family members.

# RESULTS

## Interaction of Dimebon with Biochemical Targets

Injection of NMDA into the lateral ventricle of the control mice (0.1 μg per mouse) resulted in hyperactivity of animals, expressed in running and jumping, followed by convulsions, and, ultimately, death. In the experimental group, animals were injected

with varying amounts of Dimebon before the NMDA solution was injected. The pre-injection of Dimebon prevented both development of convulsions and death of animals. Protection against NMDA toxicity by Dimebon was dose dependent. The value of $ED_{50}$ evaluated in these experiments is presented in TABLE 1.

TABLE 1. Effect of Dimebon on biochemical targets

| Inhibitor | | Antagonist | |
|---|---|---|---|
| AChE<br><br>IC50, μM | BuChE<br><br>IC50, μM | $Ca^{2+}$ channels<br><br>IC50, μM | NMDA receptors<br><br>$ED_{50}$, mg/kg, i.p. |
| 42 | 8.9 | 57 | 42 |

Calcium channel antagonist activity of Dimebon was determined using $Ca^{2+}$-dependent contraction of isolated smooth muscles of rat ileum intestine. It was shown that Dimebon suppressed contractions of smooth muscles in $Ca^{2+}$ containing media in a reversible and concentration dependent manner (TABLE 1).

The level of actetylcholine in the brain is regulated through its synthesis, transport, and degradation. Acetylcholine esterase (and to a lesser extent, butyrylcholine esterase) is the key enzyme that provides the degradation of this neurotransmitter. Inhibition of the enzyme results in the elevation of acetylcholine level associated with an improvement in cognitive functions. It was shown that Dimebon is a potent competitive and reversible inhibitor of both acetylcholine esterase and butyrylcholine esterase (SEE TABLE 1).

## Effect of Dimebon on Memory Function and Cognitive Skills

Administration of ethylcholine aziridinium ion, AF64A, in laboratory animals induces the degenerative loss of pyramidal neurons in the area CA3 of hyppocam- pus. This results in chronic cholinergic hypofunction and some neuropathological changes that are similar to changes observed in Alzheimer's disease.[10,11] A number of studies demonstrated that AF64A produced both learning and memory impairments in laboratory animals.[13-15]

We used rats treated with neurotoxin AF64A to evaluate memory- and cognition-enhancing properties of Dimebon in the active avoidance test. In our experiments, animals treated with AF64A exhibited a decrease in the performance during both the learning test and the memory test (response time to the electrostimulation and light was significantly greater). The treatment of animals in these groups with Dimebon, resulted in a remarkable improvement of learning skills and memory compared to the control group. The improvement was obvious, even in comparison with the experimental group treated with Tacrine under the same conditions (see FIGURE 2).

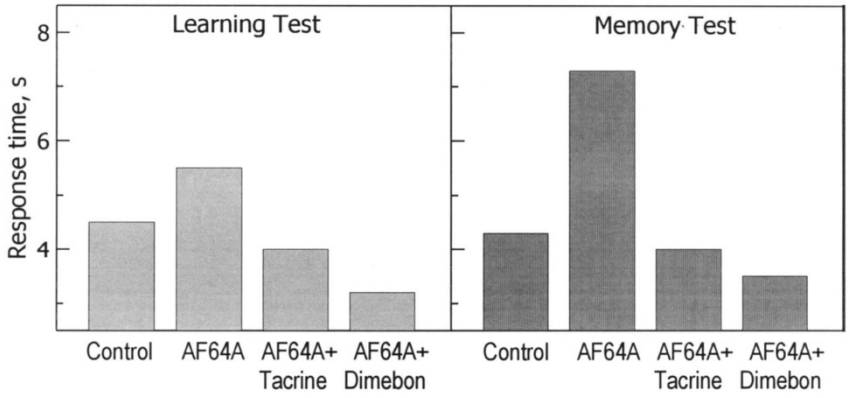


FIGURE 2. Dimebon-dependent improvement in memory and learning skills in rats treated with cholinergic toxin AF64A. Details of the experiment are provided in the text.

## Protective Effect of Dimebon Against Neurotoxicity Induced by β-amyloid Peptide in Cultured Cerebellar Granule Cells (CGC)

Incubation of mature CGC culture with Aβ25-35 led to a significant decrease in the viability of neural cells. The effect was dose-dependent ($IC_{50} = 25 \pm 8$ μM). Pronounced morphological changes, such as shrinking and fragmentation, of neurons were registered at the third day of incubation with Aβ25-35. Hence, test experiments were carried out at the fourth day of incubation of CGC with 25 μM Aβ25-35. FIGURE 3 shows that Dimebon in concentration of 25 μM increases the viability of CGC and brings the level of the survived cells up to the control.

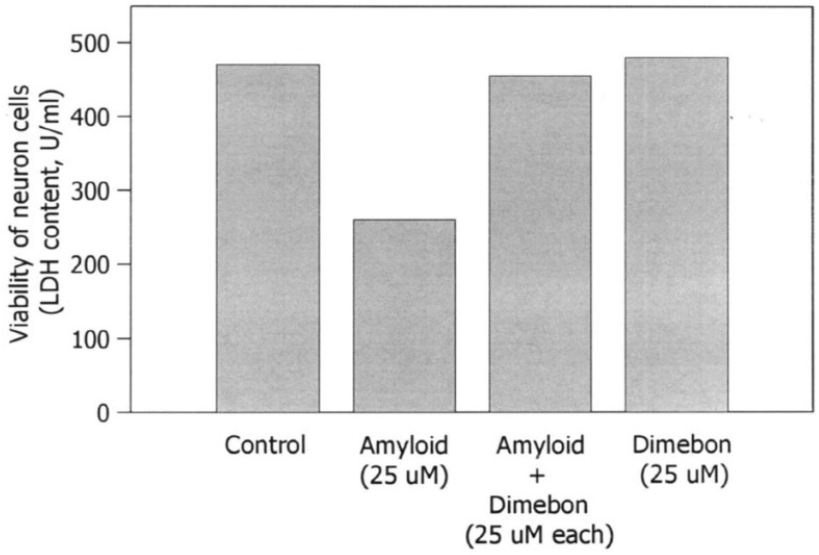


FIGURE 3. Dimebon-dependent increase of the viability of cells incubated with β-amyloid fragment Aβ25-35. Cultured neural cells were incubated for three days with either Aβ25-35, or with Dimebon, or both (25 μM each). The viability of cells incubated with Aβ25-35 is significantly decreased *(second bar)* compared to the control *(first bar).* Dimebon is not toxic to the cells *(fourth bar)* and protects them against the toxic effect of Aβ25-35 *(third bar).*

## Clinical Trial

The main objective of the study was to assess the efficacy of Dimebon in the treatment of patients with mild to moderate Alzheimer's disease.

TABLE 2. Results of the Dimebon clinical trial

| Function | Scores,[a] mean values | | | Changes in scores[b] | |
|---|---|---|---|---|---|
| | Week 0 | Week 4 | Week 8 | Week 4 | Week 8 |
| Cognition[c] | 6.29 ± 0.7 | 5.5 ± 0.79 | 3.93 ± 0.5 | +0.5 ± 0.14 | +1.79 ± 0.35 |
| Depression[c] Orientation | 1.1 ± 0.22 | 0.58 ± 0.18 | 0.58 ± 0.14 | +0.6 ± 0.11 | +0.6 ± 0.11 |
| in locality | 1.82 ± 0.19 | 1.75 ± 0.23 | 1.57 ± 0.23 | +0.11 ± 0.07 | +0.18 ± 0.08 |
| in space | 0.54 ± 0.16 | 0.32 ± 0.15 | 0.25 ± 0.13 | +0.11 ± 0.07 | +0.11 ± 0.07 |
| Memory | | | | | |
| for past | 2.34 ± 0.23 | 2.29 ± 0.21 | 1.93 ± 0.24 | +0.07 ± 0.07 | +0.29 ± 0.1 |
| for present | 2.38 ± 0.22 | 2.21 ± 0.22 | 1.86 ± 0.23 | 0 ± 0 | +0.29 ± 0.08 |
| Delirium | 0.91 ± 0.2 | 0.57 ± 0.29 | 0.5 ± 0.19 | +0.07 ± 0.09 | +0.25 ± 0.17 |
| Irritability | 0.57 ± 0.19 | 0.21 ± 0.15 | 0.14 ± 0.09 | +0.29 ± 0.13 | +0.36 ± 0.16 |
| Headaches | 1.02 ± 0.27 | 0.32 ± 0.21 | 0.64 ± 0.24 | +0.54 ± 0.21 | +0.21 ± 0.1 |
| Dizziness | 0.64 ± 0.19 | 0.71 ± 0.27 | 0.68 ± 0.25 | -0.14 ± 0.17 | -0.18 ± 0.22 |
| Tearfulness | 0.36 ± 0.18 | 0.2 ± 0.18 | 0.0 ± 0.0 | +0.14 ± 0.14 | +0.21 ± 0.15 |

[a] Bukatina scale: score 0 indicates the absence of a symptom; score 4 indicates the highest deterioration.
[b] + Indicates improvement; – indicates deterioration of function.
[c] Complex parameter that combines results of observations on relevant symptoms.

The treatment with Dimebon demonstrated a significant progressive improvement in cognitive functions of all patients participated in the trial. Mean improvements from the baseline were already observed at the fourth week of the trial, as assessed by both Hazegawa's scale and Bukatina scale. The improvements were even more profound after the eighth week of the therapy (see TABLE 2), and were more evident in patients with mild Alzheimer's disease. The improvement during the therapy is more evident on the background of dramatic deterioration in cognitive functions after the Dimebon treatment was discontinued. This was assessed at the evaluation eight weeks after the trial (see FIGURE 4).

Although the overall study was not placebo-controlled, cognitive functions were evaluated against a group of eight patients who received placebo for four weeks. The control group was not given any medication, which could influence cognitive functions of patients. The initial levels of patient dementia in both experimental and control groups were similar. After four weeks of therapy the changes in cognitive functions as evaluated by the Bukatina scale were $0.5 \pm 0.14$ and $0.12 \pm 0.12$ ($p < 0.01$) in the experimental and in the control group, respectively.

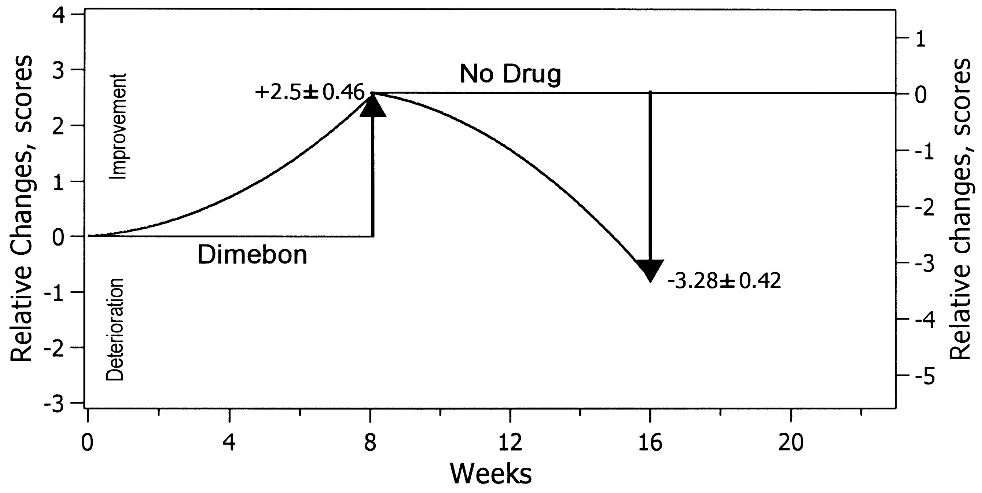


FIGURE 4. The effect of Dimebon treatment on cognitive functions of Alzheimer's patients. Patients were evaluated before the trial, at the fourth week and at the eighth week of Dimebon therapy, as well as eighth weeks after the therapy was discontinued.

Before the trial, 12 patients had various depressive symptoms. At the fourth week of therapy with Dimebon, the depressive symptoms abated in five patients. There was not a single case of deterioration or emergency depression. At the eighth week of the treatment, six other patients showed an improvement. One patient showed signs of aggravation. The mean values of depressive manifestations in 12 patients before the trial, and at the fourth and at the eighth week of the therapy were scored as 1.1 ± 0.22, 0.58 ± 0.18 and 0.58 ± 0.14, respectively (TABLE 2). The dynamics of depressive manifestations in patients suffering from evident depression prior to the treatment with Dimebon showed that the abatement of depression was significant at the eighth week of the treatment.

Ten patients complained having headaches during the observation period. Nine patients had headaches prior to the treatment. One patient had the first headache at the eighth week of treatment. Five patients (50% of patients having headaches) showed the abatement or complete cessation of headaches at the fourth week of treatment, and three more (80%) showed the same improvement after eight weeks.

Before the trial, five female patients suffered from a tearfulness (three patients had slight tearfulness). After four weeks of treatment, tearfulness symptoms were diminished in four female patients, and after eight weeks not a single female patient suffered from tearfulness. Prior to the study, and at the fourth and at the eighth week of the assessment the mean scores of tearfulness were 0.36 ± 0.18, 0.2 ± 0.18, and 0 ± 0.0, respectively (TABLE 2).

Overall, clinically meaningful improvements in cognitive function and reduction of neuropsychiatric symptoms were demonstrated during the trial (TABLE 2). Patients became calmer and more sociable. They started to act and respond more adequately.

Psychopathic symptoms (lack of restraint, touchiness, conflict making, evil mindedness, and aggressiveness) that were documented for seven patients before the study were significantly diminished during the first two weeks of the therapy. Two patients showed improvement in spirit, and this effect was attained after eight weeks of the treatment. Four patients became more active and felt that they experienced a sense of cheerfulness and freshness. Eight patients showed a greater interest in their surroundings. Five patients even showed a positive change in their entire appearance, as assessed by the medical staff and by family members.

No pathological changes in the hematological and biochemical parameters were found during the course of the treatment. A reduction in the leukocyte count (although, within a normal limit) was observed at the fourth week of the treatment. However, by the eighth week of the treatment, the leukocyte count returned to normal.

## DISCUSSION

As we mentioned, conventional therapies aimed at improving cognitive functions involve medications that elevate the level of acetylcholine, diminished due to the loss of neural cells. Studies of the mechanism of degeneration suggest that a hyperactivation of NMDA receptors might play a central role in the degeneration of neural cells. Therefore, the development of novel neuroprotective agents is currently focused on antagonists of NMDA receptors and $Ca^{2+}$ channels.

Results from both neurochemical and animal studies presented in this report show that Dimebon combines properties of both a cognition-enhancing agent and a neuroprotective agent. Its neuroprotective properties are explained by its calcium-blocking and anti-NMDA activity. The properties of Dimebon as a cognition-enhancing agent are based on its ability to elevate the level of acetylcholine by inhibition of either acetylcholine esterase or histamine receptors.[16,17] The latter leads to stimulation of the release of the neurotransmitter.

A clinical trial performed on 14 patients with Alzheimer's disease support the results of the neurochemical and animal studies. The Dimebon treatment showed appreciative improvement in cognitive functions and psychiatric and emotional symptoms of all treated patients. A distinct antidepressive effect was also observed in those patients who suffered from depression. This effect most likely results from the ability of Dimebon to inhibit brain monoamine oxidase.[18]

Safety of the therapeutic drugs is especially important when drugs are used with older patients, the main group affected by Alzheimer's disease. Safety studies were performed when Dimebon was first introduced in Russian market in 1983 as an antihistamine agent, showed that the drug has a remarkable safety profile. It has been an over-the-counter drug for almost 20 years, and it has proven to be safe. Toxicological studies showed that administration of the drug for two months in doses that exceeded

the therapeutic dose by 100 times, did not produce any changes in physiological parameters or pathological changes in organs of rats, guinea pigs, or dogs.[19,20] Based on the results of these studies, Dimebon was classified as a low toxic substance. A pronounced antiarrhythmic effect of Dimebon and its beneficial effect in certain heart conditions have also been emphasized.[21-23]

In summary, Dimebon has a combination of pharmacological and safety properties that suggest the drug as a candidate for the use in the therapy of Alzheimer's disease. The results of the study reported here show that Dimebon has a great potential as a new medication that may not only improve cognitive functions, but, most importantly, may prevent the progression of the disease. Large-scale clinical trials performed according to the FDA standards are required to confirm its efficacy in the improvement of cognitive functions and in the prevention of the progression of the disease.

**REFERENCES**


1. Harkany, T, T. Hortobagyi, M. Sasvari, *et al*. 1999. Neuroprotective approaches in experimental models of beta-amyloid neurotoxicity: relevance to Alzheimer's disease. Proc. Neuropsychopharmacol. Biol. Psychiatry **23**: 963-1008.
2. Mattson, M.P. 1990. Antigenic changes similar to those seen in neurofibrillary tangles are elicited by glutamate and $Ca^{2+}$ influx in cultured hippocampal neurons. Neuron **2**: 105-117.
3. Mills, L.R. & S.B. Kater. 1990. Neuron-specific and state-specific differences in calcium homeostasis regulate the generation and degeneration of neuronal architecture. Neuron **2**: 149-163.
4. Schoesboe, A., B. Belhage & A. Frandsen. 1997. Role of Ca2+ and other second messengers in excitatory amino acid receptor mediated neurodegeneration: clinical perspectives. Clin. Neurosci. **4**: 194-198.
5. Muller, W.E., E. Mutschler & P. Rieder. 1995. Noncompetitive NMDA receptor antagonists with fast open-channel blocking kinetics and strong voltage-dependency as potential therapeutic agents for Alzheimer's dementia. Pharmachopsychiatry **28**: 113-124.
6. Kornhuber, J. & M. Weller. 1997. Psychogenicity and *N*-methyl-D-aspartate receptor antagonism: implications for neuroprotective pharmacotherapy. Biol. Psychiatry **41**: 135-144.
7. Palmer, G.C. & D. Widzowsky. 2000. Low affinity use-dependent NMDA receptor antagonists show promise for clinical development. Amino Acids **19**: 151-155.
8. Litchfild, J.T. & F.J. Wicoxon. 1949. Pharmacol. Exp. Therap. **96**: 99-114.
9. Schramm, M., S. Eimerl & E. Costa. 1990. Serum and depolarizing agents cause acute neurotoxicity in cultured cerebellar granule cells: role of the glutamate receptor responsive to *N*-methyl-D-aspartate. Proc. Natl. Acad. Sci. U.S.A. **87**: 11931197.
10. Fisher, A. & I. Hanin. 1986. Potential animal models for senile dementia of Alzheimer's type, with emphasis on AF64A-induced cholinotoxicity. Annu. Rev. Pharmacol. Toxicol. **26**: 161-181.
11. Lermontova, N., N. Lukoyanov, T. Serkova, et al. 1998. Effects of tacrine on deficits in active avoidance performance induced by AF64A in rats. Mol. Chem. Neuropathol. **33**: 51-61.

12. McKahn, G., D. Drachman, M. Folstein, et al. 1984. Clinical diagnosis of Alzheimer's disease: report of the NINCDS-ASRDA Work Group under the auspices of the Department of Health and Human Services Task Force on Alzheimer's Disease. Neurology **34**: 939-944.
13. Walsh, T. & K. Opello. 1994. *In* Toxin-Induced Models of Neurological Disorders. 259-279. Plenum Press, New York and London.
14. Bailey, E.L., D.H. Overstreet & A.D. Crocker. 1986. Effects of intrahippocampal injections of the cholinergic neurotoxin AF64A on open-field activity and avoidance learning in the rat. Behav. Neural. Biol. **45**: 263-274.
15. Ogura, H., Y. Yamanishi & K. Yamatsu. 1987. Effects of physostigmine on AF64A-induced impairment of learning acquisition in rats. Japan J. Pharmacol. **44**: 498-501.
16. Gankina, E.M., N.V. Porodenko, T.I. Kondratenko, *et al*. 1993. The effect of antihistaminic preparations on the binding of labelled mepyramine, ketanserin and quinuclidinyl benzilate in the rat brain. Eksp. Klin. Farmakol (Russ.). **56**: 22-24.
17. Matveeva, I.A. 1983. Action of Dimebon on histamine receptors. Farmakol. Toksikol. (Russ.). **46**: 27-29.
18. Shadurskaia, S.K., A.I. Khomenko, V.A. Pereverzev & A.I. Balaklevskii. 1986. Neuromediator mechanisms of the effect of the antihistamine agent Dimebon on the brain. Biull. Eksp. Biol. Med. (Russ.) **101**: 700-702.
19. Golubeva, M.I., L.F. Shashkina, V.A. Proinova, *et al*. 1985. Preclinical study of the safety of the antihistaminic preparation Dimebon. Farmakol. Toksikol. (Russ.) **48**: 114-119.
20. Proinova, V.A., I.V. Golovanova, M.I. Golubeva & L.F. Shashkina. 1985. Evaluation of the effect of the antihistaminic preparations Dimebon and diprazin on embryogenesis in rats. Farmakol. Toksikol. (Russ.) **48**: 89-93.
21. Galenko-Iaroshevskii, P.A., I.L. Cherednik, V.V. Bartashevich, *et al*. 1997. Comparative evaluation of the anti-arrhythmia efficacy of fencarol and Dimebon during neurogenic atrial fibrillation. Biull. Eksp. Biol. Med. (Russ.) **124**: 81-85.
22. Galenko-Iaroshevskii, P.A., E.R. Melkumova, V.V. Bartashevich, *et al*. 1996. Comparative evaluation of the effect of Dimebon, obzidan, finoptin, and cordarone on the functional state of the ischemic focus and the size of necrosis zone during experimental myocardial infarction. Biull. Eksp. Biol. Med. (Russ.) **122**: 642-644.
23. Galenko-Iaroshevskii, P.A., Iu.R. Sheikh-Zade, O.A. Chekanova, *et al*. 1996. Effect of Dimebon on coronary blood flow and myocardial contractibility. Biull. Eksp. Biol. Med. (Russ.). **121**: 506-508.

# Раздел III. Избранные работы по созданию противоопухолевых агентов

## Введение

### О.Н. Зефирова

Большая серия работ, выполненных под руководством Николая Серафимовича Зефирова, посвящена молекулярному дизайну потенциальных противоопухолевых агентов – лигандов клеточного белка тубулина. Интерес к таким исследованиям в самом начале 2000-х гг. был обусловлен широким клиническим применением противоопухолевого препарата природного происхождения – таксола, действие которого основано на способности вызывать неконтролируемую полимеризацию тубулина до стабильных микротрубочек. Необходимость получения таксола полусинтетическим путем из природных источников, и как следствие, высокая стоимость соответствующего препарата, делали важной задачу создания структурно более простых аналогов природной молекулы.

Дизайн соответствующих структур, выполненный Н.С. Зефировым, О.Н. Зефировой и сотрудником ИФАВ РАН С.Е. Ткаченко, базировался на стратегии замены остова (*scaffold hopping*) в исходной молекуле. Предполагалось заменить полициклический скелет таксола структурно «более простым» фрагментом, сохранив при этом определенное пространственное расположение важных для связывания с тубулином заместителей. В качестве таких фрагментов использовали адамантановый или бицикло[3.3.1]нонановый каркасы, химия которых интенсивно изучалась на возглавляемой в те годы Н.С. Зефировым кафедре органической химии химфака МГУ (в группе к.х.н. Н.В. Авериной). Структуры предложенных соединений представлены в работах [1, 2] настоящей главы, так же как и описание их синтеза (проведенного в МГУ Е.В. Нуриевой) и результатов биотестирования, выполненного сотрудниками университета г. Росток (Германия) в группе д.б.н. С.А. Кузнецова.

Позже аналогичная стратегия замены остова была использована для создания аналогов другого природного цитотоксичного вещества – дитерпенового гликозида элеутеробина, который, как и таксол, стимулирует полимеризацию тубулина. Эти работы выполнялись д.х.н. М.В. Проскурниной, к.х.н. Н.А. Лозинской, к.х.н. С.Е. Сосонюком под непосредственным руководством Н.С. Зефирова в его лаборатории органического синтеза и были завершены уже без Николая Серафимовича [3].

Несколько исследований акад. Н.С. Зефирова в рамках изучения противоопухолевых агентов имели целью поиск новых лигандов колхицинового сайта связывания тубулина и выполнялись в группах О.Н. Зефировой и Е.Б. Авериной [4–7]. Интересным и неожиданным результатом этих работ стало обнаружение

необычного «кластеризующего» действия на тубулин для конъюгатов колхицина с адамантаном, соединенных линкерной цепью определенной длины. Для соединения с авторским названием «тубулокластин» в экспериментах *in vivo*, выполненных в Российском онкологическом научном центре им. Н.Н. Блохина РАМН, была продемонстрирована способность в низких дозах (1 мг/кг) вызывать значимое и достоверное увеличение продолжительности жизни мышей $BDF_1$ с внутрибрюшинно трансплантированным лимфолейкозом P388. Изучение механизма кластеризующего действия тубулокластина *in vitro*, проведенное совместно с сотрудниками университетов Ростока (Германия) и Осло (Норвегия) (см. работу [5]), явилось важным теоретическим вкладом в медицинскую и биоорганическую химию тубулин-направленных противоопухолевых агентов.

## Список статей раздела

### Упрощенные аналоги таксола и элеутеробина


1. Zefirova O.N., Nurieva E.V., Lemcke H., Ivanov A.A., Zyk N.V., Weiss D.G., Kuznetsov S.A., Zefirov N.S. Design, synthesis and bioactivity of simplified taxol analogues on the basis of bicyclo[3.3.1]nonane derivatives // *Mendeleev Comm*. 2008. V.18. № 4. P. 183-185.
2. Zefirova O.N., Nurieva E.V., Lemcke H., Ivanov A.A., Shishov D.V., Weiss D.G., Kuznetsov S.A., Zefirov N.S. Design, synthesis, and bioactivity of putative tubulin ligands with adamantane core // *Bioorg. Med. Chem. Lett.* 2008. V.18. № 18. P. 5091-5094.
3. Sosonyuk S.E., Peshich A., Tutushkina A.V., Khlevin D.A., Lozinskaya N.A., Gracheva Yu.A, Glazunova V.A., Osolodkin D.I., Semenova M.N., Semenov V.V., Palyulin V.A., Proskurnina M.V., Shtil A.A., Zefirov N.S. Synthesis and cytotoxicity of novel simplified eleutherobin analogues as potential antitumour agents // *Org. Biomol. Chem*. 2019. V.17. № 10. P. 2792-2797.19


### Лиганды колхицинового сайта связывания в тубулине


4. Zefirova O.N., Nurieva E.V., Shishov D.V., Baskin I.I., Fuchs F., Lemcke H., Schroder F., Weiss D.G., Zefirov N.S., Kuznetsov S.A. Synthesis and SAR requirements of adamantane-colchicine conjugates with both microtubule depolymerizing and tubulin clustering activities // *Bioorg. Med. Chem*. 2011. V.19. № 18. P. 5529-5538.
5. Zefirova O.N., Lemcke H., Lantow M., Nurieva E.V., Wobith B., Onishchenko G.E., Hoenen A., Griffiths G., Zefirov N.S., Kuznetsov S.A. Unusual Tubulin-Clustering Ability of Specifically C7-Modified Colchicine Analogues // *Chembiochem*. 2013. V.14. № 12. P.1444-1449.
6. Zefirova O.N., Nurieva E.V., Wobith B., Gogol V.V., Zefirov N.A., Ogonkov A.V., Shishov D.V., Zefirov N.S., Kuznetsov S.A. Novel antimitotic agents related to tubuloclustin: synthesis and biological evaluation // *Mol. Divers*. 2017. V.21. № 3. P. 547-564. doi: 10.1007/s11030-017-9739-6.
7. Vasilenko D.A., Averina E.B., Zefirov N.A., Wobith B., Grishin Y.K., Rybakov V.B., Zefirova O.N., Kuznetsova T.S., Kuznetsov S.A., Zefirov N.S. Synthesis and antimitotic activity of novel 5-aminoisoxazoles bearing alkoxyaryl moieties // *Mendeleev Comm.* 2017. V. 27. № 3. P. 228-230

## Упрощенные аналоги таксола и элеутеробина

*MENDELEEV COMMUN., 2008, 18, 183-185*

# DESIGN, SYNTHESIS AND BIOACTIVITY OF SIMPLIFIED TAXOL ANALOGUES ON THE BASIS OF BICYCLO[3.3.1]-NONANE DERIVATIVES

**O.N. Zefirova, E.V. Nurieva, H. Lemcke, A.A. Ivanov, N.V. Zyk, D.G. Weiss, S.A. Kuznetsov, N.S. Zefirov**

*Department of Chemistry, M.V. Lomonosov Moscow State University, Moscow, Russian Federation*
*Institute of Physiologically Active Compounds, Russian Academy of Sciences, Chernogolovka, Moscow Region, Russian Federation*
*Institute of Biological Sciences, Cell Biology and Biosystems Technology, University of Rostock, Rostock, Germany*

Four specially designed bicyclo[3.3.1]nonane-based structures were synthesised and found to be cytotoxic at micromolar concentrations and to cause slight non-specific tubulin aggregation.

Taxol (paclitaxel), isolated from the bark extracts of *Taxus brevifolia,* and its synthetic analogue taxotere (docetaxel) are current clinically used antitumor drugs (Figure 1). The action of these compounds is based on their ability to cause spontaneous polymerisation of intracellular protein tubulin to stable microtubules and to stabilise preformed microtubules thereby preventing cell division.[1,2]

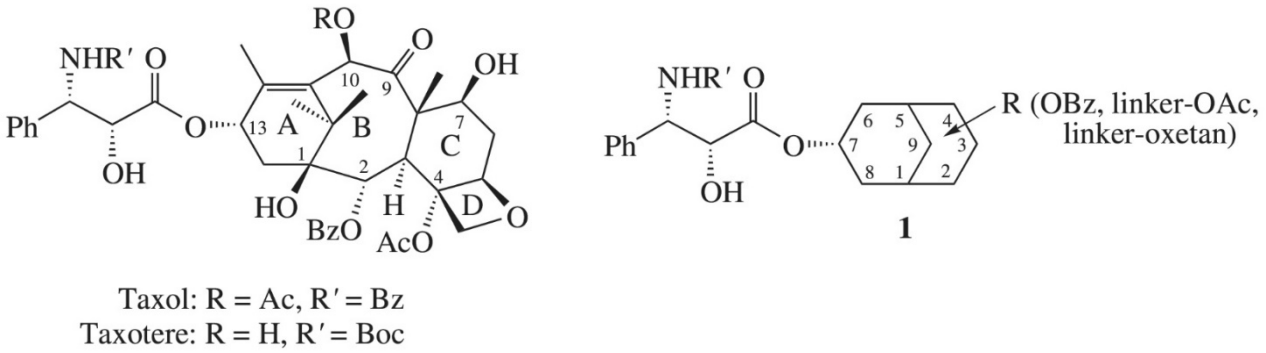


Figure 1. Taxane structures and a model of their ‘simplified’ analogues.

The intricate molecular structure of taxane compounds leads to the necessity to obtain them semi-synthetically from natural sources. Therefore, the development of taxol and taxotere analogues with a simpler structure is an important task. During the last ten years, such attempts have been reported.[3-8]

In 2002, based on the hypothesis that the main function of the taxane skeleton is to provide proper orientation of the substituents important for tubulin binding,[9] we suggested a general theoretical model of a 'simplified' taxol analogue with bicyclo[3.3.1]nonane core **(1,** Figure 1).[10] This moiety has a definite structural similarity to the AB rings of the parent molecule. Suggesting model **1**, we were guided by the fact that taxol and taxotere C(13) side chain *[i.e., N*-benzoyl- or *N-tert*-butoxycarbonyl-(2*R*,3*S*)-phenylisoseryl] makes the most important contribution to binding with tubulin, whereas C(2) (OBz), C(4) (OAc) substituents and the oxetan fragment also play a role in this binding.[1,2] Here, we present the results of molecular modeling, synthesis and biological tests of mono- and disubstituted bicyclo[3.3.1]nonanes **2**–**5**, corresponding to model compound **1.**

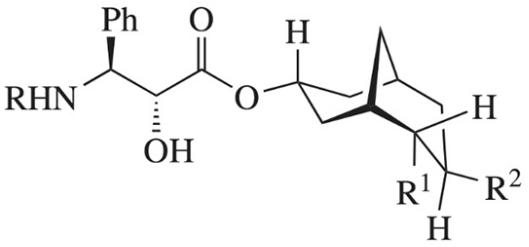


**2** R = Bz, $R^1 = R^2 = H$
**3** R = Bz, $R^1$ = OBz, $R^2$ = H
**4** R = Bz, $R^1$ = H, $R^2 = CH_2OC(O)Me$
**5** R = Boc, $R^1$ = H, $R^2$ = C(O)O 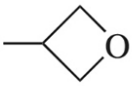

***Molecular modeling*[8].** The proper bridgehead core positions for the introduction of the substituents in model **1** were determined by the overlay of bicyclo[3.3.1]nonane with taxol in conformations with a minimal energy (chair-chair and T-conformation,[12] respectively) (Figure 2). Taking into account that the introduction of the taxol-like amino acid side chain at the 7-position of bicyclo[3.3.1]nonane brings changes to the conformation of the corresponding cyclohexane ring from chair to boat, the position of this chain in compounds **2**–**5** might differ from the one in the parent molecule. Therefore, we performed a molecular docking of two compounds (**3** and **5**) using the taxol binding site model (kindly granted to us by Professor J. Snyder[12]).

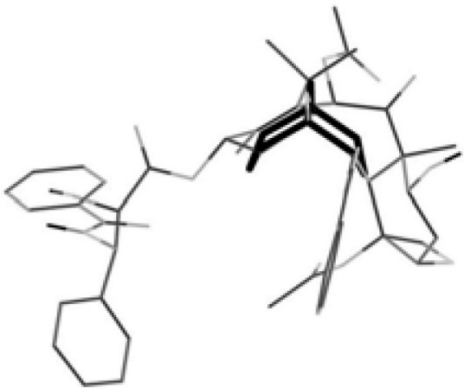

Figure 2. Overlay of bicyclo[3.3.1]nonane with the taxol molecule.

[8] The molecular docking of compounds **3** and **5** was performed automatically with the Glide program of the MacroModel package.[11] The binding site was defined as a box with a side of 29 A with a center in the centroid of taxol atoms. For all other parameters their default values were used. The full flexibility of the ligand was allowed.

This study revealed that in the case of the identical location of taxol and compound **3** *N*-benzoyl-(2*R*,3*S*)-phenylisoseryl in the protein, the aromatic ring of *endo*-benzoyloxy group in the 7-position of 3 is able to provide an important interaction with His229 (Figure 3(a)).

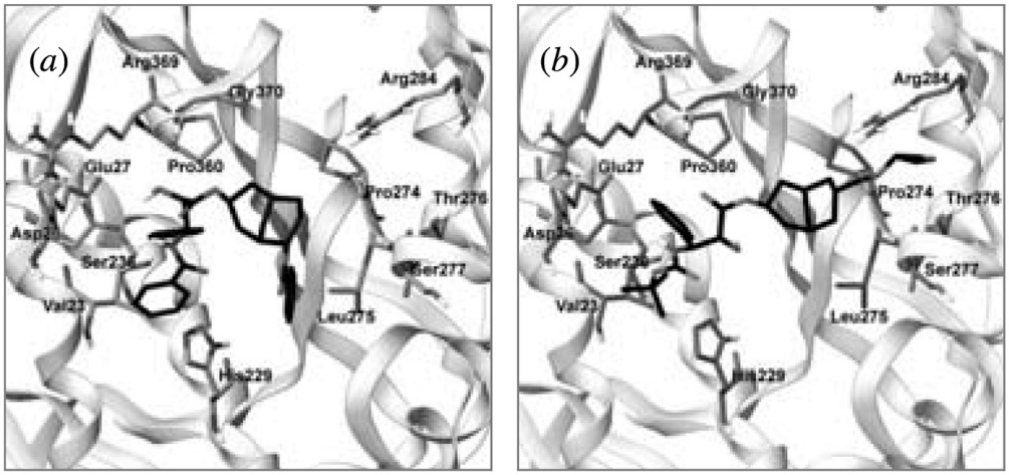


Figure 3. Structures of (*a*) **3** and (*b*) **5** inside the taxol binding site of β-tubulin (hydrogen atoms are not indicated).

The carbonyl oxygen of ester **5** can be hydrogen bonded to the Thr 276 amino group (this bond is formed by oxetan oxygen in taxol[2,12]). The oxetan oxygen of compound **5** can form a hydrogen bond with the Thr276 hydroxyl and the Arg284 side chain [Figure 3(b)].

In general, the molecular docking data confirm the expected supposition that taxol binding site, which is able to hold the tetracyclic parent molecule, is too large to hold the bridged core. Thus, many unpredictable bicyclo[3.3.1]nonane positions in the binding site are possible.

***Synthesis*[9].** Compounds **2**–**5** were synthesised by the esterification of corresponding alcohols by oxazolidine protected *N*-benzoylphenylisoserine with the subsequent opening of the oxazolidine ring.[13] Thus, ester **2** was synthesised from bicyclo[3.3.1]nonan-3-ol **7** (obtained by a five-step procedure from diol **6**[14]) (Scheme 1).

**Scheme 1**

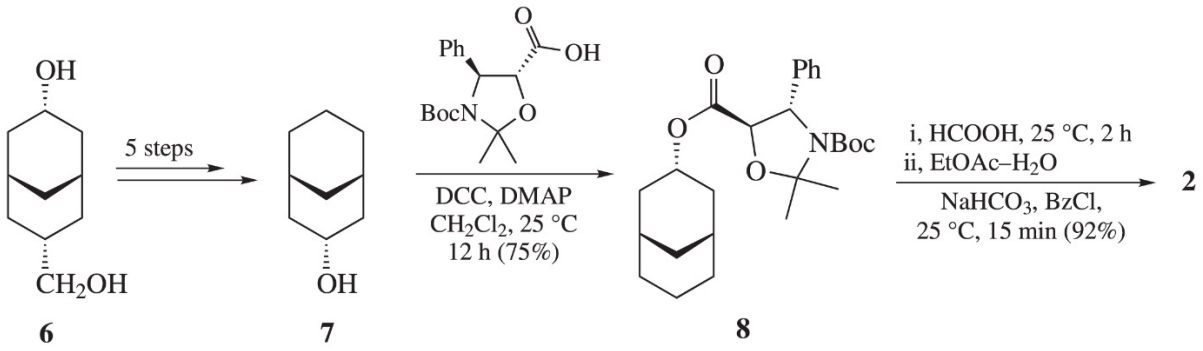


[9] For the synthetic details and the characteristics of all the compounds see Online Supplementary Materials.

The *endo:exo* isomer ratio in bicyclo[3.3.1]nonan-3-ol **7** was 9:1 but after the esterification only the wanted *endo*-isomers of esters **8** and **2** were isolated.

For the synthesis of ester **3**, *endo*-bicyclo[3.3.1]nonan-2-one **11** was obtained from bicyclo[3.3.1]nonanedione **9** as described in ref. 15 (Scheme 2).

Scheme 2

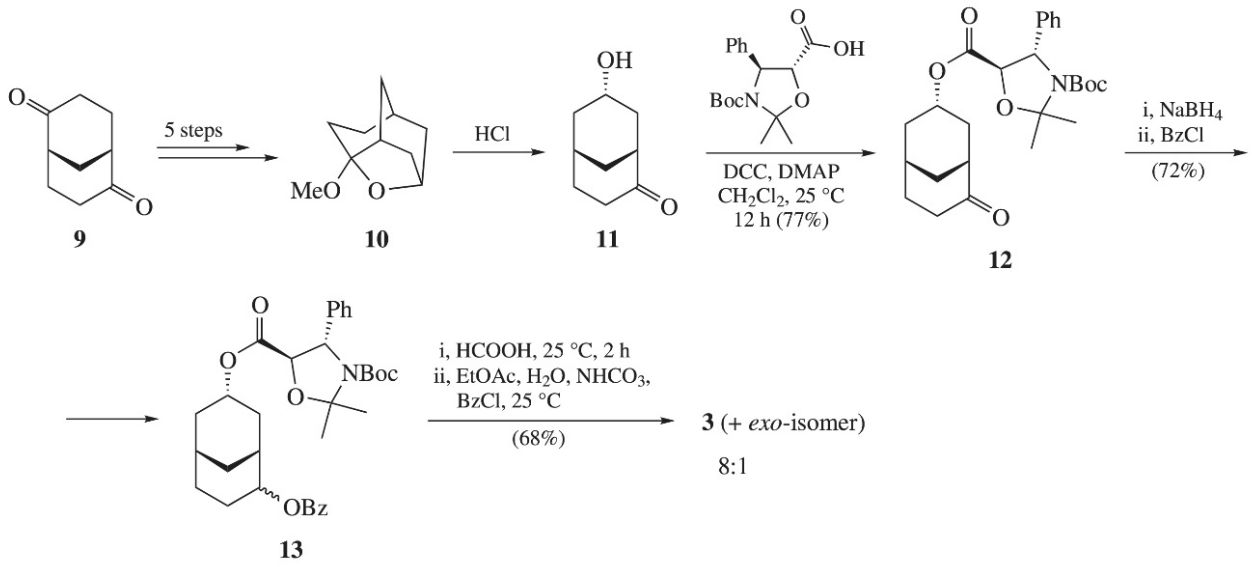


Note that key tricyclic compound **10** (its hydrolysis in acidic media leads to desired ketol **11**) can also be synthesised from 4-hydroxyadamantan-2-one.[16] The esterification of ketol **11** by protected amino acid gave product **12**, and the subsequent selective reduction of carbonyl group in **12** followed by benzoylation of the obtained hydroxyl led to the mixture of two isomeric benzoyloxy derivatives **13** with a ratio of 8:1 (*endo:exo*[17]). The same ratio was observed in final product **3**:*exo*-isomer (8:1).

Scheme 3

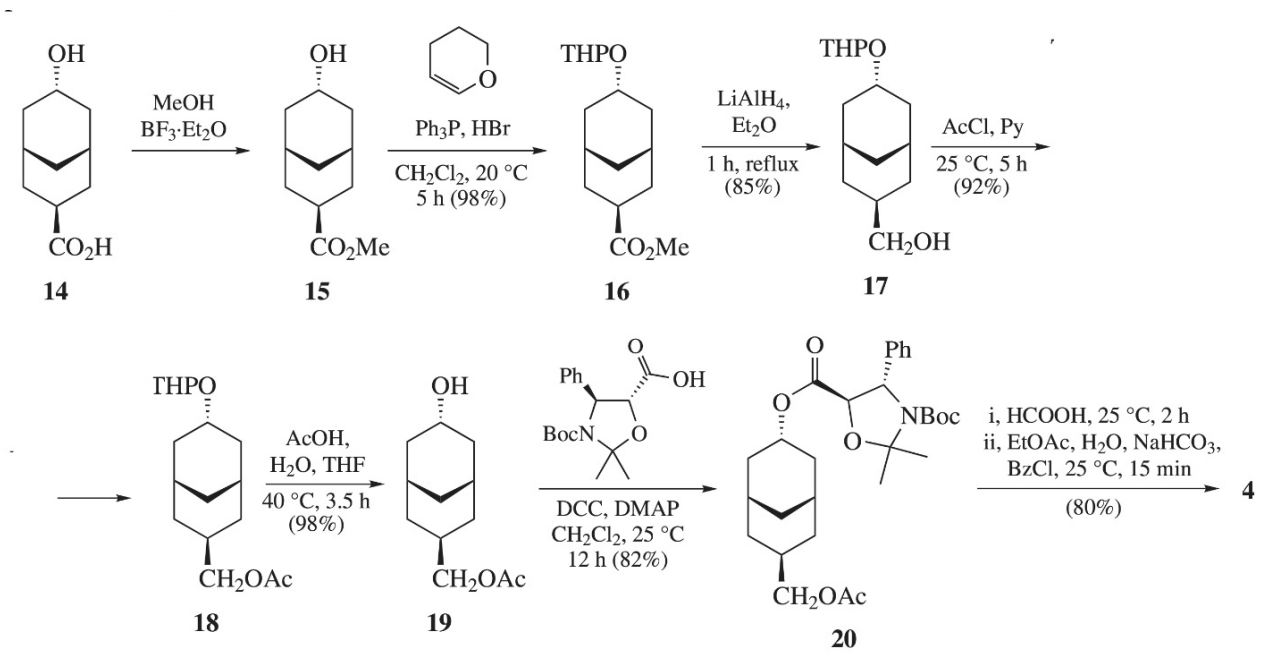

Esters **4** and **5** were synthesised from 7-*endo*-hydroxybicyclo[3.3.1]nonane carboxylic acid **14**, which was obtained by alkaline ring opening of 2-oxahomoadamantan-2-one. The resulting acid serves as a template with a proper configuration of substituents (*endo–exo*).[13,19] The synthesis of compound **4** was carried out according to Scheme 3.

To obtain compound **5**, double esterification was performed for TMS protected 7-*endo*-hydroxybicyclo[3.3.1]nonane carboxylic acid **14**, first by 3-hydroxyoxetane (obtained in five steps from glycerol)[20] and then by a protected amino acid (Scheme 4).

Note that the amino acid protection used for the synthesis of compounds **2**–**4** (Schemes 1–3) is unsuccessful in this case, because the oxetane ring undergoes destruction during amino acid regeneration from the corresponding ester. Therefore, we used a slightly different amino acid protection[21] to obtain compound **5** (Scheme 4).

Scheme 4

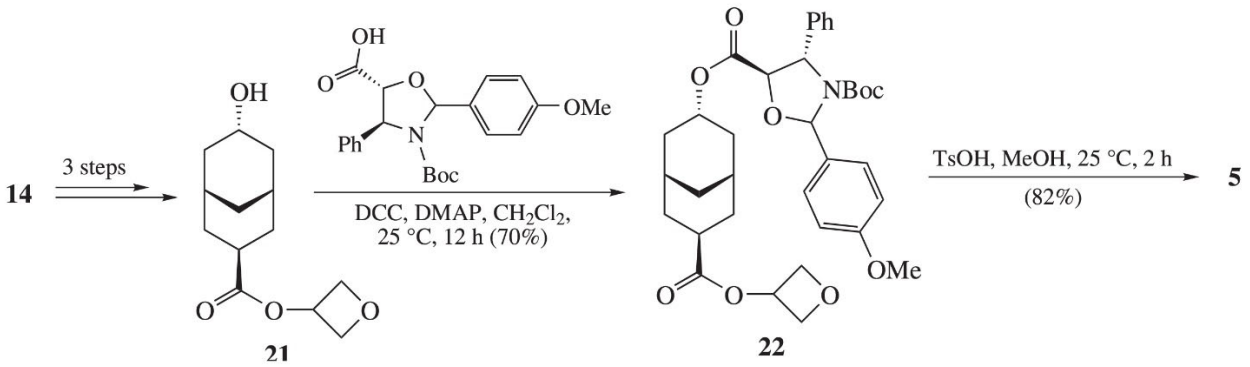


***Biotests*[10].** The results of biological activity of synthesised taxol analogues are presented in Table 1. These data indicate that, according to an estimation of $IC_{50}$ for the A549 human lung carcinoma cell line, compounds **3**-**5** exhibit cytotoxicity at a micromolar level. In spite of a noticeable (taking into account the extent of structural simplification) cytotoxicity, all compounds were found to be unable to promote microtubule assembly of purified tubulin *in vitro.* Nevertheless, a sedimentation assay revealed that compounds **2**-**5** induce slight non-specific tubulin aggregation.

Thus, the synthesised compounds display the same kind of activity as the majority of the known simplified taxol analogues, e.g., indolizidinones[5] and macrocycles.[7] The inability of compounds **2**–**5** to promote tubulin polymerization might be caused by different reasons, such as: (i) insufficiency of the two substituents in the bridgehead core, or (ii) their wrong orientation in the protein due to too bulky binding site, or (iii) the lack of the general rigidity of bicyclic framework. The results of this work indicate that the ‘simplification’ in the presented compounds is too drastic in comparison with the

[10] For biological tests of esters **2**-**5** initial solutions of these compounds and taxol in DMSO were prepared. The tests were carried out in a concentration range of 1-60 pM. A taxol solution was used as a positive control and pure DMSO as negative control. The ability of tested compounds to stimulate *in vitro* assembly of microtubules was determined using tubulin (1-2 mg $cm^{-3}$) isolated from bovine brain.[22] The formation of microtubules was monitored by light video-enhanced contract microscopy (AVEC DIC microscopy)[23] and sedimentation analysis.[24] The ability of compounds 3-5 to inhibit cell growth (IC^) was studied using phase contrast microscopy of human lung carcinoma cell line A549.

parent molecules and requires more thorough structural ‘tuning’ of the fragments to make it bioisosteric to a taxane skeleton.

Table 1 Results of biological tests.

| Compound | $IC_{50}$/μM | Tubulin sedimentation related to taxol (%) |
|---|---|---|
| Taxol | 0.002 | 100 |
| **2** | not determined | <40 |
| **3** * | 2.25 | 38 |
| **4** | 2.25 | 37 |
| **5** | 3.8 | 25 |
| DMSO | – | 12 |

*Compound **3** was tested in a mixture with its *exo*-isomer due to the small amount of the latter and the broad concentration intervals in biotests.

This work was done in the frame of a Scientific Agreement between Moscow and Rostock Universities and supported in part by German organization DAAD (the Leonard Euler Studentship program), the Russian Foundation for Basic Research (project no. 07-03-12110-ofi), the Russian Academy of Sciences, and the Russian Federation Ministry of Education.

We are grateful to Dr. Kenneth A. Jacobson (National Institute of Diabetes & Digestive & Kidney Diseases, NIH, Bethesda, MD, USA) for useful collaboration and discussion on the molecular modeling studies.

**REFERENCES**

1. D. G. I. Kingston, *Chern. Commun.,* 2001, 867.
2. O. N. Zefirova, E. V. Nurieva, A. N. Ryzhov, N. V. Zyk and N. S. Zefirov, *Zh. Org. Khim.,* 2005, **41**, 315 *(Russ. J. Org. Chem.,* 2005, **41**, 329).
3. K. Fuji, Y. Watanabe, T. Ohtsubo, M. Nuruzzaman, Y. Hamajima and M. Kohno, *Chem. Pharm. Bull.,* 1999, **47**, 1334.
4. U. Klar, H. Graf, O. Schenk, B. R6hr and H. Schulz, *Bioorg. Med. Chem. Lett.,* 1998, **8**, 1397.
5. X. Geng, R. Geney, P. Pera, R. Bemacki and I. Ojima, *Bioorg. Med. Chem. Lett.,* 2004, **14**, 3491.
6. F. Ahnqvist, S. Manner, V. Thomqvist, U. Berg, M. Wallin and T. Frejd, *Org. Biomol. Chem.,* 2004, **2**, 3085.
7. T. Ganesh, A. Norris, Sh. Sharma, S. Bane, A. A. Alcaraz, J. P. Snyder and D. G. I. Kingston, *Bioorg. Med. Chem.,* 2006, **14**, 3447.
8. J. Howarth, P. Penny, S. McDonnel and A. O’Connor, *Bioorg. Med Chem. Lett.,* 2003, **13**, 2693.
9. O. N. Zefirova, E. V. Selunina, N. V. Averina, N. V. Zyk and N. S. Zefirov, *Zh. Org. Khim.,* 2002, **38**, 1176 *(Russ. J. Org. Chem.,* 2002, **38**, 1125).

10. N. V. Averina, T. V. Lapina, O. N. Zefirova and N. S. Zefirov, *Vestnik Mosk. Univ. 2. Khim.,* 2002, **43**, 244 (in Russian).
11. F. N. Mohamadi, G. J. Richards, W. C. Guida, R. Liskamp, M. Lipton, C. Caufield, G. Chang, T. Hendrickson and W. C. Still, *J. Comput. Chem.,* 1990, **11**, 440.
12. J. P. Snyder, J. H. Nettles, B. Cornett, K. H. Downing and E. Nogales, *Proc. Nat. Acad. Sci. USA,* 2001, **98**, 5312.
13. J. D. Bourzat and A. Commerçon, *Tetrahedron Lett.,* 1993, **34**, 6049.
14. T. Momose and O. Muraoka, *Chem. Pharm. Bull.,* 1978, **26**, 228.
15. D. A. Lightner, T. C. Chang, D. T. Hefelfinger, D. E. Jackman, W. M. D. Wijekoon and J. W. Givens, *J. Am. Chem. Soc.,* 1985, **107**, 7499.
16. O. N. Zefirova, E. V. Nurieva, V. N. Nuriev, K. A. Potekhin, A. V. Maleev, N. V. Zyk and N. S. Zefirov, *Mendeleev Commun.,* 2007, **17**, 332.
17. A. C. Cope, D. L. Nealy, P. Sheiner and G. Wood, *J. Am. Chem. Soc.,* 1965, **37**, 3130.
18. G. E. Renzoni and W. T. Borden, *J. Org. Chem.,* 1983, **48**, 5231.
19. R. Partch, W. Brewser and B. Stokes, *Croat. Chem. Acta,* 1985, **58**, 661.
20. M. V. Kiryukhin, E. V. Nurieva, D. V. Shishov, V. N. Nuriev, N. V. Zyk, N. S. Zefirov and O. N. Zefirova, *Vestnik Mosk Univ. 2. Khim.,* 2007, **48**, 342 *(Moscow University Chem. Bull.,* 2007, **48**, 281).
21. E. Didier, E. Fouque, I. Taillepied and A. Commerçon, *Tetrahedron Lett.,* 1994, **35**, 2349.
22. S. A. Kuznetsov, V. I. Rodionov, A. D. Bershadsky, V. I. Gelfand and V. A. Rosenblat, *Cell Biol. Int. Rep.,* 1980, **4**, 1017.
23. D. G. Weiss, in *Cell Biology: A Laboratory Handbook,* ed. J. E. Celis, Academic Press, San Diego, 2005, vol. 3, p. 57.
24. V. I. Rodionov, F. K. Gyoeva, A. S. Kashina, S. A. Kuznetsov and V. I. Gelfand, *J. Biol. Chem.,* 1990, **265**, 5702.

*Received: 18th April 2008; Com. 08/3125*

*BIOORGANIC&MEDICINAL CHEMISTRY LETTERS, Vol. 18 (18), 5091-5094 (2008)*

# DESIGN, SYNTHESIS, AND BIOACTIVITY OF PUTATIVE TUBULIN LIGANDS WITH ADAMANTANE CORE

**Olga N. Zefirova, Evgeniya V. Nurieva, Heiko Lemcke, Andrei A. Ivanov, Dmitrii V. Shishov, Dieter G. Weiss, Sergei A. Kuznetsov, Nikolay S. Zefirov**

*Department of Chemistry, M.V. Lomonosov Moscow State University, Russian Federation*
*Institute of Biological Sciences, Cell Biology and Biosystems Technology, University of Rostock, Germany*
*Institute of Physiologically Active Compounds, Chernogolovka, Russian Federation*

Several adamantane-based taxol mimetics were synthesized and found to be cytotoxic at micromolar concentrations and to cause tubulin aggregation. The extent of the aggregation is maximal for *N*-benzoyl-(2*R*,3*S*)-phenylisoseryloxyadamantane (**5**) and is very sensitive to the structural modifications. A hybrid compound (**15**), combining adamantane-based taxol mimetic with colchicine was synthesized and found to possess both microtubule depolymerizing and microtubule bundling activities in A549 human lung carcinoma cells.

Taxol (paclitaxel, **1a**, Fig. 1), isolated from the bark extracts of *Taxus brevifolia,* and its synthetic analogue taxotere (docetaxel, **1b**) possess high antitumor activity due to their ability to cause spontaneous polymerization of the intracellular protein tubulin into stable microtubules and to stabilize preformed microtubules, thereby preventing cell division.[1,2] The most important contribution to tubulin binding is provided by the $C^{13}$ side chain taxol and taxotere (i.e., *N*-benzoyl- or *N*-*tert*-butoxycarbonyl-(2*R*,3*S*)-phenylisoseryl), while $C^2$ (–OBz), $C^4$ (–OAc) substituents, and the oxetan fragment also play a role in this binding.[1,2]

The intricate molecular structure of taxane compounds and the necessity to obtain them semi-synthetically from natural sources make the development of taxol and taxotere analogues with a simpler structure important. During the last ten years there appeared several publications about such attempts.[3-9]

In 2002, based on the hypothesis, that the main function of the taxane skeleton is to provide proper orientation of the substituents important for tubulin binding,[10] we suggested a general theoretical model of a ‘simplified’ taxol analogue with a bicyclo[3.3.1]nonane core (structurally similar to the AB rings of the parent molecule).[11] Later, we synthesized a number of such compounds, including structure **2**, and demonstrated that they possess weak cytotoxicity and can cause slight tubulin aggregation, but not polymerization to microtubules.[12] Because one of the reasons for this result might be improper substituents positions in structure **2** and similar compounds due to

the relative conformational freedom of the bicydo[3.3.1]nonane framework, we suggested to synthesize their analogues with a rigid adamantane core. Here, we present the results of molecular modeling and synthesis of structure **3** and the data of biological tests of compound **3** and two other adamantane-based taxol mimetics **4** and **5** (Fig. 1).

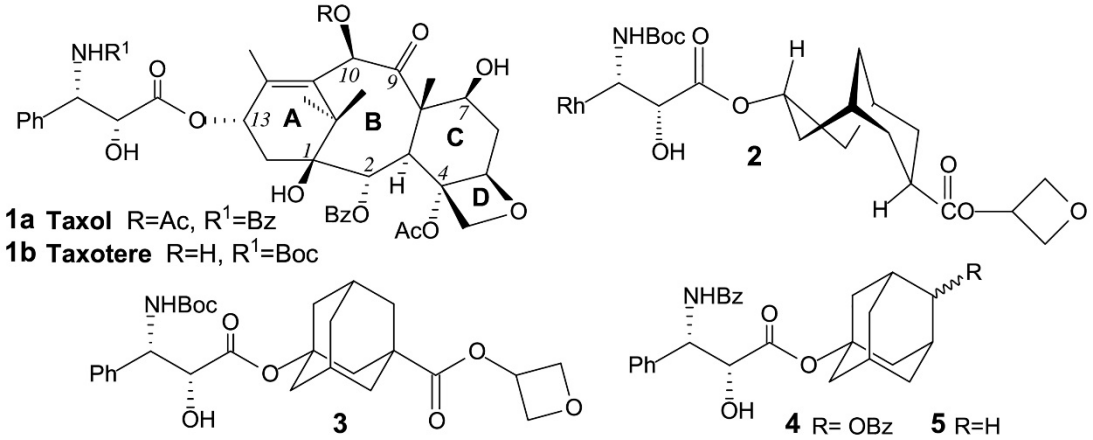


Figure 1. Structures of taxoids and their 'simplified' analogues.

The model of tubulin structure (kindly granted to us by Prof. J. Snyder, USA)[13] was used for the molecular docking of compound **3** to the taxol binding site. The obtained binding mode of ester **3** is presented in Figure 2.[1415] According to the modeling results, in case of an identical location of taxol and compound **3** side chains in the protein, the oxetan oxygen of **3** can be hydrogen bonded to the Thr 276 amino group. This interaction was not observed for the compound **2**,[12] but it corresponds exactly to the bond formed by the oxetan oxygen in taxol.[13] Moreover, the carbonyl oxygen of structure **3** ester linker can be hydrogen bonded with Arg284.

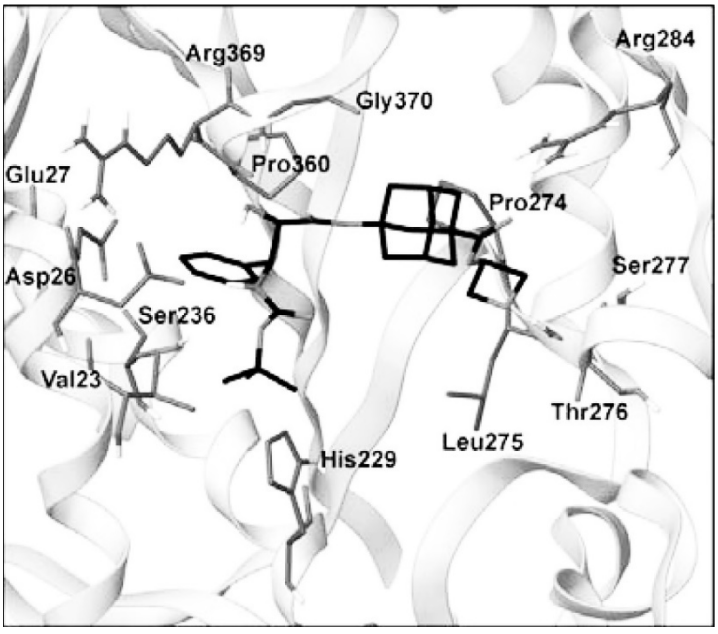


Figure 2. Structure **3** inside the taxol binding site of β-tubulin (hydrogen atoms are not indicated).

For the synthesis of compound **3** double esterification was performed for the TMS-protected 1-hydroxyadamantane-5-carboxylic acid **6**, first by 3-hydroxyoxetan (obtained in five steps from glycerin) with the formation of ester **7**,[16] and then by an oxazolidine-protected amino acid (Scheme 1).[17] The subsequent opening of the oxazolidine ring in the product **8** led to the ester **3**.[18]

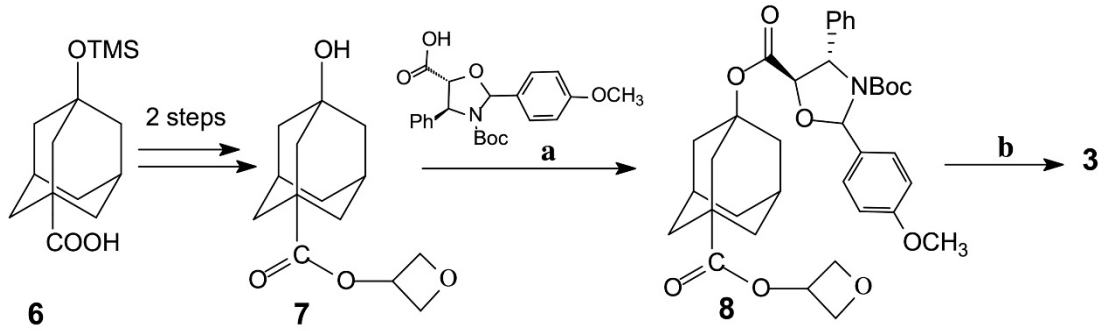


**Scheme 1.** Reagents and conditions: (a) DCC, DMAP, $CH_2Cb$, 25 °C, 12 h, 49%; (b) TsOH, MeOH, 25 °C, 2 h, 89%.

Compounds **4** and **5** were synthesized by esterification of kemantane (l-hydroxyadamantane-4-one)[19] and adamantane-1-ol[20] correspondingly using slightly different oxazolidine amino acid protections[21] (general Scheme 2). It should be noted that this type of protection is unsuitable for the synthesis of compound **3** due to the destruction of the oxetan ring during amino acid regeneration by formic acid.

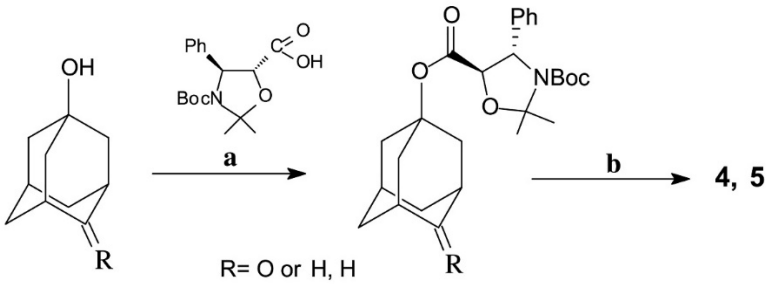


**Scheme 2.** Reagents and conditions: (a) DCC, DMAP, $CH_2C1_2$, 25°C, 12 h, 99% from kemantane, 82% from adamantanol; (b) for **4**: 1 –$NaBH_4$, MeOH, $Et_2O$, 0°C, 99%; 2 – BzCl, $Et_3N$. DMAP, $CH_2Cl_2$, 25°C, 12 h, 74%; 3 – $HCO_2H$, 25°C, 2 h, then BzCl, $NaHCO_3$, EtOAc, $H_2O$,25°C, 15 min, 83%. For **5**: $HCO_2H$, 25°C, 2 h, then BzCl, $NaHCO_3$, EtOAc, $H_2O$, 25°C, 15 min, 44%.

The synthesized adamantane-based taxol mimetics were evaluated for their *in vitro* cytotoxicity against the A549 human lung carcinoma cell line. The results are presented in Table 1. These data indicate that compounds **3**-**5** exhibit cytotoxicity at the micromolar level, that is, the same as the bicydo[3.3.1]nonane esters (e.g,, **2**)[12] and other simplified taxol analogues (e.g., indolizidinones[7] and macrocycles[9]).

To determine if the ‘adamantane taxoids’ **3**-**5** are able to cause tubulin polymerization, the samples of tubulin purified from bovine brain[23] were incubated with compounds **3**–**5** or with taxol as a positive control and studied by means of video-enhanced contrast light microscopy (AVEC-DIC microscopy).[24]

Table 1. *In vitro* cytotoxicities against the A549 cell line

| Compound | $IC_{50}$ (μM) |
|---|---|
| Taxol | 0.002 |
| **2** | 3.8 (Ref. 12) |
| **3** | 2.5 |
| **4** * | 9.5 |
| **5** | 5.6 |
| **15** | 0.0006 |

* Ester **4** was tested as a mixture of trans- and cis-isomers (in the ratio 2:1).[22]

This study showed that all tested taxol mimetics were not able to promote microtubule assembly of isolated tubulin (no microtubule bundles were observed). However, sedimentation assays[25] revealed that these compounds induced tubulin aggregation (Fig. 3A). Remarkably, ester 5 showed the highest ability to promote tubulin sedimentation – 57%, whereas for all other compounds (including **2** and similar structures)[12] it varied between 25% and 33% (Fig. 3B).

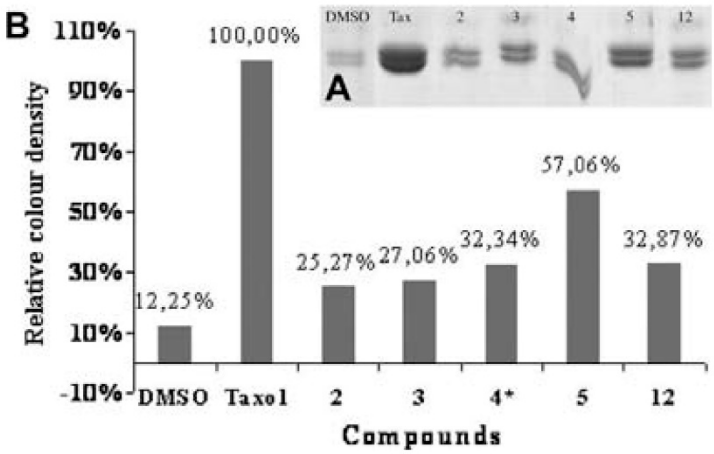


**Figure 3.** Sedimentation analysis of the tubulin after incubation in the presence of compounds **2**–**5** and **12**. (A) SDS-PAGE of tubulin pellets. (B) Estimation of the relative amount of tubulin in the sediment (100% corresponds to the amount of tubulin pelleted after incubation with taxol; DMSO was used as a negative control).

Although we were unable to observe aggregates of tubulin by AVEC-DIC microscopy in all tested adamantane ester samples (**35**), electron microscopy of these samples stained with uranyl acetate showed the presence of amorphous aggregates (data not shown). Thus, the results of the sedimentation assay and electron microscopy indicate that compounds **3**–**5** induce tubulin aggregation, and this ability is remarkably high for ester **5**. It is interesting that both unsubstituted adamantane core and taxol side chain seem to play a part in this ability, because specially synthesized esters **9**–**12** as well as **13a**–**c** demonstrate a relative amount of tubulin in the sedimentation assay of

less than 35% (e.g., **12** in Fig. 3). At the same time, the taxol side chain shift to the 2-position of adamantane (compound **14**) maintains the high level of tubulin aggregation.

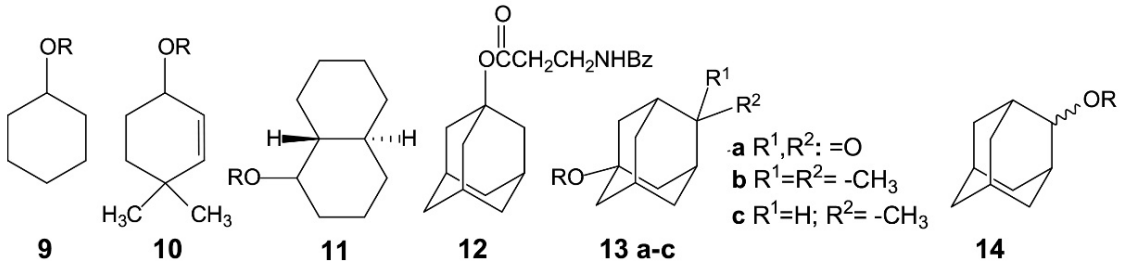


**9** **10** **11** **12** **13 a-c** **14**

R = *taxol side chain*

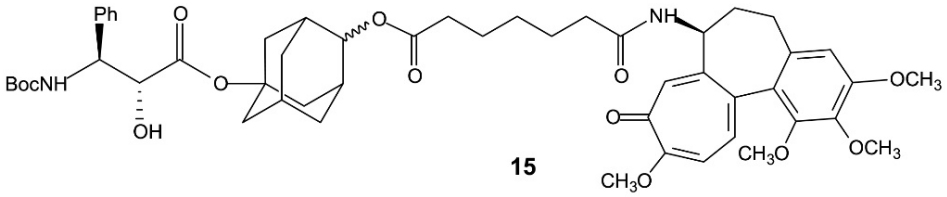


**15**

The interesting ability of structure **5** enabled us to chose taxol/taxotere side chain substituted adamantane as a structural fragment in a hybrid compound **15** analogous to recently obtained hybrid taxol-colchicine ligand colchitaxel.[26] (It is known that taxol and colchicine interact with tubulin at different binding sites and the latter inhibit the protein polymerization and microtubule formation.)[27] We hypothesized that binding of a 'colchicine part' of compound **15** with colchicine binding site might induce the 'adamantane-based taxoid mimic part' to interact effectively with the taxol binding site of tubulin.

The synthesis of the structure **15** is presented in Scheme 3. The esterification of kemantane by an oxazolidine-type-protected *N-tert*-butoxycarbonylphenylisoserine led to the ester **16**, and subsequent reduction of its keto-group by $NaBH_4$ gave the corresponding alcohol **17** (*trans*-/*cis*-isomer ratio 2:1). The further esterification of **17** by the polyanhydride of pimelinic acid led to isomeric esters **18**. Finally, deacetylcolchicine (obtained in three steps from colchicine)[27] was attached to the carboxylic group of compound **18**, and the following deprotection of amino acid in the product **19** led to compound **15** (*trans*-/*cis*-isomers ratio 2:1).

Compound **15** was found to possess very high cytotoxicity against human lung carcinoma cell line A549 (see Table 1). Though it is caused mostly by interaction with colchicine binding site, it is interesting to mention that immunefluorescent microscopy of microtubules in the A549 cells[28] revealed the existence of a small amount of microtubule bundles, characteristic for the taxol action among microtubules and their shortened aggregates in cells treated with 5 μM of **15**. This observation needs, however, additional investigation, because visually similar structures might be a result of compound **15** interacting with a vinca-alkaloid binding site on tubulin. These investigations are currently in progress.

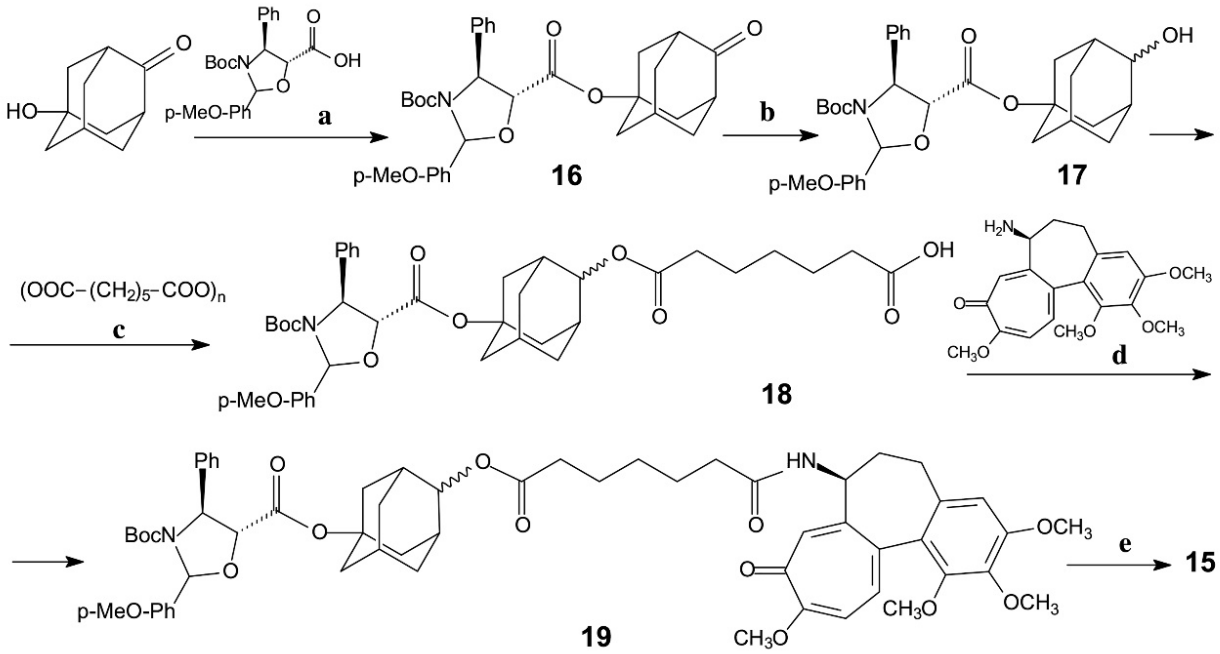


**Scheme** 3. Reagents and conditions: (a) OCC, DMAP, $CH_2C1_2$, rt, 12 h, 46%; (b) $NaBH_4$, $Et_2O$, rt, 10 h, 96%; (c) DMAP, $CH_2Cl_2$, rt, 24 h, 46%; (d) EEDQ, $CH_2C1_2$, rt, 24 h, 76%; (e) TsOH, MeOH, rt, 2 h, 63%.

In summary, the synthesized adamantane derivatives, though being cytotoxic, turned out to be unable to promote microtubule assembly of purified tubulin *in vitro* like most of the known simplified taxol analogues (e.g., Refs. 4,6,7,9,12). This indicates that the 'simplification' in the presented structures is too drastic in comparison with the parent molecule. Nevertheless, the *N*-benzoyl- (2*R*,3*S*)-phenylisoseryloxyadamantane (**5**) demonstrated the ability to cause significant aggregation of the protein, whereas the hybrid compound **15** revealed high and rather unusual cytotoxicity profile and may be considered as a structural clue for the further studies.

## Acknowledgments

We are grateful to Dr. Walter Steffen for electron microscopy. This work was done in the frame of a Scientific Cooperation Agreement between Moscow and Rostock Universities and supported in part by the German organization DAAD (the Leonard Euler Studentship program), by the Russian Foundation for Basic Research (Project No. 07-03-12110-ofi), and by grants of the Russian Academy of Sciences and Russian Federation Ministry of Education.

We thank the laboratory of Dr. Kenneth A Jacobson (National Institute of Diabetes & Digestive & Kidney Diseases, NIH, Bethesda, MD, USA) for useful collaboration on the molecular modeling studies, and for reading the manuscript.

# References and notes


1. Kingston, D. G. I. *Chem. Commun.* **2001**, 867.
2. Zefirova, O. N.; Nurieva, E. V.; Ryzhov, A. N.; Zyk, N. V.; Zefirov, N. S. *Zh. Org. Khim.* **2005**, *41,* 315 (Russ. J. *Org. Chem.* **2005**, *41*, 329).
3. Klar, U.; Graf. H.; Schenk, O.; Röhr, B.; Schulz, H. *Bioorg. Med. Chem. Lett.* **1998**, *8,* 1397.
4. Fuji, K.; Watanabe, Y.; Ohtsubo, T.; Nuruzzaman, M.; Hamajima, Y.; Kohno, M. *Chem. Pharm. Bull.* **1999**, *47,* 1334.
5. Howarth, J.; Penny, P.; McDonnel, S.; O'Connor, A. *Bioorg. Med. Chem. Lett.* **2003***, 13,* 2693.
6. Almqvist, F.; Manner, S.; Thornqvist, V.; Berg, U.; Wallin, M.; Frejd, T. *Org. Biomol. Chem.* **2004***, 2,* 3085.
7. Geng, X.; Geney, R.; Pera, P.; Bemacki, R.; Ojima, I. *Bioorg. Med. Chem. Lett.* **2004**, *14*, 3491.
8. Roussi, F.; Ngo, Q. A.; Thoret, S.; Guéritte, F.; Guédnard, D. *Eur.* J. *Org. Chem.* **2005**, 3952.
9. Ganesh, T.; Norris, A.; Sharma, Sh.; Bane, S.; Alcaraz, A. A.; Snyder, J. P.; Kingston, D. G. I. *Bioorg. Med. Chem.* **2006**, *14*, 3447.
10. Zefirova, O. N.; Selunina, E. V.; Averina, N. V.; Zyk, N. V.; Zefirov, N. S. *Zh. Org. Khim.* **2002**, *38,* 1176 (*Russ. J. Org. Chem.* **2002**, *38,* 1125).
11. Averina, N. V.; Lapina, T. V.; Zefirova, O. N.; Zefirov, N. S. *Vestnik Mosk. Univ. 2. Khim.* **2002***, 43,* 244 (in Russian).
12. Zefirova, O. N.; Nurieva, E. V.; Lemcke, H.; Ivanov, A. A.; Zyk, N. V.; Weiss, D. G.; Kuznetsov, S. A.; Zefirov, N. S. *Mendeleev Commun.* **2008**, *18*, 183.
13. Snyder, J. P.; Nettles, J. H.; Cornett, B.; Downing, K. H.; Nogales, E. Proa *Natl. Acad. Sci. USA.* **2001**, *98,* 5312.
14. The molecular docking of compound 3 was performed automatically with the Glide program of the MacroModel package.[15] The binding site was defined as a box with a side of 29 A with a centre in the centroid of taxol atoms. For all other parameters their default values were used. The full flexibility of the ligand was allowed.
15. Mohamadi, F. N.; Richards, G. J.; Guida, W. C.; Liskamp, R.; Lipton, M.; Caufield, C.; Chang, G.; Hendrickson, T.; Still, W. C. *J. Comput. Chem.* **1990**, *11*, 440.
16. Kiryukhin, M. V.; Nurieva, E. V.; Shishov, D. V.; Nuriev, V. N.; Zyk, N. V.; Zefirov, N. S.; Zefirova, 0. N. *Vestnik Mosk. Univ. 2. Khim.* **2007**. *48.* 342 *(Moscow University Chem. Bull.,* **2007**, *48,* 281).
17. Didier, E.; Fouque, E.; Taillepied, L; Commençon, A. *Tetrahedron Lett.* **1994**, *35,* 2349.
18. For the synthetic details and the characteristics of all the compounds see Online Supplementary Materials.
19. Zefirova, O. N.; Selunina, E. V.; Nuriev, V. N.; Zyk, N. V.; Zefirov, N. S. Zh. *Org. Khim.* **2003**, *39,* 880 (*Russ. J. Org. Chem.* **2003**, *39,* 831).
20. Selunina, E. V.; Zefirova, O. N.; Zyk, N. V.; Zefirov, N. S. *Vestnik Mosk. Univ. 2. Khim.* **2002**, *43,* 237 (in Russian).
21. Bourzat, J. D.; Commençon, A. *Tetrahedron Lett.* **1993**, *34*, 6049.
22. Zefirova, O. N.; Nurieva, E. V.; Chekhlov, A. N.; Aldoshin S. M.; Nesterenko, P. N.; Zyk,

N. V.; Zefirov, N. S. *Zh. Org. Khim.* **2004**, *40*, 533 (*Russ. J. Org. Chem.* **2004**, *40*, 502).

23. Kuznetsov, S. A.; Rodionov, V. L; Bershadsky, A. D.; Gelfland, V. I.; Rosenblat, V. A. *Cell Biol. Int. Rep.* **1980**, *4*, 1017.
24. Weiss, D. G. In *Cell Biology: A Laboratory Handbook;* Celis, J. E., Ed.; Academic Press: San Diego, 2006; Vol. 3, pp 57-65.
25. Rodionov, V. I.; Gyoeva, F. K.; Kashina, A. S.; Kuznetsov, S. A.; Gelfand, V. *I. J. Biol. Chem.* **1990**, *265*, 5702.
26. Bombuwala, K.; Kinstle, T.; Popik, V.; Uppal, S. O.; Olesen, J. B.; Vina, J.; Heckman, C. A. *Beilstein J. Org. Chem.* **2006**, *2*. art no 13.
27. Jordan, A.; Hadfield, J. A.; Lawrence, N.J.; McGown, A. T. *Med. Res. Rev.* **1998**, *18*, 259.
28. In this assay A549 cells were treated with compound **15**, fixed with polyformaldehyde and stained with antibodies (primary mouse anti-α-tubulin secondary fluorescent labelled rabbit anti mouse-ALEXA 488).

*ORGANIC & BIOMOLECULAR CHEMISTRY Vol. 17 (10), 2792-2797, 2019*

# SYNTHESIS AND CYTOTOXICITY OF NOVEL SIMPLIFIED ELEUTHEROBIN ANALOGUES AS POTENTIAL ANTITUMOUR AGENTS

**S.E. Sosonyuk, A. Peshich, A.V. Tutushkina, D.A. Khlevin, N.A. Lozinskaya, Yu.A. Gracheva, V.A. Glazunova, D.I. Osolodkin, M.N. Semenova, V.V. Semenov, V.A. Palyulin, M.V. Proskurnina, A.A. Shtil, N.S. Zefirov**

*Department of Chemistry, Lomonosov Moscow State University, Moscow, Russia.*
*Institute of Physiologically Active Compounds, Russian Academy of Sciences, Chernogolovka, Moscow Region, Russia*
*Blokhin National Medical Center of Oncology, Moscow, Russia*
*FSBSi "Chumakov ESC R&D IBP RAS", Poselok instituta Poliomielita, Poselenie Moskovsky, Moscow Russia*
*Institute of Translational Medicine and Biotechnology, Sechenov First Moscow State Medical University, Moscow, Russia*
*Institute of Developmental Biology, Russian Academy of Sciences, Moscow, Russia*
*Zelinsky Institute of Organic Chemistry, RAS, Moscow, Russia*

Mixed simplified structures containing the paclitaxel and eleutherobin pharmacophore moieties were analyzed using molecular docking techniques and synthesized based on adamantane and 8-oxabicyclo[3.2.1]octane scaffolds. The crucial role of substituents' stereochemistry in biological activity is discussed. At micromolar concentrations the selected analogues interfered with tubulin dynamics *in vitro* and in a living organism. Furthermore, new compounds were cytotoxic against human tumour cell lines. The simplified eleutherobin analogues may be considered as prototypes of a new class of antitumour agents.

# Introduction

Agents used in cancer chemotherapy include the compounds that inhibit ceil division by binding to tubulin and disrupting the balance between microtubule polymerization and depolymerization. Paclitaxel (Taxol®) (Fig. 1) and its synthetic analogue docetaxel (Taxotere®) have been proved to implement their effects *via* prevention of microtubule depolymerization. Eleutherobin (Fig. 1), a natural terpene isolated from the Western Australian soft coral sponge *Eleutherobia* sp., possesses a 10-fold higher antitumour potency than Taxol and docetaxel. The superposition of eleutherobin and paclitaxel in the tubulin binding site shows that different pharmacophore groups of these molecules occupy the same pockets. The taxol binding site is composed of three main pockets occupied by phenylisoserine (taxol) or *N*-methyiurocanic acid residue (eleutherobin), the benzoyloxy group of taxol and the carbohydrate moiety of eleutherobin, respectively.[1,2] The SAR analysis of eleutherobin derivatives[3] specified the groups relevant to the antimitotic activity.

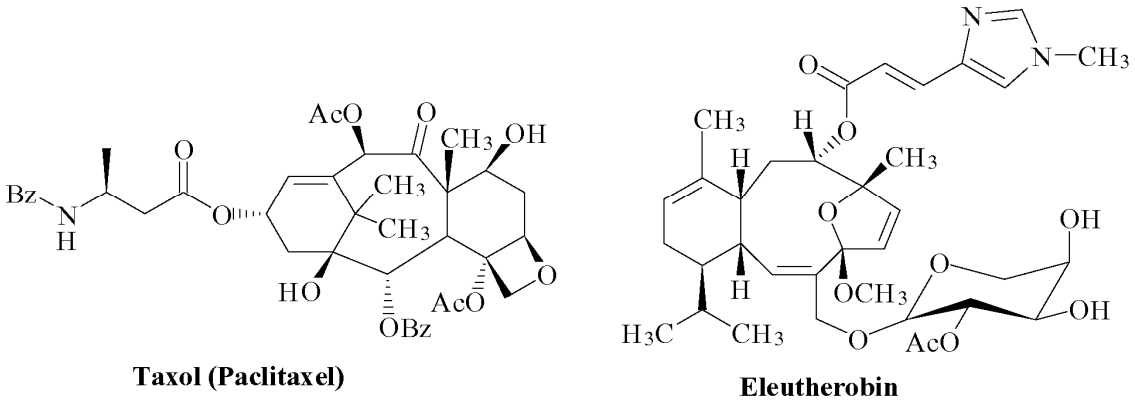


Fig. 1 Structures of paclitaxel and eleutherobin.

The *N*-methylurocanic acid residue [3-(1*H*-imidazol-4-yl]-prop-2-enic acid] is crucial for the antitumour effect of eleutherobin. Removal of *N*-methylurocanic acid residue led to the complete loss of activity.[3] However, the application of eleutherobin in clinical practice is latgely limited due to the complexity of its structure. Therefore, there is a need for isolation of this compound from natural sources or total synthesis.[4] Attempts to design the analogues of this molecule have been described in the literature. Recent approaches to the synthesis of analogues of eleutherobin have been developed based on ring closing metathesis or Claisen condensation. The reactions led to ten or nine-membered ring systems; the compounds caused microtubule destabilization and cytotoxicity at low micromolar concentrations.[1,2]

This study is aimed at the synthesis of simplified analogues of eieutherobin with an improved synthetic accessibility and retained microtubule-stabilizing properties. We describe the molecular modelling and synthesis of a series of mixed structures containing both the paclitaxel and eieutherobin pharmacophore moieties (Fig. 2).

We decided to keep in one molecule the crucial urocanic acid side chain attached to the core in combination with benzoic acid residue (taxoi pharmacophore). To arrange these groups in the tubulin binding site, a hydrophobic core was used. We chose 8-oxabieycio[3.2.1]octane and adamantane derivatives as the hydrophobic spacers. Docking of corresponding *N*-methylurocanic esters demonstrated that 2,4-disubstituted derivatives of 8-oxabicyclo[3.2.1]octane and 1,3- and 1,4-disubstituted derivatives of adamantane were the most compatible with the target (Fig. 3). We also report the cytotoxicity tests on human breast (MCF7), ovarian (SKOV), and colon carcinoma (HCT116) ceil lines.

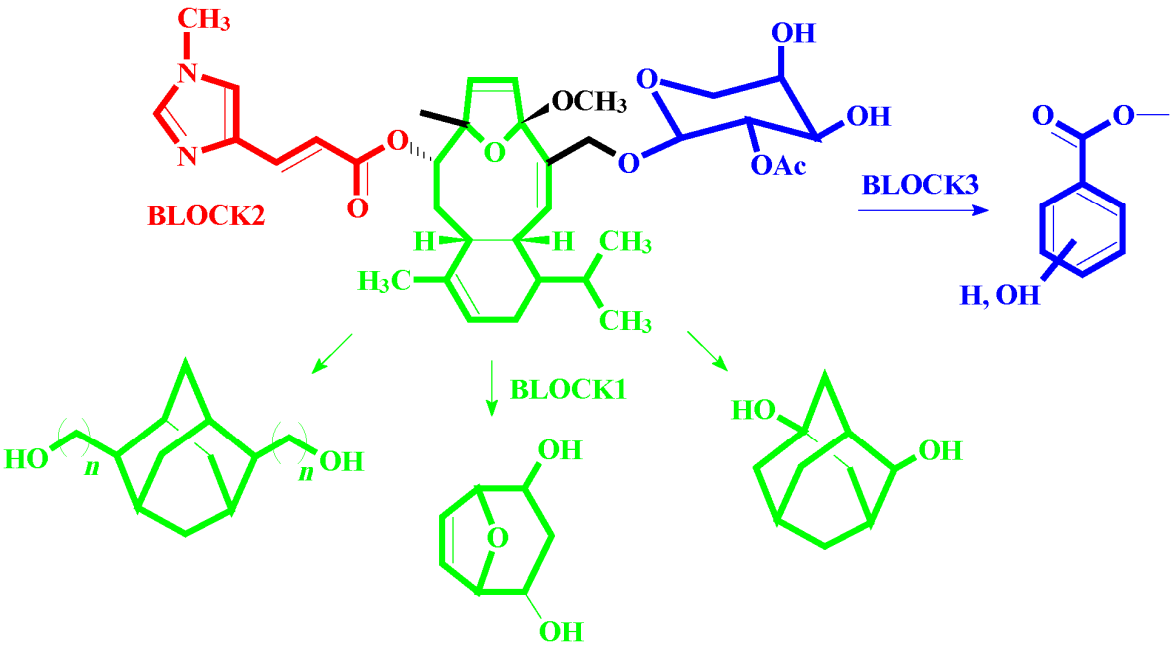


Fig. 2 Design of simplified eieutherobin analogues.

## Results and discussion

### Molecular docking and design of simplified eieutherobin analogues

The complex of tubulin co-ciystallised with paclitaxel (PDB[4] ID 1JFF, chain B[5]) was used throughout this study for docking of eieutherobin and its simplified analogues. Smail molecule conformations generation was performed in OMEGA 2.4.6 (ref. 6), docking was performed with OEDOCKING 3.0.1 (ref. 7). Both FRED[7]* and HYBRID[74] approaches were employed. The visual analysis of docked poses was performed not for a quantitative scoring but for making design decisions based on the sets of binding modes represented among the top 35 best-scored poses.

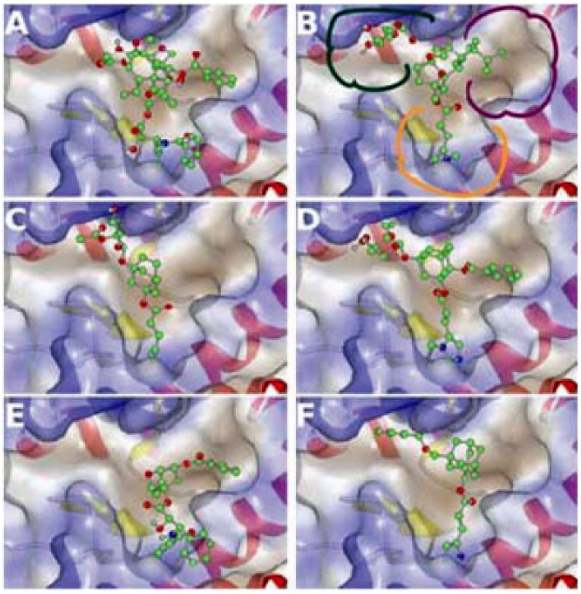


Fig. 3. Structural basis for the design of simplified analogues of eieutherobin and paclitaxel. (A) Binding mode of paclitaxel according to X-ray crystallography data (PDB ID WFF). (B) Top-scored docking pose of eieutherobin. Sub-pocket colours: 'sugar', green; 'hydrophobic', purple; 'urocanic', orange. (C) Docking pose of a virtual bicycle[3.3.1]nonane based molecule. The urocanic acid occupies its sub-pocket the ester mimicking carbohydrate is in the sugar sub-pocket. (D) Docking pose of a virtual adamantane based molecule with three warheads. All three sub-pockets are occupied by corresponding moieties. (E) Docking pose of Ba. The phenylisoserine moiety points at the urocanic subpocket similarly to the paclitaxel pose whereas the phenyl group occupies the hydrophobic sub-pocket. (F) Docking pose of **15b**. The urocanic moiety is in the corresponding pocket the phenyl group points at the hydrophobic part of the sugar pocket. The protein surface is coloured according to the Kyte-Doolittle scheme (blue for hydrophylic regions, brown for hydrophobic).[8] The figure is rendered with VIDA 4.3.0.[9]

The docked eieutherobin molecule significantly overlaps with bound paclitaxel in the tubulin binding site. The polycyclic cores occupy the same central region whereas the moieties at the peripheiy points are located at two of three smaller cavities around. The urocanic acid moiety of eieutherobin preferably occupies the same pocket as phenylisoserine fragment of paclitaxel; the sugar fragment points to a more hydrophylic pocket whereas the benzyl or isopropyl moiety are located in the hydrophobic area (Fig. 3A and B). Simplified eieutherobin analogues can be designed by substituting the central core of the molecule with smaller and more accessible 3D spacers while sparing the specific moieties from the parent molecules (Fig. 3C and D). Adamantane and 8-oxabicycIo[3.2.1]octane were chosen as spacers to substitute the eieutherobin core. According to the docking poses of *N*-methylurocanic acid esters, 2,4-disubstituted derivatives of 8-oxabicyclo[3.2.1]octane as well as 1,3- and 1,4-disubstituted derivatives of adamantane were the most compatible with the taxoi binding site (Fig. 3E and F). One can expect that the additional hydroxyls in the skeleton and the benzoic acid moiety could improve the binding due to hydrogen bond formation or mimicking the sugar

fragment. Also, the initial fusion structures combining the side chain moieties from paclitaxel and eieutherobin were designed.

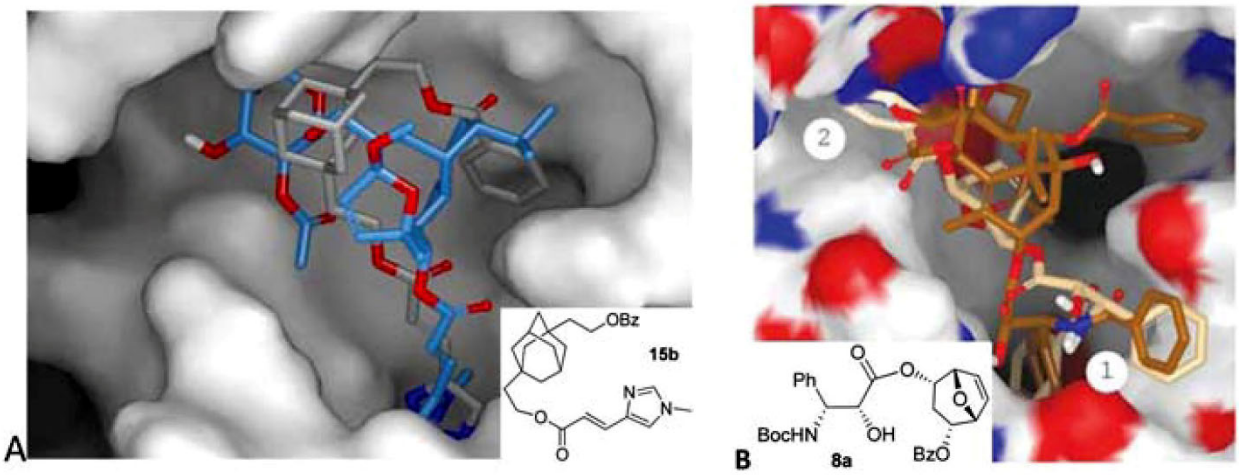


Fig. 4. Superposition of docked poses for eleutherobin and virtual bicyclic compounds. Eleutherobin is rendered blue (A) and brown (B).

The analysis of spacers showed that the introduction of additional one or two methylene groups between hydroxyl and adamantane allows to increase the volume of the hydrophobic core to better comply with the parent molecule (Fig. 4A).

## Chemistry. Synthesis of 8-oxabicyclo[3.2.1]octane derivatives

Oxabicyclooctane diols **2a** and **2b** were synthesized according to our procedure[10] in which the adduct of furan and tetrachlorocyclopropene **1** was used (Scheme 1).

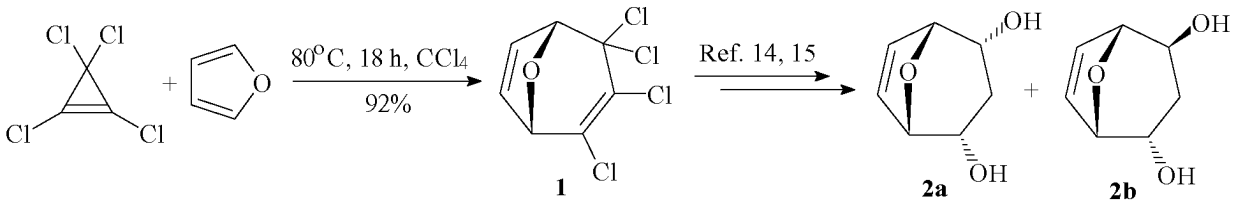


Scheme 1. Synthesis of 8-oxabicyclo[3.2.1]octane derivatives **2a** and **2b**.[10]

The reaction of diols **2a** and **2b** with a small excess of benzoyl chloride and its derivatives (1.3 equiv.) in pyridine afforded the desired monoesters as main products. Thus, the reaction of the symmetrical diol **2a** gave compound **3a**, and the reaction of the non-symmetricai diol **2b** yielded the isomers *exo*-**3b** and *endo*-**3c** in a ratio of 5:2, respectively.

Besides, dibenzoyl derivatives **4a** and **4b** were isolated as byproducts. The optimized procedure was applied to the synthesis of substituted benzoic acid esters **3d,e** (Scheme 2).

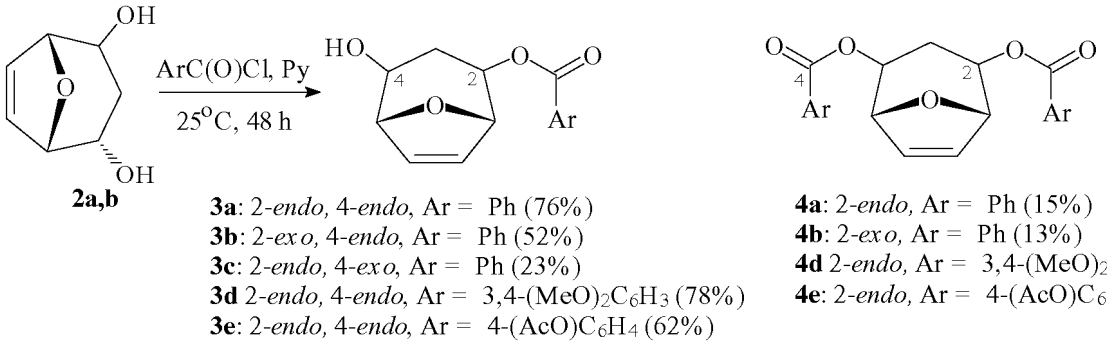


Scheme 2. Synthesis of benzoyl derivatives **3a-e**.

The resulting benzoate monoesters were subjected to esterification with *N*-methylurocanic acid in the presence of DCC and DMAP. The reaction afforded esters **5** in 60–68% yields (Scheme 3). To obtain compound **5e**, the acetate protecting group was cleaved from **5d** by treatment with hydrazine hydrate.

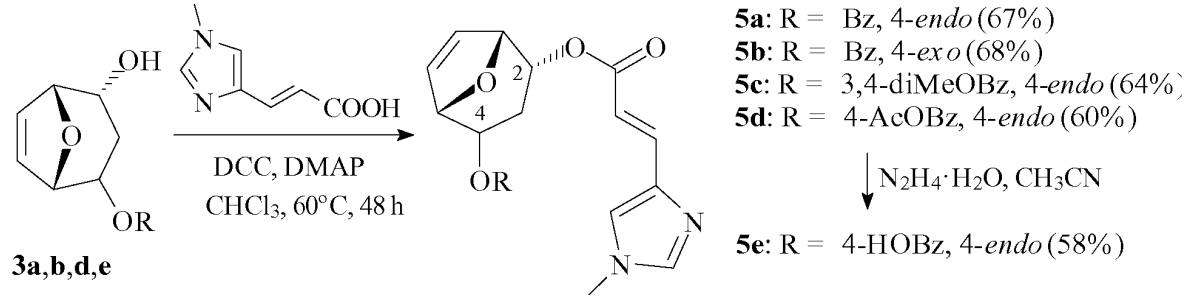


Scheme 3. Esterification of benzoate monoesters with *N*-methylurocanic acid.

The simplified structural analogue of docetaxel, *i.e.,* the ester of the bicyclic alcohol **3a** and (2*R*,3*S*)-*N*-*tert*-butoxycarbonyi-β-phenylisoserine, was synthesized according to a similar procedure. The reaction was performed using phenylisoserine derivative **6** and resulted in the formation of **7** as a mixture of diastereomers. Deprotection of **7** using *p*-toluenesuifonic acid (*p*-TSA) gave the desired ester **8** (Scheme 4). The mixture of diastereomers was separated by column chromatography, and pure compounds **8a** and **8b** were isolated.

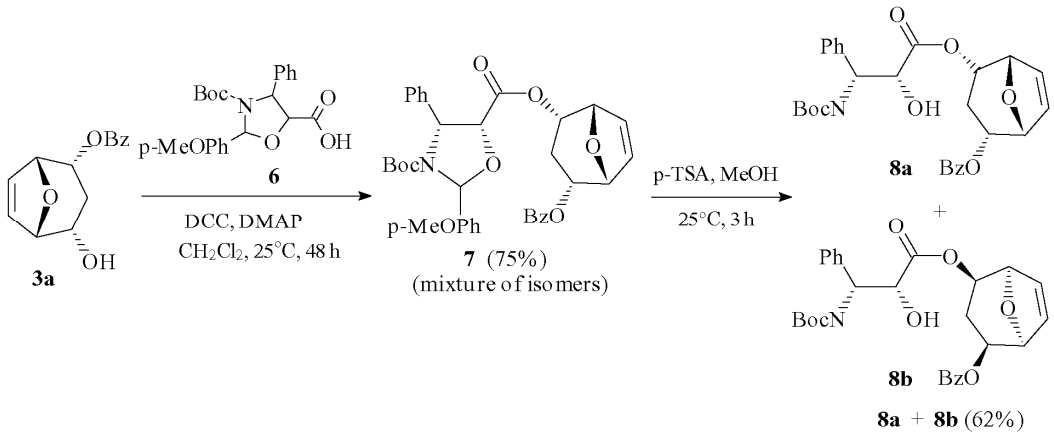


Scheme 4. Reaction of the bicyclic alcohol **3a** with (2*R*,3*S*)-*N*-*tert*- butoxycarbonyl-β-phenylisoserine derivative **6**.

## Synthesis of adamantane derivatives

The following 1,3- and 1,4-derivatives containing two hydroxy groups and 0–2 methylene spacer units were chosen as diols of the adamantane series (Fig. 5).

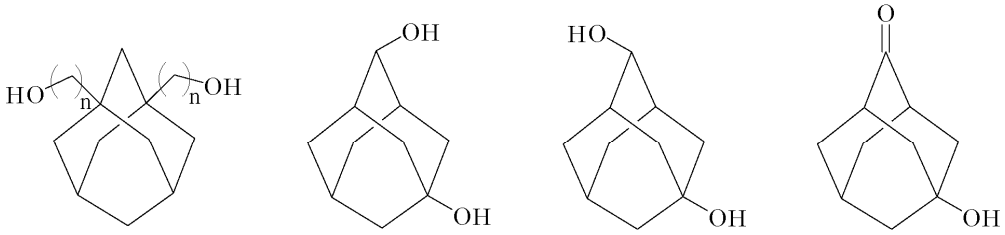


**9a** (n = 1)
**9b** (n = 2)
**10a**
**10b**
**11**

Fig. 5. Target diols **9** and **10** of the adamantane series and kemantane **11**

1,3-Adamantanediois **9a**–**b** were synthesized according to the reported procedures.[11,12] Benzoylation of primaiy diols of the adamantane series **9a**,**b** ran smoothly with a small excess of the acylating agent (Scheme 5). In the case of *p*-acetoxybenzoyl chloride an unexpected acylation yielded mono- and diacetates **12f** and **13a** as side products.

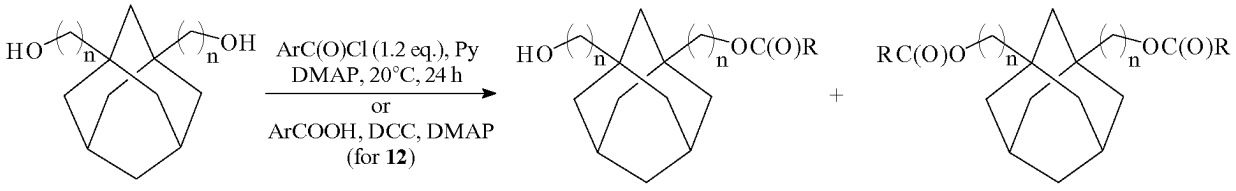


**9a** (n = 1)
**9b** (n = 2)

**12a**: n = 2, R = 3,4-$(MeO)_2C_6H_3$ (68%)
**12b**: n = 1, R = Ph (62%)
**12c**: n = 2, R = Ph (71%)
**12d**: n = 2, R = 4-$HOC_4H_4$ (20%)
**12e**: n = 2, R = 4-$AcOC_4H_4$ (56%)
**12f**: n = 2, R = $CH_3$ (20%)

**13a**: n = 2, R = $CH_3$ (12%)
**13b**: n = 1, R = Ph (13%)
**13c**: n = 2, R = Ph (15%)

Scheme 5. Synthesis of benzoyl derivatives **12a**–**f**.

Reduction of kemantane **11** with sodium borohydride resulted in a non-separabie mixture of isomeric diols **10a**,**b, 13**, **14**. To avoid the problem of isomer separation, reduction of carbonyl group was further performed after modification of hydroxyl (Scheme 6).

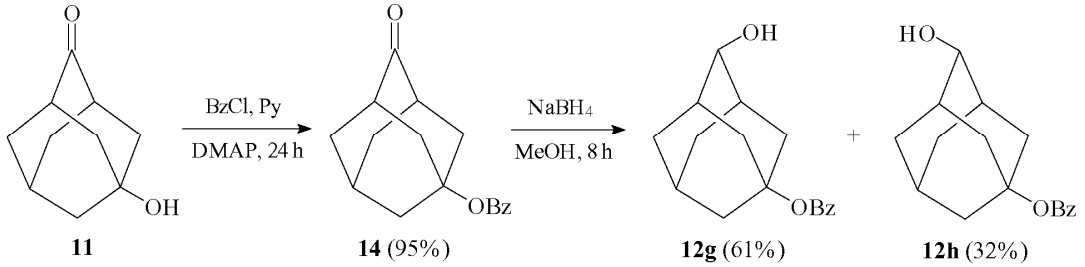


**11**
**14** (95%)
**12g** (61%)
**12h** (32%)

Scheme 6. Synthesis of 1,4-disubstituted adamantane esters.

Benzoylation of kemantane **11** followed by reduction of ketoester **14** afforded a mixture of alcohols **12g** and **12h** in a ratio of *ca.* 2:1 which could be separated into individual isomers by column chromatography. Structures of isomers were determined by NMR spectroscopy using literature data for structurally related compounds. Thus, the signal for the $H^4$ proton in cis-isomers always appears at a higher field compared with the *trans*-isomers.[15,16] Since the corresponding signals of the major/minor products **12g**/**12h** were observed at *S* 3.81/4.02 ppm, respectively, we assigned the structure of the *cis*-isomer to **12g**.

The adamantane derivatives of *N*-methylurocanic acid were synthesized by the optimized procedure from monobenzoyiated diols **12a-h** (Scheme 7). The target esters were isolated in 50–60% yields.

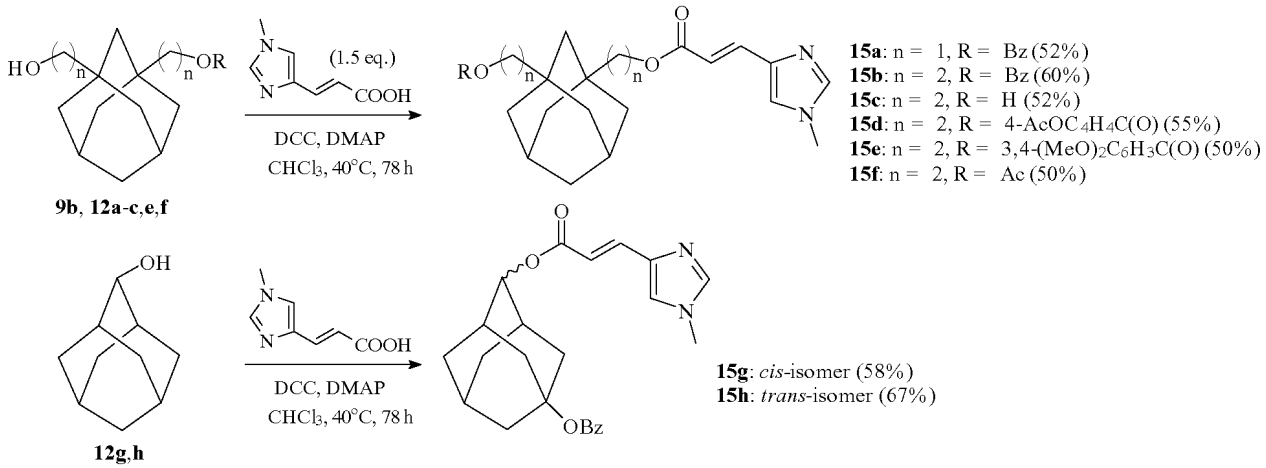


Scheme 7. Synthesis of adamantane esters of *N*-methylurocanic acid.

**Biology. Sea urchin embryo assays**

The phenylisoserine derivative **8a** and two urocanic acid isomeric derivatives **5a,b** were investigated in a sea urchin embiyo assay (Table 1).

Due to structural similarity of tubulin in animals, the sea urchin embiyo is a model for rapid 'one-pot' assessment of antiproliferative, antimitotic, and tubulin destabilizing effects of small molecules in a living organism?[7] Two processes are associated with microtubule dynamics during early sea urchin embryogenesis, namely, cleavage and ciliary swimming of hatched embryos. Compound 5a showed promising activity in causing egg cleavage arrest and the formation of tuberculate eggs typical for tubulin targeting compounds (see ESIf). Interestingly, the isomer **5b** was completely inactive in sea urchin embiyo assay which corresponds to the results of the cell-based assay (see Table 2). Compound **8a** was also inactive in the sea urchin test probably due to a low water solubility.

Table 1. Effects of simple urocanic acid derivatives and compounds **5a,b**, **8a** on sea urchin embryos
Effective concentrations, μM

| | Fertilized egg treatment | | | Hatched blastulae | |
|---|---|---|---|---|---|
| Comp. | Cleavage alteration | Cleavage arrest | Blastula malfor-mation | Developmental alteration | Toxicity, embryonic death (exposure time] |
| Urocanic acid | 800 | >800 | 800 | 200 | 800 (18 h) |
| *N*-Methyl urocanic acid methyl ester | 4 | 10 | 2 | 1 | 5.2 (12 h) |
| *N*-Methyl urocanic acid | 40 | 200 | 20 | 20 | 40 (18 h) |
| **5a** | 0.5 | 2 (TE)° | 0.5 | *2″* | >5 (24 h) |
| **5b** | >4 | >4 | >4 | >4 | >4 (24 h) |
| **8a** | >4 | >4 | >4 | >4 | >4 (24 h) |
| Taxol | 2 | 5 (TE) | 0.5 | NA[C] | 2 (8-10 h) |

Fertilized eggs and hatched blastulae were exposed to 2-fold decreasing concentrations of compounds. Triplicate measurements showed no differences in effective threshold concentration [EC] values. [a] TE: tuberculate eggs typical of microtubule destabilizing agents. [b] Embryo spinning typical of microtubule destabilizers was not observed up to 5 μM concentration. [c] NA: not available.

**Cytotoxicity against human tumour cell lines**

The cytotoxicity of ail synthesized compounds against human carcinoma ceil lines (breast MCF7, ovarian SKOV and colon HCT116) was evaluated using MIT assay[18] with paclitaxel as a reference. Compounds **15a**, **15b**, **15g** and **5a**, **5b**, **8a**, **15b** showed the highest potency against HCT116 and MCF7 ceils, respectively (Table 2). The *cis*-isomers **15g**, **5a** showed a pronounced ceil death typical for taxanes whereas the *trans*-isomers **15h**, **5b** were completely inactive. The cytotoxicity of **15f** against HCT116 ceil line dramatically increased upon doubling the concentration: at 6 pM ceils were viable whereas at 12 pM death of 100% ceils was observed. Death was preceded by ceil rounding within the initial 24 h of incubation, indicative of interaction of compounds with microtubules. It is worth mentioning that compounds **5c**, **5d**, and **15e** containing substituted benzcyl moiety were inactive. This fact indirectly supports the fitting of these substituents into the benzcyl pocket (as in taxol) rather than into the sugar one (as in eleutherobin; Fig. 2 and 3).

Table 2 Cytotoxicity ($IC_{50}$, μM) of compounds for human tumour cell lines.

| Compound | HCT116 | SCOV | MCF7 |
|---|---|---|---|
| **5a** | >50 | >50 | 20 ± 3.5 |
| **5b** | >50 | >50 | >50 |
| **5c** | >50 | >50 | >50 |
| **5e** | >50 | NA | NA |
| **8a** | >50 | >50 | 18 ± 2.6 |

| | | | |
|---|---|---|---|
| **15a** | 16.0 ± 3.2° | 14.6 ± 2.2 | 20 ± 3.5 |
| **15b** | 5.0 ± 1.5 | 4.2 ± 1.0 | 6.9 ± 1.0 |
| **15c** | >50 | NA | NA |
| **15e** | >25 | NA | NA |
| **15f** | >25 | >50 | >50 |
| **15g** | 8.0 ± 2.0 | NA | NA |
| **15h** | >50 | NA | NA |
| Paclitaxel | 0.052 ± 0.003 | 0.04 ± 0.01 | 0.04 ± 0.01 |

[a] Drug concentration that inhibited МТГ conversion by 50% after a 72 h cell exposure. Values are mean + S.D. of 3 independent experiments, each concentration tested in triplicate.

Next, *N*-methyiurocanic acid esters were tested for cytotoxicity against SCOV ceil line. Compound **15b** proved to be the most potent. It is clear though that the potency of this ligand is restricted with necessity to accept an eclipsed conformation of $CH_2CH_2$ spacer between the adamantane core and the benzcyl moiety for the best binding. Clearly, two ways can be proposed to improve the activity. First, to introduce the third substituent pointing towards the sugar pocket (as in eleutherobin; Fig. 2 and 3), and second, to change the core structure from adamantane to a less rigid moiety.

**Tubulin binding**

We assessed the effect of selected compounds on the bovine brain tubulin using a free thiol group counting assay with Eiiman's reagent[19] (Table 3). Compounds that oxidize SH groups in tubulin are known to inhibit microtubule polymerization and induce apoptosis.[20] Kinetic curves of tested compounds in Eiiman's tubulin binding assay (see ESIf for **5a**) were similar to the known tubulin binders such as colchicine, paclitaxel and vinblastine.

Therefore, the biological assays showed that the eieutherobin analogues **5a**, **8a**, **15a**, **15b** and **15g** interfere with tubulin dynamics *in vitro* and are cytotoxic against tumour cell lines at micromolar concentrations. These derivatives may serve as prototypes of a new class of eieutherobin analogues.

Table 3 Binding affinity of synthesized compounds to bovine brain tubulin

| Compound | $IC_{50}$, μM | Compound | $IC_{50}$, μM |
|---|---|---|---|
| **5a** | 21.5 | **8a** | 3.7 |
| **5c** | 12.7 | **8b** | 7.9 |
| **5e** | 5.7 | Paclitaxel | 0.12 |

Values are mean + S.D., each concentration tested in triplicate.

## Conclusions

An initial SAR exploration for a novel series of simplified eieutherobin analogues assisted in the design and synthesis of substances with eieutherobin and taxoi peripheral moieties, such as urocanic and benzoic acids residues, on adamantane and 8-oxabi-

cycio[3.2.1]octane cores. Studies of microtubule binding and cytotoxicity demonstrated that the most potent substances have W-Iike arrangement of urocanic and benzoic acids residues (**5a**, **15b** and **15g**). These compounds caused the effects typical for taxanes as assessed in a sea urchin test and tumour ceil viability. The cytotoxicity of new compounds is comparable with known eieutherobin analogues canying more complicated cores.[1,2] Thus, the simplified eieutherobin analogues emerge as a new chemotype of potential antitumour agents.

**Acknowledgements**

The academic license for OpenEye software was kindly provided by OpenEye Scientific Software Inc. to Dr Vladimir A. Paiyuiin iaboratoiy. Compound 6 was kindly provided by Prof. Olga N. Zefirova (Lomonosov Moscow State University). We thank the Russian Foundation of Basic Research (Project 17-03-01320).

## Notes and references

1. (a) G. H. Hockerman, B. Z. Peterson, B. D. Johnson and W. A. Catterall, *Annu. Rev. Pharmacol. Toxicol,* 1997, **37**, 361, DOI: 10.1146/annurev.pharmtox.37.1.361;
(b) R. Beumer, P. Bayón, P. Bugada, S. Ducki, N. Mongelli, F. R. Sirtori, J. Telsera and C. Gennari, *Tetrahedron,* 2003, **59**, 8803, DOI: 10.1016/j.tet.2003.08.057;
(c) G. C. H. Chiang, A. D. Bond, A. Ayscough, G. Pain, S. Ducki and A. B. Holmes, *Chem. Commun.,* 2005, 1860, DOI: 10.1039/b413426e;
(d) S. Chandrasekhar, V. Jagadeshwar, C. Narsihmulu, M. Sarangapani, D. R. Krishna, J. Vidyasagar, D. Vijay and G. N. Sastry, *Bioorg. Med. Chem. Lett.,* 2004, **14**, 3687, DOI: 10.1016/j. bmci.2004.05.017;
(e) S. Y. Frankie, S. Y. F. Mak, G. C. H. Chiang, E. P. James, J. E. R. Davidson, J. E. Davies, A. Ayscough, G. Pain, J. W. Burton and A. W. Holmes, *Tetrahedron: Asymmetry,* 2009, **20**, 921, DOI: 10.1016/j. tetasy.2009.03.010;
(f) O. N. Zefirova, E. V. Nurieva, D. V. Shishov, I. I. Baskin, H. Lemcke, F. Schroeder, D. G. Weiss, N. S. Zefirov and S. A. Kuznetsov, *Bioorg. Med. Chem.,* 2011, **19**(18), 5529, DOI: 10.1016/j.bmc.2011.07.040;
(g) O. N. Zefirova, H. Lemcke, M. Lantow, E. V. Nurieva, B. Wobith, G. E. Onishchenko, A. Hoenen, G. Griffiths, N. S. Zefirov and S. A. Kuznetsov, *ChemBioChem,* 2013, **14**(12), 1444, DOI: 10.1002/cbic.201300143;
(h) R. A. Stanton, K. M. Gernert, J. H. Nettles and R. Aneja, *Med. Res. Rev.,* 2011, **31**(3), 443, DOI: 10.1002/med.20242.
2. (a) D. J. Newman and G. M. Cragg, *Curr. Med. Chem.,* 2004, **11**, 1693, DOI: 10.2174/0929867043364982;
(b) F. Berrue, M. W. B. McCulloch and R. G. Kerr, *Bioorg. Med. Chem.,* 2011, **19**, 6702, DOI: 10.1016/j.bmc.2011.06.083;
(c) Y.-N. Cao, L.-L. Zheng, D. Wang, X.-X. Liang, F. Gao and X.-L. Zhou, *Eur. J. Med. Chem.,* 2018, **143**, 806, DOI: 10.1016/j.ejmech.2017.11.062;
(d) D. G. I. Kingston and J. P. Snyder, *Acc. Chem. Res.,* 2014, **47**, 2682, DOI: 10.1021/ar500203h.

3. K. C. Nicolaou, F. van Delft, T. Ohshima, D. Vourloumis, J. Xu, S. Hosokawa, J. Pfefferkom, S. Kim and T. Lee, *Angew. Chem., Int. Ed. Engl.,* 1997, **36**, 2520, DOI: 10.1002/ anie.199725201.
4. H. M. Berman, J. Westbrook, Z. Feng, G. Gilliland, T. N. Bhat, H. Weissig, I. N. Shindyalov and P. E. Bourne, The Protein Data Bank, *Nucleic Acids Res.,* 2000, **28**, 235.
5. J. Löwe, H. Li, K. H. Downing and E. Nogales, *J. Mol. Biol,* 2001, **313**(5), 1045, DOI: 10.1006/jmbi.2001.5077.
6. *(a) OMEGA, version 2.4.6,* OpenEye Scientific Software, Inc., Santa Fe, NM, USA, http://www.eyesopen.com, 2010;
(b) P. C. D. Hawkins, A. G. Skillman, G. L. Warren, B. A. Ellingson and M. T. Stahl, J. *Chem. Inf. Model,* 2010, **50**, 572-584.
7. (a) *OEDOCKING, version 3.0.1,* OpenEye Scientific Software, Inc., Santa Fe, NM, USA, http://www.eyesopen.com, 2012;
(b) M. McGann, *J. Chem. Inf. Model.,* 2011, **51**, 578-596;
(c) M. McGann, *J. Comput-Aided Mol Des.,* 2012, **26**, 897-906.
8. J. Kyte and R. Doolittle, J. *Mol. Biol.,* 1982,**157**(1), 105.
9. *VIDA, version 4.3.0,* OpenEye Scientific Software, Inc., Santa Fe, NM, USA, http://www.eyesopen.com, 2010.
10. D. A. Khievin, S. E. Sosonyuk, M. V. Proskurnina and N. S. Zefirov, *Eur. J. Org. Chem.,* 2013, 2381, DOI: 10.1002/ ej'oc.201201426; D. A. Khievin, S. E. Sosonyuk, M. V. Proskurnina and N. S. Zefirov, *Tetrahedron,* 2012, **68**, 5785, DOI: 10.1016/j.tet.2012.05.029.
11. H. Stetter and C. Wulff, *Chem. Ber.,* 1960, **93**,1366.
12. Kolocouris, R. K. Hansen and R. W. Broadhurst, *J. Med. Chem.,* 2004, **47**, 4975.
13. Y. Ishii, T. Nakano and N. Hirai, *US Patent* 6392104B1, 2002.
14. O. N. Zefirova, E. V. Selyunina, N. V. Averina, N. V. Zyk and N. S. Zefirov, *Russ. J. Org. Chem.,* 2002, **38**, 1125, DOI: 10.1023/A:1020989123733.
15. M. S. Wolfe, *Synth. Commun.,* 1997, **27**, 2975, DOI: 10.1080/ 00397919708005004.
16. S. Srivastava, CK. Cheung and W. Le Noble, *Org. Magn. Reson.,* 1985, 23, 232, DOI: 10.1002/mrc.l260230404.
17. Yu. Strobykina, M. G. Belenok, M. N. Semenova, V. V. Semenov, V. M. Babaev, I. Kh. Rizvanov, V. F. Mironov and V. E. Kataev, J. *Nat. Prod.,* 2015, **78**, 1300, DOI: 10.1021/ acsjnatprod.5b00124; M. N. Semenova, A. S. Kiselyov and V. V. Semenov, *BioTechniques,* 2006, **40**, 765, DOI: 10.2144/ 000112193.
18. W.-S. Chung, Y.-D. Liu and N.-J. Wang, J. *Chem. Soc., Perkin Trans. 2,* 1995, 581, DOI: 10.1039/p29950000581; A. E. Shchekotikhin, V. A. Glazunova, L. G. Dezhenkova, E. K. Shevtsova, V. F. Traven', J. Baizarini, H.-S. Huang, A. A. Shtil and M. N. Preobrazhenskaya, *Eur. J. Med. Chem.,* 2011, **46**, 213, DOI: 10.1016/j.ejmech.2010.11.017.
19. G. L. Ellman, Tissue sulfhydryl groups, *Arch. Biochem. Biophys.,* 1959, **82**(1), 70, DOI: 10.1016/0003-9861(59)90090-6.

20. (a) An Overview of Compounds That Interact with Tubulin and Their Effects on Microtubule Assembly, in *The role of microtubules in cell biology, neurobiology, and oncology,* ed. T. Fojo, Humana Press, 2008, ch. 1, p. 1;
(b) P. J. Britto, L. Knipling, P. Mcphie and J. Wolff, *Biochem. J.,* 2005, **389**, 549.

## Лиганды колхицинового сайта связывания в тубулине

*BIOORGANIC & MEDICINAL CHEMISTRY Vol 19 (18), 5529-5538, 2011*

# SYNTHESIS AND SAR REQUIREMENTS OF ADAMANTANE-COLCHICINE CONJUGATES WITH BOTH MICROTUBULE DEPOLYMERIZING AND TUBULIN CLUSTERING ACTIVITIES

**O.N. Zefirova, E.V. Nurieva, D.V. Shishov, I.I. Baskin, F. Fuchs, H. Lemcke, F. Schroder, D.G. Weiss, N.S. Zefirov, S.A. Kuznetsov**

*Department of Chemistry, M. V. Lomonosov Moscow State University, Moscow, Russian Federation*
*Institute of Physiologically Active Compounds, Moscow region, Chernogolovka, Russian Federation*
*Institute of Biological Sciences, Cell Biology and Biosystems Technology, University of Rostock, D-18059 Rostock, Germany*

A series of analogues of conjugate **1**, combining an adamantane-based paclitaxel (taxol) mimetic with colchicine was synthesized and tested for cytotoxicity in a cell-based assay with the human lung carcinoma cell line A549. The most active compounds (**10** $EC_{50}$ 2 ± 1.0 nM, **23** $EC_{50}$ 6±1.4 nM, **26** $EC_{50}$ 1 ± 1.8 nM, **28** $EC_{50}$ 11 ± 1.7 nM, **30** $EC_{50}$ 4.8 ± 0.5 nM) were found to interfere with the microtubule dynamics in an interesting manner. Treatment of the cells with these compounds promoted disassembly of microtubules followed by the formation of stable tubulin clusters. Structure-activity relationships for the analogues of **23** revealed the sensitivity of both cytotoxicity and tubulin clustering ability to the linker length. The presence of adamantane (or another bulky hydrophobic and non-aromatic moiety) in **23** was found to play an important role in the formation of tubulin clusters. Structural requirements for optimal activity have been partially explained by molecular modeling.

## 1. Introduction

Natural compounds such as paclitaxel (taxol), colchicine and vinca-alkaloids (vincristine and vinblastine) possess high antitumour activity due to their interaction with the intracellular protein tubulin. Although these compounds have the same target protein, their binding sites and their biological activities differ considerably. Thus, paclitaxel causes spontaneous tubulin polymerization into stable microtubules and stabilize preformed microtubules whereas colchicine and vinca-alkaloids inhibit tubulin polymerization and microtubule formation.[1,2]

Among the different approaches to the design of new antitubulin agents, studies of various hybrid ligands recently attracted much attention.[3] The rationale behind the combination of two or more tubulin ligands in a single molecule is that the hybrid ligand may have higher activity and/or better pharmacological profile than the equivalent combination of individual compounds. Besides, this approach leads sometimes to a discovery of molecules with unusual types of activity.

Earlier we synthesized a hybrid ligand combining an adamantane-based paclitaxel mimetic with colchicine (**1**, *trans/cis* 2:1, Fig. 1),[4] which possessed very high cytotoxicity against A549 human lung carcinoma cells. Moreover, the preliminary test indicated that hybrid **1** had an unusual cytotoxicity profile, namely both microtubule destabilizing activity and ability to promote the formation of stable tubulin structures resembling the action of paclitaxel with microtubule bundling or vinblastine-like activity with tubulin paracrystal formation.

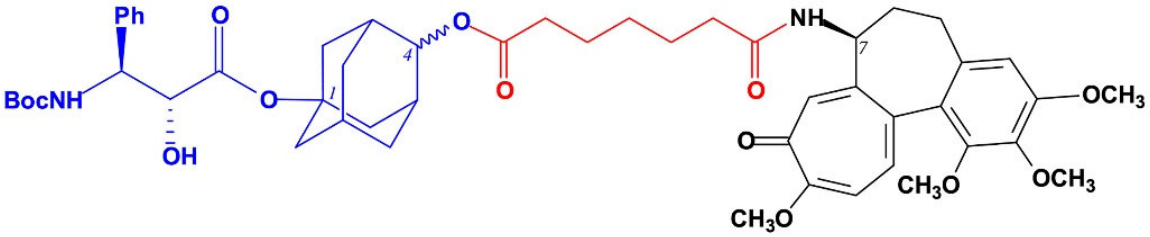


Figure 1. Adamantan-based paclitaxel mimetic-colchicine hybrid.

In the present work we carried out additional biological tests to verify the effect of 1 on tubulin and studied the structure-activity relationships for a number of analogues of the lead compound. Several aspects were suggested for the investigation: the linker length, the possibility of amino acid side chain removal, the position of the linker attachment and the role of adamantane moiety. Molecular modeling was performed for a better understanding SAR results.

## 2. Results and discussion

### 2.1. Biological assays for the lead compound

The hybrid **1** was first tested using in vitro tubulin polymerization assay.[5] Purified bovine brain tubulin was polymerized in the presence of 10% DMSO and supplemented with 10 μM of **1** or 10 μM colchicine, as positive control. After 1 h of incubation the resulting preparations were analyzed by Allen Video-Enhanced Differential Interference Contrast light microscopy.[6] According to the images obtained hybrid **1** completely inhibited the microtubule assembly *in vitro*. This effect was more pronounced than that of colchicine, in the presence of which few small aggregates and short microtubules have been detected.

Compound **1** was previously found to inhibit strongly the cell growth of human lung carcinoma cell line A549 in a cell proliferation test.[4] In this study cytotoxic properties of **1** were further evaluated by A549 cell-based viability assay with the standard MTT [3-(4,5-dimethylthiazol-2-yl)-2,5-diphenyltetrazolium bromide] assay protocol.[7] The $EC_{50}$ value was found to be close to that of colchicine (see Table 1).[11]

**Table 1**
Cytotoxicity and effect of the hybrid compounds on A549 cellular microtubules

| N | Compound | Cytotoxicity[a] $EC_{50}$ ± SD (nM) | Effect on cellular microtubules[b] at 1 μM |
|---|---|---|---|
| 1 | 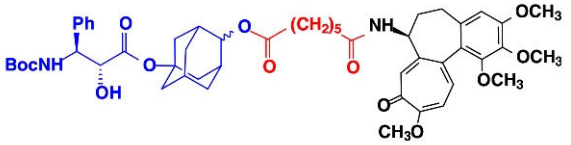 | 73± ± 2.9 | Depolymerization and tubulin clustering ++ |
| 4 | 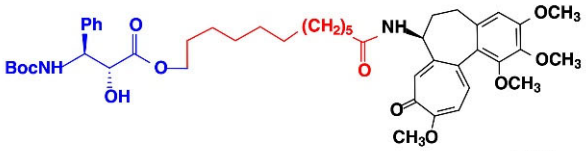 | 41 ± 9.8 | Depolymerization and tubulin clustering + |
| 10 | 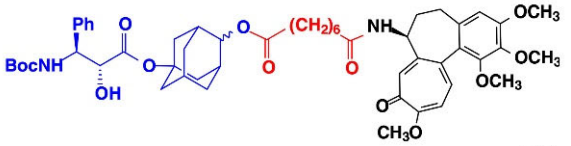 | 2 ± 1.0 | Depolymerization and tubulin clustering +++ |
| 11 | 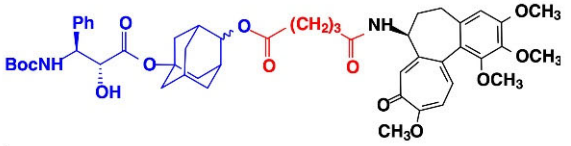 | 220 ± 12 | ND |
| Colchicine | | 27 ± 1.5 | Depolymerization only |
| Paclitaxel (Taxol) | | 4.6 ± 0.7 | Microtubule bundling |

[a] The average of three to six experiments.
[b] The number of '+' symbolizes the relative strength of the effect.

[11] It should be mentioned that this value was higher than the $IC_{50}$ value for compound 1 determined earlier by a different method (i.e. the proliferation assay, where the cells were counted directly with hemocytometer cell count calculator).[4] Actually it is not clear, why the two methods give so different absolute values, while the relative values obtained for the different compounds are in a good agreement. However in the present investigation MTT experiments were carried out under identical conditions for all the tested compounds. The differences in the effects were also confirmed by immunofluorescence microscopy.

The effect of hybrid **1** on microtubule dynamics in A549 cells was also investigated and compared to that of colchicine. Cells were incubated with 1 μM and 5 μM of **1** for 8 h, fixed in 4% paraformaldehyde and stained with primary mouse monoclonal antibodies against α-tubulin followed by incubation with ALEXA-Fluor488 labelled goat anti-mouse IgG as the secondary antibody.[8] Images of the samples were analyzed by fluorescence microscopy and are shown on Figure 2(A-D).

At a concentration of 1 μM hybrid **1** had a clearly visible destabilizing effect on the microtubule network: the samples displayed only very few small microtubule fragments. Although the effect of the tested compound was slightly weaker than that of colchicine, contrary to the latter, hybrid **1** in addition caused a formation of tubulin clusters which were detected among short microtubules and diffusely labeled tubulin (Fig. 2C). Notably, at a concentration of 5 μM no intact microtubules were observed and the clustering effect of **1** was more prominent (Fig. 2D).

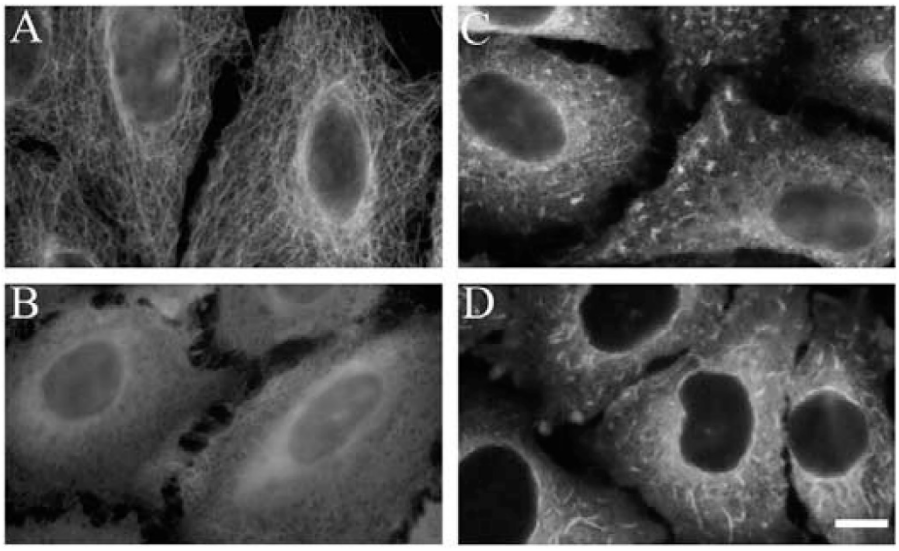


**Figure 2.** Effect of conjugate **1** on the microtubule network in A549 lung carcinoma cells analyzed by indirect immunofluorescence microscopy. Cells were treated: A – with 0.6% DMSO (negative control): B – with 1 μM of colchicine (positive control): C and D – with 1 μM and 5 μM of compound **1** respectively. Destabilizing effect of **1** on the microtubule network and tubulin clustering effect are clearly seen in C and D. Bar 20 μM.

These experiments proved the ability of hybrid **1** to cause tubulin clustering in addition to the colchicine-like activity. We named the former ability 'tubulin clustering' because the morphology of these clusters is different from paclitaxel-induced microtubule bundles and vinblastine-induced tubulin paracrystals (see also Fig. 3).

Interestingly, the 'clustering effect' cannot be caused by the simultaneous cell treatment with 5 μM paclitaxel and 5 μM colchicine for eight hours, thus being a specific property of the hybrid molecule.

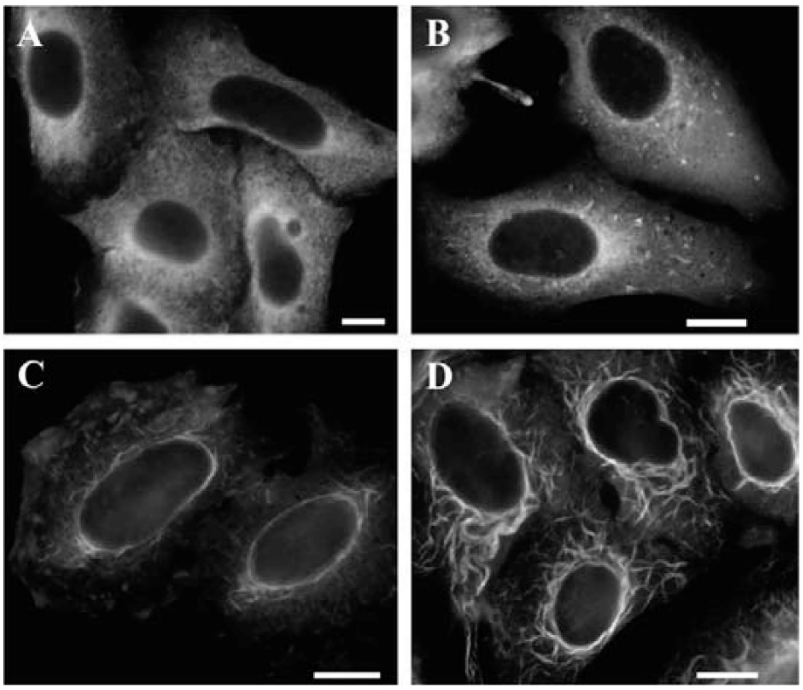


**Figure 3.** Typical patterns of tubulin distribution in treated cells used for evaluation of the effect of tested compounds on microtubules as indicated in Tables 1 and 2.
A – 'depolymerization only'; B – tubulin clustering, C – tubulin clustering *++'; D – tubulin clustering '+++'. Bar 20 μM.

## 2.2. Chemistry

To determine the structural requirements for the tubulin clustering effect and cytotoxicity a structure-activity investigation was performed for analogues of **1**. The derivative of hybrid **1** without adamantane moiety (structure **4**) was synthesized from 12-hydroxydodecanoic acid and *N*-deacetylcolchicine (prepared in three steps from colchicine[9]) as shown in Scheme 1. Esterification of the obtained amide **2** by an oxazolidine-type protected *N-tert*-butoxycarbonylphenylisoserine[10] led to the conjugate **3** and deprotection of the latter afforded the purpose compound **4**.

The synthesis of two hybrids **10**, **11** with different linker lengths was analogous to that of **1** (Scheme 2). The esterification of 1-hydroxyadamantantane-4-one by protected amino acid and subsequent reduction of the resulting keto-ester gave a mixture of isomeric alcohols **5**.[4] Further esterification of **5** by either suberic acid polyanhydride[11] or glutaric acid anhydride led to isomeric esters **6** and **7** respectively. Finally, *N*-deacetylcolchicine was attached to the carboxylic group of compounds **6** and **7**. The following deprotection of amino acid in the products **8** and **9** afforded hybrids **10** *(trans/cis* 7:3) and **11** *(trans/cis* 1:1).

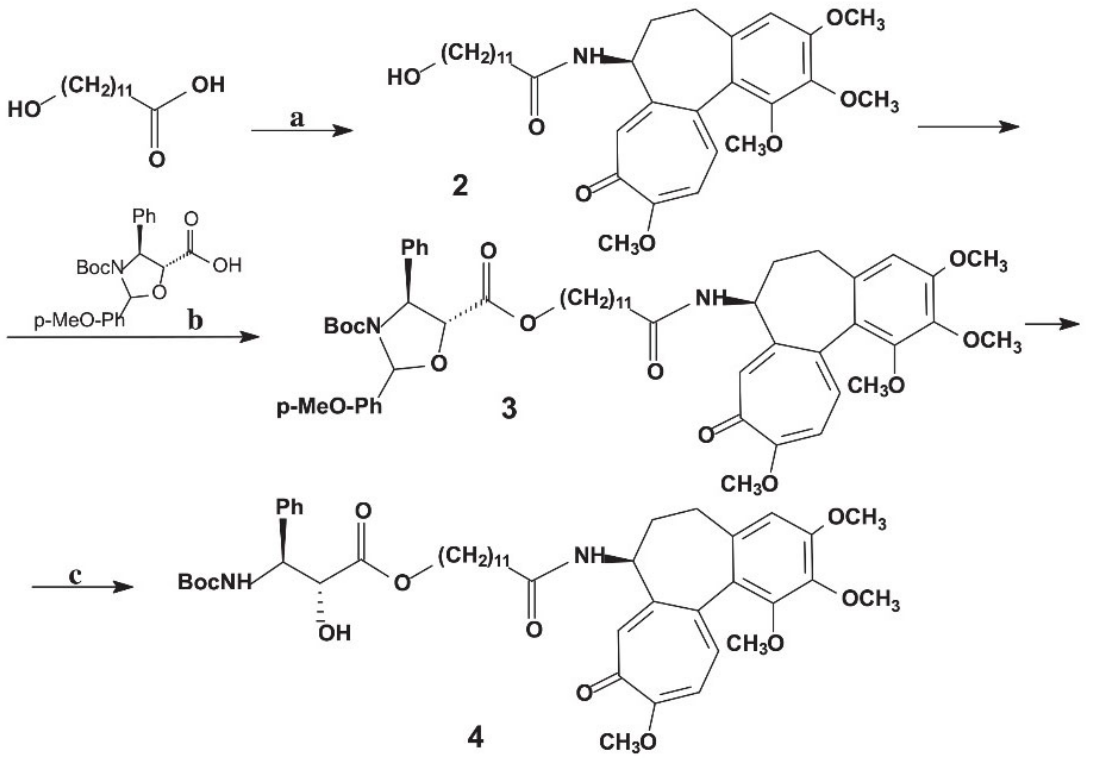

**Scheme 1.** *Reagents and conditions:* (a) EEDQ, $CH_2C1_2$, rt, 60 h; (b) DCC, DMAP, $CH_2Cl_2$, rt, 12 h; (c) *p*TSA, MeOH, rt, 2.5 h.

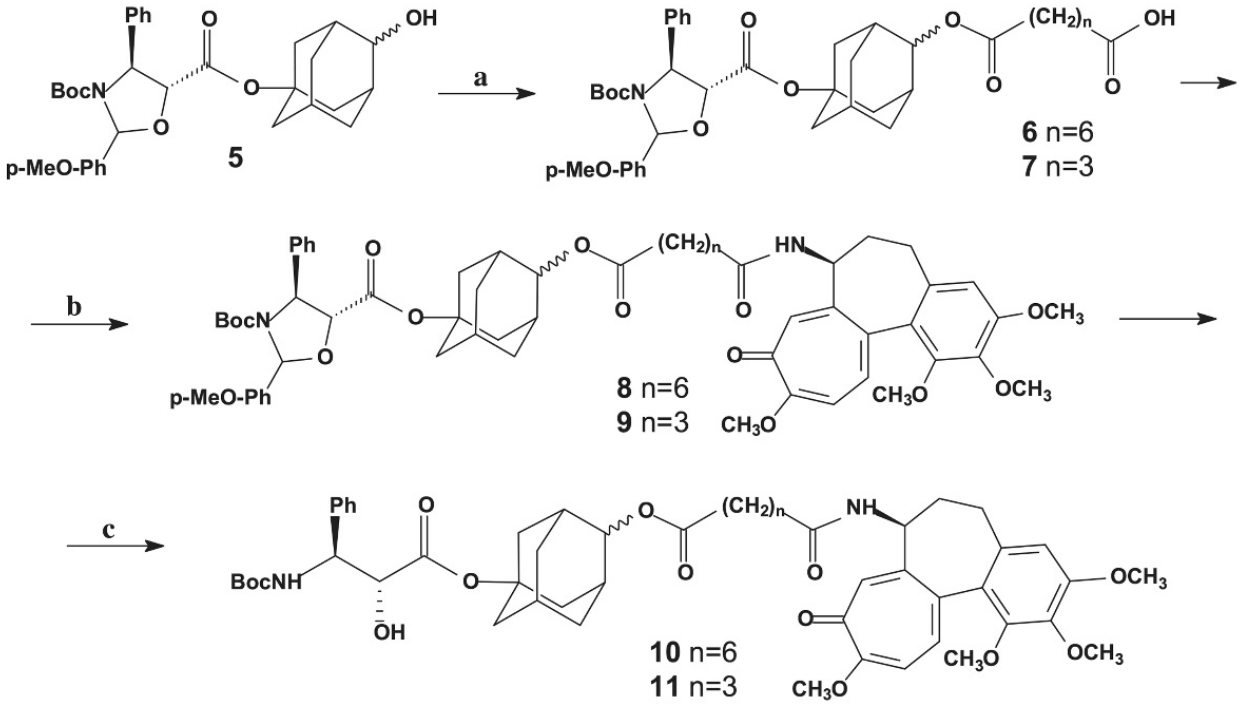

Scheme 2. *Reagents and conditions:* (a) $(OOC–(CH_2)_n–CO)_m$, DMAP, $CH_2C1_2$, rt, 24-48 h; (b) N-deacetylcolchicine, EEDQ, $CH_2C1_2$, rt, 24 h; (c) *p*TSA, MeOH, rt, 2.5 h.

All derivatives of **1** without amino acid side chain (**23**–**29**) and their analogues with hydrophobic substituents other than adamantane (**30**–**33**) were prepared from the corresponding alcohols as shown in Scheme 3.

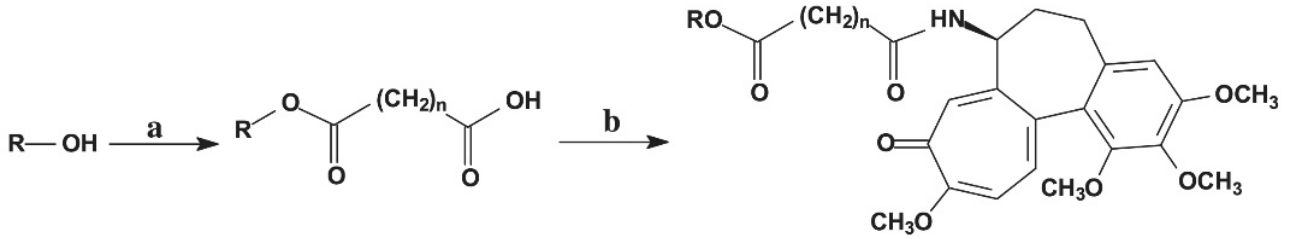


**12** R=2-Ad, n=5
**13** R=2-Ad, n=4
**14** R=2-Ad, n=3
**15** R=2-Ad, n=6
**16** R=2-Ad, n=7
**17** R=1-Ad, n=5
**18** R=1-Ad, n=7
**19** R= cyclohexyl, n=5
**20** R=Me, n=5
**21** R=i-Pr, n=5
**22** R=Ph, n=5

**23** R=2-Ad, n=5
**24** R=2-Ad, n=4
**25** R=2-Ad, n=3
**26** R=2-Ad, n=6
**27** R=2-Ad, n=7
**28** R=1-Ad, n=5
**29** R=1-Ad, n=7
**30** R= cyclohexyl, n=5
**31** R=Me, n=5
**32** R=i-Pr, n=5
**33** R=Ph, n=5

Scheme 3. *Reagents and conditions:* (a) (OOC–$(CH_2)_n$–CO)$_m$, DMAP, $CH_2C1_2$, rt, 24–36 h; (b) *N*-deacetylcolchicine, EEDQ, $CH_2C1_2$, rt, 12–24 h, (c) TEA, $CH_2C1_2$, rt, 24 h.

## 2.3. Biotests and structure-activity relationships

The inhibitory effect of the synthesized compounds on proliferation of human lung carcinoma A549 cells was evaluated using MTT test.[7] Effect on microtubule dynamics was investigated as described in section 2.1 (the typical patterns of tubulin clusters in cells treated with different compounds are shown in Fig. 3). The results of both tests are presented in Tables 1 and 2.

As evidenced from Table 1 an analogue of hybrid **1** without adamantane moiety and with the similar distance between colchicine and the amino acid (hybrid **4**) exhibited only slightly higher cytotoxicity than the parent compound and a strongly less pronounced clustering effect. Thus the adamantane fragment was maintained in the next two series of compounds.

The data for **1**, **10** and **11** clearly indicate that the elongation of the spacer length improves cytotoxity, the hybrid **10** with a six-methylene linker being one order of magnitude more potent than colchicine and as potent as paclitaxel (see Table 1).

To check the role of amino acid substituent in the parent structure we synthesized compound **23**, which is an analogue of **1** without *N*-*tert*-butoxycarbonyl-(2*R*,2*S*)-phenylisoseryl moiety. This amino acid represents a $C^{13}$ side chain of paclitaxel derivative taxoter and is known to provide the most important contribution to the paclitaxel-binding site interaction.[1,2] As seen in Table 2 conjugate **23** exhibits very high cytotoxicity and its clustering activity is improved in comparison with **1**. This result is remarkable and signifies that the clustering effect does not depend upon the presence of taxoter amino acid side chain and, consequently, is hardly connected to an interaction with the

paclitaxel binding site of tubulin. Thus, these data are in accordance with the results of our study on the morphology of the clusters.

Table 2. Cytotoxicity and effect of the colchicine conjugates on A549 cellular microtubules

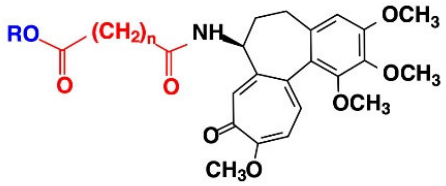


| Compound | | | Cytotoxicity[a] $EC_{50}$ ± SD (nM) | Effect on cellular microtubules[b] at 1 μM |
|---|---|---|---|---|
| N | R | *n* | | |
| **23** | | 5 | 6 ± 1.4 | Depolymerization and tubulin clustering +++ |
| **24** | | 4 | 830 ± 140 | Depolymerization and tubulin clustering ++ |
| **25** | | 3 | 200 ± 62 | depolymerization only |
| **26** | | 6 | 5 ± 1.8 | Depolymerization and tubulin clustering +++ |
| **27** | | 7 | 3800 ± 630 | Depolymerization and tubulin clustering + |
| **28** | | 5 | 11 ± 1.7 | Depolymerization and tubulin clustering +++ |
| **29** | | 7 | 29 ± 1.2 | ND |
| **30** | | 5 | 4.8 ± 0.5 | Depolymerization and tubulin clustering +++ |
| **31** | 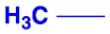 | 5 | 32 ± 2.1 | Depolymerization only |
| **32** | 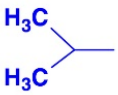 | 5 | 30 ± 2.7 | Depolymerization and tubulin clustering + |
| **33** | | 5 | 5700 ± 820 | Weak depolymerization only |
| Colchicine | | | 27 ± 1.5 | Depolymerization only |
| Paclitaxel (Taxol) | | | 4.6 ± 0.7 | Microtubule bundling |

[a] The average of three to six experiments.
[b] The number of '+' symbolizes the relative strength of the effect.

As though the structure of conjugate **23** is much simpler than that of **1**, we have chosen **23** as a new lead compound for subsequent structure-activity investigations.

A SAR study in a series of analogues of **23** with different linker length **23**–**27** (Table 2) shows a maximum of cytotoxicity for ligands with five- and six-methylene linkers (**23**, **26**). Further elongation of the spacer (**27**) or its shortening (**24**, **25**) leads to a considerable decrease of activity. Interestingly, all compounds in the series are in fact rather simple colchicine derivatives with a modified side chain at $C^7$ (it is generally accepted that substitution at this position is highly tolerated (see e.g.[12])). Nevertheless a strong dependence of both cytotoxicity and clustering effect on the length of this

substituent was observed. Thus, three-methylene ligand **25** maintains only the microtubule depolymerizing activity while its four-methylene analogue **24** possesses also a noticeable clustering effect.

The structural modification of the lead **23** next studied was a change of the position of linker attachment to adamantane. Conjugate **28** with the linker attached to a bridgehead atom possessed high cytotoxicity and clustering effect close to that of **23**, thus suggesting that the movement of the linker was tolerated. Interestingly, the two-methylene elongation of the spacer length in **28** – structure **29** – only slightly reduced the cytotoxicity, while in the pair **23**/**27** it was detrimental for the activity.

The final structure-activity relationship was established for a series of conjugates similar to **23** but with lipophilic moieties distinct from adamantane. Replacement of a bridgehead core for cyclohexane led to compound **30** with the same high cytotoxicity and close tubulin clustering effect. Unexpectedly weak activity was observed for ligand **33** with a phenyl substituent, moreover its clustering ability was lost. Cytotoxicity of methyl (**31**) and isopropyl (**32**) derivatives was almost equal to that of colchicine and for the former only the colchicine-like depolymerizing effect was observed. These results indicate, that the presence of a bulky hydrophobic and non-aromatic moiety in the studied conjugates plays an important role in the tubulin-dustering effect.

Since all the most cytotoxic compounds synthesized (**10**, **23**, **26**, **28**, **30**) possess the strongest tubulin clustering ability (see Tables 1 and 2), we suppose that this property might be an important factor in the increment of mitostatic activity. This proposition is also confirmed by comparison of the activities in the triad of structurally close compounds colchicine – **31**–**23**. A noticeably higher cytotoxicity is observed for the compound **23** with high clustering effect, while compounds with depolymerizing ability only have equal lower cytotoxicity.

It should be mentioned, that the effect of the lead compound **23** on microtubule dynamics was also studied using cancer cell line, different from A549, namely HeLa human cervical carcinoma cells. In these cells we also observed the intensive formation of tubulin clusters, which proves the fact that this ability of **23** is not only limited to A549 cancer cells.

### 2.4. Molecular modeling

To gain more knowledge about the mechanism of action of the synthesized compounds we conducted a molecular modeling study using a three-dimensional model of the structure of the tubulin dimer-colchicine-vinblastine complex (PDB ID: 1Z2B). Conjugate **23** was chosen for the modeling among the synthesized compounds with highest cytotoxicity and maximal clustering effect **(10**, **23**, **26**, **28**, **30**). As though the clustering ability of the conjugates does not depend upon the presence of taxoter side chain (see Section 2.3), molecular docking was performed to the colchicine binding site located at β-subunit at the interface of α/β tubulin subunits. The study was carried out with the

help of the AutoDock Vina program, which takes ligands flexibility into account.[13] Ligand-tubulin complexes with the best values of the corresponding scoring function calculated by AutoDock Vina were chosen. The obtained binding mode of **23** is presented in Figure 4.

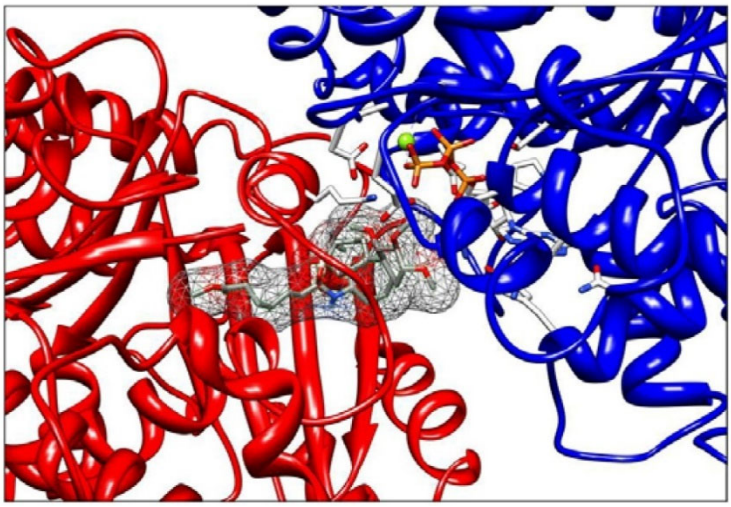

**Figure 4.** Location of compound **23** at the interface of α/β tubulin subunits (β-subunit is colored in red, α-subunit in blue, hydrogen atoms are not shown for clarity, molecular surface mesh is indicated).

According to the modeling results, while colchicine fragment of **23** binds to the corresponding site of β-subunit (formed by the residues of Cys241, Leu248, Leu255, Asn 258, Met 259 etc.), the adamantane moiety of the conjugate is located in a binding site formed by hydrophobic residues Tyr224 and Vail 77 in the α-subunit. Thus, compound **23** connects two binding sites located on two opposite surfaces of α and β tubulin subunits. It should be mentioned that if the docking study is carried out using the model of β-subunit only, then in the best binding mode of **23** its adamantane moiety is located in an additional binding site formed by hydrophobic residues Ile347 and Pro348 along with hydrophobic parts of Thr314 and Asn 349. Both carbonyl oxygens of the linker in **1** may form hydrogen bonds with Asn 258 and Met 259 residues and the importance of these bonds might be the reason for the observed dependence of activity on spacer length. However this docking study does not explain the difference in binding of compounds with and without tubulin clustering ability as it does the docking to both α- and β-subunits of the tubulin dimer (see below).

Each of oxygen atoms of the linker ester group of **23** may form a hydrogen bond with the hydroxyl of Tyr224. This hydrogen bonding seems to be important for providing the location of the adamantane moiety at the interface of two subunits and can be the reason for the observed dependence of the activity on spacer length.

A similar molecular modeling study was carried out for compound **31**, which possesses no tubulin clustering ability. The result indicates that its best binding mode is different from that of **23** (Fig. 5). The linker and methyl group of **31** are not exposed to the interface of tubulin subunits but are directed towards the inner space of the

β-subunit protein globe (Fig. 5). The analogues binding mode (i.e. the direction of the side chain to the internal area of β-subunit) was observed for conjugate **33** with phenyl substituent (data not shown).

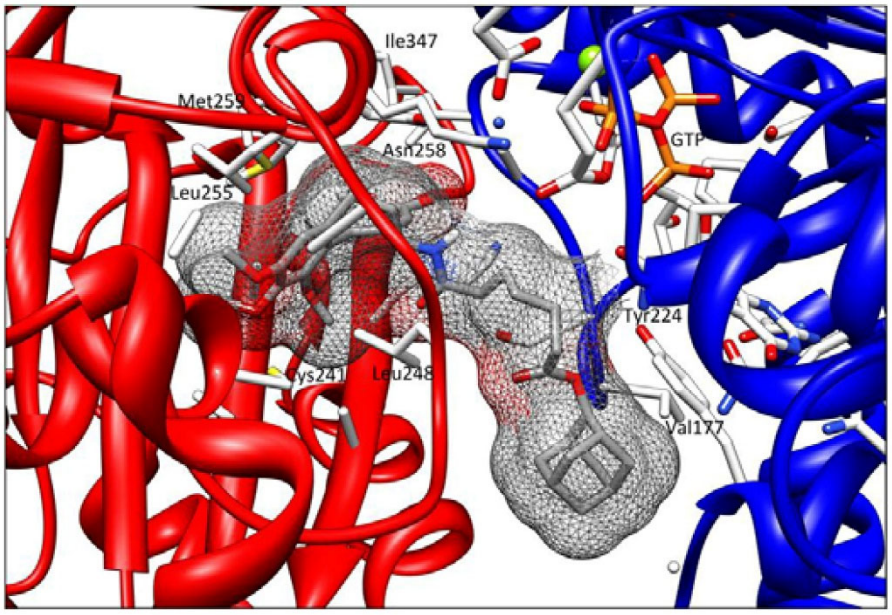


**Figure 5.** The best-binding mode of compound **31** with tubulin (β-subunit is colored in red, α-subunit in blue, hydrogen atoms are not shown for clarity, molecular surface mesh is indicated). The direction of the linker of **31** towards the inner space of the β-subunit is clearly seen.

Since compounds **31** and **33** do not exhibit the tubulin-dustering effect it is logical to propose that this property might be connected to the ability of the adamantane moiety of **23** to interact with the hydrophobic site on the α-subunit, providing a kind of 'cross-linking' of the tubulin dimer subunits. Binding of the conjugate **23** to other tubulin areas is also possible. Further experiments are ongoing to understand the details of the mechanisms by which the compounds effect microtubule dynamics and induce tubulin clustering in cultured cells and to evaluate an anti-tumor effect and an overall toxicity of the most active conjugates *in vivo*.

## Conclusion

In summary, a hybrid of adamantane-based paclitaxel mimetic with colchicine (**1**) was proved to interfere with the microtubule dynamics in an unusual manner, i.e. to promote disassembly of microtubules followed by the formation of stable tubulin clusters. This ability was found to be sensitive to the length and structure of the linker. More pronounced tubulin clustering effect was observed for the derivative of **1** without amino acid side chainconjugate **23**. Structure–activity relationships for the analogues of **23** indicate that both cytotoxicity and clustering ability are very sensitive to the linker length and much less sensitive to the shift of the position of linker attachment to adamantane. Replacement of the bridgehead core in **23** for other lipophilic groups re-

vealed, that the presence of a bulky hydrophobic and non-aromatic moiety in the studied conjugates plays an important role in bringing about the tubulin-clustering effect. These structure–activity data were partially explained by molecular modeling studies.

The most cytotoxic compounds synthesized in this work (**10**, **23**, **26**, **28**, **30**) possess activity in nanomolar concentrations and are several times more cytotoxic than colchicine.

## 3. Biology

### Cell culture

A549 human lung epithelial carcinoma cells (CCL-185™) were cultured with Dulbecco's modified Eagle medium (DMEM) containing 10% fetal bovine serum and 1% antibiotic penicillin/streptomycin at 37°C under a humidified 5% $CO_2$ atmosphere.

### MTT cytotoxicity assay

Cells were seeded in 96-well plates at a density of $3\times10^3$ cells per well. Stock solutions of test compounds were prepared in dimethylsulfoxide (DMSO). Cells were treated for 24 h with selected compounds at 1–12000 nM or with colchicine at 5–100 nM or taxol at 1–15 nM as positive controls (8 wells for each concentration). DMSO (0.4%) served as a negative control. The number of surviving cells was determined by the colorimetric MTT assay.[7] MTT (3-(4,5-dimethylthiazolyl-2)-2,5-diphenyl-2*H*-tetrazoliumbromid, Roth GmbH, Karlsruhe, Germany) was prepared at 5 mg/mL in phosphate buffered saline (PBS) and filtered through a 0.22 pm filter. 20 μL of sterile MTT solution (final concentration 0.5 mg/mL) was added to each well 2 h before the end of compound exposure. Then the supernatant was removed, and 100 μL of DMSO containing 10% SDS and 0.6% acetic acid was added to each well. Resulting formazan crystals were solubilised by thorough mixing on a plate shaker. Optical density was measured at 590 nm with 690 nm reference filter using a EL808 Ultra Microplate Reader (BioTek Instruments, Winooski, USA). Experiments for all compounds were repeated at least three times and $EC_{50}$ values were determined by sigmoidal curve fitting using Excel-based software.

### Immunofluorescence staining of cellular microtubules

For microtubule staining A549 cells were cultured in 12-well plates on small glass coverslips (11 mm diameter) at a density of $2\times10^4$ cells per coverslip. Cells were incubated with selected compounds or colchicine and taxol as positive controls at concentrations of **1** and 5 μM at 37°C and 5% $CO_2$ for 8 h. 0.5% DMSO served as a negative control. The whole process of cell fixation and staining was described previously.[8]

Fixed cells were labelled with mouse monoclonal antibody against α-tubulin at a dilution of 1:400 (Sigma, St. Louis. USA), followed by incubation of Alexa Fluor488 labelled goat anti-mouse IgG at a dilution of 1:200 (Invitrogen, Germany). Images of all samples were acquired with a Nikon Diaphot 300 inverted microscope (Nikon GmbH, Dusseldorf, Germany) equipped with a cooled charge-couple device camera system (SenSys; Photometries, Munich, Germany).

## Acknowledgements

This work was done in the frame of a Scientific Cooperation Agreement between Moscow and Rostock Universities and supported by the Alexander von Humboldt Foundation (3.4-Fokoop-Rus/ 1015567). A part of the work was supported by Russian Foundation for Basic Research (No. 00879/12088) and Russian Academy of Sciences.

## References and notes

1. Kingston, D. G. I. *Chem. Commun*. **2001**, 867.
2. Zefirova, O. N.; Nurieva, E. V.; Ryzhov, A. N.; Zyk, N. V.; Zefirov, N. S. *Russ. J. Org Chem*. **2005**, 41, 329.
3. Breen, E. S.; Walsh, J. J. *Curr. Med. Chem*. **2010**, 17, 609.
4. Zefirova, O. N.; Nurieva, E. V.; Lemcke, H.; Ivanov, A. A.; Shishov, D. V.; Weiss, D. G.; Kuznetsov, S. A.; Zefirov, N. S. *Bioorg. Med. Chem. Lett*. **2008**, 18, 5091.
5. Kuznetsov, S. A.; Rodionov, V. I.; Bershadsky, A. D.; Gelfland, V. I.; Rosenblat, V. A. *Cell Biol. Int. Rep*. **1980**, 4, 1017.
6. Weiss, D. G. In *Cell Biology*: *A Laboratory Handbook*; Celis, J. E., Ed.; Academic Press: San Diego, 2006; Vol. 3, pp 57-65.
7. Mosmann, T. *J. Immunol*. *Methods* **1983**, 65, 55.
8. Al-Haddad, A.; Shonn, M. A.; Redlich, B.; Blocker, A.; Burkhardt, J. K.; Yu, H.; Hammer, J. A., 3rd; Weiss, D. G.; Steffen, W.; Griffiths, G.; Kuznetsov, S. A. *Mol. Biol. Cell* **2001**, 12, 2742.
9. Lebeau, L.; Ducray, P.; Mioskowski, C. *Synth. Commun*. **1997**, 27, 293.
10. (a) Bourzat. J. D.; Commenjon, A. *Tetrahedron Lett*. **1993**, 34, 6049; (b) Didier, E.; Fouque, E.; Taillepied, I.; Commerçon, A. *Tetrahedron Lett.* **1994**, 35, 2349.
11. Hill, J. W.; Carothers, W. H. *JACS* **1933**, 55, 5023.
12. Zefirova, O. N.; Diikov, A. G.; Zyk, N. V.; Zefirov, N. S. *Russ. Chem. Bull., Int. Ed.* **2007**, 56, 680.
13. Trott, O.; Olson, A. J. *J. Comput. Chem*. **2010**, 31, 455.

*CHEM**BIO**CHEM, Vol. 14(12), 1444-1449, 2013*

# UNUSUAL TUBULIN-CLUSTERING ABILITY OF SPECIFICALLY C7-MODIFIED COLCHICINE ANALOGUES

**O.N. Zefirova, H. Lemcke, M. Lantow, E.V. Nurieva, B. Wobith, G.E. Onishchenko, A. Hoenen, G. Griffiths, N.S. Zefirov, S.A. Kuznetsov**

*Institute of Biological Sciences, University of Rostock, Rostock (Germany)*
*M.V. Lomonosov Moscow State University, Moscow (Russian Federation)*
*Institute of Physiologically Active Compounds, Chernogolovka (Russian Federation)*
*Department of Biosciences, University of Oslo, Oslo (Norway)*

Several colchicine analogues, variously modified at C7, not only show colchicine-like ability to promote microtubule disassembly, but also induce tubulin assembly into clusters; an example is *N*-(7-adamant-2-yloxy-7-oxoheptanoyl)-*N*-deacetylcolchicine, herein named "tubulodustin". These tubulin aggregates are morphologically distinct from microtubule bundles induced by taxol and from tubulin paracrystals induced by vinblastine. The tubulin clusters are very stable in cells: they are not affected by low temperature or by removal of tubulodustin from the culture medium. A detailed study of tubulodustin action has indicated that it inhibits binding of both [$^3$H]colchicine and [$^3$H]taxol to tubulin in vitro and induces tubulin assembly into regular wavy-shaped clusters composed of bundles of protofilaments. The compound blocks cell division at the $G_2$/M phase and induces cell apoptosis. The proposed mechanism of action of tubulodustin and its analogues, beyond that of colchicine, includes additional specific interactions with the α-tubulin subunit. This makes them interesting leads in the design of novel mitostatic drugs and useful tools for the study of microtubule dynamics.

Assemblies of the cell cytoskeletal protein tubulin are known to exhibit extensive polymorphism. Besides protofilaments and microtubules (formed by polymerisation of α,β-tubulin heterodimers), tubulin assemblies include various atypical structures, such as rings, incomplete microtubules, sheets and microtubule bundles.[1] The formation of a particular structure is strongly dependent on pH, temperature and the presence of divalent cations and GTP, as well as the activity of some drugs. Natural compounds such as taxol (paclitaxel), colchicine and vinca alkaloids (vincristine and vinblastine) interact with different binding sites of tubulin and have different effects on microtubule dynamics: taxol stabilises and promotes tubulin assembly into stable microtubule bundles, whereas colchicine and vinca alkaloids are categorised as microtubule-destabilising agents, the latter also causing formation of tubulin paracrystals. The interaction of another group of substances (dolas- tatins, cryptophycins, phomopsin, etc.) with the "vinca domain" of tubulin in some cases leads to the formation of yet different tubulin aggregates (rings, spirals etc.).[2]

Earlier, we synthesised a series of highly cytotoxic hybrid molecules of colchicine linked to an adamantane-based taxol mimetic (**1**, Scheme 1), as well as simple analogues, exempli-fied by compounds **2**–**4**.[3] These C7-modified colchicine conjugates manifested not only microtubule-depolymerisation activity (well known for colchicines) but also the ability to form tubulin clusters in human lung carcinoma cells.[3b] Interestingly, the strength of tubulin clustering correlated with the mitostatic activity of the compounds.[3b] This fact stimulated us to carry out additional experiments, to characterise the mechanism of the conjugates action on tubulin dynamics in vitro and in different cells. *N*-(7-adamant-2-yloxy-7-oxoheptanoyl)-*N*-deacetylcolchicine **2** (tubuloclustin; Scheme 1) was chosen for the further investigation.

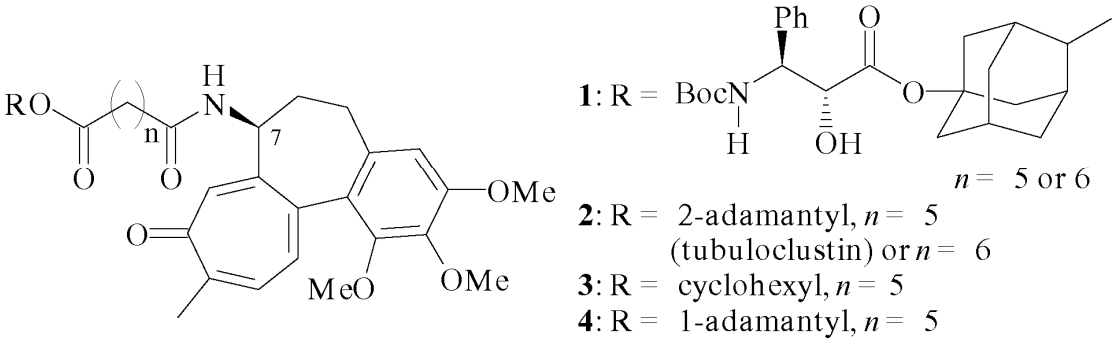


Scheme 1. Structures of C7-modified colchicine analogues. Compound **2** is named "tubuloclustin".

Immunofluorescence microscopy with different cell lines (Vero, HeLa, J774, A549) treated with tubuloclustin revealed unusual effects of the compound on microtubule dynamics and tubulin distribution, and led to the formation of large tubulin structures ("clusters"; Figure 1).

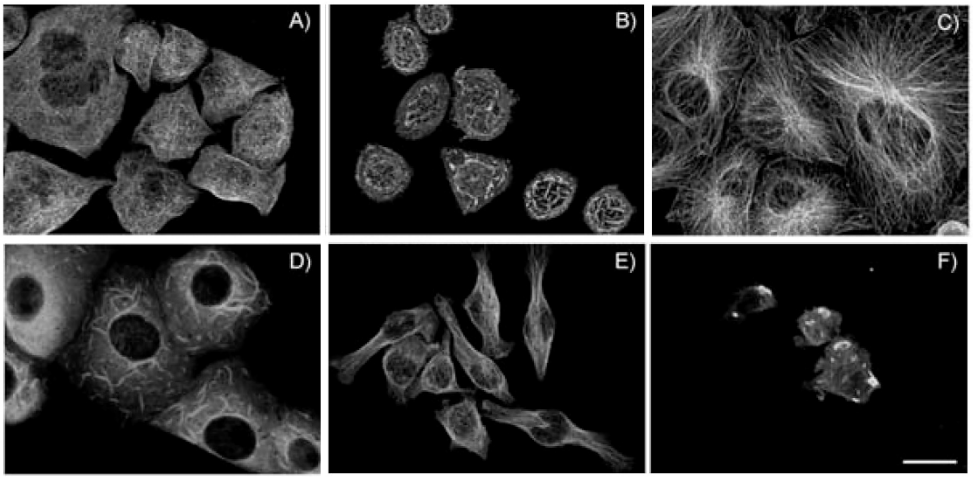


Figure 1. Effect of tubulodustin on microtubule network in different cell lines. A) and B) HeLa cells, Q and D) Vero cells, and E) and F) J774 mouse macrophages before (A, C, E) and after (B, D, F) treatment with 500 нм tubulodustin for 8 h. Disrupted microtubule networks and typical tubulin clusters are clearly visible in all cell lines. Scale bar: 20 μm.

All selected cell lines showed disrupted microtubule networks coupled with tubulin structures around the nuclei. Microtubule disassembly by tubuloclustin was also confirmed by TEM (Figure 2), as well as by the formation of large homogenous aggregates near the nuclei (Figure 2D and F). The tubulin clustering effect is highly specific: it was not observed following cell treatment with a mixture of colchicine and taxol, or colchicine and vinblastine.

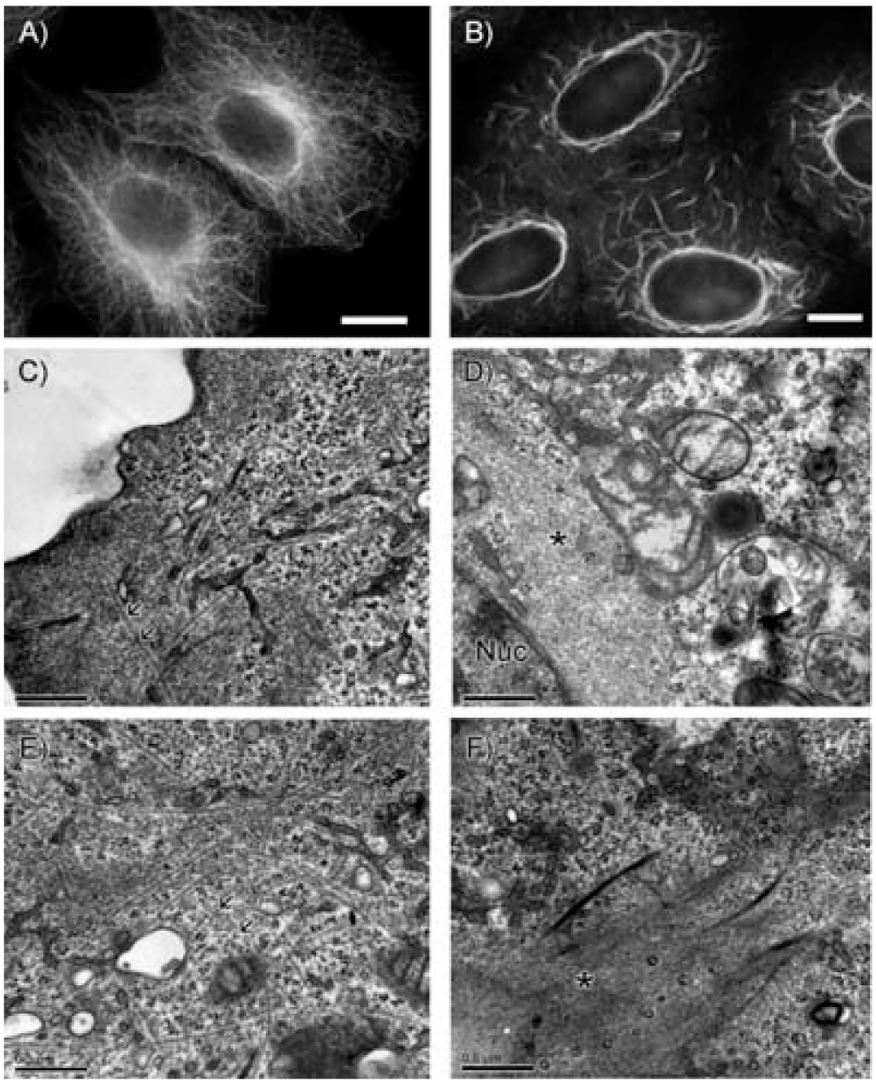


Figure 2. Effect of tubulodustin on microtubule networks in A549 cells. Cells were treated for 8 h with A), C) and E) 0.5% DMSO (negative control) or B), D) and F) 1 μm tubulodustin. A and B are immunofluorescence images, C–F are JEM images showing typical regions of DMSO (C and E) and tubulodustin (D and F) treated cells. Microtubules are indicated by arrows (C, E); the asterisk marks an area of amorphous material that might be protein aggregate. Microtubules are not observed in this area (D, F); the nucleus is identified by “Nuc" (D). Scale bars: 20 μm (immunofluorescence images A and B), 0.5 μm (TEM images).

A cytotoxicity test demonstrated that tubulodustin was highly toxic against A549 human lung carcinoma cells ($EC_{50}$ – (6±1.5) нм)[3b] and A431 human epithelial carcinoma cells ($EC_{S0}$=(8±1.3) нм, n = 3, present study); it was only half as toxic against HaCaT normal keratinocytes ($EC_{50}$=(13±2.2) нм, n = 3, present study). Similarly to

other anti-tubulin agents, tubulodustin causes cell-cycle arrest at the $G_2$/M stage, with efficacy similar to that of vinblastine and taxol (Figure 3A and B, Table 1).

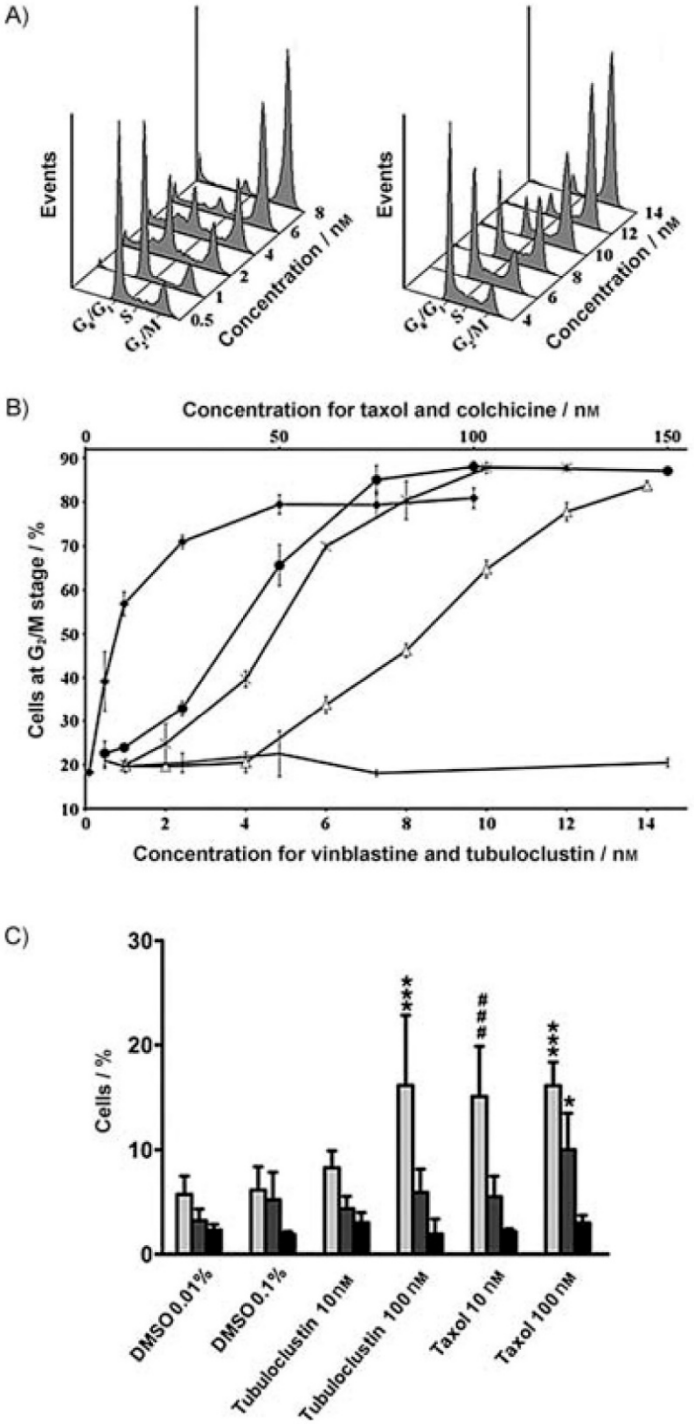


Figure 3. Effect of tubuloclustin on cell viability. A) and B) Effect of tubuloclustin on cell-cycle progression. A549 cells were treated with different concentrations of drug for 24 h. A) Flow cytometry histogram plots of left: vinblastine and right: tubuloclustin. B) Concentration-dependent cell-cycle arrest in $G_2$/M phase caused by colchicine (●), vinblastine (*), taxol (♦) and tubuloclustin (△) or 0.05% DMSO (negative control; (■). C) Flow cytometric detection of necrosis (■) and early (■)/late (■) apoptosis of A549 cells after 24 h treatment with DMSO (negative control), taxol (positive control) or tubuloclustin. Data are meaniSD of three independent experiments performed in triplicate; * significant difference from 0.01 % DMSO, # significant difference from 0.1% DMSO (control), determined by two-tailed paired Students t-test and one way ANOVA (***$p$< 0.001, *$p$<0.05, ***$p$<0.001).

In order to determine whether inhibition of cell-cycle progression by tubulodustin results in apoptosis, DNA staining was performed at different time points. A homogenous distribution of chromatin was observed by fluorescence microscopy in control cells after 72 h. After 24 h of incubation with tubuloclustin, the beginning of chromatin condensation was observed. Prolonged treatment with tubulodustin (up to 3 days) led to fragmentation of the nucleus. Double staining with annexin V-FITC and 7-AAD (7-amino actinomycin D) dyes[4] showed that tubulodustin (100 нм) significantly induces early apoptosis and, to a lesser degree, late apoptosis, without affecting necrosis. A similar result was observed with taxol (100 нм, positive control). At a lower concentration (10 нм, close to $EC_{S0}$) tubulodustin was less potent than taxol as an apoptosis-inducing agent (Figure 3C).

Table 1. Cytotoxicity of the compounds determined by an MTT assay, and effect on A549 cell-cycle arrest analysed by flow cytometry.[a]

| | $EC_{50}$±SD [нм] | |
|---|---|---|
| Compound | Cytotoxicity | $G_2$/M arrest |
| DMSO | no effect | no effect |
| vinblastine | 0.82 ±0.03 | 4.65 ±0.04 |
| colchicine | 27±1.5 | 37± 1.1 |
| taxol | 4.6 ±0.7 | 7.8 ±1.8 |
| tubulodustin | 6.4 ±1.5 | 8.4 ±0.3 |
| [a] Results of four independent experiments. | | |

Tubulin association following depolymerisation of microtubules is inhibited by low temperature, and taxol is known to stabilise microtubules against cold-induced depolymerisation.[5] Our experiments show that exposure to 0°C for 1 h triggered depolymerisation of the entire microtubule network in A549 cells, whereas cells treated with 1 μм tubulodustin prior to cold treatment retained their intracellular tubulin clusters, similarly to the situation with stable taxol-induced microtubule bundles and vinblastine paracrystals.

Further investigation of tubulodustin binding to tubulin was carried out by treatment of cells with the selected compounds, followed by replacement of the drug-containing medium. Analysis of alterations to microtubule structures at 48 h (Figure 4A) showed that tubuloclustin-induced clusters displayed high stability (Figure 4A panels a–c) in comparison with microtubule bundles formed by taxol and vinblastine paracrystals, which were not maintained in the absence of drugs (Figure 4A d–f and g–i). These data prompted us to check whether tubulodustin binds to intracellular tubulin in an irreversible and noncompetitive manner. For this, tubuloclustin-pretreated A549 cells were incubated with colchicine or vinblastine. Colchicine partially depolymerised tubuloclustin-induced tubulin accumulations after 24 h treatment (data not shown), and almost fully disassembled them after 48 h (Figure 4B b). The depolymerisation effect

of vinblastine was observed after just 24 h incubation (Figure 4B e). These data show that clusters formed by tubulodustin are very stable, but mainly reversible. Interestingly, taxol-induced tubulin bundles demonstrated much less stability against colchicine: no microtubule bundles were detected after 24 h treatment (Figure 4B d–f). Furthermore, vinblastine was able to form paracrystals in cells pretreated with taxol, but not in those pretreated with tubuloclustin (Figure 4 B c and f).

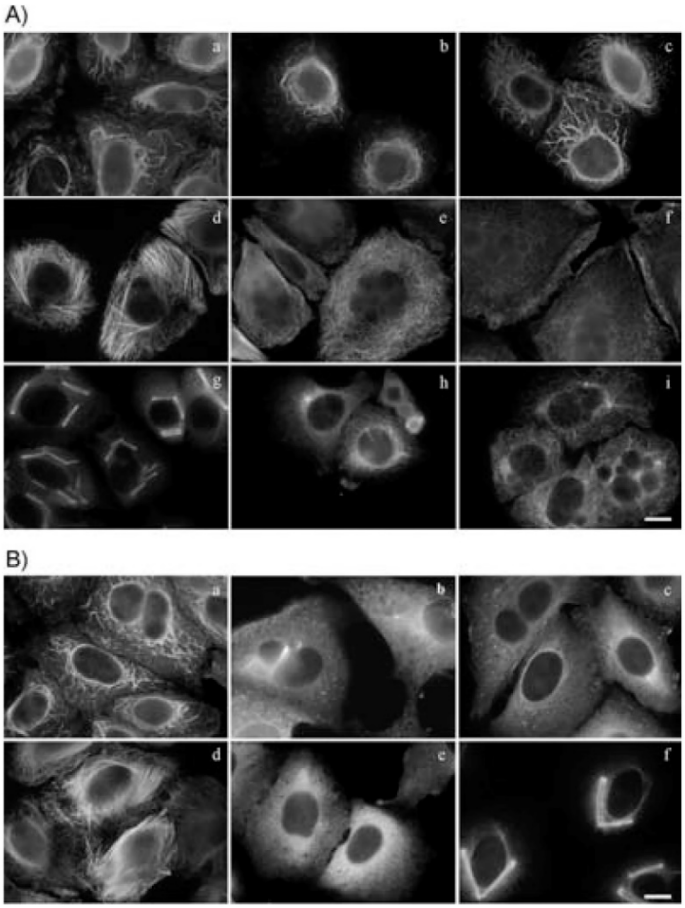


Figure 4. Stability of tubuloclustin-induced tubulin cluster in A549 cells. A) Reversibility of clusters. Cells were treated with compound (5 μm for 8 h), followed by removal of drug-containing medium and tubulin staining after 24 and 48 h. Tubuloclustin binds to tubulin in a nonreversible manner (a–c), whereas cells treated with taxol (d–f) and vinblastine (g–i) were able to restore microtubule networks in the absence of drug. B) Stability of clusters in the presence of microtubule destabilisers: a) tubuloclustin pretreated cells were exposed to b) 5 μm colchicine for 48 h and c) vinblastine for 24 h. Both microtubule-destabilising drugs strongly disrupted tubulin clusters of tubuloclustin. d) Taxol-initiated microtubule bundles were also depolymerised by e) colchicine, and f) vinblastine. Scale bars: 20 μm.

In order to study the dynamics of tubulin-cluster formation, the concentration-dependent manner of tubulodustin action was evaluated by immunofluorescence microscopy of cells incubated with the tested compound (7.5–500 нм; Figure 5A). The minimum tubulodustin concentration required for clusters formation was just 15–30 нм (Figure 5A b), whereas the maximum effect was achieved with 125 нм treatment (Figure 5A d). Alteration of the microtubule network was also studied in a time-dependent manner, by fixing cells treated with 50 нм tubuloclustin at different time

points. After 30 min of incubation, tubuloclustin induced partial depolymerisation of microtubules in the cells (Figure 5B b), and microtubules were completely disrupted 3 h before the onset of tubulin aggregate formation (Figure 5B b,e). The number and sizes of the tubulin clusters increased proportionally with increasing period of treatment (Figure 5B f). These data show that clusters are not formed in the course of increased microtubule polymerisation, but that tubuloclustin first causes depolymerisation of microtubules and subsequently initiates formation of clusters from free tubulin subunits.

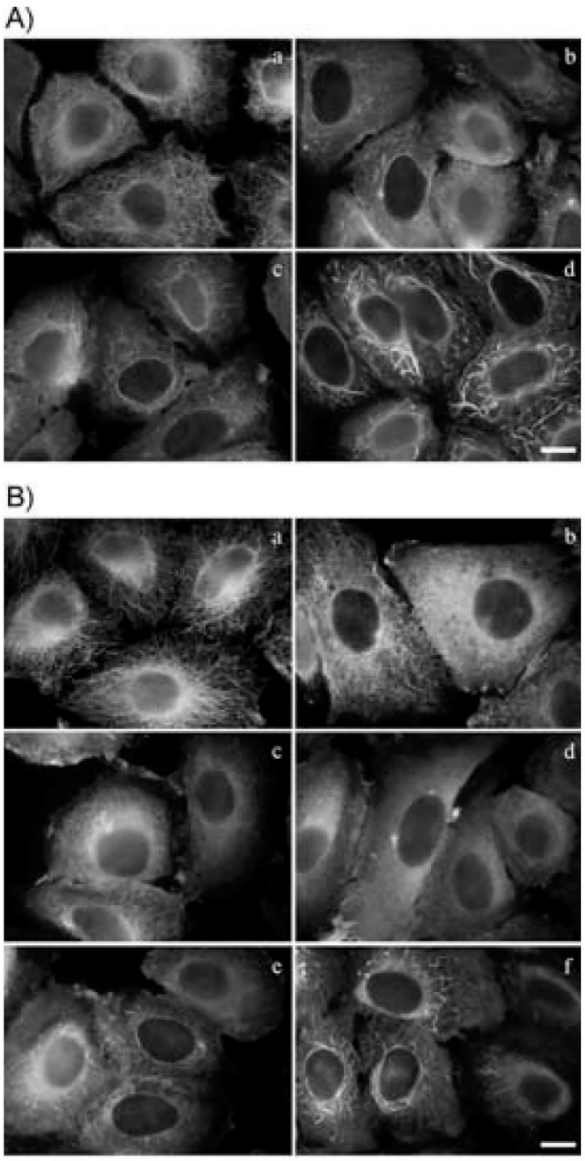


Figure 5. Dynamics of tubulin cluster formation in A549 cells. A) Concentration-dependent formation of tubuloclustin-induced tubulin structures. Cells were incubated for 3 h with tubuloclustin at a) 15 нм, b) 30 нм, c) 60 нм and d) 125 нм. Cells treated with 30 нм tubuloclustin showed no microtubules, but small tubulin structures, whose quantity and size increased at higher concentrations within 3 h; this was followed by formation of tubulin structures. B) Time-dependent formation of tubuloclustin-induced tubulin clusters. Cells were incubated with 50 нм tubuloclustin, fixed and stained after incubation periods of a) 0 min, b) 30 min, c) 1 h, d) 2 h, e) 3 h and f) 5 h. Tubuloclustin completely destroyed microtubules network within 3 h, and then initiated formation of tubulin clusters. Scale bars: 20 μm.

*In vitro* experiments with purified bovine tubulin confirmed the effect of tubuloclustin on tubulin dynamics and revealed the unique structure of the clusters (Figure 6). Microtubules in DMSO-treated samples (control) are clearly visible (Figure 6A–C), whereas tubuloclustin induced inhibition of tubulin assembly into microtubules and the formation of large regular clusters of different sizes and of similar internal composition (Figure 6D–F). All clusters were composed of layers of roughly equal-sized short bundles of wavy tubulin protofilaments (Figure 6F). The observed tubulin-tubulodustin polymers were different not only from taxol-formed microtubule bundles and vinblastine paracrystals but also from the sheet- and ribbonlike regular filamentous structures observed upon polymerisation of tubulin-colchicine complexes *in vitro*.[6] However, the wavy tubulin protofilaments were not observed within cells, as dense contrast due to other cell components made it difficult to draw any firm conclusion on this issue (Figure 2D and F).

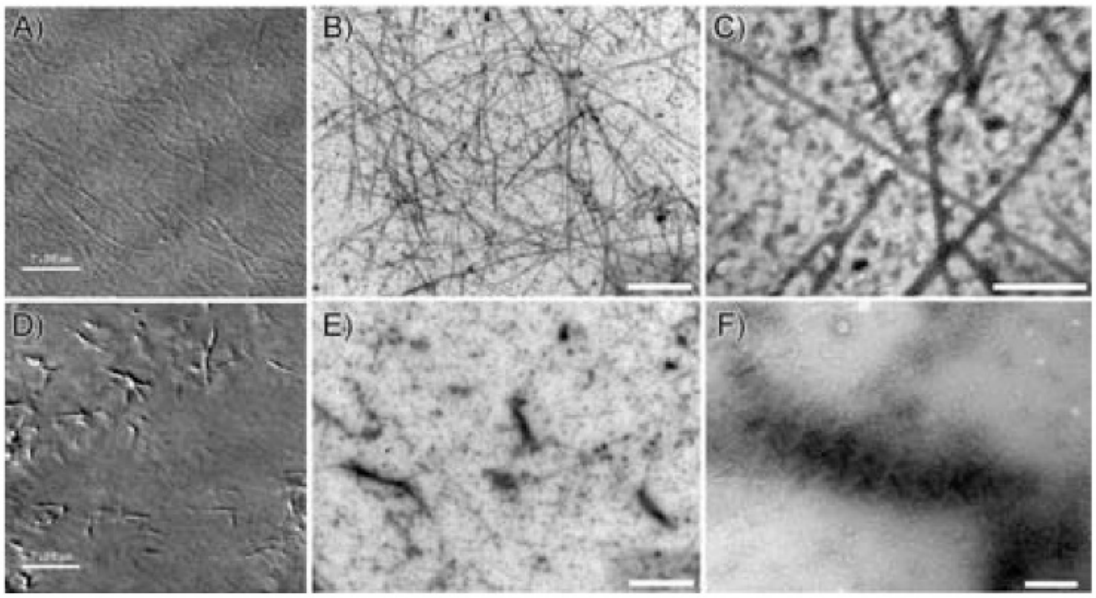


Figure 6. Effect of tubuloclustin on purified tubulin *in vitro*. Effect of tubuloclustin on purified tubulin assembly *in vitro* analysed by A) and D) VEC-DIC and B), Q, E) and F) TEM microscopy. A)-Q Samples treated with 10% DMSO (negative control) showed a large number of single microtubules. D)-F) Tubuloclustin inhibited microtubule formation, but induced formation of tubulin regular clusters consisting of helical protofilaments. Scale bars: 7 μm (A and D), 2 μm (B and E), 500 nm (C), 200 nm (F).

Competition assays revealed that tubuloclustin caused a coordinated and concentration-dependent decline in tubulin-bound [$^3$H]colchicine (Figure 7A) and [$^3$H]taxol (Figure 7B), but not [$^3$H]vinblastine (Figure 7Q). This indicates that tubuloclustin's mode of action differs from that of vinca alkaloids and vinca-domain ligands, which are well known for their ability to cause microtubule depolymerisation followed by formation of aggregates.[7]

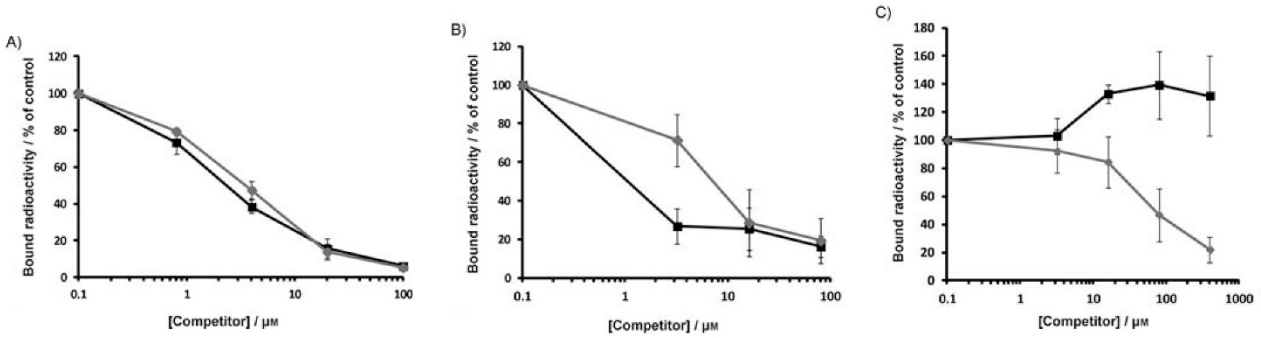


Figure 7. Competitive binding. A) Inhibition of [$^3$H] colchicine binding to tubulin heterodimers by tubuloclustin (■). Final concentrations of reagents were [$^3$H]colchicine: 0.4 μm (specific acti vity – 5 $C_i$ mmol$^{-1}$); tubulin: 2.3 μm; tubuloclustin: 0.8,4, 20 and 100 μm. B) inhibition of [$^3$H]taxol binding to microtubules preformed by tubuloclustin (■). Final concentrations of reagents were [$^3$H]taxol: 0.8 μm (specific activity – 2.5 $C_i$ mmol$^{-1}$); tubulin: 4.6 μm; tubuloclustin: 3.2,16 and 80 μm. C) Effect of tubuloclustin (■) on [$^3$H]vinblastine binding to tubulin heterodimers. Final concentrations of reagents were [$^3$H]vinblastine: 0.4 μm (specific activity 2.5 $C_i$ mmol$^{-1}$); tubulin: 2.3 μm; tubuloclustin: 3.2,16, 80 and 400 μm. Nonradioactive compounds (o) at the same concentrations as indicated were used as a positive control. The ability of the competitor to affect binding of the radioactive ligand is expressed as a percentage of control binding in the absence of competitor. Data are mean ±SD of three (B and C) or four (A) independent experiments.

The ability of tubuloclustin to compete effectively with [$^3$H]colchicine suggests that it binds to the colchicine binding site. This was confirmed by fluorescence measurements of tubulodustin-tubulin mixtures. Upon binding of tubuloclustin to tubulin, the same enhancement of fluorescence (excitation maximum 430–432 nm; Figure 8) was observed as for colchicine-tubulin complex.[8] Furthermore, as a result of its interaction with the colchicine binding site, tubuloclustin induced inhibition of microtubule assembly in vitro and causes a small stimulation of [$^3$H]vinblastine binding (Figure 7Q, an effect previously described for colchicines.[9]

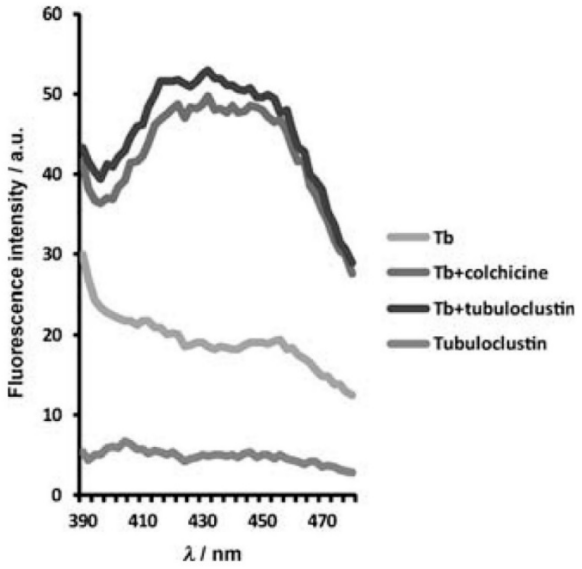


Figure 8. Fluorescence spectra of tubulin heterodimer alone (Tb), or in the presence of colchicine (Tb + colchicine) or tubuloclustin (Tb + tubuloclustin). The spectrum of tubuloclustin without tubulin is also shown.

Tubuloclustin was very effective in the inhibition of [$^3$H]taxol binding (Figure 7B). However this observation might be a result of the inability of [$^3$H]taxol to bind properly to nonmicrotubule clusters, to tubulin oligomers or to protofilaments, which could form in the reaction mixture at high tubulodustin concentrations. We assume that the ability to form tubulin aggregates is unlikely to be connected to the interaction of tubulodustin with the taxol-binding site itself, because of differences in the structure and stability between the clusters and microtubule bundles (see Figure 4).

A possible alternative mechanism of cluster formation is tubulodustin binding to the colchicine site and thereby interacting simultaneously with the hydrophobic area on the α-subunit of the tubulin dimer by its bulky adamantane group. The possibility of such subunits "cross-linking" has been demonstrated by molecular modelling.[3b] This additional interaction should enhance the binding of tubulodustin to the protein (relative to colchicine), and to change the α–β intradimer angle, thus weakening the lateral interactions in the course of tubulin polymerisation. As polymerised tubulin molecules that have lost one of their two lateral areas should preferentially form S-shaped structures,[10] formation of wavy protofilament layers under conditions where no aggregates are formed by colchicine might be a result of the tighter tubulodustin binding.

In the context of the suggested mechanism, the inhibition of [$^3$H]taxol binding by tubulodustin can be explained by long-range conformational changes, the possibility of which was demonstrated recently by computer modelling with other compounds, with suggested intradimer binding modes.[11] Interestingly, distant connection of colchicine and vinblastine binding by means of the long-range conformational changes has frequently been reported,[11] and might explain the interconnection of tubulodustin binding and the inability of vinblastine to form paracrystals in tubuloclustin-pretreated cells (Figure 4B c and F).

The suggested mechanism of cluster formation by tubuloclustin and its analogues allows us to propose that tubulin clustering is a general property of C7-modified colchicine analogues that provide appropriate interactions with the α-tubulin subunit. This hypothesis is supported by previous observations of unexpected aggregation or "microtubular fragmentation" for some colchicine derivatives.[12]

In conclusion, the effects of compounds of the "tubuloclustin family" on tubulin dynamics in cells differs from that of colchicine, taxol and vinblastine, and is proposed to be a result of specific interactions (additional to and/or distinct from those of colchicine) of C7 substituent with the α-tubulin subunit.

## Experimental Section

Tubulodustin (**2**, Scheme 1) was synthesised as described previously.[3b] For the tubulin polymerisation assay, purified tubulin isolated from bovine brain[13] was diluted (1:1) in BRB80 buffer (PIPES (80 мм, pH 6.8), $MgCl_2$ (1 mM), EGTA (1 mM)),[14] to a final tubulin concentration of 1.2 mg·mL$^{-1}$. Polymerisation was initiated by adding DMSO

(10%) and GTP (0.5 мм) in the presence of different concentrations of tubuloclustin for 1 h at 37°C. The extent and products of tubulin polymerisation were analysed by both video-enhanced contrast differential interference contrast (VEC-DIC) microscopy[15] and transmission electron microscopy (TEM). For TEM, the samples were stained with uranyl acetate (negative staining) and analysed with a CM100 transmission electron microscope (80 kV; Philips/FEI, Eindhoven, The Netherlands).

Binding of [$^3$H]colchicine (specific activity 60–87 $C_i$ mmol$^{-1}$; #NET189259UC, PerkinElmer), [$^3$H]taxol (specific activity 5.5 $C_i$ mmol$^{-1}$; #NSC125973, Moravek, Brea, CA) and [$^3$H]vinblastine sulfate (specific activity 3.7 $C_i$ mmol$^{-1}$; #NSC49842, Moravek) were assayed by the DEAE-cellulose filter method (see ref. [16]).

For fluorescence spectra detection, the reaction mixture contained tubulin (9.4 μM) and tubuloclustin (5 μM) in BBR80 buffer with GTP (0.1 μM), and was incubated for 1 h at 37°C. Fluorescence was measured with a SpectraMax M2$^e$ ($\lambda_{ex}$ 353 nm; Molecular Devices, Sunnyvale, CA).[9]

Cell lines A549 (human lung epithelial carcinoma cells), A431 (human epithelial carcinoma cells), HeLa (human epithelial adenocarcinoma cells), Vero (epithelial cells from normal monkey kidney), HaCaT (human normal keratinocytes) and J774 (mouse macrophages) were cultured in Dulbecco's Modified Eagle medium containing fetal bovine serum (10%) and antibiotic (penicillin/streptomycin (1%)) at 37°C under a 5% $CO_2$ humidified atmosphere. For all cell lines, the colorimetric MTT cytotoxicity assay[17] was performed as described in ref. [3b]. Experiments for each cell line were repeated at least three times, and $EC_{50}$ values were determined by sigmoid curve fitting in Excel-based software.

Immunofluorescence staining of cellular microtubules was carried out as described previously.[3b] For TEM, the samples were prepared as described in [18]. Ultrathin sections were cut with a Diatome diamond knife on an LKB ULTRATOM III (LKB Ultratome, Uppsala, Sweden), then contrasted with uranyl acetate and lead citrate and examined on a JEOL 100CX transmission electron microscope (JEOL, Tokyo, Japan).

Cell-cycle analysis was performed as described in ref. [19]. For apoptosis analysis, cells treated with control (DMSO (0.01 and 0.1%)), tubuloclustin (10 and 100 нм) or taxol (10 and 100 нм) were examined for the induction of apoptosis by using an Annex-in-V-FITC/7-AAD detection kit (Beckman Coulter, Krefeld, Germany) according to the manufacturer's instructions (see the Supporting Information).

## Acknowledgements

This work was undertaken in the framework of a Scientific Cooperation Agreement between Moscow and Rostock Universities and was supported by the Alexander von Humboldt Foundation (Grant 3.4-Fokoop-Rus/1015567), Russian Foundation for Basic Research (11-03-12088, 12-03-00720) and the Russian Academy of Sciences.

# References


1. a) S.A. Kuznetsov, V. I. Gelfand, V. I. Rodionov, V.A. Rosenblat, J.G. Gulyaeva, *FEBS Lett*. **1978**, *95*, 343 - 346; b) S. J. Edelstein, *Biophys. J.* **1980**, *32*, 347-360; c) P. Karecla, E. Hirst, P. Bayley, *J. Cell Sci*. **1989**, *94*, 479-488.
2. a) L. Wilson, M. A. Jordan, A. Morse, R. L. Margolis, *J. Mol. Biol*. **1982**, *159*, 125-149; b) A.-M. C. Yvon, P. Wadsworth, M. A. Jordan, *Mol. Biol. Cell* **1999**, *10*, 947-959.
3. a) O. N. Zefirova, E.V. Nurieva, H. Lemcke, A. A. Ivanov, D. V. Shishov, D. G. Weiss, S. A. Kuznetsov, N. S. Zefirov, *Bioorg. Med. Chem. Lett.* **2008**, *18*, 5091-5094; b) O. N. Zefirova, E. V. Nurieva, D. V. Shishov, 1.1. Baskin, F. Fuchs, H. Lemcke, F. Schöder, D. G. Weiss, N. S. Zefirov, S. A. Kuznetsov, *Bioorg. Med. Chem*. **2011**, *19*, 5529 - 5538.
4. Vermes, C. Haanen, H. Steffens-Nakken, C. Reutelingsperger, *J. Immunol. Methods* **1995**, *184*, 39 - 51.
5. a) D. M. Bollag, P. A. McQueney, J. Zhu, O. Hensens, L. Koupal, J. Liesch, M. Goetz, E. Lazarides, C.M. Woods, *Cancer Res*. **1995**, *55*, 2325 - 2333; b) C. A. Collins, R. B. Vallee, *J. Cell Biol*. **1987**, *105*, 2847 - 2854.
6. a) J. M. Andreu, S. N. Timasheff, *Proc. Natl. Acad. Sci. USA* **1982**, *79*, 6753-6756; b) J. M. Andreu, T. Wagenknecht, S. N. Timasheff, *Biochemistry* **1983**, *22*, 1556-1566.
7. S. Gupta, B. Bhattacharyya, *Mol. Cell. Biochem*. **2003**, *253*, 41 -47.
8. B. Bhattacharyya, J. Wolff, *Proc. Natl. Acad. Sci. USA* **1974**, *71*, 2627-2631.
9. E. Hamel, C. M. Lin, J. Plowman, H.-K. Wang, K.-H. Lee, K. D. Paull, *Biochem. Pharmacol*. **1996**, *51*, 53-59.
10. D. Saltarelli, D. Pantaloni, *Biochemistry* **1982**, *21*, 2996 - 3006.
11. a) L. Alisaraie, J. A. Tuszynski, *Chem. Biol. Drug Des*. **2011**, *78*, 535- 546; b) N. R. Watts, N. Cheng, W. West, A. C. Steven, D. L. Sackett, *Biochemistry* **2002**, *41*, 12662-12669.
12. a) R. F. Williams, C. L. Mumford, G. A. Williams, L. J. Floyd, M. J. Aivaliotis, R.A. Martinez, A. K. Robinson, L. D. Barnes, *J. Biol. Chem*. **1985**, *260*, 13794-13802; b) D. Passarella, B. Peretto, R. Blasco y Yepes, G. Cappelletti, D. Cartelli, C. Ronchi, J. Snaith, G. Fontana, B. Danieli, J. Borlak, *Eur. J. Med. Chem*. **2010**, *45*, 219-226.
13. S. A. Kuznetsov, V. I. Rodionov, A. D. Bershadsky, V. I. Gelfand, V. A. Rosenblat, *Cell Biol. Int. Rep.* **1980**, *4*, 1017-1024.
14. S. L Brenner, B. R. Brinkley, *Cold Spring Harbor Symp. Quant. Biol*. **1982**, *46*, 241-254.
15. T. Wollert, D.G. Weiss, H.-H. Gerdes, S.A. Kuznetsov, *J. Cell Biol*. **2002**, *159*, 571 -577.
16. G. G. Borisy, *Anal. Biochem*. **1972**, *50*, 373-385.
17. T. Mosmann, *J. Immunol. Methods* **1983**, *65*, 55-63.
18. C. Coulouarn, L E. Gomez-Quiroz, J.-S. Lee, P. Kaposi-Novak, E. A. Conner, T. A. Goldina, G. E. Onishchenko, V. M. Factor, S. S. Thorgeirsson, *Hepatology* **2006**, *44*, 1003-1011.
19. M. N. Semenova, A. S. Kiselyov, D. V. Tsyganov, L D. Konyushkin, S. I. Firgang, R. V. Semenov, O. R. Malyshev, M. M. Raihstat, F. Fuchs, A. Stielow, M. Lantow, A. A. Philchenkov, M. P. Zavelevich, N. S. Zefirov, S. A. Kuznetsov, V. V. Semenov, *J. Med. Chem.* **2011**, *54*, 7138-7149.

*MOLECULAR DIVERSITY, 2017, 21(3), 547-564*

# NOVEL ANTIMITOTIC AGENTS RELATED TO TUBULOCLUSTIN: SYNTHESIS AND BIOLOGICAL EVALUATION

**O.N. Zefirova, E.V. Nurieva, B.Wobith, V.V. Gogol, N.A. Zefirov, A.V. Ogonkov, D.V. Shishov, N.S. Zefirov, S.A. Kuznetsov**

*Department of Chemistry, Lomonosov Moscow State University, Russian Federation*
*Institute of Physiologically Active Compounds, Chernogolovka, Russian Federation*
*Institute of Biological Sciences, University of Rostock, Rostock, Germany*

Tubuloclustin [*N*-(7-adamant-2-yloxy-7-oxoheptanoyl)-*N*-deacetylcolchicine], a highly cytotoxic antitubulin compound is known for its ability to promote microtubule disassembly followed by the formation of tubulin clusters of unique morphology. Three series of antimitotic agents related to tubuloclustin were designed and synthesized in order to enhance the molecular diversity of "tubuloclustin-like" family of compounds. The series of compounds with modified adamantane moiety was highly potent in cytotoxic effect on human lung carcinoma A549 cells ($EC_{50}$ = 6–400 μM) and was active in affecting the microtubule arrays and induction of strong tubulin clusterization. In two other sets of compounds, the colchicine moiety of tubuloclustin was replaced by podophyllotoxin or combretastatin A-4. All combretastatin A-4 derivatives displayed noticeable cytotoxic activity ($EC_{50}$ = 0.8–1.6 μM) but their effect on microtubules depended on the position of the linker attachment. Podophyllotoxin derivatives were also toxic to A549 cells ($EC_{50}$ = 0.38–0.50 μM) and caused both microtubule depolymerization and some tubulin clustering. The data obtained gave additional evidence that the whole panel of C7-colchicine, podophyllotoxin and combretastatin derivatives could manifest clustering effect, and the strength of this effect correlated with cytotoxic activity of the compounds.

During final preparation of this manuscript Nikolay S. Zefirov sadly died. This paper is dedicated to his memory.

## Introduction

Microtubules are dynamic polymers, which consist of a heterodimeric cell protein α,β-tubulin and play a key role in cell division. A number of antineoplastic agents such as colchicine, combretastatin A-4, podophyllotoxin and others bind to tubulin at colchicine's binding domain and inhibit microtubule formation [1-3]. Over the last two decades numerous modifications of these compounds were carried out in an effort to obtain more active and/or selective tubulin-targeted agents [1].

Recently we found out that the conjugation of colchicine with the adamantane moiety using a spacer with an appropriate length (see structures **1**–**3,** Fig. 1) improved

significantly the antiproliferative activity and cytotoxic effect of the parent molecule [4]. Moreover, compounds **1**–**3** caused microtubule depolymerization typical for colchicine and stimulated the formation of tubulin clusters of unusual morphology, therefore compound **1** was referred to as *tubuloclustin* [4,5]. We showed that the strength of clustering effect correlated with antimitotic and cytotoxic activities of tubuloclustin analogues [4]. High cytotoxic and antiproliferative effects of **1** *in vitro* and *in vivo* [6] and its unusual clustering effect prompted us to examine each "region" of the molecule, i.e., the colchicine moiety, the spacer and adamantane core, to determine what modifications would lead to potent compounds. First we showed that both adamantane (or other lipophilic non-flat moiety) and a spacer with 5 or 6 methylene groups were important for potency [4].

In the present work, we synthesized a set of tubuloclustin analogues with different substituents in the adamantane core in an attempt to get additional information about the binding mode to tubulin (Fig. 1, Type 1).

We also studied two novel modifications of the lead structure 1 directed to the molecular diversity enhancement of "tubuloclustin-like" family of compounds. The main idea was to replace the colchicine moiety with structurally different podophyllotoxin and combretastatin A-4 (CA-4) (Fig. 1, Types 2 and 3), and to determine whether this replacement retains tubulin clustering ability and cytotoxicity.

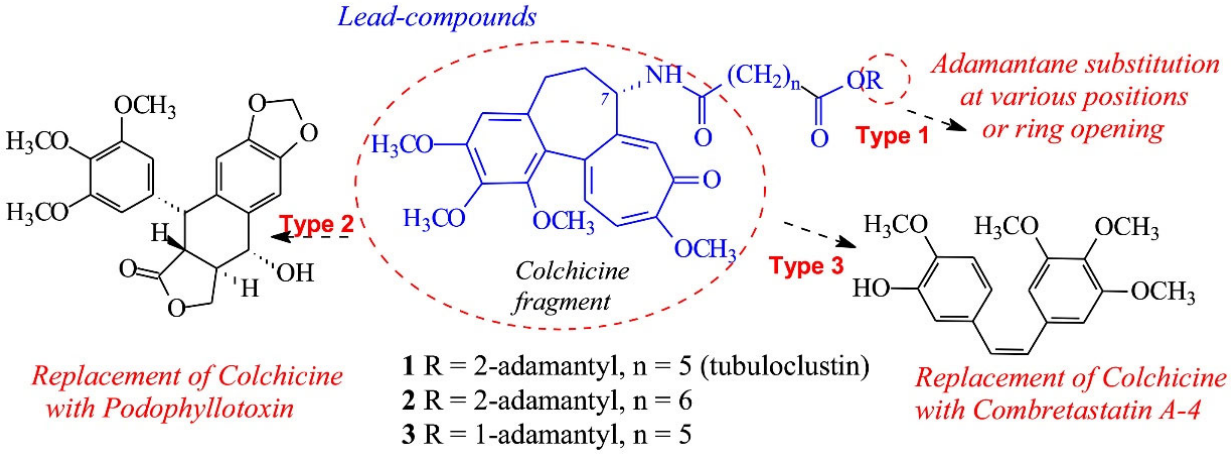


**Fig. 1.** Three types of modifications of tubuloclustin (**1**) and analogues made in the present work.

## Results and discussion

### Molecular design

The choice of substituents for the modification of the adamantane moiety in lead compounds **1** and **3** was conditioned by the diversity of their characteristics, i.e., lipophilicity, bulkiness and conformational flexibility. The positions of the substitution were also varied. The set of compounds synthesized **(4a**–**g)** is presented in Fig. 2.

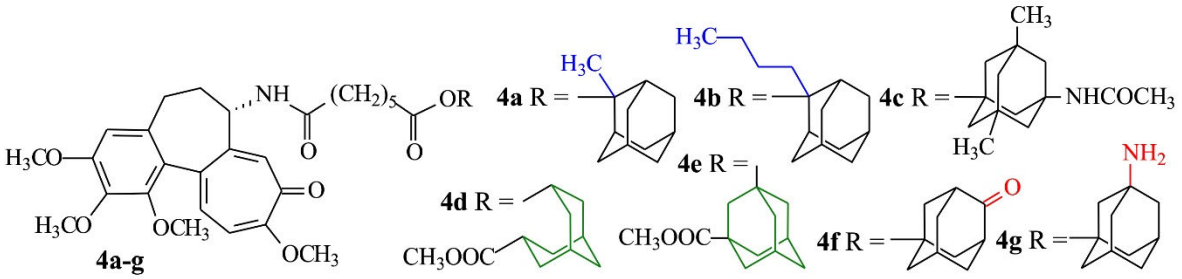


**Fig. 2.** Analogues of lead compounds **1** and **3** with different groups in the adamantane core and with a substituted bicyclo[3.3.1]nonane moiety.

The design of podophyllotoxin and CA-4 derivatives related to tubuloclustin was based on the pharmacophore model of colchicine domain inhibitors [3]. According to this model, the hydroxyl group of podophyllotoxin is located in close proximity to the nitrogen atom of the colchicine amide group (see Supplementary materials) and is shifted closer to the "border" of the β-tubulin subunit. We synthesized podophyllotoxin conjugates **5a**–**c** (Fig. 3) with a linking arm similar to that in lead compounds **1** and **2** (the linker in compound **5a** was shorter in order to take in account the mentioned shift).

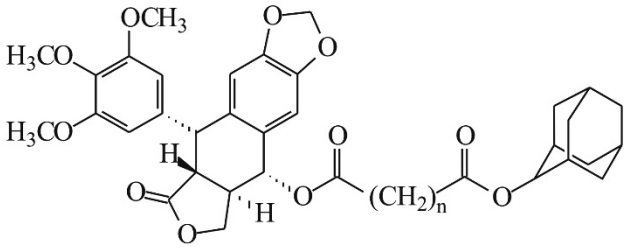

**5a** n = 4 **5b** n = 5 **5c** n = 6

**Fig. 3.** Podophyllotoxin derivatives related to tubuloclustin.

According to a common pharmacophore for colchicine site inhibitors [3], the double bond of CA-4 is positioned slightly further from the 'border" of the β-subunit than the amide group of colchicine, so the nitrogen atom of the latter is located at a certain distance from both carbon atoms of the CA-4 double bond (2.75 A to $C^2$ and 3.45 A to C') (Fig. 4). Therefore, we synthesized CA-4 conjugates **6a**–**c** and **7a**–**c** with elongated linkers compared to lead compounds **1** and **2** (Fig. 5).

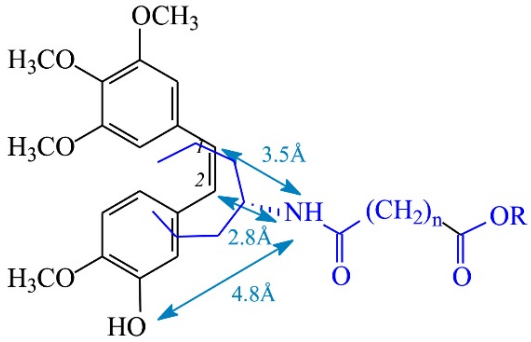


**Fig. 4.** Schematic representation of the double bond and phenol hydroxyl positions in CA-4 relative to the amide group in **1**.

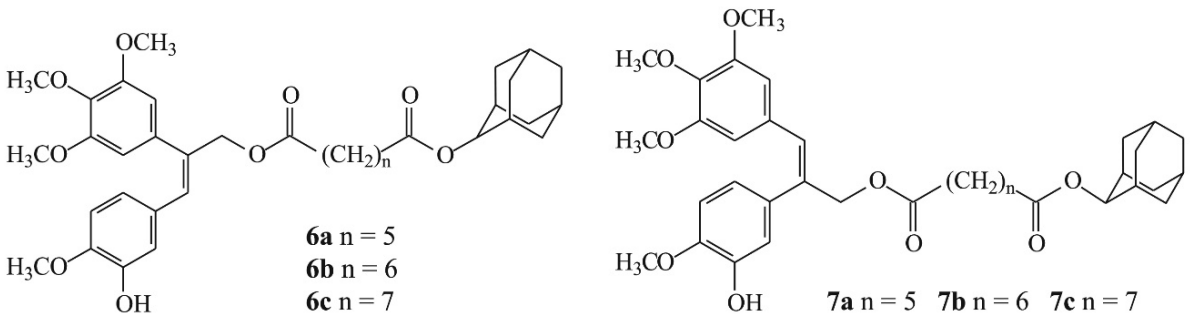


**Fig. 5.** CA-4 conjugates related to tubuloclustin with substituted double bond.

Another way to attach the substituted adamantyl moiety to CA-4 was to use the phenolic hydroxyl located at the distance ~ 4.8 Å to the nitrogen atom of the amide group of colchicine (Fig. 4).

In this case, it was taken into account that the linker bound to the phenolic ester bond would be easily hydrolyzable in cell cultures. To address this potential problem, we synthesized compounds **8a**–**c** with a more stable ether linkage (Fig. 6).

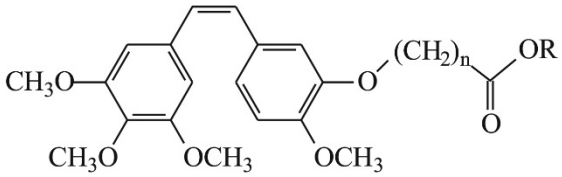


**8a** n = 6, R = 2-adamantyl; **8b** n = 6, R = 1-adamantyl;
**8c** n = 7, R = 2-adamantyl

**Fig. 6.** CA-4 conjugates related to tubuloclustin with substituted phenolic hydroxyl

## Chemistry

Compounds **4a**–**f** and **4g** were synthesized from the corresponding alcohols as outlined in Schemes 1 and 2.

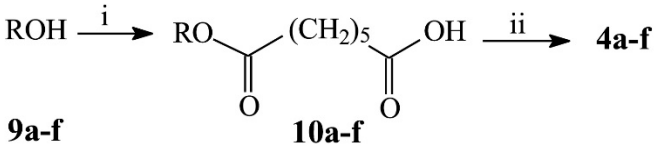


**Scheme 1.** Reagents and conditions: (i) pimelic add polyanhydride, DMAP, $CH_2Cl_2$, rt then 80–90 °C (**10a-f**: 20-53%); *N*-deacetylcolchicine, EEDQ, $CH_2Cl_2$, rt (**4a**–**f**: 52–98%)

Initial substituted alcohols **9a**–**f** were prepared according to the literature methods: 2-methyl-2-adamantanol **(9a)** and 2-*n*-butyl-2-adamantanol **(9b)** *via* reaction of adamantanone with methylmagnesium bromide [7] or butyllithium [8], respectively; l-acetamino-3,5-dimethylaminoadamantanol **(9c)** in two steps from 1,3-dimethyladamantane [9-11]; methyl 7-endo-hydroxybicyclo[3.3.1]nonane-3-exo-carboxylate (**9d**) in two steps from 2-oxahomoadamantan-3-one [12]; methyl 3-hydroxyadamantane-l-

carboxylate (**9e**) from the corresponding acid using method [13]; 5-hydroxy adamantan-2-one (**9f**) by oxidation of adamantanone with nitric add [14]. Alcohol **9g** was synthesized *via* a standard Boc protection [15] of the amino group of 1-aminoadamantan-3-ol [16]. Alcohols **9a**–**g** were subjected to esterification with polyanhydride of pimelic acid resulting in the formation of esters **10**–**g**.

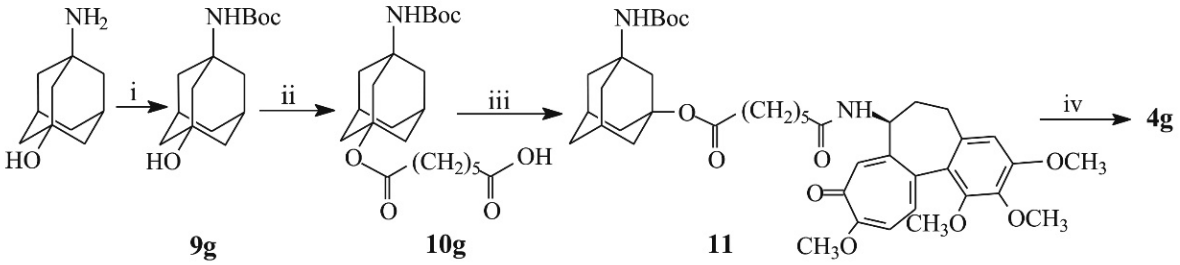


**Scheme 2.** Reagents and conditions: (i) $Boc_2O$, $NEt_3$,$CH_2Cl_2$, rt (97%); (ii) pimelic acid polyanhydride, DMAP, $CH_2Cl_2$, rt then 80-90°*C* (28%); (iii) *N*-deacetylcolchicine, EEDQ, $CH_2Cl_2$, rt (80%); (iv) 1. $CF_3COOH$, $CH_2Cl_2$, rt; 2. $NaHCO_3$ aq. (90%)

The reaction of the esters with *N*-deacetylcolchidne (obtained in three steps from colchicine [17]) in the presence of *N*-eth-oxycarbonyl-2-ethoxy-l,2-dihydroquinoline (EEDQ) afforded the target conjugates **4a-f** and compound **11.** Removal of the Boc protecting group in **11** led to the final conjugate **4g** (Scheme 2).

For the synthesis of podophyllotoxin analogues of tubuloclustin **5a**–**c** 2-adamantyl monoesters of adipic, pimelic or suberic acids were first obtained as described in [4] and then treated with podophyllotoxin in the presence of DCC and DMAP (Scheme 3) to yield the desired conjugates **5a**–**c.** The synthesis of combretastatin A-4 analogues of tubuloclustin **6a**–**c** and **7a**–**c** is outlined in Scheme 4.

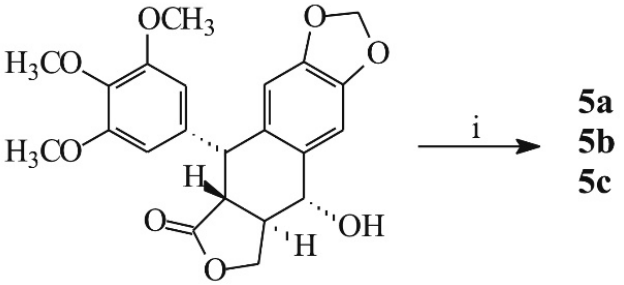


**Scheme 3.** Reagents and conditions: *(i)* 6-(2-adamantyloxy)-6-oxohexanoic add or 7-(2-adamantyloxy)-7-oxoheptanoic add or 8-(2- adamantyloxy)-8-oxooctanoic acid, DCC, DMAP, $CH_2Cl_2$, rt (**5a:** 78%, **5b:** 94%, **5c:** 97%)

Combretastatin A-4 carboxylic acids were obtained by the Perkin reaction of 3,4,5-trimethoxyphenylacetic acid and 3-hydroxy-4-methoxybenzaldehyde or from 3,4,5-trimethoxybenzaldehyde and 3-hydroxy-4-methoxyphenylacetic acid [18-20]. The acids were converted to the corresponding methyl esters **12a** and **12b** with the following TBDMS-protection of the phenolic hydroxyl group. Protected esters **13a** and **13b** were reduced with lithium aluminum hydride in THF to give alcohols **14a** and

**14b.** The reaction of these alcohols with 2-adamantyl monoesters of pimelic, suberic or azelaic acids [4] in the presence of DCC and DMAP provided esters **15a**–**c** and **16a**–**c.** Their deprotection led to the target conjugates **6a**–**c** and **7a**–**c.**

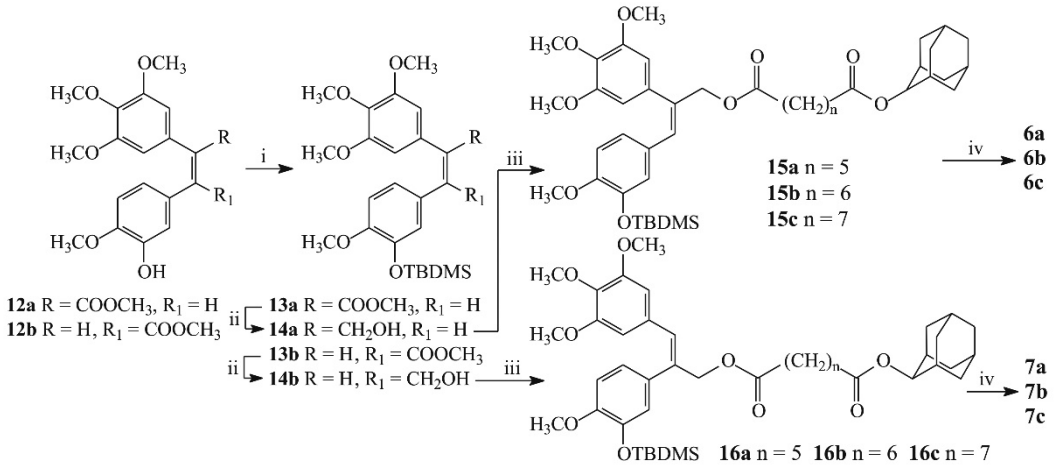


**Scheme 4.** Reagents and conditions: *(i)* TBDMSCl, imidazole, DMF, rt, **(13a:** 98%, **13b:** 95%); (*ii*) $LiAlH_4$, THF; –15°C to rt (**14a**: 81%, **14b**: 74%,); *(iii)* 7-(2-adamantyloxy)-7-oxoheptanoic acid or 8-(2-adamantyloxy)-8-oxooctanoic acid or 9-(2-adamantyloxy)-9-oxononanoic acid, DCC, DMAP, $CH_2Cl_2$, rt (**15a**: 85%, **15b**: 80%, **15c**: 78%; **16a**: 95%, **16b**: 85%, **16c**: 99%); *(iv)* DBU, $CH_3CN/H_2O$ 99:1, rt (**6a**: 75%, **6b**: 84%, **6c**: 85%; **7a**: 76%, **7b**: 83%, **7c**: 79%)

Compounds **8a-c** were synthesized in two steps from 7-bromoheptanoic **(17a)** or 8-bromooctanoic **(17b)** acids as shown on Scheme 5.

The intermediate to-bromocarboxyhc add adamantyl esters **18a-c** were conjugated with CA-4 in the presence of $K_2CO_3$ to give the target compounds in high yields.

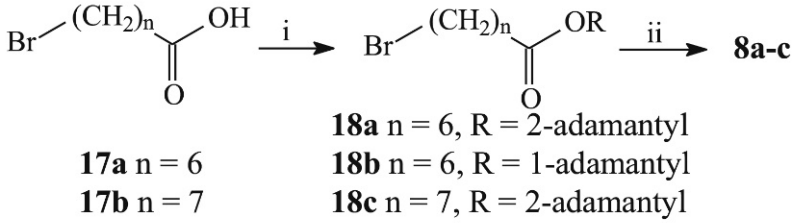


**Scheme 5.** Reagents and conditions: *(i)* 1-adamantanol or 2-adamantanol, DCC, DMAP, $CH_2CI_2$, rt, (**18a**: 76% from **17a**; **18b**: 73% from **17a**; **18c**: 56% from **17b**); (if) CA-4, $K_2CO_3$, $CH_2Cl_2$, rt. Ar (**8a**: 87% from **18a**; **8b**: 98% from **18b**; **8c**: 90% from **18c**)

## Biological activity and structure–activity relationship

All novel compounds were examined for their influence on viability of lung carcinoma cancer cells A549 in a standard colorimetric MTT assay [21] and were also evaluated by immunofluorescence microscopy recording their ability to alter microtubule arrays in these cells [22]. The results for **4a**–**g** are presented in Table 1. As can be seen from Table 1, tubuloclustin analogues with modified adamantane moiety displayed high cytotoxicity (nanomolar concentration range.).

**Table 1** Effect of the compounds **4a–g** and **11** on A549 cells

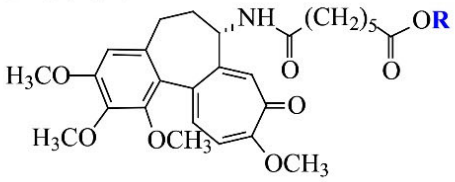


| Compound | R | Cytotoxicity[a] $EC_{50}$ ± SD (nM) | Effect on tubulin clustering[b] |
|---|---|---|---|
| **4a** | 2-Methyl-2-adamantyl | 13 ± 6 | +++ |
| **4b** | 2-*n*-Butyl-2-adamantyl | 15 ± 6 | ++ |
| **4c** | 3-Acetamido-(5,7-dimethyl)-1-adamantyl | 6 ± 2 | +++ |
| **4d** | 7-*Exo*-methoxycarbonyl-3-*endo*-bicyclo[3.3.1]nonanyl | 21 ± 7 | ++ |
| **4e** | 3-Methoxycarbonyl-1-adamantyl | 11 ± 4 | +++ |
| **4f** | 4-Oxo-1-adamantyl | 62 ± 14 | +++ |
| **4g** | 1-Amino-3-adamantyl | 400 ± 70 | ++ |
| **11** | 1-[(*Tert*-butoxycarbonyl)amino]-3-adamantyl | 38 ± 4 | ++ |
| **1** Tubuloclustin | 2-Adamantyl | 6 ± 1.4 [7] | +++ |
| **3** | 1-Adamantyl | 11 ± 1.7 [7] | +++ |
| Colchicine | | 27 ± 1.5 | No clustering |

[a] The average of three to six independent experiments

[b] All the compounds were able to induce depolymerization of microtubules, so only relative strength of the clustering effect (symbolized by the number of "+", see Fig. 7) is indicated. Cells were treated with each compound for 8 h at a 1 μM concentration

All the compounds of this series inhibited microtubule polymerization and also caused strong or mild tubulin clustering typical for tubuloclustin (Fig.7D, E). In addition, these compounds induced a nuclear fragmentation typical for cells undergoing apoptosis (after 24–48 h of culturing, Fig.7F).

2-Methyl **(4a)** and 2-*n*-butyl **(4b)** substitution of adamantane was tolerated, and the introduction of three hydrophobic and bulky substituents to different positions of adamantane core (**4c**) led to a compound with maximal cytotoxicity of the series ($EC_{50}$ = 6 nM). The activity of **4c** was higher than that of its unsubstituted structural prototype **3**. In the pair of compounds with equal substituents **4d** and **4e** the conformationally more flexible bicyclo[3.3.1]nonane derivative was only slightly less active than its rigid analogue **4e**.

The conjugates with hydrophilic groups in carcass were slightly (**4f**) or noticeably (**4g**) less active. However, the drop of activity of aminoadamantane derivative **4g** was probably connected to its low cellular permeability due to the high degree of ionization at pH 7.4. Indeed, the compounds with acylated (**4c**) or Boc-protected amino group (compound **11**, the precursor of **4g** in the synthetic scheme) displayed high cytotoxic activity.

High cytotoxic activity and clustering ability of compounds **4b**, **4c**, **4e** and **11** with diverse bulky substituents [*n*-Bu, $NHC(O)CH_3$, $C(O)OCH_3$, $NHC(O)Bu^t$] at different positions of carcass is of special interest. This indicates that the substituted adamantane moiety of the corresponding compounds is positioned inside a voluminous vacant area. It is known that colchicine binds on the β-tubulin subunit at the intradimeric interface of the heterodimer and has little direct interaction with α-subunit [2].

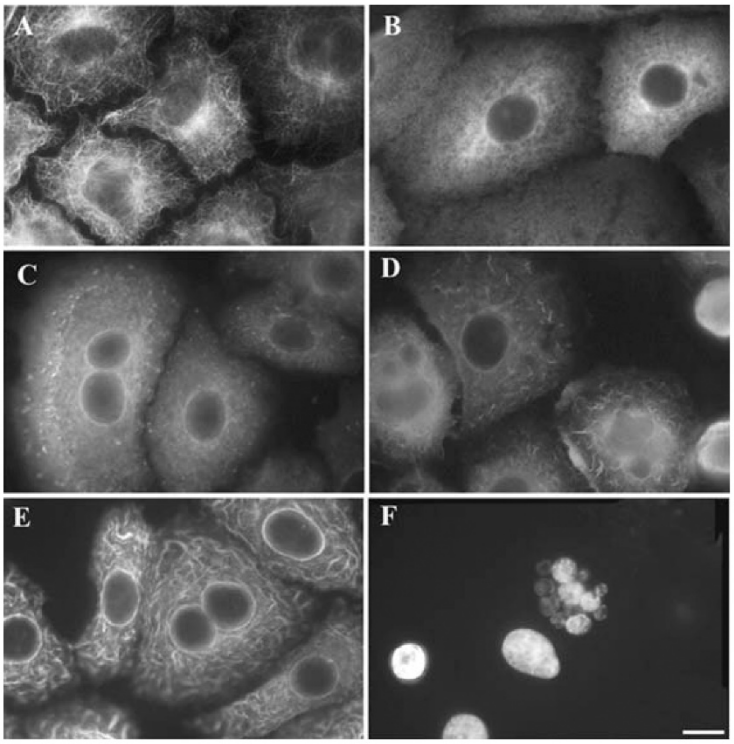


**Fig. 7.** Patterns of tubulin distribution (**A**–**E**) and nucleus fragmentation (**F**) observed in A549 cells treated with various compounds of series **4**-**8** (the depicted images were observed for the molecules indicated in *parentheses*). **A** Intact microtubules (DMSO, control); **B** diffused tubulin pattern after microtubule depolymerization without tubulin clustering (**7a**); **C** weak tubulin clustering marked as +: few tubulin clusters were found mainly at the cell periphery (**5b**); **D** medial tubulin clustering marked as ++: many tubulin clusters were located throughout the cells **(4d)**; **E** strong tubulin clustering marked as +++: many tubulin clusters were located throughout the cells and especially near the nucleus (**4e**); **F** nuclear fragmentation typical for the apoptotic cells (b). Bar 20 μM

Earlier we proposed that the adamantane moiety of tubuloclustin interacts with a hydrophobic binding region at the edge of a-tubulin subunit (formed by residues aTyr224 and aVall77) and the whole molecule 1 causes a sort of “crosslinking” of the subunits (Fig. 8) [5].

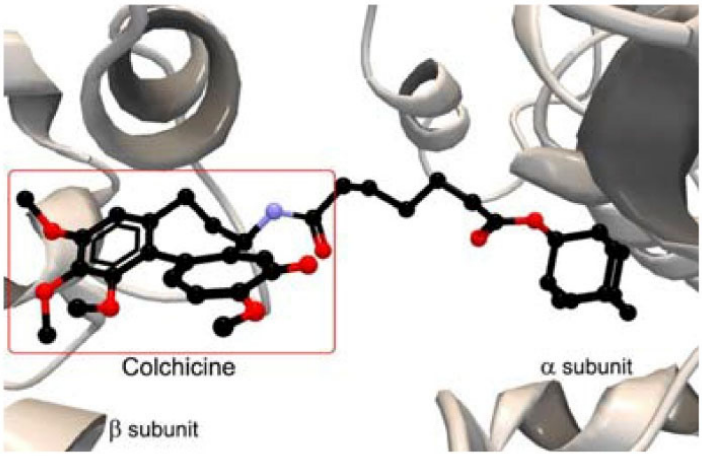


**Fig. 8.** Schematic representation of the earlier proposed mode of tubuloclustin binding with α and β subunits of tubulin

The maintaining of activity in the case of adarnantane substitution with bulky groups is in agreement with the hypothesis of its location at the intradimeric interface of the heterodimer. The data obtained confirm also the hypothesis that clustering ability is a general property of definitely modified $C^7$ colchicine analogues [5].

The results of biotests for the series of compounds **5**–**8** are presented in Table 2.

Cytotoxic activity of both podophyllotoxin and CA-4 derivatives related to tubuloclustin, although lower than that of the lead compound, was still reasonable with the $EC_{50}$ values 0.38–1.6 μM (Table 2).

Podophyllotoxin derivatives **5a**–**c** exhibited the maximal cytotoxicity, which was almost independent on the linker length of the conjugates. It should be emphasized that compounds **5a**–**c** caused not only tubulin depolymerization but also showed some tubulin clustering typical for tubuloclustin analogues with lower activity [4] (Fig.7C).

**Table 2** Effect of compounds **5a–c**, **6a–c**, **7a–c** and **8a–c** on A549 cells

| Compound | Ligand of the colchicine binding site | n in $-(CH_2)_n$-sequence in the linker | Inhibition of cell viability[a] $EC_{50} \pm$ SD (nM) | Effect on microtubules (MTs) and tubulin (Tb) clustering[b] |
|---|---|---|---|---|
| **5a** | Podophyllotoxin | 4 | 490 ± 40 | MT depolymerization and Tb clustering + |
| **5b** | Podophyllotoxin | 5 | 380 ± 60 | MT depolymerization and Tb clustering + |
| **5c** | Podophyllotoxin | 6 | 500 ± 40 | MT depolymerization and Tb clustering + |
| **6a** | CA-4 ($C^1$) | 5 | 829 ± 20 | No effect |
| **6b** | CA-4 ($C^1$) | 6 | 1400 ± 250 | No effect |
| **6c** | CA-4 ($C^1$) | 7 | 1400 ± 200 | No effect |
| **7a** | CA-4 ($C^2$) | 5 | 1300 ± 300 | MT depolymerization |
| **7b** | CA-4 ($C^2$) | 6 | 1400 ± 300 | MT depolymerization |
| **7c** | CA-4 ($C^2$) | 7 | 1600 ± 300 | MT depolymerization |
| **8a** | CA-4 (-O-) | 6 | 1040 ± 40 | MT depolymerization and Tb clustering + |
| **8b** | CA-4 (-O-) | 6 | 4440 ± 820 | MT depolymerization and Tb clustering + |
| **8c** | CA-4 (-O-) | 7 | 7260 ± 1650 | MT depolymerization and Tb clustering + |
| **CA-4-($C^2$)–COOH** | | | 240 ± 90 | MT depolymerization |
| Podophyllo-toxin | | | 10 ± 3 | MT depolymerization |
| **CA-4** | | | 9 ± 3 | MT depolymerization |

[a] The average of three to six experiments

[b] Effect on microtubules was observed in cells treated with 1) CA-4-($C^2$)-COOH, podophyllotoxin and CA-4 for 24 h at 1 μM, 2) with compounds **5a–c, 6a–c, 7a–c** for 24 h at 5 μM 3) with compound **8a** at 10 μM and **8b,c** at 50 μM for 24h (MT depolymerization) and 72 h (Tb clustering); "+" symbolizes the relative strength of the clustering effect (Fig. 7)

As follows from the data presented in Table 2, the $EC_{50}$ values for CA-4 derivatives **6a-c** and **7a-c** were very close and almost independent on the linker length or the position of its attachment. At the saturation concentration of 5 μM $C^2$-derivatives of CA-4 **7a-c** stimulated strong depolymerization of microtubules, induced the nucleus fragmentation in 20-30% cells (after 24 h of incubation) but did not display the clustering effect (Fig.7B). Interestingly, none of $C^1$-combretastatin derivatives **6a-c** rendered a noticeable effect on the microtubules. The pattern of tubulin distribution was equal to control (Fig. 7A). Thus, despite the close structural resemblance the conjugates **6a-c** and **7a-c** are essentially different in the interaction with tubulin. In this connection it is interesting to mention that the similar relationship was observed in a pair of $C^1$ and

$C^2$-carboxyl derivatives of CA-4. According to literature data [23], $C^1$-acid has no effect on microtubules and is not cytotoxic, while $C^2$-acid (as shown in the present work, see Table 2) retains rather high cytotoxic activity ($EC_{50}$ ~ 200 nM) and the ability to inhibit microtubule depolymerization. Therefore, the introduction of a substituent to $C^2$ of CA-4 is prefered both in the pair of corresponding acids and in the case of series **6a-c** and **7a-c.**

CA-4 derivatives **8a-c** with the ether linkage were less cytotoxic than **7a-c** and caused tubulin depolymerization at higher concentrations (5 μM for **7a-c,** 10 μM for **8a** and 50 μM for **8b,c**). On the other hand, conjugates **8a-c** induced a formation of tiny tubulin clusters in A549 cells (the pattern was analogues to the one caused by conjugate **5b** (Fig. 7C)). The ability of compounds **5a-c, 7a-c** and **8a-c** to inhibit tubulin polymerization indicates that podophyllotoxin or combretastatin moieties in these molecules are located in the colchicine domain. However, the exact positions of these moieties in the binding site may differ from that of the parent podophyllotoxin and CA-4 resulting in a drop of cytotoxicity of compounds **5a-c, 7a-c** and **8a-c** in comparison to tubuloclustin. In conjugates **5** and **8** this difference in arrangement in the binding site does not seem to interfere adamantane interaction with a-subunit, which eventually leads to the observed tubulin clusterization. Thus, a clustering effect is characteristic not only to certain colchicine derivatives, but it can also be manifested by structurally different ligands of colchicine domain in tubulin.

**Conclusion**

In an effort to further investigate the structural requirements associated with high cytotoxicity and unusual tubulin clustering ability of tubuloclustin (1) new types of its derivatives were designed, synthesized and tested on the lung carcinoma A549 cell line. The potency of tubuloclustin analogues with different (including bulky) substituents in adamantane core was very high and they all stimulated microtubule depolymerization and formation of prominent tubulin clusters, thus supporting the hypothesis on the location of adamantane moiety of **1** in a voluminous vacant region in the protein (most likely between two subunits). In two other sets of compounds colchicine fragment of the parent molecule was replaced with other anti-tubulin agents, namely CA-4 or podophyllotoxin. Both types of these tubuloclustin analogues inhibited cell proliferation at submicromolar concentrations and several compounds also exhibited some clustering activity. Thus, it was clearly demonstrated that the whole panel of $C^7$-modified colchicine, podophyllotoxin and combretastatin derivatives could manifest clustering effect, and the strength of this effect correlated with cytotoxic activity of the compounds.

**Experimental section**

**Chemistry**

*General method* A. To a solution of an alcohol **9a-g** in $CH_2Cl_2$ (10 mL) was added pimelic add poly anhydride (PAPA) [24], followed by catalytic amount of DMAP (0.01 g). The mixture was stirred at room temperature for 15 min, then the solvent was removed *in vacuo,* and the residue was heated on an oil bath at 80-90°C for 18 h. The reaction mixture was diluted with aqueous acetone (ca. 10% of water, 10 mL) and stirred at room temperature for 2 h, then concentrated under reduced pressure, taken up in CH2CI2 (20 mL), dried over $Na_2SO_4$, filtered and evaporated. The product was purified by column chromatography (ethyl acetate/petroleum ether (40-70°C) in a gradient ratio from 1:7 to 1:2, unless indicated otherwise).

*General method* B. To a solution of acid **10a-g** and *N*-deacetylcolchicine in $CH_2Cl_2$ (5 mL) was added EEDQ at room temperature. After stirring for 24 h, the solvent was removed under reduced pressure, and the residue was purified by column chromatography (ethyl acetate/petroleum ether (40-70°C) 1:2, then $CH_2Cl_2$/methanol in a gradient ratio from 20:1 to 10:1, unless indicated otherwise).

*General method* C. To a solution of carboxylic add in $CH_2Cl_2$ (10 mL) was added podophyllotoxin or alcohol **14a,b** or (1-, 2-)adamantanol at room temperature. The resulting mixture was treated with DCC and catalytic quantity of DMAP (0.01 g). After stirring for 12 h, acetic acid (5-10 μL) was added, and in 15 min the solvent was removed *in vacuo.* The residue was dissolved in ethyl acetate (10 mL) and kept at 4°C for 2-3 h. The solid was filtered, washed with cold ethyl acetate (2×10 mL), and the filtrate was washed with brine (10 mL), water (10 mL), dried over $Na_2SO_4$ and evaporated. The product was purified by column chromatography (ethyl acetate/petroleum ether (40-70°C) 1:8).

*General method* D. To a solution of compound **15a-c** or **16a-c** in MeCN:$H_2O$ (99:1,5 mL total volume) was added DBU. After stirring at room temperature for 24 h the reaction mixture was diluted with saturated aqueous solution of $NH_4Cl$ (1 mL) and extracted with $CH_2Cl_2$ (3 x 10 mL). The organic layers were dried over $Na_2SO_4$ and concentrated. The residue was purified by column chromatography (ethyl acetate/petroleum ether (40-70°C) 1:10).

*General method* E. To a solution of CA-4 in dry DMF (2 mL) under atmosphere of argon was added anhydrous $K_2CO_3$, followed by ω-bromocarboxylic acid ester **18a-c**. The mixture was stirred at room temperature for 12 h, then diluted with water (20 ml) and extracted with $CH_2Cl_2$ (3×10 mL). The organic layers were dried over $Na_2SO_4$ and

concentrated. The residue was purified by column chromatography (ethyl acetate/petroleum ether (40-70°C) 1:7).

**Protocols of biological tests**

**Cell culture**

A549 human lung epithelial carcinoma cells (CCL-185™) were cultured with Dulbecco's modified Eagle's medium (DMEM) containing 10% fetal bovine serum and 1% antibiotic penicillin/streptomycin at 37°C under a 5% $CO_2$ humidified atmosphere.

**MTT cell cytotoxicity assay**

A549 cells were seeded in 96-well plates at a density of 3000 cells per well. Stock solutions of test compounds were prepared in DMSO. Cells were treated for 24 h with selected compounds at 1 nM-100 μM (8 wells for each concentration). DMSO (0.5%) served as a negative control. MTT (3-(4,5-dimethylthiazolyl-2)-2,5-diphenyl-2*H*-tetrazolium bromide, Roth GmbH, Karlsruhe, Germany) was prepared at 5 mg/mL in phosphate-buffered saline (PBS) and filtered through a 0.22 μm filter. 20 μL of sterile MTT solution (final concentration 0.5 mg/mL) was added to each well 2 h before the end of compound exposure. Then the supernatant was removed, and 100 μL of DMSO containing 10% SDS and 0.6% acetic acid was added to each well. Resulting formazan crystals were solubilized by thorough mixing on a plate shaker. Optical density was measured at 590 nm with 690-nm reference filter using a EL808 Ultra Microplate Reader (BioTek Instruments, Winooski, USA). Experiments for all compounds were repeated at least 3 times and EC50 values were determined by sigmoidal curve fitting using Excelbased software.

**Immunofluorescence staining of cellular microtubules**

For microtubule staining, A549 cells were cultured in 12- well plates on small glass coverslips (11 mm diameter) at a density of 20000 cells per coverslip. Cells were incubated for 8-72 hours at different saturation concentrations of tested compounds. These concentrations lie in the range of plateau concentrations at which maximum effects on microtubules were observed (moreover, at these concentrations even in the case of partial non-specific hydrolysis of the compounds there exist enough intact molecules in the cells to interact with tubulin). DMSO (0.5% v/v) served as a negative control. The cells were fixed and stained as described in [24]. Fixed cells were labeled with mouse monoclonal antibody against a-tubulin at a dilution of 1:400 (Sigma, St. Louis. USA), followed by incubation of Alexa Fluor488 labeled goat antimouse IgG at a dilution of 1:200 (Invitrogen, Germany). Nuclei were stained with 4pM Hoechst 33258 (Sigma-Aldrich, USA). Images of all samples were acquired with a Nikon Diaphot 300 inverted microscope (Nikon GmbH, Dusseldorf, Germany) equipped with a cooled charge-couple device camera system (SenSys; Photometries, Munich, Germany).

Acknowledgements The work was supported by Russian Foundation for Basic Research (project 15-03-04894), Russian Academy of Sciences and by the German organization DAAD (German Academic Exchange Service) in the frame of a Scientific Cooperation Agreement between Moscow and Rostock Universities.

**References**

1. Stanton RA, Gemert KM, Nettles JH, Aneja R (2011) Drugs that target dynamic microtubules: a new molecular perspective. Med Res Rev 31:443-481. doi:10.1002/med.20242
2. Ravelli RBG, Gigant B, Curmi PA, Jourdain I, Lachkar S, Sobel A, Knossow M (2004) Insight into tubulin regulation from a complex with colchicines and a stathmin-like domain. Nature 428:198-202. doi:10.1038/nature02393
3. Nguyen TL, McGrath C, Hermone AR, Burnett JC, Zaharevitz DW, Day BW, Wirf P, Hamel E, Gussio R (2005) A Common pharmacophore for a diverse set of colchicine site inhibitors using a structure-based approach. J Med Chem 48:6107-6116. doi:10.1021/jm050502t
4. Zefirova ON, Nurieva EV, Shishov DV, Baskin II, Fuchs F, Lemcke H, Schröder F, Weiss DG, Zefirov NS, Kuznetsov SA (2011) Synthesis and SAR requirements of adamantine–colchicine conjugates with both microtubule depolymerizing and tubulin clustering activities. Bioorg Med Chern 19:5529-5538. doi:10.1016/j.bmc. 2011.07.040
5. Zefirova ON, Lemcke H, Lantow M, Nurieva EV, Wobith B, Onishchenko GE, Hoenen A, Griffiths G, Zefirov NS, Kuznetsov SA (2013) Unusual tubulin-clustering ability of definitely C7- modified colchicine analogues. ChemBioChem 14:1444-1449. doi: 10.1002/cbic.201300143
6. Zefirova ON, Nurieva EV, Glazkova YS, Zefirov NA, Mamaeva AV, Wobith B, Romanenko VI, Lesnaia NA, Treshalina HM, Kuznetsov SA (2014) Antiproliferative activity of tubuloclustin and its steroid analogues. Pharm Chern J 48:373-378. doi: 10.1007/si1094-014-1113-8
7. Mullen GB, Georgiev VSt (1986) Synthesis of substituted spiro[azetidin-2-one-4,2'(or 3,2')-tricyclo[3.3.1.13,7]decane] derivatives. Heterocycles 24:3441-3446. doi: 10.3987/R-1986-12-3441
8. Kolocouris A, Tzitzoglaki C, Johnson FB, Zell R, Wright AK, Cross TA, Tietjen I, Fedida D, Busath DD (2014) Aminoadamantanes with persistent in vitro efficacy against H1N1 influenza A. J Med Chem 57:4629-1639. doi:10.1021/jm500598u
9. Klimochkin YN, Bagrii EI, Dolgopolova TN, Moiseev TK (1988) Synthesis of alkoxycarbonylaminoadamantanes and acetylaminoadamantanes in nitric acid. Bull Acad Sci USSR Div Chem Sci 27:757-759. doi: 10.1007/BF01455495 (Engl. Transl.)
10. Wanka L, Cabrele C, Vanejews M, Schreiner PR (2007) ϫ- Aminoadamantanecarboxylic acids through direct C-H bond amidations. Eur J Org Chem 2007:1474—1490. doi:10.1002/ejoc.200600975
11. Lipton StA (2004) Methods for treating neuropsychiatric disorders with NMDA receptor antagonists. Patent US2004/122090 Al
12. Zefirova ON, Nurieva EV, Lemcke H, Ivanov AA, Zyk NV, Weiss DG, Kuznetsov Zefi-

rov NS (2008) Design, synthesis and bioactivity of simplified taxol analogues on the basis of bicyclo[3.3.1]nonane derivatives. Mendeleev Commun 18:183-186. doi: 10.1016 /j.mencom.2008.07.003

13. Adcock W, Kok GB (1987) Transmission of polar substituent effects in saturated systems: synthesis and fluorine-19 NMR study of 3-substituted adamant-1-yl fluorides. J Org Chem 52:356-364. doi:10.1021/jo00257a011
14. Ie Noble WJ, Srivastava S, Cheung CK (1983) 5-tert-Butyladamantan-2-one. J Org Chem 48:1099-1101. doi: 10.1021/ jo00155a034
15. Aranyi P, Bata I, Batory S, Boronkay É, Bovy P (2005) Adamantane and azabicyclo-octane and nonane derivatives, process of their preparation and their use as DPP-IV inhibitors. Patent WO/2005/021536
16. Stetter H, Gärtner J, Тасκе P (1965) Neue Möglichkeiten des Adamantan-Ringschlusses. Angew Chem 77:171-171. doi:10.1002/ange. 19650770410
17. Bagnato JD, Eilers AL, Horton RA, Grissom CB (2004) Synthesis and characterization of a cobalamin-colchicine conjugate as a novel tumor-targeted cytotoxin. J Org Chem 69: 8987-8996. doi:10.1021/ jo049953w
18. Xiao C-F, Zou Y, Du J-L, Sun H-Y, Liu X-K (2012) Hydroxyl substitutional effect on selective synthesis of cis, trans stilbenes and 3-arylcoumarins through Perkin condensation. Synth Commun 42:1243-1258. doi:10.1080/00397911.2010.538889
19. Gaukroger K, Hadfield JA, Hepworth LA, Lawrence NJ, McGown AT (2001) Novel syntheses of cis and trans isomers of combretastatin A-4. J Org Chem 66:8135-8138. doi:10.1021/jo015959z
20. Chen Y, Zou Y, Sun H-Y, Liu X-K, Xiao C-F, Sun J, He S-J, Li J (2011) Practical and green synthesis of combretastatin A-4 and its prodrug CA4P using renewable biomass-based starting materials. Synthesis 2011:217-222. doi:10.1055/s-0030-1258358
21. Mosmann T (1983) Rapid colorimetric assay for cellular growth and survival: application to proliferation and cytotoxicity assays. J Immunol Methods 65:55-63. doi:10.1016/ 0022-1759(83)90303-4
22. Al-Haddad A, Shonn MA, Redlich B, Blocker A, Burkhardt JK, Yu H, Hammer 3rd JA, Weiss DG, Steffen W, Griffiths G, Kuznetsov SA (2001) Myosin Va bound to phagosomes binds to F-actin and delays microtubule-dependent motility. Mol Biol Cell 12:2742-2755. doi:10.1091/mbc.12.9.2742
23. Borrel C, Thoret S, Cachet X, Guenard D, Tillequin F, Koch M, Michel S (2005) New antitubulin derivatives in the combretastatin A4 series: synthesis and biological evaluation. Bioorg Med Chem 13:3853-3864. doi:10.1016/j.bmc.2005.02.039
24. Hill JW, Carothers WH (1933) Studies of polymerization and ring formation. XIX. Many-membered cyclic anhydrides. J Am Chem Soc 55:5023-5031. doi:10.1021/ja01339a054
25. Al-Haddad A, Shonn MA, Redlich B, Blocker A, Burkhardt JK, YuH, Hammer, 3rd JA, Weiss DG, Steffen W, Griffiths G, Kuznetsov SA (2001) Myosin Va bound to phagosomes binds to F-actin and delays microtubule-dependent motility. Mol Biol Cell 12: 2742-2755. doi:10.1091/mbc.12.9.2742

*MENDELEEV COMMUNICATIONS, Vol. 27 (3), 228-230, 2017*

# SYNTHESIS AND ANTIMITOTIC ACTIVITY OF NOVEL 5-AMINOISOXAZOLES BEARING ALKOXYARYL MOIETIES

**Dmitry A. Vasilenko, Elena B. Averina, Nikolay A. Zefirov, Birgit Wobith, Yuri K. Grishin, Victor B. Rybakov, Olga N. Zefirova, Tamara S. Kuznetsova, Sergei A. Kuznetsov and Nikolay S. Zefirov**

*Department of Chemistry, M. V. Lomonosov Moscow State University, 119991 Moscow, Russian Federation.*
*Institute of Physiologically Active Compounds, Russian Academy of Sciences, Moscow Region, Russian Federation*
*Institute of Biological Sciences, Cell Biology and Biosystems Technology, University of Rostock, Rostock, Germany*

DOI: 10.1016/j.mencom.2017.05.003

5-Aminoisoxazoles containing trimethoxy- and methylenedioxyphenyl moieties were prepared by heterocyclization of electrophilic alkenes with tetranitromethane in the presence of triethylamine with subsequent reduction of resulting 5-nitroisoxazoles. The crystal structure of 3,4,5-tiimethoxy- benzyl 5-aminoisoxazole-3-carboxylate was determined by X-ray analysis. Two novel 5-aminoisoxazoles demonstrated moderate antimitotic activity to human lung carcinoma A549 cell Une.

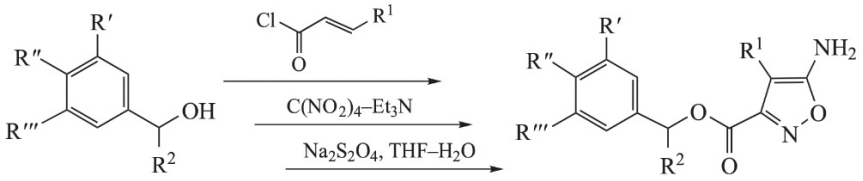


Five-membered aromatic heterocycles are often applied in drug design as classical isosteric groups of substituted or non-substituted benzene rings of the lead compounds and quite often such a replacement leads to retention of biological activity.[1-3] Earlier we reported an easily accessible regioselective synthesis of 5-nitroisoxazoles by heterocyclization of electrophilic alkenes with tetranitromethane in the presence of triethylamine[4,5] and the following reduction ($SnCl_2$/EtOH or Zn/AcOH/Pr$^i$OH) of these compounds to the corresponding 5-aminoisoxazoles.[6] Elaboration of this method encouraged us to apply substituted 5-aminoisoxazole scaffolds in the design of compounds with different types of physiological activity, including putative antineoplastic agents.

Many classical natural tubulin-targeted ligands, *e.g.* podophyllotoxin (Figure 1), interact with tubulin and inhibit its polymerization to microtubules.[7] 3,4,5-Trimethoxyphenyl and methylenedioxyphenyl moieties represent common structural fragments

often found in the molecules of these ligands.[7,8] Therefore, we decided to introduce these moieties into 5-aminoisoxazole scaffolds and to synthesize compounds **1a-f** (see Figure 1). Interestingly, compounds **1a-d** can be considered as 'open' analogues of an antineoplastic agent A-105972 obtained using classical isosteric replacement of o-toluidine fragment by a methyl-substituted or unsubstituted 5-aminoisoxazole. The parent molecule A-105972 is known to possess noticeable cytotoxicity *in vitro* ($EC_{50}$ = 0.003-0.2 μM depending on the cell line type) and to disrupt at high concentrations (100 μM) the tubulin polymerization to microtubules.[9]

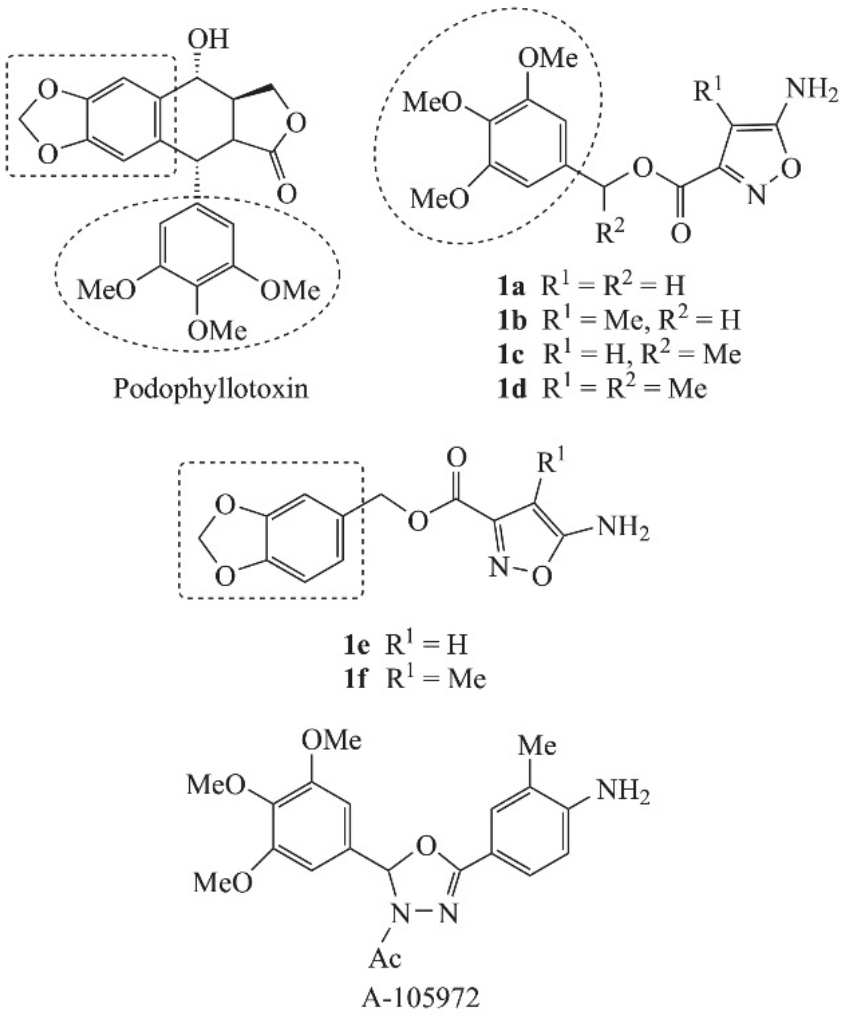


Figure 1. The structures of antineoplastic agents podophyllotoxin, A-105972 and compounds **1a-f** synthesized in the present work.

The preliminary studies showed that compounds **1a-f** could not be obtained following strictly the described procedures.[4-6] Therefore, preparation of compounds **1a-f** was the purpose of the present work. The proposed method comprised acylation of the benzylic alcohols with appropriate acyl chloride followed by heterocyclization of thus obtained unsaturated esters **2**, and the final reduction of 5-nitroisoxazoles **3** into the corresponding 5-aminoisoxazoles **1** (Scheme 1).

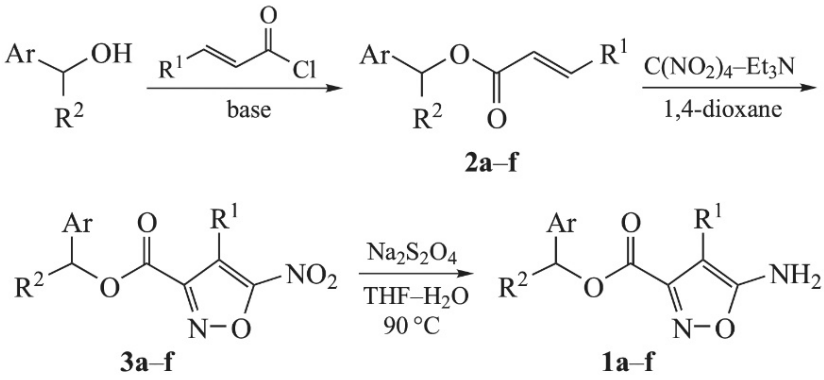


**a** Ar = 3,4,5-$(MeO)_3C_6H_2$, $R^1 = R^2 = H$
**b** Ar = 3,4,5-$(MeO)_3C_6H_2$, $R^1$ = Me, $R^2 = H$
**c** Ar = 3,4,5-$(MeO)_3C_6H_2$, $R^1 = H$, $R^2$ = Me
**d** Ar = 3,4,5-$(MeO)_3C_6H_2$, $R^1 = R^2$ = Me
**e** Ar = 3,4-methylenedioxyphenyl, $R^1 = R^2 = H$
**f** Ar = 3,4-methylenedioxyphenyl, $R^1$ = Me, $R^2 = H$

**Scheme 1**

To access the starting aryl-containing alkenes **2**, we used the synthetic protocol,[10,11] when the reaction between alcohols and acyl chlorides proceeded in the presence of $Et_3N$ as a base. Under these conditions, acrylic esters **2a,c,e** were obtained in good preparative yields and no formation of side products was observed (Table l). However, the reaction of (3,4,5-trimethoxyphenyl)- methanol or l-(3,4,5-trimethoxyphenyl)ethan-l-ol with crotonoyl chloride and $Et_3N$ occurred with the double bond migration giving isomeric vinylacetates **4a,b** without traces of crotonates **2b or 3d** (Scheme 2).

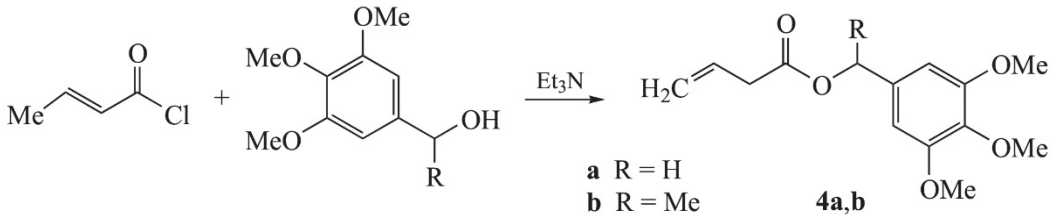


**Scheme 2**

To prepare the desired products **2b,d,f** we tried various known esterification conditions.[12-14] Such systems as Zn/benzene,[12] NaH/THF[13] or $A1_2O_3$ without solvent[14] were found to be unsuitable as they gave complex mixtures with a negligible amount of compound **2b**. We succeeded in obtaining ester **2b** as a sole product in a good preparative yield (59%, Table 1) using pyridine as a base in dichloromethane. This procedure was successfully extended onto esters **2d** and **2f** (Table 1).

Heterocyclization of electrophilic alkenes **2a-f** was performed by the action of *in situ* generated tetranitromethane-triethylamine complex [$C(NO_2)_4$-$Et_3N$] in 1,4-dioxane at 70°C. The resulting 5-nitroisoxazoles **3a-d** were obtained in moderate yields owing to partial oxidation of alkenes **2a-d** leading to 3,4,5-trimethoxy benzaldehyde

or l-(3,4,5-trimethoxyphenyl)ethanone. Lowering the reaction temperature to ambient did not raise the yield due to the formation of 3,3,3-trinitropropanoic esters as the main products.

Table 1 Synthesis of 5-aminoisoxazoles **1a-f**.

| Compounds **1-3** | Isolated yields (%) | | |
|---|---|---|---|
| | Ester **2** (base) | Nitroisoxazole **3** | Aminoisoxazole **1** |
| **a** | 70 ($Et_3N$) | 38 | 67 |
| **b** | 59 (Py) | 33 | 50 |
| **c** | 64 ($Et_3N$) | 29 | 30 |
| **d** | 34 (Py) | 37 | 50 |
| **e** | 66 ($Et_3N$) | 58 | 65 |
| **f** | 39 (Py) | 57 | 58 |

For example, compound **5** was isolated from the reaction mixture of ester **2c** and $C(NO_2)_4$–$Et_3N$ complex in 1,4-dioxane at 25°C.

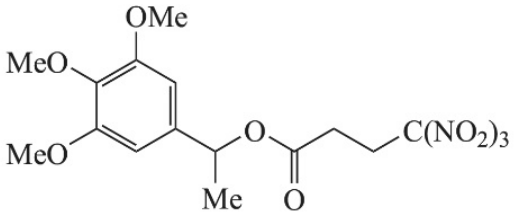


**5**

Although we previously[6] prepared a series of various 5-aminoisoxazoles in good yields, the attempts to reduce 5-nitroisoxazoles **3a-f** into target 5-aminoisoxazoles **1a-f** under previously established conditions *(i.e.* $SnCl_2$/EtOH or Zn/AcOH/ $Pr^iOH$) gave complex mixtures and no identified products were isolated. The variations of the reaction time and temperature or the amounts of reducing agents ($SnO_2$ or Zn) in the reaction of model 5-nitroisoxazole **3e** did not significantly influence the formation of the target products. The application of a neutral reducing system Zn/$NH_4C1$[15] was also shown to be inefficient. Luckily, system $Na_2S_2O_4$/THF/$H_2O$[16] allowed us to obtain the target 5-aminoisoxazoles in satisfactory yields (see Table 1). All synthesized compounds were characterized and identified using $^1H$ and $^{13}C$ NMR spectroscopy and HRMS or elemental analysis.

The structure of **1a** was unambiguously proved by X-ray diffraction analysis (Figure 2). Within the crystal lattice the molecules of **1a** arrange in a chain along the *a*-axis due to intermolecular hydrogen bonds between amino group and $sp^2$-nitrogen atom of isoxazole ring.

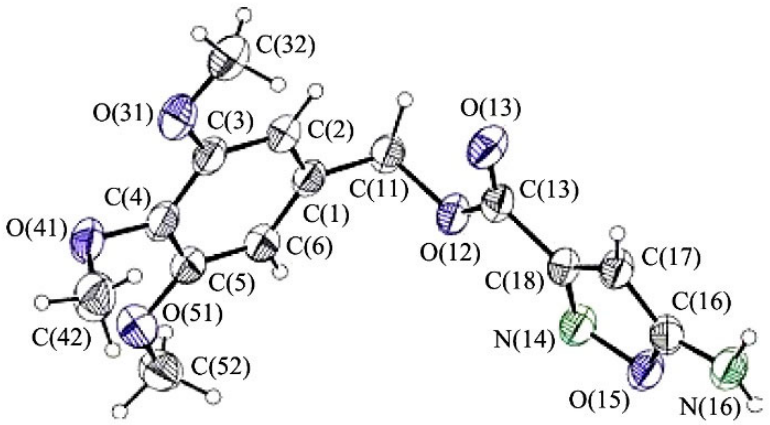


Figure 2. The general view of 3,4,5-trimethoxybenzyl 5-aminoisoxazole-3-carboxylate **1a** in representation of atoms by thermal ellipsoids (*p* = 50%).

Novel substituted 5-aminoisoxazoles were examined for their cytotoxicity to epithelial lung carcinoma cancer cells A549 in a standard colorimetric MTT assay using the procedure described[17-19] (Table 2). Their cytotoxicity turned out to be inferior to that of podophyllotoxin or A-105972. Nevertheless, two compounds of the series, namely **1a** and **1e,** were moderately cytotoxic with $EC_{50}$ values in the micromolar concentration range. The data obtained demonstrated that the introduction of methyl substituent either to the isoxazole or to the linker chain (compounds **1b-d,f**) led to a decrease in cytotoxicity. Interestingly, the equal $EC_{50}$ values for **1a** and **1e** indicated the equivalence of the trimethoxyphenyl and methylenedioxyphenyl rings for the cytotoxic activity of these compounds.

Table 2 Cytotoxicity of compounds **1a-f** to human lung carcinoma cell line A549.

| Compound | Cytotoxicity ($EC_{50}$, μM) | Cell growth inhibition (%)[a] |
|---|---|---|
| **1a** | 38 ± 4 | 91 |
| **1b** | >100 | – |
| **1c** | >100 | – |
| **1d** | >100 | – |
| **1e** | 35 ± 5 | 100 |
| **1f** | 93 ± 7 | 55 |
| Podophyllotoxin | 0.04 | – |

[a]After 48 h of culturing.

We also studied the effect of compounds **1a, 1e** and **1f** (100 pM) on cell growth using direct cell counting by microscopy over 24, 48 and 72 h of culturing (Figure 3). The compounds strongly inhibited cell proliferation, and the extent of inhibition correlated with the cytotoxicity of compounds **1a,e,f** (see Table 2). Thus, cell growth experiments confirmed the MTT data.

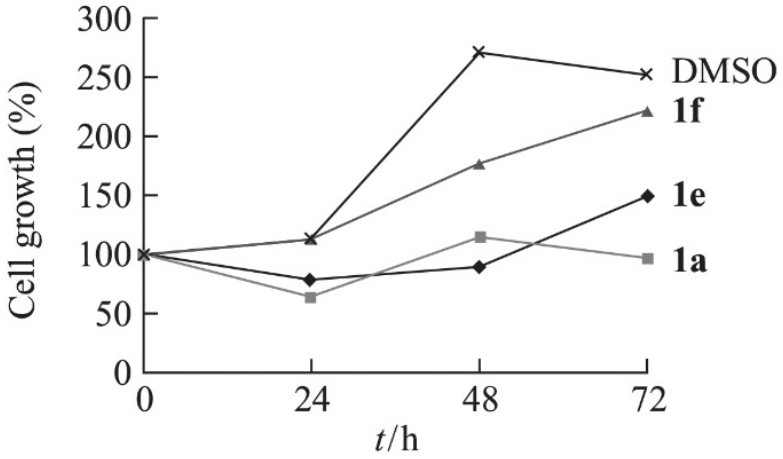


Figure 3. Effect of compounds **1a**, **1e** and **1f** on cell growth in culture. The cells were incubated with 100 μM of each compound and after resuspension were counted by phase-contrast microscopy using hemocytometer. 1% DMSO was used as a control.

In conclusion, a three-step synthetic protocol was accomplished for the preparation of substituted 5-aminoisoxazoles with polymethoxyphenyl- and methylenedioxyphenyl moieties. The optimization of the first and the third steps of the protocol was required in comparison with the earlier established conditions. A gentle reagent was found for the reduction of nitro group in isoxazole core. Two biotests revealed moderate antimitotic activity of compounds **1a** and **1e** to human lung carcinoma A549 cell line. These compounds are of interest for additional investigation of the mechanism of their antiproliferative properties.

This work was supported by the Russian Foundation for Basic Research (project nos. 14-03-00469 and 15-03-04894), the Russian Academy of Sciences (programme nos. 8P and 9) and the German Academic Exchange Service under the auspices of a collaborative agreement between Moscow and Rostock Universities. This study was fulfilled using a STOE STADI VARI PILATUS-100K diffractometer purchased by MSU Development Program.

## References

1. G. A. Patani and E. J. LaVoie, *Chem. Rev*., 1996, **96**, 3147.
2. N. A. Meanwell, *J. Med. Chem*., 2011, **54**, 2529.
3. S. G. Zlotin, A. M. Churakov, O. A. Luk'yanov, N. N. Makhova, A. Yu. Sukhorukov and V. A. Tartakovsky, *Mendeleev Commun*., 2015, **25**, 399.
4. Y. A. Volkova, E. B. Averina, Y. K. Grishin, P. Bruheim, T. S. Kuznetsova and N. S. Zefirov, *J. Org. Chem.*, 2010, **75**, 3047.
5. E. B. Averina, Y. V. Samoilichenko, Y. A. Volkova, Y. K. Grishin, V. B. Rybakov, A. G. Kutateladze, M. E. Elyashberg, T. S. Kuznetsova and N. S. Zefirov, *Tetrahedron Lett*., 2012, **53**, 1472.
6. E. B. Averina, D. A. Vasilenko, Y. V. Samoilichenko, Y. K. Grishin, V. B. Rybakov, T. S. Kuznetsova and N. S. Zefirov, *Synthesis*, 2014, **46**, 1107.
7. T. L. Nguyen, C. McGrath, A. R Hermone, J. C. Burnett, D. W. Zaharevitz, B. W. Day, P.

Wipf, E. Hamel and R Gussio, *J. Med. Chem*., 2005, **48**, 6107.
8. O. N. Zefirova, A. G. Diikov, N. V. Zyk and N. S. Zefirov, *Russ. Chem. Bull., Int. Ed.*, 2007, **56**, 680 (*Izv. Akad. Nauk, Ser. Khim*., 2007, 655).
9. J. R. Wu-Wong, J. D. Alder, L. Alder, D. J. Burns, E. K.-H. Han, B. Credo, S. K. Tahir, B. D. Dayton, P. J. Ewing and W. J. Chiou, *Cancer Res*., 2001, **61**, 1486.
10. W. Wang, Y. Li, M. Sun, C. Zhou, Y. Zhang, Y. Li and Q. Yang, *Chem. Commun*., 2012, **48**, 6040.
11. E. B. Averina, D. A.Vasilenko, Y. A. Gracheva, Y. K. Grishin, E. V. Radchenko, V. V. Burmistrov, G. M. Butov, M. E. Neganova, T. P. Serkova, O. M. Redkozubova, E. E Shevtsova, E. R. Milaeva, T. S. Kuznetsova and N. S. Zefirov, *Bioorg. Med. Chem*., 2016, **24**, 712.
12. J. S. Yadav, G. S. Reddy, D. Srinivas and K. Himabindu, *Synth. Commun.*, 1998, **28**, 2337.
13. M. Bruder, D. B. Vendramini-Costa, J. E. de Carvalho and R A. Pilli, *Bioorg. Med. Chem*., 2013, **21**, 5107.
14. V. K. Yadav and K. Ganesh Babu, *J. Org. Chem*., 2004, **69**, 577.
15. A. Pascual, *Helv. Chim. Acta*, 1991, **74**, 531.
16. M. Weiwer, J. A. Bittker, T. A. Lewis, K. Shimada, W. S. Yang, L. MacPherson, S. Dandapani, M. Palmer, B. R Stockwell, S. L. Schreiber and B. Munoz, *Bioorg. Med. Chem. Lett*., 2012, **22**, 1822.
17. O. N. Zefirova, H. Lemcke, M. Lantow, E. V. Nurieva, B. Wobith, G. E. Onishchenko, A. Hoenen, G. Griffiths, N. S. Zefirov and S. A. Kuznetsov, *ChemBioChem*, 2013, **14**, 1444.
18. A. A. Beloglazkina, B. Wobith, E. S. Barskaia, N. A. Zefirov, A. G. Majouga, E. K. Beloglazkina, N. V. Zyk, S. A. Kuznetsov and O. N. Zefirova, *Med. Chem. Res*., 2016, **25**, 1239.
19. O. N. Zefirova, E. V. Nurieva, H. Lemcke, A. A. Ivanov, N. V. Zyk, D. G. Weiss, S. A. Kuznetsov and N. S. Zefirov, *Mendeleev Commun*., 2008, **18**, 183.

*Received: 2nd September 2016;*
*Com. 16/5037*

# Раздел IV. Избранные работы в области медицинской химии препаратов для терапии нарушений окислительного статуса организма

## Введение

**Е.Р. Милаева**

Одним из важных направлений исследований в области медицинской химии, выполненных под руководством и при непосредственном участии академика Н.С. Зефирова, явились работы по синтезу и изучению взаимосвязи «структура–активность» серий соединений, которые могут представлять интерес в качестве кандидатов для терапии нарушения окислительно-восстановительного статуса организма.

Нарушение клеточного редокс-статуса является следствием окислительного стресса, и в результате в организме индуцируются процессы окислительного повреждения белков, липидов и ДНК. Окислительный стресс приводит к нарушению функций клетки, индуцирует апоптоз или некроз и участвует в патогенезе многих патологий (атеросклероз, рак, диабет, астма, болезнь Альцгеймера, болезнь Паркинсона и др.). Организм имеет собственную защитную систему, которая включает ферменты, утилизирующие образующиеся активные метаболиты кислорода и азота, а также низкомолекулярные природные антиоксиданты, поступающие в организм в виде витаминов или присутствующие в нем. Однако при нарушении баланса необходимо введение терапевтических средств, обеспечивающих борьбу с последствиями окислительного стресса и действующими на вовлеченные в эти процессы мишени.

Антиоксиданты различной природы действуют по различным механизмам. Это могут быть ингибиторы цепных радикальных реакций (в пероксидном окислении липидов), переносчики электрона (в редокс-процессах с участием металла, в частности железа) и др. Но во всех случаях добавки антиоксидантов призваны обеспечить способность организма восстановить нарушенный окислительно-восстановительный баланс.

В работах Н.С. Зефирова с коллегами разработана общая стратегия, принципы и методы создания новых комплексов биогенных металлов с функциями пролекарств и клеточных транспортеров, обладающих свойствами антиоксидантов, нейропротекторов, модуляторов апоптоза, антипролиферативных агентов, с целью получения мультитаргетных систем. Преимущества нового подхода для создания биоконъюгированных физиологически активных соединений металлов

состоят в следующем: с применением методов органического и элементоорганического синтеза обеспечивается модулирование биохимической и редокс-активности за счет вариабельности металла, лиганда, спейсера, геометрии, растворимости; введение атома металла приводит к стабилизации радикальных интермедиатов, ответственных за механизм редокс-активности; присутствие в молекуле нескольких реакционных центров позволяет создавать вещества мультитаргетного физиологического действия.

Так синтезирована серия миметиков α-токоферола, в частности производных бутилгидрокситолуола (BHT, E321), содержащих в молекулах редокс-активный фрагмент ферроцена (например, *N*-(3,5-ди-*трет*-бутил-4-гидроксифенил)-иминометилферроцен и др.) [1], для которых обнаружена высокая антиоксидантная активность, а также способность ингибировать Са-зависимое набухание митохондрий, что позволяет предположить наличие мито- и нейропротекторной активности данных субстанций.

Осуществлено сочетание в молекулах противоположных по функциональным характеристикам фрагментов, например макроциклов-биомиметиков гемов (порфирины) и 2,6-диалкилфенолов, являющихся антиоксидантами процессов окисления, что приводит к проявлению данными системами свойств полифункциональных редокс-систем [2]. Возможность комплексов меди выступать в качестве обратимых ингибиторов важной мишени – негемового фермента липоксигеназы (арахидонат : кислород 5-оксидоредуктаза), осуществляющей превращение арахидоновой кислоты по липоксигеназному пути в медиаторы воспаления – лейкотриены, продемонстрирована на примере введения в лигандное окружение нитронилнитроксильных радикалов, что подтверждено также данными молекулярного докинга [3].

Еще одним примером синтеза новых ингибиторов липоксигеназы является получение 5-гидроксиаминоизоксазолов, способных подобно известному специфическому ингибитору – препарату Эбселен (2-фенил-1,2-бензоселеназол-3(2*H*)-он) подавлять активность фермента, и обладающих также выраженной антиоксидантной активностью [4]. Производные изоксазола промотируют фосфорилирование в дыхательной цепи митохондрий и при этом не проявляют токсичности по отношению к первичной культуре нейронов коры головного мозга крыс.

В настоящей главе будут представлены избранные публикации академика Н.С. Зефирова с сотрудниками, связанные с указанным направлением в области поиска и создания лекарственных веществ для коррекции редокс-статуса организма.

**Список статей раздела**

1. Milaeva E.R, Filimonova S.I., Meleshonkova N.N., Milaeva E.R., Filimonova S.I., Meleshonkova N.N., Dubova L.G., Shevtsova E.F., Bachurin S.O., Zefirov N.S. Antioxidative activity of ferrocenes bearing 2,6-di-*tert*-butylphenol moieties // *Bioinorg. Chem. App.* V. 2010. ID 165482, 6 P. doi:10.1155/2010/165482

2. Milaeva E.R., Gerasimova O.A., Zhang Jingwei, Shpakovsky D.B., Syrbu S.A.,
Semeykin A.S., Koifman O.I., Kireeva E.G., Shevtsova E.F., Bachurin S.O., Zefirov N.S. Synthesis and antioxidative activity of metalloporphyrins bearing 2.6-di-tert-butylphenol pendants // *J. Inorg. Biochem*. 2008. V. 102. № 5-6. P. 1348-1358.

3. Милаева Е.Р., Орлова С.И., Осолодкин Д.И., Палюлин В., Фурсова Е.Ю., Овчаренко В.И., Зефиров Н.С. Комплексы меди с нитронилнитроксильными радикалами как ингибиторы липоксигеназы с антиоксидантной активностью // *Изв. АН Сер. хим.* 2011. № 12. С. 2514-2521.

4. Averina E.B., Vasilenko D.A., Gracheva Y.A., Grishin Yu.K., Radchenko Eu.V., Burmistrov V.V., Butov G.M., Neganova
M.E., Serkova T.P., Redkozubova O.M., Shevtsova E.F., Milaeva E.R., Kuznetsova T.S., Zefirov N.S. Synthesis and biological evaluation of novel 5-hydroxylaminoisoxazole derivatives as lipoxygenase inhibitors and metabolism enhancing agents // *Bioorg. Med. Chem.* 2016. V. 24. № 4. P. 712-720.

*BIOINORGANIC CHEMISTRY AND APPLICATIONS, Vol. 2010, Article ID 165482, 2010*

*Research Article*

# ANTIOXIDATIVE ACTIVITY OF FERROCENES BEARING 2,6-DI-*TERT*-BUTYLPHENOL MOIETIES

**E.R. Milaeva, S.I. Filimonova, N.N. Meleshonkova, L.G. Dubova, E.F. Shevtsova, S.O. Bachurin, and N.S. Zefirov**

*Organic Chemistry Department, M.V. Lomonosov Moscow State University, Moscow, Russia*

*Institute of Physiologically Active Compounds, Russian Academy of Sciences, Chernogolovka, Russia*

Received 28 December 2009; Accepted 30 March 2010

The antioxidative activity of ferrocenes bearing either 2,6-di-*tert*-butylphenol or phenyl groups has been compared using DPPH (1,1-diphenyl-2-picrylhydrazyl) test and in the study of the in vitro impact on lipid peroxidation in rat brain homogenate and on some characteristics of rat liver mitochondria. The results of DPPH test at 20°C show that the activity depends strongly upon the presence of phenolic group but is improved by the influence of ferrocenyl fragment The activity of N-(3,5-di-*tert*-butyl-4-hydroxyphenyl)iminomethylferrocene (**1**), for instance, was 88.4%, which was higher than the activity of a known antioxidant 2,6-di-*tert*-butyl-4-methylphenol (BHT) (48.5%), whereas the activity of N-phenyl-iminomethylferrocene **2** was almost negligible –2.9%. The data obtained demonstrate that the compounds with 2,6-di-*tert*-butylphenol moiety are significantly more active than the corresponding phenyl analogues in the in vitro study of lipid peroxidation in rat brain homogenate. Ferrocene **1** performs a promising behavior as an antioxidant and inhibits the calcium-dependent swelling of mitochondria. These results allow us to propose the potential cytoprotective (neuroprotective) effect of ditopic compounds containing antioxidant 2,6-di-*tert*-butylphenol group and redox active ferrocene fragment.

## 1. Introduction

Oxidative stress has been found to play a critical role in numerous disease conditions including neurodegeneration [1-3].

The antioxidative defense system in living organism regulates a disturbance in the prooxidant-antioxidant balance and protects the cell damage induced by high level of oxidative stress. Among the classes of well-known natural antioxidants – vitamins E group, ascorbic acid, glutathione, and so forth, α-tocopherol and its synthetic analogues, sterically hindered phenols, are of particular importance [4]. The substituted

2,6-dialkylphenols are widely used as inhibitors of free radicals formation in the oxidative destruction of natural and synthetic substrates. The mechanism of their physiological action is associated with the stable phenoxyl radicals' formation in the process of hydrogen atom abstraction by highly reactive peroxyl radicals of lipids [5].

The goal of this study was to optimize the effect of 2,6-di-*tert*-butylphenol and to increase the stability of the corresponding phenoxyl radicals responsible for their antioxidative activity. The approach based on modification of phenolic antioxidants *via* incorporation of ferrocenyl moiety in their molecules seems to be a promising one. Previously we have reported the synthesis, electrochemical characteristics, and ESR study of novel ferrocenes with redox active 2,6-di-*tert*-butylphenol fragments (compounds **1**, **3**) [6]. These compounds exhibit the properties of multistep redox systems, and the intramolecular electron transfer between two redox active sites of the molecule (the phenol and ferrocene groups) was observed. The high stability of phenoxyl radical species formed in the oxidation is in agreement with a certain degree of electronic delocalization over the molecule.

On the other hand, the ferrocene derivatives show a wide spectrum of physiological activity [7-9].

The incorporation of ferrocene into an anticancer drug tamoxifen, a selective estrogen receptor modulator, containing phenol was reported. The activity of these novel ferrocene derivatives (ferrocifens) was found to be associated with the proton-coupled electron transfer between ferrocenium ion and phenol group that occurs in their oxidized species [10-12].

The antioxidative activity in scavenging of superoxide radical-anion $O_2^{\bullet -}$ and $HO^{\bullet}$ radical was observed for recently synthesized ferrocenes containing nitroxides radicals as substituents [13].

As it has been reported earlier, diselenides having redoxactive ferrocenyl units show peroxidase-like antioxidant activity mimicking selenoenzyme glutathione peroxidase that protects the cell membranes from oxidative damage [14].

In our previous study, we have observed the modulation of the antioxidative effect of metalloporphyrins bearing 2,6-di-*tert*-butylphenol pendants by the metal nature [15].

In this study we compared the antioxidative activity of **1**-**6** presenting the pairs of compounds bearing either 3,5-di-*tert*-butyl-4-hydroxyphenyl or phenyl substituents linked to the ferrocene by various spacers (Figure 1).

## 1. Materials and Methods

*2.1. Ferrocenes. N*-(3,5-di-*tert*-butyl-4-hydroxyphenyl)-iminomethylferrocene (**1**), *N*-phenyl-iminomethylferrocene (**2**), *N*-(3,5-di-*tert*-butyl-4-hydroxybenzyl)iminome-

thylferrocene (**3**), N-benzyliminomethylferrocene (**4**), (3,5-di-*tert*-butyl-4-hydroxy-phenyl)-3-ferrocenylpropen-2-on (**5**), and phenyl-3-ferrocenylpropen-2-on (**6**) were synthesized as described previously [6,16].

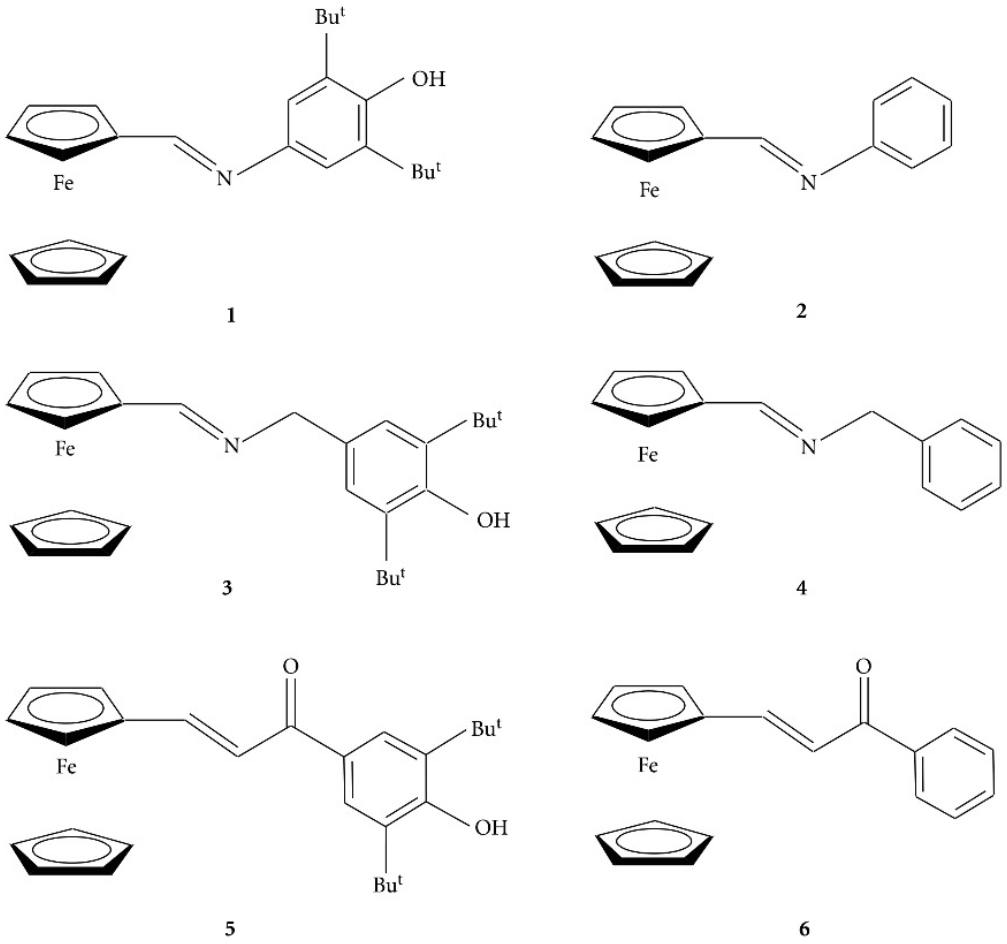


FIGURE 1: Structures of compounds **1**-**6**.

*2.2. DPPH Radical Scavenging Activity.* The free radicalscavenging activity was evaluated using the stable radical DPPH, according to the method described by Brand-Williams et al. [17] with a slight modification.

Each compound was tested for antioxidant activity against DPPH radical at a molar 1:1 ratio. One ml of antioxidant solution in methanol was added to 1 mL of DPPH solution in methanol so that the final DPPH and antioxidant concentration can be 0.1 mM. The samples were incubated for 30 minutes at 20°C in methanol and the decrease in the absorbance of DPPH solution was measured at 517 nm, using a Thermo Evolution 300 BB spectrophotometer. The results were expressed as scavenging activity, calculated as follows:

$$\text{Scavenging activity, \%} = \left[\frac{(A_0 - A_1)}{A_0}\right] \times 100. \qquad (1)$$

The concentration of antioxidant needed to decrease 50% of the initial substrate concentration ($EC_{50}$) is a parameter widely used to measure the antioxidant effect [18]. For determination of $EC_{50}$, the values of DPPH solution absorbance which decrease after 30 minutes were used. The $EC_{50}$ values were calculated graphically by plotting scavenging activity against compound concentration. Different sample concentrations (0.01, 0.02, 0.05, and 0.1 mM) were used in order to obtain kinetic curves and to calculate the $EC_{50}$ values. The lower $EC_{50}$ means the higher antioxidant activity.

*2.3. Rat Brain Homogenates (RBH) and Rat Liver Mitochondria (RIM) Preparation.* On the day of the experiment, adult Wistar male rats fasted overnight were euthanized in a $CO_2$-chamber followed by decapitation. The procedure was in compliance with the Guidelines for Animal Experiments at Institute of Physiologically Active Compounds of Russian Academy of Sciences.

The brains were rapidly removed and homogenized in 0.12 M HEPES/0.15M NaCl, pH 7.4 buffer (HBS) (10 mg/gr wet weight) and used immediately for assay.

Mitochondria were isolated from homogenates of livers of adult Wistar strain rats, fasted overnight, in a 5 mM HEPES buffer, pH 7.4, containing 210 mM mannitol, 70 mM sucrose, and 1 mM EDTA, by conventional differential centrifugation [19].

Protein concentrations in RBH and RLM were determined by the biuret assay using bovine serum albumin as a standard [20].

*2.4. $Fe^{3+}$-Induced Lipid Peroxidation Assay.* The extent of lipid peroxidation (LP) was estimated by the levels of malondialdehyde measured using the thiobarbituric acid reactive substances (TBARS) assay. Isolated mitochondria are metabolically active and tightly coupled as shown by respiratory control ratio values, which were about **4** with ghitamate-malate as substrate as measured by mitochondrial oxygen consumption at Oroboros oxygraph (Anton Paar, Austria) in a medium containing 10 mM $KH_2PO_4$ (or $NaH_2PO_4$), 60 mM KC1, 60 mM Tris, 5 mM $MgCl_2$, 110 mannitol, and 0.5 mM EDTA-$Na_2$, pH 7.4.

Study of compounds influence on LP of the RBH was carried out at 30°C for 40 minutes in 0.25 mL of the RBH in HBS (2 mg of protein $\cdot$ $mL^{-1}$) in the presence or absence of compounds or vehicle (DMSO). LP was induced by using $Fe^{3+}$ (0.5 mM $Fe(NH_4)(SO_4)_2$) as an oxidizing agent [21]. Then 0.25 mL aliquots were mixed with 0.5 mL thiobarbituric acid (TBA) medium containing 250 mM HC1, 15% trichloroacetic acid, and 3 mM TBA, heated at 95°C for 15 minutes, cooling at 4°C then probes centrifuged (10 minutes at 10 000 g) and the supernatants transferred into 96-plate and absorbance was measured at 530-620 nm at the Wallac Victor 1420 Multilabel Counter (PerkinElmer Wallac).

All the experiments were performed using four independent experiments with different brain homogenate preparations. Data are normalized to control probe with oxidant as 100% and blank probe with diluent but without oxidizing agent. Preliminary experiments were done in the absence of compounds interaction with thiobarbituric acid. The values are expressed as mean % ± SD. The concentrations of ferrocenes giving half-maximal inhibition ($IC_{50}$) of LP were determined by dose-effect analysis.

*2.5. Mitochondrial Swelling Assay.* Mitochondrial swelling caused by influx of solutes through open mitochondrial permeability transition (MPT) pores results in an increase in light transmission (i.e., a reduced turbidity). This turbidity change offers a convenient and frequently used assay of the MPT by measurement of absorbance in mitochondrial suspensions. The MPT induced by $Ca^{2+}$ was monitored by absorbance changes at 540 nm in a Beckman DU 640 spectrophotometer in 1 mL of buffer A plus 0.8 μM rotenone, 5 mM succinate, 1 mM $KH_2PO_4$, and 0.5 mg protein of isolated liver mitochondria at 30°C and continuous stirring [19]. Swelling rate is quantified as $\Delta A_{540}$/min/mg, calculated, in all cases, from a tangent to the steepest portion of the plot of $A_{540}$ versus time.

*2.6. Measurement of Mitochondrial Membrane Potential.* The same experimental conditions were used for the assessment of alterations of the mitochondrial membrane potential, except that safranine was included in incubation medium at a final concentration of 10 μM and succinate was added after the compound. This concentration of safranine was determined before hand as the optimal compromise between signal/baseline ratio and interference of safranine itself with swelling induced by Ca/Pi (safranine tended to enhance Ca/Pi-induced swelling at concentrations above 20 μM) [19]. Changes in the status of the MPT pore are assessed spectrophotometrically at 524 versus 554 nm in a Beckman DU 640 spectrophotometer at 30°C and continuous stirring.

## 2. Results and Discussion

We have compared the antioxidative activity of 1-6 presenting the pairs of compounds bearing either 3,5-di-*tert*- butyl-4-hydroxyphenyl or phenyl substituents linked to the ferrocene by various spacers (Figure 1).

The scavenging activity has been studied in the process of hydrogen atom transfer to the stable free radical DPPH [22]. The results of DPPH test at 20°C show that the activity depends strongly upon the presence of phenolic group in the presented pairs of compounds. The activity of **1**, for instance, was 88.4% that is higher than that of a known antioxidant 2,6-di-*tert*-butyl-4-methylphenol (BHT) (48.5%) whereas the activity of **2** bearing phenyl substituent was almost negligible –2.9% (Figure 2). The values of scavenging activity of compounds **3**, **5** were lower, and in the case of **3** the

decrease in activity was more pronounced. Evidently the activity extent of the compounds tested depends on their molecular structures. The HO-group of 2,6-di-*tert*-butylphenol is the key site in the molecule that is involved in hydrogen transfer to DPPH. However, despite the presence of ferrocene moiety in all the compounds they differ significantly containing linkers of various length and conjugation ability (–CH=N–, **1**; –CH=N–$CH_2$–, **2**; –CH=CH–C(O)–, **3**). The decrease of conjugation in their molecules containing either $CH_2$ or CO groups in linkers leads to the decrease of metal influence on the stability of radicals formed as it has been observed previously [6]. However, it should be mentioned that the activity of **3** is much higher than that of **5** with N atom possessing a lone electron pair in linker that improves the influence of ferrocene moiety.

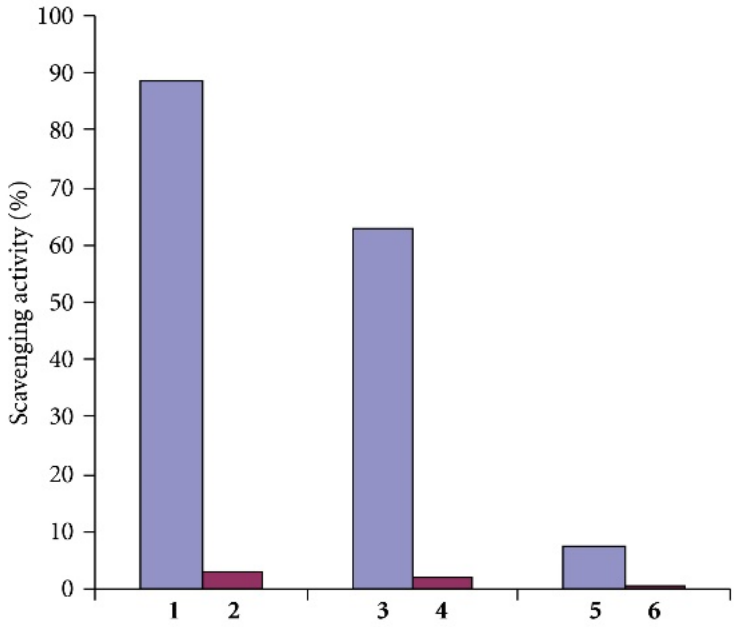


FIGURE 2: Scavenging activity for compounds 1-6 in DPPH test (MeOH, 20°C, 100 pM).

TABLE 1: The values of $IC_{50}$ in the antioxidative activity assay in rat brain homogenates for compounds **1**-**6**.

| Compound | $IC_{50}$ μM (0.5 mM $Fe(NH_4)(SO_4)_2$) |
|---|---|
| **1** | 3.7 ± 1.0 |
| **2** | 70.4 ± 11.1 |
| **3** | 47.3 ± 2.4 |
| **4** | 100 ± 15.0 |
| **5** | 3.9 ± 1.8 |
| **6** | 47.8 ± 1.6 |

To compare the activity of compounds under investigation with that of widely known antioxidant parameter, $EC_{50}$ was determined for the more efficient ferrocene **1**

and 2,6-di-*tert*-butyl-4-methylphenol (BHT). $EC_{50}$ values after 30 minutes of experiment at 20°C for **1** and BHT are 34.6 and 105.4 μM, respectively. Therefore, the result obtained shows a more pronounced effect of ferrocenyl derivative of 2,6-di-*tert*-butylphenol.

In order to study the antioxidant effect of ferrocenes **16** in biologically significant *in vitro* test system, we have investigated the compounds influence on $Fe^{3+}$-induced peroxidation of brain homogenate lipids (LP) as a nonenzymatic process by addition of $(NH_4)Fe(SO_4)_2$. The level of LP was followed by the accumulation of products that reacted with thiobarbituric acid – TBARS. The samples of Wistar strain rats homogenates were divided as following: one control homogenate and samples of homogenate with addition of compounds under investigation. TBARS concentrations were determined in homogenates by measuring the intensity of the solution color at 530 nm using UV-VIS spectroscopy [23].

The data of antioxidative activity assay of **1-6** presenting the pairs of compounds bearing either 3,5-di-*tert*-butyl-4- hydroxyphenyl or phenyl substituents linked to the ferrocene by various spacers are shown in Figure 3. The $IC_{50}$ values are summarized in Table 1.

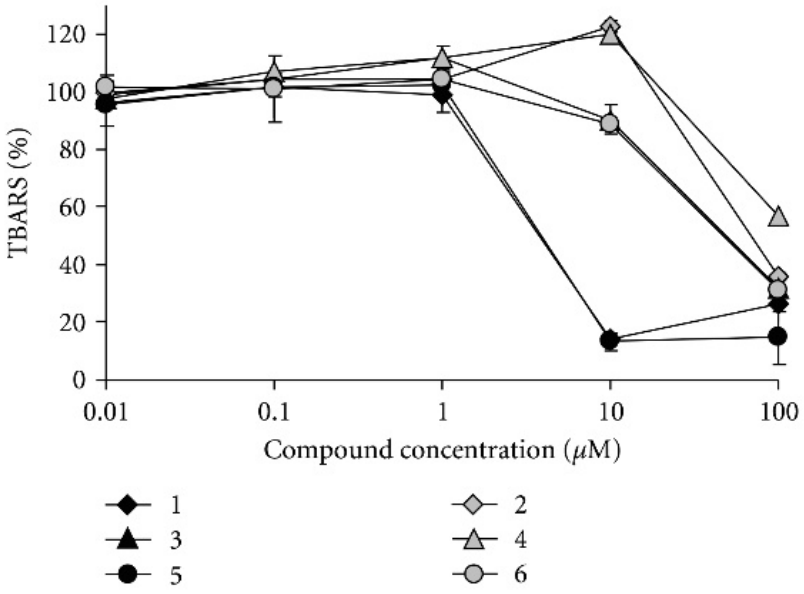


Figure 3: The relative content of TBARS in the lipid peroxidation of rat brain homogenates as nonenzymatic process in the presence of 10 μM **1-6** (0.5 mM $Fe(NH_4)(SO_4)_2$).

The data of antioxidative activity assay of ferrocenes **16** indicate the influence of 2,6-di-*tert*-butylphenol group as it was observed in DPPH test. Ferrocene **1** performs an effective inhibitory action in concentrations range at 10100 μM (Figure 3, curve 1). The decrease in peroxidation level is more that 10%.

In contrast to DPPH test, the data of this assay reveal the antioxidant activity of all studied compounds. These results allow us to suggest that the ferrocene moiety participates in antioxidative potential of these compounds. However, the compounds **1**, **3**, **5** bearing 2,6-di-*tert*-butyiphenol are significantly more active than the corresponding

phenyl analogues. This effect is most obvious at concentration 10 μM of compounds (Figure 3). Moreover, at this concentration some pro-oxidant effect of compounds **2** and **4** could be observed. This fact might be associated with the influence of iron center in the molecules of ferrocenes that participates in redox processes and therefore promotes the peroxidation.

The involvement of ferrocene group in the peroxidation process might be associated with the oxidation of $Fe^{2+}$ to $Fe^{3+}$ in the oxidative medium that leads to the formation of ferrocenium cation. As it was proved earlier [24] ferrocenium cations react easily with molecular oxygen and produce reactive peroxy radical cations. On the other hand, in the presence of antioxidant, namely BHT, ferrocenium cation can be stabilized due to the reduction that takes place between the cation and antioxidant. The principal consequence of this electron/proton coupled reaction is the reversibility of ferrocene/ferrocenium redox system. This fact might support the proposition of the intramolecular redox process in ferrocene species containing 2,6-di-*tert*-butylphenol fragment (compounds **1**, **3**, **5**).

To study proapoptotic/antiapoptotic effect of ferrocene **1** with 2,6-d-*tert*-butyiphenol group which shows the more promising activity in both tests and to compare it with the effect of its analog **2** bearing phenyl substituent, we have investigated the influence of these compounds on two main characteristics of mitochondria: calcium-induced mitochondrial swelling (SW) that represents the mitochondrial permeability pores opening (which causes cell death), and mitochondrial membrane potential.

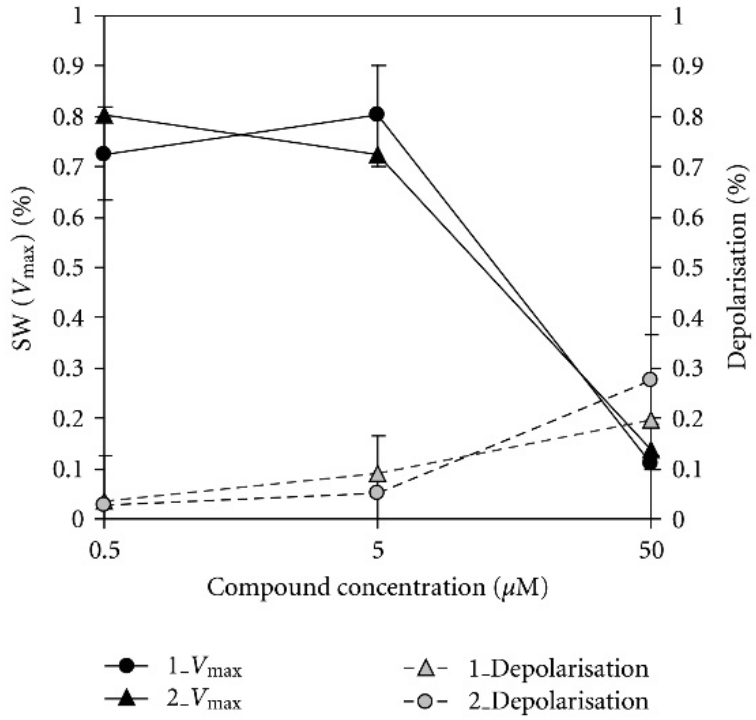


FIGURE 4: Influence of 0.1 μM ferrocenes **1** and **2** on mitochondrial swelling and transmembrane potential (the values were determined and expressed as % of control).

It was shown that at concentration 0.1 mM ferrocenes **1** and **2** slightly depolarize the mitochondria (up to 25%) (Figure 4). On the other hand, these compounds inhibit the calcium-dependent swelling of mitochondria and this effect could not be the consequence of the depolarisation only. In both cases the effects on mitochondrial swelling and mitochondrial membrane potential obtained for ferrocene **1** are less pronounced that for **2**. These data allow us to propose the potential cytoprotective (neuroprotective) effect of compounds studied.

### 3. Conclusion

The antioxidative activity of ferrocenes bearing either 2,6-di-*tert*-butylphenol or phenyl groups, studied using DPPH test, depends strongly upon the presence of phenol group and the conjugation between penoxyl radical formed and ferrocene unit. The compounds **1**, **3**, **5** bearing 2,6-di-*tert*-butylphenol are significantly more active than the corresponding phenyl analogues in the in vitro lipid peroxidation in rat brain homogenate. N-(3,5-di-*tert*-butyl-4-hydroxyphenyl)iminomethylferrocene (**1**) performs a promising behavior as an antioxidant and inhibits the calcium-dependent swelling of mitochondria. The results allow us to propose the potential cytoprotective (neuroprotective) effect of ditopic compounds containing antioxidant 2,6-di-*tert*-butylphenol group and redox active ferrocene fragment.

## Abbreviations

BHT: butylated hydroxytoluene (2,6-di-*tert*-butyl-4-methylphenol)
DPPH: 1,1-diphenyl-2-picrylhydrazyl (α,α-diphenyl-β-picrylhydrazyl)
HBS: HEPES buffered saline
LP: lipid peroxidation
MPT: mitochondrial permeability transition
RBH: rat brain homogenate
RLM: rat liver mitochondria
TBA: thiobarbituric acid
TBARS: thiobarbituric acid reactive substances.

## Acknowledgments

The financial support of RFBR (Grants 08-03-00844, 0903-00090, 09-03-12261, and 10-03-01137) and the program N9 “Biomolecular and Medicinal Chemistry” of Russian Academy of Sciences are gratefully acknowledged.

## References

1. L. Migliore and F. Coppedè, “Environmental-induced oxidative stress in neurodegenerative disorders and aging,” *Mutation Research,* vol. 674, no. 1-2, pp. 73-84, 2009.
2. H. Kozlowski, A Janicka-Klos, J. Brasun, E. Gaggelli, D. Valensin, and G. Valensin,

"Copper, iron, and zinc ions homeostasis and their role in neurodegenerative disorders (metal uptake, transport, distribution and regulation), "*Coordination Chemistry Reviews,* vol. 253, no. 21-22, pp. 2665-2685, 2009.

3. R. R. Crichton and R. J. Ward, *Metal-Based Neurodegeneration. From Molecular Mechanisms to Therapeutic Strategies*, John Wiley & Sons, Chichester, UK, 2006.
4. E. Denisov, *Handbook of Antioxidants,* CRC Press, Boca Raton, Fla, USA, 1995.
5. E. Niki, Y. Yoshida, Y. Saito, and N. Noguchi, "Lipid peroxidation: mechanisms, inhibition, and biological effects," *Biochemical and Biophysical Research Communications,* vol. 338, no. 1, pp. 668-676, 2005.
6. N. N. Meleshonkova, D. B. Shpakovsky, A V. Fionov, A V. Dolganov, T. V. Madesieva, and E. R. Milaeva, "Synthesis and redox properties of novel ferrocenes with redox active 2,6-di-*tert*-butylphenol fragments: the first example of 2,6- di-tert-butylphenoxyl radicals in ferrocene system," *Journal of Organometallic Chemistry,* vol. 692, no. 24, pp. 5339-5344, 2007.
7. G. Jaouen, Ed., *Bioorganometallics. Biomolecules, Labeling, Medicine*, Wiley-VCH, New York, NY, USA, 2006.
8. D. R. van Staveren and N. Metzler-Nolte, "Bioorganometallic chemistry of ferrocene," *Chemical Reviews,* vol. 104, no. 12, pp. 5931-5985, 2004.
9. "The bioorganometallic chemistry of ferrocene," in *Ferrocenes: Ligands, Materials and Biomolecules,* P. Stepnicka, Ed., pp. 499-639, John Wiley & Sons, New York, NY, USA, 2008.
10. E. Hillard, A. Vessières, L. Thouin, G. Jaouen, and C. Amatore, "Ferrocene-mediated proton-coupled electron transfer in a series of ferrocifen-type breast-cancer drug candidates," *Angewandte Chemie International Edition,* vol. 45, no. 2, pp. 285-290, 2005.
11. A. Vessières, S. Top, W. Beck, E. Hillard, and G. Jaouen, "Metal complex SERMs (selective oestrogen receptor modulators). The influence of different metal units on breast cancer cell antiproliferative effects," *Dalton Transactions,* no. 4, pp. 529-541, 2006.
12. A. Vessières, S. Top, P. Pigeon, et al., "Modification of the estrogenic properties of diphenols by the incorporation of ferrocene. Generation of antiproliferative effects in vitro," *Journal of Medicinal Chemistry,* vol. 48, no. 12, pp. 3937-3940, 2005.
13. X. Qiu, H. Zhao, and M. Lan, "Novel ferrocenyl nitroxides: synthesis, structures, electrochemistry and antioxidative activity," *Journal of Organometallic Chemistry,* vol 694, no. 24, pp. 3958-3964, 2009.
14. G. Mugesh, A. Panda, H. B. Singh, N. S. Punekar, and R. J. Butcher, "Diferrocenyl diselenides: excellent thiol peroxidase- like antioxidants," *Chemical Communications,* no. 20, pp. 2227-2228, 1998.
15. E. R. Milaeva, O. A. Gerasimova, Z. Jingwei, et al., "Synthesis and antioxidative activity of metalloporphyrins bearing 2,6-di-*tert*-butylphenol pendants," *Journal of Inorganic Bio chemistry,* vol. 102, no. 5-6, pp. 1348-1358, 2008.
16. V. Yu. Tyurin, A. P. Gluchova, N. N. Meleshonkova, and E. R. Milaeva, "Electrochemical method of antioxidative activity assay based on DPPH test," submitted to *Russian Chemical Bulletin.*
17. W. Brand-Williams, M. E. Cuvelier, and C. Berset, "Use of a free radical method to evaluate antioxidant activity," *Food Science and Technology,* vol. 28, no. 1, pp. 25-30, 1995.
18. P. Molyneux, "The use of the stable free radical diphenylpicrylhydrazyl (DPPH) for estimating antioxidant activity," *Songklanakarin Journal of Science and Technology,* vol 26, no. 2, pp. 211-219, 2004.
19. I. V. Serkov, E. E Shevtsova, L. G. Dubova, et al., "Interaction of docosahexaenoic acid derivatives with mitochondria," *Doklady Biological Sciences,* vol. 414, no. 1, pp. 187-189, 2007.

20. A. G. Gornall, C. J. Bardawill, and M. M. David, "Determination of serum proteins by means of the biuret reaction," *Journal of Biological Chemistry,* vol 177, pp. 751-766, 1949.
21. J. K. Callaway, P. M. Beart, and B. Jarrott, "A reliable procedure for comparison of antioxidants in rat brain homogenates," *Journal of Pharmacological and Toxicological Methods,* vol. 39, no. 3, pp. 155-162, 1998.
22. M. C. Foti, C. Daquino, I. D. Mackie, G. A. DiLabio, and K. U. Ingold, "Reaction of phenols with the 2,2-diphenyl-l-picrylhydrazyl radical. Kinetics and DFT calculations applied to determine ArO-H bond dissociation enthalpies and reaction mechanism," *Journal of Organic Chemistry,* vol 73, no. 23, pp. 9270-9282, 2008.
23. C. Paquot and A. Hantfenne, *Standard Methods for the Analysis of Oils, Fats and Derivatives,* Blockwell Scientific, Oxford, UK, 7th edition, 1987.
24. J. P. Hurvois and C. Moinet, "Reactivity of ferrocenium cations with molecular oxygen in polar organic solvents: decomposition, redox reactions and stabilization," *Journal of Organometallic Chemistry,* vol. 690, no. 7, pp. 1829-1839, 2005.

*JOURNAL OF INORGANIC BIOCHEMISTRY, Vol. 102, 1348-1358 (2008)*

# SYNTHESIS AND ANTIOXIDATIVE ACTIVITY OF METALLOPORPHYRINS BEARING 2,6-DI-*TERT*-BUTYLPHENOL PENDANTS

**E.R. Milaeva, O.A. Gerasimova, Zhang Jingwei, D.B. Shpakovsky, S.A. Syrbu, A.S. Semeykin, O.I. Koifman, E.G. Kireeva, E.F. Shevtsova, S.O. Bachurin, N.S. Zefirov**

*Organic Chemistry Department, Moscow State Lomonosov University, Moscow, Russian Federation*
*Ivanovo State Academy of Chemical Technology, Ivanovo, Russian Federation*
*Institute of Physiologically Active Compounds of Russian Academy of Sciences, Chernogolovka, Russian Federation*

*Received 28 September 2007*

The novel metalloporphyrins (M = HH, Fe, Mn, Co, Cu, Zn) bearing 2,6-di-*tert*-butylphenol pendants as antioxidant substituents, and a long chain hydrocarbon palmitoyl group have been synthesized. The oxidation of compounds by $PbO_2$ leads to the formation of the corresponding 2,6-di-*tert*-butylphenoxyl radicals studied by EPR. The activity of porphyrins in lipid peroxidation has been examined using (1) *in vitro* lipid peroxidation induced by *tert*-butylhydroperoxide in respiring rat liver mitochondria, (2) *in vitro* lipid peroxidation in liver homogenates of Wistar strain rats, and (3) a model process of peroxidation of (Z)-octadec-9-enic (oleic) acid as a structural fragment of lipids. The activity of these compounds depends dramatically

on the nature of metal and might be changed from antioxidative (M = HH, Mn, Cu, Zn) to indifferent (M = Co), and to pro-oxidative one (M = Fe). The anti- or pro-oxidative action of these compounds may be derived from the concurrence between the involvement of 2,6-di-*tert*-butylphenol pendants acting as radical scavengers and redox active metal center promoting oxidation processes. The results of this study suggest that the polytopic compounds combining in one molecule 2,6-di-*tert*-butylphenol pendants, metalloporphyrin moiety, and a palmitoyl group, are membrane active compounds and might be studied in an effort to find novel pharmaceutical agents.

## 4. Introduction

The formation of reactive oxygen species (ROS) in various enzymatic and non-enzymatic processes in living organisms is associated with the oxidative damage of DNA, proteins, lipids, and mitochondrial dysfunction [1]. The oxidative stress is one of the causes of various pathologies including neurodegenerative diseases [2]. Recent results suggest that the mitochondria-mediated neurodegenerative diseases, for which toxic ROS are implicated, might be treated with antioxidants and free radical scavenging agents [3,4].

Since α-tocopherol acts as an effective radical scavenger, stabilizes cell membranes, and prevents the oxidative stress, there is an increasing interest in the application of its synthetic analogues based on lipophilic 2,6-dialkylphenols [5].

On the other hand, it is well known that endogenous porphyrins play a significant role in a variety of physiological processes in living organisms such as electron and oxygen transport, and respiration [6]. A wide spectrum of synthetic porphyrins reactivity provides their applications as catalytic antioxidants mimicking superoxide dismutase (SOD) and catalase [7-9], pro-oxidants in iron-induced lipid peroxidation [10].

It has been shown recently that synthetic metallopor- phyrins such as palladium *meso*-tetra(4-carboxyphenyl)porphyrin, accumulate in the mitochondria of several cell lines [11], water soluble manganese porphyrins bearing pyridinium residues such as Mn(III) *meso*-tetra(2-*N*-ethylpyridinium)porphyrin accumulate in mitochondrial fractions in intact cultured cortical neurons [12]. To improve cellular permeability, current synthetic efforts include increasing the lipophilicity of substituted porphyrins, achieved by lengthening alkyl or methoxyethyl side chains [13-15].

The metalloporphyrins capability of acting as biomimetics of SOD and antioxidants has been used to inhibit lipid peroxidation and to scavenge the highly reactive ROS [1618]. The comparative study of the role of metal site in metalloporphyrins neuroprotection has been performed using redox active Mn and redox innocent Zn derivatives [19].

Earlier we have studied the antioxidant activity of metalloporphyrins bearing four 2,6-di-*tert*-butylphenol fragments [20,21]. The pro- or antioxidant activity of these porphyrins depends upon the nature of metal. Free base tetra(3,5-di-*tert*-butyl-4-hydroxyphenyl)porphyrin performs the highest antioxidant activity in model reaction of peroxidation of (*Z*)-octadec-9-enic (oleic) acid.

The aims of this study were (1) to synthesize the polytopic compounds **1a-f**, **2a-f** combining in one molecule 2,6-di-*tert*-butylphenol pendants as antioxidant substituents, metalloporphyrin moiety, and a long chain hydrocarbon palmitoyl group as a lipophilic fragment compatible with membranes lipid bilayer, and (2) to study their *in vitro* activity in lipid peroxidation.

## 5. Experimental

### *5.1. General*

All reagents of high purity grade were purchased from Sigma, Fluka, Merck and used as supplied without further purification. All solvents were dried using molecular sieves. All buffers were prepared using doubly distilled, deionized water.

The electron absorption spectra were recorded on a Varian Cari-219 spectrophotometer. The Fourier transform IR absorption spectra were recorded on a IR200 Thermo Nicolet spectrophotometer in KBr pellets. The NMR spectra were registered on a Bruker AMX-400 spectrometer in $CDCl_3$ ($^1H$, 400 MHz; $^{13}C$, 100 MHz).

The MALDI TOF mass spectra were acquired using a Autoflex II (Bruker daltonics) mass spectrometer. The samples were dissolved in $CHCl_3$ with 2,5-dihydroxybenzoic acid (DHB) as matrix and put at target.

Thin-layer chromatography was performed on the Silufol UV-254 plates. Column chromatography was performed with the use of aluminum oxide (neutral, Brockmann). Elemental analysis was recorded with a Perkin Elmer elemental analyzer.

X-band EPR spectra were recorded on Bruker ELEXSYS E-500-10/12 EPR spectrometer (9.853 GHz, $\lambda$ 3 cm) running WinEPR software.

Thiobarbituric acid reactive substances (TBARS) in mitochondria suspension were measured at the Wallac Victor 1420 Multilabel Counter (Perkin Elmer Wallac).

### *5.2. Antioxidative activity assay*

#### *Peroxidation of (Z)-octadec-9-enic (oleic) acid in the presence of porphyrins* **1a-f** *and* **2a-f**

(*Z*)-Octadec-9-enic (oleic) acid was chosen as a model substrate LH for lipid peroxidation. The monitoring of oleic acid peroxidation level was performed by the determination of the total concentration of the corresponding isomeric hydroperoxides LOOH and TBARS.

The hydroperoxides content was determined by an iodometric method [24] based on the titration of iodine released from potassium iodide by the peroxides in a biphasic system with a thiosulfate solution. The oxidation of oleic acid (4.45 mg, 5 ml) was carried out in a thermostatic cell using airflow with the constant rate of **2** 4 ml $min^{-1}$ at 37°C. Since oleic acid oxidation proceeds as an autooxidation, the air has been passed through for 2 h before the addition of the compounds under investigation. The concentrations of the additives **1a**-**f** and **2a**-**f** were 1 mM compared with the initial concentration of hydroperoxides LOOH in the reaction mixture or 0.125, 0.25, 0.5, 1 mM for **1c**, **2c**. The monitoring of the total concentration of TBARS as markers of carbonyl compounds (malondialdehyde and other products) formed after LOOH decomposition, has been performed by the procedure with the thiobarbituric acid (TBA) reagent [25,26]. The intensity of the solution color in *tris*-buffer was measured at $\lambda_{max}$ 530 nm using UV-vis spectrophotometry.

The porphyrins **1a**-**f** and **2a**-**f** were purified by thin-layer chromatography on Silufol with methanol as eluent before use in antioxidative activity assay.

### *The in vitro effect of porphyrins* 1a-f *and* **2a-f** *on lipid peroxidation level in rat liver homogenates*

The level of lipid peroxidation was measured in rat liver homogenates as non-enzymatic process by the addition of ascorbic acid and $(NH_4)_2Fe(SO_4)_2$. Twelve liver samples of Wistar strain rats were divided in three experimental groups of four samples each and homogenized. The samples were divided as following: one control homogenate and three samples of homogenate with the addition of porphyrins under investigation. The concentration of porphyrins in the medium was 1 mM; TBARS concentrations were determined in tissue homogenates by measuring the intensity of the solution color at $\lambda_{max}$ 530 nm using UV-vis spectrophotometry [26].

### *Evaluation of porphyrins* **1a-f** *and* **2a-f** *influence on mitochondrial membranes oxidative damage induced by* $^{t}$*BHP*

Mitochondria were isolated by conventional differential centrifugation from the livers of adult Wistar strain rats fasted overnight [27] in a 5 mM Hepes buffer, pH 7.4, containing 210 mM mannitol, 70 mM sucrose, and 1 mM EDTA. Since mannitol binds hydroxyl ions, it was omitted during the final centrifugation and resuspension of mitochondria.

Protein concentrations were determined by the microbiuret assay using bovine serum albumin as a standard [28].

The experiments were carried out at 30°C for 40 min in 0.25 ml of the reaction medium containing 125 mM sucrose, 65 mM KCl, 10 mM Hepes buffer, pH 7.4, 5.0 1M rotenone, 5 mM succinate and mitochondria (2 mg of protein · $ml^{-1}$) in the presence

or the absence of porphyrins or vehicle (DMSO). The final concentrations of porphyrins in the reaction medium varied in the range 0.01-100 l M. The final concentration of DMSO in the suspension was 0.2% v/v that did not show appreciable interference to the reaction as evidenced by control experiments. Mitochondrial membranes oxidative damage (lipid peroxidation) was induced by using 0.4 mM *tert*-butylhydroxyperoxide ($^t$BHP) as an oxidizing agent.

Lipid peroxidation in mitochondrial suspension was followed by the accumulation of TBARS, and monitored spectrophotometrically according to the procedure described previously and modified for the plate reader measurements [29]. After the incubation the mitochondrial suspension was mixed with 0.5 ml TBA medium containing 250 mM HCl, 15% trichloroacetic acid and 3 mM TBA. The color was allowed to develop in the dark for 12 h, then probes were centrifuged (10 min at 10,000 g) and the supernatants were transferred to 96-plate. The absorbance was measured at $\lambda_{max}$ 530 nm at the Wallac Victor 1420 Multilabel Counter (Perkin Elmer Wallac). The amount of TBARS formed was calculated using a molar extinction coefficient $1.49\times10^5$ $M^{-1}$ $cm^{-1}$. All the experiments were performed using four independent experiments with different mitochondrial preparations. The values are expressed as means ± SEM.

## 6. Results

### *6.1. Synthesis*

Acylation of free base porphyrin **1a** at non-hindered phenolic group with palmitoyl chloride leads to free base porphyrin **2a** with a long chain hydrocarbon moiety [23] (Fig. 1). The metal complexes **1b-f** and **2b-f** were prepared by standard method [30] by treatment of the free base porphyrins with the corresponding metal salts in refluxing DMF.

Compounds **1b-f** and **2b-f** are crystalline substances stable in the air and in solutions. The compounds were characterized by IR, UV-vis, $^1$H and $^{13}$C NMR spectroscopy (**1e, 1f, 2e, 2f**), MALDI TOF mass spectrometry, as well as by analytical data.

The sharp absorption bands are observed in IR spectra in the 3630-3640 cm $^1$ region corresponding to the stretching vibrations of the O–H bond of the sterically hindered unassociated phenol group and in the 3300-3400 $cm^{-1}$ region (associated OH group of phenol in the case of **1b-f**). The absorption bands characteristic of the metalloporphyrins are observed in UV-vis spectra (Table 1). The spectra consist of an intense Soret band in the ~400 nm region and two Q-bands of lower intensity in the ~500–600 nm region respectively, which confirms the formation of the porphyrin ring. Introduction of a long chain hydrocarbon substituent into the porphyrin molecule results in the slight shift of the absorption bands toward the shortwave region. $^1$H and $^{13}$C NMR spectroscopic data available for Cu and Zn complexes confirm the structures of the

compounds obtained. The MALDI TOF mass spectra show the intense peaks of metalloporphyrins molecular ions, which confirm the porphyrins structures as well.

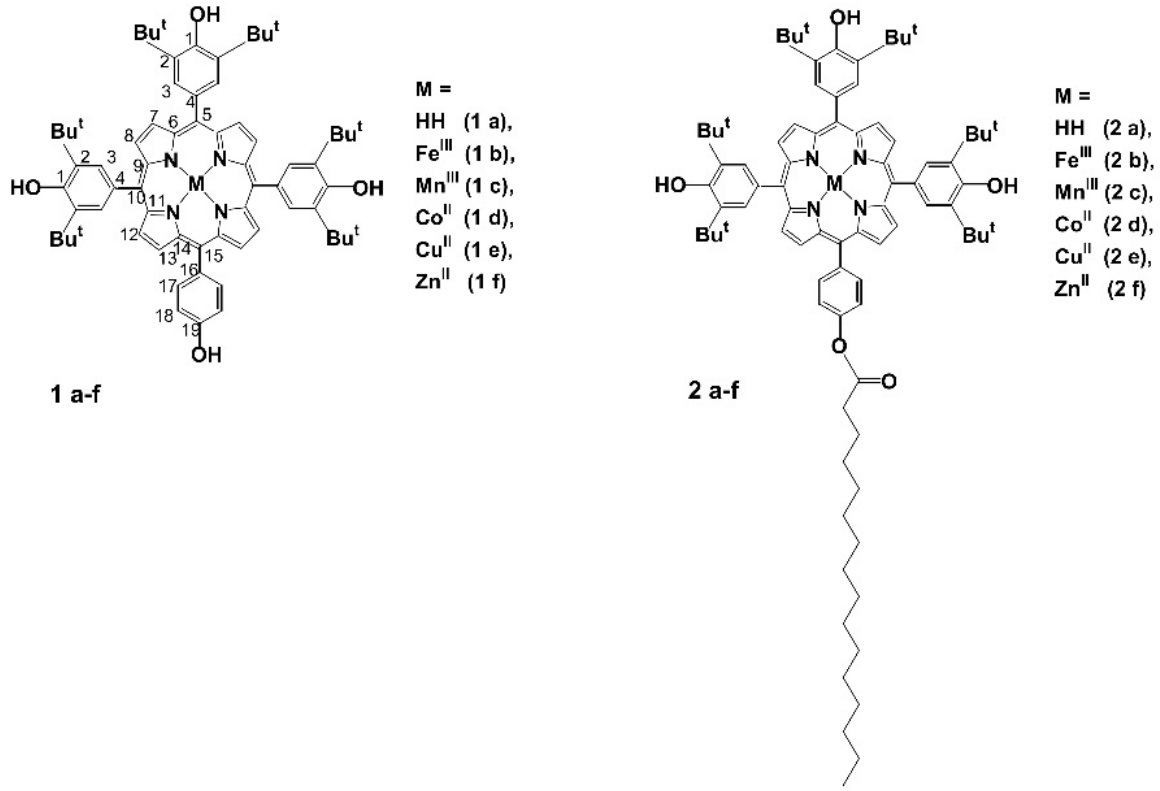


Fig. 1. Structures of porphyrins **1a-f** and **2a-f** bearing 2,6-di-*tert*-butylphenol pendants.

Table 1. UV-vis spectral data for porphyrins **1a-f**, **2a-f**, $\lambda_{max}$, nm (lg$\varepsilon$), ($CHC1_3$)

| Porphyrin (M) | Soret | Q-bands |
|---|---|---|
| **1a** (HH) | 425 (5.63) | 522 (4.15); 560 (4.09); 595 (3.75); 652 (3.86) |
| **1b** (Fe) | 423 (4.98) | 515.5 (4.96); 579 (3.20) |
| **1c** (Mn) | 386 (5.64); 407 (5.65) | 483 (5.82); 628 (5.19) |
| **1d** (Co) | 436.5 (5.89) | 477 (5.38); 544 (5.16) |
| **1e** (Cu) | 422.5 (5.75) | 541.5 (5.25); 582.5 (4.47) |
| **1f** (Zn) | 423.5 (4.67); 480 (4.82) sh | 619 (4.13); 679 (4.21) |
| **2a** (HH) | 424 (5.64) | 521 (4.22); 558 (4.11); 593 (3.87); 650 (3.93) |
| **2b** (Fe) | 420.9 (5.03) | 512.9 (4.28), 551 (4.02) |
| **2c** (Mn) | 387 (4.91); 408 (4.92) | 482 (5.12); 628 (4.44) |
| **2d** (Co) | 436.5 (4.61) | 477.5 (3.99) 549 (3.79) |
| **2e** (Cu) | 421 (5.19) | 541 (3.79); 582 (2.32) |
| **2f** (Zn) | 427 (4.62); 474 (3.88) sh | 620 (3.78); 671 (3.85) |

### *6.2. Oxidation of porphyrins 1a-f and 2a-f to the corresponding radicals 1a'-f and 2a'-f*

Porphyrins **1a-f** and **2a-f** were oxidized in anhydrous toluene by the tenfold excess of $PbO_2$ at 293 K using diphenylpicrylhydrazyl as a standard in the determination of *g*-factor. The experimental X-band EPR spectra of radicals **1a'-f'** and **2a'-f'** show triplets

typical for organic phenoxyl radicals [31,32] characterizing interaction of a spin of the unpaired electron with two equivalent *meta*-protons in phe- noxyl residue (Fig. 2). No interaction of the unpaired electron with metal nuclei is observed in the spectra of metal complexes. Radicals **1a˙-f˙** and **2a˙-f˙** are stable in solution in the absence of oxygen at the room temperature for a few days. The values of isotropic *g*-factor and the superfine coupling constant values on the $a_{2H}$ ($^1$H) nuclei are presented in Table 2.

Table 2. Parameters of X-band EPR spectra for radicals **1a˙-f˙**, **2a˙-f˙** (toluene, 295 K)

| Radical (M) | *g*-values | a2H (1H) (mTl) |
|---|---|---|
| **1a˙˙** (HH) | 2.0041 | 0.18 |
| **1b˙˙** (Fe) | 2.0041 | 0.17 |
| **1c˙˙** (Mn) | 2.0040 | 0.17 |
| **1d˙˙** (Co) | 2.0040 | 0.17 |
| **1e˙˙** (Cu) | 2.0041 | 0.15 |
| **1f˙˙** (Zn) | 2.0041 | 0.17 |
| **2a˙˙** (HH) | 2.0040 | 0.18 |
| **2b˙˙** (Fe) | 2.0040 | 0.17 |
| **2c˙˙** (Mn) | 2.0040 | 0.17 |
| **2d˙˙** (Co) | 2.0039 | 0.18 |
| **2e˙˙** (Cu) | 2.0040 | 0.16 |
| **2f˙˙** (Zn) | 2.0041 | 0.17 |

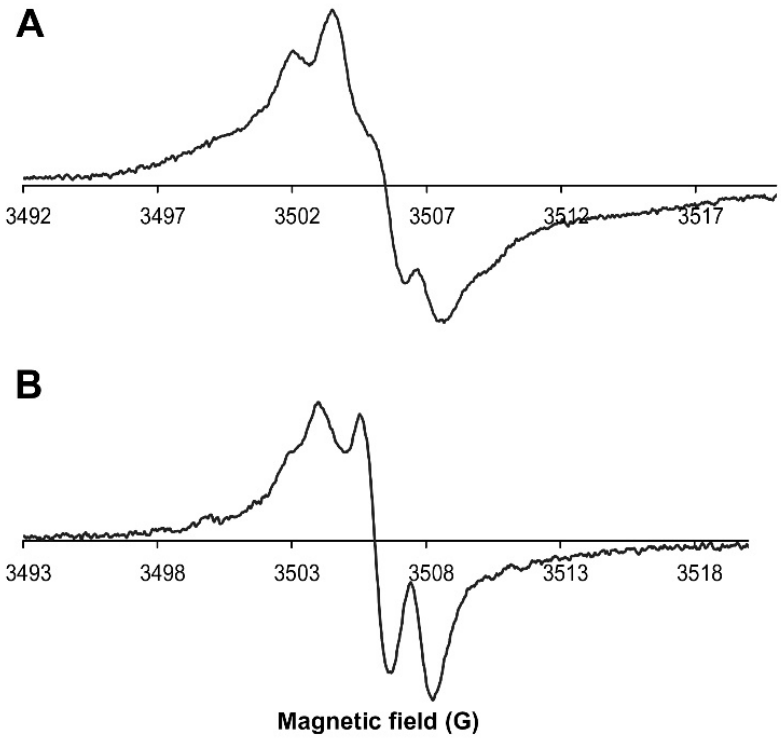


Fig. 2. EPR spectra of radicals **1e˙** (A) and **2e˙** (B) (toluene, 295 K).

### *6.3. Antioxidative activity assay*

The comparative study of activity of a series of porphyrins **1a-f** and **2a-f** in lipid peroxidation has been carried out using mitochondria isolated from the livers of adult Wistar strain rats, rat liver homogenates and (*Z*)-octadec-9-enic (oleic) acid as a structural fragment of lipid bilayer.

#### *6.3.1. Evaluation of porphyrins 1a-f and 2a-f influence on mitochondrial membranes oxidative damage induced by $^t$BHP*

The level of lipid peroxidation in mitochondrial suspension was followed by the accumulation of products that reacted with thiobarbituric acid-TBARS, and monitored spectrophotometrically at $\lambda_{max}$ 530 nm [29]. Mitochondrial membranes oxidative damage (lipid peroxidation) was induced by $^t$BHP. The concentrations of porphyrins in the reaction medium under investigation varied in the range 0.01-100 μM. The data of antioxidative activity assay of porphyrins **1a-f** and **2a-f** are shown in Fig. 3. The content of TBARS in the presence of 2.5 μM porphyrins **1a-f** and **2a-f** are summarized in Table 3.

Table 3. TBARS production in lipid peroxidation of rat liver mitochondria in the presence of porphyrins **1a-f** and **2a-f** (the data are presented for the concentration of porphyrins 2.5 μM).

| Porphyrin (M) | TBARS, nmol mg$^{-1}$ mitochondrial protein |
|---|---|
| **1a** (HH) | 1.264 ±0.064 |
| **1b** (Fe) | 2.914 ± 0.115 |
| **1c** (Mn) | 1.331 ± 0.073 |
| **1d** (Co) | 1.633 ± 0.089 |
| **1e** (Cu) | 1.328 ± 0.023 |
| **1f** (Zn) | 1.582 ± 0.076 |
| **2a** (HH) | 1.421 ± 0.036 |
| **2b** (Fe) | 1.798 ± 0.133 |
| **2c** (Mn) | 1.161 ± 0.110 |
| **2d** (Co) | 1.615 ± 0.065 |
| **2e** (Cu) | 1.466 ± 0.074 |
| **2f** (Zn) | 1.351 ± 0.084 |
| Control with 0.4 mM $^t$BHP | 1.716 ± 0.037 |
| Control without $^t$BHP | 0.468 ± 0.069 |

The results presented in Fig. 3(a, c-f) indicate that the free base porphyrins **1a, 2a** and Mn, Co, Cu, Zn porphyrins **1c-f, 2c-f** act as inhibitors of mitochondrial membranes lipid peroxidation, whereas Fe porphyrins **1b, 2b** (Fig. 3b) display a high pro-oxidant effect. 5-(4-Palmitoyloxyphenyl)-10,15,20-tris(3,5-di-*tert*-butyl-4-hydroxyphenyl)-porphyrins **2a-f** with a long chain hydrocarbon substituent have an analogous mode of action as their unsubstituted analogues **1a-f**. However their effect on membranes lipid peroxidation in intact mitochondria is more pronounced (Fig. 3).

The *in vitro* effect of porphyrins **1b, 2b** on lipid peroxidation level was measured in liver homogenates of Wistar strain rats as non-enzymatic process by the addition of ascorbic acid and $(NH_4)_2Fe(SO_4)_2$.

The accumulation of TBARS was determined in tissue homogenates by the known method using UV-vis spectrophotometry at $\lambda_{max}$ 530 nm [25, 26]. Both compounds perform pro-oxidative activity (Fig. 4).

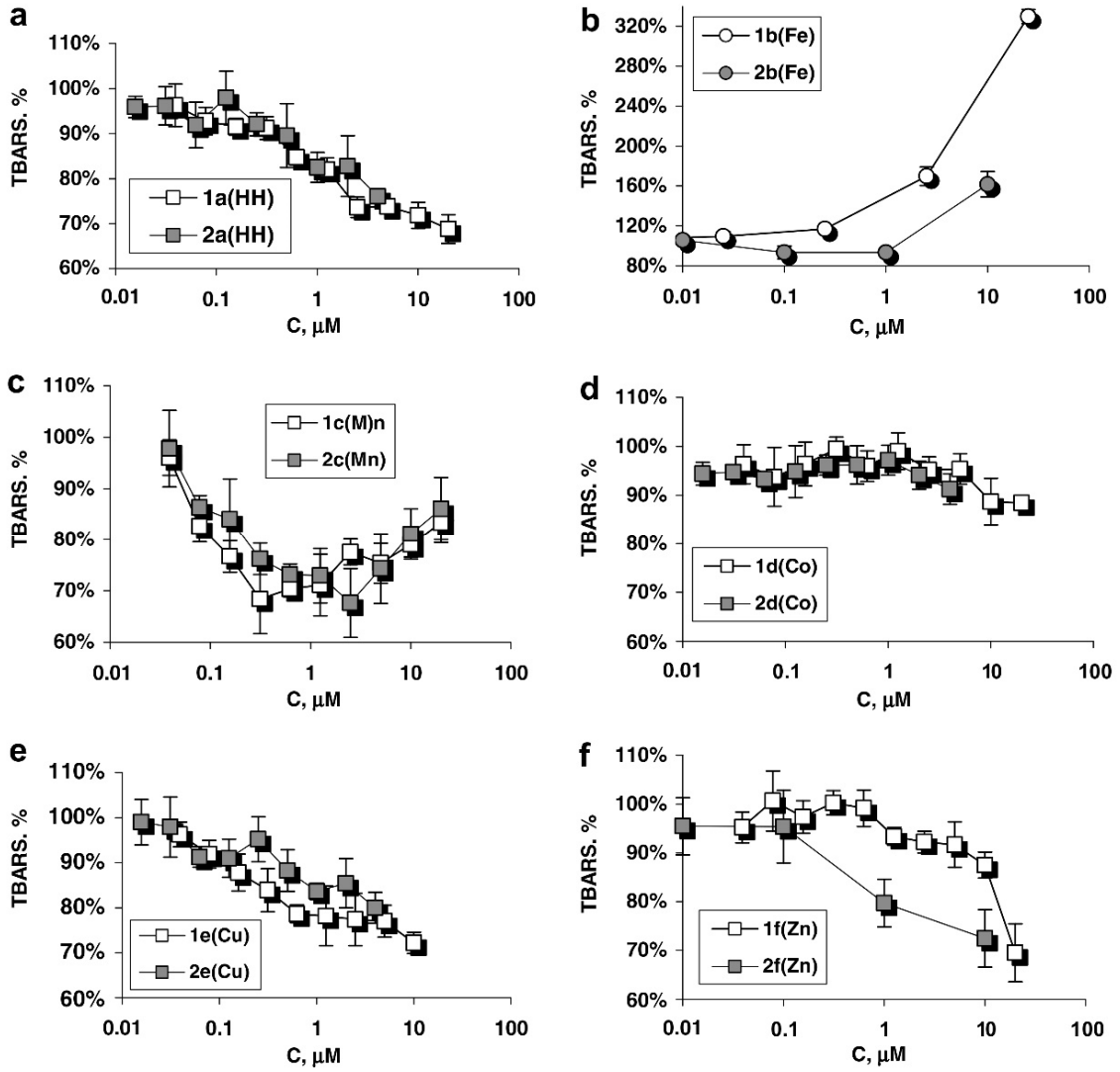


Fig. 3. Concentration-response curves for the inhibitory effects of metalloporphyrins **1a-f** and **2a-f** on lipid peroxidation in isolated rat liver mitochondria; (2 mg mitochondrial protein were incubated for 40 min with shaking at 30°C in a reaction medium as described in Section 2; then TBARS were determined and expressed as % of control, metal is given in parentheses).

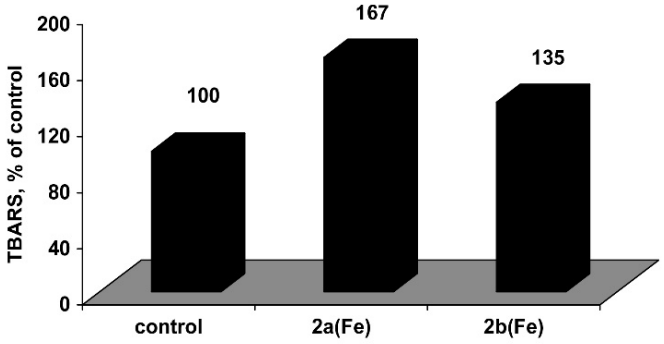


Fig. 4. The relative content of TBARS in the peroxidation of liver homogenates as non-enzymatic process in the presence of porphyrins **1b, 2b**; (the concentration of porphyrins were 1 μM in the reaction medium; the absolute control value for TBARS concentration was 62.1 ± 0.06 nmol g 1 wet wt., the absolute values in the presence of **2a** and **2b** were 103.7 ± 0.2 and 83.8 ± 0.2 nmol g 1 wet wt., respectively).

### *6.3.2. Peroxidation of (Z)-octadec-9-enic acid in the presence of porphyrins **1a-f** and **2a-f***

The influence of the free base porphyrins **1a** and **2a** and their metal complexes **1b-f** and **2b-f** upon the radical chain oxidation of (*Z*)-octadec-9-enic (oleic) acid as model substrate LH of lipid peroxidation has been studied.

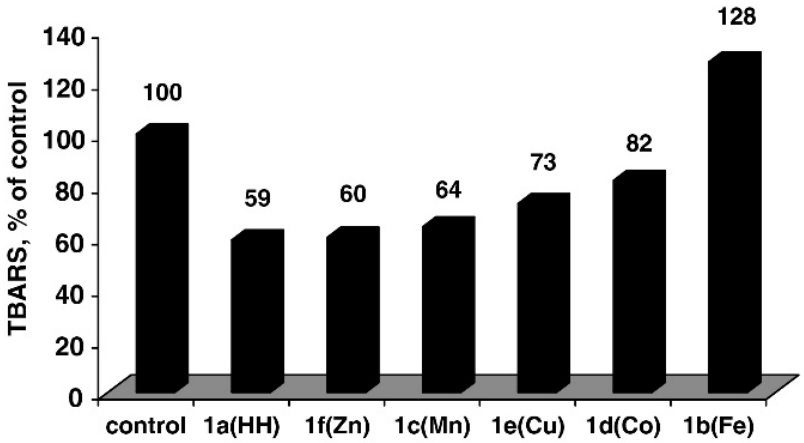


Fig. 5. The relative content of TBARS in the peroxidation of oleic acid in the presence of porphyrins **1a-f** (porphyrins were dissolved at 37°C in a reaction medium as described in Section 2; the concentration of porphyrins was 1 mM in the reaction medium; then TBARS were determined after 4 h; the absolute control value for TBARS concentration was 1.21 ±0.04 μM, the absolute values in the presence of **1a-f** were 0.71 ±0.04, 1.55 ±0.05, 0.77 ± 0.06, 0.99 ± 0.06, 0.88 ± 0.07 and 0.73 ± 0.03 μM, respectively).

The comparative study has been carried out using the monitoring of isomeric hydroperoxidis LOOH and TBARS. Hydroperoxides are primary products of oleic acid peroxidation and carbonyl compounds, which react with thiobarbituric acid, are formed

as products of LOOH decomposition [33]. The results show that free bases and Mn, Co, Cu, Zn porphyrins exhibit a pronounced inhibitory effect on the formation of TBARS at 37°C (Fig. 5). On the other hand, Fe porphyrins act as pro-oxidants in LH peroxidation.

The comparative TBARS analysis of the effect of two pairs of Fe and Mn porphyrins **1b, 2b, 1c, 2c** shows that the influence of a long chain palmitoyl substituent that is compatible with the substrate's structure increases the pro-oxidative effect of metalloporphyrins.

In the accumulation of primary formed hydroperoxides LOOH Mn porphyrins **1c, 2c** act as inhibitors. The content of LOOH decreased significantly in the presence of both compounds (Fig. 7). The attachment of palmitoyl group to the porphyrin core increased the antioxidative effect of Mn porphyrins.

## 7. Discussion

Among the well known antioxidants – vitamin E in the form of a-tocopherol and its synthetic analogues, sterically hindered phenols, are of particular importance. The substituted 2,6-dialkylphenols and especially 2,6-di-*tert*-butylphenols are widely used as inhibitors of free radical formation in the oxidative destruction of natural and synthetic substrates [5]. In this regard, the molecular design and synthesis of novel biomimetic antioxidants based on 2,6-di-*tert*-butylphenols seem to be of importance. In this study, we have focused our attention on the construction of a series of novel polytopic compounds combining in their molecules the organism friendly scaffold – porphyrin core, antioxidant pendant – 2,6-di-*tert*-butylphenol, and a lipophilic long chain hydrocarbon substituent compatible with membranes lipid bilayer.

The principal peculiarity of porphyrins synthesized in this study is the presence of 2,6-di-*tert*-butylphenol pendants in the periphery of porphyrin ring. Thus, an important aspect of these compounds behavior is their ability to manifest the activity of porphyrins **1a-f** and **2a-f** as radical chain reaction inhibitors. The phenol groups are capable of acting as antioxidants due to the transfer of hydrogen atom to the lipid peroxyl radicals [5].

The action of known metalloporphyrins either as anti- or pro-oxidants is explained by the properties of redox active metal ion.

The prooxidant activity of iron porphyrins in lipid peroxidation is attributed to the $Fe^{II}/Fe^{III}$, $Fe^{III}/Fe^{IV}$, and $Fe^{II}/Fe^{IV}$ redox chemistry [34]. The antioxidative activity of hydrophilic manganese porphyrins with various positively charged pyridyl and imidazolyl substituents has been interpreted as a function of $Mn^{II}/Mn^{III}$ redox transition [11-18]. Recently, a new series of lipophilic manganese porphyrins with aryl, benzoyl, alkyl, trifluoromethyl and nitro groups as substituents in *meso*-positions has been synthesized in an effort to design catalytic SOD mimics [35]. The significant SOD-like activity has been observed for lipophilic manganese *meso*-tetrabenzoylporphyrin.

A large series of highly efficient catalytic antioxidants mimicking SOD activity based on manganese porphyrins with *N*-alkylpyridyl-, carboxy- and sulfo-groups has been studied [36]. The reversibility of the redox transformations of Mn(II)/Mn(III) couple allows to use these compounds as multicyclic electron acceptors towards the $O_2$. Manganese(III) *meso*-tetrakis(*N*-methyl-2-pyridyl)porphyrin showed the antioxidative and protective effect against synergistic toxicity of iron and arachidonic acid, however, this compound itself does not peroxidize the arachidonic acid [37]. Metalloporphyrins are known to inhibit iron/ascorbate-induced lipid peroxidation [38]. The pro- and antiapoptotic potentials of *meso*-tetracarboxyporphyrins of Fe(III), Mn(III), Co(III), Zn(II) in rat cardiomyocytes exposed to anticancer drug that forms $O^{\bullet-}_2$ and $H_2O_2$ and promotes the oxidative stress have been investigated [19]. It has been observed that $O_2$ was effectively scavenged by Fe and Mn porphyrins but not by Co and Zn porphyrins. The authors proposed that mechanisms other than ROS scavenging may be involved in their antiapoptotic activity.

The attachment of 2,6-di-*tert*-butylphenol groups to the periphery of porphyrin ring opens up the possibility to tune the properties of the polyfunctional compounds described herein utilizing the reactivity of 2,6-di-*tert*-butylphenol in oxidation processes.

On the other hand, it is well known that phenolic antioxidants and natural polyphenols may have both anti- and pro-oxidant activity [39-43]. The advantage of phenols with bulky 2,6-di-*tert*-butyl substituents over other antioxidants like Trolox and polyphenols is the high stability of the corresponding phenoxyl radicals and the reversibility of the oxidation reactions [31,32]. The main pathways which are typical for 2,6-di-*tert*-butylphenols are hydrogen atom transfer and the reversible formation of phenoxyl radicals. The transfer of electron from 2,6-di-*tert*-butylphenol center to oxygen occurs in basic conditions at pH > 10 only [22,31]. Therefore, the potential formation of superoxide does not seem to be a major process in the reaction conditions of this study.

The antioxidant activity of 2,6-di-*tert*-butylphenols depends on the properties of the corresponding phenoxyl radicals. The substituents in *para*-position of 2,6-di-*tert*-butylphenols affect the stability and reactivity of the radicals formed [5]. In this connection, we carried out the oxidation of compounds **1a**-**f** and **2a**-**f** and studied the radicals formed by EPR method.

It has been shown earlier [20,22,31] that the free base tetra(3,5-di-*tert*-butyl-4-hydroxyphenyl)porphyrin and the corresponding metalloporphyrins form a biradical upon oxidation, which is converted during the fast step into a diamagnetic derivative of porphodimethenediquinomethide. The oxidation steps are reversible and porphodimethenediquinomethide and porphyrinogene derivatives can be reduced back to the starting porphyrin. The presence of three sterically hindered phenol groups in molecules of **1a**-**f** and **2a**-**f** suggests that the second step of oxidation is associated with the

monoradical formation **1a**$^{\bullet}$-**f**$^{\bullet}$ and **2a**$^{\bullet}$-**f**$^{\bullet}$. Indeed, we have observed the formation of monoradical species with the isotropic *g*-factors 2.0040-2.0041 that are characteristic of organic radicals. The experimental EPR spectra (Fig. 2) of phenoxyl radicals **1e**$^{\bullet}$ (A) and **2e**$^{\bullet}$ (B), given as examples, exhibit three lines. The values $a_{2H}$ ($^1$H) indicating the interaction of unpaired electron with *meta*-protons of phenoxyl ring are equal to 0.15-0.17 mTl, that are comparable with the $a_{2H}$ ($^1$H) of known phenoxyls with electron-donating *para*-substituents [43,44]. The stability of radicals **2a**$^{\bullet}$-**f**$^{\bullet}$ bearing palmitoyl group is higher due to the presence of hydrocarbon moiety that is not involved in the secondary step of oxidation. The nature of metal in the porphyrin macrocycle does not influence significantly either the parameters or the stability of radical species formed.

In an effort to extend further the area of possible application of the synthesized polytopic compounds as antioxidants, our attention was focused on the comparative study of the activity of porphyrins **1a-f** and **2a-f** in lipid peroxidation. The *in vitro* mitochondrial membranes oxidative damage (lipid peroxidation induced by $^t$BHP in respiring rat liver mitochondria) was compared with the *in vitro* lipid peroxidation of liver homogenates of Wistar strain rats as non-enzymatic process, and with the peroxidation of (*Z*)-octadec-9-enic (oleic) acid as a structural fragment of lipids.

Lipid peroxidation in the membranes of respiring mitochondria isolated from Wistar rat liver was induced by $^t$BHP – a pro-oxidant that can induce cell death via apoptosis or necrosis [45].

The data of antioxidative activity assay of porphyrins **1a-f** and **2a-f** indicate the dramatic influence of metal. Free base porphyrins **1a**, **2a** and Mn, Cu, Zn porphyrins **1c**, **1e**, **1f**, **2c**, **2e**, **2f** perform an inhibitory activity in concentrations near 10 μM (Fig. 3a,c,e,f). The decrease in peroxidation level is more than 30%. For Mn porphyrins **1c**, **2c** the concentration dependence shows a minimum at concentration value ~1 μM (Fig. 3c). Therefore, Mn porphyrins inhibit $^t$BHP-induced mitochondrial lipid peroxidation in the concentration near 1 μM with the decreasing of the antioxidant properties at higher concentrations.

The influence of Co porphyrins **1d**, **2d** is insignificant up to 20 μM, the curves are comparable with the control ones: the decrease of peroxidation level is 5-10%.

Fe porphyrins **1b**, **2b** (Fig. 3b) produce a high prooxidant effect on lipid peroxidation. These compounds significantly increase the $^t$BHP-induced mitochondrial lipid peroxidation at concentrations more than 1 μM without any antioxidative effects in concentration range of 0.0001-20 μM. The same effect was observed for *meso*-tetra-(4-*N*-methylpyridinium)porphyrin of iron, which promoted lipid peroxidation in mitochondrial suspension in the same concentration range of 5-20 μM [46].

5-(4-Palmitoyloxyphenyl)-10,15,20-tris(3,5-di-*tert*-butyl-4-hydroxyphenyl)porphyrins **2a**, **c-f** with a long chain hydrocarbon substituent perform the analogous behavior in mitochondrial membranes lipid peroxidation as their precursors **1a**, **c-f**. The

increase in activity was observed for Cu and Zn porphyrins **2e** and **2f**. Moreover, the prooxidative activity of Fe porphyrin **2b** decreases when compared with the activity of **1b**. Thus, the attachment of palmitoyl group slightly improves the antioxidant capacity of porphyrins studied herein.

The relative content of TBARS in the peroxidation of liver homogenates as non-enzymatic process in the presence of porphyrins **1b**, **2b** follows the same order. The prooxidative effect of **2b** is ~20% lower than that of **1b** (Fig. 4).

Redox-active metal ions (Fe, Co, Mn) can generate oxidative stress by production of ROS [2]. This results in peroxidation of polyunsaturated fatty acids and membrane damage. The metal incorporated into the porphyrin core influences the activity of porphyrins as either antioxidants or pro-oxidants. In oxidation reactions, dioxygen may be activated by the coordination to the metal center in porphyrins [47]. Previously we have shown that iron *meso*-tetra(3,5-di-*tert*-butyl-4-hydroxyphenyl)porphyrin is an effective catalyst in model oxidation of hydrocarbons, whereas manganese *meso*-tetra(3,5-di-*tert*-butyl-4-hydroxy- phenyl)porphyrin acts as inhibitor [48]. The mode of iron porphyrin action is associated with the formation of a highly reactive species $(P^{+\cdot})Fe^{IV}@O$, which we have observed by EPR [50]. The 2,6-di-*tert*-butylphenol group attached to the porphyrin macrocycle increases the stability of this intermediate by intramolecular mechanism, however, it deactivates the active species of manganese porphyrin [48]. We have proposed that the results of the present investigation might be explained by the same effect of porphyrins mode of action. The concurrence between the reactivity of 2,6-di-*tert*-butylphenol groups as antioxidants and metal center as pro-oxidant leads to the pronounced pro-oxidative effect of metal site in **1b** and **2b**. The effect of cobalt porphyrins **1d** and **2d** is almost insignificant. Free bases **1a** and **2a**, and Mn, Cu and Zn porphyrins **1c, 1e, 1f** and **2c, 2e, 2f** show the inhibitory effect.

The present investigation was undertaken also in an effort to explore whether the porphyrins **1a-f** and **2a-f** act as inhibitors or pro-oxidants in the model oxidation of unsaturated fatty acids, namely (*Z*)-octadec-9-enic (oleic) acid. The oxidation of oleic acid as substrate LH by molecular oxygen involves the generation of substituted allyl radicals, which interact with $O_2$ to produce peroxyl radicals $LOO^{\cdot}$. The corresponding *cis*- and trans-isomeric hydroperoxides (LOOH) are the main products of initial reaction period [33]. The rate of $LOO^{\cdot}$ transformation to hydroperoxides LOOH might be used as a criterion of the initial rate of the peroxidation [49]. The TBARS are markers of carbonyl compounds formation following the hydroperoxides decomposition. The monitoring of oleic acid peroxidation level has been performed by measuring the total concentration of isomeric hydroperoxides LOOH as well as TBARS.

The accumulation of TBARS in the presence of porphyrins **1a-f** studied by UV-vis spectrophotometry follows the same order as observed for lipid peroxidation in mitochondria (Fig. 5). The activity of compounds as antioxidants or pro-oxidants depends on the metal nature. This experimental fact might be attributed to the catalytic character

of iron porphyrins in the LOOH decomposition. On the other hand, the attachment of a long chain palmitoyl group improves the pro-oxidative effect of porphyrins (Fig. 6) that is in agreement with the high stability of radicals **2b**$^{\cdot}$ and **2c**$^{\cdot}$.

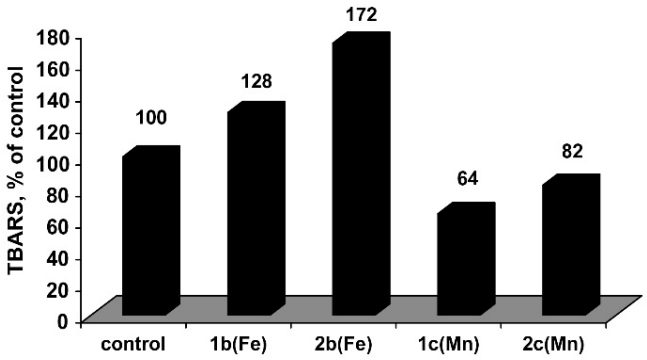


Fig. 6. The relative content of TBARS in the peroxidation of oleic acid in the presence of porphyrins **1b**, **2b**, **1c**, **2c**; (porphyrins were dissolved at 37°C in a reaction medium as described in Section 2; the concentration of porphyrins was 1 μM in the reaction medium; then TBARS were determined after 4 h; the absolute control value for TBARS concentration was 1.21 ± 0.04 μM, the absolute values in the presence of **1b**, **2b**, **1c**, **2c** were 1.55 ±0.05, 2.08 ± 0.04, 0.77 ± 0.06 and 0.99 ± 0.02 μM, respectively).

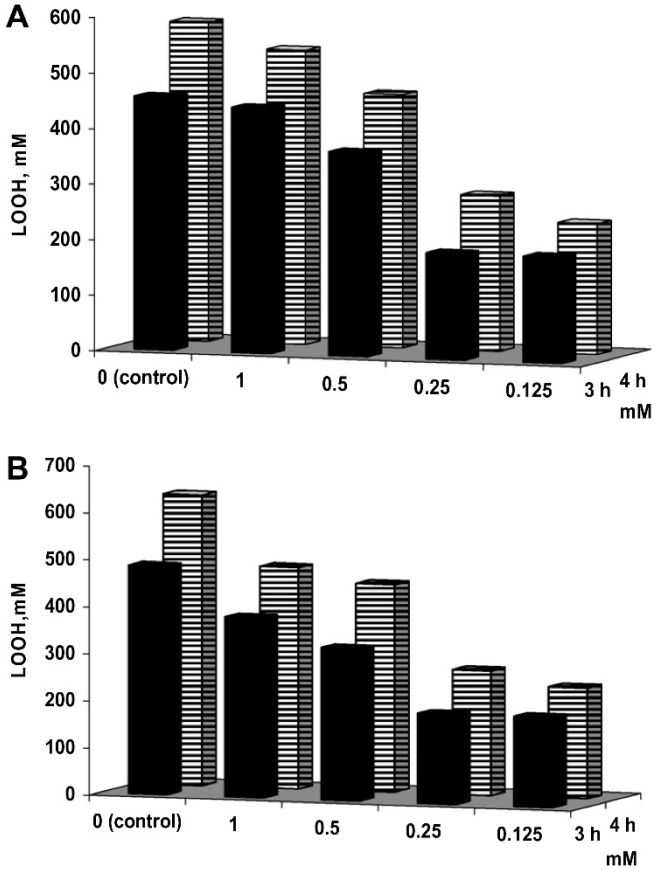


Fig. 7. The concentration-response for the inhibitory effects of Mn porphyrins $_{1c}$(a), $_{2c}$(b) on peroxidation of oleic acid; (porphyrins were dissolved at 37°C in a reaction medium as described in Section 2; then LOOH were determined after 3 h and 4 h).

Metalloporphyrins and the corresponding free bases perform the antioxidative activity due to the involvement of 2,6-di-*tert*-butylphenol groups as main reactive centers in the reaction of hydrogen atom transfer to radicals $LOO^{\bullet}$. The inhibitory effect of Mn porphyrins **1c**, **2c** on peroxidation of oleic acid depends on concentration (Fig. 7). The activity of both compounds decreases with the increase of concentration. This effect might be explained by the concurrence of two processes: inhibition of hydroperoxides formation and the promotion of hydroperoxides decomposition. The reactivity of phenol pendant is responsible for the first process, the reactivity of metal site – for the second one. The presence of lipophilic palmitoyl group improves the antioxidative activity of manganese porphyrin.

## 8. Conclusion

In conclusion, our results suggest that the polytopic compounds combining in one molecule 2,6-di-*tert*-butylphenol pendants as antioxidant substituents, metalloporphyrin moiety, and a long chain hydrocarbon palmitoyl group as a lipophilic fragment, are membrane active compounds and might be studied in an effort to find novel pharmaceutical agents. The activity of these compounds depends dramatically on the nature of metal incorporated in the porphyrin macrocycle and might be changed from antioxidative (free bases, Mn, Cu, Zn complexes) to indifferent (Co complex), and to pro-oxidative one (Fe complexes). The anti- or pro-oxidative properties of these compounds may be derived from different pathways according to the specific side groups or porphyrin core. The concurrence between the involvement of phenol pendants acting as radical scavengers and redox-active metal center promoting oxidation processes plays an important role in their mode of action.

## Abbreviations

$^{t}$BHP *tert*-butylhydroxyperoxide
MDA malondialdehyde
ROS reactive oxygen species
SOD superoxide dismutase
TBA thiobarbituric acid
TBARS thiobarbituric acid reactive substances

**Acknowledgements**

The financial support of RFBR (08-03-00844, 07-0300818, 06-03-32773, 07-03-00751, 07-03-12110), the Program ‘‘Biomolecular and Medicinal Chemistry” of Russian Academy of Sciences, Russian-Greek Program ‘‘Biomaterials”; NATO (PDD(CP)-CBP.NR.CLG 982211) is gratefully acknowledged.

## References


1. H. Sies (Ed.), Oxidative Stress, Academic Press, New York, 1985.
2. R.R. Crichton, R.J. Ward, Metal-based Neurodegeneration: From Molecular Mechanisms to Therapeutic Strategies, John Wiley & Sons, Chichester, 2006.
3. B.J. Day, Drug Discov. Today 9 (2004) 557-566.
4. S.-S. Shey, D. Nauduri, M.V. Anders, Biochim. Biophys. Acta 1762 (2006) 256-265.
5. E. Denisov, Handbook of Antioxidants, CRC Press, Boca Raton, New York, 1995.
6. M.R. Moore, Clin. Dermatol. 16 (1998) 203-223.
7. K. Faulkner, S.I. Liochev, I. Fridovich, J. Biol. Chem. 269 (1994) 23471-23479.
8. J. Milano, B.J. Day, Nucleic Acids Res. 28 (2000) 968-973.
9. H. Sheng, J.J. Enghild, R. Bowler, M. Patel, I. Batinic-Haberle, C.L. Calvi, B.J. Day, R.D. Pearlstein, J.D. Crapo, D.S. Warner, Free Radical Biol. Med. 33 (2002) 947-953.
10. M.J. Perez, A.I. Cederbaum, Free Radical Biol. Med. 33 (2002) 111-117.
11. Y. Kabe, M. Ohmori, K. Shinouchi, Y. Tsuboi, S. Hirao, M. Azuma, H. Watanabe, I. Okura, H. Handa, J. Biol. Chem. 281 (2006) 31729-31735.
12. Q.Y. Li, C. Pedersen, B.J. Day, M. Patel, J. Neurochem. 78 (2001) 746-755.
13. A. Trostchansky, G. Ferrer-Sueta, C. Batthyany, H. Botti, I. Batinic- Haberle, R. Radi, H. Rubbo, Free Radical Biol. Med. 35 (2003) 1293-1300.
14. A. Okado-Matsumoto, I. Batinic-Haberle, I. Fridovich, Free Radical Biol. Med. 37 (2004) 401-410.
15. I. Batinic-Haberle, I. Spasojevic, R.D. Stevens, P. Hambright, P. Neta, A. Okado- Matsumoto, I. Fridovich, Dalton Trans. 11 (2004) 1696-1702.
16. B.J. Day, I. Batinic-Haberle, J.D. Crapo, Free Radical Biol. Med. 26 (1999) 730-736.
17. A. Bloodsworth, V.B. O'Donnell, I. Batinic-Haberle, P.H. Chumley, J.B. Hurt, B.J. Day, J.P. Crow, B.A. Freeman, Free Radical Biol. Med. 28 (2000) 1017-1029.
18. J.P. Crow, Free Radical Biol. Med. 28 (2000) 1487-1494.
19. E.A. Konorev, S. Kotamraju, H. Zhao, S. Kalivendi, J. Joseph, B. Kalyanaraman, Free Radical Biol. Med. 33 (2002) 988-997.
20. E. Milaeva, D. Shpakovsky, Yu. Gracheva, O. Gerasimova, V. Tyurin, V. Petrosyan, J. Porphyr. Phthalocya. 8 (2003) 701-706.
21. E. Milaeva, V. Tyurin, D. Shpakovsky, O. Gerasimova, Zhang Jingwei, Yu. Gracheva, Heteroatom Chem. 17 (2006) 475-480.
22. L.R. Milgrom, N. Mofidi, C.C. Jones, A. Harriman, J. Chem. Soc., Perkin Trans. 2 4 (1989) 301-312.
23. O.A. Gerasimova, E.R. Milaeva, D.B. Shpakovsky, A.S. Semeykin, S.A. Syrbu, Russ. Chem. Bull. Int. Ed. 56 (2007) 831-834.
24. K. Helrich, AOCS Official Methods of Analysis, first ed., Arlington, AOAC, 1990, p. 956.
25. H. Ohkawa, N. Ohishi, K. Yagi, Anal. Biochem. 95 (1979) 351-358.
26. C. Paquot, A. Hantfenne, Standard Methods for the Analysis of Oils, Fats and Derivatives, seventh ed., Blockwell Scientific Publ. Ltd., Oxford, 1987.
27. R. Ramsay, R. Mehlhorn, T. Singer, Biochem. Biophys. Res. Commun. 159 (1989) 983-990.
28. A.G. Gornall, C.J. Bardawill, M.M. David, J. Biol. Chem. 177 (1949) 751-766.
29. W.L. Erdahl, R.J. Krebsbach, D.R. Pfeiffer, Arch. Biochem. Biophys. 285 (1991) 252-260.
30. P. Rothemund, J. Am. Chem. Soc. 57 (1935) 2010-2021.

31. L.R. Milgrom, C.C. Jones, A. Harriman, J. Chem. Soc., Perkin Trans. 2 (1988) 71-84.
32. L.R. Milgrom, C.J. Palmer, Chem. Res. Synop. (1990) 66-74.
33. N.A. Porter, K.A. Mills, R.L. Carter, J. Am. Chem. Soc. 116 (1994) 6690-6698.
34. C.U. Carlsen, J.K.S. M0ller, L.H. Skibsted, Coordin. Chem. Rev. 249 (2005) 485-498.
35. D. Lahaye, K. Muthukumaran, Chen-Hsiung Hung, D. Gryko, J.S. Reboucas, I. Spasojevic, I. Batinic-Haberle, J.S. Lindsey, Bioorg. Med. Chem. 15 (2007) 7066-7086.
36. I. Spasojevic, I. Batinic-Haberle, Inorg. Chim. Acta 317 (2001) 230-242.
37. M.J. Perez, A.I. Cederbaum, Free Radical Biol. Med. 33 (2002) 111-118.
38. B.J. Day, I. Batinic-Haberle, J.D. Crapo, Free Radical Biol. Med. 26 (1999) 730-739.
39. M.J. Burkitt, L. Milne, FEBS Lett. 379 (1996) 51-54.
40. C. Hoelzl, J. Bichler, F. Ferk, T. Simič, A. Nersesyan, L. Ebing, V. Ehrlich, A. Chakraborty, S. Knasműller, J. Phys. Pharmacol. 56 (2005) 49-64.
41. B. Halliwell, Cardiovasc. Res. 73 (2007) 341-347.
42. R. Apak, K. Güçlü, B. Demirata, M. Özyürek, S.E. Çelik, B. Bektaşoğlu, K.I. Berker, D. Özyurt, Molecules 12 (2007) 1496-1547.
43. E. Manda, T. Shimura, Bull. Chem. Soc. Jpn. 49 (1976) 1431-1438.
44. E. Manda, Bull. Chem. Soc. Jpn. 47 (1974) 2727-2735.
45. C.H. Kim, K. Yasumoto, T. Suzuki, M. Yoshida, J. Nutr. Sci. Vitaminol. 34 (1988) 481-490.
46. M.F. Nepomuceno, M. Tabak, A.E. Vercesi, J. Bioenerg. Biomembr. 34 (2002) 41-47.
47. K. Faulkner, S.I. Liochev, I. Fridovich, J. Biol. Chem. 269 (1994) 23471-23478.
48. E.R. Milaeva, O.A. Gerasimova, A.L. Maximov, E.A. Ivanova, E.A. Karachanov, N. Hadjiliadis, M. Louloudi, Catal. Commun. 8 (2007) 2069-2073.
49. E.N. Frankel, in: M. Simic, M. Karel (Eds.), Autooxidation in Food and Biological Systems, Plenum Press, New York, 1980, p. 141.
50. K.C. Christoforidis, M. Louloudi, E.R. Milaeva, Y. Sanakis, Y. Deligiannakis, Mol. Phys. 105 (2007) 2185-2194.

*Известия Академии наук. Серия химическая, 2011, № 12, стр. 2514-2521*

УДК 546.562+541.515+577.152.133

# КОМПЛЕКСЫ МЕДИ С НИТРОНИЛНИТРОКСИЛЬНЫМИ РАДИКАЛАМИ – ИНГИБИТОРЫ ЛИПОКСИГЕНАЗЫ С АНТИОКСИДАНТНОЙ АКТИВНОСТЬЮ[12]

**Е.Р. Милаева, С.И. Орлова, Д.И. Осолодкин, В.А. Палюлин, Е.Ю. Фурсова, В.И. Овчаренко, Н.С. Зефиров**

*Московский государственный университет им. М. В. Ломоносова, Москва, Российская Федерация*

*Институт физиологически активных веществ Российской академии наук, Черноголовка, Российская Федерация*

*Международный томографический центр Сибирского отделения Российской академии наук, Российская Федерация, Новосибирск*

Исследовано влияние комплексов $Cu(L^RH)_2(NO,)_2$ (K = H, Me) с нитронилнитроксильными радикалами $L^RH$ на активность фермента липоксигеназы (LOX-1) в процессе пероксидного окисления линолевой кислоты. Изученные комплексы являются обратимыми ингибиторами фермента, причем для комплекса с метилзамещенным лигандом наблюдается конкурентный тип ингибирования, а для комплекса с незамещенным лигандом – неконкурентный. Результаты молекулярного докинга показывают, что для изученных комплексов характерно расположение в гидрофобном кармане активного центра LOX-1, а изменение типа ингибирования можно объяснить введением дополнительной метильной группы в имидазольный фрагмент лиганда, что обеспечивает несколько более выгодное взаимодействие ингибитора с ферментом и приводит к реализации неконкурентного механизма ингибирования. Исходные диамагнитные соединения ($L^RH_2$), нитронилнитроксильные радикалы ($L^RH$) и комплексы $Cu^{II}$ проявляют высокую антиоксидантую активность в неферментативном пероксидном окислении линолевой кислоты, а также в процессе генерирования супероксид анион-радикала $O_2^{-\bullet}$ в системе ксантин–ксантиноксидаза.

Липоксигеназы образуют семейство негемовых железосодержащих диоксигеназ, которые катализируют регио- и стереоселективное окисление полиненасыпценных жирных кислот (арахидоновой, линолевой, линоленовой), содержащих один или несколько (1*Z*,4*Z*)-пентадиеновых фрагментов, до соответствующих (1*S*,2*E*,4*Z*)-гидропероксидов[1,2]. Эта реакция относится к радикальным процессам

[12] Посвящается академику Российской академии наук Р.З. Сагдееву в связи с его 70-летием.

пероксидного окисления и является первой стадией биосинтеза лейкотриенов – медиаторов различных воспалительных процессов и аллергических реакций, участвующих в патогенезе опухолевых заболеваний, астмы и атеросклероза[3-7]. Кроме того, побочными продуктами липоксигеназной реакции являются активные метаболиты кислорода (АМК) – супероксид анион-радикал и пероксид водорода, что также обусловливает роль липоксигеназы в патогенезе заболеваний, индуцированных окислительным стрессом[8].

Таким образом, липоксигеназа является важной фармацевтической мишенью, вследствие чего в последние годы было предпринято множество попыток найти селективный ингибитор липоксигеназы[9-12]. Однако на рынок вышел только препарат Zileuton® (см. лит.[13]) для лечения астмы; этот препарат оказался неэффективным при лечении других заболеваний, патогенез которых связан с участием лейкотриенов. Поэтому задача поиска новых соединений, которые будут эффективно, но обратимо ингибировать липоксигеназу, является весьма актуальной.

Поиск ингибиторов ведется в ряду органических соединений, однако в последнее время получены также данные о способности комплексов металлов, например комплексов меди с диеновыми и гетероциклическими лигандами[14], проявлять ингибиторную активность по отношению к липоксигеназе[15].

В последние годы внимание исследователей привлекают стабильные нитроксильные радикалы – ингибиторы образования АМК, антиоксиданты, радиопротекторы, контрастные реагенты, антипролиферативные агенты[16]. Достигнуты большие успехи в разработке методов получения и исследовании широкого спектра свойств комплексов металлов с лигандами – нитроксильными радикалами[17–19].

Целью настоящей работы является исследование влияния комплексов $Cu^{II}$ с нитронилнитроксильными радикалами $Cu(L^RH)_2(NO_3)_2$ (**1a**,**b**) на ферментативную активность липоксигеназы в процессе пероксидного окисления линолевой кислоты, а также в процессе генерирования супероксид анион-радикала $O_2^{-\cdot}$ в системе ксантин–ксантиноксидаза. Для сравнения исследована активность нитронилнитроксильных радикалов $L^RH$ (**2a**,**b**) в этих же процессах, а также их диамагнитных предшественников $L^RH_2$ (**3a**,**b**) в процессе переноса атома водорода с использованием 1,1-дифенил-2-пикрилгидразила (ДФПГ).

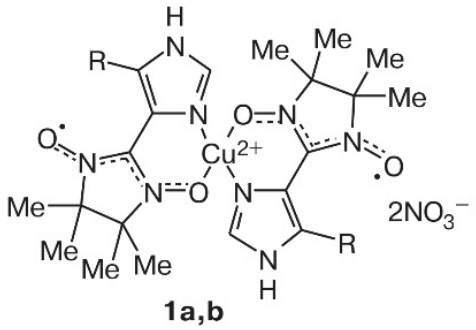


**1a,b**

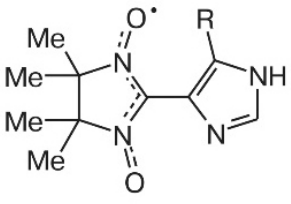


**2a,b**

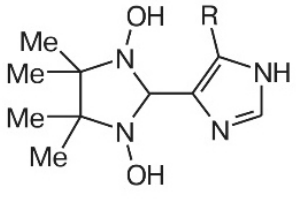


**3a,b**

**a**: R = H, **b**: R = Me

## Экспериментальная часть

Соединения **1a**,**b**, **2a**,**b** и **3a**,**b** получали по известным методикам[20–22]. В работе использованы следующие вещества и реагенты: ДФПГ («Aldrich»), этанол (96%), хлорид меди(II) («х.ч.»), неокупроин (2,9-диметил-1,10-фенантролин, «Aldrich»), соевая липоксигеназа (Lipoxidase from Glycine max (soybean), Type I-B, «Sigma»), линолевая кислота («Sigma», >99%), ксантин («Sigma»), ксантиноксидаза («Sigma»), хлорид тетразолия синего («Merck»), бычий сывороточный альбумин, тиобарбитуровая кислота (ТБК, «Sigma–Aldrich»), ионол (2,6-ди-*трет*-бутил-4-метилфенол, «Aldrich»), тролокс (Trolox, «Acros Organics»), ЭДТА («х.ч.»), трихлоруксусная кислота («х.ч.»), диметилсульфоксид (ДМСО, «х.ч.»). Растворители очищали по стандартным методикам[23]. Для приготовления буферных растворов использовали дистиллированную воду и ацетат аммония, борную кислоту, бикарбонат натрия, гидрофосфат натрия, дигидрофосфат натрия («х.ч.»).

В работе использовано следующее оборудование: кюветный спектрофотометр «Thermo Evolution 300 BB» (Великобритания), 96-луночный планшетный спектрофотометр «Zenyth200rt» (Австрия), термостат «Термит» (Россия), центрифуга «Hettich Universal 320R» (Германия).

Определение активности липоксигеназы проводили спектрофотометрически[24]. Измеряли содержание гидропероксида (продукта окисления линолевой кислоты) при $\lambda_{max}$ = 234 нм. Анализируемый раствор содержал 2 мл раствора линолевой кислоты ($0.3 \cdot 10^{-3}$ моль $\cdot$ л$^{-1}$), 0.89 мл боратного буфера (pH 9.0) и 0.01 мл раствора исследуемого соединения в ДМСО. Реакцию запускали добавлением 0.1 мл раствора фермента (500 единиц), измерение проводили в течение 10 мин при 25°C. Для каждого вещества измерения проводили с использованием шести концентраций в диапазоне (10–100) $\cdot 10^{-6}$ моль $\cdot$ л$^{-1}$. Все эксперименты повторяли трижды.

Степень ингибирования липоксигензы ($A$(%)) определяли по формуле

$$A\ (\%) = (v_0/v_0') \bullet 100\%,$$

где $v_0$ и $v_0'$ – соответственно значения начальной скорости ферментативной реакции в присутствии и в отсутствие (контроль) исследуемых соединений.

Значение начальной скорости ($v_0$ и $v_0'$) рассчитывали по формуле

$$v_0 = \Delta C/\Delta t = \Delta A/(\Delta t \bullet \varepsilon) = \mathrm{tg}\alpha/(\Delta t \bullet \varepsilon),$$

где $C$ – концентрация продукта, $t$ – время реакции, $\varepsilon$ – молярный коэффициент поглощения, $\alpha$ – угол наклона кинетической кривой (зависимость концентрации продукта от времени).

Значения ингибирующей концентрации $IC_{50}$ находили аппроксимацией полученных данных логистической кривой общего вида

$$A\ (\%) = (1/(1 + [I]/IC_{50})) \bullet 100\%,$$

где [*I*] – концентрация ингибитора.

В серии экспериментов по определению обратимости ингибирования реакционная смесь содержала 0.89 мл боратного буфера (pH 9.0), 0.01 мл раствора ингибитора в ДМСО и 0.1 мл раствора фермента (500 единиц). Далее раствор выдерживали различные промежутки времени (1,5 и 10 мин) и запускали реакцию добавлением 2 мл раствора линолевой кислоты (0.45 ммоль $\cdot$ л$^{-1}$).

**Определение типа ингибирования фермента липоксигеназы**. Определение кинетических параметров и типа ингибирования липоксигеназы проводили согласно работе[25], изменяя концентрацию линолевой кислоты в диапазоне (10–1000) • $10^{-6}$ моль • л$^{-1}$ в присутствии неизменной концентрации ингибитора, близкой к значению $IC_{50}$ для данного соединения[25]. Значения кинетических параметров $K_m$ (константа Михаэлиса) и $V_{max}$ (скорость реакции при насыщении фермента субстратом) определяли графически в координатах Лайнуивера–Берка (метод двойных обратных координат)[25].

**Ферментативное генерирование супероксид анион-радикала $O_2^{-\cdot}$ в системе ксантин–ксантиноксидаза**. Оценку влияния соединений **1a**,**b** на процесс ферментативного генерирования супероксид анион-радикала $O_2^{-\cdot}$ в системе ксантин–ксантиноксидаза проводили по скорости восстановления тетразолия синего до формазана[26]. Состав реакционной смеси: 2.7 мл карбонатного буфера (40 ммоль • л$^{-1}$, pH 10.0), содержащего 0.1 ммоль • л$^{-1}$ ЭДТА, 0.06 мл раствора ксантина (10 ммоль • л$^{-1}$), 0.03 мл 0.5%-ного бычьего сывороточного альбумина, 0.03 мл тетразолия синего (2.5 ммоль • л$^{-1}$) и 0.06 мл раствора исследуемого соединения в ДМСО. К смеси при 25°C добавляли 0.12 мл ксантиноксидазы (0.04 единицы) и измеряли поглощение при $\lambda_{max}$ = 560 нм в течение 300 с. Контрольный эксперимент проводили в присутствии 0.06 мл ДМСО. Для каждого вещества измерения проводили с использованием шести концентраций. Все эксперименты повторяли трижды.

Была также проведена серия экспериментов по оценке активности фермента ксантиноксидазы в присутствии исследуемых веществ путем определения скорости образования мочевой кислоты. Состав реакционной смеси: 2.76 мл карбонатного буфера (40 ммоль • л$^{-1}$, pH 10.0), содержащего 0.1 ммоль • л$^{-1}$ ЭДТА, 0.06 мл раствора ксантина 10 ммоль • л$^{-1}$ и 0.06 мл раствора исследуемого соединения в ДМСО. Реакцию инициировали добавлением 0.12 мл ксантиноксидазы (0.04 единицы) и измеряли поглощение при $\lambda_{max}$ = 293 нм в течение 300 с.

**Неферментативное пероксидное окисление линолевой кислоты**. Оценку влияния соединений **2a**,**b** и **3a**,**b** на процесс неферментативного пероксидного окисления линолевой кислоты проводили по известному методу[27]. К 0.034 мл линолевой кислоты в 1.97 мл этанола добавляли 2 мл фосфатного буфера (pH 7.4). Реакционная смесь содержала 0.33 мл раствора линолевой кислоты, 0.066 мл рас-

твора $FeCl_2$ (4 ммоль • л$^{-1}$), 0.164 мл фосфатного буфера и 0.1 мл раствора исследуемого соединения (30 ммоль • л$^{-1}$) в этаноле[28]. Полученный раствор инкубировали 30 мин при 37°C. Далее добавляли 0.84 мл раствора, содержащего 0.25 *M* HC1, 10% трихлоруксусной кислоты и 0.6% ТБК. Смесь нагревали 15 мин при 95°C, центрифугировали и измеряли оптическую плотность при $\lambda_{max}$ = 532 нм на 96-луночном планшетном спектрофотометре.

**ДФПГ-тест**. Оценку восстановительной активности соединений **2a**,**b** и **3a**,**b** с использованием ДФПГ проводили спектрофотометрически при длине волны 517 нм (см. лит.[29]). Реакцию проводили в ячейках 96-луночного планшета. Реакционная смесь содержала 0.1 мл ДФПГ (0.2 ммоль • л$^{-1}$) и 0.1 мл раствора исследуемых веществ различной концентрации (0.01–0.2 ммоль • л$^{-1}$). Реакцию проводили 30 мин при 25°C. Из полученных данных рассчитывали значение антиоксидантной активности в процентах ($I$(%)) по формуле

$$I\,(\%) = (A_0 - A_1)/A_0 \bullet 100\%,$$

где $A_0$ – поглощение контрольного раствора ДФПГ, $A_1$ – поглощение раствора реакционной смеси.

Значения эффективной концентрации $EC_{50}$ находили аппроксимацией полученных данных логистической кривой общего вида:

$$I\,(\%) = 100 \bullet (1/(1 + [C]/EC_{50})),$$

где [$C$] – концентрация исследованных соединений.

**CUPRAC-тест**. Оценку окислительно-восстановительной активности соединений **2a**,**b** и **3a**,**b** проводили по методу CUPRAC (см. лит.[30]). Регистрацию результатов проводили по увеличению поглощения раствора при длине волны 450 нм, соответствующей максимуму поглощения комплекса меди(I) с неокупроином. Измерения проводили при 25°C с использованием 96-луночного планшетного спектрофотометра. Реакционная смесь содержала 0.05 мл ацетатного буфера (pH 7.0), 0.05 мл раствора $CuCl_2$ (0.01 моль • л$^{-}$), 0.05 мл раствора неокупроина (7.5 ммоль • л$^{-1}$) и 0.05 мл раствора исследуемого соединения (2 ммоль • л$^{-1}$) в этаноле.

Результаты представляли в тролокс-эквивалентах (TEAC). Значение тролокс-эквивалента определяли графически по величине поглощения с использованием калибровочного графика – концентрационной зависимости количества восстановленного комплекса меди от содержания тролокса.

**Молекулярный докинг**. Докинг молекул ингибиторов в активный центр липоксигеназы осуществляли с помощью программы Auto Dock 4.2, в которой реализован генетический алгоритм[31,32].

Подготовку структуры белка (код доступа в банке белковых структур PDB[33] 1IK3[34]) путем удаления кристаллизационных молекул воды и структур лигандов, добавления полярных атомов водорода и минимизации энергии (100 итераций

методом Пауэлла в силовом поле Tripos[35]) осуществляли в программном комплексе Sybyl 8.0 (см. лит.[36]).

Координаты атомов лигандов были извлечены из файлов рентгеноструктурных данных[20,21] (CCDC 199137) с помощью программы PLATON (см. лит.[37]), после чего оптимизированы с помощью комплекса Sybyl. Поскольку рассмотрение радикальных частиц методами молекулярной механики невозможно в силу отсутствия параметров для них в силовых полях, соответствующие фрагменты молекул были представлены как *N*-оксиды. Нитрат-ионы были удалены из структур комплексов перед проведением докинга.

Подготовку систем к докингу проводили с использованием программного пакета MGLTools 1.5.4 (см. лит.[38]). Заряды на атомах при докинге рассчитывали по схеме Гастайгера[39], атому железа был присвоен заряд +3, атому меди был присвоен заряд +2. Значение ван-дер-ваальсова радиуса для атома меди было установлено равным 1.4 Å. Сеточные поля строили для области пространства, включающей только каталитический центр фермента. При докинге проводили 100 запусков генетического алгоритма для каждого комплекса, результаты кластеризовали, используя пороговое значение среднеквадратичного отклонения 2.0 Å.

## Обсуждение полученных результатов

Соевая липоксигеназа-1 (LOX-1) часто используется как модельный фермент при исследовании гомологичного семейства липоксигеназ (КФ 1.13.11.12), в частности 5-липоксигеназы, функционирующей в организме человека. 5-Липоксигеназа и LOX-1 катализируют окисление линолевой кислоты до 9-(*S*)-гидропероксо-10*E*,12*Z*-октадекадиеновой кислоты (HPOD). В настоящей работе исследование активности комплексов меди с нитронилнитроксильными радикалами **1a**,**b** и лигандов **2a**,**b** проводили на примере LOX-1. В качестве субстрата использовали линолевую кислоту. Мониторинг реакции осуществляли спектрофотометрически при $\lambda_{max}$ = 234 нм по образованию 9-(*S*)-гидропероксо-10*E,*12*Z*-октадекадиеновой кислоты ($\varepsilon = 2.5 \cdot 10^4$ л • моль$^{-1}$ • см$^{-1}$) (см. лит.[2,20]).

**Ингибирование фермента LOX-1.** Влияние комплексов **1a**,**b** на активность фермента LOX-1 иллюстрируют рис. 1–5. Важно отметить, что полученные в настоящей работе экспериментальные данные свидетельствуют об отсутствии влияния исходных органических лигандов – стабильных нитронилнитроксильных радикалов **2a**,**b** – на окисление линолевой кислоты, катализируемое липоксигеназой. Значения скоростей ферментативной реакции в присутствии лигандов **2a**,**b** отличаются от таковых для контрольной реакции без добавок на 1 ± 0.3%.

Экспериментальные кинетические кривые накопления HPOD при постоянной концентрации субстрата и различных концентрациях комплексов **1a**,**b** приведены на рис. 1 и 2.

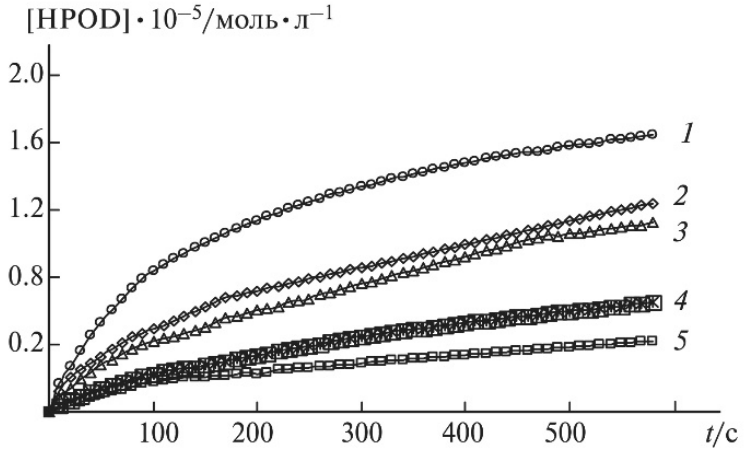


Рис. 1. Кинетические кривые накопления HPOD в отсутствие ингибитора (*1*) и в присутствии комплекса **1a** в концентрации 1.1 • $10^{-5}$ (*2*), 1.4 • $10^{-5}$ (*3*), 2.1 • $10^{-5}$ (*4*) и 3.3 • $10^{-5}$ моль • $л^{-1}$ (*5*).

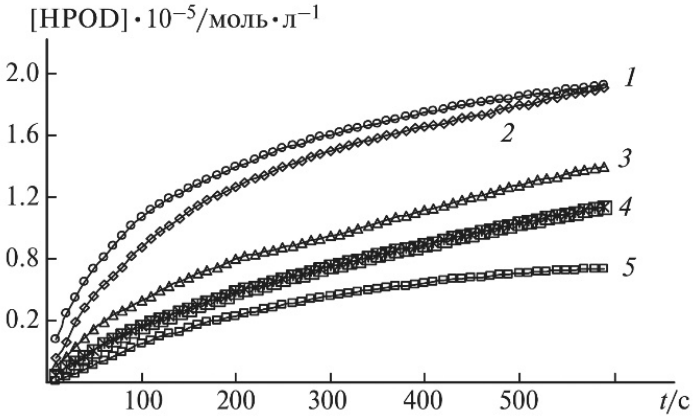


Рис. 2. Кинетические кривые накопления HPOD в отсутствие ингибитора (*1*) и в присутствии комплекса **1b** в концентрации 1.1 • $10^{-5}$ (*2*), 1.4 • $10^{-5}$ *(3),* 2.7 • $10^{-5}$ (*4*) и 3.3 • $10^{-5}$ моль • $л^{-1}$ (*5*).

Значения $IC_{50}$ определены путем аппроксимирования концентрационной зависимости логистической кривой. Полученные кривые представлены на рис. 3, кинетические данные приведены в табл. 1. Значения $IC_{50}$ для комплексов **1a**,**b** составляют (29.2±4.7) • $10^{-6}$ и (20.1±3.9) • $10^{-6}$ моль • $л^{-1}$ соответственно.

Таблица 1. Кинетические параметры ингибирования LOX-1 комплексами **1a,b***

| Комплекс | $C$ • $10^{-6}$ | $K_m$ • $10^3$ /моль • $л^{-1}$ | $K_{max}$ • $10^{-5}$ /моль • $л^{-1}$ • $с^{-1}$ | Тип ингибирования |
|---|---|---|---|---|
| **1a** | 12.5 | 0.113 | 7.8 | Конкурентный |
| | 20.0 | 0.156 | 7.5 | |
| | 30.0 | 0.200 | 7.2 | |
| **1b** | 12.5 | 0.039 | 4.7 | Неконкурентный |
| | 20.0 | 0.039 | 3.1 | |
| | 30.0 | 0.039 | 2.0 | |

*В отсутствие комплексов $K_m$ = 0.040 • $10^{-3}$ моль • $л^{-1}$, $K_{max}$ = 8.4 • $10^{-5}$ • моль • $л^{-1}$ • $с^{-1}$.

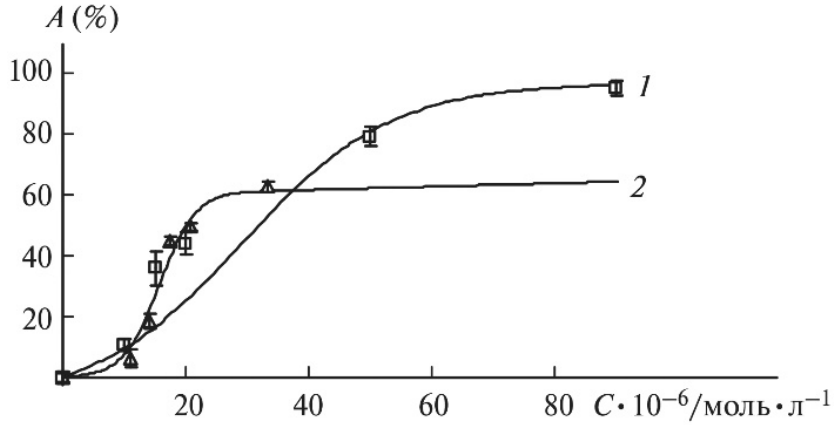


Рис. 3. Зависимости изменения степени ингибирования LOX-1 от концентрации комплексов **la** *(1)* и **1b** *(2)*.

Для установления обратимости ингибирования LOX-1 комплексами меди **1a**,**b** фермент инкубировали в буферном растворе в присутствии комплекса и фиксировали кинетические кривые через различные промежутки времени (1, 5, 10 мин), добавляя к смеси раствор линолевой кислоты в буфере. Предварительное инкубирование LOX-1 с комплексами **1a**,**b** не изменяет начальной скорости ферментативной реакции, что свидетельствует об обратимом характере ингибирования фермента.

Экспериментальные кинетические кривые, полученные для различных концентраций субстрата в координатах Лайнуивера–Берка, представлены на рисунках 4 и 5 и демонстрируют характер ингибирования липоксигеназы комплексами **1a,b** в зависимости от концентрации субстрата.

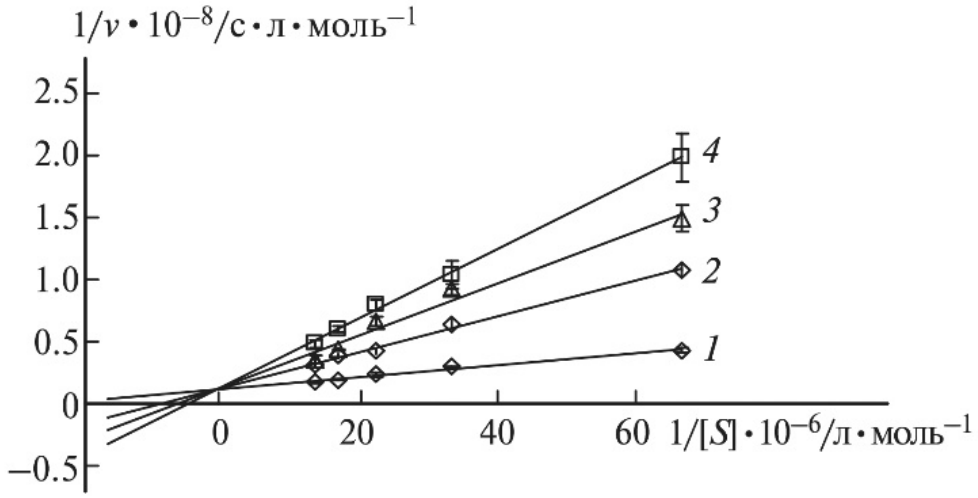


Рис. 4. Кинетические кривые ингибирования липоксигеназы (LOX-1) в координатах Лайнуивера–Берка в отсутствие ингибитора (*1*) и в присутствии комплекса **1a** в концентрации $1 \cdot 10^{-5}$ (*2*), $2 \cdot 10^{-5}$ (*3*) и $3 \cdot 10^{-5}$ моль • $л^{-1}$ (*4*).

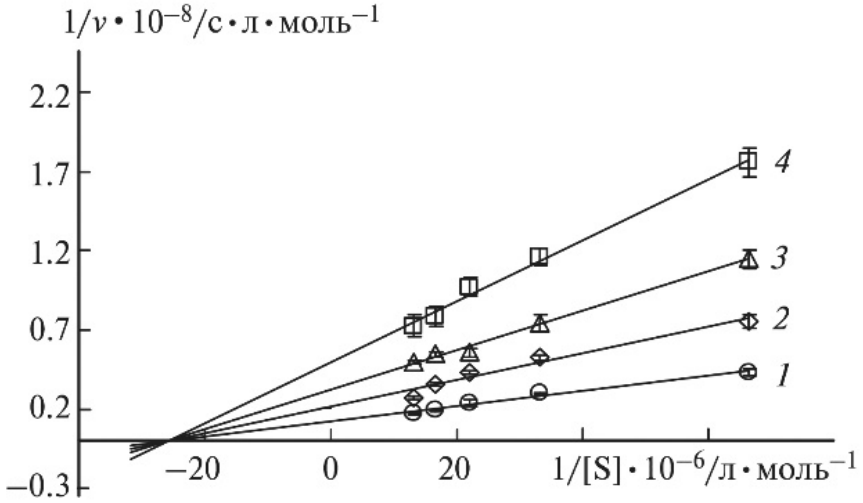


Рис. 5. Кинетические кривые ингибирования липоксигеназы (LOX-1) в координатах Лайнуивера–Берка в отсутствие ингибитора (*1*) и в присутствии комплекса **1b** в концентрации $1 \cdot 10^{-5}$ (*2*), $2 \cdot 10^{-5}$ *(3)* и $3 \cdot 10^{-5}$ моль • $л^{-1}$ (*4*).

Пересечение прямых в одной точке на ординате (см. рис. 4) указывает на то, что комплекс **1a** ингибирует фермент, конкурируя с субстратом за участок связывания с ферментом, тогда как из рис. 5 следует, что комплекс **1b** не конкурирует с линолевой кислотой как субстратом за центр связывания с ферментом и, следовательно, проявляет неконкурентный тип ингибирования.

Таким образом, полученные данные свидетельствуют об обратимом характере ингибирования LOX-1 как для соединения **1a**, так и для соединения **1b**; конкурентном механизме ингибирования в случае комплекса **1a**; а также неконкурентном механизме ингибирования для комплекса **1b**.

**Молекулярный докинг.** С целью интерпретации полученных экспериментальных данных о типе ингибирования, характерном для комплексов **1a**,**b**, мы провели молекулярный докинг. Результаты докинга соединений **1a**,**b** приведены на рис. 6. Для обоих соединений характерно расположение в гидрофобном кармане активного центра, аналогичном идентифицированному ранее[40].

Тем не менее ориентации двух исследованных соединений заметно отличаются. Для соединения **1b** характерно наличие большего числа гидрофобных взаимодействий, чем для соединения **1a**, вследствие наличия двух метильных групп, вступающих в контакты с аминокислотными остатками Val372 (минимальное расстояние $r_{C}\ldots_{C}(\min) = 3.27$ Å) и Val571 $r_{C}\ldots_{C}(\min) = 2.10$ Å). При этом возникают также гидрофобные взаимодействия с остатками Thr728 ($r_{C}\ldots_{C}(\min) = 2.1$ Å), Leu773 ($r_{C}\ldots_{C}(\min) = 2.26$ Å) и Leu565 ($r_{C}\ldots_{C}(\min) = 2.43$ Å), лишь последнее из которых присутствует в случае ориентации, предлагаемой для комплекса LOX-1 с **1a** ($r_{C}\ldots_{C}(\min) = 2.67$ Å). Кроме того, в комплексе LOX-1 с **1a** имеется гидрофобное взаимодействие лиганда и аминокислотного остатка Ile770

($r_{C…C}$(min) = 2.62 Å), отсутствующее в комплексе LOX-1 с **1b**. Для нитроксильной группы комплекса **1b** возможно образование водородных связей с остатками Arg726 (расстояние $r_{O…N}$ = 4.29 Å), Ser510 ($r_{O…O}$ = 3.26 Å) иThr575 ($r_{N…O}$ = 3.69 Å). Амидные группы остатков глутамина Gln716 и Gln514 при связывании комплекса **1b** могут переориентироваться таким образом, чтобы обеспечить взаимодействие с атомом меди, однако такие связи не были идентифицированы при докинге вследствие того, что подвижность боковых цепей белка не изучали.

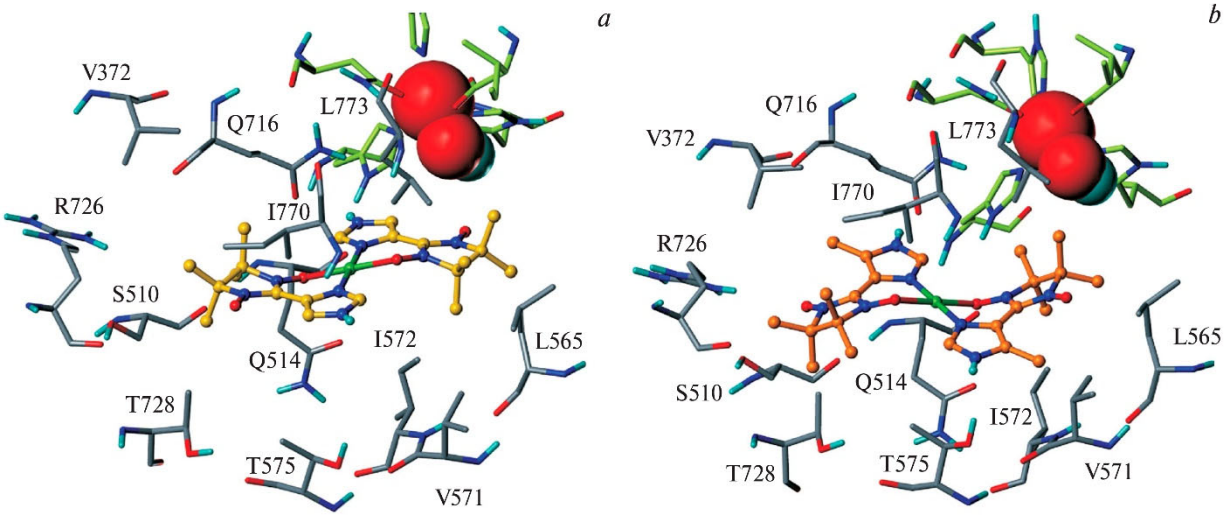


Рис. 6. Результаты докинга соединений **1a** (*a*) (атомы углерода окрашены желтым цветом) и **1b** (*b*) (атомы углерода окрашены оранжевым цветом). Комплексы меди изображены с использованием шаростержневой модели. Фрагмент [FeOH] в активном центре изображен с сохранением ван-дер-ваальсовых радиусов атомов. Атомы углерода аминокислотных остатков, координирующих атом железа, окрашены зеленым цветом, атомы углерода аминокислотных остатков, контактирующих с ингибитором – серым, атомы азота – синим, атомы водорода – голубым, атомы кислорода – красным, атомы меди –салатовым.

Комплекс **1a** расположен в связывающей полости таким образом, что образование побочных взаимодействий маловероятно. Кроме того, у этого комплекса имеется неблагоприятный близкий контакт с аминокислотным остатком His518, участвующим в комплексообразовании с атомом железа, однако ориентация, аналогичная ориентации комплекса **1b**, не была найдена при докинге. Между тем, при взаимодействии с ингибитором принципиально возможно взаимодействие этого остатка гистидина не только с атомом железа активного центра, но и с атомом меди ингибитора. Образование водородных связей между комплексом меди и областью связывания в белке маловероятно в силу высокой гидрофобности области связывания и жесткости структуры комплекса меди, что, в свою очередь, не допускает возможности образования водородных связей. Однако следует отметить, что присутствует водородная связь между протоном имидазольного цикла NH комплекса **1a** и амидным атомом кислорода основной цепи Gln514 (на рис. 6, *a* не показана). Ни одна из предложенных структур комплексов

«фермент–ингибитор» не предполагает непосредственного взаимодействия ингибиторов с атомом железа либо гидроксид-ионом, расположенным в его координационной сфере.

Расстояния между атомом меди и атомом железа активного центра фермента (рис. 7) для комплексов **1a** и **1b** составляют 7.37 и 9.15 Å соответственно. Эти данные не позволяют рассматривать комплексы **1a**,**b** как редокс-ингибиторы[12], активность которых основана на транспорте электрона от иона $Cu^{2+}$ к иону $Fe^{3+}$ в области связывания ингибитора. Однако значительная область полости, занимаемая нативными субстратами LOX-1, в данном случае занята комплексами меди, что, по-видимому, и подтверждает их ингибиторную активность.

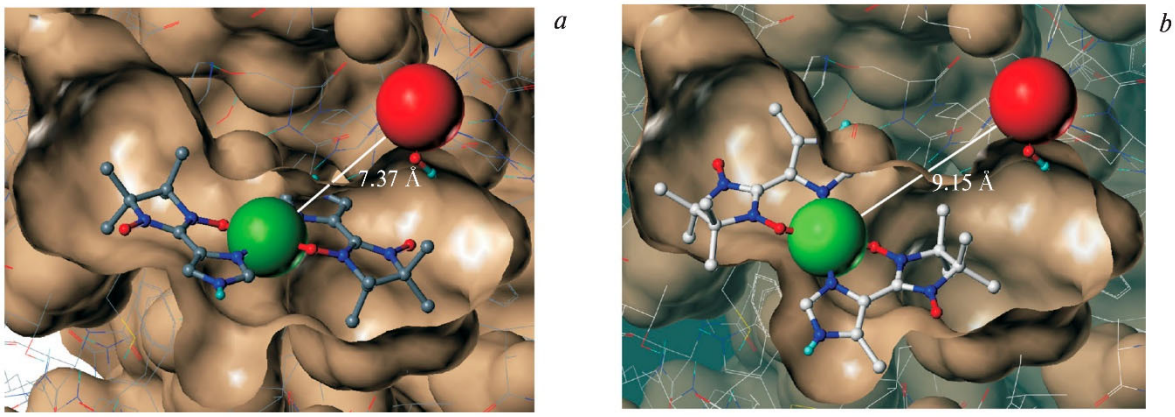


Рис. 7. Результаты докинга соединений **1a** *(a)* и **1b** *(b)*. Указаны расстояния между атомами меди (показаны зеленым цветом) в комплексах **1a**,**b** и атомом железа (показаны красным цветом) в активном центре липоксигеназы.

Необычный эффект изменения типа механизма ингибирования при переходе от **1a** к **1b** не может быть надежно объяснен без привлечения метода рентгеновской кристаллографии. Тем не менее на основании результатов докинга можно предположить, что при введении дополнительной метильной группы в имидазольный фрагмент (комплекс **1b**) становится возможной ориентация комплекса меди в полости связывания LOX-1, характеризующаяся наличием большего числа гидрофобных контактов, чем ориентация, характерная для **1a**. Как следствие, взаимодействие ингибитора с липоксигеназой становится несколько более выгодным и приводит к реализации неконкурентного механизма в исследуемом диапазоне концентраций субстрата.

**Неферментативное пероксидное окисление линолевой кислоты.** С целью исследования влияния комплексов **1a**,**b**, а также соответствующих лигандов – стабильных нитронилнитроксильных радикалов **2a**,**b** и их восстановленных форм **3a**,**b** – на неферментативное пероксидное окисление субстрата использовали окисление линолевой кислоты, индуцированное ионами $Fe^{2+}$. Спектрофотометрически определяли содержание ТБК-зависимых продуктов – карбонильных соединений, образующихся при распаде гидропероксиоктадекадиеновой кислоты в присутствии кислорода воздуха. Результаты представлены на

рис. 8 в процентах содержания ТБК-зависимых продуктов (TBARS) от контроля. Для сравнения использовали известный антиоксидант – ионол (2,6-ди-*трет*-бутил-4-метил фенол).

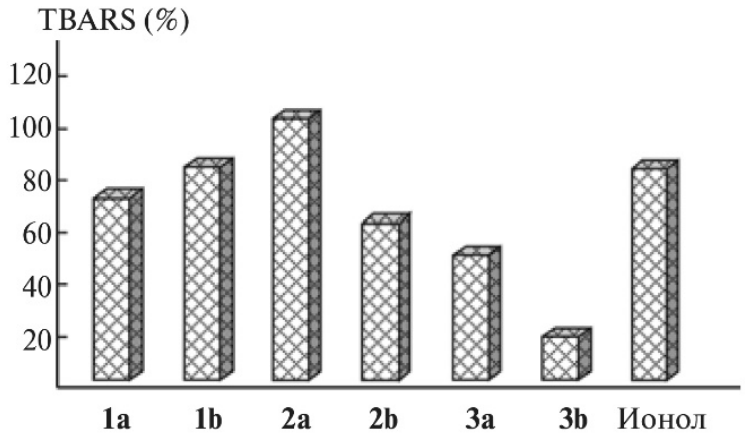


Рис. 8. Содержание ТБК-зависимых продуктов пероксидного окисления линолевой кислоты в присутствии комплексов **1a,b**, **2a,b** и **3a,b** (концентрация исследуемых соединений 1.6 ммоль • $л^{-1}$ • (мг линолевой кислоты)$^{-1}$, 37°C, $FeSO_4 \cdot 4H_2O$, 30 мин).

Присутствие в растворе соединения **2a** не оказывает влияния на процесс пероксидного окисления линолевой кислоты. Для радикала **2b** и комплексов меди **1a**,**b** антиоксидантная активность сопоставима с ионолом (~61, 70, 82 и 81% соответственно). Как видно из рисунка 8, максимальной активностью, значительно превышающей активность ионола, обладают соединения **3a**,**b** (48 и 17% соответственно), что позволяет предположить *их* высокую эффективность как перспективных антиоксидантов.

**ДФПГ-тест**. Для оценки неспецифической антиоксидантной активности соединений **3a**,**b** проявивших максимальный эффект при ингибировании цепного радикального процесса пероксидного окисления линолевой кислоты, был проведен тест с использованием модельной реакции отрыва атома водорода стабильным радикалом 1,1-дифенил-2-пикрилгидразилом (ДФПГ) от молекулы потенциального антиоксиданта. Контроль осуществляли по изменению максимума характеристичной полосы поглощения ДФПГ при $\lambda_{max}$ ~517 нм в электронных спектрах поглощения. На рис. 9 представлены концентрационные зависимости восстановления радикала ДФПГ в присутствии соединений **3a**,**b**.

Значения $EC_{50}$ для соединений **3a**,**b** составляют 41.7 и 33.7 • $10^{-6}$ моль • $л^{-1}$ соответственно. Значения $EC_{50}$ для тролокса и ионола составляют 46.4 и 101.7 • $10^{-6}$ моль • $л^{-1}$ соответственно, что также подтверждает высокую антиоксидантную активность лигандов **3a**,**b**.

**CUPRAC-тест.** С целью изучения способности соединений **1a**,**b**, **2a**,**b** и **3a**,**b** проявлять антиоксидантную активность в качестве медиаторов в процессе переноса электрона в настоящей работе использовали метод CUPRAC. Эксперимен-

тальные данные в эквивалентах тролокса (TEAC)[30] представлены на рис. 10. Соединения **3a**,**b** проявляют умеренную активность в процессе восстановлении $Cu^{2+}$ в условиях эксперимента, значения TEAC составляют 65 ± 3 и 66 ± 3% от активности тролокса соответственно. Комплексы меди **1a**,**b** и соответствующие лиганды – стабильные радикалы **2a**,**b** – проявляют крайне низкую активность. Значения TEAC составляют 10 ± 1, 38 ± 1, 1 ± 1 и 28 ± 2% для **2a**, **2b**, **1a** и **1b** соответственно.

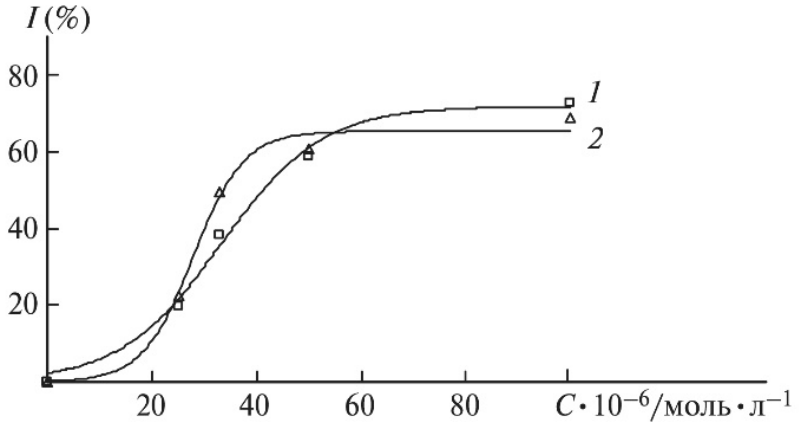


Рис. 9. Концентрационные зависимости восстановления радикала ДФПГ в присутствии соединений **3a** (*1*) и **3b** *(2)* (25°C, EtOH, 30 мин).

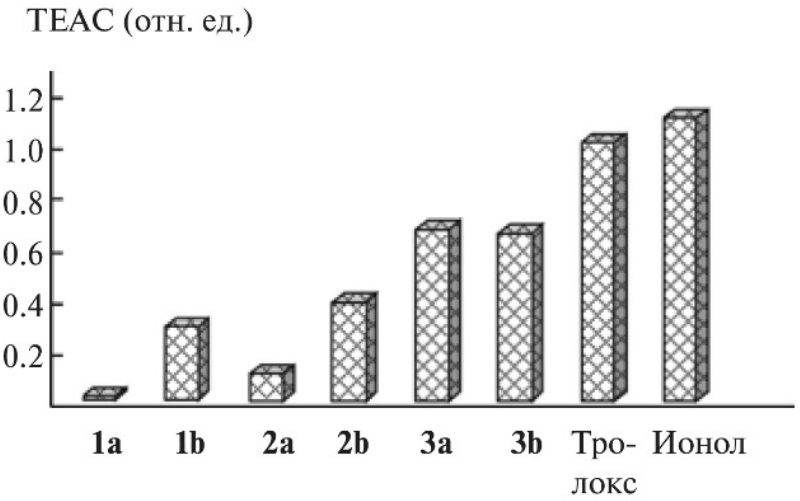


Рис. 10. Значения антиоксидантной активности исследованных соединений, полученные методом CUPRAC.

Таким образом, полученные данные также не позволяют предположить, что редокс-механизм является ответственным за активность комплексов **1a**,**b**.

Ферментативное генерирование супероксид анион-радикала $O_2^{-\cdot}$ в системе ксантин–ксантиноксидаза. Известно, что сопряженным процессом окисления, катализируемого липоксигеназой, является образование супероксид анион-радикала[12,40,41]. Способность восстанавливать супероксид анион-радикал была опре-

делена[26] для исследуемых соединений с использованием системы ксантин–ксантиноксидаза, в которой генерируется $O_2^{-\cdot}$. Отдельно были проведены эксперименты по оценке влияния комплексов **1a**,**b** на активность ксантиноксидазы, которую определяли по скорости образования мочевой кислоты[26]. Показано, что соединения **1a**,**b** не оказывают влияния на активность фермента. Радикалы **2a**,**b** не оказывают влияния на скорость образования формазана в реакционной смеси. В то же время комплексы меди на их основе **1a**,**b** обладают выраженной способностью связывать супероксид анион-радикал. Зависимости изменения скорости накопления формазана в системе ксантин–ксантиноксидаза от концентрации комплексов **1a**,**b** приведены на рис. 11.

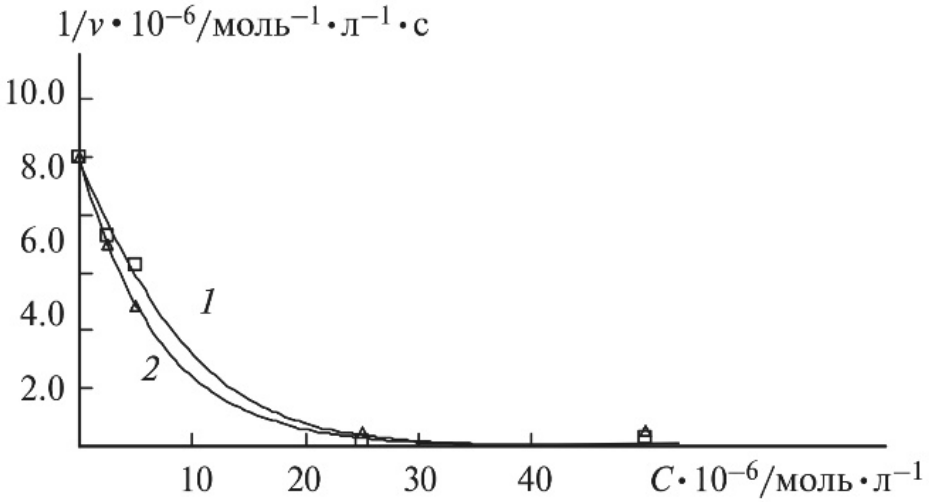


Рис. 11. Изменение скорости накопления формазана в системе ксантин–ксантиноксидаза в зависимости от концентрации комплексов **1a** (*1*) и **1b** (*2*).

Для комплексов **1a**,**b** значения $IC_{50}$ составляют (8.7±0.8) • $10^{-6}$ и (4.4+0.5) • $10^{-6}$ моль • $л^{-1}$ соответственно. Полученные величины характеризуют данные комплексы как активные восстановители супероксид анион-радикала, что позволяет предположить их антиоксидантную эффективность в процессах генерирования активных метаболитов кислорода, в частности $O_2^{-\cdot}$.

Таким образом, комплексы меди со стабильными нитронилнитроксильными радикалами являются обратимыми ингибиторами LOX-1, а также обладают высокой антиоксидантной активностью в процессах радикального пероксидного окисления субстратов и в процессе образования супероксид анион-радикала.

Работа выполнена при финансовой поддержке Российского фонда фундаментальных исследований (проекты № 09-03-00090, № 11-03-12088-офи-м и№ 11-03-01165), Отделения химии и наук о материалах Российской академии наук (проект по программе № 9 «Медицинская химия»), Междисциплинарного интеграционного проекта Сибирского отделения РАН (проект № 93).

## Список литературы


1. C. D. Funk, *Science,* 2001, **294**, 1871.
2. A. Andreou, I. Feussner, *Phytochem.,* 2009, **70**, 1504.
3. H. Nakano, T. Inoue, N. Kawasaki, H. Miyataka, H. Matsumoto, T. Taguchi, N. Inagaki, H. Nagai, T. Satoh, *Bioorg. Med. Chem.,* 2000, **8,** 373.
4. H. Hussain, L. P. Shornick, V. R. Shannon, J. D. Wilson, C. D. Funk, A P. Pentland, M. J. Holtzman, *Am. I. Physiol.,* 1994, **266**, C243.
5. D. Harats, A. Shaish, J. George, M. Mulkins, H. Kurihara, H. Levkovitz, E. Sigal, *Arterioscler. Thromb. Vasc. Biol.,* 2000, **20**, 2100.
6. V. E. Steele, C. A. Holmes, E. T. Hawk, L. Kopelovich, R. A. Lubet, J. A Crowell, C. C. Sigman, G. J. Kelloff, *Cancer Epidemiol. Biomarkers Prev.,* 1999, **8**, 467.
7. I. Avis, S. H. Hong, A. Martinez, T. Moody, Y. H. Choi, J. Trepel, R. Das, M. Jett, J. L. Mulshine, *FASEB J.,* 2001, 15, U277.
8. B. Halliwell, J. M. C. Gutterridge, *Free Radicals in Biology and Medicine,* 2nd ed., Clarendon, Oxford, 1989.
9. O. K. Mirzoeva, G. F. Sud'ina, M. A. Pushkareva, G. A. Korshunova, N.V. Sumbatyan, S. D. Varfolomeev, *Bioorg. Khim,* 1995, **21**, 143 [*Russ. J. Bioorg. Chern. (Engl. Transl.),* 1995, **21**, No. 2].
10. O. K. Mirzoeva, G. F. Sud'ina, M. A. Pushkareva, S. D. Varfolomeev, *FEBS Lett.,* 1995, **377**, 306.
11. G. F. Sud'ina, O. K. Mirzoeva, M. A. Pushkareva, G. A. Korshunova, N. V. Sumbatyan, S. D. Varfolomeev, *FEBS Lett.,* 1993, **329**, 21.
12. O. Weiz, D. Steinhilber, *Pharmacol. Therapeut.,* 2006, **112**, 701.
13. G. W. Carter, P. R. Young, D. H. Albert, J. Bouska, R. Dyer, R. L. Bell, *J. Pharmacol. Exp. Therapeut.,* 1991, **256**, 929.
14. P. C. Christidis, Z. D. Georgousis, D. Hadjipavlou-Litina, C. A. Bolos, *J. Mol. Struct.,* 2008, **872**, 73.
15. C. T. Dillon, T. W. Hambley, B. J. Kennedy, P. A Lay, J. E. Weder, *Met. Ions Biol. Syst.,* 2004, **41**, 253.
16. B. P. Soule, F. Hyodo, K. Matsumoto, N. L. Simone, J. A. Cook, M. C. Krishna, J. B. Mitchell, *Free Radical Biol. Med.,* 2007, **42**, 1632.
17. V.I. Ovcharenko, R.Z. Sagdeev, *Usp. Khim*., 1999, **68**, 381 [*Russ. Chem. Rev.* (*Engl. Transl*.)*,* 1999, **68**, 345].
18. V.I. Ovcharenko, K. Yu. Maryunina, S. V. Fokina, E. V. Tret'yakov, G. V. Romanenko, V. N. Ikorskii, *Isv. Akad. Nauk, Ser. Khim.*, 2004, 2304 [*Russ. Chern. Bull., Int. Ed.,* 2004, **53**, 2406].
19. V. I. Ovcharenko, in *Stable Radicals: Fundamentals and Applied Aspects of Odd-Electron Compounds*, Ed. R. Hicks, Wiley-VCH, 2010, p. 461.
20. E. Fursova, G. Romanenko, V. Ikorskii, V. Ovcharenko, *Polyhedron,* 2003, **22**, 1957.
21. E. Fursova, G. Romanenko, V. Ikorskii, V. Ovcharenko, *IV Phys.,* 2004, **114**, 621.
22. V. I. Ovcharenko, E. Yu. Fursova, T. G. Tolstikova, K. N. Sorokina, A. Yu. Letyagin, A.A. Savelov, *Dokl. Akad. Nauk*, 2005, **404**, 198 [*Dokl. Chem.* (*Engl. Transl.*), 2005, **404**, 171].
23. A. J. Gordon, R. A. Ford, *The Chemist's Companion,* Wiley, New York, 422 pp.
24. M. N. Xanthopoulou, S. K. Hadjikakou, N. Hadjiliadis, E. R. Milaeva, J. A. Gracheva, V. Yu. Tyurin, N. Kourkoumelis, K. C. Christoforidis, A. K. Metsios, S. Karkabounas, K. Charalabopoulos, *Eur. J. Med. Chern.,* 2008, **43**, 327.
25. I. Ozturk, S. Filimonova, S. K. Hadjikakou, N. Kourkoumelis, V. Dokorou, M. J. Manos,

A J. Tasiopoulos, M. M. Barsan, I. S. Butler, E. R. Milaeva, J. Balzarini, N. Hadjiliadis, *Inorg. Chem.,* 2010, **49**, 488.
26. I. Kubo, N. Masuoka, T. J. Ha, K. Tsujimoto, *Food Chem.,* 2006, **99**, 555.
27. J. K. Callaway, P. M. Beart, B. Jarrott, *J. Pharmacol. Toxicol. Meth.,* 1998, **39**, 155.
28. I. Gulcin, *Chem. Biol. Interact.,* 2009, **179**, 71.
29. P. Molyneux, *J. Sci. Technol.,* 2004, **26**, 211.
30. R. Apak, K. Guglu, M. Ozyurek, S. Karademir, *J. Agric. Food Chem.,* 2004, **52**, 7970.
31. G. M. Morris, D. S. Goodsell, R. S. Halliday, R. Huey, W. E. Hart, R. K Belew, A J. Olson, *J. Comput. Chem.,* 1998, **19**, 1639.
32. R. Huey, G. M. Morris, A. J. Olson, D. S. Goodsell, *J. Comput. Chem.,* 2007, **28**, 1145.
33. H. M. Berman, J. Westbrook, Z. Feng, G. Gilliland, T. N. Bhat, H. Weissig, I. N. Shindyalov, P. E. Bourne, *Nucleic Acids Res.,* 2000, **28**, 235.
34. E. Skrzypczak-Jankun, R. A. Bross, R. T. Carroll, W. R. Dunham, M. O. Funk, Jr., *J. Am. Chem. Soc.,* 2001, **123**, 10814.
35. M. Clark, R. D. Cramer III, N. Van Opdenbosch, *J. Comput. Chem.,* 1989, **10**, 982.
36. *SYBYL 8.0,* Tripos Inc., 1699 South Hanley Rd., St. Louis (MI), 63144, USA.
37. A. L. Spek, *Acta Crystallogr., Sect. D: Biol. Crystallogr*., 2009, **65**, 148.
38. M. F. Sanner, *J. Mol. Graphics Modell.,* 1999, **17**, 57.
39. J. Gasteiger, M. Marsili, *Tetrahedron,* 1980, **36**, 3219.
40. E. Pontiki, D. Hadjipavlou-Litina, K. Litinas, O. Nicolotti, A. Carotti, *Eur. J. Med. Chem.,* 2011, **46**, 191.
41. E. Novo, M. Parola, *Fibrogenesis Tissue Repair,* 2008, **1**, No. 1, 5.

*Поступила в редакцию 23 июня 2011;*
*после доработки – 18 ноября 2011*

*Bioorganic & Medicinal Chemistry. Vol. 24 (4), 712-720, 2016*

# SYNTHESIS AND BIOLOGICAL EVALUATION OF NOVEL 5-HYDROXYLAMINOISOXAZOLE DERIVATIVES AS LIPOXYGENASE INHIBITORS AND METABOLISM ENHANCING AGENTS

**E.B. Averina, D.A. Vasilenko, Yu.A. Gracheva, Yu.K. Grishin, E.V. Radchenko, V.V. Burmistrov, G.M. Butov, M.E. Neganova, T.P. Serkova, O.M. Redkozubova, E.F. Shevtsova, E.R. Milaeva, T.S. Kuznetsova, N.S. Zefirov**

*Lomonosov Moscow State University, Department of Chemistry, Moscow, Russia*
*Institute of Physiologically Active Compounds of the Russian Academy of Sciences, Chernogolovka, Moscow Region, Russia*
*Volgograd State Technical University, Volgograd, Russia*

A versatile synthesis of novel 5-hydroxylaminoisoxazoles bearing adamantane moieties has been accomplished using the heterocyclization reactions of readily available unsaturated esters by the treatment with tetranitromethane in the presence of triethylamine and subsequent reduction of resulting 5-nitroisoxazoles by $SnCl_2$ with the participation of THF. A number of obtained isoxazole derivatives were evaluated for their antioxidative activity, inhibition of lipoxygenases and impact on the rat liver mitochondria. The majority of tested compounds demonstrated moderate antiradical activity in DPPH test (up to $EC_{50}$ 16 μM). The same compounds strongly inhibited soybean lipoxygenase (up to $IC_{50}$ 0.4 μM) and $Fe^{2+}$- and $Fe^{3+}$-induced lipid peroxidation (LP) of rat brain cortex homogenate (up to $IC_{50}$ 0.3 μM). All tested isoxazole derivatives promoted the phosphorylating respiratory activity simultaneously with maximal stimulated respiratory activity of mitochondria and do not reveal any toxicity towards the primary culture of rat cortex neurons.

## 1. Introduction

Oxidative stress induced by reactive oxygen species has been implicated in the pathogenesis of various diseases and disorders. One of the main features and biomarkers for oxidative stress is the lipid peroxidation, which may be induced through non-enzymatic or enzymatic pathways involving lipoxygenase, cyclooxygenase or cytochrome P450. Lipoxygenases (LOXs) are non-heme iron-containing dioxygenases which catalyze the conversion of unsaturated fatty acids containing one or more *cis*,*cis*-pentadiene fragments into hydroperoxy fatty acids.[1-4] This process is the first step in a series of reactions producing inflammatory-mediating leukotrienes (LTs) and hydroxyeicosatetraenoic acids (HETEs) which are associated with a variety of disease states including asthma, rheumatoid arthritis, inflammatory bowel disease, psoriasis, and allergy.[1] The human lipoxygenases are indisputably involved in human pathology not only due to

their essential role in LTs and HETEs biosynthesis, but also due to their involvement in induction of lipid peroxidation. Therefore, a search for selective lipoxygenase inhibitors and multitarget antioxidants with LOXinhibiting and antioxidant activities is of a considerable interest. Although many attempts to develop selective LOX inhibitors have been made.[5-10] Zileuton, which is an iron-binding 5-LOX inhibitor with antiasthmatic action, remains the only approved drug product.

Recently we described the first synthesis of previously unknown 5-[hydroxy(tetrahydrofuran-2-yl)amino]isoxazoles **1** via unusual reduction of 5-nitroisoxazoles with the participation of THF used as solvent,[11] as well as the novel approach to hardly accessible functionalized 5-nitroisoxazoles based on the heterocyclization of electrophilic alkenes under the action of tetranitromethane (TNM) – triethylamine complex[1213] (Scheme 1).

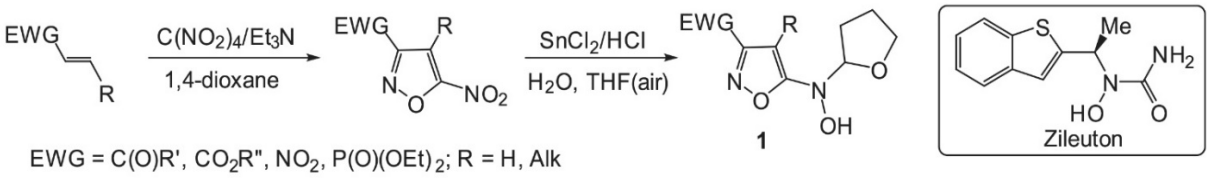


Scheme 1. A described procedure[11-13] for the synthesis of *N*-hydroxy lam inoisoxazoles **1**.

In the present work we proposed a new scaffold for structure design of LOXs inhibitors – novel N-hydroxylaminoisoxazoles 1 possessing the fragment of THF which appear to be certain structural analogue of Zileuton.

All lipoxygenases are homologues and contain the same two domains: N-terminal 'C2-like' domain and a larger C-terminal catalytic domain containing a single atom of non-heme iron.[1] Indeed, it was shown in various investigations that the molecules with bulky lipophilic fragments generally exhibit an efficient inhibition of enzymes, including LOXs.[14-19] Particularly adamantane-based compounds, due to their specific conformation, frequently demonstrated the enhanced interaction with the target enzyme's active site.[20] Moreover, the introduction of adamantane moieties increases the membrane permeability of the modified compound.[20] Therefore we introduced the adamantane framework in target heterocycles 1 employing synthetically available α,β-unsaturated esters for heterocyclization. The versatility of our synthetic methodology allowed to prepare a library of compounds 1 by varying the substituents in the 3-position of isoxazole core.

Herein, we report the design and synthesis of novel adamantane-containing 5-[hydroxy(tetrahydrofuran-2-yl)amino]isoxazoles **1** and evaluation of their antioxidative potential, as well as LOX inhibition and mitochondria functional characteristics.

**Table 1**
Synthesis of 5-[hydroxy(tetrahydrofuran-2-yl)amino]isoxazoles **1a**–**h** from adamantane-containing alcohols

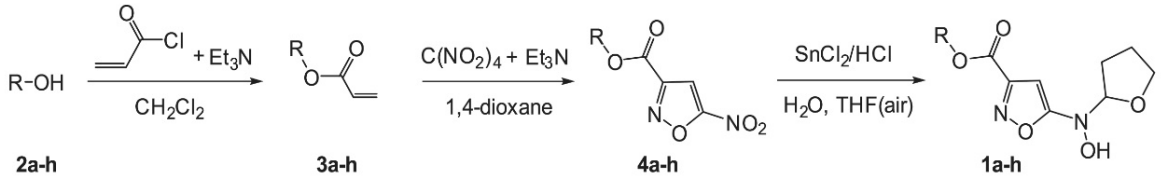


| Entry | Compound | R | Yield[a] % | | |
|---|---|---|---|---|---|
| | | | **3** | **4** | **1** |
| 1 | **a** | 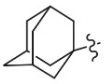 | 84 | 57 | 46 |
| 2 | **b** | 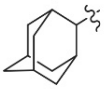 | 90 | 58 | 50 |
| 3 | **c** | 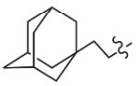 | 78 | 84 | 47 |
| 4 | **d** | 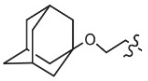 | 72 | 55 | 52 |
| 5 | **e** | 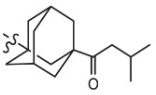 | 61 | 33 | 54 |
| 6 | **f** | 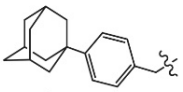 | 82 | 36 | 62 |
| 7 | **g** | | 54 | 63 | 60 |
| 8 | **h** | 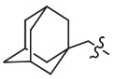 | 78 | 68 | 75 |

[a] Isolated yields.

## 2. Results and discussion

### *2.1. Chemistry*

For the synthesis of novel hydroxylamines la-h, we proposed a three-step scheme including the acylation of adamantane-containing alcohols **2a-h** by acryloyl chloride followed by the heterocyclization of unsaturated esters **3a-h** employing our previously published procedure[12,13] (Table 1). Subsequent reduction of 5-nitroisoxazoles **4a-h** by $SnCl_2$–HCl in THF resulted in desired heterocycles **1a-h.**

The preparation of the starting alkenes **3a-h** from the alcohols bearing the adamantane moieties proceeds smoothly under reported conditions[21] using equimolar amounts of acryloyl chloride and $Et_3N$. Somewhat poorer yield was obtained for alkene **3g** (Table 1, entry 7) due to low solubility of corresponding alcohol in $CH_2Cl_2$. Dilution of the reaction mixture or the use of ether solvents ($Et_2O$, THF, 1,4-dioxane) did not provide any substantial increase in the alkene yield. The electrophilic alkenes **3a-h** were involved in the heterocyclization upon the treatment by *in situ* generated

$C(NO_2)_4$–$Et_3N$ complex resulting in 5-nitroisoxazoles **4a-h** with satisfactory yields. In some cases the decrease in yields of the heterocycles **4e,** f may result from the partial oxidation of alkene **3f** (Table 1, entry 6) under the reaction conditions or from the formation of small amount of trinitropropanoic acid esters[12] (Table 1, entry 5). For the successful transformation of 5-nitroisoxazoles **4a**-**h** into desired 5-[hydroxy(tetrahydrofuran-2-yl)amino]isoxazoles **1a**-**h**, THF, previously distilled from NaOH, must be bubbled by air for 20 h. All synthesized compounds were characterized and identified using $^1H$ and $^{13}C$ NMR and HRMS.

### *2.2.Biological evaluation*

#### *2.2.1. Lipoxygenase inhibitory assessment*

Since peroxyl radical is formed in all LOX-catalyzed reactions, LOX activation evokes lipid peroxidation. During oxidative stress, LOX can exhibit uncontrolled activity and may cause cell membrane destruction by phospholipid oxidation. Thus, lipoxygenase inhibition under pathologic conditions helps to decrease the level of total oxidative stress.[22] The LOX inhibition activity of the studied compounds was evaluated in order to determine capacity of compounds to decrease oxidative stress level. Lipoxygenase-1 from soybeans (LOX-1) has been used in the present study since it shares many important characteristics with LOXs from other sources and represents a routine model for studies on animal system.[23-25]

Compounds **1a-c,g,h** (Table 2, entries 1-3, 7, 8) demonstrate $IC_{50}$ values lower than 50 μM and can be considered as promising lipoxygenase inhibitors. The most active compounds were **1b,c,g** (Table 2, entries 2, 3, 7), the $IC_{50}$ values for these compounds were in the range from 0.4 to 4 μM. In the presence of **1g** – one of the most

**Table 2** Redox activity and LOX-inhibition (soybean lipoxygenase LOX-1) of 5-[hydroxy(tetrahydrofuran-2-yl)amino]isoxazoles **1a**-**h**

| Entry | Compound | LP, $Fe^{3+}$ $IC_{50}$ μM | LP, $Fe^{2+}$ $IC_{50}$ μM | DPPH ($EC_{50}$ μM) | LOX-1 inhibition ICso, μM |
|---|---|---|---|---|---|
| 1 | **1a** | 137 ± 0.32 | 033 ± 0.19 | 16 ± 2 | 25 ± 3 |
| 2 | **1b** | 121 ± 0.20 | 10.54 ± 134 | 71 ± 8 | 4 ± 0.6 |
| 3 | **1c** | 525 ± 0.8 | 3.15 ± 0.93 | 21 ± 3 | 0.4 ± 0.1 |
| 4 | **1d** | 35 ± 2 | na[a] | >100 | na[a] |
| 5 | **1e** | 1.58 ± 0.07 | 2.74 ± 1.79 | >100 | 277 ± 6 |
| 6 | **1f** | 5.45 ± 1.52 | 3.41 ± 1.04 | >100 | na[a] |
| 7 | **1g** | 1.48 ± 023 | 5.16 ± 2.4 | 38 ± 5 | 1 ± 0.4 |
| 8 | **1h** | 22 ± 3 | 6.58 ± 1.44 | 70 ± 5 | 16 ± 2 |

[a] No active.

active compounds – the activity of LOX was inhibited almost completely at 50 μM of **1g** (Fig. 1). According to literature data[26] and our experimental results ($IC_{50}$ >100 μM) the reference compound Zileuton does not inhibit the soybean LOX, but its inhibitory activity towards human LOX-5 ($IC_{50}$ = 1.1 μM)[7,26] is similar to that of isoxazoles **1b,c,g** towards soybean.

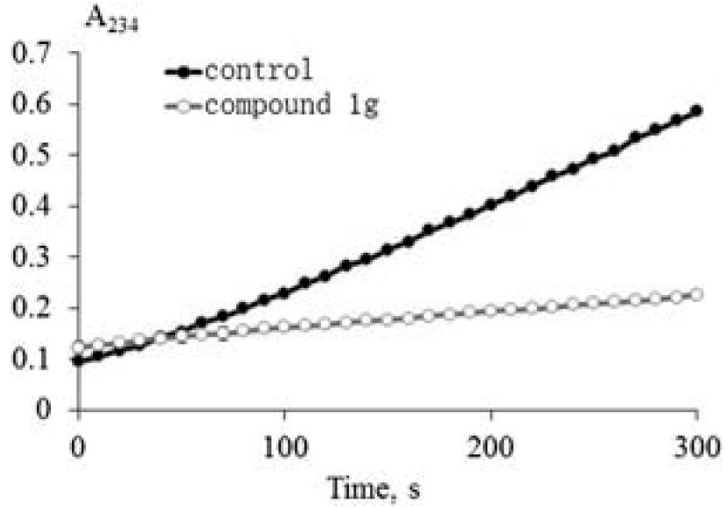


**Figure 1.** Kinetic curves of linoleic acid hydroperoxide formation in the presence of 50 μM **1g.**

*2.2.2. DPPH radical scavenging activity*

The radical scavenging activity of compounds **1a-h** has been studied in the process of hydrogen atom transfer from the molecule to the stable free radical 2,2-diphenyl-1-picrylhydrazyl (DPPH) producing diphenylpicrylhydrazine and radicals which can undergo further reactions such as coupling, fragmentation and addition. The reaction is accompanied by a color change from violet to yellow, which can be monitored spectrophotometrically by measuring the decrease in absorbance at 517 nm.[27] Antiradical activity was evaluated as the amount of antioxidant necessary to decrease the initial concentration of DPPH by 50% (Efficient Concentration = $EC_{50}$). The $EC_{50}$ values reflect the reactivity of a compound toward DPPH but give limited information on the mechanistic outcome of the reaction. The results of the DPPH test at 20°C show that the most active compounds were **1a-c, g** (Table 2, entries 1-3, 8). The antiradical activity was the highest for compound la (Table 2, entry 1) which completed the reaction with DPPH after several seconds at equimolar ratio of reagents. The compounds **1a-c,g,h** were found to demonstrate high antiradical activity. To compare the antioxidative properties of the tested compounds with the standard, the antioxidative potency of Zileuton was estimated in our experimental conditions. The obtained data clearly indicate that the antiradical activity of Zileuton (this work: $EC_{50}$ = 14 μM; for comparison, literature data: $IC_{50}$ = 43 μM[28]) is also similar to that of isoxazoles **1a-c, g, h.**

### *2.2.3. Influence on lipid peroxidation*

Not only lipoxygenases (LOX), but also the mitochondrial respiratory chain, nitric oxide synthase, NADPH oxidase and cyclooxygenases (COX) are the main sources of reactive oxygen species in the cells. It was shown that noncompetitive LOX inhibitors may act as reducing agents or iron ligands which affect not only the LOX activity, but also the LOX-independent oxidative stress.[28] Inhibitors of LOX also possess the antioxidant activity, not only by inhibiting the enzymatic activity of LOXs, but also directly by scavenging free radicals. Zileuton, an iron-chelating inhibitor of 5-LOX, was a rather weak free radical scavenger and antioxidant with $IC_{50} > 50$ μM against $Fe^{2+}$-induced lipid peroxidation in rat brain homogenate.[28] However, the new 5-hydroxylaminoisoxazoles **1a**-**h** reveal significant antioxidant properties. We have studied the influence of these compounds on oxidative degradation of lipids in rat brain homogenate induced by ferrous and ferric ions. All synthesized compounds inhibit $Fe^{2+}$- and $Fe^{3+}$-induced lipid peroxidation (LP) of rat brain cortex homogenate. The most active was compound **1a**, but a structurally similar compound **1h** reveals lower activity and the compound **1d** is the weakest inhibitor of LP. The inhibition of ferric and ferrous ion-induced lipid peroxidation by 5-hydroxylaminoisoxazoles for all compounds except le and If has some correlation with their free radical scavenging capacity (Table 2).

### *2.2.4. Cell viability*

At the next step of our work we have studied the influence of the compounds **1a**-**h** on the viability of the cultured tumor cells (neuroblastoma SH-SY5Y) and primary neuron culture from rat brain cortex (Fig. 2). Cell viability was measured by standard MTT (3-(4,5-dimethyl-2-thiazolyl)-2,5-diphenyl-2-tetrazolium bromide) assay after 24 h incubation with 30 μM of isoxazoles **1a**-**h**. Cell viability significantly decreased in neuroblastoma cells (to 22 ± 1% at 30 μM of **1h** in comparison with the control). In primary cortex neurons only compound 1c decreased the viability of cells (to 77 ± 5%). Moreover, for compounds **1d**-**h** a statistically significant increase in the MTT-connected activity was observed. MTT is a tetrazolium salt reduced to purple formazan crystals mainly by mitochondrial succinate dehydrogenase. Thus the use of this assay as an indicator of metabolically active mitochondria may overestimate the number of viable cells due to increasing activity of succinate dehydrogenase or other cellular dehydrogenases in response to some compounds. Thus we have studied the direct influence of our compounds on mitochondrial respiration and other mitochondrial functions.

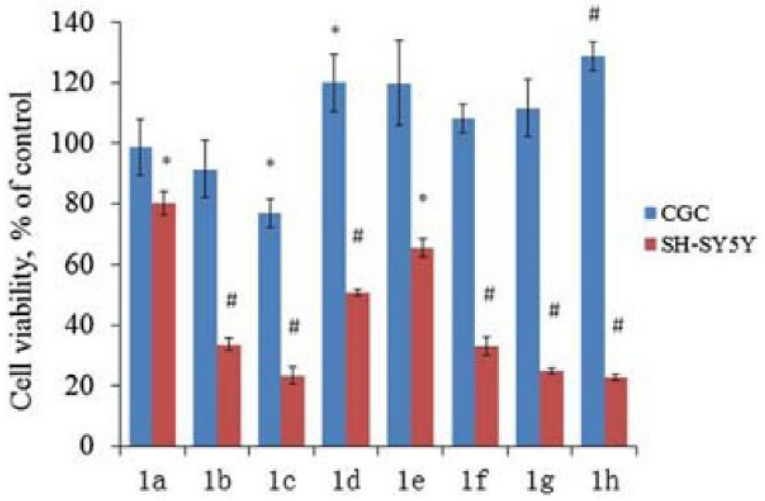


**Figure 2.** Influence of isoxazoles **1a-h** on the viability of rat cerebellar granule cells (CGC) and neuroblastoma SH-SY5Y. Control samples contain DMSO (≤1%). Indicates $p < 0.05$, $*p < 0.01$ compared to the control cultures (T-test).

### *2.2.5. Mitochondrial function measurements*

Oxygen consumption rate (OCR) by mitochondria was determined using the Seahorse extracellular flux (XF-96) analyzer (Seahorse Bioscience, Chicopee, MA, USA). Respiration of the mitochondria (0.5 mg protein/well) with or without 5-hydroxylaminoisoxazoles **1a,c-h** was sequentially measured in a coupled state with substrate of complex **II** succinate and rotenone to inhibit complex **I** of respiratory chain present (basal respiration), followed by phosphorylating respiration, in the presence of ADP and substrate, nonphosphorylating or resting respiration induced with the addition of oligomycin and then maximal uncoupler-stimulated respiration after addition of uncoupler FCCP, followed by nonrespiratory oxygen consumption in the presence of inhibitor of complex **II** antimycin A (Fig. 3a).

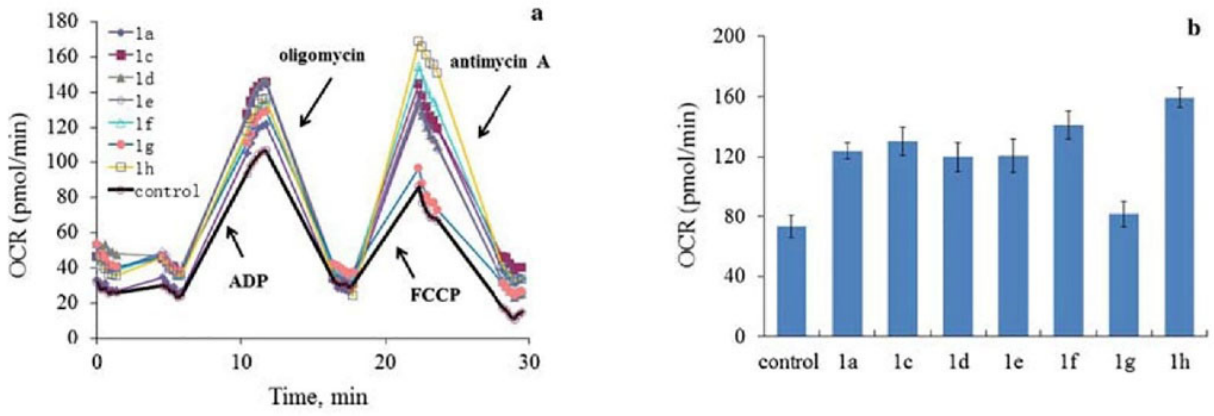


**Figure 3.** Influence of 5-[hydroxy(tetrahydrofuran-2-yl)amino] isoxazoles on representative respirometric profile of mitochondria isolated from rat liver in the presence of 10 μM of compounds **1a**,**c-h** (*a*) and FCCP-stimulated OCR (*b*). Final concentrations of additives after port injections were 4 mM ADP; 2,5 μg/ml oligomycin; 4 μM FCCP; and 4 μM antimycin A. Calculated RCR was 7.95 ± 0.8.

Treatment of mitochondria with isoxazoles **1a,c-h** led to an increase in phosphorylating respiration and moreover, in maximum stimulated respiration after uncoupling of oxygen consumption (or electron transport) and ATP synthesis with FCCP treatment (Fig. 3b). But there was no noted increase in OCR in the presence of oligomycin and we cannot propose the uncoupling mode of action of the compounds on mitochondrial respiratory chain.

The electron transport along the mitochondrial respiratory chain is accompanied by the formation of electrochemical gradient of hydrogen ions at the inner mitochondrial membrane. The electrical part of electrochemical potential, i.e. $\Delta\Psi$, can be measured in isolated mitochondria by changing the absorbance of the cationic dye safranine. We have shown that compounds **1a**-**h** do not influence $\Delta\Psi$ and calcium-induced depolarization of mitochondria regardless of the used substrates of mitochondrial respiration: succinate and rotenone or glutamate/malate (data not shown). These results are in agreement with the above mentioned absence of any change in oligomycin-dependent oxygen consumption. The increase of the phosphorylating respiration (with succinate as substrate) and of the maximal stimulated respiration caused by the studied compounds may be the reason of the overestimated MTT-dependent index of cell viability. However, more significantly, these results allow one to suggest that 5-[hydroxy(tetrahydrofuran-2-yl)amino]isoxazoles **1a**-**h** may be useful as a scaffold for the development of novel metabolic enhancers.

### *2.3.Structure-activity relationships and physico-chemical properties*

Analysis of this limited series of compounds suggests that their biological activity is defined by a common structural scaffold. The elongation of the linker between adamantane and isoxazole moieties (**1d**,**f**) as well as the enlarging of the adamantane core (**1e**) lead to a decrease in antiradical activities and inhibition of lipoxygenase.

We have performed a preliminary computational estimation of some physicochemical and pharmacokinetic properties of the studied compounds that may be relevant in the drug development context. In particular, the lipophilicity (logP) and aqueous solubility values were predicted as well as the blood-brain barrier permeability (LogBB), human intestinal absorption and cardiotoxicity potential (hERG affinity). The predicted values are presented in the Supplementary Material. No direct correlations between the physicochemical parameters and *in vitro* biological results can be discerned. However, for most of the compounds (except **1f**) the properties seem quite acceptable for a lead candidate. Their logP values are about 2–2.5 and the solubility is about $10^{-4}$ M that is significantly higher than $IC_{50}$. LogBB for all compounds is close to zero that corresponds to about 50% brain penetration, intestinal absorption is about 80–100%, and hERG p$K_i$ is about 4.5. In fact, the properties of the studied compounds are comparable or better than those of the reference compounds (Zileuton, BW-B 70C

and Phenidone). In particular, the predicted blood-brain barrier permeability of the adamantane derivatives is significantly higher than that of Zileuton and BW-B 70C, which may be important in the therapy of the brain oxidative stress.

## 3. Conclusions

In conclusion, we have developed a universal synthetic methodology for the synthesis of isoxazole derivatives with a wide range of substituents based on the heterocyclization of readily available unsaturated esters by the treatment of TNM-TEA complex and subsequent reduction of the resulting 5-nitroisoxazoles by $SnCl_2$ with the participation of THF (solvent). A number of 5-[hydroxy(tetrahydrofuran-2-yl)amino]isoxazoles containing a bulky adamantane framework were synthesized using this method. The obtained compounds were evaluated for their antioxidative activity, inhibition of lipoxygenase and impact on rat liver mitochondrial function. The compounds **1a-c,g,h** were found to demonstrate high antioxidative activity, as well as high inhibitory activity towards lipoxygenase. All tested compounds promote the phosphorylating respiratory activity simultaneously with maximal stimulated respiratory activity of mitochondria and do not reveal any toxicity towards the primary culture of rat cortex neurons. The attempt to correlate the *in vitro* biological results with some estimated physicochemical and pharmacokinetic properties was not quite successful. In particular, lipophilicity does not have a significant influence on the biological activity while the steric requirements are more important. However, the predicted properties are comparable or better than those of the reference compounds and seem quite acceptable for a lead candidate. Thus, novel 5-[hydroxy(tetrahydrofuran-2-yl)amino]isoxazoles may be considered as promising and useful scaffold for the creation of novel drugs with antioxidant and metabolic enhancing properties.

## 4. Experimental

### *4.1. Chemistry*

*General experimental details*

NMR spectra were recorded on spectrometer Agilent 400-MR (400.0 MHz for $^1H$; 100.6 MHz for $^{13}C$) at room temperature; chemical shifts were measured with reference to the solvent ($CDCl_3$, ($\delta_H$ = 7.24 ppm, $\delta_C$ = 77.0 ppm). Chemical shifts ($\delta$) are given in ppm; *J* values are given in Hz. When necessary, assignments of signals in NMR spectra were made using 2D techniques. Accurate mass measurements (HRMS) were measured on Jeol GCMate II mass spectrometer (70 eV). Analytical thin layer chromatography was carried out with Silufol silica gel plates (supported on aluminum); the detection was done by UV lamp (254 and 365 nm). Column chromatography was performed on silica gel (230-400 mesh, Merck). Compounds: **2a,**[29] **2b,**[30] **2c,**[31] **2d,**[32] **2e,**[33,34]

**2f,**[35] **2g, 2h,**[37] **3h,**[21] **4h,**[11] **1h,**[11] were synthesized by known procedures. All other starting materials were commercially available. All reagents except commercial products of satisfactory quality were purified by literature procedures prior to use.

### *4.2. Biological studies*

#### *4.2.1. Animals*

The experiments were carried out on outbreed albino male rats weighing 200–300 g. The animals had free access to food and water.

#### *4.2.2. Brain homogenate*

The animals were narcotized with carbon dioxide and decapitated using a guillotine. The procedure is in compliance with the Guidelines for Animal Experiments at IPAC RAS. Their brains were removed and homogenized in 120 mM KCl/20 mM HEPES on ice. For isolation of the subcellular fraction, the brain homogenate was centrifuged at 4000 rpm and supernatant was used in further experiments on the same day. The protein content in brain homogenate and mitochondria extracts was measured using a microbiuret method.[38]

#### *4.2.3. Mitochondria*

Mitochondria were isolated by conventional differential centrifugation from the livers of adult Wistar strain rats fasted overnight as in this work.[39] The standard mitochondrial fraction contained 130–150 mg of protein per liver. The mitochondria were stored at 4°C. Functional activity of the rat liver mitochondria remained constant for 2.5 to 4 h.

#### *4.2.4. Redox activity*

Lipid peroxidation intensity in brain homogenate was assayed using a modified TBA test.[40]

Fe(II)-chelatmg activity was evaluated using a modified method described elsewhere.[41]

The free radical scavenging activity was evaluated using the stable radical DPPH, according to the method described by Brand-Williams et al.[42] with a slight modification. All compounds were tested in 1:1 ratio expressed as moles of compound per mole of DPPH radical. A 1 mL sample of compound solution in methanol was added to 1 mL of DPPH solution in methanol so that the initial DPPH concentration in the cuvettes was 0.1 mM. The samples were incubated for 30 min at 20°C in methanol and the decrease in the absorbance values of DPPH solution was measured at 517 nm on the Thermo Scientific Multiscan Go microplate spectrophotometer. Results were expressed as scavenging activity, calculated as follows:

$$\text{Scavenging activity, \%} = [(A_0 - A_1)/A_0] \times 100$$

The concentration of the compound needed to decrease 50% of the initial substrate concentration ($EC_{50}$) is a parameter widely used to measure the antioxidant effect.[27] For determination of $EC_{50}$, the values of DPPH decrease after 30 min were used. The $EC_{50}$ values were calculated graphically by plotting scavenging activity against compound concentration. Different sample concentrations (0.01, 0.02, 0.05 and 0.1 mM) were used in order to obtain kinetic curves and to calculate the $EC_{50}$ values.

### *4.2.5. Lipoxygenase activity*

Lipoxidase (LOX) type 1-B from *Glycine max* (soybean), boric acid, linoleic acid, NaOH, ethanol (96%) were used with no further purification. LOX inhibition activity was determined spectrophotometrically by measuring the increase in absorbance at 234 nm for the oxidation of linoleic acid[43] The reaction mixture contained (final concentration) the test compounds, dissolved in DMSO at concentrations of 1-100 μM, or the solvent (control) and linoleic acid 100 μM, in borate buffer (pH = 9.0). The reaction was started by adding a lipoxygenase in amount of 500 units. Six different concentrations of each complex were used for the inhibition activity experiments. The increase in absorbance was recorded every 10 s during 10 min under controlled temperature 25°C.

The degree of LOX activity ($A$, %) in the presence of the complexes was calculated according to the following.[44]

$$A, \% = (\nu_0 \text{ in the presence of inhibitor}/\nu_0 \text{ in the absence of inhibitor}) \times 100,$$

where $\nu_0$ is the initial rate.

The value of the initial rate ($\nu_0$, μM $min^{-1}$) was calculated according to the formulas:

$$V_0 = \Delta C/\Delta t = \Delta A/\Delta t\varepsilon = \mathrm{tg}\alpha/\Delta t\varepsilon,$$

where $C$ is the product concentration (hydroperoxylinoleic add), $t$ is the reaction time, $\varepsilon$ is molar absorbance coefficient of hydroperoxylinoleic acid, $\mathrm{tg}\alpha$ is the slope of the kinetic curve plotted as absorbance versus time.

$IC_{50}$ values were obtained graphically by plotting logistic curve in coordinates inhibition activity ($A$, %) versus inhibitor concentration ([$I$], μM). The general curve equation is the following:

$$A, \% = 100 \times (1/(1+[I]/IC_{50}))$$

### *4.2.6. Mitochondrial membrane potential*

Mitochondrial membrane potential of isolated rat liver mitochondria was measured using potential-dependent indicator Safranine A at 25°C as in our previous work.[45]

### *4.2.7. Mitochondrial $O_2$ consumption rate (OCR) measurements*

Mitochondrial $O_2$ consumption measurements were made using an XF96 Extracellular Flux Analyzer (Seahorse Bioscience) as described.[46] Mitochondria were added to XF96 Analyzer plate with 30 μM of compounds in the presence of succinate (5 mM) and rotenone (1 μM) and then the measurement of the oxygen consumption was started. Final concentrations of the additives after port injections were 4 mM ADP; 2.5 μg/ml oligomycin; 4 μM FCCP; and 4 μM antimycin A. Calculated RCR was 7.95 ± 0.8. OCR was automatically calculated and recorded by the Seahorse XF96 software.

### *4.2.8. Viability of cultured neuroblastoma SH-SY5Ycells and rat cerebellar granule cells (CGC)*

Cell viability was evaluated with the 3-(4,5-dimethylthiazol-2-yl)-2,5-diphenyltetrazolium bromide (MTT) assay.[47] Briefly, the SH-SY5Y cells or primary culture of rat cerebellar granule cells were incubated with 30 μM of compounds or equal volume of vehicle (less than 1% of the total volume of medium under the cell layer) during 24 h. Then 20 μL of MTT (2mg/mL in PBS) were added to each well and the cells were incubated at 37°C for 2 h. The supernatants were aspirated carefully, 200 μl of DMSO were added to each well to dissolve the precipitate, and absorbance was measured at 570 nm using a microplate reader Victor (Perkin Elmer).

### *4.2.9. Statistics*

Data are presented as the mean ± SD. Statistical comparisons were made by Student's t-test. Values of $P < 0.05$ and $P < 0.01$ were considered significant.

## Acknowledgments

This work was partially supported by the RFBR (grant nos. 14-03-00469, 13-03-01151, 15-03-03057) and the Presidium of RAS (Program N 8). The research work was carried out using NMR spectrometer Agilent 400-MR purchased under the program of MSU development. The equipment of Center for Collective Use IPAC RAS (agreement N14.621.21.0008, ID RFMEFI62114X0008) was used in the biological experiments.

## References and notes

1. Haeggström, J. Z.; Funk, C. D. *Chern. Rev.* **2011**, *111*, 5866.
2. Gilbert, N. C.; Bartlett, S. G.; Waight, M. T.; Neau, D. B.; Boeglin, W. E.; Brash, A. R.; Newcomer, M. E. *Science* **2011**, *331*, 217.
3. Charlier, C.; Michaux, C. *Eur. J. Med. Chem*. **2003**, *38*, 645.
4. Brash, A. R. *J. Biol Chem*. **1999**, *274*, 23679.
5. Pergola, C.; Werz, O. *Expert Opin. Ther. Pat*. **2010**, *20*, 355.

6. Elkady, M.; Nieß, R.; Schaible, A. M.; Bauer, J.; Luderer, S.; Ambrosi, G.; Werz, O.; Laufer, S. *A. J. Med. Chem*. **2012**, *55*, 8958.
7. Wu, Y.; He. C.; Gao, Y.; He. S.; Liu. Y.; Lai. L. *J. Med. Chem*. **2012**, *55*, 2597.
8. Liedtke, A. J.; Keck, P. R. W. E. F.; Lehmann, F.; Koeberle, A.; Werz, O.; Laufer, S. A. *J. Med. Chem*. **2009**, *52*, 4968.
9. Chowdhury, M. A.; Abdellatif, K. R. A.; Dong, Y.; Das, D.; Suresh, M. R.; Knaus, E. E. *J. Med. Chem*. **2009**, *52*, 1525.
10. Peduto, A.; Bruno, F.; Dehm, F.; Krauth, V.; de Caprariis, P.; Weinigel, C.; Barz, D.; Massa, A.; De Rosa, M.; Werz, O.; Filosa, R. *Eur. J. Med. Chem*. **2014**, *81*, 492.
11. Averina, E. B.; Vasilenko, D. A.; Samoilichenko, Y. V.; Grishin, Y. K.; Rybakov, V. B.; Kuznetsova, T. S.; Zefirov, N. S. *Synthesis* **2014**, *46*, 1107.
12. Volkova, Y. A.; Averina, E. B.; Grishin, Y. K.; Bruheim, P.; Kuznetsova, T. S.; Zefirov, N. S. *J. Org. Chem*. **2010**, *75*, 3047.
13. Regiochemistry reported in Ref. 12 has been revised in Ref 13: Averina, E. B.; Volkova, Y. A.; Samoilichenko, Y. V.; Grishin, Y. K.; Rybakov, V. B.; Kutateladze, A. G.; Elyashberg, M. E.; Kuznetsova, T. S.; Zefirov, N. S. *Tetrahedron Lett*. **2012**, *53*, 1472.
14. Ulbrich, H.; Fiebich, B.; Dannhardt, G. *Eur. J. Med. Chem*. **2002**, 37, 953.
15. Pontiki, E.; Hadjipavlou-Litina, D.; Litinas, K.; Nicolotti, O.; Carotti, A. *Eur. J. Med. Chem*. **2011**, *46*, 191.
16. Pavi, K.; Perkovi, I.; Cindri, M.; Pranji, M.; Martin-Kleiner, I.; Kralj, M.; Schols, D.; Hadjipavlou-Litina, D.; Katsori, A.-M.; Zorc, B. *Eur. J. Med. Chem*. **2014**, *86*, 502.
17. Pontiki, E.; Hadjipavlou-Litina, D. *Med. Res. Rev*. **2008**, *28*, 39.
18. Milaeva, E. R.; Orlova, S. L; Osolodkin, D. I.; Palyulin, V. A.; Fursova, E. Yu.; Ovcharenko, V. I.; Zefirov, N. S. *Russ. Chem. Bull Int Ed*. 2011, *60*, 2564.
19. Milaeva, E. R.; Meleshonkova, N. N.; Shpakovsky, D. B.; Paulavets, V. V.; Orlova, S. I.; Osolodkin, D. I.; Palyulin, V. A.; Loginov, S. V.; Storozhenko, P. A.; Zefirov, N. S. *Doklady Chem*. **2012**, *443*, 77.
20. Wanka, L.; Iqbal, K.; Schreiner, P. R. *Chem Rev*. **2013**, *113*, 3516.
21. Wang, W.; Li, Y.; Sun, M.; Zhou, C.; Zhang, Y.; Lia, Y.; Yang, Q. *Chem. Commun*. **2012**, *48*, 6040.
22. Novo, E.; Parola, M. Fibrogenesis *Tissue Repair* **2008**, *1*, 58.
23. Ribeiro, D.; Freitas, M.; Tome, S. M.; Silva, A. M. S.; Porto, G.; Cabrita, E. J.; Marques, M. M. B.; Fernandes, E. *Eur. J. Med. Chem*. **2014**, *72*, 137.
24. Kouatly, O.; Geronikaki, A.; Kamoutsis, C.; Hadjipavlou-Litina, D.; Eleftheriou, P. *Eur. J. Med. Chem*. **2009**, *44*, 1198.
25. Lomnitski, L.; Bar-Natan, R.; Sklan, D.; Grossman, S. *Biochim. Biophys. Acta* **1993**, *1167*, 331.
26. Chan, K. Y.; Mohamad, K.; Ooi, A. J. A.; Imiyabir, Z.; Chung, L. Y. *Fitoterapia* **2012**, *83,* 961.
27. Molyneux, P. Songklanakarin *J. Set TechnoL* **2004**, *26*, 211.
28. Czapski, G. A.; Czubowicz, K.; Strosznajder, R. P. *Pharmacol Rep*. **2012**, *64*, 1179.
29. Baklan, V. F.; Khil'chevskii, A. N.; D'yakovskaya, V. M.; Sologub, L. S.; Kukhar, V. P. *Russ. J. Org. Chem*. **1993**, *29*, 454.
30. Schraml, J.; Vcelak, J.; Chvalovsky, V.; Engelhardt, G.; Jancke, H.; Vodicka, L.; Hlavaty, *J. Collect Czech. Chem. Commun*. **1978**, *43*, 3179.
31. Takahashi, N.; Mochizuki, D. US Patent; 5658923,1997; *Chem. Abstr*. **1997**, *127*, 248269.
32. Reznikov, A. N.; Skomorokhov, M. Y.; Klimochkin, Y. N. *Russ. J. Org. Chem*. **2010**, *46*, 1741.

33. Anderson, G.; Burks, W.; Harruna, I. *Synth. Commun*. **1988**, *18*, 1967.
34. Kadaba, P. *Synthesis* **1971**, 316.
35. Stepanov, F. N.; Dikolereko, E. J.; Danilenko, G. J.; *Russ, J. Org. Chem*. **1966**, *2*, 640.
36. Avdeev, M. V.; Bagrii, E. I.; Maravin, G. B.; Korolev, Y. M.; Borisov, R. S. *Petroleum Chem*. **2000**, *40*, 391.
37. Augeri, D. J.; Robi, J. A.; Betebenner, D. A.; Magnin, D. R.; Khanna, A.; Robertson, J. G.; Wang, A.; Simpkins, L M.; Taunk, P.; Huang, Q.; Han, S.-P., et al. *J. Med. Chem*. **2005**, *48*, 5025.
38. Dawson, R. M. C.; Elliott, D. C.; Elliott, W. H.; Jones, K. M. *Data for Biochemical Research*, 3rd ed.; Clarendon Press, 1991.
39. Whipps, D. E.; Halestrap, A. P. *Biochem. J*. **1984**, *221*, 47.
40. Armstrong, D.; Browne, R. *Adv. Exp. Med. Biol*. **1994**, *366*, 43.
41. Perez, C. A.; Wei, Y.; Guo, MJ. Inorg. Biochem. 2009, *103*, 326.
42. Brand-Williams, W.; Cuvelier, M. E.; Berset, C. *Food Sci. Technol* **1995**, *28*, 25.
43. Ozturk, I.; Filimonova, S.; Hadjikakou, S. K.; Kourkoumelis, N.; Dokorou, V.; Manos, M. J.; Tasiopoulos, A. J.; Barsan, M. M.; Butler, I. S.; Milaeva, E. R.; Balzarini, J.; Hadjiliadis, N. *Inorg. Chem*. **2010**, *49*, 488.
44. Xanthopoulou, M. N.; Hadjikakou, S. K.; Hadjiliadis, N.; Milaeva, E. R.; Gracheva, J. A.; Tyurin, V. Y.; Kourkoumelis, N.; Christoforidis, K. C.; Metsios, A. K.; Karkabounas, S.; Charalabopoulos, K. *Eur. J. Med. Chem*. **2008**, *43*, 327.
45. Milaeva, E. R.; Shpakovsky, D. B.; Gracheva, Y. A.; Antonenko, T. A.; Osolodkin, D. I.; Palyulin, V. A.; Shevtsov, P. N.; Neganova, M. E.; Vinogradova, D. V.; Shevtsova, E. F. *J. Organomet. Chem*. **2015**, *782*, 96.
46. Rogers, G. W.; Brand, M. D.; Petrosyan, S.; Ashok, D.; Elorza, A. A.; Ferrick, D. A.; Murphy, A. N. *PLoS One* **2011,** *6*, e21746. http://dx.doi.org/10.1371/joumal.pone.0021746.
47. Niks, M.; Otto, M. *J. ImmunoL Methods* **1990**, *130*, 149.

# Раздел V. Избранные работы по созданию веществ с различными видами биологической активности

## Введение

### О.Н. Зефирова

В некоторых исследованиях по медицинской химии, выполненных под руководством Николая Серафимовича Зефирова, для создания структур физиологически активных веществ использовались интересные комбинации классических приемов дизайна или их редкие разновидности, а также выбирались нетривиальные молекулярные мишени.

Так, Н.С. Зефировым были инициированы работы по созданию аналогов природного гормона мелатонина в качестве потенциальных регуляторов циркадных ритмов. Основным приемом дизайна лигандов рецепторов мелатонина изначально было ограничение конформационной подвижности боковой цепи природной молекулы, которое достигалось различными путями – формированием дополнительного цикла или введением заместителей в определенное положение индольного фрагмента. В работе [1] разрабатывалась идея об объединении этих двух подходов и создании оригинального структурного класса конформационно ограниченных аналогов мелатонина на основе индольных производных, аннелированных с замещенными бициклическими каркасами.

Другие исследования проводились в рамках программы по разработке эффективных ингибиторов фермента синтазы оксида азота (NOS). Эта программа была инициирована сотрудниками Медицинского радиологического научного центра им. А.Ф. Цыба и кафедры радиохимии химфака МГУ, в середине 2000-х гг. обратившихся непосредственно к Н.С. Зефирову с просьбой помочь решить проблему пролонгирования действия известного ингибитора индуцибельной изоформы NOS – 2-амино-5,6-дигидро-4*H*-1,3-тиазина, для которого в экспериментах *in vivo* было продемонстрировано кратковременное антигипотензивное и радиопротекторное действие. Для решения проблемы Н.С. Зефировым и О.Н. Зефировой было предложено два подхода – получение более липофильных производных исходной молекулы, сконструированных с использованием оригинальной стратегии «включения» моноцикла в бициклическую систему (см. один из примеров в работе [2]), а также создание пролекарств. Исследование активности последних на модели септического шока *in vivo*, показало, что антигипотензивный эффект одного пролекарства приблизительно вдвое более длителен по сравнению с таковым для исходной молекулы. Это соединение стало предметом патента RU 2338538 C1 «Антигипотензивное средство» от 28.11.2008 [*авторы* А.А. Мандругин, С.Я. Проскуряков, Т.П. Трофимова, Ю.Г. Верховский, Н.С. Зефиров, О.Н. Зефирова, В.М. Федосеев].

В 2010-х гг. под руководством Н.С. Зефирова на Химическом факультете МГУ сотрудниками группы Е.Б. Авериной совместно с коллегами из Института полиомиелита и вирусных энцефалитов им. М.П. Чумакова стали разрабатываться новые противофлавивирусные агенты. Важность этих исследований определяется тем обстоятельством, что для лечения и профилактики вызываемых флавивирусами заболеваний (клещевой энцефалит, желтая лихорадка, лихорадка денге и пр.) вплоть до настоящего момента отсутствуют специфические противовирусные препараты прямого действия. В работе [3] авторами представлен синтез серии производных 4-аминотетрагидрохиназолина, среди которых были обнаружены соединения с заметной активностью против штамма вируса клещевого энцефалита, действующие, по всей вероятности, на гликопротеин Е оболочки вириона. Исследования по созданию новых противофлавивирусных агентов в настоящее время продолжают ученики Николая Серафимовича Зефирова.

## Список статей раздела


1. Zefirova O.N., Baranova T.Y., Ivanova A.A., Ivanov A.A., Zefirov N.S. Application of the bridgehead fragments for the design of conformationally restricted melatonin analogues // *Bioorg. Chem*. 2011. V. 39. № 2. P. 67-72.

2. Плотникова Е.Д., Нуриева Е.В., Перегуд Д.И., Онуфриев М.В., Гуляева Н.В. Н.В., Макарчук В.М., Филимонова М.В., Зефиров Н.С., Зефирова О.Н. Молекулярное моделирование, рентгеноструктурный анализ и изучение *i*NOS-ингибирующей активности гидрохлорида 3-имино-2,4-диазабицикло[3.3.1]нонан-1-ола // *ЖОрХ.* 2013. Т. 49. №. 8. С. 1128-1131.

3. Sedenkova K.N., Dueva E.V., Averina E.B., Grishin Yu.K., Osolodkin D.I., Kozlovskaya L.I., Palyulin V.A., Savelyev E. N., Orlinson B.S., Novakov I.A., Butov G.M., Kuznetsova T.S., Karganova G. G., Zefirov N.S. Synthesis and assessment of 4-aminotetrahydroquinazoline derivatives as tick-borne encephalitis virus reproduction inhibitors // *Org. Biomol. Chem.* 2015. V. 13. №. 11 C. 3406-3415.

*Bioorganic Chemistry, 2011 Apr; 39(2): 67-72*

# APPLICATION OF THE BRIDGEHEAD FRAGMENTS FOR THE DESIGN OF CONFORMATIONALLY RESTRICTED MELATONIN ANALOGUES

**Olga N. Zefirova, Tatiana Yu Baranova, Anna A. Ivanova, Andrei A. Ivanov, Nikolay S. Zefirov**

*Department of Chemistry, MV. Lomonosov Moscow State University, Moscow, Russian Federation*
*Institute of Physiologically Active Compounds, Chernogolovka, Moscow region, Russian Federation*
*Department of Biochemistry, Emory University School of Medicine, Atlanta, USA*

Conformationally constrained analogues of the hormone melatonin with a side chain incorporated into the bicyclic bridgehead core were synthesized based on the homology modeling and molecular docking studies performed for the $MT_2$ melatonin receptor. The methoxy-indole derivative fused with *exo*-N-acetamino-substituted bicyclo[2.2.2]octane was found to possess nanomolar $MT_2$ receptor affinity.

## 1. Introduction

Bicyclic bridgehead fragments are used in drug design mainly when these moieties are initially present in the lead compounds (such as atropine, cocaine, and epibatidine). Other attempts to apply these fragments, e.g. as lipophilic groups or as templates, providing a proper space orientation of the substituents, are less common (e.g. [1]). Relative conformational rigidness of the bridgehead bicycles makes them also suitable for the design of conformationally restricted compounds (a classical method for the enhancement of ligand selectivity and/or affinity to a biological target).

For the structures having a rigid core and a flexible side chain, conformational restriction of the latter is usually achieved by introduction of bulky substituents, double bonds, small cycles or by partial or whole incorporation of a flexible fragment into the cycle. In the present work we have chosen the structure of the endogenous hormone melatonin for modification using bicyclic bridgehead moieties as the conformationally constricting elements and suggested to synthesize melatonin analogues with a side chain incorporated into the bicyclic bridgehead cores (Fig. 1).

Melatonin (N-acetyl-5-methoxytryptamine) is an endocrine hormone produced by the pineal gland, which plays an important role in regulation of circadian rhythms, in modulation of sleepwake cycle and in functioning of multiple other biochemical pathways in humans [2]. Physiological effects of melatonin generally result from the activation of G protein-coupled $MT_1$ and $MT_2$ receptors (there exists also a melatonin-

sensitive form of the enzyme quinone reductase, termed $MT_3$) [3]. The ligands of melatonin receptors are proposed as agents for the treatment of depression, insomnia, circadian rhythm dysfunction, etc.

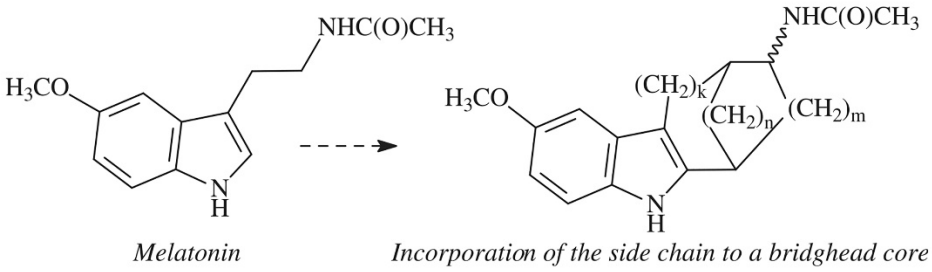


Figure 1. The general idea of the study/

In this study we intended to check if the abovementioned conformational restriction, simultaneously providing an introduction of the lipophilic substituent to the $C^2$ position of melatonin (one of the typical modifications for $MT_2$ selectivity [4]) could lead to the ligands with affinity and selectivity to $MT_2$ receptors.

## 4. Results and discussion

### *2.1. Molecular docking studies*

The choice of the exact structures was initially based on their synthetic availability, and the structures with bicycles containing a six-membered ring fused with an indole fragment were chosen. Based on these structural targets, a molecular modeling study was carried out.

For a long time, the only crystal structure of a G protein-coupled receptor available was bovine rhodopsin. Recently, a number of other GPCRs were crystallized including $\beta_1$- and $\beta_2$-adrenergic receptors, and the $A_{2A}$ adenosine receptor [5]. In addition, a crystal structure of opsin, a ligand-free form of rhodopsin, in its activated, G protein-coupled form was solved [6]. Since the opsin structure seems to be more related to an active state of other GPCRs, in the present study we used it as a template to build a homology model of the $MT_2$ melatonin receptor transmembrane domain. The molecular modeling was performed with the Modeller software [7] (the following parameters were used: number of models to generate – 50; library_schedule – autosched.slow; max_varjnteractions – 10,000; mdjevel – refine.very slow). The best model was selected based on the *moldpf* and *DOPE* scoring functions calculated by the Modeller. The general quality of the model was also confirmed by a Ramachandran plot calculated with the Schrodinger suite [8] (Fig. 2a).

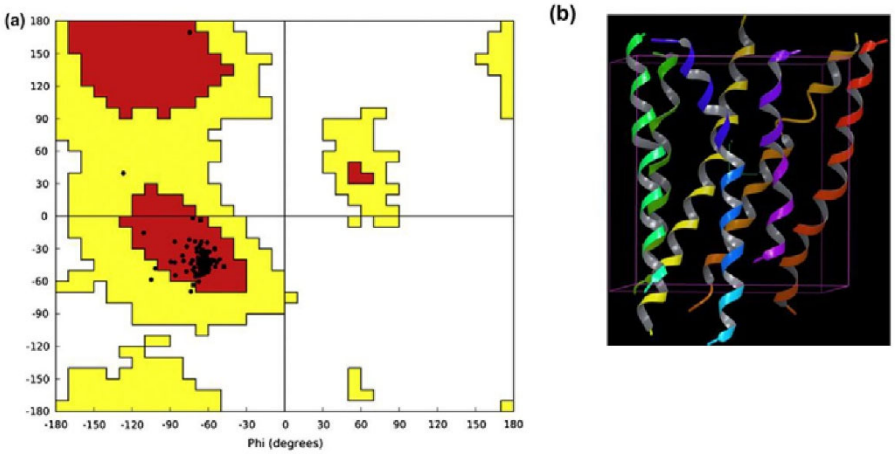


**Fig. 2.** (a) The Ramachandran plot obtained with the Schrodinger suite for the molecular model of the $MT_2$ receptor. The most favorable region is colored in red, the allowed regions – in yellow, and the disallowed regions are in white. No amino acid residues were found in the disallowed region, (b) The molecular model of the transmembrane domain of the $MT_2$ receptor colored by residue positions: TM1 in orange, TM2 in ochre, TM3 in yellow, TM4 in green, TM5 in lime, TM6 in blue, TM7 in purple. For the molecular docking the receptor grid generation was performed for a box covering almost the entire receptor (shown in purple). (For interpretation of the references to color in this figure legend, the reader is referred to the web version of this article.)

The $MT_2$ receptor model obtained was subjected to refinement with the standard procedure of the Protein Preparation Wizard implemented in the Schrodinger suite. In particular, all hydrogen atoms were added, and partial charges were assigned. Then, a fully automated molecular docking of melatonin as well as methoxyindoles fused with N-acetamino-substituted bicyclo[3.3.1]nonane, bicyclo[3.2.1]octane, bicyclo[2.2.2]-octane was carried out with the Glide program of the Schrodinger suite. The receptor grid generation was performed for a box with a center in the centroid of the receptor. The box size was determined automatically as 32 Å and, thus, covered almost the entire receptor (Fig. 2b).

The binding mode of the studied compounds docked to the $MT_2$ receptor was in excellent agreement with the available data of site-directed mutagenesis, and with the recently published rhodopsin-based models of melatonin receptors [9,10]. As shown in Fig. 3b, the oxygen atom of the ligand methoxy group can form a hydrogen bond with His208 (5.47), and the oxygen atom of the ligand amide moiety is hydrogen bonded to Asnl75 (4.60) (the numbers in parentheses correspond to the Ballesteros-Weinstein indexing system). An additional H-bond between the NH-group of amide moiety and the backbone oxygen atom of Alai 17 (3.29) was observed for melatonin and compound **3**, but not for **1** and **2**. As analogues to melatonin, the indole core of compounds **1**-**3** was surrounded by Trp264 (6.48), Vall24 (336) and Leu267 (6.51). The docking results clearly indicated that only the *endo*-isomers were able to interact with $MT_2$ binding site in the case of bicyclo[3.3.1]nonane and bicyclo[3.2.1]octane derivatives **1** and **2**, while their *exo*-analogues could not provide an energetically favorable binding mode. An

opposite situation was observed for the bicyclo[2.2.2]octane derivative **3**, the *exo*-configuration of the bridgehead being preferable in this case (Fig. 3a and b).

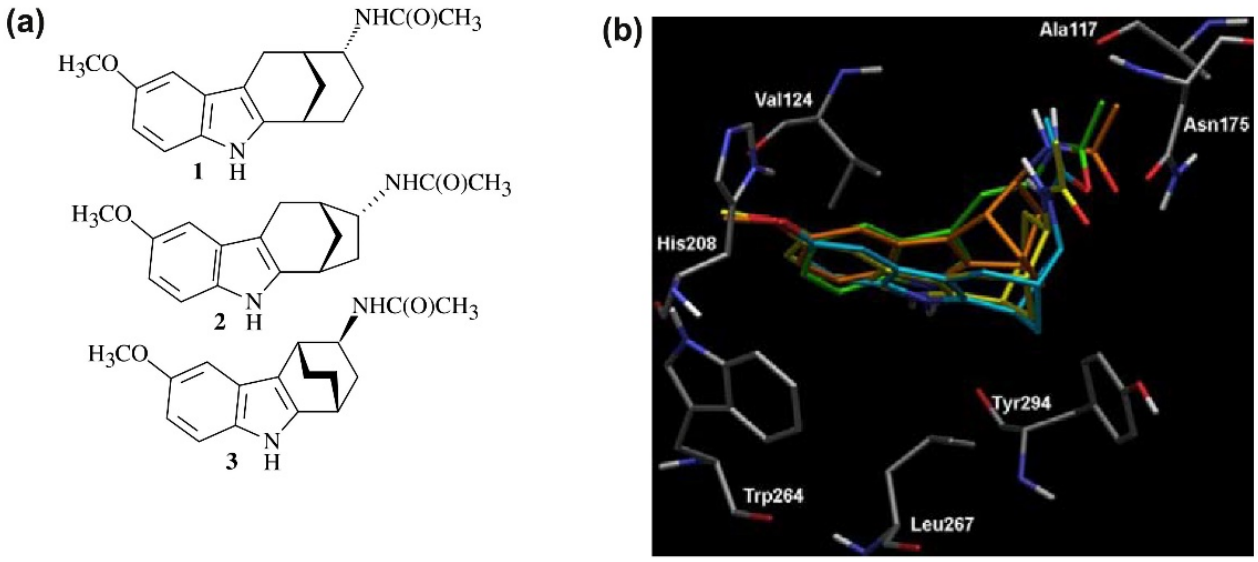


**Fig. 3.** (a) The newly synthesized bicyclo[3.3.1]nonane, bicyclo[3.2.1]octane, and bicyclo[2.3.2]octane derivatives of melatonin, (b) The superimposition of melatonin and compounds **1**-**3** docked to the $MT_2$ melatonin receptor. The carbon atoms of melatonin are colored in green, *1* – yellow, *2* – cyan, *3* – orange. (For interpretation of the references to color in this figure legend, the reader is referred to the web version of this article.)

Overlay of compounds **1**-**3** and melatonin (Fig. 3) shows that their binding modes are rather similar, and there were no significant differences in their energy scoring functions. But the values of Root Mean Square Deviation (RMSD) calculated for the heteroatoms of melatonin and **1**-**3** inside the receptor binding site were found to be of 0.67 Å for **3**, 1.08 Å for **1** and 0.84 Å for **2**, indicating that the binding mode of **3** is closer to the one of melatonin than the binding modes of **1** and **2**. Thus, the results of molecular modeling allowed us to expect better binding of **3** at the $MT_2$ receptor than **1** and **2**.

### *2.2. Chemistry*

Synthesis of the compounds **1**-**3** was performed by the indole fragment formation on the bicyclic core using a Fisher reaction. Compound **1** was synthesized from the corresponding oxime **4** obtained in five steps from the Meerwein ester as described in [11].

The oxime **4** was reduced by lithium aluminum hydride to give a mixture of diastereomeric amines **5a,b** (5:1) from which each diastereomer was separated by column chromatography. *N*-acetylation of the *endo*-isomer **5a** led to the desired *endo*-amide **1** (Scheme 1).

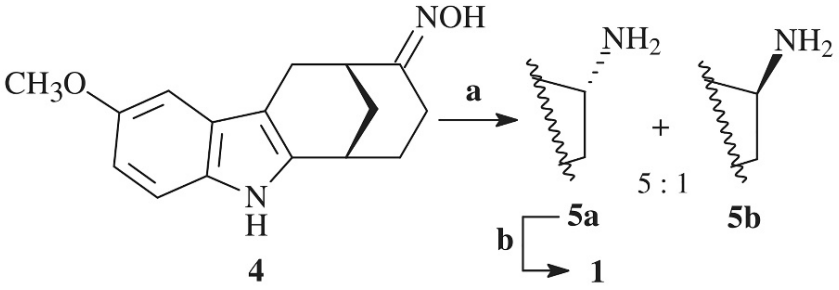


**Scheme 1.** *Reagents and conditions:* (a) $LiAlH_4$, THF, 69% (total yield); (b) $Ac_2O$, $NEt_3$, $CH_2C1_2$, 72%.

To obtain the structure **2** initially methyl *endo*-2-oxo-bicyclo[3.2.1]octan-6-carboxylate was synthesized in four steps as shown at Scheme 2.[13] Formylation of ketal **6** followed by a diazo transfer reaction with tosyl azide gave the corresponding α-diazoketone **8**. Photochemical Wolff rearrangement of the latter [13] led to the isomeric esters **9** and concomitant protection cleavage – to isomeric methyl 2-oxobicyclo-[3.2.1]octan-6-carboxylate (12:1, *endo*-:*exo*-).

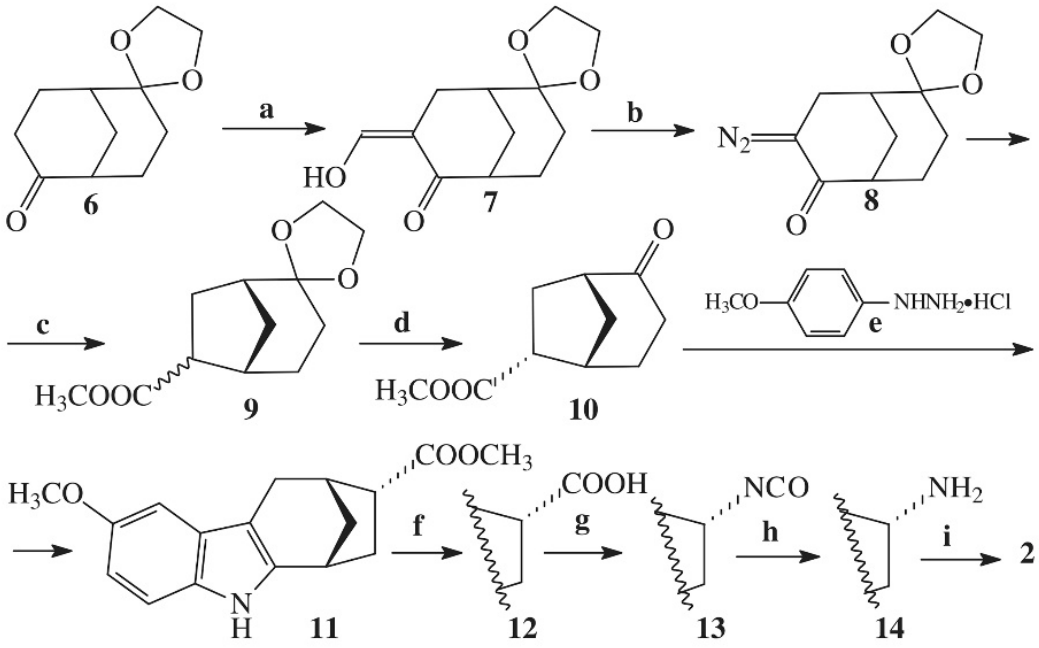


**Scheme 2.** *Reagents and conditions:* (a) NaH, HCOOEt, $Et_2O$, 75%; (b) $TsN_3$, $NEt_3$, $CH_2C1_2$, 84%; (c) *hv,* $CH_3OH$, 74%; (d) PTSA, acetone, column chromatography, 80%; (e) $CH_3COOH$, 67%; (f) HC1, $H_2O$, 70%; (g) ClCOOEt, $NEt_3$. $CH_2Cl_2$, then $NaN_3$, $H_2O$, toluene, reflux, 89%; (h) HC1, $H_2O$, 50%; (i) $Ac_2O$, $NEt_3$. $CH_2C1_2$, 65%.

The *endo*-isomer **10** was isolated by column chromatography at 95% purity and its reaction with 4-methoxyphenylhydrazine hydrochloride in glacial acetic acid led to the *endo*-isomer of the indole **11**. While the hydrolysis of the ester group in **11** under

[13] Interestingly, the isomeric methyl *exo*-2-oxo-bicyclo[3.2.1]octan-6-carboxylate can be regioselectively prepared by ring constriction in bicyclo[3.3.1]nonan-2,6-dione by tallium nitrate, that makes the stereoselective synthesis of *exo*-isomer of **2** (described in our previous work [12]) easier than that of **2**.

alkaline conditions caused epimerization, it was carried out smoothly in the presence of hydrochloric acid to afford the *endo*-acid **12**. The latter was then converted to *endo*-amine **14** in two steps and *N*-acetylation of the amine **14** with acetic anhydride gave a conformationally restricted melatonin analogue **2**.

For the synthesis of the indole derivative fused with bicyclo[2.2.2]octane **3**, a ketal of methyl *endo*-5-oxobicyclo[2.2.2]octane-2-carboxylate **16a** (obtained by reaction of cyclohexenone and methyl actylate with further protection [14,15]) was epimerized in the reaction with lithium diisopropylamide (Scheme 3).[14]

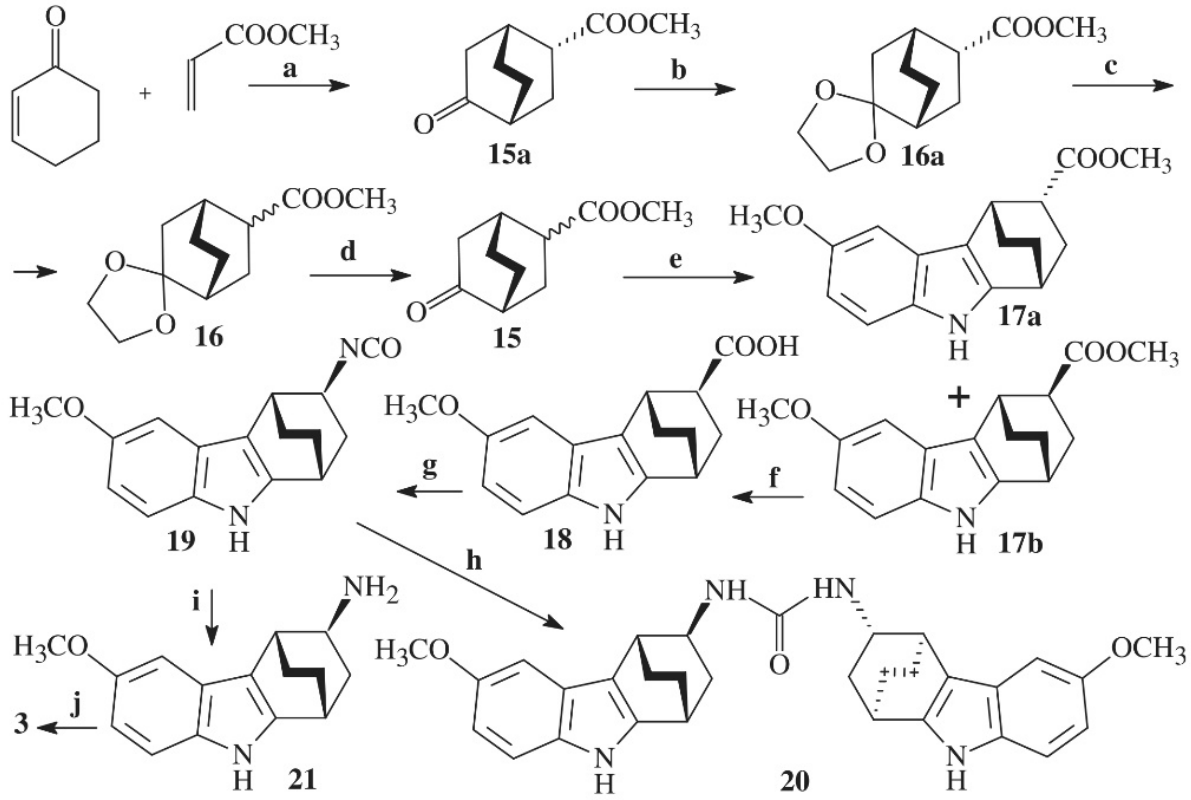


**Scheme 3.** *Reagents and conditions:* (a) LDA. THF, –23°C, 60%; (b) $HOCH_2CH_2OH$, PTSA, 90%; (c) LDA. THF, –78 °C → –20 °C, 76%; (d) PTSA, acetone, 80%; (e) $CH_3OPhNHNH_2$.HCl, $CH_3COOH$; column chromatography, 56% (total yield); (f) NaOH, $CH_3OH/H_2O$, 79%; (g) ClCOOEt, $NEt_3$. $CH_2Cl_2$, then $NaN_3$, $H_2O$, toluene, reflux, 90%; (h) NaOH, 40–50°C, $PhCH_3/H_2O$, 71%; (i) NaOH, 0–5°C, $THF/H_2O$, 55%; 0) $Ac_2O$, $NEt_3$. $CH_2C1_2$, 61%.

The mixture of deprotected esters **15** (*endo*-:*exo*- ratio 1:1) was subjected to Fischer reaction conditions and transformed to the isomeric indoles **17a** and **17b**, separated by column chromatography (the isomers configuration was determined by homonuclear $^1H$ double resonance spectroscopy and proved by comparison with the spectrum of indole derivative **17a** directly obtained from **15a**). After the conversion of *exo*-ester **17b** to the corresponding acid **18** and isocyanate **19**, the latter was hydrolyzed

[14] An attempt to subject a ketal of bicyclo[2.2.2]octane-2,5-dione to a Fisher reaction conditions (in the presence of $CH_3COOH$, HCl or ZnCCl) led to the protective group cleavage and a formation of a hard to separate mixture, from which the corresponding methoxyindol derivative fused with bicyclo[2.2.2]octanone was isolated in a very low yield.

by 2 N NaOH at 0–5°C in THF to the corresponding amine **21**. (Hydrolysis of isocyanate **19** under acidic conditions led to the degradation of the indole system, while an analogous reaction with 3 N NaOH at 40–50°C in toluene gave disubstituted urea **22** as the only product). Acetylation of the amine **21** led to the desired compound **3**.

### *2.3. $MT_1$ and $MT_2$ affinity results*

The synthesized confbrmationally constrained melatonin analogues **1**-**3** were evaluated for their *in vitro* affinity to the recombinant human $MT_1$, and $MT_2$ subtypes expressed in CHO-K1 cells in a radioligand-binding assay using [$^{125}$I]2-iodomelatonin as a labeled ligand [16,17] according to standard protocols of the MDS Pharma Services (Taipei, Taiwan). K) values were calculated from $IC_{50}$ values, obtained from competition curves by the method of Cheng and Prusoff. Melatonin and 4-phenyl-2-propionamidotetralin (4P-PDOT, $MT_2$ antagonist) were tested as the reference compounds in the $MT_1$ and $MT_2$ assays correspondingly (melatonin $MT_1$: $IC_{50}$ 034 nM, $K_i$ ~ 0.18 nM; 4P-PDOT $MT_2$: $IC_{50}$ ~ 0.42 nM, $K_i$ ~ 0.22 nM). It should be mentioned, that CHO-h$MT_2$ binding affinity of 4P PDOT is very close to that of melatonin [18].

The results indicate that methoxyindole annelated with the acetamino-substituted bicyclo[2.2.2]octane (**3**) has the highest $MT_2$ binding affinity ($MT_2$: $IC_{50}$ ~2.75 nM, $K_i$ ~ 1.43 nM), which is about one order of magnitude lower than that of melatonin, but still in nanomolar range. Taking into account that **3** was tested as racemic mixture, its $MT_2$ binding affinity is rather high and proves our predictions made on the basis of molecular modeling. Compound **3** demonstrated also a noticeable selectivity to $MT_2$ subtype ($MT_1$: $IC_{50}$ ~ 54.6 nM, $K_i$ ~ 28.3 nM), though it was less then expected: $K_i(MT_1)/ K_i(MT_2)$ ~ 20.

The affinity of an analogous compound with bicyclo[3.3.1]nonane fragment (**1**) drops to a micromolar range, but it still retains $MT_2$ selectivity ($MT_2$: $IC_{50}$ > 1.1 μM, $K_i$ ~ 0.57 μM; $MT_1$: $IC_{50}$ > 10 μM). No significant affinity was observed for bicyclo[3.2.1]octane derivative **2** at both receptors subtypes ($MT_1$, $MT_2$: $IC_{50}$ > 10 μM). These results confirm the positive effect of the bulk of the $C^2$-substituent in the indole core on $MT_2$ selectivity, but indicate that there is no linear dependence between the $MT_2$ binding affinity and the bridgehead core size among the tested compounds.

The considerable decrease in affinity of bicyclo[3.3.1]nonane and bicyclo[3.2.1]octane derivatives **1** and **2** in comparison with **3** could be partially explained by close location (3.8 Å) of hydrophobic bridge carbon atoms of **1** and **2** from the hydroxyl group of Tyr294 (7.40) in the $MT_2$ binding site. This proximity might be enough to produce undesired changes in the protein structure or decrease the binding properties of compounds. In contrast the closest carbon atom of bicyclo[2.2.2]octane fragment of **3** is positioned at a distance of 4.6 Å from the Tyr294 (7.40) OH-group.

The drop of affinity of **1** and **2** conforms to the observations, that conformational constriction leading to the movement of melatonin side chain towards the $C^2$ atom of

the indole ring often leads to the decrease of potency [19]. Nevertheless bicyclo-[2.2.2]octane analogue **3** with the same type of constriction retains good $MT_2$ binding affinity. Obviously, additional study is needed to find out if the bridgehead moiety of **3** plays its part in this case.

In summary, bridgehead bicycles were applied for the design of conformationally restricted melatonin analogues. The experimentally determined binding affinity of methoxyindole derivative fused with *exo*-N-acetamino-substituted bicyclo[2.2.2]octane (**3**) confirmed the molecular docking predictions. To our knowledge, this is the first bridgehead melatonin analogue with nanomolar $MT_2$ affinity. Further molecular modeling and experimental studies are ongoing to evaluate the functional activity of the compounds, to better understand the dependence between $MT_2$ binding affinity and the bridgehead core size and to extend the application of the bridgehead moieties as conformationally constricting elements to other classes of substrates.

## Acknowledgments

This work was supported by the Russian Foundation for Basic Research (Projects Nos. 09-03-879 and 09-03-12110-ofi).

We thank the laboratory of Dr. Ichiro Matsumura (Department of Biochemistry, Emory University School of Medicine, USA) and the laboratoty of Dr. Kenneth A. Jacobson (National Institute of Diabetes 8i Digestive 8i Kidney Diseases, Bethesda, MD, USA) for useful collaboration on the molecular modeling studies, and for reading the manuscript.

We are grateful to the MDS Pharma Services (Taipei, Taiwan) for the effective collaboration concerning the receptors binding experiments.

## References

[1] For examples of these works see: (a) Y. Chen, Q. Zhang, B. Zhang, P. Xia, Y. Xia, Z. Yang, N. Kilgore, C. Wild, S.L. Morris-Natschkeb, K. Leeb, Bioorg. Med. Chem. 12 (2004)6383-63874;
(b) R.S. Muthyala, S. Sheng, K.E. Carlson, B.S. Katzenellenbogen, J.A Katzenellenbogen, J. Med. Chem. 46 (2003) 1589-1602;
(c) O.N. Zefirova, E.V. Nurieva, H. Lemcke, AA. Ivanov, D.V. Shishov, D.G. Weiss, S.A. Kuznetsov, N.S. Zefirov, Bioorg. Med. Chem. Lett. 18 (2008) 5091-5094;
(d) M. Zurcher, F. Diederich, J. Org. Chem. 73 (2008) 4345-4361.

[2] P. Pevet, B. Botherel. H. Slotten, M. Saboureau, Cell Tissue Res. 309 (2002) 183-191.

[3] D.P. Zlotos, Arch. Pharm. Chem. Life Sci. 338 (2005) 229-247.

[4] S. Rivara, M. Mor, C. Silva, V. Zuliani, F. Vacondio, G. Spadoni, A Bedini, G. Tarzia, V. Lucini, M. Pannacci, F. Fraschini, P.V. Plazzi, J. Med. Chem. 46 (2003) 1429-1439.

[5] S. Topiol, M. Sabio, Biochem. Pharmacol. 78 (2009) 11-20.

[6] P. Scheerer, J.H. Park, P.W. Hildebrand, Y.J. Kim, N. Krauß, H.-W. Choe, K.P. Hofmann, O.P. Ernst, Nature 455 (2008) 497-502.

[7] A. Šali, T.L. Blundell, J. Mol. Biol. 234 (1993) 779-815.
[8] F.N. Mohamadi, G.J. Richards, W.C. Guida, R. Liskamp, M. Lipton, C. Caufield, G. Chang, T. Hendrickson, W.C. Still, J. Comput. Chem. 11 (1990) 440-467.
[9] M. Gerdin, F. Mseeh, M.L. Dubocovich, Biochem. Pharmacol. 66 (2003) 315-320.
[10] A. Farce, A.O. Chugunov, C. Loge, A Sabaouni, S. Yous, S. Billy, N. Renault, G. Vergoten, R.G. Efremov, D. Lesieur, P. Chavatte, Eur. J. Med. Chem. 43 (2008) 1926-1944.
[11] T.Yu. Baranova, O.N. Zefirova, N.V. Averina, V.V. Boyarskikh, G.S. Borisova, N.V. Zyk, N.S. Zefirov, Russ. J. Org. Chem. 43 (2007) 1196-1201.
[12] T.Yu. Baranova, N.V. Averina, N.V. Zyk, N.S. Zefirov, K.A. Lyssenko, M.Yu. Antipin, O.N. Zefirova, Mend. Commun. 19 (2009) 10-11.
[13] E.P. Butkus, A.I. Zilinskas, N.S. Zefirov, P.P. Kadziauskas, Zh. Org. Khim. (Russ.) 22 (1986) 871.
[14] N.H. Werstiuk, S. Yeroushalmi, H. Guan-Lin, Can. J. Chem. 70 (1992) 974-980.
[15] M. Nakazaki, H. Chikamatsu, T. Fujii, Y. Sasaki, S. Ao, J. Org. Chem. 48 (1983) 4330-4337.
[16] P. Paul, C. Lahaye, P. Delagrange, J.P. Nicolas, E. Canet, J.A Boutin, J. Pharmacol. Exp. Ther. 290 (1999) 334-340.
[17] M.L. Dubocovich, K. Yun, W.M. Al-Ghoul, S. Benloucif, M.L. Masana, FASEB J. 12 (1998) 1211-1220.
[18] V. Audinot, F. Mailliet, Ch. Lahaye-Brasseur, A Bonnaud, A Le Gall, Ch. Amossé, S. Dromaint, M. Rodriguez, N. Nagel, J.-P. Galizzi, B. Malpaux, G. Guillaumet, D. Lesieur, F. Lefoulon, P. Renard, Ph. Delagrange, J.A Boutin, Naunyn- Schmiedeberg's Arch. Pharmacol. 367 (2003) 553-561.
[19] M. Mor, S. Rivara, C. Silva, F. Bordi, P.V. Plazzi, G. Spadoni, G. Diamantini, C. Balsamini, G. Tarzia, F. Fraschini, V. Lucini, R. Nonno, B.M. Stankov, J. Med. Chem. 41 (1998) 3831-3844

*Журнал органической химии. 2013. Т. 49. Вып. 8, 1128-1131*

УДК. 547.518

# МОЛЕКУЛЯРНОЕ МОДЕЛИРОВАНИЕ, РЕНТГЕНОСТРУКТУРНЫЙ АНАЛИЗ И ИЗУЧЕНИЕ INOS-ИНГИБИРУЮЩЕЙ АКТИВНОСТИ ГИДРОХЛОРИДА 3-ИМИНО-2,4-ДИАЗАБИЦИКЛО[3.3.1]НОНАН-1-ОЛА[15]

**Е.Д. Плотникова, Е.В. Нуриева, Д.И. Перегуд, М.В. Онуфриев, Н.В. Гуляева, В.М. Макарчук, М.В. Филимонова, Н.С. Зефиров, О.Н. Зефирова**

*Московский государственный университет им. М.В.Ломоносова, Москва,*
*Национальный научный центр наркологии Росздрава, Москва*
*Институт Высшей нервной деятельности и нейрофизиологии РАН, Москва*
*Медицинский радиологический научный центр Минздрава России, Обнинск*
*Институт физиологически активных веществ РАН, Черноголовка*

На основании молекулярного моделирования предсказана *i*NOS-ингибирующая активность гидрохлорида 3-имино-2,4-диазабицикло[3.3.1]нонан-1-ола, которая подтверждена в экспериментах *in vitro*. Представлены результаты изучения молекулярной и кристаллической структуры этого соединения методом РСА.

В ходе работ по созданию ингибиторов индуцибельной изоформы фермента синтазы оксида азота (*i*NOS), обладающих пролонгированным антигипотензивным эффектом за счет высокой липофильности, нами получены бициклические мостиковые дигидротиазины (I, II) [1, 2]. Соединение (II) проявило высокую ингибирующую активность по отношению к *i*NOS *in vitro.*

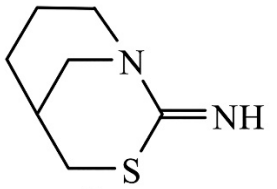


I

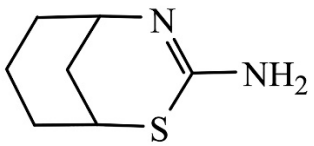


II

Это соединение, по-видимому, обладает также селективностью к указанной изоформе фермента, так как проведенные в данной работе эксперименты *in vivo*

[15] Посвящается памяти академика АН Г.А. Толстикова – талантливого и разностороннего ученого, автора серии публикаций в области создания физиологически активных веществ.

не выявили у него признаков вазопрессорного действия на модели геморрагического шока (см. экспериментальную часть), характерного для ингибиторов эндотелиальной изоформы NOS.

Несмотря на обнадеживающие данные по активности и селективности тиазина (II), его получение требует реализации многостадийной схемы синтеза [2]. Поэтому мы провели литературный поиск синтетически более доступных структурных аналогов этого соединения. При этом мы руководствовались также расчетными значениями липофильности (log*P*) таких аналогов, с тем, чтобы оно попадало в интервал от –0.3 [для соединения (I)] до 0.35 [для соединения (II)].

В результате нами был выявлен гидрохлорид 3-имино-2,4-диазабицикло[3.3.1]нонан-1-ола (III) [3], близкий по строению тиазину (II) и содержащий дополнительную гидроксильную группу в узловом положении бицикла. Расчетное значение log*P* для этого соединения составило –0.01. Докинг структуры (III) в оксидазный домен индуцибельной изоформы NOS (PDB ID: 4NOS) показал удачное расположение молекулы и возможность образования водородных связей гуанидиновой группировки с аминокислотными остатками Glu377 и Trp372 (рис. 1), играющими центральную роль в связывании субстрата *i*NOS L-аргинина. По данным моделирования, еще две водородные связи возможны между соединением (III) и активным центром фермента, а именно между атомом водорода при $N^2$ и атомом азота одного из пиррольных колец гема, а также между атомом водорода гидроксила при $C^1$ и карбонильным атомом кислорода боковой цепи остатка аминокислоты Pro350.

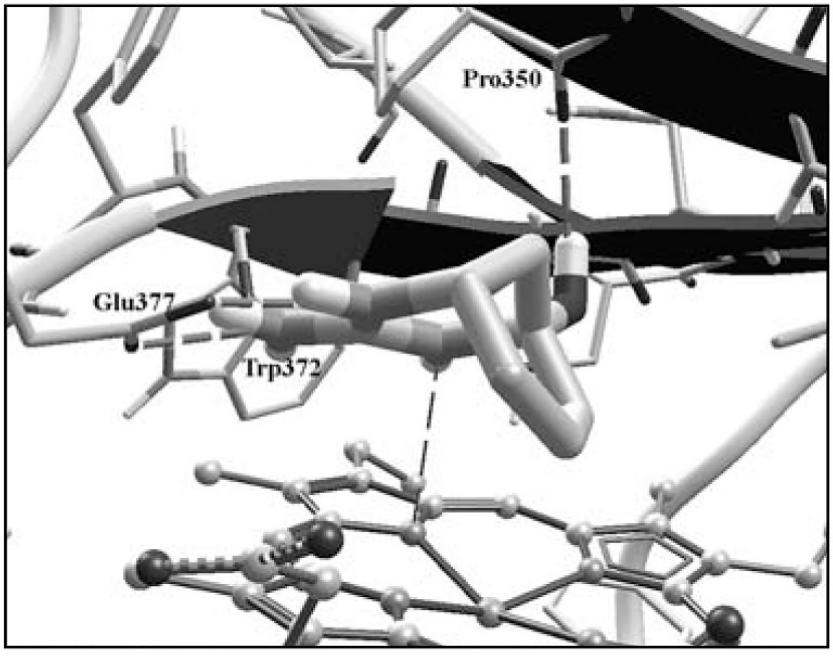


Рис. 1. Расположение молекулы (III) в активном центре *i*NOS.

Соединение (III) синтезировали из циклогексенона и сульфата гуанидина по модифицированной методике [3] (схема 1).

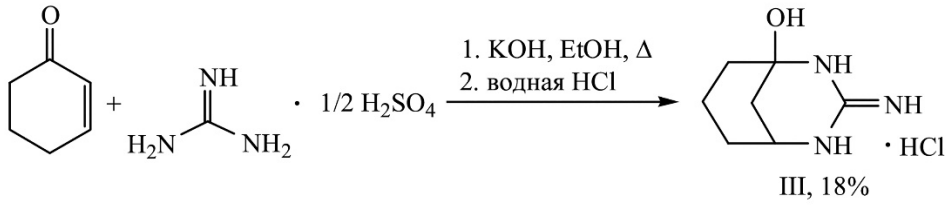


Схема 1

Полученный мостиковый гуанидин (III) был полностью охарактеризован нами с помощью данных ЯМР спектроскопии, масс-спектрометрии и рентгеноструктурного анализа. В спектре ЯМР $^1$H сигнал протона при $C^5$ проявляется в виде мультиплета в области 3.90 м.д. В спектре ЯМР $^{13}$C сигнал иминного атома углерода наблюдается при 154.8 м.д., а сигналы узловых атомов $C^1$ и $C^5$ – при 79.4 и 47.4 м.д. соответственно. В масс-спектре гуанидина (III) присутствует пик молекулярного иона, *m/z* 155.

Исследование молекулярной и кристаллической структуры соединения (III) (рис. 2) позволило выявить особенности конформаций колец мостикового фрагмента, наличие гетероатомов в котором приводит к искажению наиболее стабильной конформации *двойного кресла* бицикло[3.3.1]нонана.

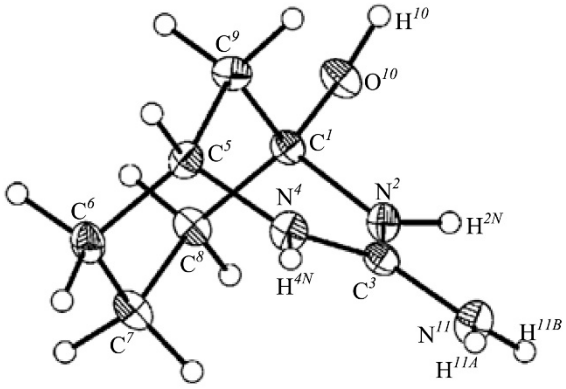


Рис. 2. Молекулярное строение 1-гидрокси-2,4-диазабицикло[3.3.1]нонан-3-иминиумхлорида в кристалле в представлении тепловыми эллипсоидами колебаний вероятностью 50%.

Согласно данным РСА и результатам расчетов параметров складчатости Зефирова–Палюлина *(ZP)* и Кремера–Попла (*CP*) по программе RICON [4], цикл $C^1$–$C^9$–$C^5$–$C^6$–$C^7$–$C^8$ в структуре (ГП) имеет конформацию *искаженного кресла (ZP: S* 1.168, θ 4.5, $\psi_2$ 9.8, σ 0.31; *CP: Q* 0.593, θ 8.71, $\varphi_2$ 7.3), но это искажение незначительно. Кольцо с двумя гетероатомами $C^1$–$N^2$–$C^3$–$N^4$–$C^5$–$C^9$ сильно уплощено из-за наличия $sp^2$-гибридизованного атома углерода и заместителя при $C^3$. Оно принимает конформацию идеального *конверта (ZP: S* 9.774, θ 49.9, $\psi_2$ 2.3, σ 1.94; *CP: Q* 9.533, θ 54.9, $\psi_2$ 1.9), то есть максимально плоскую из всех конформаций, наблюдавшихся для аналогичных циклов в ранее изученных нами гете-

роаналогах бицикло[3.3.1]нонана [5]. Двойная связь в гуанидиновой группировке структуры (III) делокализована между тремя атомами азота, на что указывают значения длин связей $N^2$–$C^3$ 1.336 (3), $C^3$–$N^{11}$ 1.341 (3), $C^3$–$N^4$ 1.330 (3) Å.

Соединение (III) кристаллизуется в виде полугидрата (молекула воды занимает частное положение на оси 2) в ахиральной пространственной группе P2/n. В кристалле водородные связи между катионом и анионом объединяют молекулы в бесконечные цепи, направленные вдоль кристаллографической оси *b* [$N^2$–$H^{2N\cdots}$Cl 2.45 Å, $N^4$–$H^{4N}$…Cl 2.78 Å, $N^{11}$–$H^{11A\cdots}$Cl 2.45 Å], а водородные связи с участием молекулы воды или гидроксила, в свою очередь, объединяют цепи в слои, параллельные плоскости *ab* ($O^{1W}$–$H^{1WA\cdots}$Cl 2.17 Å, $O^{10}$–$H^{10\cdots}$Cl 2.21 Å, $N^{11}$–$H^{11B\cdots}O^{1W}$ 2.97 Å) (рис. 3).

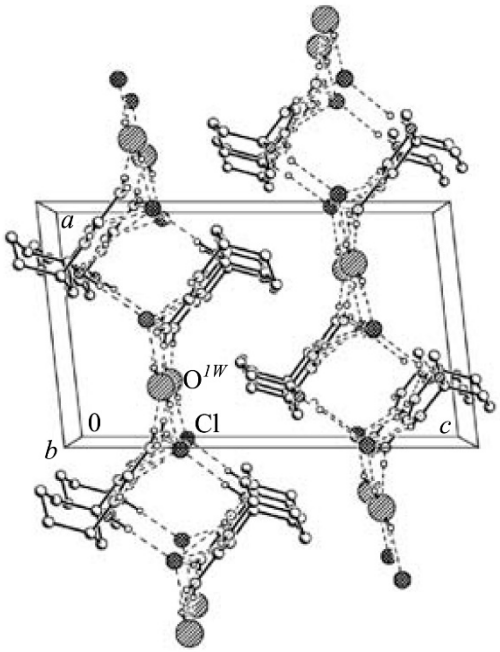


Рис. 3. Слои в кристалле соединения (III), образованные за счет водородных связей (молекулы воды показаны увеличенными шариками).

Полученный мостиковый гуанидин (III) в виде рацемической смеси был испытан *in vitro* на способность ингибировать *i*NOS, выделенную из стимулированных липополисахаридом макрофагов мыши, радиометрическим методом по скорости накопления [$^3$H]-L-цитруллина в катализируемой NOS реакции окисления субстрата этого фермента [$^3$H]-L-аргинина (см. экспериментальную часть). По данным тестирования в концентрации 1 μM относительная ингибиторная активность гуанидина (III) составляет ~20%, то есть является промежуточной между значениями активности соединений (I) и (II) (<1 и 76% соответственно). Способность соединений (II) и (III) ингибировать *i*NOS в экспериментах *in vivo* в настоящее время изучается.

## Экспериментальная часть

Спектры ЯМР $^{1}H$ и $^{13}C$ регистрировали на приборе VXR-400 (Varian) с рабочей частотой 400 и 100 МГц соответственно (химические сдвиги приведены относительно остаточного сигнала растворителя). Контроль протекания реакций проводили с помощью ТСХ на пластинах Silufol UV-254, а хроматографическое разделение выполняли на колонках с силикагелем Acros (40–60 мкм). Масс-спектры регистрировали на квадрупольном масс-спектрометре Finnigan MAT Ineos 50 с энергией ионизирующих электронов 70 эВ, температура ионизационой камеры 200°C, система прямого ввода. *rac*-2-тиа-4-азабицикло[3.3.1]нон-3-ен-3-амин гидрохлорид (III) получен по методике [2].

**Тестирование *in vivo.*** Вазопрессорное действие соединения (II) на модели тяжелого геморрагического шока изучали на крысах Wistar (самцы, масса 250–320 г). Наркотизированному животному (тиопентал натрия 60 мг/кг, в/б) устанавливали трахеостому, катетеризировали яремную вену и обе сонные артерии, подключали инвазивный датчик артериального давления (АД) и электроды регистрации ЭКГ. После стабилизации состояния животного регистрировали (полиграф Nihon Kohden RM-6000) исходные показатели частоты сердечных сокращений, дыхательных движений, систолического и диастолического АД в левой сонной артерии. Шок вызывали путём забора крови из правой сонной артерии (2.5 мл на 100 г массы животного), по окончании кровопотери повторяли регистрацию физиологических показателей. Затем животным вводили внутрибрюшинно соединение (II): в первой группе – в дозе 10 мг/кг в 0.2 мл 5%-ного этанола, во второй группе – в дозе 20 мг/кг в 0.2 мл 10%-ного раствора Tween-80. Дальнейший мониторинг показателей в течение 60 мин не выявил в обеих группах значимого повышения тонуса сосудов и роста АД.

**Молекулярное моделирование** проводили в полуавтоматическом режиме с помощью программы Molegro Virtual Docker Version 5.5 (пробная версия) с приложением Molecular Viewer 2.5. Отбор наиболее качественной модели проводили на основе скоринг-функций, рассчитанных с помощью Molegro.

***rac*-3-Имино-2,4-диазабицикло[3.3.1]нонан-1-ол гидрохлорид (III).** К раствору 0.25 г (2.6 ммоль) циклогексенона в этаноле прибавили 0.9 г (4 ммоль) гуанидин сульфата $[(H_2N)_2C{=}NH]_2 \cdot H_2SO_4 \cdot 0.5\ H_2O$ и 0.7 г (12.5 ммоль) KOH, кипятили 12 ч. Нейтрализовали 2 н. HCl и упарили, остаток перекристаллизовали из этанола и хроматографировали (элюент – $CH_2Cl_2$–метанол, 25:1). Выход 0.09 г (18%), бесцветные кристаллы, т.пл. 198–200°C (198–201°C [3]).

Кристаллы соединения (III) $[(C_7H_{14}N_3O)Cl \cdot 0.5\ H_2O$, $M$ 200.67, кристаллизованы из водного метанола] моноклинные, пространственная группа $P2/n$, при 100 K. Интенсивности 5921 отражения измерены на дифрактометре Bruker APEX II Dual CCD [l($MoK_a$) 0.71072 Å, 20<56°], 2320 независимых отражений ($R_{int}$

0.0521) использованы в дальнейшем уточнении. Структура решена прямым методом и уточнена полноматричным МИК по $F^2$ в анизотропно-изотропном приближении. Атомы водорода групп NH, $NH_2$ и OH, а также молекулы воды локализованы из разностных синтезов электронной плотности, а положения атомов водорода H(C) рассчитаны геометрически. Все атомы водорода уточнены в изотропном приближении по модели *наездника.* Окончательное значение факторов недостоверности $wR_2$ 0.1320, *GOF* 1.066 для всех независимых отражений [$R_1$ 0.0480 рассчитывали по *F* для 1837 отражений с $I > 2s(1)$]. Все расчеты проведены с помощью комплекса программ SHELXTL PLUS 5.0. Полностью данные РСА доступны в Кембриджской кристаллографической базе данных (CCDC № 913723).

**Тестирование *i*NOS-ингибирующей активности для соединения (III) *in vitro.*** Активность *i*NOS, выделенной из стимулированных липополисахаридом макрофагов мыши (Cayman chemical, США, каталожный номер 60862; 22.43 Ед/мг; 4.97 мг/мл; 111.5 Ед/мл), определяли радиометрическим методом по скорости накопления [$^3$H]-L-цитруллина в катализируемой NOS реакции окисления [$^3$H]-L-аргинина (0.37 Ки/ммоль) по методике, описанной в работе [1].

Работа выполнена при финансовой поддержке Российского фонда фундаментальных исследований (проект 12-03-00720) и Отделения химии и наук о материалах Российской Академии наук (программа 9). Авторы выражают глубокую благодарность д.х.н. К.А.Лысенко за помощь в работе.

## Список литературы

1. Zefirova O.N., Nurieva E.V., Chupakhin V.I, Semenova I.S., Peregud D.I, Onufriev M.V., Gulyaeva N.V. *Mendeleev Commun.* **2010**, *20,* 323.
2. Zefirova O.N., Plotnikova E.D., Nurieva E.V., Peregud D.I., Onufriev M.V., Gulyaeva N.V. *Mendeleev Commun.* **2013**, *23,* 76.
3. Wendelin W., Kern W. *Monatsh. Chem.* **1979**, *110,* 861.
4. Zotov A.Yu., Palyulin V.A., Zefirov N.S. *J. Chem. Inf. Comput. Sci.* **1997**, *37,* 766.
5. Zefirova O.N., Moisseeva N.N., Nurieva E.V., Trofimova T.P., Proshin A.N., Slovokhotov Y.L. *Mendeleev Commun.* **2011**, *21,* 247.

*Organic & Biomolecular Chemistry Org. Biomol. Chem., 2015, 13, 3406-3415*

# SYNTHESIS AND ASSESSMENT OF 4-AMINOTETRAHYDRO-QUINAZOLINE DERIVATIVES AS TICK-BORNE ENCEPHALITIS VIRUS REPRODUCTION INHIBITORS

**K.N. Sedenkova, E.V. Dueva, E.B. Averina, Yu.K. Grishin, D.I. Osolodkin, L.I. Kozlovskaya, V.A. Palyulin, E.N. Savelyev, B.S. Orlinson, I.A. Novakov, G.M. Butov, T.S. Kuznetsova, G.G. Karganova and N.S. Zefirov**

*Department of Chemistry, Lomonosov Moscow State University, Moscow Russia.*
*Institute of Physiologically Active Compounds, Russian Academy of Sciences, Chernogolovka, Moscow Region, Russia*
*Chumakov Institute of Poliomyelitis and Viral Encephalitides, Moscow Russia*
*Volgograd State Technical University, Volgograd, Russia*
*Department of Biology, Lomonosov Moscow State University, MoscowRussia*

Received 22nd December 2014, Accepted 26th January 2015

Tick-borne encephalitis virus (TBEV) belonging to Flavivirus genus causes severe infection in humans. The search for therapeutically relevant compounds targeting TBEV requires the exploration of novel chemotypes. A versatile synthesis of previously unknown 4-aminopyrimidines and 4-aminopyrimidine N-oxides based on a fluorosubstituted heterocyclic core is described. A representative series of 4-aminotetrahydro- quinazoline derivatives, containing aliphatic and aromatic substituents as well as the adamantane framework, was obtained and their activity against tick-borne encephalitis virus reproduction was studied. Nine compounds were found to inhibit TBEV entry into the host cells. A bulky hydrophobic adamantyl group was identified to be important for the antiviral activity. The developed synthetic route allowed an easy access to a consistent compound library for further structure-activity relationship studies.

## Introduction

Tick-borne encephalitis (TBE) is a severe neuroinvasive viral zoonotic infection, occurring in humans after a bite of an infected tick.[1] The case fatality rate varies in a wide range (0.5-2% for the European subtype and up to 17.5% for the Far East subtype),[2] a long-term post-encephalitic syndrome appears in up to 75% cases leading to the prolonged disability[1] that negatively affects the patients' quality of life. A causative agent of TBE, the tick-borne encephalitis virus (TBEV), belongs to the genus Flavivirus (family Flaviviridae) along with the dengue virus (DENV), West Nile virus (WNV), yellow fever virus (YFV), Japanese encephalitis virus (JEV), and a number of rare viruses transmitted by ticks or mosquitoes.[3] TBE prevention can be successfully

achieved by the vaccination;[4] immunoglobulin treatment is widely used for a TBE prophylaxis or symptomatic treatment,[5] and recently a chimeric anti-TBEV antibody was introduced.[6] Nevertheless, the applicability domain of effective post-infection treatments is restricted, thus justifying the need for new small molecule based treatment schemes.

We have recently reported the potent TBEV reproduction inhibitors based on 1,4-dihydropyridine (compound **1**) and pyrido[2,1-b][1,3,5]thiadiazine (compound **2**) scaffolds (Fig. 1).[7] These scaffolds were identified with the help of docking-based virtual screening against the detergent binding pocket in the homology model of the flavivirus envelope protein E, which plays the leading role in the process of the pH-driven membrane fusion between the virus particle and the host cell.[8] Despite these compounds showing significant antiviral activity and acceptable toxicity, clear structure–activity relationships could not be established for them due to insufficient coverage of analogues' space. Additional complications could be introduced by a limited solubility of the compounds. Therefore, for further rational structure design we needed a novel core, which could be readily functionalized in order to obtain a consistent compound library. For this purpose we exploited a series of 4-fluorosubstituted pyrimidine N-oxides and pyrimidines which are excellent substrates for the aromatic nucleophilic substitution and possess a high potential of functionalization providing many possibilities for designing new molecular scaffolds. In previous papers we described the first synthesis of previously unknown 4-fluoropyrimidine 1-oxides **3** via novel three-component heterocyclization involving gem-bromofluorocyclopropane **4**, $NOBF_4$ and organic nitrile,[9] as well as the approach to 4-fluoropyrimidines **5** based on the reduction of the corresponding N-oxides under the treatment of $PCl_3$ (Scheme 1).[10] It should be noted that it is the only general method of construction of the 4-fluoropyrimidine pattern via a direct cyclization. All other described approaches to 2-, 4- or 6-fluoropyrimidines are based on the transformations of previously constructed heterocycles, among them more used being (1) the transhalogenation of other halogenopyrimidines,[11] and rarer (2) the displacement of trimethylammonio or hydroxyl groups to fluorine,[12] (3) the diazotization of appropriate aminopyrimidines[13] or (4) the selective fluorination of the C–H bond adjacent to nitrogen.[14]

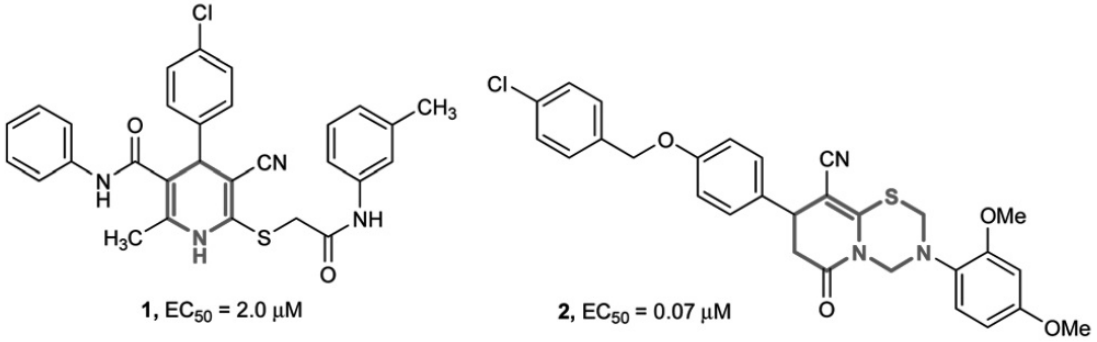


**Fig. 1.** Potent compounds showing antiviral activity against TBEV.

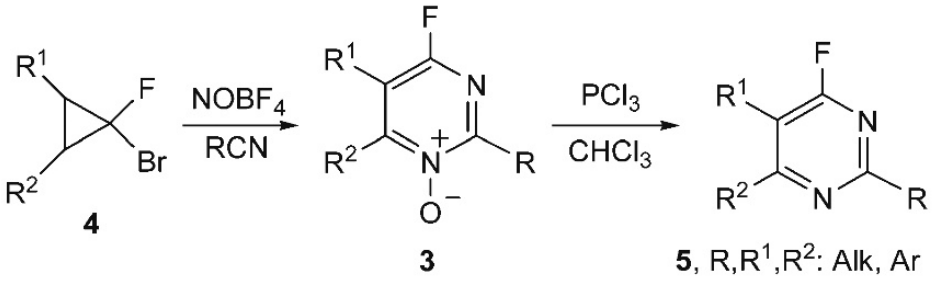


**Scheme 1.** Synthesis of 4-fluorosubstituted pyrimidine N-oxides and pyrimidines.

It is well-known that the treatment of halogen substituted pyrimidines with amines is a prevalent method of synthesis of aminopyrimidines, proceeding under mild conditions.[11a]

Nevertheless, though fluorine is the most effective leaving group in $S_NAr$ processes in the line of halogens,[13a] fluoropyrimidine derivatives are not of common use in the aminolysis reactions, due to their limited availability.[14b,15]

In the present work we have described the study of 4-fluoropyrimidine N-oxides **3** and 4-fluoropyrimidines **5** in SNAr reactions with primary and secondary amines, the targeted synthesis of a large series of 4-aminotetrahydroquinazoline derivatives, and analysis of their anti-TBEV activity and mechanism of action.

## Results and discussion

We performed a molecular docking study of a virtual library of 4-fluoropyrimidine N-oxides **3** to analyse possible directions of the scaffold decoration for the achievement of better binding. Molecules were docked into the detergent *n*-octyl-β-D-glucoside (β-OG) binding pocket of the TBEV E protein model constructed in the previous study.[7]

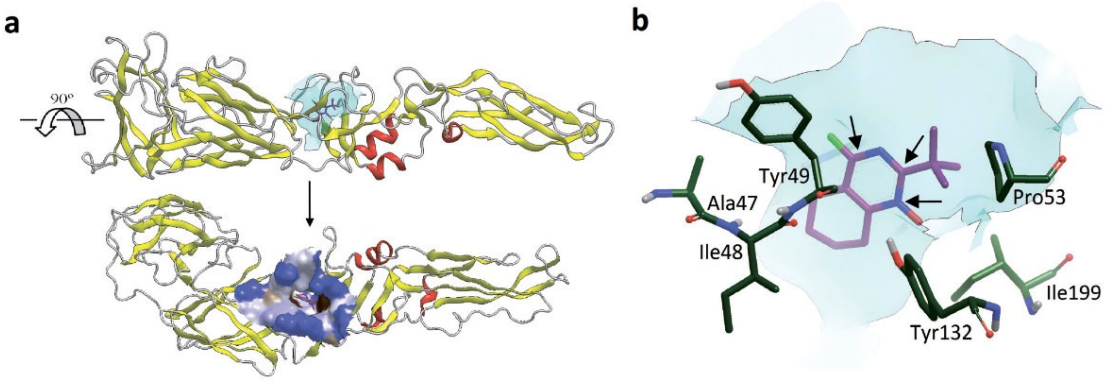


**Fig. 2.** (a) Localisation of the β-OG binding pocket (surface representation) in the monomeric TBEV E ectodomain (cartoon representation): upper panel – side view; lower panel – top view (perpendicular to the viral membrane). The docked pose of compound **3c** is shown as a reference; (b) docked pose of **3c**. Arrows show points of substituent variations explored in this study.

The binding mode of **3c** (see Scheme 2) appeared to be promising, showing the interaction of the *tert*-butyl group with the hydrophobic region (Pro53, Ile199) and the tetramethylene ring buried in the binding pocket (Fig. 2). The fluorine atom is directed towards the wide region near the binding site, thus allowing almost unrestricted variations in this position. A series of bulkier analogues **7a-ab** varied in positions 1, 2, and 4, was designed, synthesized and assessed against TBEV reproduction *in vitro*.

## Chemistry

4-Fluorotetrahydroquinazoline N-oxides **3a-c** were synthesized in good yields via heterocyclization of bromofluorocyclopropane **4a** in the presence of different nitriles (Scheme 2).[9] A brief optimization of conditions for the $S_NAr$ reaction was carried out on the model N-oxide **3a** and primary N-butylamine **6a** (Table 1). Varying the additional base and solvent we have found that the most effective method is to carry out the reaction in ethanol at room temperature using either diisopropylethylamine (DIPEA) or triethylamine to capture hydrogen fluoride formed. Using excess amino-component **6a** also affords 4-aminotetrahydroquinazoline N-oxide **7a** in high yield; nevertheless, in the case of less available amines this method is not practical.

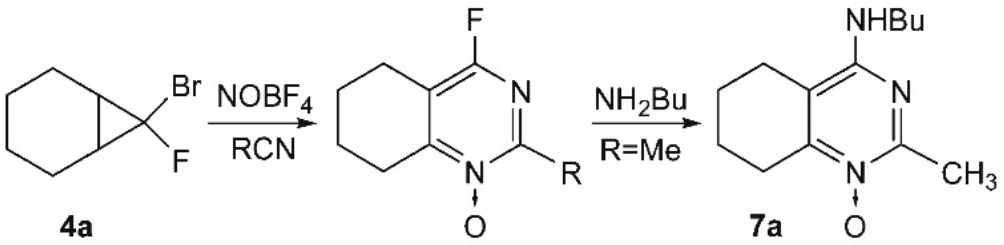


**Scheme 2.** Synthesis of 4-aminotetrahydroquinazoline N-oxide **7a**.

**Table 1** Condition variations for the synthesis of **7a**

| Entry | Conditions | Yield[a] **7a**/% |
|---|---|---|
| 1 | 1 eq. $NH_2Bu$, EtOH, 25°C | 44 |
| 2 | 2 eq. $NH_2Bu$, EtOH, 25°C | 64 |
| 3 | 3 eq. $NH_2Bu$, EtOH, 25°C | 83 (36)[b] |
| 4 | 1 eq. $NH_2Bu$, 2 eq. $Et_3N$, EtOH, 25°C | 89 (32)[b] |
| 5 | 1 eq. $NH_2Bu$, 2 eq. DIPEA, EtOH, 25°C | 90 (30)[b] |
| 6 | 1 eq. $NH_2Bu$, 2 eq. $K_2CO_3$, EtOH, 25°C | 68 |
| 7 | 1 eq. $NH_2Bu$, 2 eq. $K_2CO_3$, dioxane, 25°C | 50 |
| 8 | 1 eq. $NH_2Bu$, 2 eq. $K_2CO_3$, DMF, 25°C | 80 (28)[b] |
| 9 | 1 eq. $NH_2Bu$, 2 eq. $Cs_2CO_3$, DMF, 25°C | 73 |

[a] Yields were determined for crude products.
[b] Isolated yield after chromatographic purification.

We studied a series of aliphatic and aromatic amines, as well as those amines containing the bulky adamantane framework, **6a-q**, in the reaction with tetrahydroquinazoline derivatives **3a-c**, **5a** under the optimal conditions, and obtained a series of 4-aminosubstituted tetrahydroquinazolines and tetrahydroquinazoline N-oxides **7a-ab** (Scheme 3, Table 2).

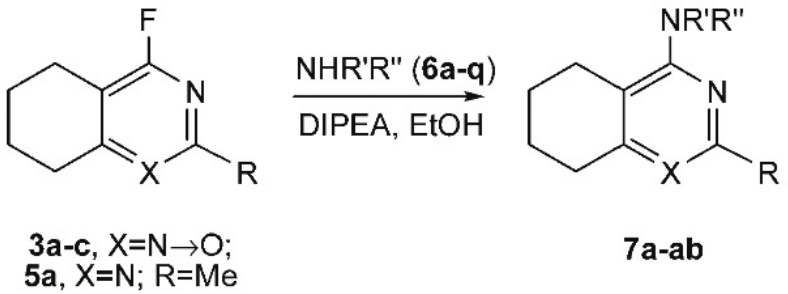


**Scheme 3.** Synthesis of 4-aminosubstituted tetrahydroquinazolines and tetrahydroquinazoline N-oxides **7a**-**ab**.

**Table 2** Structures of synthesised compounds

| Entry | X | R | NHR′R″ | R′ | R″[a] | Product | Yield[b]/% |
|---|---|---|---|---|---|---|---|
| 1 | N→O | Me | **6a** | H | *n*-Bu | **7a** | 36 |
| 2 | N→O | Me | **6b** | H | $CH_2Ph$ | **7b** | 50 |
| 3 | N→O | *t*-Bu | **6b** | H | $CH_2Ph$ | **7c** | 68 |
| 4 | N→O | Me | **6c** | H | $CH_2(4\text{-OMe-}C_6H_4)$ | **7d** | 40 |
| 5 | N→O | Me | **6d** | H | $CH_2(3\text{-OH-}4\text{-OMe-}C_6H_3)$ | **7e** | 42 |
| 6 | N→O | Me | **6e** | | 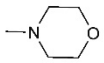 | **7f** | 85 |
| 7 | N | Me | **6e** | | 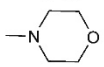 | **7g** | 65 |
| 8 | N→O | *t*-Bu | **6e** | | 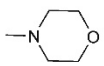 | **7h** | 43 |
| 9 | N→O | Me | **6f** | | 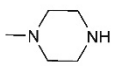 | **7i** | 90 |
| 10 | N | Me | **6f** | | 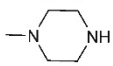 | **7j** | 59 |
| 11 | N→O | *t*-Bu | **6f** | | 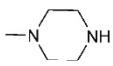 | **7k** | 32 |
| 12 | N→O | Me | **6g** | H | Ph | **7l** | 48 |
| 13 | N→O | *t*-Bu | **6g** | H | Ph | **7m** | 31 |
| 14 | N→O | Me | **6h** | H | $4\text{-Me-}C_6H_4$ | **7n** | 15 |
| 15 | N→O | Me | **6i** | H | $2\text{-OH-}C_6H_4$ | **7o** | 36 |
| 16 | N→O | Me | **6j** | H | $2\text{-Me-}5\text{-F-}C_6H_3$ | — | — |
| 17 | N→O | Me | **6k** | H | $CH_2$-(1-Ad) | **7p** | 20 |
| 18 | N→O | *t*-Bu | **6k** | H | $CH_2$-(1-Ad) | **7q** | 26 |
| 19 | N→O | Me | **6l** | H | $CH(1\text{-Ad})CH_3$ | **7r** | 15 |
| 20 | N→O | Me | **6m** | H | $(CH_2)_2$-(1-Ad) | **7s** | 36 |
| 21 | N→O | Et | **6m** | H | $(CH_2)_2$-(1-Ad) | **7t** | 47 |
| 22 | N→O | *t*-Bu | **6m** | H | $(CH_2)_2$-(1-Ad) | **7u** | 34 |
| 23 | N→O | Me | **6n** | H | $(CH_2)_2$-(2-Ad) | **7v** | 65 |
| 24 | N→O | *t*-Bu | **6n** | H | $(CH_2)_2$-(2-Ad) | **7w** | 62 |
| 25 | N→O | Me | **6o** | H | $(CH_2)_2O$-(1-Ad) | **7x** | 23 |
| 26 | N→O | Me | **6p** | H | CH(1-Ad)Ph | **7y** | 51 |
| 27 | N→O | *t*-Bu | **6p** | H | CH(1-Ad)Ph | **7z** | 25 |
| 28 | N→O | Me | **6q** | | 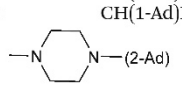 | **7aa** | 29 |
| 29 | N→O | *t*-Bu | **6q** | | 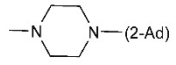 | **7ab** | 51 |

[a] Ad = Adamantyl [b] Isolated yields after chromatographic purification.

Generally, the reaction followed the common tendencies of nucleophilic substitution and proceeded in good yields in most cases. The aromatic amine with an electron-withdrawing group (**6j**) could not be involved in the reaction; even after increasing the time of reaction to 7 days, the conversion of the starting compound was low and the only product observed was ethoxy substituted N-oxide **8**, the product of solvolysis (Scheme 4). The decrease of isolated yields of products **7** is caused by the partial decomposition of pyrimidine N-oxides during the chromatographic separation from admixtures of starting amines and byproduct **8**.

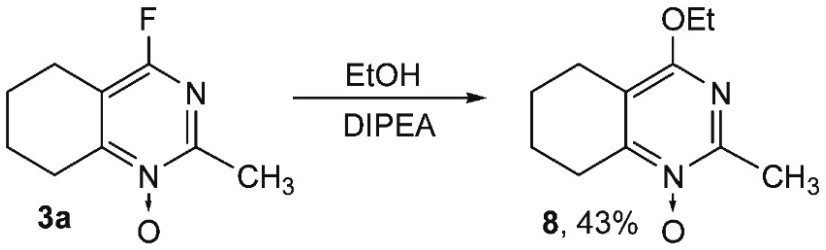


**Scheme 4.** Solvolysis of tetrahydroquinazoline N-oxide **3a** in ethanol.

## Assessment of cytotoxicity and antiviral activity

Most of the studied compounds revealed satisfactory solubility while preparing stock solutions in DMSO with a concentration of 25 mM with the exception of compounds **7q**, **7s**, **7t** and **7x**, which showed varying signs of precipitation at this concentration.

An acute (24 hours) and chronic (7 days) 50% cytotoxic concentration ($CC_{50}$) in porcine embryo kidney (PEK) cells were initially determined for all compounds (Table 3). Both acute and chronic toxicity were generally lower for those compounds which did not contain the adamantyl moiety. Cytotoxicity values varied significantly for both tetrahydroquinazoline and tetrahydroquinazoline N-oxide derivatives, but for all studied compounds 24 hours $CC_{50}$ values were over 10 μM. Based on these data, all compounds were sent for further assessment of antiviral activity.

**Table 3** Cytotoxicity, antiviral activity against TBEV and calculated octanol-water partition coefficient[16] ($_c \log P$) for compounds **7a**-**ab**

| Compound | $CC_{50}$ (24 h)/μM | $CC_{50}$ (7 d)/μM | $EC_{50}$/HM | *c* log *P* |
|---|---|---|---|---|
| **7a** | 172 | 97 | 12 ± 1 | 2.55 |
| **7b** | 432 | 93 | >50 | 3.34 |
| **7c** | 283 | 98 | 46 ± 3 | 4.61 |
| **7d** | 220 | 87 | >50 | 3.20 |
| **7e** | >500 | 214 | >50 | 2.54 |
| **7f** | >500 | >125 | >50 | 1.21 |
| **7g** | >500 | >500 | >50 | 0.93 |
| **7h** | >500 | 282 | >50 | 2.48 |
| **7i** | >500 | >500 | >50 | 1.08 |

| Compound | $CC_{50}$ (24 h)/μM | $CC_{50}$ (7 d)/μM | $EC_{50}$/HM | *c* log *P* |
|---|---|---|---|---|
| **7j** | >500 | 305 | >50 | 0.80 |
| **7k** | >500 | 213 | >50 | 2.35 |
| **7l** | >500 | >250 | >50 | 2.80 |
| **7m** | >500 | >500 | >50 | 4.07 |
| **7o** | >500 | 340 | 5.60 ± 0.09 | 1.91 |
| **7p** | 142 | 47 | >50 | 4.48 |
| **7q** | >500 | 419 | >50 | 5.75 |
| **7r** | 101 | 40 | >50 | 5.01 |
| **7s** | 54 | 12 | >50 | 4.97 |
| **7t** | 109 | 64 | 33.1 ± 0.2 | 5.33 |
| **7u** | 43 | 12 | 7.4 ± 0.5 | 6.24 |
| **7v** | 46 | 16 | >50 | 4.66 |
| **7w** | 54 | 35 | 6.6 ± 0.4 | 5.94 |
| **7x** | 183 | 85 | >50 | 3.83 |
| **7y** | 48 | 14 | 11 ± 3 | 6.03 |
| **7z** | 24 | 11 | 5.5 ± 0.2 | 7.03 |
| **7aa** | 391 | 90 | >50 | 3.77 |
| **7ab** | 271 | 211 | 14.1 ± 0.6 | 5.04 |

The antiviral activity of compounds **7a-m**, **7o-ab** was initially assessed by the 50% plaque reduction test ($PRT_{50}$) at a fixed concentration of 50 μM against 200 plaque forming units per mL (PFU $mL^{-1}$) of the TBEV strain Absettarov in the PEK cell line. The values of 50% effective concentration ($EC_{50}$) were determined for nine compounds that inhibited the growth of at least 50% of plaques at 50 μM, using the same procedure with sequential compound dilutions (Table 3). The compounds tested showed the dose-dependent inhibition of the viral reproduction (Fig. 3).

Compound **7a** showed moderate activity with $EC_{50}$ of 12 μM. To probe the electronic and steric effects, the butyl moiety was replaced by various substituents. A series of morpholine containing compounds (with the hydrogen bond acceptor function) **7f-h**, piperazine derivatives **7i-k** (hydrogen bond donors, given the protonation of the secondary amine at the physiological pH level), and compounds derived from the primary aromatic amines, showed no antiviral activity with the exception of **7o** ($EC_{50}$ = 5.60 μM) and barely active **7c**.

The potent compounds **7u**, **7w**, **7z**, and **7ab** contained a bulky hydrophobic adamantyl group in R" and a *tert*-butyl moiety in the R position. The removal of the adamantyl group led to significant activity decrease (**7z** vs. **7c**) or to its loss (**7ab** vs. **7k**). The replacement of the *tert*-butyl substituent with smaller groups also impaired the potency (**7s**, **7t**, **7v**, **7y**, **7aa**). Shortening of the linker between the adamantyl and the central moiety (**7q**) also resulted in the loss of activity. The efficacy of these adamantane derivatives correlated with their hydrophobicity (see c log*P* values in Table 3),

being in good agreement with the presence of large hydrophobic regions in the β-OG pocket of the TBEV E protein.

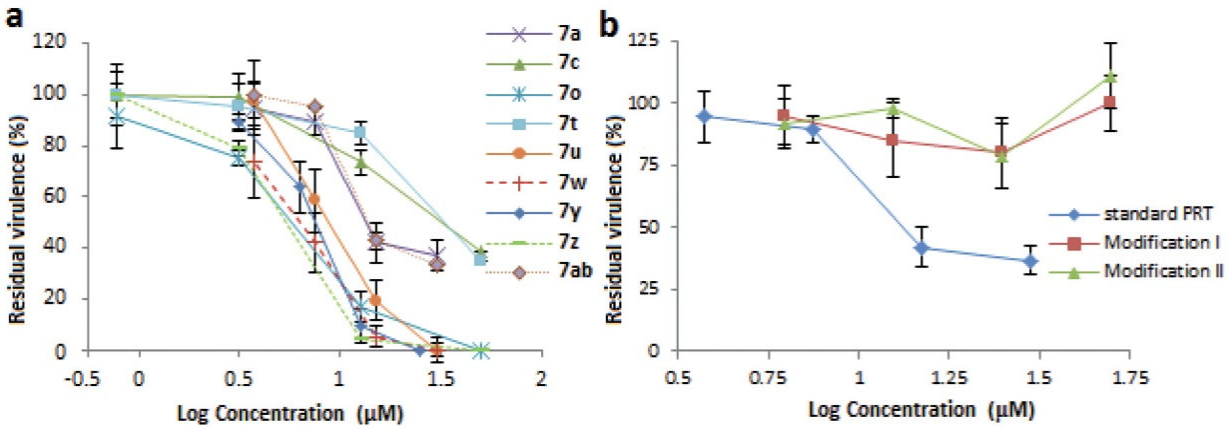


**Fig. 3.** (a) Dose-dependent responses of potent compounds in the standard $PRT_{50}$; (b) typical dose-dependent response of compound **7a** in the standard $PRT_{50}$ (virus suspension was preliminary incubated with the compound dilutions and then added to the cells) and the lack of the effect in the time-of-addition assay (compound dilutions were added to the cells 1 h before or after infection: on the graph modifications I and II respectively). Percent of residual virulence was calculated as a ratio of PFU in compound-treated well to DMSO-treated control well, multiplied by 100%. The data are the averages for duplicate wells for at least 3 independent experiments, and the error bars represent standard deviations from the mean.

## Identification of the infection stage associated with the reproduction inhibition

The mechanism of antiviral activity of the hit compounds was explored in this study by the time-of-addition assay as previously described.[17] In addition to a standard $PRT_{50}$ experiment, where the virus had been preliminarily incubated with the compounds and after that added to the cells, two additional experiments were performed: compounds were added to the cells 1 h before or after infection. No inhibition of viral reproduction was observed in these additional experiments, and only the standard $PRT_{50}$ led to the demonstration of dose dependent antiviral activity of the compounds (Fig. 4). Consequently, the compounds should interact with the virion surface prior to or at the stage of the virion entry into the host cell, but inhibition of reproduction does not take place on the later stages of the viral life cycle or due to interactions with the cells.

## Interaction with unrelated viruses

Specificity of compounds' interaction with Flaviviruses was also confirmed by a study of antiviral activity against completely unrelated non-enveloped poliovirus type 1 strain Sabin1 in human muscle rhabdomyosarcoma (RD) cell line. The TBEV reproduction inhibitors identified in this study did not show any inhibitory effect against poliovirus (data not shown), thus confirming our hypothesis about the specific interaction with the TBEV envelope.

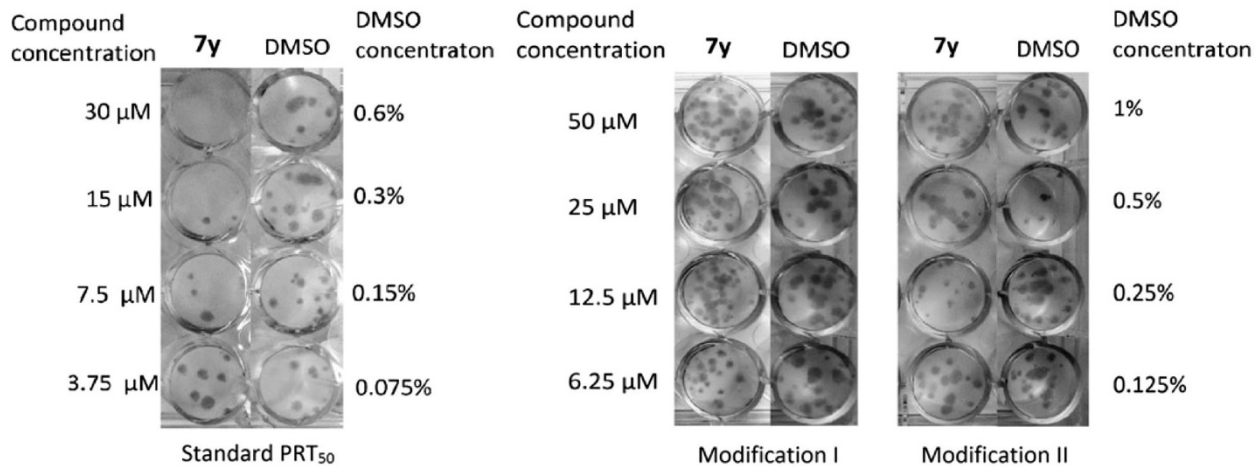


**Fig. 4.** Results of the standard $PRT_{50}$ test and the time-of-addition assay for compound **7y**. Dose-dependent number of foci in standard $PRT_{50}$ and comparable with DMSO-control number of foci in $PRT_{50}$ modification I (when cells were pre-incubated with the compounds for 1 h, and then the virus was added to the cells) and modification II (when cells were pre-incubated with the virus for 1 h, then compounds were added to the cells) are shown.

## Docking studies

Further docking studies were performed in an attempt to rationalize the data obtained in the experiments. A number of different binding modes were observed throughout the series (Fig. 5), thus showing the possible incompleteness of the initial hypothesis but still opening ways for further optimization of the scaffold. Two flipped orientations of the scaffold were observed most often, with N-oxide oxygen atoms pointing in opposite directions (Fig. 5a,c). Specific orientations were found for **7o** and **7ab**, which does not attain the pose similar to others.

The docked poses of **7a** and **7c** are similar to each other and characterised by hydrogen bonds with His275 and Tyr132 (Fig. 5a). The condensed cyclohexyl rings are pointed into the pocket similar to the binding mode of **3c** (Fig. 2). Docked poses of inactive compounds **7b**, **7d**, **7e**, **7l**, and **7m** are similar to the one of **7c**, but due to the presence of hydrophilic substituents in positions 3 and 4 of a phenyl ring **7d** and **7e** are scored lower compared to **7c**, because these groups form unfavourable interactions with a hydrophobic region. Compounds **7l** and **7m**, bearing phenyl instead of benzyl, cannot adopt a favourable conformation with a planar amino group; consequently, their lack of activity cannot be unexpected. Compound **7b** bears a smaller methyl group instead of a tert-butyl and forms fewer interactions with the binding site than **7c**.

Adamantyl groups of **7u** (Fig. 5a) and **7w**, similarly placed in the site, perfectly fit the hydrophobic cavity formed by Ile199, Ala212, and Ala274, while *t*-Bu groups contact Ala47. Hydrogen bonds with His275 and Tyr132 are also formed. Replacement of *t*-Bu with a smaller moiety (**7s**, **7t**, **7v**) and decrease of length of the aliphatic linker to adamantyl (**7q**, **7p**) impair these interactions.

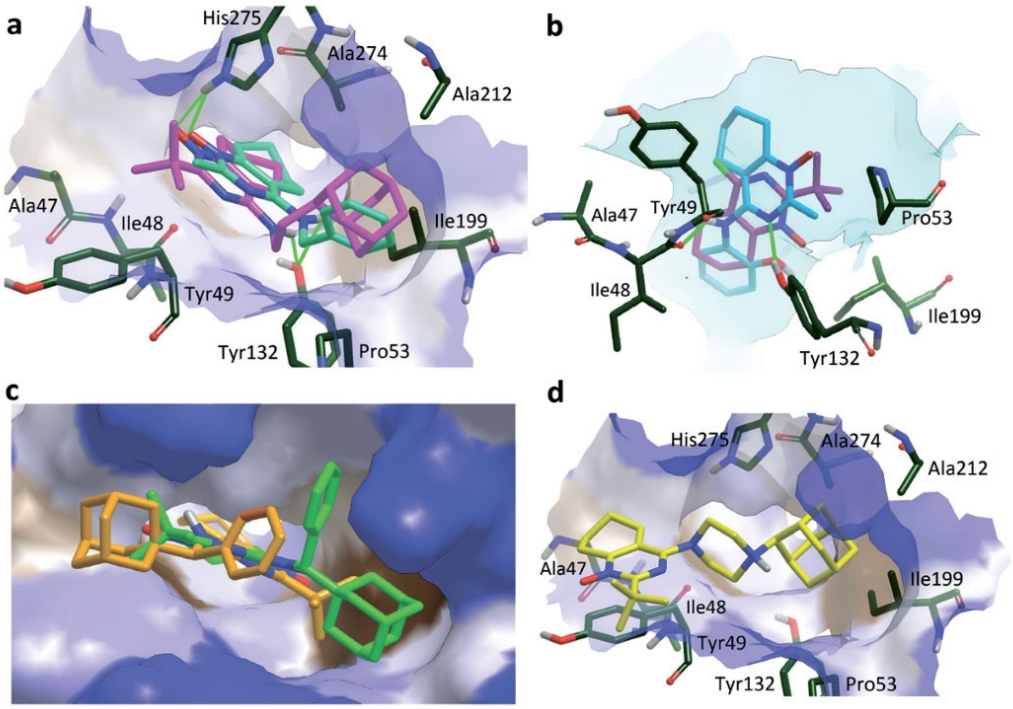


**Fig. 5.** Docking of tetrahydroquinazoline N-oxides into the β-OG pocket of the TBEV E protein model: (a) docked poses of **7c** (sea-green) and **7u** ( purple), top view; (b) docked poses of **3c** (mauve) and **7o** (light-blue), side view. Surface is coloured cyan; (c) docked poses of (*R*)-**7z** (yellow) and (*S*)-**7z** (light-green); (d) docked pose of **7ab**, top view. The surface is coloured according to the Kyte-Doolittle hydrophobicity scheme[31] (blue for the most hydrophilic regions, to white, to brown for the most hydrophobic), if not stated otherwise; hydrogen bonds are coloured light-green.

The best scored pose of one of the most active compounds **7o** differs significantly from the poses of all other active compounds with tetramethylene pointing to the deep regions of the β-OG pocket (Fig. 5b): hydrogen bonds can be formed between the hydroxyl group of Tyr132 and the nitrogen atom at position 3 of the pyrimidine ring, and between the carbonyl oxygen atom of Ile48 and the amino group of **7o**.

Hydrogen bonding seems to have a significant impact on the affinity of the aforementioned compounds, whereas for the chiral compound **7z** the key role should be played by the hydrophobic interactions. Two enantiomers of **7z** (Fig. 5c) are predicted to bind in hydrophobic regions of the pocket in opposite ways. Further enantiomer separation and activity measurements should be conducted to design a new generation of **7z** analogues.

The predicted binding pose of **7ab** differs significantly from the other compounds poses due to π-π stacking interactions between Tyr49 and the pyrimidine N-oxide ring (Fig. 5d), while existing hydrophobic interactions between the adamantyl moiety of compound **7ab** and the cavity of Ile199, Ala212 and Ala274, and between the cyclohexyl ring and Ala47 take place.

Several ways of further SAR exploration in the pyrimidine N-oxide were pointed out based on the docking results. The first method, not considered in this study, is a modification of the condensed cyclohexyl fragment by the introduction of various

small groups and/or ring size adjustment for better exploration of the deeper cavities of the pocket and solubility improvement. These modifications should be accompanied by the analysis of substituents in the R position of the most active compounds **7u**, **7w**, **7ab**, **7o** with the aim to optimize the toxicity and activity of the compounds. Distinct binding modes of **7o** and **7ab** open a separate branch for structure optimization, which can be initially explored by the analysis of substituted phenyl moieties.

## Conclusions

In conclusion, we have developed a simple and efficient methodology for the synthesis of 4-aminopyrimidines and pyrimidine N-oxides with a wide range of substituents based on the heterocyclization of the readily available 1-bromo-1-fluorocyclopropanes and an aromatic nucleophilic substitution in the resulting fluoropyrimidine core. A number of 4-aminotetrahydroquinazoline derivatives containing aliphatic and aromatic substituents as well as a bulky adamantane framework were synthesized by employing this method. We performed an initial SAR exploration for a novel series of antiviral heterocyclic compounds, inhibiting the reproduction of tick-borne encephalitis virus and possessing good solubility. Substituents were varied in positions 1, 2 and 4 of the tetrahydroquinazoline fragment, and several compounds with an anti-TBEV activity on a micromolar level were identified. Preliminary mechanism studies proved the interaction of compounds with the viral envelope. The highest antiviral activity was observed for the adamantane containing molecules. This study opens possibilities for further optimization of the scaffold with the aim of designing the fusion inhibitors of the tick-borne encephalitis virus.

## Experimental section

### Chemistry

**General experimental details.** NMR spectra were recorded on an Agilent 400-MR spectrometer (400.0 MHz for $^{1}$H; 100.6 MHz for $^{13}$C) at room temperature; chemical shifts were measured with reference to the solvent ($CDC1_3$, $\delta_H$ = 7.24 ppm, $\delta_C$ = 77.13 ppm). Chemical shifts (3) are given in ppm; *J* values are given in Hz. When necessary, assignments of signals in NMR spectra were made using 2D techniques. Accurate mass measurements (HRMS) were done on a JEOL GCMate II mass spectrometer (70 eV). Elemental analyses were performed on a Carlo Erba 1106 instrument. Analytical thin layer chromatography was carried out with Silufol silica gel plates (supported on aluminum); the detection was done by using a UV lamp (254 and 365 nm). Column chromatography was performed on silica gel (230–400 mesh, Merck). Starting compounds **3a-c**,**9 4a**,[9] **5a**,[10] **6m**,[18] **6n**,[19] **6o**,[20] **6p**,[21] **6q** [22] were synthesized by known procedures.

All other starting materials were commercially available. All reagents except commercial products of satisfactory quality were purified by literature procedures prior to use.

**General procedure for the preparation of compounds 7a-ab**. A mixture of tetrahydroquinazoline derivatives **3a-c**, **5** (0.5 mmol), the corresponding amine (0.5 mmol) and DIPEA (129 mg, 1.0 mmol) in ethanol (1 mL) was stirred for 24 h at room temperature. The solvent was evaporated in vacuo, the product was isolated via column chromatography ($SiO_2$). Only characterization data for chosen representative compounds are presented here as they were chosen for biomedical assays. Complete characterization of all novel compounds along with NMR spectra can be found in the ESI.

## Docking studies

Rigid docking of multi-conformer compound libraries was performed in the open-state detergent-binding pocket A of the TBEV E protein dimer model obtained earlier.[7] OpenEye software suite was used in the course of molecular docking. The docking procedure consisted of the following steps: (1) tautomeric and protonation state cleanup in QUACPAC 1.5.0;[23] (2) exhaustive conformer and enantiomer generation in OMEGA 2.4.6;[24] (3) MMFF charge[25] assignment in QUACPAC 1.5.0; (4) rigid molecular docking of the pregenerated conformer ensembles into the rigid protein site in FRED 2.2.5[26] with Chem- gauss3 scoring function[27] used during the pose selection, 10 alternative poses were generated for each ligand; (5) scoring of alternative poses with Chemgauss4;[28] (6) visual analysis of the binding modes in VIDA 4.2.1.[16a]

## Virological studies

**Cells and viruses.** Porcine embryo kidney (PEK) cell line was maintained at 37°C in medium 199 (FSUE IPVE) supplemented with 5% fetal bovine serum (FBS, Gibco).

Human muscle rhabdomyosarcoma (RD) cell line was maintained at 36°C in a minimal essential medium with double quantity of minerals and amino acids (2x MEM) (FSUE IPVE) with 5% fetal bovine serum (FBS, Gibco).

TBEV strain Absettarov (GenBank access no. AF091005) from laboratory collection of Chumakov IPVE was isolated in the Leningrad region in 1951 from the blood of a patient with acute TBE. Reference vaccine strain Sabin 1 of poliovirus type 1 (GenBank access no. V01150) from Moscow RRL Polio collection originated from NIBSC (UK).

Viruses were stored as aliquots of infected cultural fluid at –70°C.

**Cytotoxicity test in PEK cells.** A cytotoxicity test in PEK cells was performed as described previously.[7] In brief, PEK cells were seeded and incubated for 72 hours at 37°C. Stock solutions of the compounds with the concentration of 25 mM were prepared in 100% DMSO (Sigma). Two-fold dilutions of studied compounds were prepared in medium 199 on Earle solution to obtain final concentrations starting from 500 μM. Equal volumes of compound dilutions were added in three replicates to the

cells. Cell control was treated with the same sequential concentrations of DMSO, as in compounds dilutions, and the culture medium with no additions to mark the possible non-specific effect of DMSO on the cell line. After incubation at 37°C on days 1 or 7 the cultural supernatant was gently removed and the cells were washed with phosphate buffered saline (PBS, Sigma) twice. A solution of 0.0002% neutral red in PBS was added to the washed cells, and the cells were incubated for 30 minutes at 37°C, so the live cells would consume dye in endosomes. Afterwards cells were gently washed with PBS twice and fixed with 96% ethanol. Dye absorption was counted using MultiScan FC (Thermo) at 450 nm. $CC_{50}$ was calculated according to the Reed and Muench method.[29]

**50% Plaque reduction tests ($PRT_{50}$).** $PRT_{50}$ was performed in PEK cells as described previously.[7] Briefly, PEK cells were seeded and incubated for 72 hours at 37°C. Stock solutions of the compounds with a concentration of 5 mM were prepared in 100% DMSO (Sigma). For initial activity screening solutions of studied compounds with a final concentration of 50 pM were prepared in medium 199 on Earle solution. For further $EC_{50}$ determination four sequential dilutions of studied compounds were prepared with concentrations starting from 50 pM (**7c**, **7o**, **7t**, **7z**) or 30 pM (**7a**, **7u**, **7y**, **7w**, **7ab**). Equal volumes of TBEV suspension, containing approximately 200 PFU $mL^{-1}$, were added to each compound dilution. For virus control, a virus was added to the same sequential dilutions of DMSO, as in compound dilutions, to mark the possible nonspecific effect of DMSO on viral incorporation into the cells. Virus control and virus + compound were incubated at 37°C for 1 hour. Equal aliquots of control virus or virus + compound were added in four replicates to the cells, and incubated at 37°C for 1 hour with gentle shaking for virus adsorption. Negative cell control was treated with the same sequential dilutions of compounds. Then, each well was overlaid with 0.85% methylcellulose (Sigma) containing 2% FBS (Gibco). After incubation at 37°C for 3 days cells were fixed with 96% ethanol, and foci were immunostained. Percent of residual virulence was calculated as a ratio of PFU in compound-treated well to DMSO-treated control well, multiplied by 100%. $EC_{50}$ was calculated according to the Reed-and-Muench method.[29]

**Time of addition test.** Two additional modifications of the initial $PRT_{50}$ were performed to establish the stage of viral infection which the studied compounds inhibited. At first, cells were pre-incubated with the compounds, and then virus was added to the cells – to find out whether the compounds affect cells that inhibit viral reproduction. Secondly, cells were pre-incubated with the virus, after that the compounds were added to the cells – to understand if the compound affects virus reproduction after virion incorporates the cell:

1. Stock solutions of the compounds with a concentration of 5 mM were prepared in 100% DMSO (Sigma). Compound dilutions and the same sequential dilutions of DMSO as a virus control were added to the cells in two replicates

(with concentrations corresponding to those in cell wells at initial experiment) and incubated at 37°C for 1 hour. Then, cells were washed twice with medium 199 on Earle solution and the virus suspension equivalent to initial experimental PFU was added. Negative cell control was treated with the same volume of medium 199 on Earle solution.

2. The virus suspension was added to the cells and incubated at 37°C for 1 hour. Negative cell control was treated with medium 199 on Earle solution. After two rinses with medium 199 on Earle solution four compound dilutions and the equivalent concentrations of DMSO as in the first experiment were added to the cells. Negative cell control was treated with the same dilutions of the compounds. After 1 hour of incubation at 37°C, cells were washed twice with medium 199 on Earle solution.

Then, cells were overlaid with 0.85% methylcellulose (Sigma) containing 2% FBS (Gibco). After incubation at 37°C for 3 days cells were fixed with 96% ethanol, and foci were immunostained.

**Selectivity control with poliovirus (PV).** Stock solutions of the compounds with a concentration of 5 mM were prepared in 100% DMSO (Sigma). Eight 2-fold dilutions of studied compounds were prepared in 2x MEM medium to obtain a final concentration series starting from 50 pM. Compound dilutions were mixed with equal volume of the PV suspension containing 100 $TCID_{50}$ (50% tissue culture infective dose) in four replicates. For virus control the same sequential dilutions of DMSO, as in compound dilutions, were mixed with the virus suspension. For cell control, the same sequential concentrations of DMSO were mixed with equal volume of the culture medium. After 1 hour incubation at 36°C the RD cell suspension in 2x MEM medium containing 5% FBS was added to experimental mixtures.

To confirm the PV dose the back titration of the virus suspension was performed.

Following a 5-day incubation at 37°C, cytopathic effect (CPE) was visually assessed. The virus titre was calculated according to the Karber method.[30]

## Acknowledgements

This work was partially supported by the Russian Foundation for Basic Research (grants no. 14-03-00469, 14-03-31566, 13-0300572, 15-04-08365) and the Presidium of RAS (Program no. 8). The research work was carried out using an Agilent 400-MR NMR spectrometer purchased under the program of MSU development.

## Notes and references

1 (*a*) J. Süss, *Ticks Tick-Borne Dis.,* 2011, **2**, 2-15; (*b*) K. L. Mansfield, N. Johnson, L. P. Phipps, J. R. Stephenson, A. R. Fooks and T. Solomon, *J. Gen. Virol.*, 2009, **90**, 1781-1794.

2 G. J. Sips, J. Wilschut and J. M. Smit, *Rev. Med. Virol.*, 2012, **22**, 69-87.

3 T. C. Pierson and M. S. Diamond, in *Fields Virology*, ed. D. M. Knipe and P. Howley, Lippincott

Williams & Wilkins, Philadelphia, 6th edn, 2013, ch. 26, pp. 747-794.

4 (*a*) M. S. Vorob'eva, M. N. Rasshchepkina and I. P. Ladyzhenskaia, *Vopr. Virusol.*, 2007, **52**, 30-36; (*b*) F. X. Heinz and K. Stiasny, *Vaccine*, 2012, **30**, 4301-4306.

5 N. A. Pen'evskaia and N. V. Rudakov, *Med. Parazitol.*, 2010, 53-59. [PMID 20361640].

6 I. K. Baykov, A. L. Matveev, O. V. Stronin, A. B. Ryzhikov, L. E. Matveev, M. F. Kasakin, V. A. Richter and N. V. Tikunova, *Vaccine*, 2014, **32**, 3589-3594.

8 D. I. Osolodkin, L. I. Kozlovskaya, E. V. Dueva, V.V. Dotsenko, Y. V. Rogova, K. A. Frolov, S. G. Krivokolysko, E. G. Romanova, A. S. Morozov, G. G. Karganova, V. A. Palyulin, V. M. Pentkovski and N. S. Zefirov, *ACS Med. Chem. Lett.*, 2013, **4**, 869-874.

9 S. Mukhopadhyay, R. J. Kuhn and M. G. Rossmann, *Nat. Rev. Microbiol.*, 2005, **3**, 13-22.

10 K. N. Sedenkova, E. B. Averina, Y. K. Grishin, A. G. Kutateladze, V. B. Rybakov, T. S. Kuznetsova and N. S. Zefirov, *J. Org. Chem.*, 2012, **77**, 9893-9899.

11 K. N. Sedenkova, E. B. Averina, Y. K. Grishin, T. S. Kuznetsova and N. S. Zefirov, *Tetrahedron Lett.*, 2014, **55**, 483-485.

12 (*a*) D. J. Brown, in *The Chemistry of Heterocyclic Compounds: The Pyrimidines*, ed. E. C. Taylor and A. Weissberger, John Wiley & Sons, Inc. N.-Y., Chichester, Brisbane, Toronto, Singapore, 1994, vol. 52, pp. 545-546; (*b*) S. D'Errico, G. Oliviero, N. Borbone, J. Amato, D. D'Alonzo, V. Piccialli, L. Mayol and G. Piccialli, *Molecules*, 2012, **17**, 13036-13044; (*c*) A. M. Shestopalov, A. E. Fedorov, L. A. Rodinovskaya, A. A. Shestopalov and A. A. Gakh, *Tetrahedron Lett.*, 2009, **50**, 5257-5259; (*d*) H. Sun and S. G. DiMagno, *Angew. Chem., Int. Ed.*, 2006, **45**, 2720-2725; (e) M. Darabantu, T. Lequeux, J.-C. Pommelet, N. Plé, A. Turck and L. Toupet, *Tetrahedron Lett.*, 2000, **41**, 67636767.

13 (*a*) T. Fujimoto, F. Becker and T. Ritter, *Org. Process Res. Dev.*, 2014, **18**, 1041-1044; (*b*) H. Cai, D. Yin, L. Zhang and Y. Wang, *J. Fluorine. Chem.*, 2006, **127**, 837-841; (*c*) V. Gurvich, H.-Y. Kim, R. P. Hodge, C. M. Harris and T. M. Harris, *Nucleosides Nucleotides*, 1999, **18**, 2327-2333.

14 (*a*) J. Liu and M. J. Robins, *J. Am. Chem. Soc.*, 2007, **129**, 5962-5968; (*b*) N. Yoneda and T. Fukuhara, *Tetrahedron*, 1996, **52**, 23-36.

15 (*a*) P. S. Fier and J. F. Hartwig, *Science*, 2013, **342**, 956-960; (*b*) P. S. Fier and J. F. Hartwig, *J. Am. Chem. Soc.*, 2014, **136**, 10139-10147.

16 For examples see: (*a*) Y. Inouye and Y. Higuchi, *J. Fluorine Chem.*, 1985, **27**, 231-236; (*b*) L. M. Popova and E. P. Studentsov, *Russ. J. Org. Chem.*, 1996, **32**, 1376-1381; (*c*) T. J. Delia, D. P. Anderson and J. M. Schomaker, *J. Heterocycl. Chem.*, 2004, **41**, 991-993; (*d*) E. L. Parks, G. Sandford, D. S. Yufit, J. A. K. Howard, J. A. Christopher and D. D. Miller, *Tetrahedron*, 2010, **66**, 6195-6204; (*e*) K. M. Lovell, A. S. Felts, A. L. Rodriguez, D. F. Venable, H. P. Cho, R. D. Morrison, F. W. Byers, J. S. Daniels, C. M. Niswender, P. J. Conn, C. W. Lindsley and K. A. Emmitte, *Bioorg. Med. Chem. Lett.*, 2013, **23**, 3713-3718.

17 (*a*) *VIDA, version 4.2.1*, OpenEye Scientific Software, Inc., Santa Fe, NM, USA, www.eyesopen.com, 2010; (*b*) R. Wang, F. Ying and L. Lai, *J. Chem. Inf. Comput. Sci.*, 1997, **37**, 615-621.

18 E. V. Dueva, D. I. Osolodkin, L. I. Kozlovskaya, V. A. Palyulin, V. M. Pentkovski and N. S. Zefirov, *Mol. Inf.*, 2014, **33**, 695-708.

19 I. A. Novakov, I. A. Kulev, S. S. Radchenko, K. A. Birznieks, E. I. Boreko, G. V. Vladyko and L. V. Korobchenko, *Pharm. Chem. J.*, 1987, **21**, 287-291.

20 Y. V. Popov, V. M. Mokhov and N. A. Tankabekyan, *Russ. J. Appl. Chem.*, 2013, **86**, 404-409.

21 B. Gopalan, A. Thomas and D. M. Shah, *WO* 2006090244, 2006; *Chem. Abstr.*, 2006, **145**, 292604.
22 A. D. Averin, E. R. Ranyuk, S. L. Golub, A. K. Buryak, E. N. Savelyev, B. S. Orlinson, I. A. Novakov and I. P. Beletskaya, *Synthesis*, 2007, 2215-2221.
23 N. V. Klimova, L. N. Lavrova, G.V. Pushkar, M. I. Shmar'yan, A. P. Arendaruk and A. P. Skoldinov, *Khim.-Farm. Zh.*, 1975, **9**, 8-11; N. V. Klimova, L. N. Lavrova, G. V. Pushkar, M. I. Shmar'yan, A. P. Arendaruk and A. P. Skoldinov, *Chem. Abstr.*, 1976, **84**, 43963.
23 *QUACPAC, version 1.5.0*, OpenEye Scientific Software, Inc., Santa Fe, NM, USA, www.eye-sopen.com, 2010.
24 (*a*) *OMEGA, version 2.4.6*, OpenEye Scientific Software, Inc., Santa Fe, NM, USA, www.eye-sopen.com, 2010; (*b*) P. C. D. Hawkins, A. G. Skillman, G. L. Warren, B. A. Ellingson and M. T. Stahl, *J. Chem. Inf. Model.*, 2010, **50**, 572-584.
25 T. A. Halgren, *J. Comput. Chem.*, 1996, **17**, 520-552.
26 (*a*) *FRED, version 2.2.5*, OpenEye Scientific Software, Inc., Santa Fe, NM, USA, www.eye-sopen.com, 2010; (*b*) M. McGann, *J. Comput. Aided Mol. Des.*, 2012, **26**, 897-906.
27 M. R. McGann, H. R. Almond, A. Nicholls, J. A. Grant and F. K. Brown, *Biopolymers*, 2003, **68**, 76-90.
28 M. McGann, *J. Chem. Inf. Model.*, 2011, **51**, 578-596.
29 L. J. Reed and H. Muench, *Am. J. Epidemiol.*, 1938, **27**, 493-497.
30 WHO, *Polio laboratory manual*, 4th edn, 2004, WHO, Geneva, WHO/IVB/04/10.
31 J. Kyte and R. Doolittle, *J. Mol. Biol.*, 1982, **157**, 105-132.

# Раздел VI. Избранные работы в области развития методов компьютерного молекулярного моделирования и QSAR

## Введение

### В.А. Палюлин

Важным направлением работ, выполненных под руководством и при непосредственном участии академика Н.С. Зефирова, явились обширные исследования как по разработке и развитию новых методов анализа количественной связи между структурой и физиологической активностью веществ, развитию методов молекулярного моделирования биомишеней, по разработке новых моделей для прогнозирования параметров ADMET, так и по их применению для направленного дизайна структур новых веществ с заданной биологической активностью и определенным набором свойств.

Первые исследования в этих областях были начаты еще во второй половине 80-х годов и уже к середине 90-х годов в лаборатории Н.С.Зефирова были разработаны на тот момент одни из лучших в мире нейросетевых программых комплексов, позволяющих строить надежные модели, связывающие свойства и биологическую активность органических соединений с особенностями их строения, а также осуществлять автоматическую генерацию и отбор наиболее перспективных структур. Разработанные в те годы методы и основанные на них модели и компьютерные программы наряду с новыми разработками успешно применяются и в настоящее время для моделирования связи структура–активность и успешного прогнозирования целого ряда свойств, необходимых для дизайна лекарственных веществ. Достаточно сказать, что компьютерная программа, занявшая первое место в мире в 1995 году по точности прогнозирования липофильности лекарственных веществ, и по сей день остается одной из наиболее надежных.

В конце 90-х – начале 2000-х годов благодаря развитию компьютерной техники и появлению ключевых экспериментальных данных о пространственном строении ряда белков появилась возможность молекулярного моделирования важнейших биомишеней, экспериментальные данные о строении которых полностью отсутствовали. В результате сотрудниками лаборатории Н.С.Зефирова на Химическом факультете МГУ были построены первые корректные модели важнейших рецепторов, определяющих функционирование центральной нервной системы человека – всех подтипов метаботропных глутаматных рецепторов, всех доменов N-метил-D-аспартатного рецептора (см. главу 2), внеклеточных доменов рецепторов $ГАМК_A$ и $ГАМК_C$, аденозиновых рецепторов всех подтипов и ряда других. Появлявшиеся позже в литературе экспериментальные данные под-

тверждали высокую точность построенных моделей, а использование этих моделей для дизайна новых физиологически активных соединений позволило найти целый ряд новых веществ, обладающих высокой физиологической активностью.

Дальнейшие детальные исследования по молекулярному моделированию ионотропных глутаматных рецепторов AMPA-типа, включая методы молекулярной динамики, позволили осуществить дизайн целых классов совершенно новых модуляторов, проявляюших активность в электрофизиологических экспериментах в субнаномолярных концентрациях и обладающих когнитивно-стимулирующими свойствами в исследованиях на лабораторных животных (подробнее эти результаты рассмотрены в главе 2). Несколько веществ из этих серий успешно прошли полные циклы доклинических исследований.

Следствием обширных исследований в перечисленных областях стала публикация более ста статей в ведущих научных журналах, материалы которых, к сожалению, совершенно невозможно рассмотреть в рамках данной небольшой главы. Поэтому мы решили ограничиться лишь несколькими из последних работ, в которых Н.С. Зефиров принимал активное участие. Две статьи относятся к применению новых методов при моделировании ингибиторов киназы гликогенсинтазы GSK-3, которая участвует в важнейших сигнальных путях. Селективные ингибиторы этой киназы могут быть полезны в сочетании с другими препаратами при лечении диабета второго типа, а также в качестве противоопухолевых препаратов. В работе [1] при моделировании связи структура–активность для ингибиторов киназы GSK-3 с помощью 3D QSAR успешно использованы разработанные в лаборатории Н.С. Зефирова новые методы расчета частичных атомных зарядов и показана их высокая эффективность при проведении моделирования. В работе [2] предложен и детально рассматривается метод одноклассовой классификации на основе структур лигандов для виртуального скрининга ингибиторов киназы GSK-3. Работы [3–6] посвящены прогностическим моделям важнейших свойств лекарственных веществ – их абсорбции в желудочно-кишечном тракте, проникновению через гематоэнцефалический барьер и действию на известную антимишень hERG. Для всех трех свойств были построены лучшие на тот период модели, позволяющие их оценивать с помошью компьютерных программ, доступных на веб-сайте лаборатории.

В заключение подчеркнем, что многочисленные работы Н.С.Зефирова и его соавторов, посвященные разработке и развитию новых методов в области молекулярного моделирования, QSAR и математической химии получили широкое мировое признание и высокое цитирование. К сожалению, объем данной книги позволил представить лишь очень небольшую часть таких работ. Тем не менее, ссылки на другие работы Н.С. Зефирова легко могут быть найдены как в системе «ИСТИНА» МГУ, так и в других поисковых системах.

## Список статей раздела

1. Tsareva D.A., Osolodkin D.I., Shulga D.A., Oliferenko A.A., Pisarev S.A., Palyulin V.A., Zefirov N.S. General Purpose Electronegativity Relaxation Charge Models Applied to CoMFA and CoMSIA Study of GSK-3 Inhibitors // *Mol. Informatics*. 2011. V. 30. № 2-3, P. 169-180.

2. Karpov P.V., Osolodkin D.I., Baskin I.I., Palyulin V.A., Zefirov N.S. One-class classification as a novel method of ligand-based virtual screening: The case of glycogen synthase kinase 3 beta inhibitors // *Bioorg. Med. Chem. Lett.* 2011. V. 21. № 22. P. 6728-6731.

3. Радченко Е.В., Дябина А.С., Палюлин В.А., Зефиров Н.С. Прогнозирование всасывания лекарственных веществ в кишечнике человека // *Изв. АН Сер. Хим.* 2016. № 2, С. 576-580.

4. Дябина А.С., Радченко Е.В., Палюлин, Н.С. Зефиров. Прогнозирование проникновения органических веществ через гематоэнцефалический барьер. // *Доклады Академии наук. Биохимия, Биофизика, Молекулярная биология*. 2016. Т. 470. № 6. С. 301-723.

5. Радченко Е.В., Рулев Ю.А., Сафаньяев А.Я., Палюлин В.А., Зефиров Н.С. Компьютерная оценка риска hERG-опосредованной кардиотоксичности потенциальных лекарственных веществ // *Доклады Академии наук. Биохимия, Биофизика, Молекулярная биология*. 2017. Т. 473. № 4. С. 301-497.

6. Zefirov N.S., Palyulin V.A. Molecular modelling of central nervous system receptors // *Mendeleev Commun*., 2010. V. 20. P. 243-248.

*MOLECULAR INFORMATICS. Vol. 30 (2-3), 169-180 (2011)*

DOI: 10.1002/minf.201000141

# GENERAL PURPOSE ELECTRONEGATIVITY RELAXATION CHARGE MODELS APPLIED TO COMFA AND COMSIA STUDY OF GSK-3 INHIBITORS

**D.A. Tsareva, D.I. Osolodkin, D.A. Shulga, A.A. Oliferenko, S.A. Pisarev, V.A. Palyulin, N.S. Zefirov**

*Department of Chemistry, Moscow State University, Moscow, Russia*
*Institute of Physiologically Active Compounds, Russian Academy of Sciences, Chernogolovka, Moscow Region, Russia*

Presented at the 18th European Symposium on Quantitative Structure Activity Relationships, EuroQSAR 2010, Rhodes, Greece

Two fast empirical charge models, Kirchhoff Charge Model (KCM) and Dynamic Electronegativity Relaxation (DENR), had been developed in our laboratory previously for widespread use in drug design research. Both models are based on the electronegativity relaxation principle *(Adv. Quantum Chem.* 2006, *51,* 139-156) and parameterized against ab initio dipole/quadrupole moments and molecular electrostatic potentials, respectively. As 3D QSAR studies comprise one of the most important fields of applied molecular modeling, they naturally have become the first topic to test our charges and thus, indirectly, the assumptions laid down to the charge model theories in a case study. Here these charge models are used in CoMFA and CoMSIA methods and tested on five glycogen synthase kinase 3 (GSK-3) inhibitor datasets, relevant to our current studies, and one steroid dataset. For comparison, eight other different charge models, ab initio through semiempirical and empirical, were tested on the same datasets. The complex analysis including correlation and cross-validation, charges robustness and predictability, as well as visual interpretability of 3D contour maps generated was carried out. As a result, our new electronegativity relaxation-based models both have shown stable results, which in conjunction with other benefits discussed render them suitable for building reliable 3D QSAR models.

## 1. Introduction

The electrostatic interactions play a crucial role in biomolecular environment, where a delicate interplay between polar and nonpolar parts governs the biological functions of the species. The electrostatic forces are long range, and in most biomolecular applications it is sufficient to use atom-centered charges to account for much of the molecular electrostatics. Thus, development and testing of charge calculation methods is a very important topic in modern molecular modeling.

Three-dimensional quantitative structure-activity relationship (3D QSAR) studies are widely used in biomolecular modeling and in searching for prospective drug candidates due to the ease of visual interpretation.[1] The Comparative Molecular Field Analysis[2] (CoMFA) and Comparative Molecular Similarity Indices Analysis[3] (CoMSIA) are the most popular 3D QSAR methods based on the spatial alignment of molecules. For both methods electrostatic and steric (in CoMSIA additionally hydrophobic and hydrogen bond donor and acceptor) molecular fields are implemented. The atomic charges are used to describe the electrostatic field in both methods.

Different types of charge calculation methods find their use: (i) in population analysis of wavefunctions,[4-6] (ii) in fitting atomic charges to reproduce the ab initio calculated molecular electrostatic potential (MEP),[7-11] (iii) in Bader's electron density analysis,[12,13] (iv) in corrected semiempirical methods like AM1-BCC,[14] and (v) in the Hückel method.[15] The methods (i)–(iii) are computationally expensive, so a number of fast empirical and semiempirical methods have been designed. The very early accomplishments were the Sanderson equalization of electronegativity[16] and the Del Re semiempirical model.[17] The Sanderson electronegativity equalization principle gave rise to a multitude of modern charge models including the Gasteiger–Marsili[18] method, the full equalization of orbital electronegativity,[19,20] the QEq method by Rappe and Goddard,[21] Zefirov's charges,[22,23] the Kirchhoff Charge Model,[24-26] the VC scheme by Gilson et al.[27] and the QTPIE (charge transfer with polarization current equilibration) method by Martinez and coworkers.[28] The Del Re model was combined by Pullman[29] with the Hückel method to reproduce dipole moments of aromatic and conjugated compounds. In a similar way, by combining the Gasteiger-Marsili σ-charges and the Hückel π-charges, the Gasteiger-Hückel model was introduced and implemented in the Sybyl program.[30] Among the other charge models, the RESidual CHArges[31] and the MMFF94 force field charges[32] should be mentioned. The Kirchhoff Charge Model (KCM) has been developed by us based on the application of Kirchhoff's electrical circuit laws to equalize atomic electronegativities in a molecule.[25,26] Later it was reformulated as a discrete Laplace equation with Dirichlet boundary conditions to establish the electronegativity relaxation principle.[33] The KCM model was parameterized to reproduce ab initio calculated dipole and quadrupole moments and finally implemented in a virtual screening routine.[24] The most recent extension of the Kirchhoff Charge Model is the Dynamic Electronegativity Relaxation[35] (DENR), which provides a unified description framework for several known charge schemes based on incomplete electronegativity equalization. DENR parameters were fitted to reproduce ab initio (HF/6-31G*) calculated MEP. The latter makes the charges directly applicable to modeling with majority of classical biochemical force fields such as AMBER, GROMACS, and MMFF94.

Currently no particular atomic charge model has been recommended as standard for using in 3D QSAR studies. The common practice is to use any readily available atomic charges based on very different assumptions such as AM1,[36] AM1-ESP,[37]

AM1-BCC,[38] ESP,[39] Gasteiger–Marsili,[40,41] Gasteiger–Hückel,[42-44] MMFF94[42] Hückel,[45] and Pullman.[45] This could be regarded as a sign of relatively low sensitivity of 3D QSAR results to the choice of charge derivation method.

Comparative analysis of the different atomic charges influence on CoMFA or CoMSIA results is infrequent but it would be very instructive. The early analysis by Kroemer et al.[46] was based on the dataset of 37 compounds. The study revealed that MEP-fitting methods based on semiempirical or ab initio wavefunctions provided higher predictive ability than the Mulliken and Gasteiger–Marsili charges. A few similar studies can be found in the literature.[47,48] In the recent study,[47] common semiempirical charges such as MNDO, AM1, and PM3 were used and it was found that in CoMFA and CoMSIA they were superior to the Gasteiger–Marsili and Gasteiger–Hückel methods. The authors recommended the use of MMFF94 charges if the former ones were not available.

Despite the wavefunction-based charges have become increasingly affordable recently, they still have well known inherent drawbacks hindering their massive application in molecular modeling, such as: a) low calculation speed, which impedes processing of huge molecule sets; b) exaggerated dependence of charges on molecular geometry; c) generally small relevance of charges to the description of intermolecular electrostatic interactions (except ESP-based methods);[11] d) instability of ESP-based charges as the consequence of intrinsically ill-defined ESP-charge fitting procedure;[11] e) high sensitivity to the quantum chemical level used. The account of the above factors has been incorporated into the design and choice of parameters for KCM and DENR so that they are suitable for wide range of molecular modeling approaches.

The aim of this work is to investigate to which extent KCM and DENR schemes are suited to 3D QSAR modeling as implemented in CoMFA and CoMSIA. Thus the indirect assessment of the underlying assumptions in our charge schemes is intended. To provide a proper context for comparison of charge performance in our 3D QSAR studies, five GSK-3 inhibitor and one steroid datasets were selected. Despite the choice of target activities is rather arbitrary and focused on our current research interests, we hope that certain generalizations could be derived based on this study. A number of other available charge models were also tested on the same datasets. There are indications of little charge dependence of certain CoMFA models in the literature.[49,50] To assess the statistical significance of the use of charges, models with excluded electrostatic descriptors were additionally derived. The charge models selected for comparison were the Gasteiger-Hückel (GH), Merck Molecular Force Field 94 (MMFF94), the Pullman model (PLM), the AM1 with Bond Charge Corrections (AM1-BCC, the Lowdin charges (LOWD), the Mulliken charges (MULL), the Merz-Kollman Electrostatic Potential charges (MK-ESP), and the Restrained Electrostatic Potential fit charge model (RESP). The prediction accuracy of the 3D QSAR models built was analyzed in terms of the $R^2$ and $Q^2$ values. A detailed graphical analysis of 3D molecular fields was

also carried out, as visual interpretability of 3D QSAR models gives direct drug design decision guidance.

## 2. Materials and Methods

### 2.1. Datasets

Six datasets used in this study are described in Table 1. Five of them are inhibitors of glycogen synthase kinase 3 (GSK-3): aloisines (ALOIS for short), indirubins (INDIRU), maleimides (MALEI), paullones (PAULL), and N-phenyl-4-pyrazolo[1,5-b]pyridazin-3-ylpyrimidin-2-amines (PYRID). The sixth dataset represents steroid structures[2] (STERO). The datasets were sketched and maintained with Instant JChem 5.0.0.[51] Three-dimensional coordinates for all structures were generated with a Concord 8.0 program,[52] with 2,000 optimization steps taken and other parameters set to the default values. The structure alignment (according to the common substructure criterion) was done with the Sybyl 8.0 software.[53]

**Table 1.** Dataset specifications

| Dataset | N | Activity | Activity range[a] | Structure | Ref |
|---|---|---|---|---|---|
| ALOIS | 35 | GSK-3 | 4.07 – 7.00 | 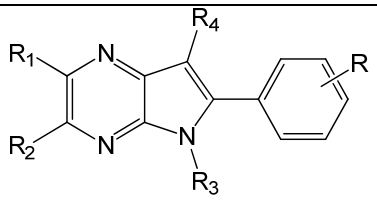 | 49 |
| INDIRU | 85 | GSK-3 | 3.70 – 8.66 | 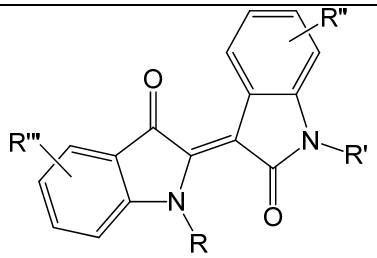 | 50-54 |
| MALEI | 107 | GSK-3 | 7.69 – 9.74 | 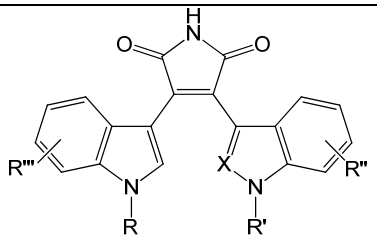 | 55-61 |
| PAULL | 77 | GSK-3 | 3.00 – 8.40 | 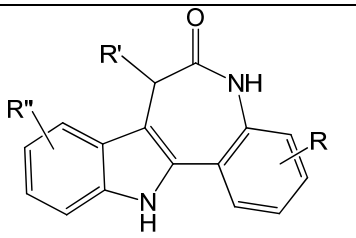 | 62-64 |

| | | | | | |
|---|---|---|---|---|---|
| PYRIDAZ | 70 | GSK-3 | 4.50 — 8.30 | 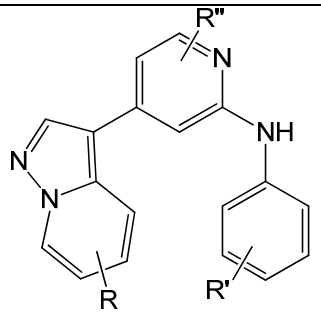 | 65 |
| STERO | 21 | TBG | 5.32 – 9.74 | 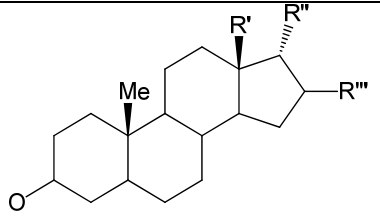 | 2 |

[a]All activity values are collected from the literature and given in p$IC_{50}$ units; in the case of MALEI the Cheng-Prusoff equation was used to convert $IC_{50}$ values to p$Ki_{20}$, with $K_M$ = 20μM[66].

## 2.2. Atomic Charge Calculation

Ten different charge calculation schemes were evaluated. KCM and DENR charges were calculated with in-house programs. Parameters for KCM are published and can be found elsewhere,[34] while the DENR parameters are given in the Supporting Information. The calculation of GH, MMFF94 and PLM charges was done with Sybyl. AM1-BCC charges were calculated with Antechamber 1.27.[72] The MK- ESP and RESP charges were generated using the resp program.[73] PC-GAMESS/Firefly software[74] was employed to calculate atomic charges by the Löwdin and Mulliken population analyses. All quantum chemical calculations were performed at the RHF/6-31G* level of theory without structure optimization.

## 2.3. 3D QSAR Modeling

### *2.3.1. CoMFA Settings*

All analyses were performed with Sybyl software with all parameters set to default: Tripos force field, $C_{sp3}$ hybridized probe atom with formal charge +1.0, grid spacing 2.0 A, steric and electrostatic cutoffs 30.0 kcal/mol, distance-dependent dielectric constant ($1/r^2$), no smoothing.

### *2.3.2. CoMSIA Settings*

Five molecular fields were used for the calculation of similarity indices within Sybyl software: steric, electrostatic, hydrophobic, H-bond donor and H-bond acceptor. The parameters for probe atom and grid spacing were the same as in CoMFA. Attenuation factor was set to 0.3.

*2.3.3. Statistical Analysis*

Partial least squares (PLS) calculations both for CoMFA and CoMSIA were performed with Sybyl 8.0. In case of both CoMFA and CoMSIA the 'leave-one-out', 'cross-validation' and 'no validation' procedures were the same. The 'leave- one-out' procedure was conducted with the number of components ranging from 10 to 20 (depending on the number of compounds in the dataset) in order to identify the optimal number of components to be used next, in 'cross-validation' and 'no validation' analyses. The column filtering threshold was set to 2.0. The number of groups in 'cross-validation' analysis was taken five for ALOIS, eleven for INDIRU, fifteen for MALEI, ten for both PAULL and PYRID, and five for STERO. Ten 'cross-validation' analyses with random splitting for each model were carried out, and the mean $Q^2$ values were used for comparison. Strong outliers were excluded from the datasets, with respective models rebuilt and additional analyses done over again.

## 3. Results

Three types of statistical models for both CoMFA and CoMSIA were generated for each of the six datasets. The first type is "All Fields Included". This is a default model where electrostatic and steric fields (CoMFA) and electrostatic, steric, hydrophobic, and hydrogen bond donor/acceptor fields (CoMSIA) are turned on. Two other types of models are "No electrostatics" (electrostatic field turned off) and "Only electrostatics" (all molecular fields except electrostatic are turned off). Thus, given six datasets, ten charge models, and two 3D QSAR techniques, CoMFA and CoMSIA, in total 252 statistical models were generated: ten default models and ten "Only Electrostatics" models plus one "No electrostatics" model for each dataset multiplied by 2, the number of methods involved. All numerical statistical data (leave-one-out correlation coefficient $R^2_{LOO}$, number of components NoC, cross-validation correlation coefficient $Q^2$, correlation coefficient $R^2$, standard error *S,* Fischer criterion *F*) are given in the Supporting Information. Generally, one can observe that the quality of 3D QSAR models is datasetdependent: the best statistically consistent results ($Q^2$>0.5) are achieved for the datasets MALEI, PAULL, PYRIDAZ and STERO, both for CoMFA and CoMSIA. Particular results depending on the types of models and technique used are presented in the graphical form and described in the forthcoming sections.

### 3.1. CoMFA Models

*3.1.1. CoMFA All Fields Included*

The results of CoMFA analyses with all fields included are shown in Figure 1 ($Q^2$) and in the Supporting Information. The best structure-biological activity correlations were obtained for datasets PYRIDAZ and STERO for which the $R^2$ values are 0.95–0.98.

For the other datasets $R^2$ values were generally not less than 0.8, with PAULL as the only exception. Investigation of cross-validation helps to estimate the internal consistency and predictive ability of the model under study. Thus in terms of $Q^2$ the results are somewhat different. The PYRIDAZ dataset still demonstrates the best $Q^2$ values ranging from 0.70 to 0.78, while the models for MALEI and STERO are characterized by lower but still acceptable values. Rather low $Q^2$ values for ALOIS, INDIRU and PAULL are in accord with the presence of a few strong outliers (see Supporting Information).

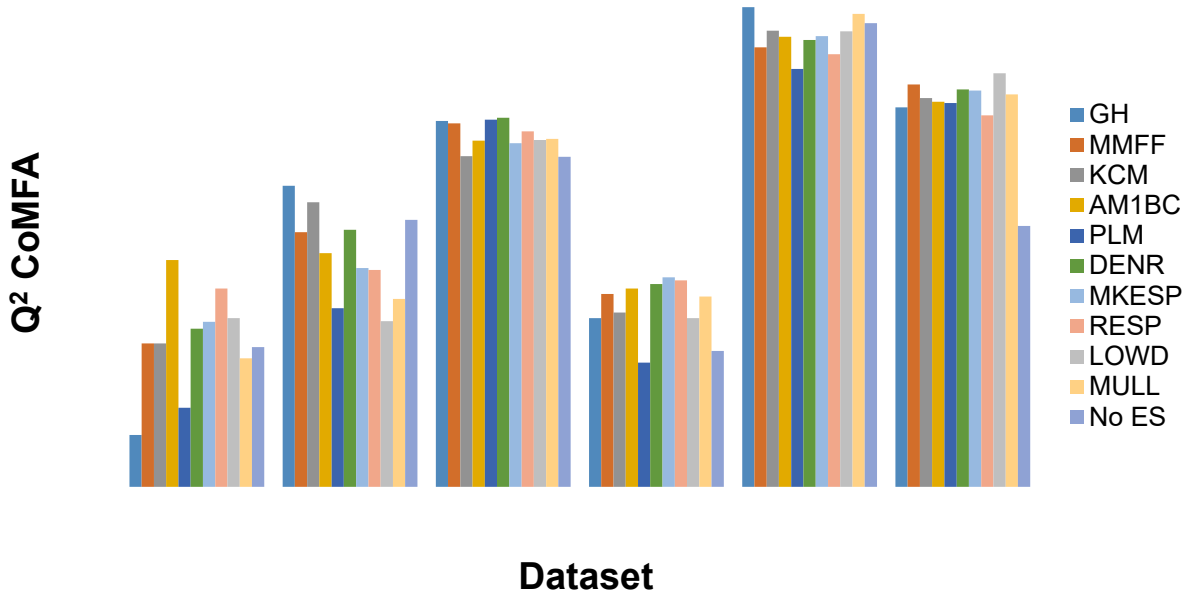


**Figure 1**. Cross-validation correlation coefficients for CoMFA (All Fields Included and No Electrostatics).

In terms of the charge models, the correlation and internal consistency quality is rather similar across the datasets, though with a few notable exceptions, especially when $Q^2$ values are considered. GH and PLM charges show the lowest $Q^2$ values for the ALOIS dataset. The Pullman (PLM) model is particularly less performing than the other charge models for the following datasets: ALOIS, INDIRU, PAULL, and PYRIDAZ, both in terms of $R^2$ and $Q^2$. PLM is not the only charge model demonstrating unstable results: LOWD charges perform greatly for STERO, but are the poorest for the INDIRU dataset. One observes that in many cases the "best" charge model only slightly improves the performance of the model compared to the most popular GH or MMFF94 charges, whereas the 'worst' model (most frequently PLM) leads to a notable decrease in $Q^2$.

Another observation of interest is that the models built with the use of charge calculation methods tending to reproduce the MEP (KCM, DENR, MMFF94, and AM1-BCC) provide higher correlation coefficients and fewer number of outliers compared to the models built with GH charges. A substantial improvement was achieved with the use of these charges in the datasets ALOIS and PAULL. The "true" MEP-fitted charges such as MK-ESP and RESP are also performing rather well, with the

INDIRU dataset being the only exception. This reiterates again the necessity of an adequate MEP representation in CoMFA modeling. Despite only subtle improvements are achieved in datasets MALEI and STERO, one could see that molecular fields generated with the above-mentioned MEP-reproducing methods are more stable and consistent.

### *3.1.2. CoMFA No Electrostatics*

Turning electrostatics off (shown in Figure 1 with the rightmost bars) led to substantial decreases in $Q^2$ for the ALOIS, PAULL, and STERO datasets. The other three datasets showed only insignificant drop in both $R^2$ and $Q^2$. Thus, the electrostatic field may seem far less important comparing to the steric one for the INDIRU, MALEI, and PYRIDAZ datasets. As shown below, this is not necessarily true.

### *3.1.3. CoMFA Only Electrostatics*

Here only electrostatic descriptors are taken into account, with no steric, which enables one to approximate differences in binding energy in the set by electrostatic contributions only and to compare the performance of different charge models in terms of correlation with biological activity (Figure 2).

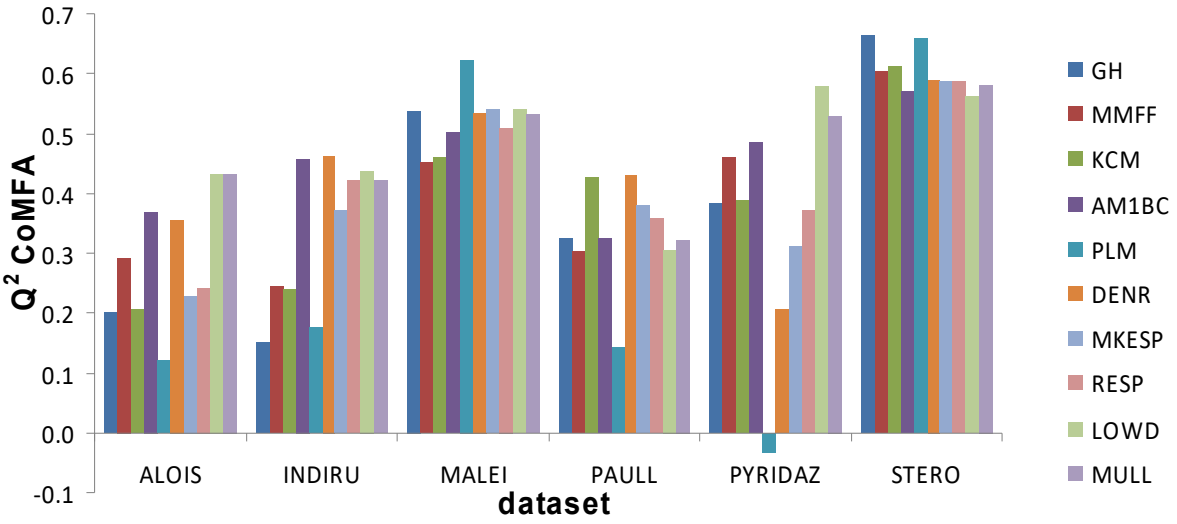


**Figure 2**. Cross-validation correlation coefficients for CoMFA (Only Electrostatics).

The PLS fit in some cases is not affected by the turning electrostatic and steric fields on and off, instead a slight increase in $R^2$ may take place. This is illustrative in the INDIRU dataset where both purely steric and electrostatic models with the AM1-BCC, DENR, RESP, LOWD, and MULL charges are of comparable statistical quality. For this dataset, the two molecular fields can be thought of as mutually replaceable or highly correlated. In the case of the MALEI dataset, only DENR provides $R^2$ higher than does the "No Electrostatics" model. Electrostatics is vitally important for successful correlation of PAULL, as the $R^2$ value drops down dramatically if the electrostatic

field is excluded, and conversely: purely electrostatic models with the KCM, PLM, DENR, MK-ESP, RESP, and LOWD charges are comparable to those with both molecular fields. Only on the PYRIDAZ dataset the purely steric model sufficiently outperforms the purely electrostatic ones according to their $R^2$ values.

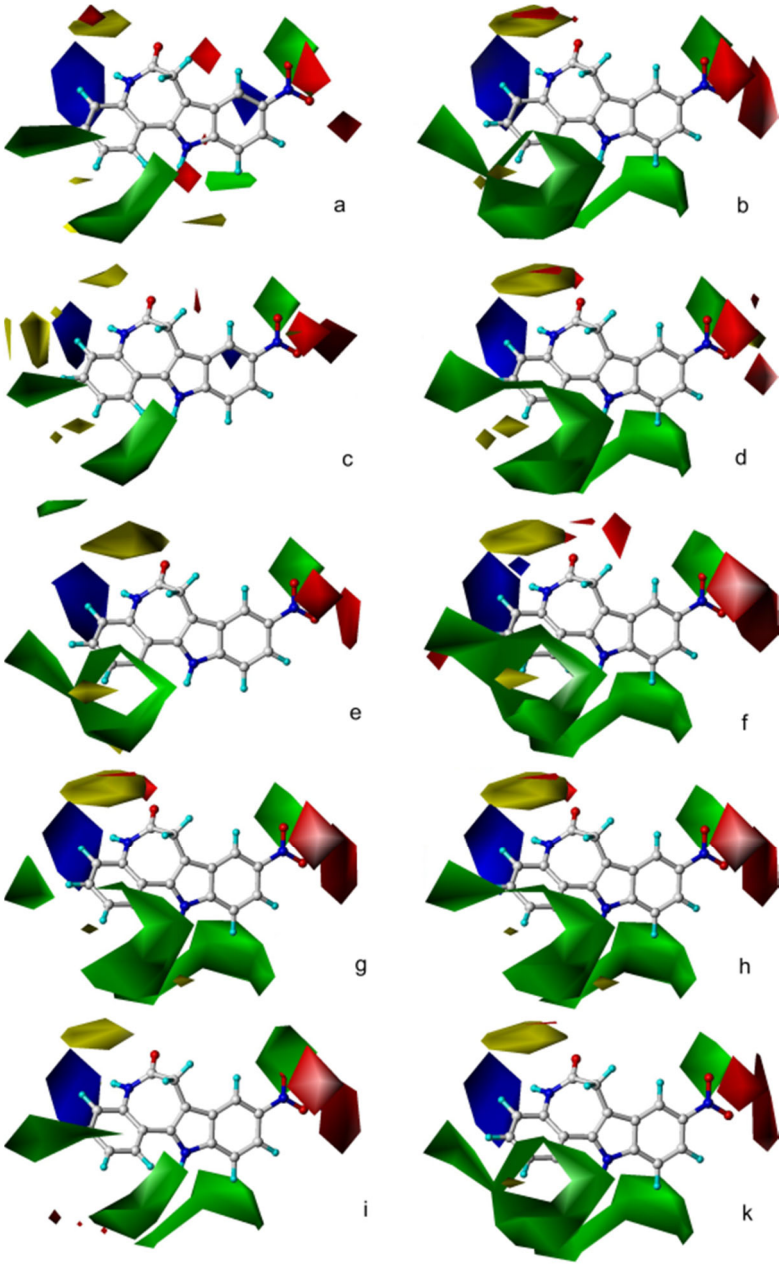


**Figure 3.** CoMFA contour maps of steric and electrostatic interaction fields. The charge models are: a) GH; b) MMFF94; c) PLM; d) AM1-BCC; e) LOWD; f) MULL; g) MK-ESP; h) RESP; i) KCM; k) DENR. The fields are displayed around the structure of alsterpaullone. Green areas correspond to favored steric bulk, yellow ones – to disfavored, blue areas – to favored positive charge, and red – to favored negative charge.

The cross-validation comparison (presented by Figures 1 and 2) is less straightforward. The models with PLM and GH charges are less stable, showing significant spread of $Q^2$ values with the highest values for MALEI and STERO. ALOIS, INDIRU, and PYRIDAZ demonstrate different patterns of the $Q^2$ distribution: empirical (GH, MMFF94, KCM, PLM) and MEP-fitted (MK-ESP and RESP) charges lead to rather

low $Q^2$. The models for the MALEI and STERO datasets show more consistent results with lower dependence on charge scheme. The most surprising finding is that the nonempirical charges, both Mulliken and Lowdin, provide the highest cross-validation coefficients on all datasets.

### *3.1.4. Contour Maps*

Contour maps analysis is illustrated (Figure 3) by PAULL dataset since the influence of charge scheme on the prediction quality for this set is substantial. The conclusions made on the contour maps analysis for this set are nevertheless general. The interpretation of contour maps of interactions is easier for the MEP-fitted (MK-ESP and RESP) and MEP-reproducing (KCM and DENR) charges due to the presence of large continuous fields, that in turn facilitates the design of new inhibitors. On the contrary, the contour maps of GH and PLM models are quite different: the interaction fields are notably smaller and split, that implies a lower variation of the electrostatic potential with biological activity, lack of which has to be compensated by nonelectrostatic contributions.

## 3.2. CoMSIA Models

### *3.2.1. CoMSIA All Fields Included*

The results of the CoMSIA analyses (Figure 4) differ from CoMFA results significantly. First, the CoMSIA correlation coefficients (see Supporting Information) are higher and more evenly distributed over datasets and charge models than those of CoMFA. Second, cross-validation results are more affected by the choice of electrostatics compared to CoMFA.

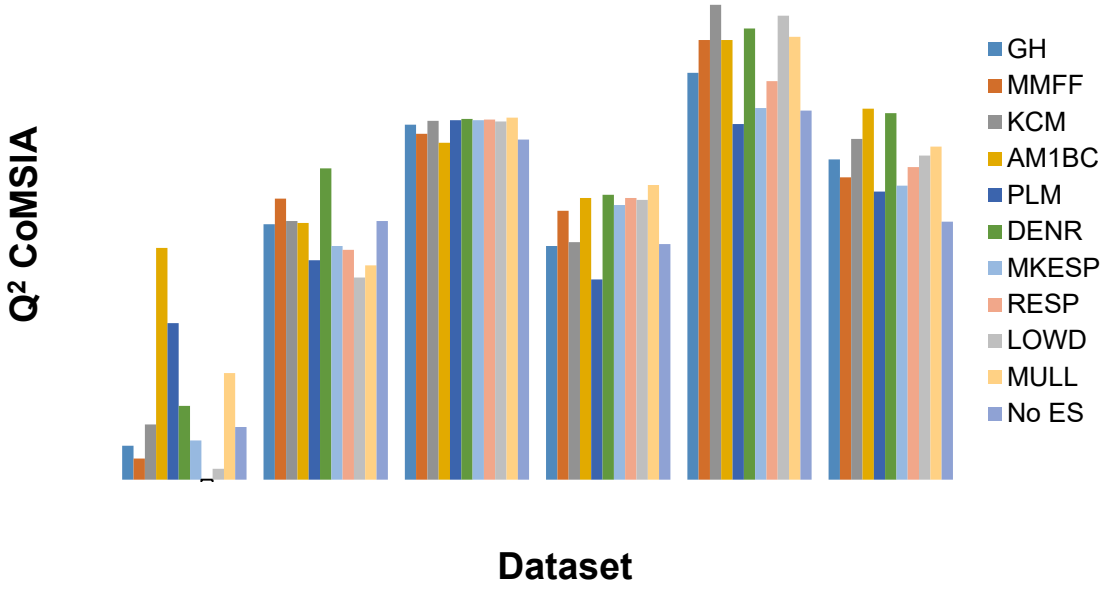


**Figure 4.** Cross-validation correlation coefficients for CoMSIA (all fields included and no electrostatics).

### *3.2.2. CoMSIA No Electrostatics*

Correlation and cross-validation results without electrostatics are shown in the histograms with the rightmost bars. The omission of explicit electrostatics has only a negligible effect on the $R^2$ values (Supporting info). In case of the $Q^2$ data, this results in a more substantial decrease, especially for the ALOIS, PAULL, PYRIDAZ, and STERO datasets. Seemingly, the "no electrostatics" model works well only for the INDIRU dataset, as its $Q^2$ is slightly higher than the average. The set of five fields used in CoMSIA seems to be exhaustive at least on our data sets in a sense that the fields are sufficiently correlated so that the lack of each of them is easily compensated with the others. Very uniform cross-validation results are obtained for the MALEI dataset. The most consistent charge models for CoMSIA are KCM, DENR, AM1-BCC, and MULL.

### *3.2.3. CoMSIA Only Electrostatics*

In this case the results become more diverse and generally inferior to both the CoMFA and the standard, five-field CoMSIA. In terms of correlation ($R^2$), high values are achieved with all charge models for the ALOIS, MALEI, and STERO datasets (see Supporting Information). The PYRIDAZ dataset is best described by the nonempirical LOWD and MULL models. The INDIRU dataset exemplifies inadequacy of using electrostatics alone for CoMSIA studies: the only charge model able to provide a sensible correlation is MK- ESP.

Cross-validation analysis (Figure 5) only exaggerates the picture: none of the charge models except KCM showed a positive $Q^2$ value for the INDIRU dataset.

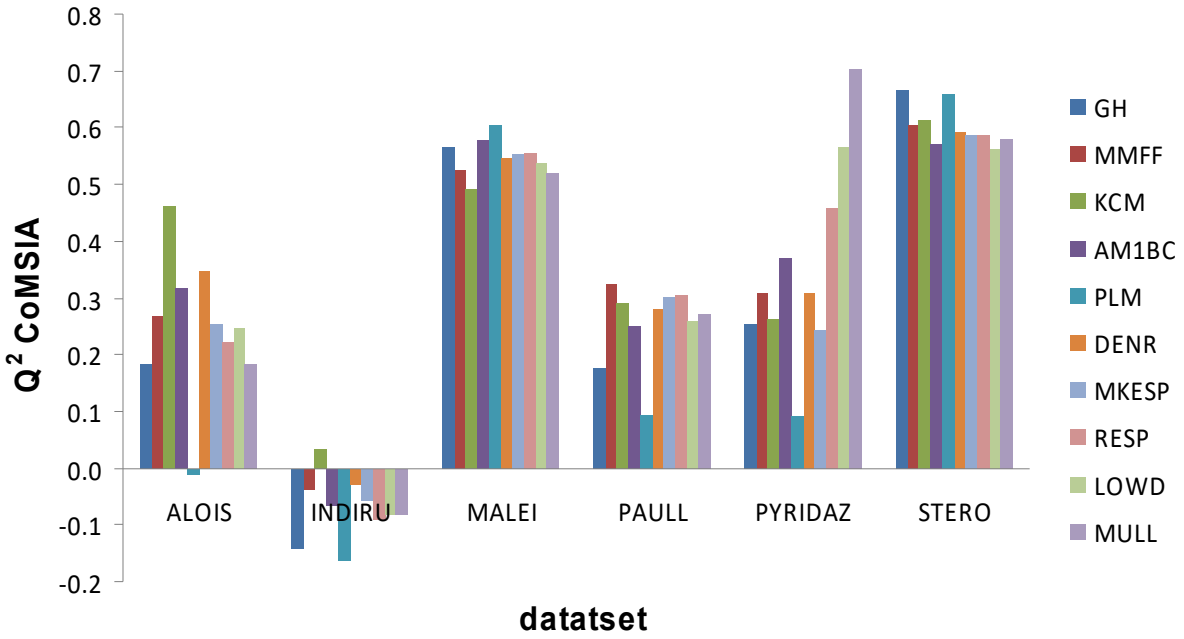


**Figure 5.** Cross-validation correlation coefficients for CoMSIA (Only Electrostatics).

The ALOIS, PAULL, and PYRIDAZ datasets are also examples of insufficiency of purely electrostatic CoMSIA models. Only KCM and DENR charges show reasonable cross-validation being applied to the ALOIS dataset, while MEP-fitted and especially nonempirical LOWD and MULL charge models are the best for PYRIDAZ. The PLM charge model performs worst for the ALOIS, INDIRU, PAULL, and PYRIDAZ datasets, but is surprisingly good in case of the MALEI and STERO datasets, which confirms the observed instability of this charge model.

### *3.2.4. Contour Maps*

Contour maps of CoMSIA steric and electrostatic interactions shown in Figure 6 are more continuous than those of CoMFA. Despite MK-ESP and RESP methods should provide better electrostatic description, the models built with them are more fragmented in the vicinity of the alsterpaullone nitro group. Notably, the KCM and DENR charge models result in a more tractable contour map picture.

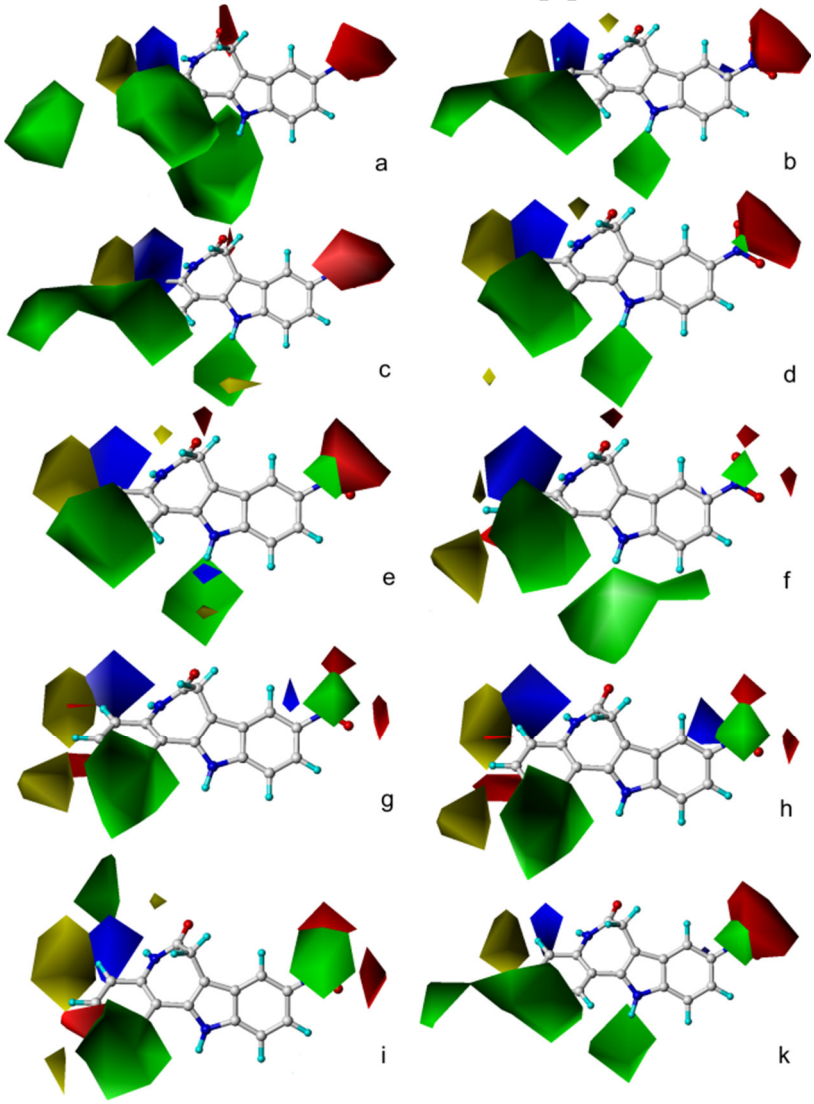


**Figure 6.** CoMSIA contour maps of steric and electrostatic interaction fields; the following charge models are designated by the letters: a) GH; b) MMFF94; c) PLM; d) AM1-BCC; e) LOWD; f) MULL; g) MK-ESP; h) RESP; i) KCM; k) DENR). The fields are displayed on the structure of alsterpaullone. The color coding is the same as in Figure 3.

### 3.3. Outliers

The CoMFA and CoMSIA models built with MEP-fitted techniques (MK-ESP and RESP) and nonempirical charges (LOWD and MULL) are generally characterized by a greater number of outliers. This is particularly relevant for the INDIRU and MALEI datasets. The least numbers of outliers were obtained with the GH, MMFF94, KCM, AM1-BCC, and PLM charge models. A detailed analysis of outliers and the protocol are given in the Supporting Information.

## 4. Discussion

### 4.1. CoMFA and CoMSIA Results

According to the data shown in Figure 1, the influence of charge calculation scheme on CoMFA cross-validation results is not large if both electrostatic and steric fields are included. Notable differences between the charge models are observed for the datasets possessing small $Q^2$ values (ALOIS, INDIRU, and, to a lesser degree, PAULL), but datasets with higher $Q^2$ are less charge-dependent and may have good correlation even if the electrostatic descriptor is not taken into account. Interestingly, all kinase inhibitor datasets studied are characterized by a substantial contribution (approximately 40-50%, see Tables S2 and S3 and Figures S6 and S7) of the electrostatic field to the overall correlation. Nevertheless, the difference between charge schemes does not exceed 10% for any dataset, so definitive conclusions cannot be made based on these observations.

Poor internal predictivity, i.e. small $Q^2$ values occurred in some analyses can be described by several reasons. ALOIS dataset consists of small molecules spanning a narrow activity range (2.93 log units) that increases probability of chance correlations. Good internal predictivity appears due to a greater number of compounds and a broader structural variance (MALEI) or more consistent structure–activity relationships (PYRID) in the datasets. Influence of charge scheme choice is less pronounced for the same datasets. A balanced model can be obtained, provided the steric descriptors supplement the electrostatic ones if the latter fail to account much of the variance. In its extreme this effect is manifested in the "No Electrostatics" models, when subtle steric differences between various atom types seem to be sufficient to achieve a good correlation for a structurally homogeneous dataset.

Almost all charge models studied lead to negative values of $Q^2$ for the "only electrostatics" CoMSIA models for the INDIRU dataset, whereas analogous CoMFA models do not fail so terrifically. Lack of the steric descriptors consideration in these CoMSIA models cannot be compensated with the electrostatic descriptors, and it also shows that the steric descriptors are not correlated with the electrostatic ones. On the other hand, the CoMFA fields take the molecule shape into account implicitly by the use of cutoff values.[2,3]

PYRIDAZ dataset is an example of almost purely "steric" dataset: consideration of the charges influences the quality of correlation slightly. Consequently, the "only electrostatics" CoMFA models for this dataset differ significantly depending on the extent to which steric effects could be captured with the electrostatic descriptors of each charge scheme.

Another reasoning applies to the STERO dataset. It is a small dataset of 21 compounds with a very consistent structure-activity relationship and high contribution of electrostatics. Consequently, virtually any electrostatic model leads to a substantial improvement (compared to the "no electrostatics" option) of the corresponding CoMFA/CoMSIA models, and their predictivity does not depend strongly on particular charge model, which is reflected by high $Q^2$ values for all charges. Although such a straightforward situation does not seem quite general, it should not be completely discarded.

In cases where statistical characteristics of otherwise good CoMFA models appear to be weakly charge-dependent, notable differences can be revealed by looking at contour maps of the interaction fields. Even for the same dataset, contour maps obtained with different charges, differ in the information they convey. For example, it is seen in Figure 3 that the GH charge model is characterized by a number of split contours, whereas DENR charges produce more continuous contour maps. The MMFF94 charges demonstrate a good correlation, but the contours are also small and split. This may be confusing if one is aimed to design new structures on the basis of such contour maps.

In contrast to CoMFA, the effect of atomic charges on CoMSIA predictivity is more pronounced. Only the MALEI dataset is virtually unaffected by the choice of the charge model, whereas for other datasets certain charge models perform better than others. The latter is particularly true for the ALOIS and INDIRU datasets.

## 4.2. Effects of Different Charge Models

For the datasets studied none of the charge models appears to be absolutely superior. Some of them work well on some datasets but fail on others. Actually the only charge model whose performance was inferior to the others' is the Pullman method. Though this method was parameterized to reproduce resonance-related dipole moments of aromatic compounds and was not intended for general description of molecular electrostatics. The Gasteiger-Hückel method, though widely used in 3D QSAR studies, demonstrated ambiguous results in this work. It may miss certain important MEP features because it was not especially fitted to reproduce the MEP. On the other hand, it is a fast nondemanding method available in commercial as well as open-source software.

As a general conclusion, charge models fitted to the MEP (MK-ESP and RESP) or parameterized to reproduce it in some way (AM1-BCC, KCM, DENR, and MMFF94) mainly perform better. This is in accordance with the previous research.[46–48] It is also the result to be anticipated from theoretical considerations, as the molecular electrostatic potential is known[75-78] to define the electrostatic part of

intermolecular interactions thus affecting many physicochemical properties and biological activity.

It has been also observed that empirical MEP-based schemes such as MMFF94, KCM and DENR generally provide better statistical results than their nonempirical counterparts (MK-ESP and RESP). Empirical charge models are largely based on the transferability principle, which means the same sets of parameters are applied to different molecules. These models provide a twofold advantage of using in 3D QSAR studies. First, they calculate atomic charges orders of magnitudes faster than semiempirical and nonempirical methods. Second, empirical charges are more robust in the sense they are much less dependent on the molecule's conformation: the charges remain generally valid until the geometry is reasonable. In contrast to the "true" MEP-based charges (MK-ESP and RESP), there are no such problems as "buried atoms" or underdetermined matrices.[11]

The purely empirical MMFF94, KCM and DENR models appear to be more robust partly in exchange for a certain degree of accuracy. As our study shows, these charge models are a good choice for mass calculations. Of them the simplest one is MMFF94, which is based on predefined bond charge increments, and does not account explicitly the inductive effects of remote substituents. As such, MMFF94 generates less diverse charges and thus may be less accurate, although more consistent. The new generation models KCM and DENR are based on a solid theory, the electronegativity relaxation principle.[33] All bonded pairwise atomic interactions are taken into account and the final charge distribution is solved using a linear simultaneous equations. In addition, these charge models are parameterized against important components of the MEP or the MEP itself. The individual performance of KCM and DENR in the CoMFA and CoMSIA modeling tasks is notable both in terms of high correlation/predictivity and wide applicability. The attempt to use them on an external test set of paullones proved their prominent predictive ability.[79] The contour maps produced by the KCM and DENR are clear and easily interpretable, which is indicative of a consistent description of molecular electrostatics. Moreover, the robustness of charges to geometry change provides additional benefits resulting in more consistent models.

## 5. Conclusions

The main aim of the study was to test in CoMFA and CoMSIA tasks two new charge calculation methods KCM and DENR, which were developed for general use in molecular modeling and proven to be highly efficient in terms of speed and robustness. Our results for six structural datasets convince that these charge models are also performing well, that indirectly supports the theory behind the charge models and parameter choice proposed for general use without special reference to 3D QSAR studies.

We have also tested eight widely used charge models (empirical, semiempirical and nonempirical) in the same CoMFA and CoMSIA tasks. Based on this comparative

study one can conclude that charge models either directly or indirectly fitted to the MEP are most successful. The additional advantages of KCM, and DENR are the unparalleled speed of calculation and invariance to the conformational changes of the molecules.

## Acknowledgements

The study was financially supported by The Russian Foundation for Basic Research (Grant no. 08-03-00783) and The Ministry of Education and Science of Russian Federation (Project no. P-714).

## References

[1] S. Cross, G. Cruciani, *Drug Discov. Today* **2010**, *15,* 23-32.
[2] R. D. Cramer III, D. E. Patterson, J. D. Bunce, *J. Am. Chem. Soc* **1988**, *110,* 5959-5967.
[3] G. Klebe, U. Abraham, T. Mietzner, *J. Med. Chem.* **1994**, *37,* 4130-4146.
[4] R. S. Mulliken, *J. Chem. Phys.* **1955**, *23,* 1833-1840.
[5] P. O. Löwdin, *J. Chem. Phys.* **1953**, *21,* 374-382.
[6] P. Politzer, R. R. Harris, *J. Am. Chem. Soc.* **1970**, *92,* 6451-6454.
[7] L. Baumer, G. Sala, G. Sei Io, *J. Comp. Chem.* **1990**, *11,* 694-699.
[8] L. E. Chirlian, M. M. Frand, *J. Comp. Chem.* **1987**, *8,* 894-905.
[9] K. B. Wiberg, P. R. Rablen, *J. Comp. Chem.* **1993**, *14,* 1504-1518.
[10] B. H. Besler, K. M. Merz Jr., P. A. Kollman, *J. Comp. Chem.* **1990**, *11,* 431-439.
[11] C. I. Bayly, P. Cieplak, W. Cornell, P. A. Kollman *J. Phys. Chem.* **1993**, *97,*10269-10280.
[12] J. Hinze, H. H. Jaffe, *J. Am. Chem. Soc.* **1962**, *84,* 540-546.
[13] R. F. W. Bader, *Atoms in Molecules: A Quantum Theory,* Wiley, Oxford, **1990**, p. 532.
[14] A. Jakalian, D. B. Jack, C. I. Bayly, *J. Comp. Chem.* **2002**, *23,* 1623-1641.
[15] A. Streitwieser Jr., *Molecular Orbital Theory for Organic Chemists,* Wiley, New York, **1961**, p. 489.
[16] R. T. Sanderson, *J. Am. Chem. Soc* **1983**, *105,* 2259-2261.
[17] G. Del Re, *J. Chem. Soc.* **1958**, 4031-4040.
[18] J. Gasteiger, M. Marsili, *Tetrahedron* **1980**, *36*, 3219-3288.
[19] J. Mullay, *J. Am. Chem. Soc.* **1986**, *108,* 1770-1775.
[20] W. J. Mortier, K. V. Genechten, J. Gasteiger, *J. Am. Chem. Soc.* **1985**, *107,* 829-835.
[21] A. K. Rappe, W. A. Goddard III, *J. Phys. Chem.* **1991**, *95*, 3358-3363.
[22] N. S. Zefirov, M. A. Kirpichenok, F. F. Ismailov, M. I. Trofimov, *Dokl. Akad. Nauk SSSR* **1987**, *296*, 883-887.
[23] M. A. Kirpichenok, N. S. Zefirov, *Zh. Org. Khim.* **1987**, *23,* 673-691.
[24] A. A. Oliferenko, V. A. Palyulin, N. S. Zefirov, *Dokl. Chem.* **1999**, *368*, 209-212.
[25] A. A. Oliferenko, V. A. Palyulin, A. V. Neiman, N. S. Zefirov, *Dokl. Chem.* **2000**, *375,* 281-284.
[26] A. A. Oliferenko, V. A. Palyulin, S. A. Pisarev, A. V. Neiman, N. S. Zefirov, *J. Phys. Org. Chem.* **2001**, *14,* 355-369.
[27] M. K. Gilson, H. S. R. Gilson, M. J. Potter, *J. Chem. Inf. Comp. Sci.* **2003**, *43*, 1982-1997.
[28] J. H. Chen, D. Hundertmark, T. J. Martinez, *J. Chem. Phys.* **2008**, *129,* 214-113.
[29] H. Berthod, C. Giessner-Prettre, A. Pullman, *Theor. Chem. Acta* **1967**, *8*, 212-222.

[30] *Tripos Bookshelf* 8.0, Tripos International, 1699 South Hanley Rd., St. Louis, MO 63144. USA.
[31] L. Baumer, G. Sala, G. Sello, *Tetrahedron Comp. Meth.* **1989**, *2,* 37-46.
[32] T. A. Halgren, *J. Am. Chem. Soc.* **1990**, *112,* 4710-4723.
[33] A. A. Oliferenko, S. A. Pisarev, V. A. Palyulin, N. S. Zefirov, *Adv. Quant. Chem.* **2006**, *51,* 139-156.
[34] O. Yakovenko, A. A. Oliferenko, V. G. Bdzhola, V. A. Palyulin, N. S. Zefirov, *J. Comp. Chem.* **2008**, *29,*1332-1343.
[35] D. A. Shulga, A. A. Oliferenko, S. A. Pisarev, V. A. Palyulin, N. S. Zefirov, *SAR&QSAR Env. Res.* **2008,** *19,* 153-165.
[36] K. H. Kim, Y C. Martin, *J. Org. Chem.* **1991**, *56*, 2723 - 2729.
[37] P. Datar, P. Desai, E. Coutinho, K. Iyer, *J. Mol. Model.* **2002**, *8*, 290-301.
[38] V. N. Viswanadhan, Y. Sun, M. H. Norman, *J. Med. Chem.* **2007**, *50*, 5608-5619.
[39] S. Puri, J. S. Chickos, W. J. Welsh, *J. Chem. Inf. Comp. Sci.* **2002**, *42,* 109-116.
[40] E. A. Amin, W. J. Welsh, *J. Med. Chem.* **2001**, *44,* 3849-3855.
[41] S. Puri, J. S. Chiekos, W. J. Welsh, *J. Chem. Inf. Comp. Sci.* **2002**, *42,* 299-304.
[42] H. Luo, Y.-K. Cheng, *QSAR Comb. Sci.* **2005**, *24,* 968-975.
[43] E. A. Amin, W. J. Welsh, *J. Chem. Inf. Model.* **2006**, *46*, 17751783.
[44] Shagufta, A. Kumar, G. Panda, M. I. Siddiqi, *J. Mol. Model.* **2007**, *13*, 99-109.
[45] L.-L. Zhu, X.-J. Xu, *Acta Phys.-Chim. Sin.* **2002**, *18*, 1087-1092.
[46] R. T. Kroemer, P. Hecht, K R. Liedl, *J. Comput. Chem.* **1996**, *17*, 1296-1308.
[47] R. R. Mittal, L. Harris, R. A. McKinnon, M. J. Sorich, *J. Chem. Inf. Model.* **2009**, *49,* 704-709.
[48] K.-C. Tsai, Y.-C. Chen, N.-W. Hsiao, C.-L. Wang, C.-L. Lin, Y.-C. Lee, M. Li, B. Wamg, *Eur. J. Med. Chem.* **2010**, *45*, 1544-1551.
[49] P. R. N. Jayatilleke, A. C. Nair, R. Zauhar, W. J. Welsh, *J. Med. Chem.* **2000**, *43*, 4446-4451.
[50] Y. Peng, S. M. Keenan, Q. Zhang, W. J. Welsh, *J. Mol. Graph. Model.* **2005**, *24,* 25-33.
[51] *Instant J Chem* 5.0.0, **2010**, ChemAxon (**www.chemaxon.com**).
[52] R. S. Pearlman, *Chem. Des. Auto. News.* **1987**, *2*, 1-7.
[53] *SYBYL* 8.0, Tripos International, 1699 South Hanley Rd., St. Louis, MO 63144. USA.
[54] Y. Mettey, M. Compel, V. Thomas, M. Garnier, M. Leost, I. Ceballos-Picot, M. Noble, J. Endicott, J.-M. Vierfond, L. Meijer, *J. Med. Chem.* **2003**, *46*, 222-236.
[55] P. Polychronopoulos, P. Magiatis, A.-L. Skaltsounis, V. Myrianthopoulos, E. Mikros, A. Tarricone, A. Musacchio, S. M. Roe, L. Pearl, M. Leost, P. Greengard, L. Meijer, *J. Med. Chem.* **2004**, *47*, 935-946.
[56] A. Beauchard, Y. Ferandin, S. Frère, 0. Lozach, M. Blairvacq, L. Meijer, V. Thiéry, T. Besson, *Bioorg. Med. Chem.* **2006**, *14*, 6434-6443.
[57] S. Leclerc, M. Garnier, R. Hoessel, D. Marko, J. A. Bibb, G. L. Snyder, P. Greengard, J. Biernat, Y.-Z. Wu, E.-M. Mandelkow, G. Eisenbrand, L. Meijer, *J. Biol. Chem.* **2001**, *276*, 251-260.
[58] F. P. Guengerich, J. L. Sorrells, S. Schmitt, J. A. Krauser, P. Aryal, L. Meijer, *J. Med. Chem.* **2004**, *47*, 3236-3241.
[59] Z.-L. Wu, P. Aryal, 0. Lozach, L. Meijer, F. P. Guengerich, *Chem. Biodiversity.* **2005**, *2*, 51-65.

[60] L. Shen, C. Prouty, B. R. Conway, L. Westover, J. Z. Xu, R. A. Look, X. Chen, M. P. Beavers, J. Roberts, W. V. Murray, K. T. Demarest, G. H. Kuo, *Bioorg. Med. Chem.* **2004**, *12*, 1239-1255.

[61] A. P. Kozikowski, I. N. Gaisina, P. A. Petukhov, J. Sridhar, L.T. King, S. Y. Blond, T. Duka, M. Rusnak, A. Sidhu, *ChemMedChem.* **2006**, *1*, 256-266.

[62] A. P. Kozikowski, I. N. Gaisina, H. Yuan, P. A. Petukhov, S. Y. Blond, A. Fedolak, B. Caldarone, P. McGonigle, *J. Am. Chem. Soc.* **2007**, *129*, 8328-8332.

[63] T. A. Engler, J. R. Henry, S. Malhotra, B. Cunningham, K Furness, J. Brozinick, T. P. Burkholder, M. P. Clay, J. Clayton, C. Diefenbacher, E. Hawkins, P. W. Iversen, Y. Li, T. D. Lindstrom, A. L. Marquart, J. McLean, D. Mendel, E. Misener, D. Briere, J. C. O'Toole, W. J. Porter, S. Queene, J. K. Reel, R. A. Owens, R. A. Brier, T. E. Eessalu, J. R. Wagner, R. M. Campbell, R. Vaughn, *J. Med. Chem.* **2004**, *47*, 3934-3937.

[64] H.-C. Zhang, C. K. Derian, D. F. McComsey, K. B. White, H. Ye, L. R. Hecker, J. Li, M. F. Addo, D. Croll, A. J. Eckardt, C. E. Smith, Q. Li, W.-M. Cheung, B. R. Conway, S. Emanuel, K. T. Demarest, P. Andrade-Gordon, B. P. Damiano, B. E. Maryanoff, *J. Med. Chem.* **2005***, 48,* 1725-1728.

[65] J. O'Neill, L. Shen, C. Prouty, B. R. Conway, L. Westover, J. Z. Xu, H. C. Zhang, B. E. Maryanoff, W. V. Murray, K. T. Demarest, G. H. Kuo, *Bioorg. Med. Chem.* **2004**, *12*, 3167-3185.

[66] T. A. Engler, S. Malhotra, T. P. Burkholder, J. R. Henry, I. D. Mende, W. J. Porter, K. Furness, C. Diefenbacher, A. Marquart, J. K. Reel, Y. Li, J. Clayton, B. Cunningham, J. McLean, J. C. O'Toole, J. Brozinick, E. Hawkins, E. Misener, D. Briere, R. A. Brier, J. R. Wagner, R. M. Campbell, B. D. Anderson, R. Vaughn, D. B. Bennett, T. I. Meier, J. A. Cook, *Bioorg. Med. Chem. Lett.* **2005**, *15*, 899-903.

[67] M. Leost, C. Schultz, A. Link, Y. Z. Wu, J. Biernat, E. M. Mandelkow, J. A. Bibb, G. L. Snyder, P. Greengard, D. W. Zaharevitz, R. Gussio, A. M. Senderowicz, E. A. Sausville, C. Kunick, L. Meijer, *Eur. J. Biochem.* **2000**, *267*, 5983-5994.

[68] C. Kunick, K. Lauenroth, K. Wieking, X. Xie, C. Schultz, R. Gussio, D. Zaharevitz, M. Leost, L. Meijer, A. Weber, F. S. Jorgensen, T. Lemcke, *J. Med. Chem.* **2004**, *47*, 22-36.

[69] X. Xie, T. Lemcke, R. Gussio, D. W. Zaharevitz, M. Leost, L. Meijer, C. Kunick, *Eur. J. Med. Chem.* **2005**, *40*, 655-661.

[70] F. X. Tavares, J. A. Boucheron, S. H. Dickerson, R. J. Griffin, F. Preugschat, S.A. Thomson, T. Y. Wang, H.-Q. Zhou, *J. Med. Chem.* **2004**, *47*, 4716-4730.

[71] Y. Cheng, W. H. Prusoff, *Biochem. Pharmacol.* **1973**, *22*, 3099-3108.

[72] J. Wang, W. Wang, P. A. Kollman, D. A. Case, *J. Mol. Graph. Model.* **2006**, *25*, 247-260.

[73] http://ambermd.org/Questions/resp.html

[74] A. A. Granovsky, *PC GAMESS,* version 7.0, http://classic.chem.msu.su/gran/gamess/index.html

[75] P. Politzer, J. S. Murray, *Theor. Chem. Acc.* **2002**, *108*, 134-142.

[76] G. Naray-Szabo, G. G. Ferenczy, *Chem. Rev*. **1995**, *95,* 829-847.

[77] C. E. Dykstra, *Chem. Rev*. **1993**, *93,* 2339-2353.

[78] D. Mackerell Jr., *J. Comp. Chem.* **2004**, *25*, 1584-1604.

[79] A. A. Osolodkin, D. A. Shulga, D. A. Tsareva, A. A. Oliferenko, V. A. Palyulin, N. S. Zefirov, *Dokl. Biochem. Biophys.* **2010**, *434*, 274-278. BIOORGANIC & MEDICINAL CHEMISTRY LETTERS. Vol. 21 (22), 6728-6731 (2011)

# ONE-CLASS CLASSIFICATION AS A NOVEL METHOD OF LIGAND-BASED VIRTUAL SCREENING: THE CASE OF GLYCOGEN SYNTHASE KINASE 3β INHIBITORS

**P.V. Karpov, D.I. Osolodkin, I.I. Baskin, V.A. Palyulin, N.S. Zefirov**

*Department of Chemistry, Moscow State University, Moscow, Russia*
*Laboratoire d'lnfochimie, UMR 7177 CNRS, Strasbourg, France*
*Institute of Physiologically Active Compounds, RAS, Chernogolovka, Moscow Region, Russia*

A virtual screening system based on one-class classification with molecular fingerprints as descriptors is developed and tested on a series of 1226 inhibitors and 209 noninhibitors of glycogen synthase kinase 3β (GSK-30). The suggested system outperforms the ones based on pharmacophore hypothesis and molecular docking in a retrospective study. However, in a prospective study it should not be used as a sole classifier. The system is exceptionally useful for the identification of new scaffolds among the virtual screening results obtained with other methods.

The main task of a virtual screening (VS) is to discriminate putative active compounds from inactive ones. The main requirement of major classification methods is to use both classes of active and inactive compounds during the ligand-based model construction, allowing one to find a hyperplane in a feature space that would separate active samples from inactive ones. The problem is that data for the inactive samples should be collected in the same conditions as for the active ones, but usually information on inactive compounds is not available, and researchers are obliged to create decoy datasets by themselves using their own rules (e.g., Refs. 1,2), that leads to several disadvantages. First, certain decoys may be really active. Second, the performance of a model is influenced by the quality of data and chemical diversity of the training dataset. Therefore, usage of standard classification procedures is methodologically incorrect when the decoy set is not rigorously defined.

The simplest and fastest VS method is the similarity search when a reference molecule with the desired biological activity is selected and all compounds from a database are ranked in ascending order of similarity to the reference molecule.[3] This procedure generally does not require building a model and using the negative samples, but recently it has been shown that the similarity search works only when the structure/activity surface is smooth enough and there are no 'activity cliffs'.[4] This condition is difficult to meet because such information is unattainable a priori, so the new methods of similarity search have to be proposed.

All these problems could be successfully resolved using the one- class classification (OCC) method,[5-7] the main idea of which is to construct the model based on the active compounds exclusively. In this Letter, we demonstrate the application of OCC

to the VS of glycogen synthase kinase 3β (GSK-3β) inhibitors (for a recent review of this target see Ref. 8).

The reconstruction methods of the OCC approach include the auto-encoder neural networks, self-organizing maps (SOM) and principal component analysis (PCA). Auto-encoder (replicator, bottleneck or sand-glass) networks[9] are feed forward neural networks which have at least one hidden layer with the number of neurons many times smaller than in the other layers (Fig. 1). This layer acting as a compressing element attempts to reconstruct the input data to the output layer. The number of neurons in this layer can be roughly correlated with the number of features that are responsible for the biological activity.

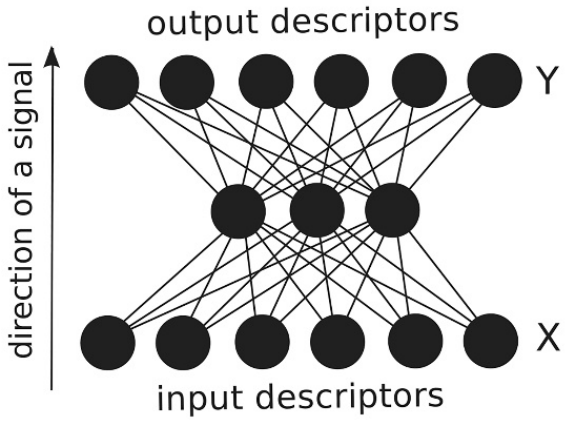


**Figure 1.** Typical scheme of an auto-encoder neural network.

Biological activity of an organic compound is defined by the constellation of its pharmacophoric features, encoded in the chemical structure, but it is very difficult to guess a priori which features are responsible for a certain activity. Moreover, one structure can possess several biological activities and have different features related to them. One way to predict the probability for a molecule to be biologically active is to compare features of the ligand with those for the target. If they are similar, the compound can be considered as potentially active. The auto-encoder network does actually the same: it tries to reconstruct the target features. In other words, auto-encoders work like the nonlinear PCA and sometimes similarly to pseudo-receptor models, implicitly reconstructing the binding cavity from the ligand features. PCA acts as a linear method, but auto-encoder networks perform the nonlinear transformation in data.

The second layer in Figure 1 is comprised of three neurons which filter only desired features. The reconstructed descriptors (Y) at the output layer should be the same as the input descriptors (X), thus the size of the output layer is also the same as the size of the input layer. The network can be divided into two parts: the first part encodes input information into the vector of features, whereas the second part acts as a decompressor which reconstructs this vector into the output one. The well trained network produces the output very similar to the input for those samples that possess the same characteristics that were in the training data, and for such samples the reconstruction

error defined by the dissimilarity between the input and the output vectors would be minimal. If the reconstruction error is relatively high then the sample was reconstructed poorly and one can conclude that it is out of the space of the training data and is supposed to be inactive.

The OpenBabel FP2 1024-bit fingerprints[10] were used as descriptors for this study. The auto-encoder neural network software was adapted from our in-house package. The learning algorithm is a standard back-propagation procedure; leave-20%-out cross-validation was employed during the learning (Fig. 2). One- class classification method uses only active samples for model construction so modification in the standard cross-validation procedure is to be made. The set of active ligands is divided into five parts. The first part is excluded and the model is built on the remaining data. Then values of the excluded samples are predicted and the procedure is repeated with all data parts. Then the model is built on all positive samples and all negative samples are predicted. Using both positive and negative results of modeling it is possible to build a receiver operating characteristic (ROC) curve and calculate the area under the curve (AUC).[11,12]

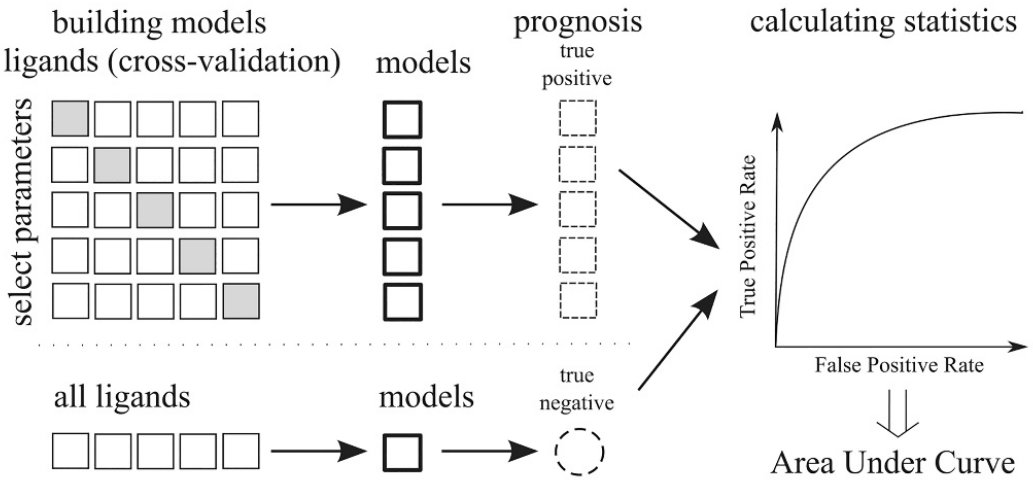


**Figure 2.** The workflow for choosing parameters of OCC models.

The reconstruction error was estimated with the Tanimoto coefficients (Tc) between the input and the output vectors. ROC analysis implemented in StAR server[13] was employed in order to find the optimal thresholds for each model and assess the performance of the classifier using AUC. Due to the stochastic nature of neural network's learning procedures ten models were built and average statistics were calculated. Such method is thought to give more accurate results than one model can do. The datasets used for the retrospective VS analysis are thoroughly described by us earlier[14]; briefly, the set of true actives (TA) contained 1226 compounds representing all classes of known GSK-3β inhibitors, the set of true inactives (TI) consisted of 209 compounds which did not show inhibitory activity in the assay conditions, NCI Diversity Set (DS, 2000 compounds[15]) was employed as a decoy set without explicit structure restrictions, and DUD CDK2 decoy set (2073 structures[16]) was used due to high similarity between

the CDK2 and GSK-3β inhibitors. Prospective study was performed with subset of ZINC database[17] obtained by pre-filtering the whole database with OpenEye lead-like filter[18] modified to select features needed for the interaction with kinases (i.e., one hydrogen bond donor and one acceptor; Table 1); the filtered subset contained 1,204,522 structures.

**Table 1.** Criteria of ZINC pre-filtering

| Parameter | Minimum | Maximum |
|---|---|---|
| Molecular weight | 150 | 500 |
| Number of heavy atoms | 10 | 30 |
| Number of cycles | 1 | 4 |
| Number of hydrogen bond donors | 1 | 4 |
| Number of hydrogen bond acceptors | 1 | 6 |
| Number of rotatable bonds | 0 | 10 |
| Number of rigid bonds | 0 | 25 |
| Heteroatoms count | 2 | 12 |
| Calculated logP | –5 | 4 |
| Formal charge | –2 | +2 |

The simplest architecture of the network leads to the most acceptable solution. We checked the performance of auto-encoder networks with simple three-layered architecture varying the size of the hidden layer from 3 to 15 neurons. Cross-validation studies showed that five hidden neurons are the best choice. Due to stochastic nature of the models, simple voting system was utilized in the final model: the mean prediction of the five best models was used as the final compound score.

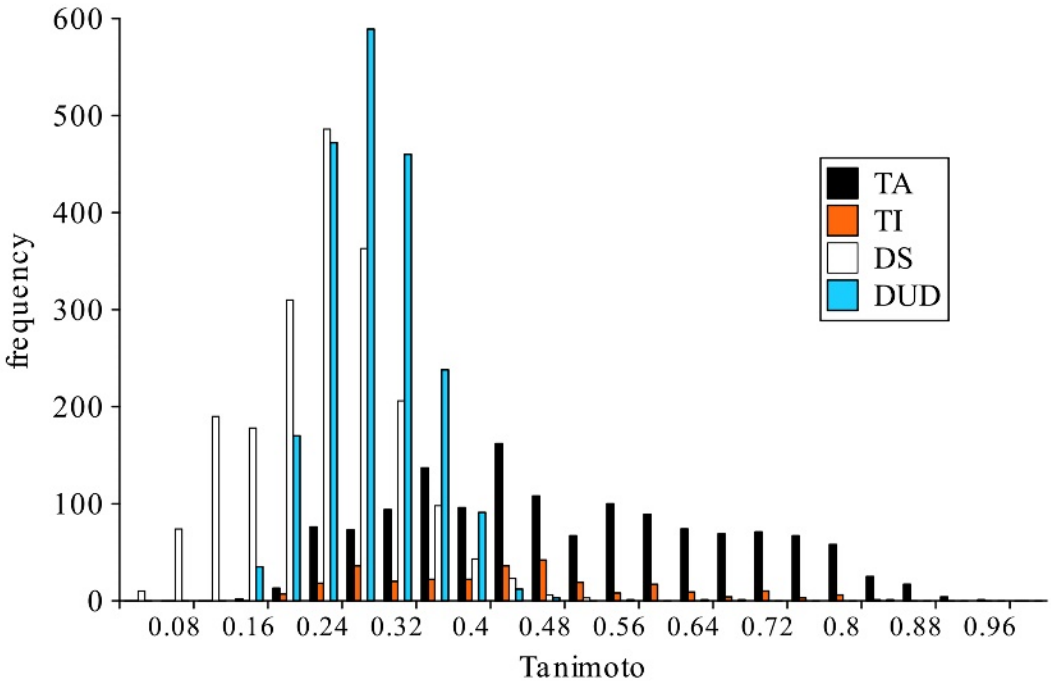


**Figure 3.** Distribution of scores for the retrospective VS. The [0,1] range was uniformly divided into 26 bins. TA, true actives; TI, true inactives; DS, NCI Diversity Set; DUD, Directory of Useful Decoys; see also Ref. 13.

The distribution of OCC Tc's (Fig. 3) clearly shows that they are widely distributed for TA (from 0.16 to 0.96), whereas for the decoy sets only single compounds get the score higher than 0.5. TI compounds occasionally get much higher scores than decoys, usually owing to small changes needed to cancel compound activity, for example, insertion of a single methyl group in the hinge-interacting region of the ligand. Nevertheless, because the main task of VS is the scaffold identification, the presence of such compounds in the hit list is acceptable.

ROC analysis (Fig. 4) revealed that enrichment with OCC is the best of studied methods (AUC 0.892, compare with pharmacophore search (0.862[19]; see Fig. 5) and docking (0.824 with Chemscore scoring; see also Ref. 14)), especially in the top part of the hit list, and optimal threshold of 0.4 can be used for the prospective VS.

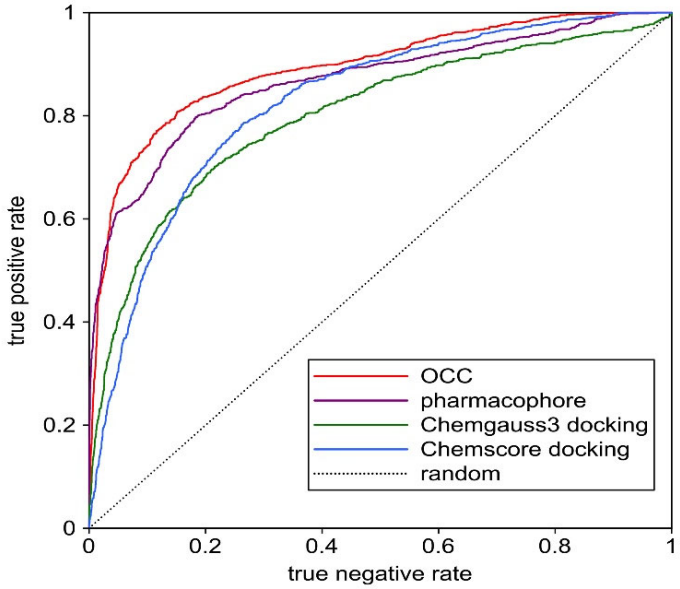


**Figure 4**. Rock curves for the different VS approaches

Only 8757 compounds of 1.2 million passed the optimal threshold, 435 of them having Tc >0.5, and six with Tc >0.6. The latter compounds are shown in Table 2. Five of them are not very similar to common kinase inhibitors, and compound 6 is a well-known GSK-3β inhibitor aloisine.[25] On the other hand, 2580 compounds passed the optimal threshold derived for the pharmacophore hypothesis, and only 73 of them passed the OCC threshold. Thus, OCC gives many false positives upon screening of large diverse databases that can be eliminated by simple visual analysis (like compound 1) or by subsequent more specific screening procedure, such as docking or pharmacophore search, but it may be used as a very effective postprocessing step, selecting only compounds very similar to the known inhibitors or allowing to identify less similar (i.e., 'newer') inhibitors in a large hit list. Very strict criteria of presence of cycles during pre-filtration could be another reason for rather poor performance and low scores of OCC in prospective VS, because many known GSK-3β inhibitors contain more than four rings, that makes them less lead-like.

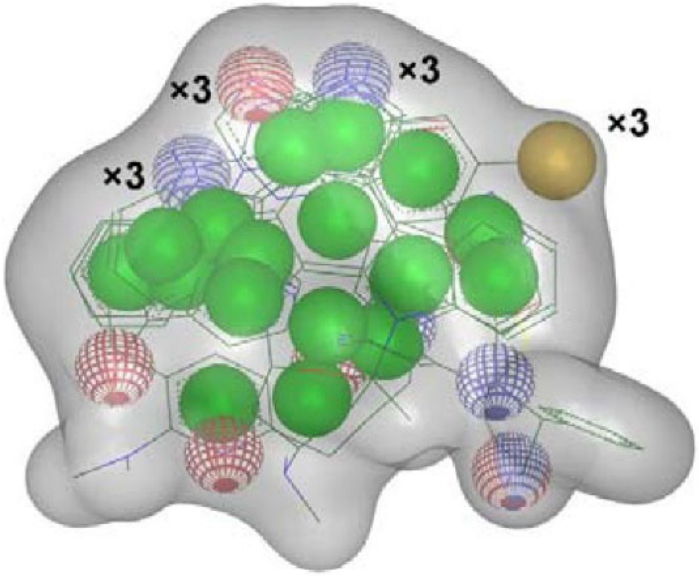


**Figure 5.** Pharmacophore model for GSK-3 inhibitors[19] is built by ROCS based on the co-crystal structures of hinge-aligned GSK-3-inhibitor complexes (PDB IDs 1Q3D,[20] 1UV5,[21] 2OW3,[22] 3F88,[23] and 3I4B[24]). The model was chosen from the series of the best ones owing to presence of hydrophobic feature (yellow ball) and maximal allowed molecular volume (grey cloud). Weight tripling for the features corresponding to the interaction of the inhibitor with the hinge (two hydrogen bond donors (blue balls), hydrogen bond acceptor (red balls)) and gatekeeper (hydrophobic) led to maximal *AUC* increase. Green balls correspond to the presence of ring features in the ligands.

**Table 2.** Top six hits of ZINC OCC screening

| Tc | # | Structure | Tc | # | Structure |
|---|---|---|---|---|---|
| 0.648 | 1 | 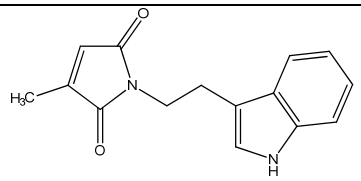 | 0.614 | 4 | 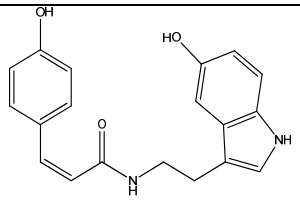 |
| 0.639 | 2 | 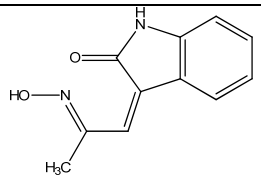 | 0.614 | 5 | 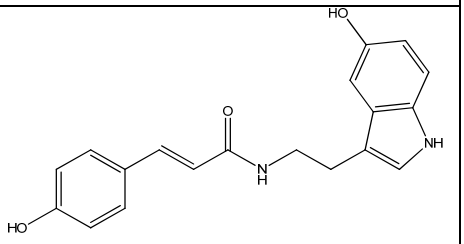 |
| 0.622 | 3 | 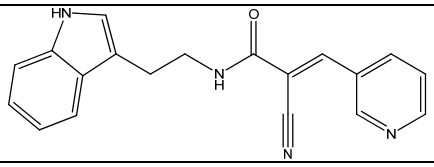 | 0.610 | 6 | 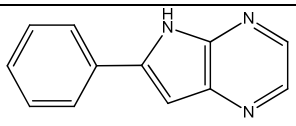 |

In this study, we have shown that one-class classification based on auto-encoder neural networks is a powerful method of ligand-based virtual screening, the best served in conjunction with other methods, such as pharmacophore search or molecular docking.

## Acknowledgments

The academic licence for ROCS and FILTER was kindly provided by OpenEye Scientific Software Inc. This work was financially supported by the Grants of Russian Academy of Sciences and of Russian Foundation for Basic Research (Grant 11-03-01174).

## References and notes

1. Bruno-Blanch, L.; Gálvez, J.; García-Domenech, R. *Bioorg. Med. Chem. Lett*. **2003**, *13*, 2749.
2. Tikhonova, I. G.; Baskin, I. I.; Palyulin, V. A.; Zefirov, N. S. *Russ. Chem. Bull*. **2004**, *53*, 1335.
3. Varnek, A.; Tropsha, A. *Chemoinformatics Approaches to Virtual Screening*; RCS Publishing: Cambridge, 2008.
4. Guha, R.; Drie, J. *J. Chem. Inf. Model.* **2008**, *48*, 646.
5. Tax, D. M. J. Ph.D. Thesis, Technische Universiteit Delft, 2001.
6. Baskin, I. I.; Kireeva, N.; Varnek, A. *Mol. Inf.* **2010**, *29*, 581.
7. Karpov, P. V.; Baskin, I. I.; Palyulin, V. A.; Zefirov, N. S. *Dokl. Chem*. **2011**, *437*, 107.
8. Phukan, S.; Babu, V. S.; Kannoji, A.; Hariharan, R.; Balaji, V. N. Br. *J. Pharmacol.* **2010**, *160*, 1.
9. Thomson, B. B.; Marks, R. J.; Choi, J. J. *IEEE Proc. 2002 Int. Joint Conf. Neural Netw*. **2002**, *3*, 2878.
10. Guha, R.; Howard, M. T.; Hutchison, G. R.; Murray-Rust, P.; Rzepa, H.; Steinbeck, C.; Wegner, J. K.; Willighagen, E. L. *J. Chem. Inf. Model*. **2006**, *46*, 991.
11. Swets, J. A. *Science* **1988**, *240*, 1285.
12. Triballeau, N.; Acher, F.; Brabet, I.; Pin, J.-P.; Bertrand, H.-O. *J. Med. Chem*. **2005**, *48*, 2534.
13. Vergara, I. A.; Norambuena, T.; Ferrada, E.; Slater, A. W.; Melo, F. *BMC Bioinformatics* **2008**, *9*, 265.
14. Osolodkin, D. I.; Palyulin, V. A.; Zefirov, N. S. *Chem. Biol. Drug. Des*. **2011**, *78*, 378.
15. Diversity Set II Information [http://dtp.nci.nih.gov/branches/dscb/div2_explanation.html].
16. Huang, N.; Shoichet, B. K.; Irwin, J. J. *J. Med. Chem*. **2006**, *49*, 6789.
17. Irwin, J. J.; Shoichet, B. K. *J. Chem. Inf. Model.* **2005**, *45*, 177.
18. OpenEye Scientific Software. 9 Bisbee Court, Suite D. Santa Fe, New Mexico 87508, USA.
19. Osolodkin, D. I. Ph.D. Thesis, Moscow State University, 2011.
20. Bertrand, J. A.; Thieffine, S.; Vulpetti, A.; Cristiani, C.; Valsasina, B.; Knapp, S.; Kalisz, H. M.; Flocco, M. *J. Mol. Biol*. **2003**, *333*, 393.
21. Meijer, L; Skaltsounis, A.-L. L.; Magiatis, P.; Polychronopoulos, P.; Knockaert, M.; Leost, M.; Ryan, X. P.; Vonica, C. A. A.; Brivanlou, A.; Dajani, R.; Crovace, C.; Tarricone, C.; Musacchio, A.; Roe, S. M.; Pearl, L.; Greengard, P. *Chem. Biol.* **2003**, *10*, 1255.
22. Zhang, H.-C.; Boñaga, L. V. R.; Ye, H.; Derian, C. K.; Damiano, B. P.; Maryanoff, B. E. *Bioorg. Med. Chem. Lett*. **2007**, *17*, 2863.
23. Saitoh, M.; Kunitomo, J.; Kimura, E.; Hayase, Y.; Kobayashi, H.; Uchiyama, N.; Kawamoto, T.; Tanaka, T.; Mol, C. D.; Dougan, D. R. *Bioorg. Med. Chem*. **2009**, *17*, 2017.
24. Aronov, A. M.; Tang, Q.; Martinez-Botella, G.; Bemis, G. W.; Cao, J.; Chen, G.; Ewing, N. P.; Ford, P. J.; Germann, U. A.; Green, J.; Hale, M. R.; Jacobs, M.; Janetka, J. W.; Maltais, F.; Markland, W.; Namchuk, M. N.; Nanthakumar, S.; Poondru, S.; Straub, J.; ter Haar, E.; Xie, X *J. Med. Chem*. **2009**, *52*, 6362.

25. Mettey, Y.; Compel, M.; Thomas, V.; Garnier, M.; Leost, M.; Ceballos-Picot, I.; Noble, M.; Endicott, J.; Vierfond, J.-M.; Meijer, L. *J. Med. Chem*. **2003**, *46*, 222.

*ИЗВЕСТИЯ АКАДЕМИИ НАУК. СЕРИЯ ХИМИЧЕСКАЯ, 2016, №2, 576-580*

УДК 544.165:615.033

# ПРОГНОЗИРОВАНИЕ ВСАСЫВАНИЯ ЛЕКАРСТВЕННЫХ ВЕЩЕСТВ В КИШЕЧНИКЕ ЧЕЛОВЕКА

**Е.В. Радченко, А.С. Дябина, В.А. Палюлин, Н.С. Зефиров**

*Московский государственный университет им. М. В. Ломоносова, Химический факультет, Москва, Российская Федерация*
*Институт физиологически активных веществ Российской академии наук, Черноголовка Московской обл., Российская Федерация .*

Всасывание в тонком кишечнике – один из ключевых процессов, определяющих биодоступность лекарства при пероральном введении. С использованием фрагментных дескрипторов и искусственных нейронных сетей построена предсказательная модель связи структуры органических соединений и их способности к всасыванию в кишечнике человека, а также проанализированы структурные факторы, влияющие на легкость всасывания. Эта модель превосходит по точности прогноза и области применимости другие известные модели и может быть использована при оптимизации фармакокинетических параметров в ходе разработки лекарств.

Характеристики всасывания, распределения, метаболического изменения, выведения и токсичности лекарственных веществ (ADMET – Absorption, Distribution, Metabolism, Excretion, Toxicity) оказывают решающее влияние на эффективность, фармакологический профиль, способ применения и безопасность действия лекарств. Оптимизация этих свойств является важной частью поиска и разработки лекарств, причем возможность их прогнозирования *in silico* для новых структур позволяет значительно ускорить такую разработку и повысить ее эффективность[1].

При пероральном введении лекарства одним из ключевых фармакокинетических процессов, определяющих его биодоступность, является всасывание в тонком кишечнике[2]. Способность вещества к всасыванию в кишечнике человека (HIA — Human Intestinal Absorption) обычно количественно выражается как часть введенной дозы, которая достигает воротной вены:

$$HIA = D_{blood}/D_{oral},$$

где $D_{blood}$ – количество вещества, достигшее воротной вены, а $D_{oral}$ – общее количество перорально введенного вещества. Тем самым исключается эффект метаболического изменения при первом прохождении вещества через печень до его попадания в системную циркуляцию.

В последние годы были достигнуты значительные успехи в развитии малоинвазивных экспериментальных методов определения всасывания *in vivo* и его оценки *in vitro*[3-5], однако задача компьютерного прогнозирования величины всасывания для новых, пока не синтезированных или не изученных соединений остается весьма актуальной. В то же время, несмотря на большое число исследований в этой области, представленные в литературе модели[4-8] имеют ограничения по точности и области применимости.

Цель данной работы – построение предсказательных моделей количественной связи структуры лекарственных веществ и их способности к всасыванию в кишечнике, а также анализ структурных факторов, влияющих на легкость всасывания.

## Модели и методы

В ходе работы на основе анализа большого числа литературных источников[9-24] была подготовлена обширная база данных по всасыванию органических соединений в кишечнике человека. Для формирования базы данных применяли программный комплекс Instant JChem[27]. В качестве базового параметра использовали величину доли всасывания *HIA,* выраженную в процентах. В общей сложности обучающая выборка включает 708 соединений различных химических классов и, по-видимому, является наиболее полной и точной среди известных в литературе и основанных на открытых данных. К сожалению, в некоторых публикациях приводятся лишь оценки параметра *HIA* на основе косвенных данных, например, по величине общей биодоступности или по различиям в количестве выводимого из организма вещества при пероральном и внутривенном введении[9], что может приводить к завышению величин всасывания, а также вносит в них дополнительную неопределенность. Кроме того, детальные исследования всасывания нередко проводились преимущественно для перспективных соединений с высокой оральной активностью и биодоступностью. По-видимому, именно эти факторы объясняют неравномерность охвата различных интервалов значений *HIA* (более 60% соединений выборки имеют величину *HIA* > 80%). Тем не менее в условиях, когда более полные и надежные данные недоступны, целесообразно использовать выборку с максимально широким покрытием химического пространства, чтобы обеспечить возможно более широкую область применимости моделей, хотя это может несколько ограничивать их точность.

Для построения моделей связи структуры и доли всасывания использовали метод искусственных нейронных сетей в рамках программного комплекса NASAWin 2.0[28,29]. При построении моделей были использованы следующие группы дескрипторов молекулярной структуры: число вхождений в структуру соединения структурных фрагментов различных типов, содержащих не более восьми атомов (цепочки, циклы и разветвленные фрагменты с многоуровневой классификацией атомов, учитывающей их тип, валентное состояние, набор связей и число присоединенных атомов водорода)[28,30]; комбинации свойств атомов для коротких цепочек атомов[31]; рассчитанные с помощью нейросетевых моделей дескрипторы Абрахама, описывающие растворимость и способность к образованию водородных связей для органических молекул[32], и значение липофильности соединения[33]. Из анализа исключали редкие фрагменты, встречающиеся лишь в пяти или меньшем числе соединений, а затем отбирали наиболее значимые дескрипторы с помощью метода пошаговой множественной линейной регрессии. При построении нейросетевых моделей рассматривали сети трехслойной архитектуры с различным числом нейронов в скрытом слое и применяли процедуру 5×4-кратного двойного перекрестного контроля, использующую независимые подвыборки данных для обучения нейронной сети, выбора ее оптимальной конфигурации и оценки предсказательной способности моделей[34].

Поскольку для большинства соединений отсутствуют достаточно полные и точные данные о роли различных механизмов пассивного и активного транспорта в их переносе через стенку кишечника[2], эти параметры не включали в модель в явном виде, однако связанные с ними особенности влияния структуры соединений на всасывание должны косвенно учитываться нейросетевой фрагментной моделью. Принимая во внимание неравномерность распределения соединений обучающей выборки по величине *HIA,* а также сложность самого процесса всасывания в кишечнике, в качестве целевых параметров при построении моделей рассматривали не только непосредственно значение *HIA,* но и его нелинейные функции. Параметр *LogHIAm* качественно соответствует коэффициенту проницаемости кишечника $P_{\text{eff}}$,[35] а параметр *LogHIAratio* – логарифму коэффициента распределения вещества между желудочно-кишечным трактом и кровью:

$$LogHIAm = 2 - \lg(101 - HIA),$$

$$LogHIAratio = \lg[(1 + HIA)/(101 - HIA)].$$

## Обсуждение полученных результатов

Для каждой из целевых функций в таблице 1 представлены характеристики оптимальных моделей, построенных по всей обучающей выборке (708 соедине-

ний). Поскольку функции сильно различаются по диапазону изменения прогнозируемого параметра, для корректного сравнения прогнозируемые значения приводили в шкалу *HIA* (включая их нормализацию к допустимому диапазону значений от 0 до 100), а затем рассчитывали характеристики качества моделей. Как видно, параметр *LogHIAm* не обеспечивает какого-либо выигрыша в качестве прогноза по сравнению с другими рассмотренными моделями. Модель для параметра *HIA* превосходит по характеристикам модель для *LogHIAratio,* хотя различие между ними не очень велико. Анализ графиков соответствия экспериментальных и прогнозируемых значений *HIA* для моделей *HIA* и *LogHIAratio* (рис. 1) также подтверждает отсутствие существенных различий в качестве прогноза, несмотря на несколько меньшие отклонения для соединений с очень низким и очень высоким всасыванием в модели *LogHIAratio.*

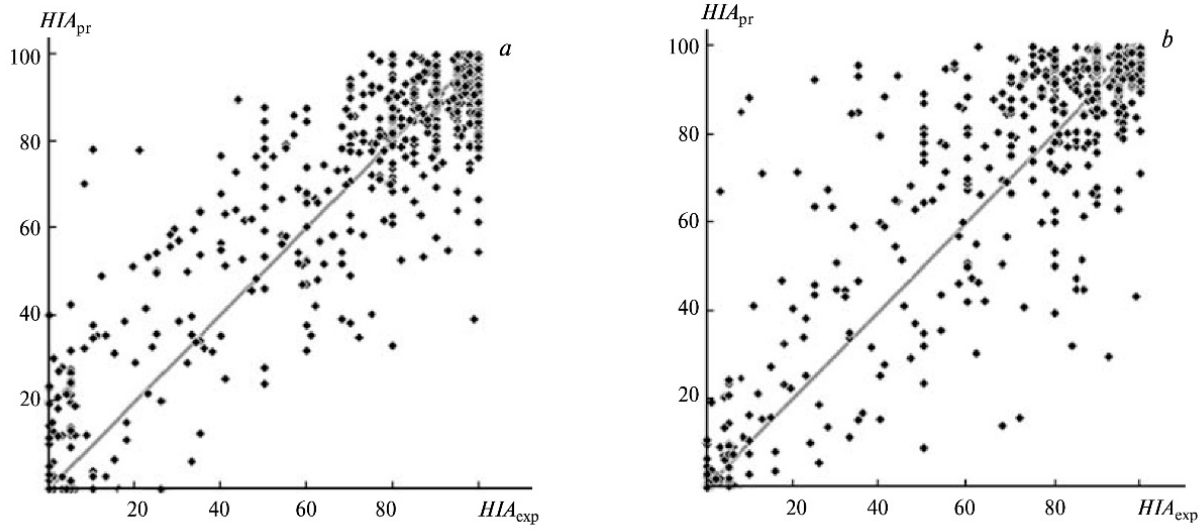


**Рис. 1.** Соответствие экспериментальных ($HIA_{exp}$) и прогнозируемых в ходе процедуры перекрестного контроля ($HIA_{pr}$) величин всасывания в кишечнике для соединений обучающей выборки в модели *HIA* (*a*) и *LogHIAratio (b).*

В то же время для модели *HIA* меньше соединений прогнозируются со значительными ошибками (около 10 соединений для модели *HIA* и около 30 – для модели *LogHIAratio).* Скорее всего, такие отклонения от модели связаны с шумом в исходных данных, однако исключение этих соединений из обучающей выборки было признано нецелесообразным, хотя оно могло бы привести к построению моделей с более высокими итоговыми показателями качества. Благодаря использованию значительно более представительной обучающей выборки построенная нами модель превосходит по точности прогноза и области применимости лучшие из ранее предложенных моделей. Например, для обучающей выборки, содержащей 380 соединений, получена[36] модель с коэффициентом корреляции $R^2 = 0.66$ (для контрольной выборки из 172 соединений $R^2 = 0.77$) и сред-

неквадратической ошибкой (RMSE) 16.0, а для обучающей выборки из 638 соединений получены[37] значения: RMSE 10.2 и параметр перекрестного контроля ($Q^2$) 0.67.

Таблица 1. Характеристики нейросетевых моделей связи структуры органических соединений и величины всасывания в кишечнике

| Модель | $N_d$ | $N_h$ | $Q^2$ | *RMSEcv* | $Q^2$*(HIA)* | *RMSEcv(HIA)* |
|---|---|---|---|---|---|---|
| *HIA* | 120 | 2 | 0.79 | 14.2 | 0.80 | 13.8 |
| *LogHIAm* | 140 | 2 | 0.68 | 0.39 | 0.64 | 18.6 |
| *LogHIAratio* | 140 | 2 | 0.76 | 0.51 | 0.77 | 14.7 |

*Примечание.* Модели построены по обучающей выборке, содержащей 708 соединений различных классов. $N_d$ – число дескрипторов, $N_h$ – число нейронов в скрытом слое архитектуры нейронной сети, $Q^2$ – параметр перекрестного контроля, *RMSEcv* – среднеквадратическая ошибка при перекрестном контроле, $Q^2$*(HIA)* – параметр перекрестного контроля в шкале *HIA, RMSEcv(HIA)* – среднеквадратическая ошибка при перекрестном контроле в шкале *HIA*.

Для дополнительной оценки моделей рассчитывали показатели точности качественной классификации соединений обучающей выборки. Рассматривали три класса всасывания: хорошее – HIA+ *(HIA* > 70%), среднее – HIA± (30% < *HIA* < 70%) и плохое – HIA– *(HIA* < 30%). В таблицах 2 и 3 представлены матрицы неточностей, построенные на основе прогнозируемых в ходе процедуры перекрестного контроля значений *HIA* для моделей *HIA* и *LogHIAratio,* а также рассчитанные по ним параметры общей точности распознавания, доли грубых ошибок (ситуаций, когда для соединения с плохим всасыванием прогнозируется хорошее, и наоборот), чувствительности для класса HIA+ (точности распознавания соединений с хорошим всасыванием) и специфичности для класса HIA+ (точности распознавания соединений со средним и плохим всасыванием). Как видно, точность классификации с помощью этих моделей весьма близка, хотя модель *HIA* несколько надежнее распознает соединения с невысоким всасыванием. Кроме того, модель *HIA* более проста и понятна, что позволяет достаточно уверенно использовать ее для прогнозирования всасывания новых соединений.

Таблица 2. Матрицы неточностей для классов всасывания, прогнозируемых в ходе процедуры перекрестного контроля по моделям *HIA* и *LogHIAratio*

| Эксперимент | Прогноз | | | | | |
|---|---|---|---|---|---|---|
| | *HIA* | | | *LogHIAratio* | | |
| | HIA+ | HIA± | HIA– | HIA+ | HIA± | HIA– |
| HIA+ | 493 | 28 | 0 | 494 | 25 | 2 |
| HIA± | 25 | 61 | 6 | 37 | 45 | 10 |
| HIA– | 3 | 25 | 67 | 5 | 14 | 76 |

*Примечание.* Классы всасывания: HIA+ *(HIA* > 70%) – хорошее, HIA± (30% < *HIA* < 70%) – среднее, HIA– *(HIA* < 30%) – плохое всасывание.

Для целей качественного анализа и интерпретации влияния различных дескрипторов на прогнозируемые с помощью нейросетевой модели величины целевого параметра использовали численно определяемые значения частных производных такого параметра по дескрипторам, усредненные по обучающей выборке[38]. Чтобы учесть различия в диапазонах изменения дескрипторов, рассчитывали нормированный относительный отклик модели

$$RR_i = \mathrm{avg}\left(\frac{\partial y}{\partial x_i}\right) \times \frac{\mathrm{range}(x_i)}{\mathrm{range}(y)},$$

где $\mathrm{avg}\left(\frac{\partial y}{\partial x_i}\right)$ – среднее значение производной целевого параметра $y$ по дескриптору $x_i$, range ($x_i$) – диапазон изменения дескрипторах $x_i$, а range ($y$) – диапазон изменения параметра $y$.

Фрагменты, оказывающие наиболее сильное положительное и отрицательное влияние на величину всасывания, представлены на рисунке 2. Многие из них допускают простую интерпретацию, которая согласуется с известными представлениями о структурных факторах, влияющих на проникновение вещества через биологические барьеры[39]. Так, при прочих равных условиях всасывание выше для умеренно полярных соединений, в том числе замещенных аминов и амидов, простых и сложных эфиров, ароматических сульфонамидов. В то же время всасывание уменьшается при наличии сильнополярных или малополярных групп: гидрокси- и аминогрупп, фрагментов четвертичных алкиламмониевых солей, фосфоновых кислот и фосфонатов, амидов, сульфонов, циклобутановых и ароматических циклов. Тем не менее следует иметь в виду, что модель включает также большое число других дескрипторов, влияющих на прогнозируемую величину всасывания, поэтому для оптимизации фармакокинетических свойств лекарственного вещества целесообразно использовать подход, основанный на виртуальном скрининге.

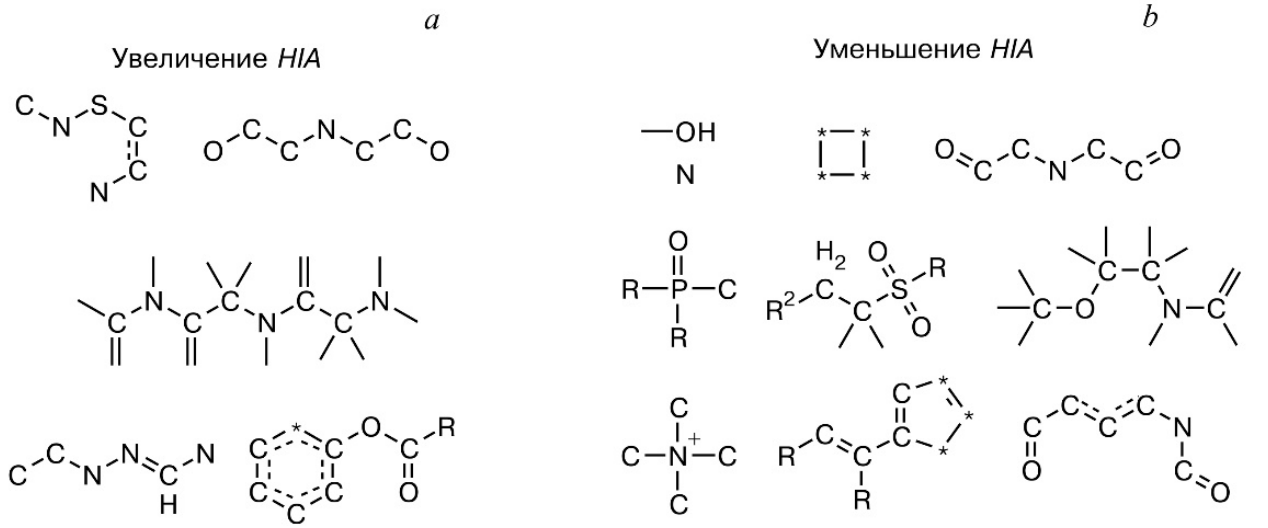


Рис. 2. Фрагменты, оказывающие наиболее сильное положительное (а) и отрицательное (*b*) влияние на прогнозируемую величину всасывания в модели *HIA* (звездочка – любой атом).

Построенная нами модель для прогнозирования всасывания лекарственных веществ в кишечнике человека включена в интегрированную веб-службу для прогнозирования ADMET-параметров лекарственных веществ, разрабатываемую в лаборатории медицинской химии Химического факультета МГУ (http://qsar.chem.msu.ru/admet/)[40].

Таблица 3. Параметры качества распознавания классов всасывания, прогнозируемых в ходе процедуры перекрестного контроля по моделям *HIA* и *LogHIAratio (%)*

| Параметр | *HIA* | *LogHIAratio* |
|---|---|---|
| Общая точность | 88 | 87 |
| Грубые ошибки | 0.4 | 1.0 |
| Чувствительность HIA+ | 95 | 95 |
| Специфичность HIA+ | 85 | 78 |

Таким образом, с использованием фрагментных дескрипторов и искусственных нейронных сетей нами построена предсказательная модель связи структуры органических соединений и их способности к всасыванию в кишечнике человека, а также проанализированы структурные факторы, влияющие на легкость всасывания. Эта модель превосходит по точности прогноза и области применимости ранее опубликованные в литературе модели и может найти применение при оптимизации фармакокинетических параметров в ходе разработки лекарств.

Работа выполнена при финансовой поддержке Российского фонда фундаментальных исследований (проект № 15-03-09084) и Министерства образования и науки Российской Федерации (проект RFMEFI60414X0144).

## Список литературы

1. A. Ruiz-Garcia, M. Bermejo, A. Moss, V. G. Casabo, J. *Pharm. Sci.,* 2008, **97**, 654.
2. J. Keldenich, *Chem. Biodivers.,* 2009, **6**, 2000.
3. S. Alqahtani, L. A. Mohamed, A. Kaddoumi, *Expert Opin. Drug Metab. Toxicol.,* 2013, **9**, 1241.
4. E. Sjögren, B. Abrahamsson, P. Augustijns, D. Becker, M. B. Bolger, M. Brewster, J. Brouwers, T. Flanagan, M. Harwood, C. Heinen, R. Holm, H. P. Juretschke, M. Kubbinga, A. Lindahl, V. Lukacova, U. Münster, S. Neuhoff, M. A. Nguyen, A. van Peer, C. Reppas, A. R. Hodjegan, C. Tannergren, W. Weitschies, C. Wilson, P. Zane, H. Lennernäs, P. Langguth, *Eur. J. Pharm. Sci.,* 2014, **57**, 99.
5. E. S. Kostewicz, B. Abrahamsson, M. Brewster, J. Brouwers, J. Butler, S. Carlert, P. A. Dickinson, J. Dressman, R. Holm, S. Klein, J. Mann, M. McAllister, M. Minekus, U. Muenster, A. Müllertz, M. Verwei, M. Vertzoni, W. Weitschies, P. Augustijns, *Eur. J. Pharm. Sci.,* 2014, **57**, 342.
6. T. Hou, Y. Li, W. Zhang, J. Wang, *Comb. Chem. High Throughput Screen.,* 2009, **12**, 497.
7. J. Zhu, J. Wang, H. Yu, Y. Li, T. Hou, *Comb. Chem. High Throughput Screen.,* 2011, **14**, 362.
8. F. T. Silva, G. H. Trossini, *Med. Chem.,* 2014, **10**, 441.

9. Y. H. Zhao, J. Le, M. H. Abraham, A. Hersey, P. I. Eddershaw, C. N. Luscombe, D. Butina, G. Beck, B. Sherborne, I. Cooper, J. A. Platts, *J. Pharm. Sci.,* 2001, **90**, 749.
10. K. Palm, P. Stenberg, K. Luthman, P. Artursson, *Pharm. Res.,* 1997, **14**, 568.
11. T. Hou, J. Wang, Y. Li, *J. Chem. Inf. Model.,* 2007, **47**, 2408.
12. T. Hou, J. Wang, W. Zhang, X. Xu, *J. Chem. Inf. Model.,* 2007, **47**, 208.
13. M. Kansy, F. Senner, K. Gubernator, *J. Med. Chem.,* 1998, **41**, 1007.
14. M. D. Wessel, P. C. Jurs, J. W. Tolan, S. M. Muskal, *J. Chem. Inf. Comput. Sci.,* 1998, **38**, 726.
15. W. L. Chiou, H. Y. Jeong, S. M. Chung, T. C. Wu, *Pharm. Res.,* 2000, **17**, 135.
16. M. L. Weaver, B. A. Orwig, L. C. Rodriguez, E. D. Graham, J. A. Chin, M. J. Shapiro, J. F. McLeod, J. B. Mangold, *Drug. Metab. Dispos.,* 2001, **29**, 415.
17. G. Klopman, L. R. Stefan, R. D. Saiakhov, *Eur. J. Pharm. Sci.,* 2002, **17**, 253.
18. Y. H. Zhao, M. H. Abraham, J. Le, A. Hersey, C. N. Luscombe, G. Beck, B. Sherborne, I. Cooper, *Eur. J. Med. Chem.,* 2003, **38**, 233.
19. M. A. Pérez, M. B. Sanz, L. R. Torres, R. G. Avalos, M. P. González, H. G. Díaz, *Eur. J. Med. Chem.,* 2004, **39,** 905.
20. M. V. Varma, K. Sateesh, R. Panchagnula, *Mol. Pharm.,* 2005, **2**, 12.
21. *Pharmacogenomics Knowledgebase* (*PharmGKB*); http://www.pharmgkb.org.
22. T. Hou, J. Wang, W. Zhang, X. Xu, *J. Chem. Inf. Model.,* 2007, **47**, 460.
23. E. Deretey, M. Feher, J. M. Schmidt, *Quant. Struct.-Act. Relat.,* 2002, **21**, 493.
24. S. B. Gunturi, R. Narayanan, *QSAR Comb. Sci.*, 2007, **26**, 653.
25. У. H. Zhao, M. H. Abraham, J. Le, A. Hersey, C. N. Luscombe, G. Beck, B. Sherborne, I. Cooper, *Pharm. Res.,* 2002, **19**, 1446.
26. K. Balon, B. U. Riebesehl, B. W. Müller, *Pharm. Res.,* 1999, **16**, 882.
27. *Instant JChem 6.3.3,* 2014, ChemAxon Ltd; http://www.chemaxon.com.
28. Н. В. Артеменко, И. И. Баскин, В. А. Палюлин, Н. С. Зефиров, *Изв. АН. Сер. хим.,* 2003, 19 [N. V. Artemenko, I.I. Baskin, V. A. Palyulin, N. S. Zefirov, *Russ. Chem. Bull.* (*Engl. Transl.*)*,* 2003, **52**, 20].
29. I. I. Baskin, N. M. Halberstam, N. V. Artemenko, V. A. Palyulin, N. S. Zefirov, in *Euro QSAR 2002 Designing Drugs and Crop Protectants: Processes, Problems and Solutions,* Blackwell, Oxford, 2003, 260.
30. N. S. Zefirov, V. A. Palyulin, *J. Chem. Inf. Comput. Sci.,* 2002, **42**, 1112.
31. Н. И. Жохова, И. И. Баскин, А. Н. Зефиров, В. А. Палюлин, Н. С. Зефиров, *Докл. АН,* 2010, **430**, 635 [N. I. Zhokhova, I.I. Baskin, A. N. Zefirov, V. A. Palyulin, N. S. Zefirov, *Dokl. Chem.* (*Engl. Transl.*), 2010, **430**, 39].
32. M. H. Abraham, *Chem. Soc. Rev.,* 1993, **22**, 73.
33. Н. В. Артеменко, В. А. Палюлин, Н. С. Зефиров, *Докл. АН,* 2002, **383**, 771 [N. V. Artemenko, V. A. Palyulin, N. S. Zefirov, *Dokl. Chem.* (*Engl. Transl.*), 2002, **383**, 114].
34. Н. И. Жохова, И. И. Баскин, В. А. Палюлин, А. Н. Зефиров, Н. С. Зефиров, *Докл. АН,* 2007, **417**, 639 [N. I. Zhokhova, I. I. Baskin, V. A. Palyulin, A. N. Zefirov, N. S. Zefirov, *Dokl. Chem.* (*Engl. Transl.*), 2007, **417**, 282].
35. N. Petri, C. Tannergren, B. Holst, F. A. Mellon, Y. Bao, G. W. Plumb, J. Bacon, K. A. O' Leary, P. A. Kroon, L. Knutson, P. Forsell, T. Eriksson, H. Lennernas, G. Williamson, *Drug Metab. Dispos.,* 2003, **31**, 805.
36. A. Yan, Z. Wang, Z. Cai, *Int. J. Mol. Sci.,* 2008, **10**, 1961.
37. T. L. Moda, A. D. Andricopulo, *Bioorg. Med. Chem. Lett.,* 2012, **22**, 2889.
38. I. I. Baskin, A. O. Ait, N. M. Halberstam, V. A. Palyulin, N. S. Zefirov, *SAR QSAR Environ. Res.,* 2002, **13**, 35.

39. C. A. Lipinski, F. Lombardo, B. W. Dominy, P. J. Feeney, *Adv. Drug Deliv. Rev*., 2001, **46**, 3.
40. Е. В. Радченко, П. В. Карпов, С. Б. Соснин, В. А. Палюлин, Н. С. Зефиров, в кн. *XXII Российский национальный конгресс «Человек и лекарство», Москва, 6—10 апреля 2015,* 250.

*Поступила в редакцию 12 мая 2015;*
*после доработки — 5 ноября 2015*

*ДОКЛАДЫ АКАДЕМИИ НАУК, 2016, том 470, № 6, с. 720-723*

*БИОХИМИЯ, БИОФИЗИКА, МОЛЕКУЛЯРНАЯ БИОЛОГИЯ*

УДК 544.165

# ПРОГНОЗИРОВАНИЕ ПРОНИКНОВЕНИЯ ОРГАНИЧЕСКИХ ВЕЩЕСТВ ЧЕРЕЗ ГЕМАТОЭНЦЕФАЛИЧЕСКИЙ БАРЬЕР

**А. С. Дябина, Е. В. Радченко, В. А. Палюлин, академик РАН Н. С. Зефиров**

*Московский государственный университет им. М.В. Ломоносова*
*Институт физиологически активных веществ Российской Академии наук, Черноголовка Московской обл.*

С использованием фрагментных дескрипторов и искусственных нейронных сетей построена предсказательная модель связи структуры органических соединений и их способности к проникновению через гематоэнцефалический барьер, а также проанализированы структурные факторы, влияющие на легкость такого проникновения. Эта модель *(*$N$= 529, $Q^2$ = 0.82, $RMSE_{cv}$ = 0.32) превосходит по точности прогноза и области применимости ранее опубликованные в литературе модели и ее можно использовать при оптимизации фармакокинетических параметров в ходе разработки лекарств.

DOI: 10.7868/S0869565216300253

Проникновение лекарств и других физиологически активных веществ через гематоэнцефалический барьер (ГЭБ) принадлежит к числу важнейших фармакокинетических процессов, которые определяют их биодоступность в центральной нервной системе и оказывают решающее влияние на эффективность, фармакологический профиль, способ применения и безопасность действия лекарств. Для соединений, действующих на центральную нервную систему, такое проникновение должно быть максимальным, тогда как для лекарств периферического действия его следует минимизировать, чтобы избежать побочных эффектов [1,2]. Несмотря на значительные успехи в развитии эффективных и малоинвазивных

экспериментальных методов оценки проникновения веществ через ГЭБ, весьма актуальной остается потребность в надежных методах его прогнозирования *in silico* для новых структур в ходе поиска и оптимизации соединений-лидеров. Этой проблеме были посвящены многочисленные исследования с использованием методов хемоинформатики [3,4], однако представленные в литературе модели не обладают достаточно широкой областью применимости и/или высокой точностью для прогнозирования проникновения разнообразных органических соединений.

С учетом этого целью настоящей работы явилось построение более надежных предсказательных моделей количественной связи структуры потенциальных лекарственных веществ и их проникновения через гематоэнцефалический барьер, а также анализ структурных факторов, влияющих на легкость такого проникновения. Предварительные результаты исследования были представлены нами ранее [5].

В ходе работы на основе анализа большого числа литературных источников была подготовлена обширная база данных по способности органических соединений проникать через ГЭБ, представленной в виде логарифма эффективного коэффициента распределения вещества между мозгом и кровью $LogBB = \lg(C_{brain}/C_{blood})$. Для формирования базы данных применяли программный комплекс Instant JChem [6]. В общей сложности обучающая выборка включает 529 соединений различных химических классов и охватывает широкий диапазон значений *LogBB*. По-видимому, она является наиболее полной и точной среди описанных в литературе выборок, содержащих открытые количественные данные.

Для построения моделей связи структуры соединений с параметром *LogBB* использовали метод искусственных нейронных сетей в рамках программного комплекса NASAWin 2.0 [7,8]. Молекулярную структуру описывали с помощью фрагментных (подструктурных) дескрипторов, отражающих число вхождений в структуру соединения фрагментов различных типов, содержащих не более 10 атомов (цепочки, циклы и разветвленные фрагменты с многоуровневой классификацией атомов, учитывающей их тип, валентное состояние, набор связей и число присоединенных атомов водорода) [8,9]. Из анализа исключали редкие фрагменты, встречающиеся лишь в одном или двух соединениях, а затем из полученного множества, включающего несколько тысяч дескрипторов, отбирали от 60 до 160 наиболее значимых дескрипторов с помощью метода пошаговой множественной линейной регрессии. При построении нейросетевых моделей рассматривали сети трехслойной архитектуры с различным числом нейронов в скрытом слое и применяли процедуру 5×4-кратного двойного перекрестного контроля, использующую независимые подвыборки данных для обучения нейронной сети, выбора оптимальной ее конфигурации и оценки предсказательной способности моделей [10]. Поскольку для большинства соединений отсут-

ствуют достаточно полные и точные данные о роли различных механизмов пассивного и активного транспорта в их переносе через ГЭБ, а также связывания вещества с белками плазмы крови и тканями мозга [1], эти параметры не включали в модель в явном виде, однако связанные с ними особенности влияния структуры на проникновение через ГЭБ должны косвенно учитываться нейросетевой фрагментной моделью.

Характеристики оптимальных моделей, построенных с использованием различных подмножеств фрагментных дескрипторов, представлены в табл. 1. Как видно, наилучшая модель опирается на фрагменты, включающие не более 9 атомов. По своим статистическим параметрам ($Q^2$ = 0.82, $RMSE_{cv}$ = 0.32) она сопоставима с наиболее надежными представленными в литературе моделями или превосходит их [4,11], а средняя ошибка прогноза близка к ошибке экспериментального определения *LogBB* (0.3 логарифмических единицы [12]).

Таблица 1. Характеристики нейросетевых моделей связи структуры органических соединений и их способности к проникновению через ГЭБ.

| Размер фрагментов | $N_d$ | $N_h$ | $Q^2$ | $RMSE_{cv}$ |
|---|---|---|---|---|
| 5 | 120 | 4 | 0.78 | 0.35 |
| 6 | 160 | 6 | 0.81 | 0.33 |
| 7 | 120 | 6 | 0.80 | 0.34 |
| 8 | 160 | 2 | 0.80 | 0.33 |
| 9 | 160 | 3 | 0.82 | 0.32 |
| 10 | 120 | 2 | 0.76 | 0.36 |

Модели построены по обучающей выборке, содержащей 529 соединений различных классов. $N_d$ – число дескрипторов, $N_h$ – число нейронов в скрытом слое архитектуры нейронной сети, $Q^2$ – параметр перекрестного контроля, $RMSE_{cv}$ – среднеквадратическая ошибка при перекрестном контроле.

При этом значительно бóльшая представительность обучающей выборки обеспечивает более широкую область применимости модели, охватывающую более разнообразные соединения. Сравнение экспериментальных значений *LogBB* со значениями, прогнозируемыми в ходе процедуры двойного перекрестного контроля, также подтверждает высокую точность прогноза для подавляющего большинства соединений (рис. 1).

Для дополнительной проверки модели использовали контрольную выборку, включающую 2053 соединения с качественной (классификационной) оценкой проникновения через ГЭБ [13]. Рассматривали два класса: проникающие соединения (BBB+) и непроникающие соединения (BBB–). Среди этих соединений лишь 247 (12%) присутствовали в нашей обучающей выборке. Как и в работе [13], прогнозируемые с помощью нейросетевой модели количественные значе-

ния *LogBB* преобразовывали в качественную шкалу с использованием порогового значения *LogBB* = –1, соответствующего проникновению в мозг около 10% вещества.

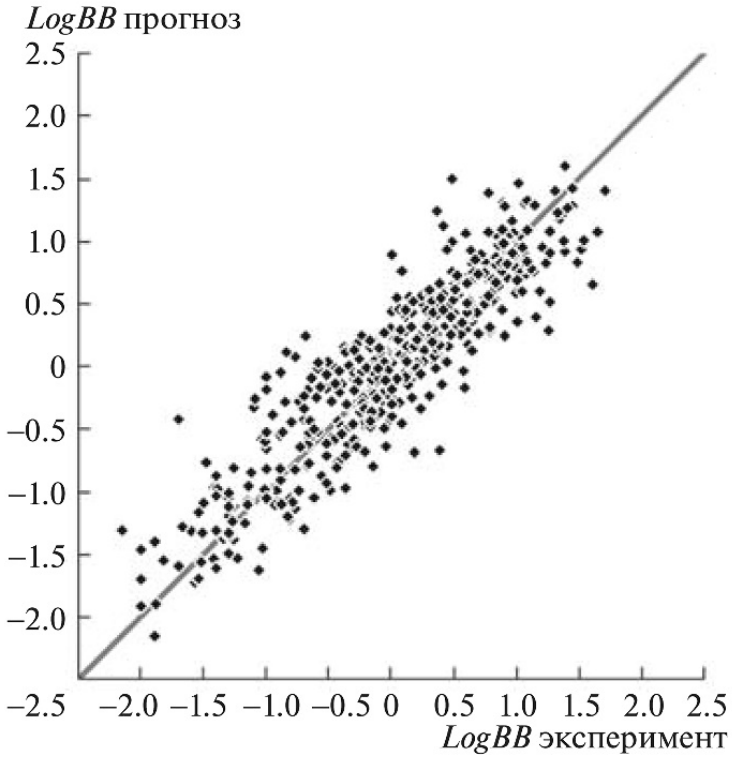


Рис. 1. Соответствие экспериментальных и прогнозируемых в ходе процедуры перекрестного контроля величин проникновения через ГЭБ для соединений обучающей выборки.

В табл. 2 представлены матрицы неточностей классификации, а также рассчитанные по ним параметры общей точности распознавания, чувствительности (точности распознавания проникающих соединений) и специфичности (точности распознавания непроникающих соединений) для всей контрольной выборки и для ее подвыборки, не перекрывающейся с обучающей выборкой. Как видно, построенная нами модель правильно определяет более 90% проникающих через ГЭБ соединений в независимой контрольной выборке. Для класса BBB– качество распознавания (специфичность) ниже. Отчасти это может быть связано с тем, что отнесение многих соединений к нему опиралось на косвенные данные об отсутствии наблюдаемой активности в отношении центральной нервной системы, которое может объясняться не только отсутствием проникновения через ГЭБ, но и другими факторами. Параметры для полной и неперекрывающейся контрольных выборок весьма близки, что дополнительно подтверждает надежность и широкую область применимости нашей модели и позволяет достаточно уверенно использовать ее для прогнозирования проникновения через ГЭБ новых соединений.

**Таблица 2.** Матрицы неточностей и параметры качества классификации соединений по проникновению через ГЭБ для контрольной выборки.

| Показатель | Прогноз, полная выборка | | Прогноз, неперекрывающаяся выборка | |
|---|---|---|---|---|
| Эксперимент | BBB+ | BBB– | BBB+ | BBB– |
| BBB+ | 1464 | 105 | 1255 | 100 |
| BBB- | 281 | 203 | 259 | 192 |
| Всего | 2053 | 2053 | 1806 | 1806 |
| Общая точность | 81% | | 80% | |
| Чувствительность | 93% | | 93% | |
| Специфичность | 42% | | 43% | |

Для целей качественного анализа и интерпретации влияния различных дескрипторов на прогнозируемые с помощью нейросетевой модели величины целевого параметра использовали численно определяемые значения частных производных такого параметра по дескрипторам, усредненные по обучающей выборке [14]. Чтобы учесть различия в диапазонах изменения дескрипторов, рассчитывали нормированный относительный отклик модели

$$RR_i = \mathrm{avg}\left(\frac{\partial y}{\partial x_i}\right) \cdot \frac{\mathrm{range}(x_i)}{\mathrm{range}(y)},$$

где $\mathrm{avg}\left(\frac{\partial y}{\partial x_i}\right)$ – среднее значение производной целевого параметра $y$ по дескриптору $x_i$, $\mathrm{range}(x_i)$ – диапазон изменения дескриптора $x_i$, $\mathrm{range}(y)$ – диапазон изменения параметра $y$.

Фрагменты, оказывающие наиболее сильное положительное и отрицательное влияние на величину параметра *LogBB,* представлены на рис. 2. Многие из них допускают простую интерпретацию, которая согласуется с известными представлениями о структурных особенностях, влияющих на проникновение вещества через ГЭБ [12]. Так, при прочих равных условиях проникновение ухудшается при наличии в структуре сильнополярных групп (гидроксильной, карбоксильной, гуанидиновой). В то же время гидрофобные фрагменты (алкильные или ароматические) способствуют проникновению вещества. Значительный положительный вклад фрагмента, включающего гидроксил в α-положении к карбонильной группе, по-видимому, отражает роль активного транспорта замещенных монокарбоновых кислот, который обеспечивает хорошее их проникновение, хотя пассивный транспорт этих соединений затруднен присутствием в молекуле

полярных групп. Тем не менее при анализе наиболее значимых вкладов фрагментов следует иметь в виду, что модель включает также большое число других фрагментных дескрипторов, влияющих на прогнозируемую величину проникновения через ГЭБ, поэтому для оптимизации фармакокинетических свойств лекарственного вещества целесообразно использовать подход, основанный на виртуальном скрининге.

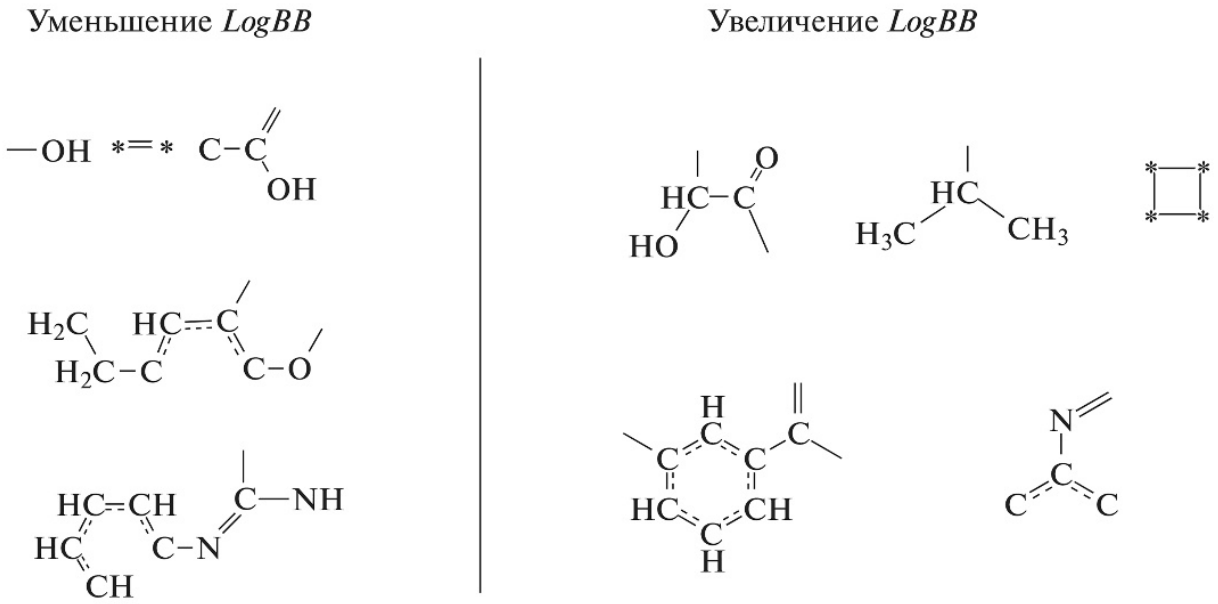


Рис. 2. Фрагменты, оказывающие наиболее сильное отрицательное и положительное влияние на прогнозируемую величину проникновения вещества через ГЭБ.

Построенная нами модель для прогнозирования проникновения лекарственных веществ через гематоэнцефалический барьер включена в интегрированную веб-службу для прогнозирования ADMET-параметров лекарственных веществ, разрабатываемую в лаборатории медицинской химии Химического факультета МГУ (http://qsar.chem.msu.ru/admet/) [15].

Таким образом, с использованием фрагментных дескрипторов и искусственных нейронных сетей нами построена предсказательная модель связи структуры органических соединений и их способности к проникновению через гематоэнцефалический барьер, а также проанализированы некоторые структурные факторы, влияющие на легкость такого проникновения. Эта модель превосходит по точности прогноза и области применимости ранее опубликованные в литературе модели и может использоваться при оптимизации фармакокинетических параметров в ходе разработки лекарств.

Авторы признательны фирме «ChemAxon» за предоставление лицензий на программное обеспечение для работы со структурными данными.

Работа выполнена при поддержке Министерства образования и науки Российской Федерации (проект № RFMEFI60414X0144).

# СПИСОК ЛИТЕРАТУРЫ


1. *Di L., Rong H., Feng B.* // J. Med. Chem. 2013. V. 56. № 1. P. 2-12.
2. *Wager T.T., Liras J.L., Mente S., Trapa P.* // Expert Opin. Drug Metab. Toxicol. 2012. V. 8. № 5. P. 531-542.
3. *Garg P, Verma J., Boy N. In silico* Modeling for Blood-Brain Barrier Permeability Predictions. In: Drug Absorption Studies. N.Y.: Springer, 2008. P. 510-556.
4. *Lanevskij K., Japertas P., Didziapetris B.* // Expert Opin. Drug Metab. Toxicol. 2013. V. 9. № 4. P. 473-486.
5. *Patyulin V.A., Dyabina A.S., Radchenko E.V., Zefirov N.S.* In: ISMC EFMC XXII Intern. Symp. on Medicinal Chemistry. Berlin, September 2-6, 2012. B., 2012. P. 374-375.
6. Instant JChem 16.4.11, 2016. ChemAxon Ltd. (http://www.chemaxon.com).
7. *Baskin I.I., Halberstam N.M., Artemenko N.V., Palyulin V.A., Zefirov N.S.* In: EuroQSAR 2002 Designing Drugs and Crop Protectants: Processes, Problems and Solutions. Oxford: Blackwell, 2003. P. 260-263.
8. *Артеменко Н.В., Баскин И.И., Палюлин В.А., Зефиров Н.С.* // Изв. РАН. Сер. хим. 2003. Т. 52. С. 19-28.
9. *Zefirov N.S., Palyulin V.A. //* J. Chem. Inf. Comput. Sci. 2002. V. 42. № 5. P. 1112-1122.
10. *Жохова Н.И., Баскин И.И., Палюлин В.А., Зефиров А.Н., Зефиров Н.С.* // ДАН. 2007. Т. 417. № 5. С. 639-641.
11. *Muehlbacher M., Spitzer G.M., Liedl K.R., Kornhuber J.* // J. Comput.-Aided Mol. Des. 2011. V. 25. № 12. P. 1095-1106.
12. *Clark D.E.* // Drug Discov. Today. 2003. V. 8. № 20. P. 927-933.
13. *Martins I.F., Teixeira A.L., Pinheiro L., Falcao A.O. //* J. Chem. Inf. Mod. 2012. V. 52. № 6. P. 1686-1697.
14. *Baskin I.I., Ait A.O., Halberstam N.M., Palyulin V.A., Zefirov N.S.* // SAR QSAR Environ. Res. 2002. V. 13. № 1. P. 35-41.
15. *Радченко Е.В., Карпов П.В., Соснин С.Б., Палюлин В.А., Зефиров Н.С.* В кн.: XXII Рос. нац. конгресс “Человек и лекарство”. Москва, 6-10 апреля 2015. М., 2015. С. 250.


*Поступило 29.04.2016 г.*

*ДОКЛАДЫ АКАДЕМИИ НАУК, 2017, том 473, № 4, с. 494-497*

*БИОХИМИЯ, БИОФИЗИКА, МОЛЕКУЛЯРНАЯ БИОЛОГИЯ*

УДК 544.165

# КОМПЬЮТЕРНАЯ ОЦЕНКА РИСКА hERG-ОПОСРЕДОВАННОЙ КАРДИОТОКСИЧНОСТИ ПОТЕНЦИАЛЬНЫХ ЛЕКАРСТВЕННЫХ ВЕЩЕСТВ

**Е.В. Радченко, Ю.А. Рулев, А.Я. Сафаньяев, В.А. Палюлин, академик РАН Н.С. Зефиров**

*Московский государственный университет им. М.В. Ломоносова*
*Институт физиологически активных веществ Российской Академии наук, Черноголовка Московской обл.*

Калиевый канал hERG представляет собой одну из важнейших анти-мишеней, определяющую кардиотоксичность потенциальных лекарственных веществ. С использованием фрагментных дескрипторов и искусственных нейронных сетей построены предсказательные модели связи структуры органических соединений и их активности по отношению к hERG, а также проанализированы влияющие на нее структурные факторы. Эти модели ($N$ = 1000, $Q^2$ = 0,77, $RMSE_{cv}$ = 0,45 для аффинности и $N$= 2886, $Q^2$ = 0,60, $RMSE_{cv}$ = 0,55 для ингибирования канала) превосходят по предсказательной способности и области применимости ранее опубликованные в литературе модели и могут использоваться для минимизации риска кардиотоксичности в ходе разработки лекарств.

**DOI:** 10.7868/S0869565217040235

Потенциалзависимый калиевый канал задержанного выпрямления hERG (по традиционному названию кодирующего его гена Human Ether-à-go-go Related Gene, систематическое обозначение канала $K_v11.1$) экспрессируется главным образом в кардиомиоцитах сердечной мышцы и обеспечивает реполяризацию желудочков в ходе развития потенциала действия. Нарушение функционирования канала под влиянием низкомолекулярных соединений (в частности, лекарственных средств) или в результате некоторых заболеваний вызывает замедление реполяризации и удлинение потенциала действия (интервала QT на электрокардиограмме), что может приводить к желудочковой аритмии и внезапной смерти. В связи с этим канал hERG относят к числу важнейших анти-мишеней (мишеней, опосредующих побочные эффекты лекарств). Активность по отношению к нему стала причиной прекращения исследований или снятия с рынка многих перспективных препаратов, поэтому в настоящее время исключению риска его ингиби-

рования уделяется огромное внимание при разработке новых лекарств [1]. Несмотря на значительные успехи в развитии эффективных экспериментальных методов для оценки *in vitro* действия соединений на hERG, весьма актуальной остается потребность в надежных методах *in silico* прогнозирования связанных с ним рисков для новых структур в ходе поиска и оптимизации соединений-лидеров. Этой проблеме были посвящены многочисленные исследования с использованием методов анализа связи «структура–активность», фармакофорного поиска, молекулярного моделирования и докинга [2], однако представленные в литературе модели не обладают достаточно высокой точностью и/или широкой областью применимости для прогнозирования активности разнообразных органических соединений. Дополнительные сложности связаны с возможностями реализации разных способов связывания ингибиторов в структуре канала [3], а также с влиянием соединений на экспрессию и внутриклеточный транспорт hERG, а не непосредственно на его функционирование [4].

В то же время модели связи «структура–активность», построенные на основе фрагментных дескрипторов и искусственных нейронных сетей, часто позволяют добиться достаточно высокой точности прогнозирования взаимодействия биологических мишеней с лигандами в широких рядах соединений, различающихся по структуре и механизму действия [5].

С учетом этого целью настоящей работы явилось построение более надежных предсказательных моделей количественной связи структуры потенциальных лекарственных веществ и их активности по отношению к каналу hERG, а также анализ влияющих на активность структурных факторов. Предварительные результаты исследования были представлены нами ранее [6].

В ходе работы на основе анализа большого числа литературных источников была подготовлена обширная база данных по активности органических соединений по отношению к каналу hERG, которая может оцениваться на двух уровнях. Связывание вещества с каналом (аффинность) обычно характеризуют константой диссоциации комплекса $K_i$, определяемой методом конкурентного радиолигандного связывания, а блокирование прохождения ионов калия через канал – концентрацией $IC_{50}$, обеспечивающей 50%-ное снижение калиевого тока, которое определяется электрофизиологическим методом на экспрессирующих канал клетках. К сожалению, для большинства соединений доступны данные, определенные лишь одним из методов, хотя значения этих параметров, как правило, хорошо коррелируют. При дальнейшем анализе использовали логарифмические величины $pK_i = \lg(1/K_i)$ и $pIC_{50} = \lg(1/IC_{50})$. Для формирования базы данных применяли программный комплекс Instant JChem [7]. В общей сложности обучающая выборка для $K_i$ включала 1000 соединений, а для $IC_{50}$ – 2886 соединений различных химических классов, охватывая широкий диапазон значений активности. По-видимому, она является наиболее полной и точной среди описанных в литературе выборок, содержащих открытые количественные данные.

Для построения моделей связи структуры соединений с параметрами $pK_i$ и $pIC_{50}$ использовали метод искусственных нейронных сетей в рамках программного комплекса NASAWin 2.0 [8, 9]. Молекулярную структуру соединений описывали с помощью фрагментных дескрипторов, отражающих число вхождений в нее подструктурных фрагментов разных типов, содержащих не более 12 атомов (цепочки, циклы и разветвленные фрагменты с многоуровневой классификацией атомов, учитывающей их тип, валентное состояние, набор связей и число присоединённых атомов водорода) [9, 10]. Из анализа исключали редкие фрагменты, встречающиеся менее чем в 3% обучающей выборки (30 соединений для $pK_i$ и 100 соединений для $pIC_{50}$), поскольку они непригодны для построения предсказательных моделей с широкой областью применимости. Затем из полученного множества, включающего несколько тысяч дескрипторов, отбирали от 100 до 200 наиболее значимых дескрипторов с помощью метода пошаговой множественной линейной регрессии. При построении нейросетевых моделей рассматривали сети трехслойной архитектуры с различным числом нейронов в скрытом слое и применяли процедуру 5×4-кратного двойного перекрёстного контроля, использующую независимые подвыборки данных для обучения нейронной сети, выбора оптимальной ее конфигурации и оценки предсказательной способности моделей [11].

Характеристики оптимальных моделей, построенных с использованием разных подмножеств фрагментных дескрипторов, представлены в табл. 1. Как видно из таблицы, наилучшие модели опираются на фрагменты, включающие не более 11 атомов. По своим статистическим параметрам ($Q^2$ = 0,77, $RMSE_{cv}$ = 0,45 для $pK_i$ и $Q^2$ = 0,60, $RMSE_{cv}$ = 0,55 для $pIC_{50}$) они сопоставимы с лучшими представленными в литературе моделями или превосходят их [2]. Так, в работе [12] для одной из наиболее широких обучающих выборок, включающей 1312 соединений, получены модели со значениями параметра $Q^2$ от 0,33 до 0,54, в то же время большинство опубликованных моделей опирается на обучающие выборки, содержащие лишь несколько десятков или сотен соединений [2]. Сравнение экспериментальных значений $pK_i$ и $pIC_{50}$ со значениями, прогнозируемыми в ходе процедуры двойного перекрестного контроля, также подтверждает высокую точность прогноза для подавляющего большинства соединений (рис. 1), хотя для отдельных соединений ошибки оказываются значительными (7 соединений с ошибкой более 1,5 логарифмических единиц для модели $pK_i$ и 46 соединений для модели $pIC_{50}$). Скорее всего, такие отклонения связаны с шумом в исходных данных, однако исключение этих соединений из обучающей выборки было признано нецелесообразным, хотя оно могло бы привести к построению моделей с более высокими итоговыми показателями качества. При этом значительно бóльшая представительность обучающей выборки (особенно для $pIC_{50}$) обеспечивает бо-

лее широкую область применимости моделей, охватывающую более разнообразные соединения, а их точность достаточна для полуколичественной оценки риска кардиотоксичности соединений.

**Таблица 1.** Характеристики нейросетевых моделей связи структуры органических соединений и их активности по отношению к каналу hERG

| Размер фрагментов | $pK_i$ ($N$= 1000) | | | | $pIC_{50}$ ($N$= 2886) | | | |
|---|---|---|---|---|---|---|---|---|
| | $N_d$ | $N_h$ | $Q^2$ | $RMSE_{cv}$ | $N_d$ | $N_h$ | $Q^2$ | $RMSE_{cv}$ |
| 6 | 200 | 6 | 0,74 | 0,48 | 200 | 3 | 0,56 | 0,58 |
| 7 | 160 | 3 | 0,72 | 0,50 | 200 | 5 | 0,57 | 0,57 |
| 8 | 200 | 6 | 0,74 | 0,48 | 200 | 6 | 0,59 | 0,56 |
| 9 | 160 | 2 | 0,76 | 0,46 | 200 | 6 | 0,60 | 0,56 |
| 10 | 180 | 2 | 0,76 | 0,46 | 200 | 5 | 0,59 | 0,56 |
| 11 | 200 | 4 | 0,77 | 0,45 | 200 | 3 | 0,60 | 0,55 |
| 12 | 160 | 2 | 0,76 | 0,46 | 200 | 5 | 0,60 | 0,55 |

Примечание. $N$ – число соединений в обучающей выборке, $N_d$ – число дескрипторов, $N_h$ – число нейронов в скрытом слое архитектуры нейронной сети, $Q^2$ – параметр перекрестного контроля, $RMSE_{cv}$ – среднеквадратическая ошибка при перекрёстном контроле.

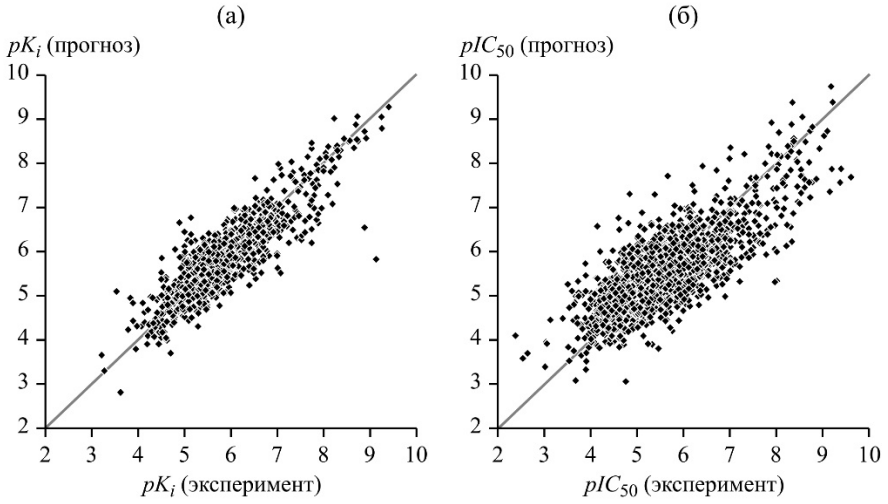


**Рис.** 1. Соответствие экспериментальных и прогнозируемых в ходе процедуры перекрёстного контроля величин активности $pK_i$ (а) и $pIC_{50}$ (б) по отношению к каналу hERG для соединений обучающей выборки.

Для целей качественного анализа и интерпретации влияния различных дескрипторов на прогнозируемые с помощью нейросетевой модели величины целевого параметра использовали численно определяемые значения частных производных такого параметра по дескрипторам, усредненные по обучающей выборке [13]. Чтобы учесть различия в диапазонах изменения дескрипторов, рассчитывали нормированный относительный отклик модели

$$RR_i = \text{avg}\left(\frac{\partial y}{\partial x_i}\right) \times \frac{\text{range}(x_i)}{\text{range}(y)},$$

где $\text{avg}\left(\frac{\partial y}{\partial x_i}\right)$ – среднее значение производной целевого параметра $y$ по дескриптору $x_i$, range ($x_i$) – диапазон изменения дескрипторах $x_i$, а range ($y$) – диапазон изменения параметра $y$.

Фрагменты, оказывающие наиболее сильное положительное и отрицательное влияние на величину параметра $pK_i$, представлены на рис. 2. Многие из них допускают простую интерпретацию, которая согласуется с известными представлениями о структурных особенностях сайта связывания ингибиторов hERG, имеющего преимущественно гидрофобный характер [2, 3], а также с фармакофорными моделями ингибиторов, большинство из которых включает положительно заряженную группу и несколько гидрофобных групп на расстоянии 5–7 Å от нее [14]. Так, при прочих равных условиях связыванию с hERG способствуют большие гидрофобные фрагменты (алкильные или ароматические), а также аминогруппы с длинными алкильными заместителями. В то же время полярные группы и близкое расположение аминогруппы и ароматического фрагмента снижают связывание. Тем не менее при анализе наиболее значимых вкладов фрагментов следует иметь в виду, что модель включает также большое число других фрагментных дескрипторов, влияющих на прогнозируемую величину активности по отношению к hERG, поэтому для оптимизации свойств лекарственного вещества целесообразно использовать подход, основанный на виртуальном скрининге.

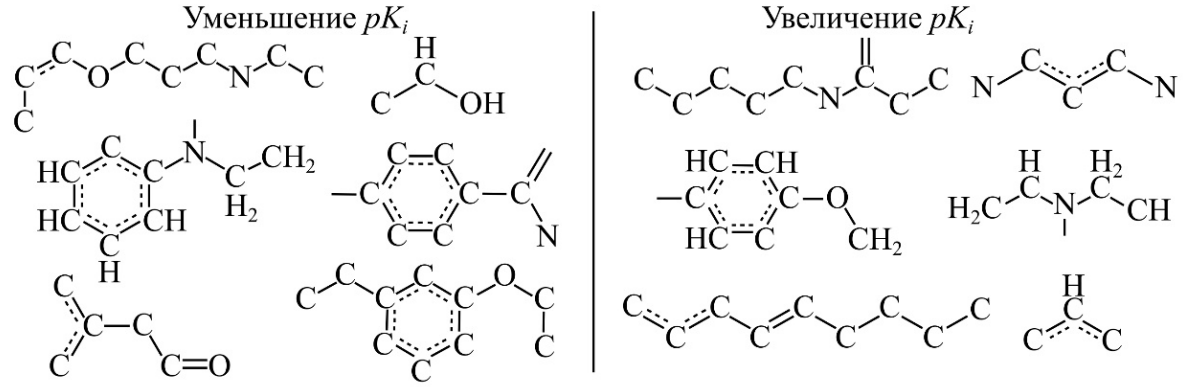


**Рис. 2.** Фрагменты, оказывающие наиболее сильное отрицательное и положительное влияние на прогнозируемую величину аффинности к каналу hERG.

Построенные модели для прогнозирования активности потенциальных лекарственных веществ по отношению к каналу hERG свободно доступны для использования по адресу http://qsar.chem.msu.ru/admet/ [15].

Таким образом, с использованием фрагментных дескрипторов и искусственных нейронных сетей нами построены предсказательные модели связи структуры органических соединений и их активности по отношению к каналу hERG,

а также проанализированы некоторые влияющие на нее структурные факторы. Эти модели превосходят по предсказательной способности и области применимости ранее опубликованные в литературе модели и могут использоваться для минимизации риска кардиотоксичности в ходе разработки лекарств.

Авторы признательны фирме «ChemAxon» за предоставление лицензий на программное обеспечение для работы со структурными данными.

Работа выполнена при поддержке Министерства образования и науки Российской Федерации (проект № RFMEFI60414X0144).

## СПИСОК ЛИТЕРАТУРЫ

1. *Gintant G., Sager P. T., Stockbridge N.* // Nat. Rev. Drug Discov. 2016. V. 15. № 7. P. 457-471.
2. *Jing Y., Easter A., Peters D., Kim N., Enyedy I. J.* // Future Med. Chem. 2015. V. 7. № 5. P. 571-586.
3. *Saxena P., Zangerl-Plessl E.M., Linder T., Windisch A., Hohaus A., Timin E., Hering S., Stary-Weinzinger A.* // Sci. Rept. 2016. V. 6. P. 24182.
4. *Nogawa H, Kawai T.* // Europ. J. Pharmacol. 2014. V. 741. P. 336-339.
5. *Курило М. Н., Рыжков Ф. В., Карпов П. В., Радченко Е. В., Палюлин В. А., Зефиров Н. С.* // ДАН. 2015. Т. 461. № 6. С. 720-723.
6. *Рулев Ю. А., Сафаньяев А. Я., Радченко Е. В., Палюлин В. А., Зефиров Н. С.* В кн.: XX Рос. национальный конгресс “Человек и лекарство”. Москва, 15—19 апреля 2013. М., 2013. С. 419—420.
7. Instant JChem 16.4.11, 2016, ChemAxon Ltd. http://www.chemaxon.com.
8. *Baskin I. I., Halberstam N. M., Artemenko N. V., Palyulin V.A., Zefirov N. S.* In: EuroQSAR 2002 Designing Drugs and Crop Protectants: Processes, Problems and Solutions. Oxford: Blackwell, 2003. P. 260-263.
9. *Артеменко Н. В., Баскин И. И., Палюлин В. А., Зефиров Н. С.* // Изв. АН. Сер. хим. 2003. Т. 52. С. 19-28.
10. *Zefirov N. S., Palyulin V. A.* // J. Chem. Inf. Comput. Sci. 2002. V. 42. № 5. P. 1112-1122.
11. *Жохова Н. И., Баскин И. И., Палюлин В. А., Зефиров А. Н., Зефиров Н. С.* // ДАН. 2007. Т. 417. № 5. С. 639-641.
12. Gavaghan C. L., Arnby C. H., Blomberg N., Strandlund G., Boyer S. // J. Comput.-Aided Mol. Des. 2007. V. 21. № 4. P. 189-206.
13. *Baskin I. I., Ait A. O., Halberstam N. M., Palyulin V.A., Zefirov N. S.* // SAR QSAR Environ. Res. 2002. V. 13. № 1. P. 35-41.
14. *Kratz J. M., Schuster D., Edtbauer M., Saxena P., Mair C. E., Kirchebner J., Matuszczak B., Baburin I., Hering S., Rollinger J. M.* // J. Chem. Inf. Model. 2014. V. 54. № 10. P. 2887-2901.
15. *Радченко Е. В., Карпов П. В., Соснин С. Б., Дябина А. С., Соснина Е.А., Палюлин В. А., Зефиров Н. С.* В кн.: XX Менделеевский съезд по общей и прикладной химии. Екатеринбург, 2016. Т. 4. С. 432.

*Mendeleev Commun., 2010, 20, 243-248*

# MOLECULAR MODELLING OF CENTRAL NERVOUS SYSTEM RECEPTORS

**Nikolay S. Zefirov and Vladimir A. Palyulin**

*Department of Chemistry, M. V. Lomonosov Moscow State University, Moscow, Russian Federation*

*The Editorial Board and Staff of Mendeleev Communications take an opportunity to congratulate Academician N. S. Zefirov on the occasion of his 75th birthday and wish him all the very best.*

The molecular models of ionotropic and metabotropic glutamate receptors, ionotropic γ-aminobutyric acid receptors, adenosine and melatonin receptors are discussed; the developed models were used in the design of new neuroprotective compounds.

| | |
|---|---|
| | Professor **Nikolay S. Zefirov** graduated from M. V. Lomonosov Moscow State University (MSU) in 1958. For more than 50 years, he holds various positions at the Department of Chemistry of the MSU; since 1994, he is the head of Organic Chemistry Division. He received PhD and Dr. Sci. degrees in 1961 and 1966, respectively. Professor Zefirov was elected a corresponding member and a full member of the USSR Academy of Sciences in 1981 and 1987, respectively. Since 1987, he is the head of the Laboratory of Mathematical Chemistry and Computer-Assisted Synthesis at the N. D. Zelinsky Institute of Organic Chemistry of the Russian Academy of Sciences (RAS). In 1989-2006, he was the director of the Institute of Physiologically Active Compounds of the RAS; in 2006, he was appointed as a scientific supervisor at this institute. Professor Zefirov was awarded the Prize of the Government of the Soviet Union (1989) and Russia (2001). He received the Lomonosov Award (1983) and Butlerov Award (1994). Professor Zefirov is a member of the International Academy of Mathematical Chemistry. In 1974—1991, he headed the Division of Organic Chemistry at the D. I. Mendeleev USSR Chemical Society; currently, he is the president of the Medicinal Chemistry Section of D. I. Mendeleev Russian Chemical Society. His research interests cover theoretical and synthetic organic chemistry, medicinal chemistry, mathematical chemistry and computer-aided molecular design. |
| | Dr. **Vladimir A. Palyulin** graduated from M. V. Lomonosov Moscow State University in 1974. Since that time, he occupied research positions at the Department of Chemistry of the MSU; since 1998, he is a leading researcher. He received PhD degree in 1985 under the supervision of Professor Zefirov. Since 1988, he is the head of a research group. In 2008, he was elected a member of the International Academy of Mathematical Chemistry. He received the first prize of the D. I. Mendeleev USSR Chemical Society. His research interests include theoretical organic chemistry, mathematical chemistry, computer-aided molecular design of physiologically active compounds and medicinal chemistry. |

The functioning of central nervous system (CNS) involves the activation of numerous receptors. In the case of neurodegenerative diseases, usually, some corrections of that activation are necessary. For this purpose, the selective agonists and antagonists, as well as the positive and negative modulators of receptors, could be considered as drug candidates. For their efficient design as potential drugs, the detailed knowledge of the 3D structure of CNS receptors is necessary. However, despite a great amount of X-ray data available for various proteins, the 3D structure of the majority of CNS receptors can currently be obtained only using molecular modelling.[1]

Here, we consider the molecular modelling of ionotropic and metabotropic glutamate receptors, ionotropic γ-aminobutyric acid (GABA) receptors, adenosine and melatonin receptors.

## Ionotropic glutamate receptors

The glutamatergic system is of vital importance for learning and memory functioning.[2,3] It includes both metabotropic glutamate receptors $mGluR_{18}$ and ligand-gated ionotropic receptors, which are subdivided into several types: NMDA receptors, AMPA receptors and KA receptors (or kainate receptors) named after their agonists *N*-methyl-D-aspartate **1**, 2-amino-3-(3-hydroxy-5-methylisoxazol-4-yl)propionic acid **2** and kainic acid **3,** respectively. The kainate receptors are often considered as a subtype of AMPA receptors.

NMDA receptors are involved in neuronal signalling processes, memory consolidation and synaptic plasticity. NMDA receptor hyperactivation induces neurotoxic effects leading to a number of pathological conditions including neurodegenerative diseases. Thus, NMDA receptor antagonists or reversible ion channel blockers could be used for the cure of such diseases.

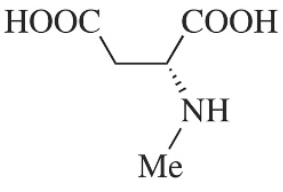


**1**

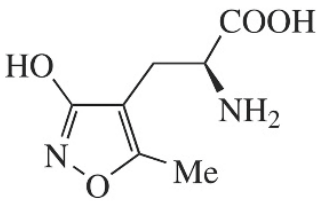


**2**

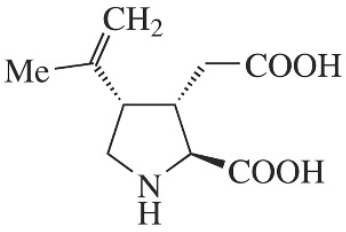


**3**

An NMDA receptor is composed of two NR1 and two NR2 subunits. Each NR2 subunit belongs to one of its four subtypes, NR2A-NR2D, leading to the heterogeneity of the wild-type NMDA receptors. NR1 and all NR2 subunits have similar four domain structures: (*a*) the N-terminal extracellular modulatory domain, (*b*) the agonist/coagonist binding domain, which holds the glycine (or D-serine) binding site in an NR1 subunit and the glutamate binding site in an NR2 subunit, (*c*) the transmembrane channel-forming region, which hosts several binding sites, and *(d)* the C-terminal intracellular regulatory domain.

The NMDA receptor ion channel is an important target for compounds exhibiting neuroprotective properties. The reversible channel blockers decreasing the $Ca^{2+}$ influx into neurons could be used for the cure of neurodegenerative diseases. However, the 3D molecular structure of the channel was not considered in the literature before our modelling studies. The first 3D model of a closed form of NMDA receptor ion channel was constructed[4] on the basis of its homology with the potassium channel KscA.[5] For the construction[6] of the open form of the channel, the X-ray data on the potassium channel of *Methanothermobacter* were used. The latter model is important as far as it was demonstrated[7] that the ion channel blockers influence the receptor in the presence of its agonists; that is, they interact with the open form of the channel. The channel consists of four subunits surrounding a pore having a narrow neck with carbonyl groups involved in the intermediate binding of the cations passing through the channel. The carbonyl group of an asparagine side chain at the neck inlet should be involved in the dehydration of $Ca^{2+}$ cations [Figure 1(a)].

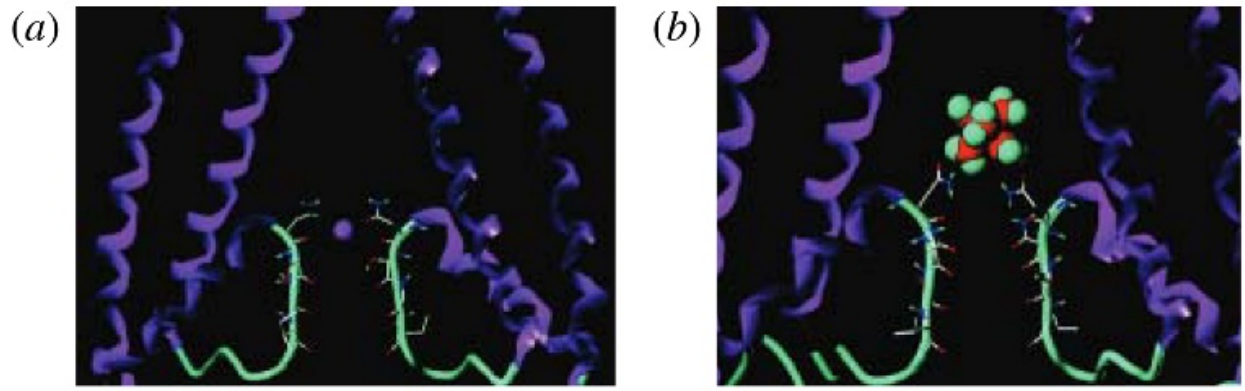


**Figure 1** *(a)* Model of $Ca^{2+}$ ion transport through the NMDA receptor ion channel, and *(b)* channel blocking by the hydrated $Mg^{2+}$ ion.

The hydrated magnesium ion binds with this asparagine residue and serves as a natural channel blocker [Figure 1(h)]. The binding mode of memantine **4** (a drug used for the cure of neurodegenerative diseases) is somewhat similar to that of magnesium; its protonated form also should generate a hydrogen bond with asparagines (Figure 2).

Thus, the ligand-bound asparagine cannot be involved in the cation dehydration, which is a necessary step for passing cations through the neck of the channel. Other known channel blockers like phencyclidine **5** or MK-801 **6** not only form a hydrogen bond with asparagine but also stick tightly to the hydrophobic walls of the channel and occupy the hydrophobic pocket (Figure 3). Thus, their binding becomes excessively high to cause serious side effects. The design of flexible analogs of MK-801 to decrease the binding could be a reasonable outcome.[4]

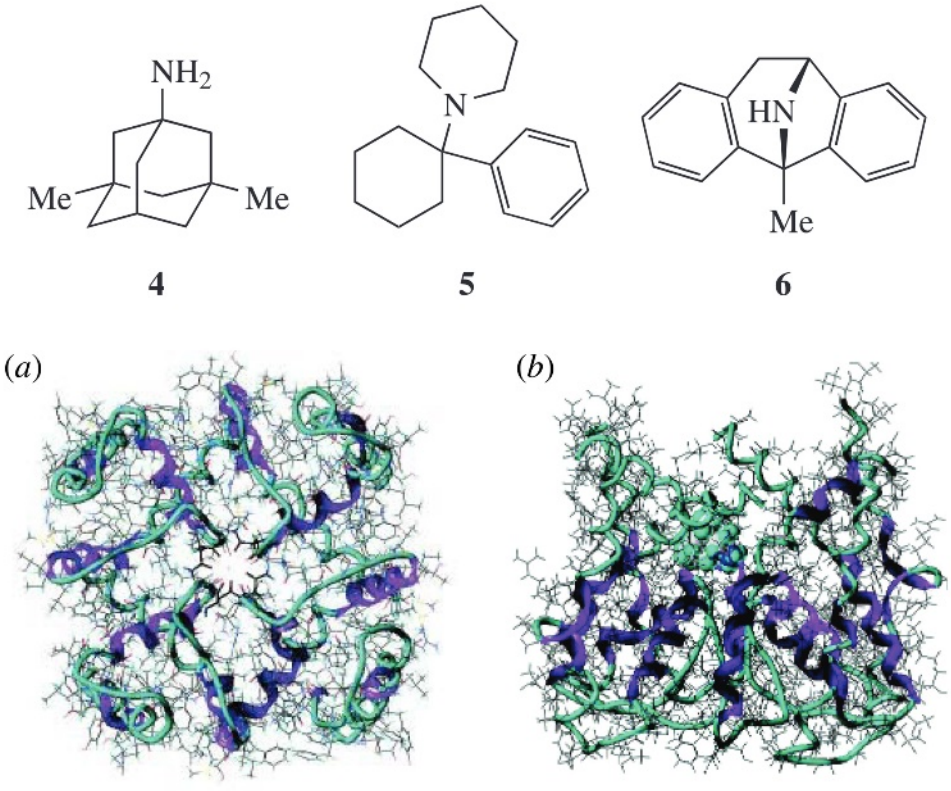


**Figure 2** *(a)* NMDA receptor ion channel (top view), and *(b)* its blocking by memantine (side view).

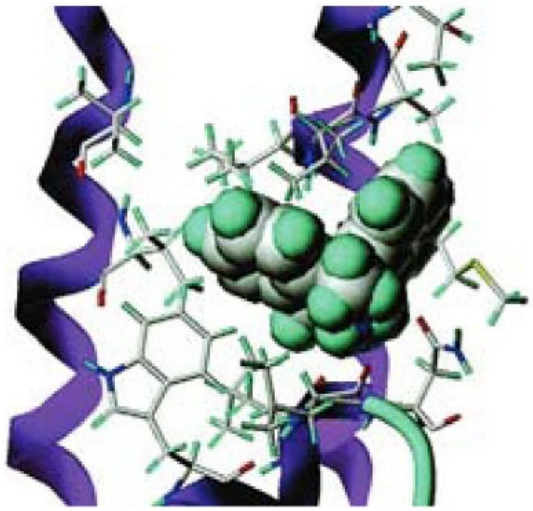

**Figure 3** Docking of MK-801 into an NMDA receptor ion channel.

Extracellular agonist and co-agonist binding domains host the binding sites of a natural agonist (glutamic acid **7**) or a co-agonist (glycine **8** or D-serine **9).** The glutamate and glycine binding sites of the NMDA receptor have similar 3D structures and are localized in NR2 and NR1 subunits, respectively. The simultaneous binding of an agonist and a co-agonist together with membrane depolarization to relieve magnesium block leads to receptor activation[8,9] and opening of the ion channel as a result of conformational reorganization.

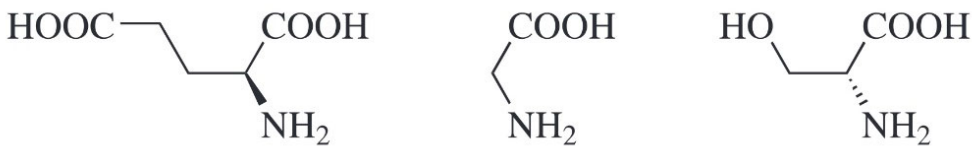


**7** **8** **9**

The models of the glutamate binding site (in closed and open forms) of the NMDA receptor NR2B subunit have been constructed[10,11] on the basis of comparative modelling with the GluR2 ligand binding core.[12] These models allowed us to analyse the binding modes of agonists and antagonists (Figure 4) and to explain known structure-activity relationships for them like a switch between the agonist and antagonist activity of ligands upon lengthening the chain between the amino acid moiety and the distal anionic group, the preference for the D-configuration in some agonists (like NMDA) and antagonists, *etc*.

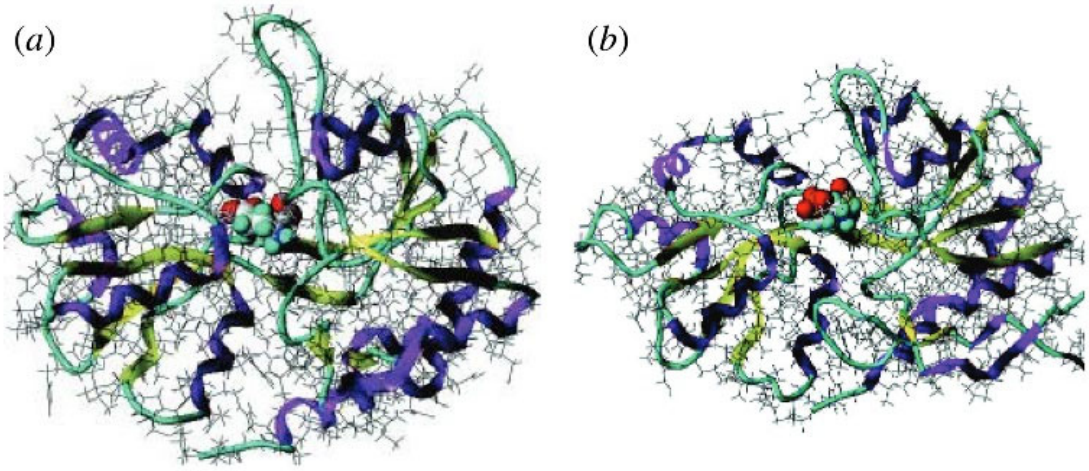


**Figure 4** *(a)* Docking of agonist glutamate 7 into the closed form, and *(b)* docking of antagonist AP5 **10** into the open form of NMDA receptor glutamate binding domain.

Interest in the glycine binding site of NMDA receptor significantly increased after the discovery of the fact that antagonists of this site may lack certain undesirable side effects observed for many noncompetitive and competitive antagonists. The modelling of the glycine binding site of NMDA receptor[13,14] was based on the same template as for the glutamate binding site. The docking of agonists and antagonists to the models (Figure 5) was used to analyse their binding modes and to explain structure-activity relationships. Note that, after the first publication of our model, X-ray data for the glycine binding site of NMDA receptor[15] with the same antagonist **11** as in our model were published. All main structural features in our model were confirmed experimentally including the binding mode of the antagonist.[15] Subsequently, we suggested the concept of selectivity fields, which was demonstrated using data on the binding of antagonists of the glycine site of NMDA receptor and glutamate site of AMPA receptor.[16]

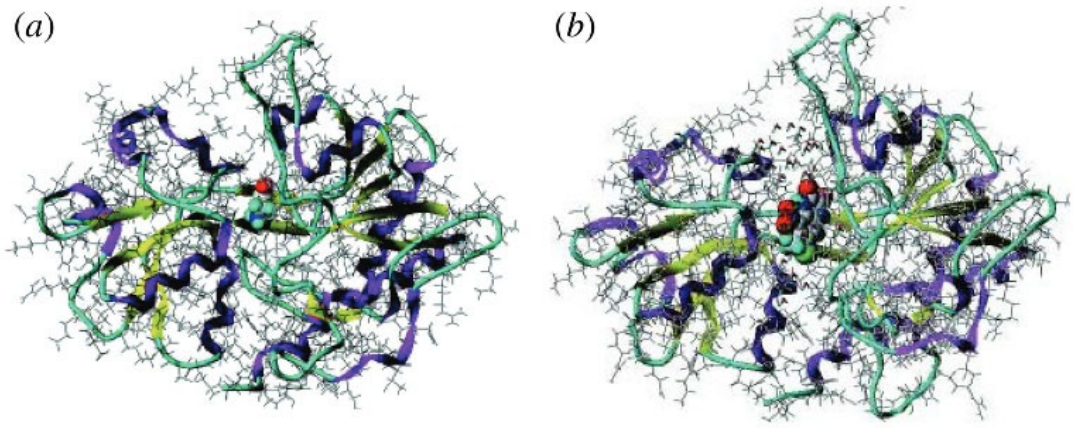


**Figure 5** *(a)* Docking of agonist glycine **8** into the closed form, and *(b)* docking of antagonist 11 into the open form of NMDA receptor glycine binding domain.

NMDA receptor N-terminal domains are of considerable interest as potential targets for the treatment of neurodegenerative diseases: the binding sites for many pharmacologically significant compounds affecting CNS are localized in these domains. The modelling of the 3D structure of N-terminal domains of NR1 and NR2B subunits[17] was based on their homology with the N-terminal domain of metabotropic glutamate receptor mGluRp[18] The constructed models were used for the evaluation of putative binding sites of ifenprodil-like compounds. It was shown that, in the N-terminal domains of NR2B subunits, the side chains of the amino acid residues involved in binding of modulator ifenprodil **12** (according to site-directed mutagenesis data) are exposed to the space between globules while for NR1 subunit the amino acid residues important for ifenprodil binding are exposed to the outer surface of the globule and do not form a certain binding site.

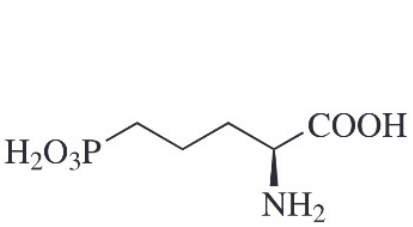


**10**

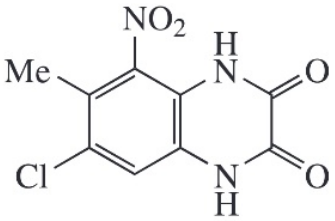


**11**

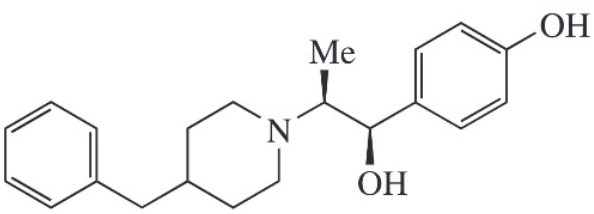


**12**

As far as ifenprodil-like compounds are considered as selective antagonists of the NR2B subunit of NMDA receptor, it can be supposed that the main binding site of ifenprodil is located in the N-terminal domain of the NR2B subunit, while the NR1 subunit is additionally involved in the binding process. The molecular models of

NMDA receptor N-terminal domains together with 3D QSAR studies allowed us to evaluate the structural features of ifenprodil-like compounds important for binding to NMDA receptor.[17]

The constructed models of NMDA receptor domains together with X-ray data for AMPA receptors and our QSAR studies for their ligands[16,19] allowed us to develop a virtual screening system for the design of ligands of NMDA and AMPA receptors.[20]

Recently, a model of the tetrameric structure of ionotropic GluR6 was built[21] and the crystal structure of the AMPA-sensitive, homotetrameric, rat GluA2 receptor at 3.6 Å resolution in complex with a competitive antagonist was reported,[22] which means a considerable success in the experimental studies of ionotropic glutamate receptors. The latter structure can serve as a good template for modelling a complete NMDA receptor structure.

The positive modulators of AMPA receptors could be effective as cognition enhancers. The docking studies[23] for a series of positive AMPA receptor modulators and a detailed analysis of their binding modes served as a basis for the design of new molecules optimally fitting to the modulator binding site. After the synthesis and biological studies, the compounds with picomolar activity were found,[24] which are significantly more potent than any other known positive modulators.

## Metabotropic glutamate receptors

Metabotropic glutamate receptors[25] are considered as targets for the cure of various CNS disorders. Eight subtypes of metabotropic glutamate receptors are known ($mGluR_{1\text{-}8}$), which belong to type 3 G protein-coupled receptors (GPCRs). They may be divided into three groups with respect to the signal transduction mechanism, pharmacological properties and the amino acid sequence homology. The receptors of the first group ($mGluR_1$ and $mGluR_5$) activate phospholipase C, while the receptors of the second group ($mGluR_2$ and $mGluR_3$) and the third group ($mGluR_4$, $mGluR_6$, $mGluR_7$ and $mGluR_8$) inhibit adenylate cyclase but differ in pharmacological properties.[25] All mGluRs function as dimeric structures, whose monomers incorporate N-terminal, cysteine-rich (CRD) and transmembrane domains. Agonists and competitive antagonists bind to N-terminal domain (to the glutamate binding site), while non-competitive antagonists bind to transmembrane domain. The first our model[26] of the open form of an N-terminal domain revealed the importance of Arg78 for ligand binding in the $mGluR_1$ subtype (unlike published modelling results). This hypothesis was confirmed experimentally[27] and later by an X-ray study of the N-terminal domain of $mGluR_1$[18] The model for the closed form of $mGluR_1$ (Figure 6) was built by a threading method[28] The earlier hypothesis of antagonist binding had also been corrected[29] as a result of our simulation. Using the $mGluR_1$ structure as a template, the models of other seven sub-

types of mGluRs were constructed, the comparative analysis of structures for all subtypes of metabotropic glutamate receptors was carried out[30] and the results of their ligands docking were analysed.[31]

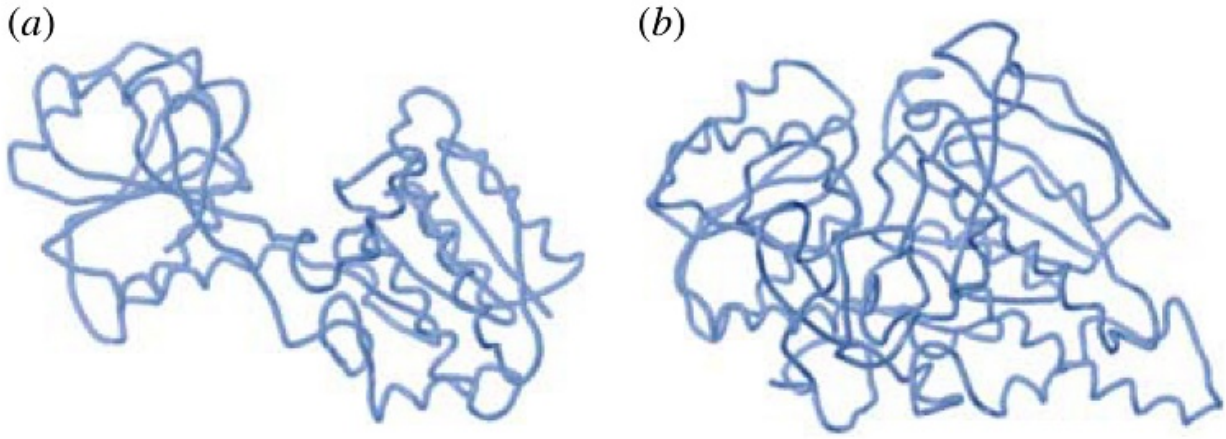


**Figure 6** *(a)* Open and *(b)* closed forms of the mGluR, N-terminal domain.

The transmembrane domain of mGluRs hosts the binding site of highly active non-competitive antagonists. The structure of this domain in $mGluR_1$ was constructed using the rhodopsin structure as a template.[32] The CRD is located between N-terminal and transmembrane domains, its fold type was estimated, the first 3D models were constructed and the role of CRD in receptor functioning was considered.[33]

## Adenosine receptors

The adenosine receptors ($A_1$, $A_{2A}$, $A_{2B}$ and $A_3$)[34,35] are activated by natural agonist adenosine **13** and have been classified as GPCRs of the rhodopsin family (type 1 GPCRs). They consist of seven transmembrane α-helices connected by three intracellular and three extracellular hydrophilic loops. Adenosine receptors are present in various tissues and involved in the regulation of various processes. The activation of $A_1$ and $A_3$ receptors decreases the cAMP level, while the activation of $A_{2A}$ and $A_{2B}$ receptors increases it. Adenosine $A_1$ receptor activation induces the inhibition of the dopamine D receptors, and stimulation of the $A_{2A}$ receptor leads to functional inhibition of the $D_2$ dopamine receptors. Antagonists of the $A_{2A}$ receptor can be used to increase the effect of dopaminergic neurotransmission in the treatment of Parkinson's disease. Other adenosine receptor ligands could be used in treatment of Alzheimer's disease and schizophrenia. The antagonist of $A_{2B}$ receptor theophylline **14** is a strong antiasthmatic drug. $A_3$ receptor agonists reduce myocardial ischemia/reperfusion injury.

Our molecular models for all subtypes of adenosine receptors[36-41] were built using the bovine rhodopsin structure as a template. The structure of $A_{2B}$ receptor is shown in Figure 7.

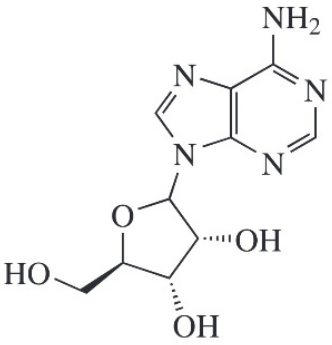

13

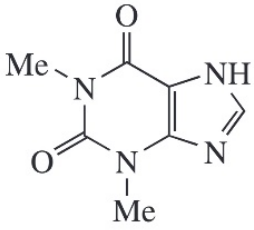

14

The detailed analysis of docking results both for antagonists and for agonists (which are located between transmembrane α-helices) allowed us to evaluate the main features of the ligands structures responsible for the activity. Recently, after the publication of the $A_{2A}$ receptor X-ray structure,[42] it has been shown that the crystallographic structure of $A_{2A}$ receptor has been reasonably approximated using rhodopsin-based modelling [43,44] though the ligand positions are most accurate when water molecules are taken into account or some constraints (like at least one H-bond) are applied. A comparison of the $A_{2B}$ receptor models based on the X-ray structures of bovine rhodopsin, the $\beta_2$-adrenergic receptor and the human $A_{2A}$ receptor was performed.[45]

**Figure** 7 Molecular model of $A_{2B}$ adenosine receptor.

## Melatonin receptors

Melatonin **15,** the natural agonist of melatonin receptors,[46] is widely used to treat daily rhyme disorders, migraine and seasonal depressions. Melatonin receptors belong to the same family of GPCRs as adenosine receptors (type 1 GPCRs). Like other GPCRs, they consist of seven transmembrane α-helices linked by three extracellular and three intracellular hydrophilic loops. The models of two subtypes of melatonin receptors

based on the bovine rhodopsin structure were published.[47-52] The binding site of melatonin is located between α-helices, the oxygen atom of the methoxy group, as well as the acetamido group of melatonin, form hydrogen bonds with the receptor. However, the results of the docking of melatonin and its analogues showed the absence of any direct interactions of the nitrogen atom in the indol fragment of melatonin with the receptor. It allows one to conclude that the indol fragment is not necessary for the manifestation of activity, and it may be replaced with other fragments. This conclusion is confirmed by the existence of a great number of ligands without the indol fragment. The results of modelling were used in the design of melatonin receptor ligands incorporating new scaffolds.[53]

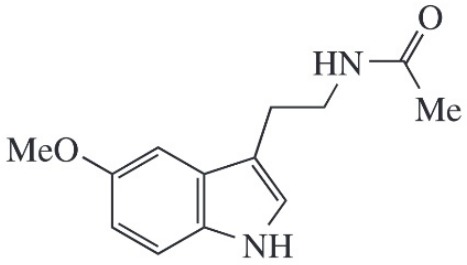


**15**

## Receptors of γ-aminobutyric acid $GABA_A$ and $GABA_C$

γ-Aminobutyric acid (GABA) **16** is the main inhibitory neurotransmitter in the vertebrate CNS.[54-57] GABA activates three types of receptors, $GABA_A$, $GABA_B$, and $GABA_C$. The $GABA_C$ receptor is sometimes considered as a subtype of $GABA_A$ receptors, and it is designated as $GABA_{A0r}$.[54] The $GABA_B$ receptor belongs to the type 3 GPCR, and it will not be considered in this article. $GABA_A$ and $GABA_C$ receptors are pentameric ligand-gated ion channels belonging to a nicotinicoid (Cys-loop) family. Several drugs like benzodiazepines and barbiturates bind with $GABA_A$ receptors. New ligands affecting $GABA_A$ receptors may find application in the treatment of epilepsy, schizophrenia, Alzheimer's and Parkinson's diseases, *etc.*

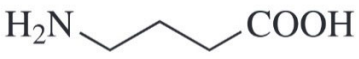


**16**

$GABA_A$ and $GABA_C$ receptors consist of five subunits forming the ion channel. Each subunit includes an N-terminal domain and four transmembrane α-helices. The extracellular domain consists of an α-helical region and a β-sandwich. Several types and subtypes of subunits composing the pentameric structure of $GABA_A$ receptors have been identified, the composition $\gamma_2\beta_2\alpha_1\beta_2\alpha_1$ [Figure 8(a)] is the most common in brain, and for this composition (as well as for a few other compositions with different α-

subunit types) our modelling[58,59] was performed for open and closed forms of the receptor using acetylcholine-binding protein (AChBP) as a template. Similarly, the models of $GABA_C$ receptor consisting of $\rho_1$ subunits were built.[59-61] The picture of the model of extracellular domain of $GABA_A$ receptor is shown in Figure 8. This domain hosts the main binding sites for the neurotransmitter GABA (located between α and β subunits) and benzodiazepines (located between α and γ subunits). The analysis of the docking of GABA into the closed form of the receptor allowed us to suggest the mechanism of the receptor activation: GABA binds to the $GABA_A$ receptor and interacts with αArg120 and βGlu155 to weaken the salt bridge between βGlu155 and βArg207. Thus, the latter may interact with αGlu183 and αAsp184. This can lead to conformational rearrangements finally causing the channel opening. The detailed analysis of the GABA binding site allowed us to design new potent structures.

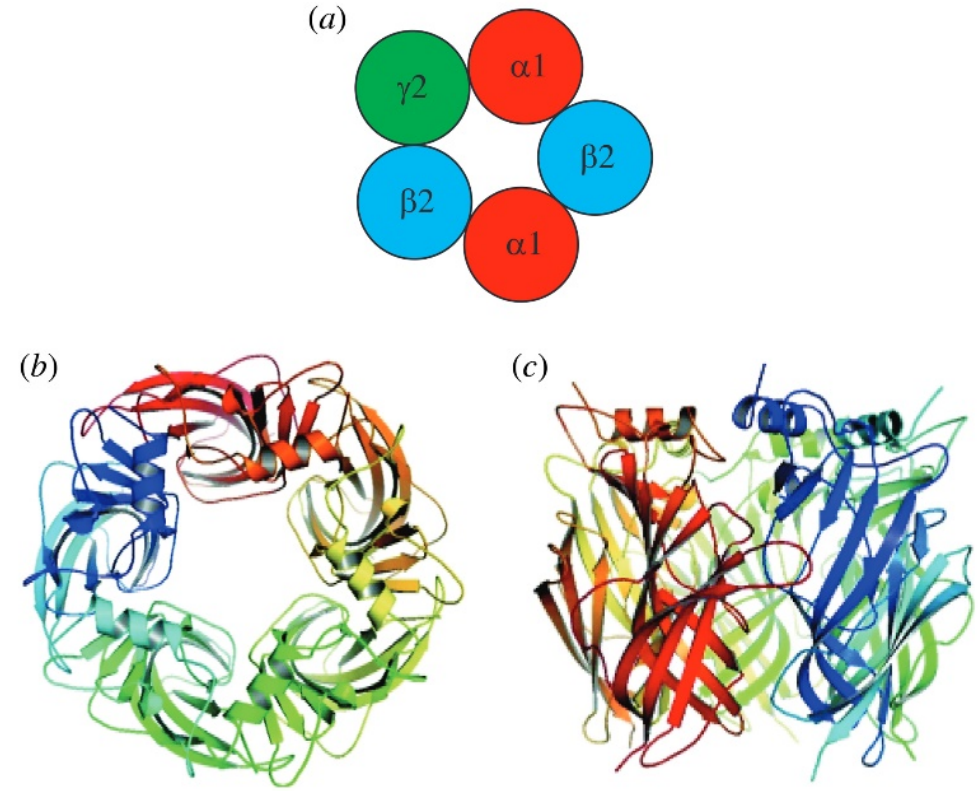


**Figure 8** Extracellular domain of $GABA_A$ receptor: *(a)* arrangement of domains, *(b)* top view, and *(c)* side view.

Our molecular modelling of $GABA_A$ and $GABA_C$ receptors and molecular dynamics simulation[58-61] together with other modelling studies[62-72] had revealed the receptor structures in different forms and putative binding modes of many known ligands.

The docking studies for the benzodiazepine-binding site in several $GABA_A$ receptor subtypes jointly with QSAR studies[73-76] have shown the ligand structural features responsible for the activity variation and selectivity with respect to those subtypes.

In conclusion, note that the molecular modelling of receptors and the detailed analysis of their binding sites is an important step in the design of new drugs. Dozens

of receptors ligands computationally designed by our group had demonstrated exclusively high activity, and some of them are now at the preclinical stages of pharmacological studies.

## References


1. I. I. Baskin, V. A. Palyulin and N. S. Zefirov, *Usp. Khim.,* 2009, **78**, 539 (*Russ. Chem. Rev.,* 2009, **78**, 495).
2. C. G. Parsons, W. Danysz and G. Quack, *Drug News Perspect.,* 1998, **11**, 523.
3. N. S. Nakanishi, *Science,* 1992, **258**, 31.
4. S. Bachurin, S. Tkachenko, I. Baskin, N. Lermontova, T. Mukhina, L. Petrova, A. Ustinov, A. Proshin, V. Grigoriev, N. Lukoyanov, V. Palyulin and N. Zefirov, *Ann. New York Acad. Sci.,* 2001, **931**, 219.
5. D. A. Doyle, J. M. Cabral, R. A. Pfuetzner, A. Kuo, J. M. Gulbis, S. L. Cohen, B. T. Chait and R. MacKinnon, *Science,* 1998, **280**, 69.
6. I. G. Tikhonova, I. I. Baskin, V. A. Palyulin and N. S. Zefirov, *Dokl. Akad Nauk,* 2004, 396, 551 [*Dokl. Biochem. Biophys.* (*Engl. Transl.*), 2004, **396**, 181].
7. K. Kashiwagi, T. Masuko, C. D. Nguyen, T. Kuno, I. Tanaka, K. Igarashi and K. Williams, *Mol. Pharmacol.,* 2002, **61**, 533.
8. M. L. Mayer, G. L. Westbrook and P. B. Guthrie, *Nature,* 1984, **309**, 261.
9. J. W. Johnson and P. Ascher, *Nature,* 1987, **325**, 529.
10. I. G. Tikhonova, I. I. Baskin, V. A. Palyulin and N. S. Zefirov, *Dokl. Akad. Nauk,* 2002, **382**, 550 [*Dokl. Biochem. Biophys.* (*Engl. Transl.*), 2002, **382**, 38].
11. *(a)* I. G. Tikhonova, I. I. Baskin, V. A. Palyulin, N. S. Zefirov and S. O. Bachurin, *J. Med. Chem.,* 2002, **45**, 3836; *(b)* I. G. Tikhonova, I. I. Baskin, V. A. Palyulin, N. S. Zefirov and S. O. Bachurin, *J. Med, Chem.,* 2002, **45**, 5608.
12. N. Armstrong and E. Gouaux, *Neuron,* 2000, **28**, 165.
13. I. G. Tikhonova, I. I. Baskin, V. A. Palyulin and N. S. Zefirov, *Dokl. Akad. Nauk,* 2002, **382**, 840 [*Dokl. Biochem. Biophys.* (*Engl. Transl.*), 2002, **382**, 67].
14. I. G. Tikhonova, I. I. Baskin, V. A. Palyulin and N. S. Zefirov, *J. Med. Chem.,* 2003, **46**, 1609.
15. H. Furukawa and E. Gouaux, *EMBO J.,* 2003, **22**, 2873.
16. I. I. Baskin, I. G. Tikhonova, V. A. Palyulin and N. S. Zefirov, *J. Med. Chem.,* 2003, **46**, 4063.
17. I. G. Tikhonova, I. I. Baskin, V. A. Palyulin and N. S. Zefirov, *Dokl. Akad. Nauk,* 2004, **397**, 549 [*Dokl. Biochem. Biophys. (Engl. Transl.*), 2004, **397**, 242].
18. N. Kunishima, Y. Shimada, Y. Tsuji, T. Sato, M. Yamamoto, S. Kumasaka, S. Nakanishi, H. Jingami and K. Morikawa, *Nature,* 2000, **407**, 971.
19. I. G. Tikhonova, I. I. Baskin, V. A. Palyulin and N. S. Zefirov, *Dokl. Akad. Nauk,* 2003, **389**, 123 [*Dokl. Biochem. Biophys.* (*Engl. Transl.*), 2003, **389**, 75].
20. I. G. Tikhonova, I. I. Baskin, V. A. Palyulin and N. S. Zefirov, *Izv. Akad. Nauk, Ser. Khim.,* 2004, 1282 (*Russ. Chem. Bull., Int. Ed.,* 2004, **53**, 1335).
21. A. A. Kaczor, U. A. Kijkowska-Murak, C. Kronbach, K. Unverferth and D. Matosiuk, *J. Chem. Inf. Model.,* 2009, **49**, 1094.
22. A. I. Sobolevsky, M. P. Rosconi and E. Gouaux, *Nature,* 2009, **462**, 745.
23. I. G. Tikhonova, M. I. Lavrov, V. A. Palyulin and N. S. Zefirov, *Dokl. Akad. Nauk,* 2004, **399**, 268 [*Dokl. Biochem. Biophys.* (*Engl. Transl.*), 2004, **399**, 351].

24. S. O. Bachurin, V. V. Grigor'ev, N. S. Zefirov, M. I. Lavrov, V. L. Lapteva and V. A. Palyulin, *RF Patent* RU 2333211, 2008.
25. D. D. Schoepp, D. E. Jane and J. A. Monn, *Neuropharmacology,* 1999, **38**, 1431.
26. I. I. Baskin, M. S. Belenikin, E. V. Ekimova, G. Costantino, V. A. Palyulin, R. Pellicciari and N. S. Zefirov, *Dokl. Akad. Nauk,* 2000, **374**, 347 [*Dokl. Chem.* (*Engl. Transl.*), 2000, **374**, 191].
27. A. A. Jensen, P. O. Sheppard, P. J. O'Hara, P. Krogsgaard-Larsen and H. Brauner-Osborne, *Eur. J. Pharmacol.,* 2000, **397**, 247.
28. M. S. Belenikin, I. I. Baskin, V. A. Palyulin and N. S. Zefirov, *Dokl. Akad. Nauk,* 2002, **383**, 643 [*Dokl. Chem.* (*Engl. Transl.*), 2002, **383**, 97].
29. M. S. Belenikin, I. I. Baskin, V. A. Palyulin and N. S. Zefirov, *Dokl. Akad. Nauk,* 2002, **384**, 113 [*Dokl. Biochem. Biophys.* (*Engl. Transl.*), 2002, **384**, 131].
30. M. S. Belenikin, I. I. Baskin, G. Costantino, V. A. Palyulin, R. Pellicciari and N. S. Zefirov, *Dokl. Akad. Nauk,* 2002, **386**, 261 [*Dokl. Biochem. Biophys.* (*Engl. Transl.*), 2002, **386**, 251].
31. M. S. Belenikin, A. Macciarulo, G. Costantino, V. A. Palyulin, R. Pellicciari and N. S. Zefirov, *Vestn. Mosk. Univ., Ser. 2: Khim.,* 2002, **43**, 221 (in Russian).
32. M. S. Belenikin, G. Costantino, V. A. Palyulin, R. Pellicciari and N. S. Zefirov, *Dokl. Akad. Nauk,* 2003, **393**, 827 [*Dokl. Biochem. Biophys.* (*Engl. Transl.*), 2003, **393**, 341].
33. M. S. Belenikin, V. A. Palyulin and N. S. Zefirov, *Dokl. Akad. Nauk,* 2004, **394**, 259 [*Dokl. Biochem. Biophys.* (*Engl. Transl.*), 2004, **394**, 21].
34. B. B. Fredholm, J. F. Chen, S. A. Masino and J. M. Vaugeois, *Annu. Rev. Pharmacol. Toxicol.,* 2005, **45**, 385.
35. B. B. Fredholm, A. P. IJzerman, K. A. Jacobson, K. N. Klotz and J. Linden, *Pharmacol. Rev.,* 2001, **53**, 527.
36. A. A. Ivanov, V. A. Palyulin and N. S. Zefirov, *J. Mol. Graph. Model.,* 2007, **25**, 740.
37. A. A. Ivanov, I. I. Baskin, V. A. Palyulin, P. G. Baraldi and N. S. Zefirov, *Mendeleev Commun.,* 2002, 211.
38. A. A. Ivanov, I. I. Baskin, V. A. Palyulin, L. Piccagli, P. G. Baraldi and N. S. Zefirov, *J. Med. Chem.,* 2005, **48**, 6813.
39. V. A. Palyulin, A. A. Ivanov, P. G. Baraldi and N. S. Zefirov, *Purinergic Signalling,* 2006, **2**, 262.
40. A. A. Ivanov, I. I. Baskin, V. A. Palyulin and N. S. Zefirov, *Dokl. Akad. Nauk,* 2002, **386**, 548 [*Dokl. Biochem. Biophys* (*Engl. Transl.*), 2002, **386**, 271].
41. A. A. Ivanov, I. I. Baskin, V. A. Palyulin and N. S. Zefirov, *Dokl. Akad. Nauk,* 2003, **389**, 404 [*Dokl. Biochem. Biophys.* (*Engl. Transl.*), 2003, **389**, 94].
42. V.-P. Jaakola, M. T. Griffith, M. A. Hanson, V. Cherezov, E. Y. T. Chien, J. R. Lane, A. P. IJzerman and R. C. Stevens, *Science,* 2008, **322**, 1211.
43. A. A. Ivanov, D. Barak and K. A. Jacobson, *J. Med. Chem.,* 2009, **52**, 3284.
44. S.-K. Kim, Z.-G. Gao, P. Van Rompaey, A. S. Gross, A. Chen, S. Van Calenbergh and K. A. Jacobson, *J. Med. Chem.,* 2003, **46**, 4847.
45. F. F. Sherbiny, A. C. Schiedel, A. Maaß and C. E. Müller, *J. Comput. Aided Mol. Des.,* 2009, **23**, 807.
46. R. Jockers, P. Maurice, J. A. Boutin and P. Delagrange, *Br. J. Pharmacol.,* 2008, **154**, 1182.
47. A. A. Ivanov, A. E. Voronkov, I. I. Baskin, V. A. Palyulin and N. S. Zefirov, *Dokl. Akad. Nauk,* 2004, **394**, 822 [*Dokl. Biochem. Biophys.* (*Engl. Transl.*), 2004, **394**, 49]
48. A. E. Voronkov, A. A. Ivanov, I. I. Baskin, V. A. Palyulin and N. S. Zefirov, *Dokl. Akad. Nauk,* 2005, **403**, 409 [*Dokl. Biochem. Biophys.* (*Engl. Transl.*), 2005, **403**, 284]

49. (*a*) P. Mazna, V. Obsilova, I. Jelinkova, A. Balik, K. Berka, Z. Sovova, R. Ettrich, P. Svoboda, T. Obsil and J. Teisinger, *J. Neurochem.,* 2004, **91**, 836; (*b*) P. Mazna, V. Obsilova, I. Jelinkova, A. Balik, K. Berka, Z. Sovova, R. Ettrich, P. Svoboda, T. Obsil and J. Teisinger, *J. Neurochem.,* 2004, **91**, 1505.
50. S. Rivara, M. Mor, S. Lorenzi, A. Lodola, P. V. Plazzi, G. Spadoni, A. Bedini and G. Tarzia, *ARKIVOC,* 2006, Part 8, 8.
51. A. O. Chugunov, A. Farce, P. Chavatte and R. G. Efremov, *J. Biomol. Struct. Dyn.,* 2006, **24** (2), 91.
52. A. Farce, A. O. Chugunov, C. Logé, A. Sabaouni, S. Yous, S. Dilly, N. Renault, G. Vergoten, R. G. Efremov, D. Lesieur and P. Chavatte, *Eur. J. Med. Chem.,* 2008, **43**, 1926.
53. T. Yu. Baranova, O. N. Zefirova, N. V. Averina, V. V. Boyarskikh, G. S. Borisova, N. V. Zyk and N. S. Zefirov, *Zh. Org. Khim.,* 2007, **43**, 1201 (*Russ. J. Org. Chem.,* 2007, **43**, 1196).
54. G. Michels and S. J. Moss, *Crit. Rev. Biochem. Mol. Biol.,* 2007, **42**, 3.
55. M. Chebib and G. A. Johnston, *J. Med. Chem.,* 2000, **43**, 1427.
56. M. Chebib, *Clin. Exp. Pharmacol. Physiol*., 2004, **31**, 800.
57. C. D'Hulst, J. R. Atack and R. F. Kooy, *Drug Discov. Today,* 2009, **14**, 866.
58. V. I. Chupakhin, V. A. Palyulin and N. S. Zefirov, *Dokl. Akad. Nauk,* 2006, **408**, 693 [*Dokl. Biochem. Biophys.* (*Engl. Transl.*), 2006, **408**, 169].
59. D. I. Osolodkin, V. I. Chupakhin, V. A. Palyulin and N. S. Zefirov, *Dokl. Akad. Nauk,* 2007, **412**, 404 [*Dokl. Biochem. Biophys.* (*Engl. Transl.*), 2007, **412**, 25].
60. D. I. Osolodkin, V. I. Chupakhin, V. A. Palyulin and N. S. Zefirov, *J. Mol. Graph. Model.,* 2009, **27**, 813.
61. V. I. Chupakhin, *PhD Thesis,* M. V. Lomonosov Moscow State University, 2010.
62. B. A. Cromer, C. J. Morton and M. W. Parker, *Trends Biochem. Sci.,* 2002, **27**, 280.
63. M. Ernst, D. Brauchart, S. Boresch and W. Sieghart, *Neuroscience,* 2003, **119**, 933.
64. M. Ernst, D. Brauchart, S. Boresch and W. Sieghart, *Mol. Pharmacol.,* 2005, **68**, 1291.
65. C. L. Padgett, A. P. Hanek, H. A. Lester, D. A. Dogherty and S. C. Lummis, *J. Neurosci.,* 2007, **26**, 760.
66. Y. Mokrab, V. N. Bavro, K. Mizuguchi, N. P. Todorov, I. L. Martin, S. M. Dunn, S. L. Chan and P. L. Chau, *J. Mol. Graph. Model.,* 2007, **26**, 760.
67. J. R. Trudell and E. Bertaccini, *Br. J. Anaesth.,* 2002, **89**, 32.
68. V. Canpagna-Slater and D. F. Weaver, *J. Mol. Graph. Model.,* 2007, **25**, 721.
69. M. O'Mara, B. Cromer, M. Parker and S. H. Chung, *Biophys. J.,* 2005, **88**, 3286.
70. A. Sedelnikova, C. D. Smith, S. O. Zakharkin, D. Davis, D. S. Weiss and Y. Cheng, *J. Biol. Chem.,* 2005, **280**, 1535.
71. N. J. Harrison and S. C. Lummis, Z *Mol. Model.,* 2006, **12**, 317.
72. H. Abdel-Halim, J. R. Hanrahan, D. E. Hibbs, G. A. Johnston and M. A. Chebib, *Chem. Biol. Drug. Des.,* 2008, **71**, 306.
73. V. I. Chupakhin, S. V. Bobrov, E. V. Radchenko, V. A. Palyulin and N. S. Zefirov, *Dokl. Akad. Nauk,* 2008, **422**, 204 [*Dokl. Chem.* (*Engl. Transl*.), 2008, **422**, 227],
74. E. V. Radchenko, V. A. Palyulin and N. S. Zefirov, in *Chemoinformatics Approach to Virtual Screening,* ed. A. Vamek and A. Tropsha, RSC, Cambridge, 2008, pp. 150-181.
75. V. A. Palyulin, E. V. Radchenko and N. S. Zefirov, *J. Chem. Inf. Comput. Sci.,* 2000, **40**, 659.
76. E. V. Radchenko, V. A. Palyulin and N. S. Zefirov, *Zh. Khim. Ob-va im. D. I. Mendeleeva* (*Ross. Khim. Zh.),* 2006, **50** (2), 76 (in Russian).

# Оглавление

**Введение ..... 3**

**Раздел I. Предмет и стратегии медицинской химии ..... 7**

МЕДИЦИНСКАЯ ХИМИЯ (MEDICINAL CHEMISTRY). I. КРАТКИЙ ИСТОРИЧЕСКИЙ ОЧЕРК, ОПРЕДЕЛЕНИЯ И ЦЕЛИ ..... 8

МЕДИЦИНСКАЯ ХИМИЯ (MEDICINAL CHEMISTRY). II. МЕТОДОЛОГИЧЕСКИЕ ОСНОВЫ СОЗДАНИЯ ЛЕКАРСТВЕННЫХ ПРЕПАРАТОВ ..... 17

**Раздел II. Избранные работы в области медицинской химии препаратов для лечения нейродегенеративных заболеваний ..... 33**

МЕДИЦИНСКАЯ ХИМИЯ ДЛЯ КОРРЕКЦИИ ФУНКЦИЙ МОЗГА ..... 37

Structural Basis for Understanding Structure- Activity Relationships for the Glutamate Binding Site of the NMDA Receptor ..... 46

Neuroprotective and Cognition-Enhancing Properties of MK-801 Flexible Analogs Structure-Activity Relationships ..... 61

МОЛЕКУЛЯРНЫЙ ДИЗАЙН ПРОНЕЙРОГЕННЫХ И НЕЙРОПРОТЕКТОРНЫХ СОЕДИНЕНИЙ – АЛЛОСТЕРИЧЕСКИХ МОДУЛЯТОРОВ РЕЦЕПТОРА NMDA ..... 78

НОВЫЙ БИВАЛЕНТНЫЙ ПОЛОЖИТЕЛЬНЫЙ АЛЛОСТЕРИЧЕСКИЙ МОДУЛЯТОР AMPA-РЕЦЕПТОРОВ ..... 84

Синтез «трипептида памяти» (Arg–Glu–Arg, RER) и реакция Кабачника–Филдса с ди- и трипептидами как метод синтеза фосфор- содержащих производных пептидов ..... 89

Combined QSAR studies of inhibitor properties of O-phosphorylated oximes toward serine esterases involved in neurotoxicity, drug metabolism and Alzheimer's disease ..... 97

Antihistamine Agent Dimebon As a Novel Neuroprotector and a Cognition Enhancer ..... 119

**Раздел III. ИЗБРАННЫЕ РАБОТЫ ПО СОЗДАНИЮ ПРОТИВООПУХОЛЕВЫХ АГЕНТОВ ..... 131**

Design, synthesis and bioactivity of simplified taxol analogues on the basis of bicyclo[3.3.1]-nonane derivatives ..... 133

Design, synthesis, and bioactivity of putative tubulin ligands with adamantane core ..... 140

Synthesis and cytotoxicity of novel simplified eleutherobin analogues as potential antitumour agents ..... 147

Synthesis and SAR requirements of adamantane-colchicine conjugates with both microtubule depolymerizing and tubulin clustering activities ..... 159

Unusual Tubulin-Clustering Ability of Specifically C7- Modified Colchicine Analogues ..... 172

Novel antimitotic agents related to tubuloclustin: synthesis and biological evaluation ..... 184

Synthesis and antimitotic activity of novel 5-aminoisoxazoles bearing alkoxyaryl moieties ..... 198

**Раздел IV. Избранные работы в области медицинской химии препаратов для терапии нарушений окислительного статуса организма ..... 205**

Antioxidative Activity of Ferrocenes Bearing 2,6-Di-*Tert*-Butylphenol Moieties ..... 208

Synthesis and antioxidative activity of metalloporphyrins bearing 2,6-di-*tert*-butylphenol pendants ..... 218

Комплексы меди с нитронилнитроксильными радикалами – ингибиторы липоксигеназы с антиоксидантной активностью ..... 236

Synthesis and biological evaluation of novel 5-hydroxylaminoisoxazole derivatives as lipoxygenase inhibitors and metabolism enhancing agents ..... 252

**Раздел V. Избранные работы по созданию веществ с различными видами биологической активности ..... 266**

Application of the bridgehead fragments for the design of conformationally restricted melatonin analogues ..... 268

МОЛЕКУЛЯРНОЕ МОДЕЛИРОВАНИЕ, РЕНТГЕНОСТРУКТУРНЫЙ АНАЛИЗ И ИЗУЧЕНИЕ iNOS-ИНГИБИРУЮЩЕЙ АКТИВНОСТИ ГИДРОХЛОРИД А 3-ИМИНО-2,4-ДИАЗАБИЦИКЛО[3.3.1]-НОНАН-1-ОЛА ..... 277

Synthesis and assessment of 4-aminotetrahydroquinazoline derivatives as tick-borne encephalitis virus reproduction inhibitors ..... 283

**Раздел VI. Избранные работы в области развития методов компьютерного молекулярного моделирования и QSAR ..... 299**

General Purpose Electronegativity Relaxation Charge Models Applied to CoMFA and CoMSIA Study of GSK-3 Inhibitors ..... 302

One-class classification as a novel method of ligand-based virtual screening: The case of glycogen synthase kinase 3β inhibitors ..... 320

Прогнозирование всасывания лекарственных веществ в кишечнике человека ..... 327

ПРОГНОЗИРОВАНИЕ ПРОНИКНОВЕНИЯ ОРГАНИЧЕСКИХ ВЕЩЕСТВ ЧЕРЕЗ ГЕМАТОЭНЦЕФАЛИЧЕСКИЙ БАРЬЕР ..... 335

КОМПЬЮТЕРНАЯ ОЦЕНКА РИСКА hERG-ОПОСРЕДОВАННОЙ КАРДИОТОКСИЧНОСТИ ПОТЕНЦИАЛЬНЫХ ЛЕКАРСТВЕННЫХ ВЕЩЕСТВ ..... 342

Molecular modelling of central nervous system receptors ..... 348

**Избранные труды академика Н.С. Зефирова**
**в области медицинской химии**

Под общей редакцией
академика С.О. Бачурина и профессора О.Н. Зефировой

Сдано в печать 16.05.2025. Подписано в печать 09.06.2025.
Формат 60×90/16. Объем 22,75 п.л.  Заказ 74. Тираж 100

Отпечатано в ФИЦ ПХФ и МХ РАН
142432, Московская обл., г. Черноголовка, пр-т ак. Семенова, 5
Тел. 8(496)522-44-71

Книга содержит избранные статьи в области медицинской химии с авторством академика Н.С. Зефирова, опубликованные в открытой печати (в российских и зарубежных научных журналах).

Материал в книге систематизирован по разделам:

- предмет и стратегии медицинской химии;
- избранные работы в области медицинской химии препаратов для лечения нейродегенеративных заболеваний;
- избранные работы по созданию противоопухолевых агентов;
- избранные работы в области медицинской химии препаратов для терапии нарушений окислительного статуса организма;
- избранные работы по созданию веществ с различными видами биологической активности;
- избранные работы в области развития методов компьютерного молекулярного моделирования и QSAR.

Во *Введении* кратко описана научная деятельность академика Н.С. Зефирова.

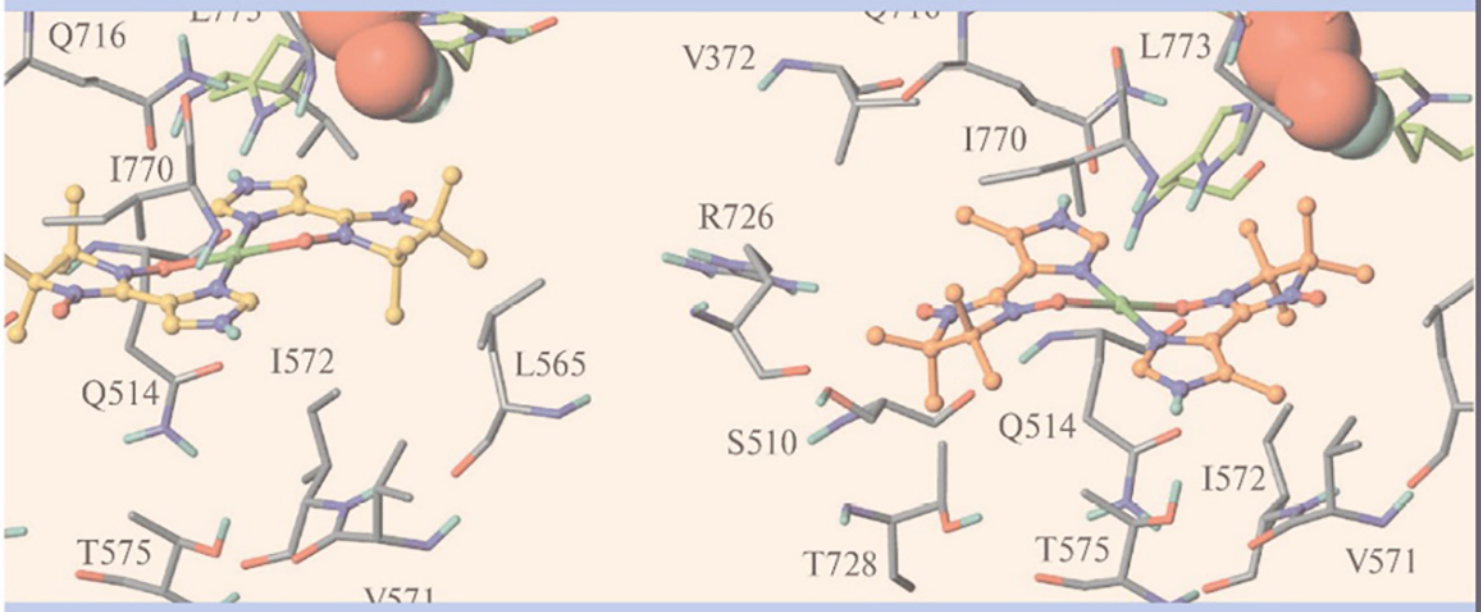


ISBN 978-5-91845-122-9